Conséquences de la surexpression des formes solubles de l'APP dans les mécanismes de mémoire : application à la maladie d'Alzheimer

Romain Fol

UNIVERSITE PARIS DESCARTES

THESE DE DOCTORAT

pour obtenir le grade de Docteur de l'Université Paris Descartes
Ecole Doctorale : Bio Sorbonne Paris Cité
Département : « Développement, Génétique, Neurobiologie, Reproduction et Vieillissement
Discipline : Neurobiologie

Conséquences de la surexpression des formes solubles de l'APP dans les mécanismes de mémoire : Application à la maladie d'Alzheimer.

Présentée et soutenue publiquement par
Romain Fol
le 21 septembre 2016

M. le Professeur Charles DUYCKAERTS	Président
Mme. le Docteur Sylvie CLAEYSEN	Rapportrice
Mme. le Docteur Cécile DELARASSE	Rapportrice
Mme. le Professeur Bernadette ALLINQUANT	Examinatrice
M. le Docteur Alexandre URANI	Examinateur
Mme. le Professeur Nathalie CARTIER	Directrice de thèse

« In the race for excellence, there is no finish line »

David T. Kearns

REMERCIEMENTS :

Je tiens d'abord à remercier les membres de mon jury pour avoir accepté d'examiner mon travail de thèse et pour leur participation à ma soutenance. C'est un véritable plaisir pour moi d'exposer mon travail de thèse devant un jury de cette qualité. Je remercie tout particulièrement les Docteur Sylvie Claeysen et Cécile Delarasse pour avoir accepté d'être rapportrices de mon manuscrit. Un grand merci au Professeur Charles Duyckaerts, président de ce jury, ainsi qu'au Professeur Bernadette Allinquant et au Docteur Alexandre Urani pour l'évaluation de ce travail comme examinateurs.

Je remercie chaleureusement ma directrice de thèse, le Professeur Nathalie Cartier, de m'avoir donné l'opportunité de réaliser cette thèse. Je vous remercie de m'avoir laissé cette grande autonomie et d'avoir eu la chance de profiter de cette fructueuse collaboration franco-allemande.

Un grand merci aux membres, passés ou présents, du bureau INSERM : Jérôme, Mickaël, Benoit, Marie-Anne, Sandro, Satoru & Nicola. Merci à Jérôme pour les discussions extra-scientifiques et sans qui cette thèse n'aurait pas été possible. Merci à mes confrères doctorants, Micka et Benito, pour leur aide et les bons moments passés.

Merci à Françoise et Gaëlle pour l'aide apportée au cours de ma thèse. Merci aux autres membres de l'U1169 : Aurélie, Benoit G, Caroline S, Christine, Cyndie, Emilie, Fathia, Laetitia, Morgane, Sylvie, Vanja, Yasemin, et bien sûr Léa. J'en profite aussi pour remercier les directeurs de l'unité : le Pr Patrick Aubourg et le Pr Pierre Bougnères.

Je remercie énormément mes collaborateurs du consortium ERANET : Ulrike, Christian, Martin, Anton, Sascha, Tobias, Susann et Jan-Peter. Cette collaboration fut fructueuse et le sera encore.

Merci aux membres de MIRCen, qui ont permis d'agrémenter cette thèse tant scientifiquement qu'au niveau extra-professionnel. Je remercie tout particulièrement Alexis et son équipe : Charlène, Noëlle et Gwen pour les prods virales et leur sortie du A2.

Il me sera difficile de citer tout le monde, mais je tiens à remercier grandement le personnel avec lequel il a été agréable d'interagir. Merci à Juliette, Laetitia, Lucille, Matthias, Emilie. Marie-Claude, Karine, Maria, Mylène, Dimitri, Julien, Charlotte, Noémie, Marie, Yael, Kelly, Sandrine, Brice, Clémence, Caroline, Fanny, Pauline, Camille, Didier, Aude, Laurent, Sylvie, Martine, Léopold, Che, Laurent W, Lev, Claire-Maëlle, Joanna, Marie-Christine, Marie-Laure, sans oublier les chefs d'équipes : Philippe, Emmanuel, Marc, Carole, Gilles & Frédéric. Un gros merci également à toute l'équipe indispensable au bien-être de nos animaux : Julien, Lambert, David & Jean-Marie.

Merci aux sportifs de MIRCen (Clémence, Juliette, Mylène, Séverine, Fanny, Micka, Benoit, Brice, Yael entre autres) pour les bons moments passés entre volley-ball, course à pieds et fractionné/freeletics pour les plus courageux !

Merci aux Magistériens pour les soirées et escapades européennes au cours de ces 3 dernières années. Enfin merci à mes parents & Xénia sans qui je n’en serais pas là aujourd’hui.

RESUME :

Une des principales caractéristiques de la maladie d'Alzheimer (MA) est l'accumulation intracérébrale du peptide neurotoxique Amyloïde β (Aβ) sous forme oligomérique et sous forme agrégée en plaques amyloïdes. Ce peptide est le produit du clivage de l'**Amyloid Precursor Protein** (**APP**) selon la voie amyloïdogène, voie pathologique suractivée dans la MA. La majorité des recherches, au cours des 25 dernières années, se sont concentrées sur les conséquences pathologiques de cette dérégulation, mettant au second plan la compréhension des fonctions physiologiques de l'APP. Cependant, de nombreuses études montrent que ses fonctions physiologiques pourraient être médiées par ses formes solubles (APPs). Dans la voie de clivage physiologique, la voie non-amyloïdogène, l'APP est clivé par l'α secrétase pour libérer l'**APPsα**, peptide disposant de propriétés neuroprotectrices et synaptotrophiques, essentielles au bon fonctionnement cérébral. Dans le contexte de la MA, la suractivation de la voie amyloïdogène va aboutir à la production de l'**APPsβ** au détriment de celle d'APPsα. Les conséquences fonctionnelles associées à la maladie d'Alzheimer pourraient ainsi être dues à la diminution de la production d'APPsα associée à une augmentation de la production d'APPsβ.

Mon projet de thèse porta sur les conséquences mnésiques et fonctionnelles de la surexpression de ces deux formes et à leur potentiel thérapeutique dans la maladie d'Alzheimer.

Nous avons tout d'abord surexprimé l'APPsα dans les neurones de l'hippocampe de souris transgéniques APP/PS1ΔE9, modèle de la MA, qui présentent des déficits cognitifs et synaptiques. L'expression continue d'APPsα, à l'aide de vecteurs AAV, permet la **restauration des performances mnésiques des souris, de la potentialisation à long terme (LTP) ainsi que du nombre d'épines dendritiques** dans l'hippocampe. Ce sauvetage phénotypique s'accompagne de la **diminution conjointe des niveaux d'Aβ et des plaques amyloïdes**. Ceci serait en partie la conséquence de l'**activation de la microglie**, type cellulaire ayant la capacité d'internaliser et de dégrader l'Aβ.

Mon second axe de recherche a consisté à étudier l'APPsβ dont l'implication dans la MA reste méconnue. Sa surexpression dans le modèle murin APP/PS1ΔE9 n'induit pas de restauration de la LTP ni de la mémoire spatiale. Néanmoins, l'injection d'APPsβ aboutit à la **diminution de la concentration en Aβ solubles** sans cependant réduire le nombre de plaques amyloïdes. Ce défaut pourrait-être la conséquence de l'absence d'activation microgliale.

En résumé, mon travail de thèse montre que, contrairement à l'APPsβ, la surexpression d'APPsα pourrait contrecarrer l'évolution inéluctable de la maladie et en particulier en réduisant l'atteinte synaptique et mnésique caractéristique de la MA. **Ces résultats renforcent une nouvelle voie d'action pour lutter contre la progression de la MA. L'utilisation de l'APPsα en tant qu'agent thérapeutique pourrait ainsi s'avérer être un élément important dans l'arsenal clinique de ces prochaines années.**

Mots-clés : Maladie d'Alzheimer, Thérapie génique, AAV, APP, APPsα, APPsβ, Mémoire spatiale, Plasticité synaptique, Epines dendritiques, Microglie.

ABSTRACT :

One of the main characteristic of Alzheimer's Disease (AD) is the intracerebral accumulation of the neurotoxic Amyloid β peptide (Aβ) either as oligomeric or aggregated forms known as the amyloid plaques. This peptide is produced via the **Amyloid Precursor Protein (APP)** processing following the amyloidogenic pathway, pathological pathway overactivated in AD. Most of the research performed during the last 25 years focused on pathogenic consequences of this dysregulation, deprioritizing the understanding of the APP physiological functions. Nonetheless, numerous studies show that these physiological functions might be mediated via APP soluble forms (APPs). In the physiological APP processing pathway, the non-amyloidogenic pathway, APP is cleaved by the α secretase, releasing the **APPsα** which display neuroprotective and synaptotrophic properties, essential for brain normal functions. In the context of AD, the amyloidogenic pathway overactivation leads to **APPsβ** overproduction at the expense of APPsα. Therefore, AD harmful consequences could be due to the decrease of APPsα concentration associated with an increase of APPsβ.

My thesis project aimed to characterize mnemonic and functional properties following the overexpression of these two soluble forms of APP and their therapeutic potential in AD.

We firstly overexpressed APPsα in hippocampal neurons of APP/PS1ΔE9 mice, animal model of AD, which display cognitive and synaptic deficits. The continual expression of APPsα, mediated via AAV viruses, enabled **restoration of spatial memory, long-term potentiation and dendritic spines density** in the hippocampus. This phenotypic rescue was accompanied with the **decrease of both Aβ levels and amyloid plaques**. This might be due to the **activation of microglia**, cell type able to internalize and degrade Aβ.

In a second hand, I studied the involvement of APPsβ in AD, which remains poorly known. Its overexpression in APP/PS1ΔE9 did not induce neither LTP nor spatial memory restoration. However, APPsβ injection lead to the **decrease of Aβ levels** without reducing amyloid plaques. This default might be due to the lack of microglial activation.

In conclusion, my thesis work show that, unlike APPsβ, APPsα overexpression might overcome the AD inevitable evolution by reducing synaptic and memory alterations, typical of AD. **These results reinforce a new way of treatment to cope with AD progression. The use of APPsα as therapeutic agent might be an important tool for future AD therapies.**

Key words: Alzheimer's disease, Gene therapy, AAV, APP, APPsα, APPsβ, Spatial memory, Synaptic plasticity, Dendritic spines, Microglia.

I. TABLE DES MATIERES

II. ABREVIATIONS :

AAIC: Alzheimer's Disease Internationnal Conference

ABCA7: Transporteur de cholestérol, de l'anglais « ATP-Binding Cassette sub-family A member 7 »

AD/PD: Alzheimer's Disease / Parkinson's Disease Conference

ADAM10: α-secrétase, de l'anglais « A Disintegrin And Metalloproteinase domain-containing protein 10 »

ADN: Acide DésoxyriboNucléique

AICD: Domaine intracellulaire de l'APP, de l'anglais "APP IntraCellular Domain »

APL: Homologue de l'APP chez Caenorhabditis elegans

APLP1/2: Homologues de l'APP chez les mammifères, de l'anglais « Amyloid β Precursor-Like Protein 1/2

APOE: Apolipoprotéine E »

APP/PS1ΔE9: Modèle murin classiquement utilisé de la MA présentant une mutation Swedish de l'APP et la PS1 délestée de l'exon 9.

APP: Protéine précurseuse du peptide amyloïde β, de l'anglais « Amyloid β Precursor Protein »

APPL: Homologue de l'APP chez la drosophile

APPsβ/α: Formes N-terminales solubles de l'APP

ARN: Acide RiboNucléique

Aβ: Peptide Amyloïde β, de l'anglais « Amyloid β »

BHE: Barrière Hémato-Encéphalique

BIN1: Gène de susceptibilité pour la MA, de l'anglais « Bridging INtegrator 1 »

C57Bl6/j: Souris de laboratoire de type sauvage

CA1/2/3: Sous-structures de l'hippocampe, Corne d'Ammon 1/2/3

CAG: promoteur synthétique fort, de l'anglais « Cytomegalovirus βActin βGlobin »

CD2AP: Gène de susceptibilité pour la MA, de l'anglais « Cluster of Differentiation 2 Associated Protein »

CD33: Gène de susceptibilité pour la MA, de l'anglais « Cluster of Differentiation 33 »

Cdk5: Principale kinase de tau, de l'anglais "Cyclin Depedant Kinase 5"

CLU: Gène de susceptibilité pour la MA, Clusterin ou Apolipoprotéine J

CR1: Gène de susceptibilité pour la MA, de l'anglais « Complement Receptor type 1 »

CuBD: Domaine de liaison au cuivre et au zinc de l'APP, de l'anglais « Copper Binding Domain »

CYP46A1: Cytochrome 46A1, gène codant pour la cholestérol 24-hydroxylase

DNF: Dégénérescence NeuroFibrillaire, « Tangles » en anglais

DYRK1A: Kinase de tau, de l'anglais « Dual specificity Tyrosine (Y) phosphorylation Regulated Kinase 1A

EGF: Facteur de croissance épidermique, de l'anglais « Epidermal Growth Factor »

EPHA1: Gène de susceptibilité pour la MA, de l'anglais « EPHrin Receptor A1 »

FDG: Analogue radiopharmaceutique du glucose, de l'anglais « FluoroDesoxyGlucose »

GAPDH: Gène de ménage, de l'anglais « GlycérAldéhyde-3-Phosphate DésHydrogénase »

G-CSF: Facteur de croissance hématopoïétique spécifique de la lignée granulocytaire, de l'anglais Granulocyte – Colony Stimulating Factor

GFAP: Marqueur astrocytaire, de l'anglais « Glial fibrillary acidic protein »

GSK3β: Principale kinase de tau, de l'anglais « Glycogen Synthase Kinase 3 β »

GWAS: Etudes d'associations pangénomiques, de l'anglais « Genome Wide Association Studies »

HAS: Haute Autorité de Santé

HBD: Domaine de liaison de l'APP à l'héparine, de l'anglais « Heparin Binding Domain »

IBA1: Marqueur microglial, de l'anglais « Ionized calcium Binding Adaptor molecule 1 »

IDE : Enzyme de dégradation de l'insuline et de l'amyloïde β, de l'anglais « Insulin Degrading Enzyme »

iNOS : Enzyme productrice d'oxyde nitrique, de l'anglais « inducible Nitric Oxide Synthase »

INPP5D: Gène de susceptibilité pour la MA, de l'anglais « INositol PolyPhosphate-5-phosphatase D »

IRM: Imagerie par Résonance Magnétique

IWG: International Work Group criteria for the diagnosis of Alzheimer's disease

kb : kilobases, unité de mesure de longueur de l'ADN

kDa : kiloDaltons, unité de masse atomique

KPI: Domaine de l'APP, de l'anglais « Kunitz-type Protease Inhibitor »

LCR: Liquide Céphalo-Rachidien ou liquide cérébro-spinal

LRP : Lipoprotein Receptor-related Proteins

LTD : Dépression à long terme, de l'anglais « Long-Term Depression »

LTP : Potentialisation à long terme, de l'anglais « Long-Term Potentiation »

MA: Maladie d'Alzheimer

MAP/ERK : Voie de signalisation, de l'anglais "Mitogen Activated Protein kinases / Extracellular signal-Regulated Kinases"

MAPT: Gène codant tau, de l'anglais « Microtubule-Associated Protein Tau »

MEF2C: Gène de susceptibilité pour la MA, de l'anglais « Myocyte Enhancer Factor 2C »

MMSE: Test d'évaluation des fonctions cognitives, de l'anglais « Mini Mental State Examination »

MS4A: Gène de susceptibilité pour la MA, de l'anglais « Membrane-Spanning 4-domain A »

NEP : Neprilysine, enzyme de dégradation l'Aβ

NeuN: Marqueur nucléaire, de l'anglais « NEUronal Nuclei »

NGF: Facteur de croissance, de l'anglais « Nerve Growth Factor »

NMDA: acide N-méthyl-D-aspartique

PDAPP: Modèle souris de la MA surexprimant l'APP sous le promoteur PDGF « Platelet Derived Growth Factor »

PGK : promoteur fort, de l'anglais « PhosphoGlycerate Kinase »

PHF: Structures agrégées de tau, de l'anglais Paired Helical Filaments

PICALM: Gène de susceptibilité pour la MA, de l'anglais « PhosphatidylInositol binding Clathrin Assembly Protein »

PLD3: Gène de susceptibilité pour la MA, de l'anglais « PhosphoLipase D3 »

PPF : Facilitation neuronale, de l'anglais Paired Pulse Facilitation

PSD-95: PostSynaptic Density protein 95

PSEN1 / PS1: Préséniline 1

PSEN2 / PS2: Préséniline 2

PTK2B: Gène de susceptibilité pour la MA, de l'anglais « Protein Tyrosine Kinase 2 β »

RIN3: Gène de susceptibilité pour la MA, de l'anglais « Ras INteraction-interference protein 3 »

Ser: Sérine

SFFV : promoteur viral fort, de l'anglais « Spleen Focus-Forming Virus »

SLC24A4: Gène de susceptibilité pour la MA, de l'anglais « Solute Carrier Family 24 member 4 »

SNC: Système Nerveux Central

SNP: Système Nerveux Périphérique

SORL1: Gène de susceptibilité pour la MA, de l'anglais « SORtilin-related receptor L1 »

TEP: Tomographie par Emission de Positons

Tg : Transgénique

Tg2576 : Un des premier modèle souris de la MA présentant une mutation Swedish de l'APP

Thr: Thréonine

Thyr: Thyrosine

TIP60 : Histone acetyl-transferase, de l'anglais « Tat-Interactive Protein 60 kDa »

TREM2: Gène de susceptibilité pour la MA, de l'anglais « Triggering Receptor Expressed on Myeloid cells 2 »

WT: Sauvage, de l'anglais « Wild Type »

β/α-CTF: Fragments carboxy-terminaux de l'APP, de l'anglais « Carboxy Terminal Fragment »

III. LISTE DES FIGURES :

Mon travail de thèse porta sur la meilleure compréhension de la physiologie de l'APP par la surexpression de ses formes solubles. Leur potentiel thérapeutique dans la maladie d'Alzheimer fut aussi exploré. Dans cette introduction, je présenterai tout d'abord la maladie d'Alzheimer dans son ensemble. Je m'intéresserai dans une seconde partie à l'APP puis à ses deux formes solubles présentement décrites et leur potentiel thérapeutique. Dans une ultime partie, je traiterai de la thérapie génique et de ses applications à la maladie d'Alzheimer.

IV. INTRODUCTION :

A. La maladie d'Alzheimer

1. Définition de la démence

Bien qu'il existe différents types de démences comme les démences à corps de Lewy ou les démences fronto-temporales, **la maladie d'Alzheimer (MA)** est la forme la plus commune **représentant entre 50 et 80% des cas**. La démence est un terme général regroupant un large panel de symptômes associés avec un déclin de la mémoire et des capacités cognitives et motrices **portant atteinte à la réalisation des tâches quotidiennes**. Bien que ces symptômes puissent grandement différer entre deux patients, au moins deux des altérations cognitives suivantes doivent être touchées pour que le patient soit considéré comme étant atteint d'une démence (www.alz.org):

- Affection de la mémoire
- Perturbations de la communication et du langage
- Incapacité de se concentrer et de porter attention
- Altération du résonnement et du jugement
- Troubles de la perception visuelle

Cette liste est très certainement non-exhaustive et représente des grandes catégories d'altérations qui peuvent être encore subdivisées. Je reviendrai plus en détails sur le diagnostic de la MA dans la partie clinique (voir partie IV.A.6).

2. Historique d'une découverte

Aloysius **« Alois » Alzheimer (1864-1915) était un médecin et pathologiste allemand**. Il obtint son doctorat de médecine à l'université de Würzburg en 1887 avant de travailler à l'hôpital psychiatrique de Francfort. C'est à partir du 25 novembre 1901 qu'il commença à interagir avec une patiente nouvellement admise, **Auguste Deter (1850-1906)**. Sa condition se matérialisa tout d'abord par une jalousie exacerbée envers son mari suivi ensuite par des défauts de mémoires, des désorientations spatiales, une aphasie, une apraxie, une agnosie et des hallucinations. Alois Alzheimer l'examina fréquemment pendant 5 mois, avant de quitter son poste pour rejoindre l'hôpital psychiatrique royal de Munich. Bien qu'éloigné, celui-ci demanda fréquemment des renseignements sur l'évolution de son état jusqu'en 1906, année du **décès d'Auguste**

Deter, à l'âge de 55 ans. C'est à ce moment qu'il sollicita l'hôpital de Francfort afin d'obtenir son dossier clinique ainsi que son cerveau.

Max Bielschowsky venait alors de publier une technique d'imprégnation à l'argent permettant de révéler les neurofibrilles et portant toujours son nom (Bielschowsky 1902, Bielschowsky 1903). Alois Alzheimer l'utilisa afin de donner une **première description histopathologique de la maladie** qui portera bientôt son nom. Il présenta pour la première fois ses découvertes à la 37ème réunion des psychiatres du sud-ouest de l'Allemagne puis publia peu après, en 1907, un article s'intitulant « Sur une maladie inhabituelle du cortex cérébral »(Alzheimer, Stelzmann et al. 1995, Engelhardt and Gomes Mda 2015). Lors de l'analyse post-mortem, Alois Alzheimer note tout d'abord **l'atrophie globale** du cerveau d'Auguste Deter. La technique d'imprégnation à l'argent lui permit de mettre en évidence les deux grandes caractéristiques histopathologiques de la maladie. Tout d'abord **les dégénérescences neurofibrillaires** intracellulaires ainsi que des agrégats extracellulaires ; **les plaques amyloïdes**.

C'est en 1910 qu'est mentionné pour la première fois par Emil Kraepelin, directeur de l'hôpital psychiatrique royal de Munich, le terme de maladie d'Alzheimer dans la 8ème édition du Manuel de Psychiatrie. En 1911, Alois Alzheimer publia un article dans lequel sont dessinés les modifications des neurofibrilles observées dans le cerveau d'Auguste Deter ainsi que la description d'un nouveau cas de démence, Joanna F (Figure 1).

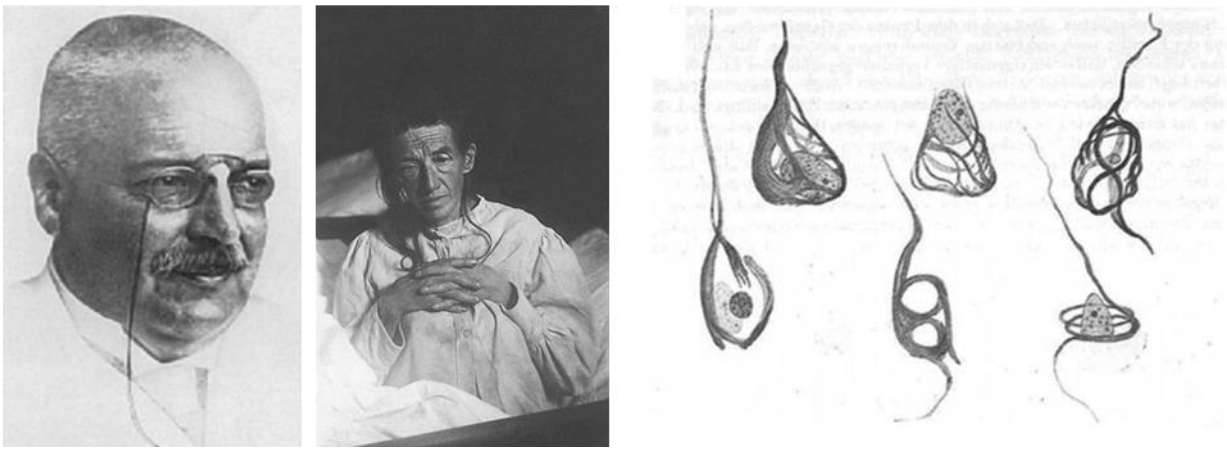

Figure 1: Alois Alzheimer, Auguste Deter et les premiers dessins des neurofibrilles caractéristiques. A gauche ; portrait d'Alois Alzheimer. Au centre ; portrait d'Auguste Deter. A droite ; dégénérescences neurofibrillaires dessinées par Alois Alzheimer

Les travaux d'Alois Alzheimer furent cependant sous-considérés pendant la majeure partie du XXème siècle. Durant ces cent dernières années, la MA passa d'un

statut de maladie rare à la maladie neurodégénérative la plus fréquente du XXIème siècle jusqu'à être considérée comme une épidémie.

3. Incidence, prévalence et coûts de la MA

a. Dans le monde

L'un des principaux facteurs expliquant la fulgurance de « l'épidémie globale de démence » est le vieillissement de la population mondiale. Selon le rapport mondial Alzheimer 2015, il y a aujourd'hui près de 900 millions de personnes de plus 60 ans dans le monde. Et cette catégorie devrait plus que doubler dans les pays à bas revenus dans les 40 prochaines années.

10 millions de nouveaux cas de démences se sont déclarés en 2015. La moitié de ces cas provenaient d'Asie et 18% d'Europe. Au total, près de **50 millions de personnes vivent avec une démence** en 2015. Et on estime que ce chiffre va doubler tous les 20 ans pour dépasser les **130 millions de personnes atteintes en 2050** (Figure 2). Une tendance forte est à noter puisque 58% des personnes atteintes d'une démence vivent actuellement dans des pays à revenus faibles et moyens et cette tendance ne va faire que s'accentuer pour atteindre 68% en 2015. La démence, et la maladie d'Alzheimer en particulier, n'est plus seulement un problème dans les pays développés mais devient une épidémie à l'échelle globale.

Bien que les conséquences sociales et humaines de la maladie d'Alzheimer soient à mettre au premier plan, les répercussions économiques sont écrasantes. Toujours selon le rapport mondial Alzheimer 2015, les coûts globaux de la démence ont augmenté de 35% entre 2010 et 2015 pour atteindre **818 milliards de dollars** soit 1% du PIB global. Ceci correspondrait à un PIB équivalent à celui de la Turquie ou des Pays-Bas ou bien à la valorisation boursière numéro un au monde devant Apple (742 milliard de dollars en 2015). Il est estimé que ce chiffre double en moins de 15 ans pour dépasser les deux milliards de dollars d'ici à 2030. A l'opposé, il est important de noter que le financement de la recherche sur la MA progresse aussi. Aux Etats-Unis par exemple, Barack Obama annonça fin 2015 une augmentation de 60% du budget alloué à la recherche sur la MA pour 2016 (Alzforum).

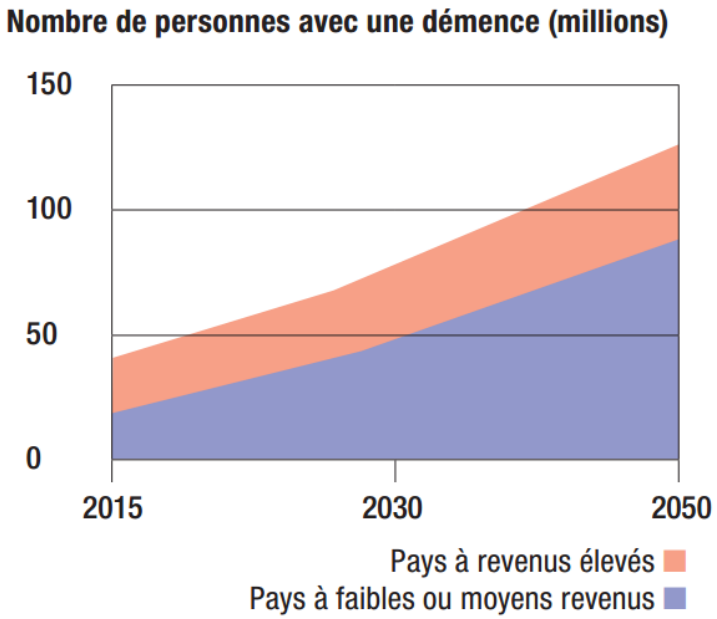

Figure 2: Estimation du nombre de personnes avec une démence entre 2015 et 2050. Bien que le nombre de personnes touchées par la démence augmente déjà substantiellement dans les pays à revenu élevé (+ 216% sur la période 2015-2050), ce nombre triple dans les pays à revenus plus modestes (+ 327%). Cette partie du monde comptera ainsi 68% des personnes touchées par la maladie en 2050.

b. En France

La majorité des données démographiques sur la MA en France proviennent de l'étude PAQUID (QUID des Personnes Agées) réalisée en Aquitaine. Cette cohorte populationnelle a été constituée en 1988 pour suivre sur le long terme 3777 personnes de plus de 65 ans (Letenneur, Commenges et al. 1994, Ramaroson, Helmer et al. 2003).

L'incidence de la MA est fortement impactée par l'âge. Il y a en effet un facteur 35 entre la tranche 65-69ans et les plus de 90ans. On estime ainsi à **225 000 nouveaux cas par an** l'incidence de la MA en France (Fratiglioni, Launer et al. 2000).

Les dernières estimations font état de **860 000 personnes touchées par la MA** chez les plus de 65 ans en France. Cette population équivaudrait à la 2ème plus grande ville française. Ces chiffres seront, comme à l'échelle mondiale, en forte hausse dans les années à venir ; 1 275 000 de malades en 2020 et 2 150 000 en 2040 (France Alzheimer). De plus, on estime actuellement que seulement **1 personne sur 2 serait diagnostiquée**. Plusieurs raisons peuvent expliquer cela comme par exemple les premiers stades légers de la maladie ou les outils diagnostiques disponibles comme le MMSE (Mini Mental State Examination) pas toujours adaptés. De plus, rappelons que les critères ne permettent d'établir qu'un diagnostic probable. Le diagnostic de certitude ne peut être effectué qu'au moment de l'analyse anatomopathologique (Ankri 2006).

Concernant les coûts, un rapport très récent de la fondation Médéric estime ceux-ci à plus de **30 milliards d'euros** pour la seule France (Fondation Médéric). Dans ce total, l'aide informelle (par une personne de l'entourage) est estimée à elle seule à 14 milliards d'euros. Le plan Alzheimer, lancé par le précédent gouvernement, arrivé à son terme en 2012, a quant à lui été prolongé sous le terme « **plan maladies neurodégénératives** » jusqu'en 2019. Ce dernier alloue un total de 470 millions d'euros pour améliorer le diagnostic et la prise en charge, la qualité de vie des patients et des aidants et le développement de la recherche.

La maladie d'Alzheimer est la 5ème cause de décès dans le monde. Sa prévalence et ses coûts ne font qu'augmenter exponentiellement depuis 40 ans. La compréhension en profondeur des mécanismes physiopathologiques mis en jeu se fait donc de en plus en plus pressante et essentielle pour le futur développement de thérapies efficaces.

4. Neuropathologie de la MA

Dès sa découverte par le Dr Alois Alzheimer au début du XXème siècle, trois caractéristiques neuropathologiques majeures ont pu être mises en évidence après l'analyse post-mortem du cerveau d'Auguste Deter ; **l'atrophie cérébrale, les plaques amyloïdes et la dégénérescence neurofibrillaire**. Cependant, elles s'accompagnent d'autres aspects essentiels comme la **perte synaptique et neuronale, la réactivité astrocytaire et microgliale et l'angiopathie amyloïde cérébrale**.

a. L'atrophie cérébrale

L'atrophie cérébrale est la première caractéristique visible d'un cerveau de patient décédé de la MA. La structure la plus atrophiée est le cortex, les circonvolutions de celui-ci se font ainsi plus visibles. L'atrophie de cette structure peut faire **perdre jusqu'à 10% du poids total** du cerveau d'un patient. Les autres structures sévèrement touchées sont **l'hippocampe** (essentiel pour les processus de mémorisation) ou l'amygdale (Figure 3). L'élargissement des ventricules est aussi aisément visible (de la Monte 1989).

Cette atrophie globale peut-être mise en évidence grâce à des techniques **d'imagerie *in vivo***, notamment l'imagerie par résonance magnétique (IRM). Cependant, elle n'est pas une caractéristique propre à la maladie d'Alzheimer. Elle touche les patients atteints

d'autres maladies neurodégénératives mais peut être aussi dû à l'âge chez des personnes saines. Ces éléments en font donc un **marqueur spécifique perfectible**. Cependant de nombreux groupes réussirent à corréler l'atrophie hippocampique ou la dilatation des ventricules avec la maladie (Thompson, Hayashi et al. 2004).

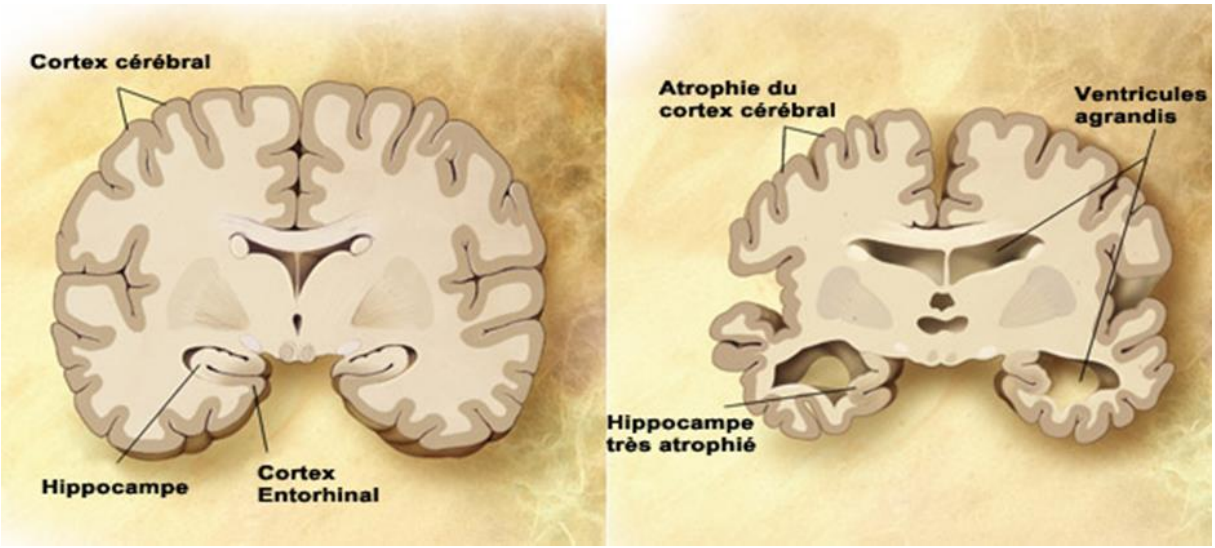

Figure 3: Cerveau de sujet sain (à gauche) comparé à un patient atteint de la MA (à droite). A noter, l'atrophie massive du cortex et de l'hippocampe ainsi que la dilatation des ventricules. lecerveau.mcgill.ca

b. Les plaques amyloïdes

Les plaques amyloïdes sont une des deux marques pathologiques de la MA découvertes par le Dr Aloïs Alzheimer. Celui-ci les décrit en effet comme des « foyers miliaires causés par le dépôt d'une substance particulière dans le cortex » (Alzheimer, Stelzmann et al. 1995). Cependant, l'origine de cette « substance » resta inconnue pendant près de 80 ans. La perte progressive des capacités cognitives et les marqueurs neuropathologiques de la MA avaient pu entre-temps être mis en évidence dans des individus porteurs de la **trisomie 21** (Ellis 1974, Glenner 1983). C'est en 1984 que George Glenner isola **le peptide Amyloïde β (Aβ)** du cerveau d'individus porteurs de la trisomie 21 ou atteints de la MA. Plus précisément, le peptide fut isolé à partir de dépôts amyloïdes cérébrovasculaires et fut ensuite séquencé (Glenner and Wong 1984, Glenner and Wong 1984). L'année suivante, le peptide fut identifié comme le **composant essentiel des plaques amyloïdes** (Masters, Simms et al. 1985).

Il est possible de mettre en évidence les plaques amyloïdes selon deux moyens :

- Tout d'abord, les **marquages de type chimique**. Ceux-ci ne sont pas spécifiques des plaques amyloïdes et permettent aussi de mettre en évidence les autres agrégats protéiques spécifiques de la MA (la DNF, voir plus bas). Dès 1927, Paul Divry utilisa le **rouge Congo** (Figure 4.A) pour mettre en évidence les plaques amyloïdes (Divry 1927). Une autre méthode classique, que j'ai réalisé pendant ma thèse, est l'utilisation de la Thioflavine T ou **Thioflavine S** (Vassar and Culling 1959, Schwartz, Kurucz et al. 1964). A noter que ces trois composés (rouge Congo, Thioflavine T et S) reconnaissent les structures de type feuillets β plissés.

- **Les anticorps** les plus couramment utilisés sont les clones **4G8 et 6E10** (Figure 4.B). On peut également citer BAM10 qui a lui été développé pour détecter les oligomères d'Aβ.

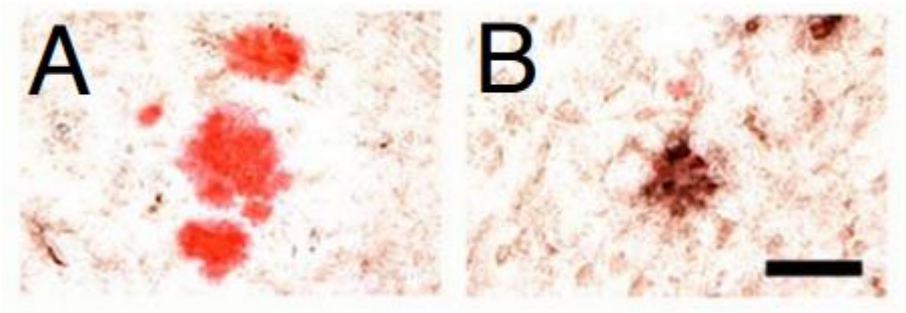

Figure 4: Plaques amyloïdes d'une souris transgénique (Tg2576, (Hsiao, Chapman et al. 1996)) marquées grâce au rouge Congo (A) ou immunomarquées avec l'anticorps 6E10. (Thakker, Weatherspoon et al. 2009)

Dans leur papier *princeps* décrivant les différents stades d'évolution de la pathologie Alzheimer, Braak & Braak ne purent corréler la diffusion de l'Aβ et la progression de la maladie. En revanche, c'est en 2002 que **Thal** décrit cette corrélation (Thal, Rub et al. 2002). Celle-ci se divise en cinq phases caractéristiques (Figure 5):

- Dans la phase I, l'Aβ se dépose de manière diffuse dans le néocortex.

- Il diffuse ensuite dans le cortex entorhinal, la région CA1 de l'hippocampe et le cortex insulaire (Phase II).

- La phase III est caractérisée par des dépôts amyloïdes dans le noyau caudé, le putamen, le claustrum, le noyau basal, le thalamus, l'hypothalamus et la substance blanche.

- Les structures touchées en phase IV sont le noyau olivaire inférieur, la formation réticulée, la substance noire, le CA4, le colliculus supérieur et inférieur et noyau rouge.

- Finalement, les dépôts d'Aβ se localisent dans le cervelet, le noyau pontin, le locus cœruleus, le noyau réticulo-tegmental, le noyau dorso-tegmental et le noyau raphé.

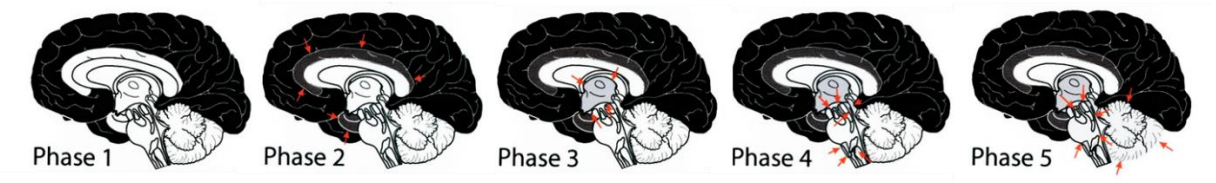

Figure 5: Evolution spatio-temporelle de la déposition d'Aβ dans la maladie d'Alzheimer ; Les 5 stades de Thal (Thal, Rub et al. 2002).

c. La dégénérescence neurofibrillaire

La dégénérescence neurofibrillaire (DNF), comme l'a décrite le Dr Alois Alzheimer, est caractérisée par des enchevêtrements épais de neurofilaments dans le cytoplasme des neurones corticaux (Alzheimer, Stelzmann et al. 1995, Engelhardt and Gomes Mda 2015). La DNF est composée de **filaments appariés en hélice** (Paired Helical Filaments, PHF). Ces structures furent observées pour la première fois par Kidd en 1963 (Kidd 1963). L'isolation de DNF de patients et la séparation par gradients de Ficoll permirent l'identification d'une protéine d'approximativement 50 kDa grâce au SDS-PAGE (Iqbal and Tellez-Nagel 1972, Iqbal, Wisniewski et al. 1974). Grâce à la production d'anticorps dirigés contre ces bandes, il a été possible de déterminer que cette protéine était une **composante des microtubules** (Grundke-Iqbal, Johnson et al. 1979, Grundke-Iqbal, Johnson et al. 1979).

Indépendamment, une nouvelle protéine composante des microtubules fut identifiée par le groupe de Marc Kirschner dans le milieu des années 1970. **Celle-ci fut nommée tau** (Tubulin-Associated Unit) (Weingarten, Lockwood et al. 1975, Cleveland, Hwo et al. 1977). Mais ce n'est qu'en 1985 que l'équipe de Jean-Pierre Brion identifia que des anticorps dirigés contre la **protéine tau permettent de mettre en évidence les PHF** (Brion, Couck et al. 1985). D'autres équipes confirmaient ces résultats et démontraient

peu après que sa **forme hyperphosphorylée** était responsable de la formation des PHF (Grundke-Iqbal, Iqbal et al. 1986, Grundke-Iqbal, Iqbal et al. 1986, Kosik, Joachim et al. 1986, Wood, Mirra et al. 1986).

De manière similaire aux plaques amyloïdes, il existe deux moyens courants pour mettre en évidence la DNF :

- Tout d'abord les techniques utilisant des **composés chimiques**. Il est ainsi important de citer la **coloration à l'argent de Gallyas** utilisée par Braak et Braak (Braak and Braak 1991, Iqbal, Braak et al. 1991). Il est aussi possible d'utiliser le **rouge Congo**, découvert par Paul Divry, afin de marquer la dégénérescence neurofibrillaire (Divry 1927, Ball 1976). Enfin, la **thioflavine S et la thioflavine T**, composés fluorescents, sont capables de reconnaitre les feuillets β plissés et permettent de marquer celle-ci (Arnold, Hyman et al. 1991).

- Depuis que tau fut démontré comme étant à l'origine de la DNF, de **nombreux anticorps** ont été développés afin de marquer celle-ci. Ils sont généralement spécifiques d'un **épitope phosphorylé**. Deux anticorps couramment utilisés sont **AT8** (Alzheimer Tau 8), spécifique des sites pS202/pT205 (Sites de phosphorisation plus ou moins pathologiques) et **AT100** (Figure 6), spécifique des sites pT212/ pS214 (plus spécifiques de la pathologie Alzheimer) (Biernat, Mandelkow et al. 1992, Mercken, Vandermeeren et al. 1992, Goedert, Jakes et al. 1995, Augustinack, Schneider et al. 2002).

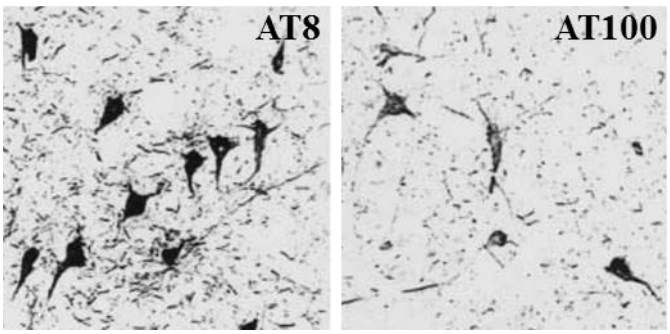

Figure 6: Immunomarquage de la dégénérescence neurofibrillaire avec les anticorps AT8 (gauche) et AT100 (droite). Images prises dans le cortex entorhinal d'une patiente décédée à l'âge de 86 ans de la MA (Augustinack, Schneider et al. 2002).

Grâce à ces anticorps, différents stades de maturité de la DNF ont ainsi pu être mis en évidence. Chaque stade est corrélé à des niveaux d'hyperphosphorylation différentiels de la protéine tau. Ainsi, différents sites spécifiques de chaque stade ont pu être mis en évidence (Morishima-Kawashima, Hasegawa et al. 1995, Kimura, Ono et al. 1996, Augustinack, Schneider et al. 2002) (Figure 7):

- Le stade « Pré-DNF » (Pre-NFT en anglais) correspond à un stade pré-PHF c'est-à-dire avec une tau phosphorylée mais non fibrillisée. Le marquage est en général décrit comme diffus.

- Le stade « DNF intraneuronale » apparait à un stade plus avancé de la pathologie. Il se caractérise par un marquage dense de la protéine tau fibrillaire au niveau du soma.

- Enfin le stade « DNF extraneuronale » est défini par un marquage filamentaire caractéristique d'un neurone atrophique.

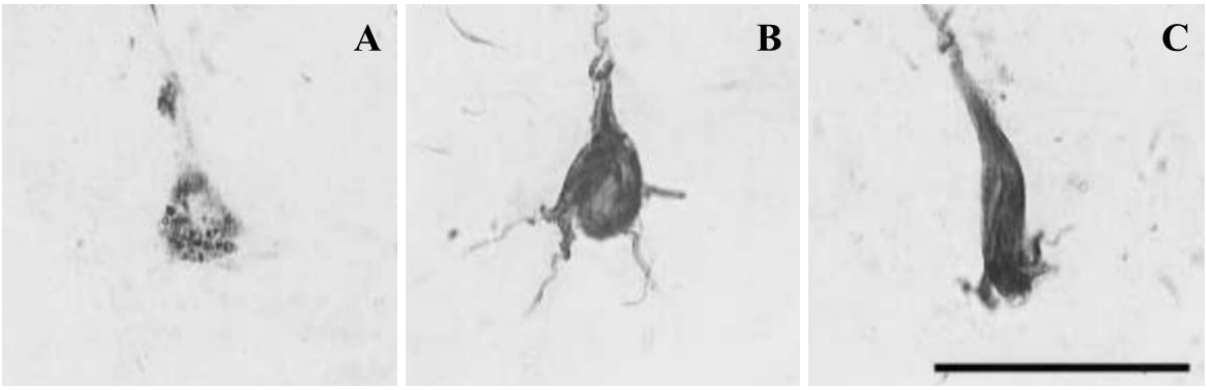

Figure 7: Les trois stades de la DNF. (A) Stade Pré-DNF. **(B)** Stade DNF intraneuronale. **(C)** Stade DNF extraneuronale. Immunohistochimie d'un cerveau de patient Alzheimer marqué avec l'anticorps TG3. Bar d'échelle : 50 µm. (Augustinack, Schneider et al. 2002)

Enfin, la diffusion spatio-temporelle de la DNF dans le cerveau des patients atteints de la MA a permis de mettre en évidence différents stades de la pathologie corrélés au déclin cognitif. Ces six stades sont aujourd'hui connus sous le nom de **stades de Braak** (Braak and Braak 1991) (Figure 8):

- Les stades I-II. La DNF commence au niveau de la région trans-entorhinale.

- Les stades III-IV. La DNF progresse dans le cortex trans-entorhinal et se propage à la région entorhinale.

- Les stades V-VI. Ils correspondent à une élévation de la DNF dans les structures précédemment citées et à l'extension au néocortex.

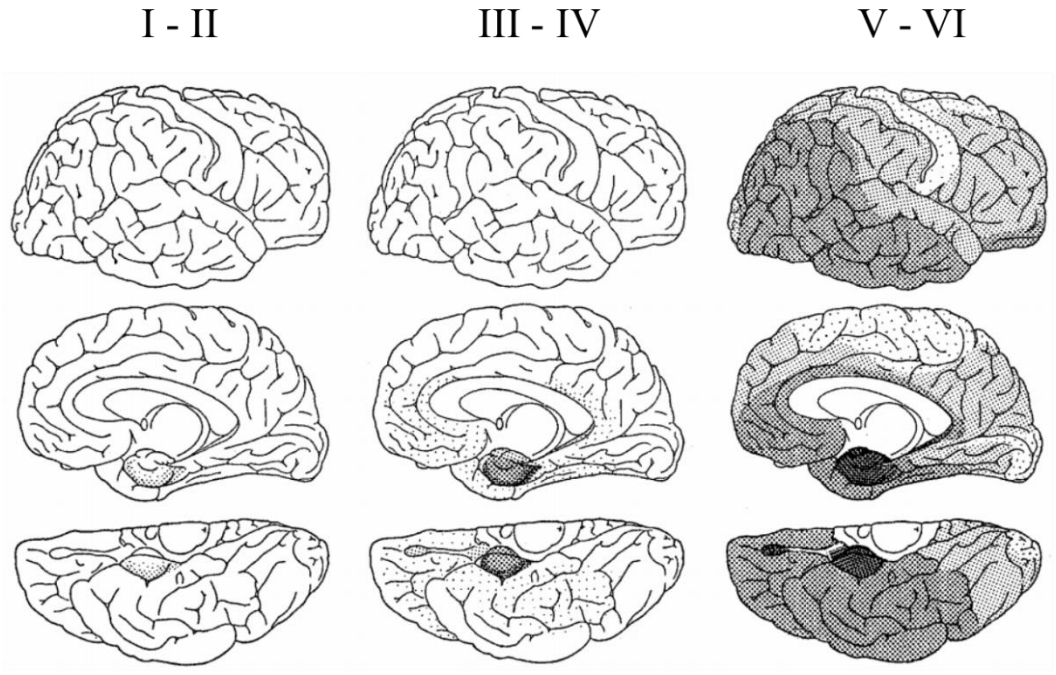

Figure 8: Progression spatiale de la DNF dans le cerveau des patients atteints de la MA. (Braak and Braak 1991)

d. Perte synaptique et neuronale

L'atrophie cérébrale présente dans la MA a pour origines principales les pertes synaptiques et neuronales. Il est généralement considéré que **la perte synaptique précède la mort neuronale**. La disparition des synapses dans la MA est facilement identifiable par des techniques de biochimie ou d'immunohistochimie. Deux grands types de marqueurs permettent de la mettre en évidence ; les **marqueurs pré-synaptiques** (par exemple, synapsine ou synaptophysine) et **post-synaptiques** (PSD-95 étant très couramment utilisé, Figure 9). Bassoon permet quant à lui de marquer la zone active de la synapse. De manière intéressante, la perte synaptique est très **bien corrélée au déclin cognitif** survenant dans la MA (DeKosky and Scheff 1990, Scheff, DeKosky et al. 1990, Scheff, Price et al. 2006).

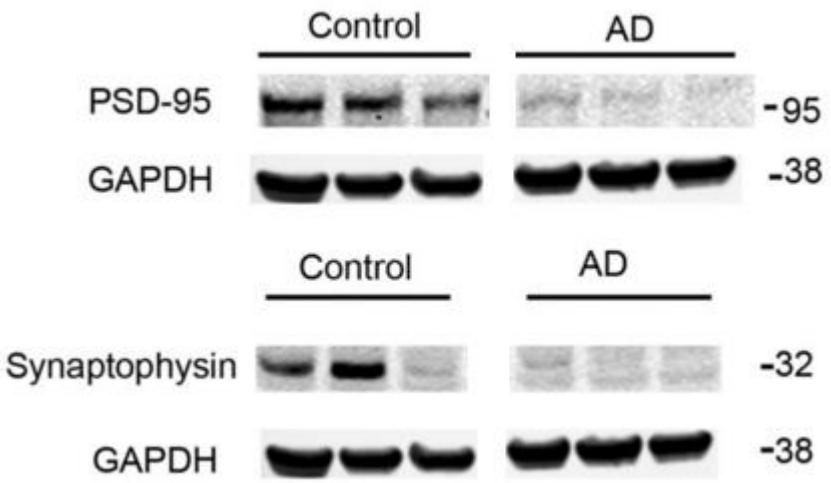

Figure 9: Analyse par western blot des protéines PSD-95 et synaptophysine dans le cerveau de sujets sains et de patients atteints de la MA. A noter la diminution des deux protéines dans les cerveaux de patients diagnostiqués déments avant leur mort avec une forte suspicion de MA (AD). (Perez-Nievas, Stein et al. 2013)

La perte neuronale peut être mise en évidence par une simple coloration à l'**hématoxyline et à l'éosine**. De plus, le marqueur **NeuN** (Neuronal Nuclei) peut être utilisé afin de réaliser des immunomarquages spécifiques des neurones. La DNF intra-neuronale est une cause prédominante de la mort neuronale (Rissman, Poon et al. 2004). Cependant, la toxicité de l'Aβ extraneuronal et la contrainte mécanique imposée par les plaques amyloïdes sont des causes importantes de la perte neuronale (Forloni, Chiesa et al. 1993, LaFerla, Tinkle et al. 1995, Yang, Sun et al. 1998, Gervais, Xu et al. 1999, Arends, Duyckaerts et al. 2000).

e. La réactivité astrocytaire et microgliale

L'activation des cellules gliales est une composante essentielle de la MA. Celle-ci fut déjà mise en évidence par le Dr. Alois Alzheimer lors de l'analyse histo-pathologique du cerveau d'Auguste Deter (Alzheimer, Stelzmann et al. 1995). **Deux populations** de cellules gliales sont trouvées réactives dans le cerveau de patients ; **les astrocytes et la microglie**. Elles participent ainsi activement à la neuroinflammation découlant de la pathologie. La microglie réactive peut être mise en évidence grâce aux marqueurs **IBA1** ou CD68 et les astrocytes par la **GFAP** ou la vimentine (Figure 10).

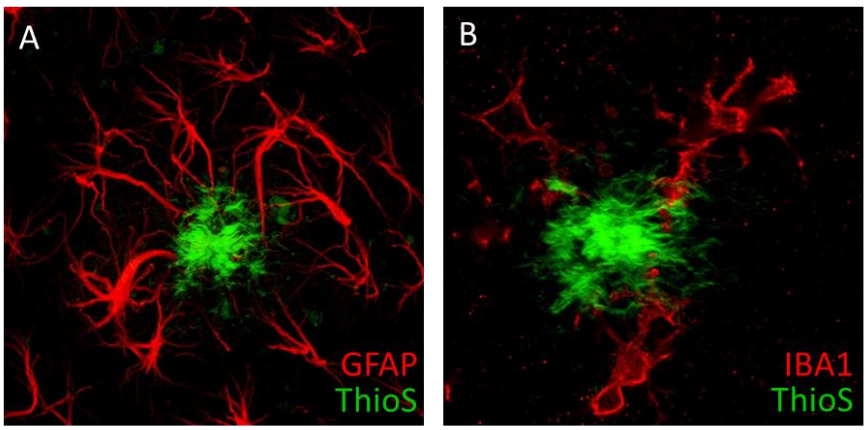

Figure 10: Plaques amyloïdes associées aux astrocytes réactifs (A) ou à la microglie réactive (B). Les plaques sont marquées grâce à la thioflavine S, les astrocytes réactifs avec l'anticorps anti-GFAP et la microglie réactive avec un anti-IBA1. (Fol, Braudeau et al. 2016)

La réactivité gliale fut d'abord considérée comme un épiphénomène accompagnant les phases tardives de la MA. Cependant, elle serait impliquée de manière active soit de manière délétère soit au contraire, de **manière bénéfique** (Heneka, Kummer et al. 2014, Heppner, Ransohoff et al. 2015). Les astrocytes réactifs et la microglie activée sont classiquement associés aux plaques et permettent leur **phagocytose** (Frackowiak, Wisniewski et al. 1992, Akiyama, Schwab et al. 1996, Shao, Gearing et al. 1997).

f. L'angiopathie amyloïde cérébrale

Outre que dans le parenchyme, l'**Aβ peut aussi se déposer dans les vaisseaux sanguins**. Ceux-ci sont la cause d'une autre composante caractéristique de la MA ; l'angiopathie amyloïde cérébrale. Bien qu'aussi présente chez certaines personnes âgées asymptomatiques, cette pathologie est très fortement reliée à la MA puisque plus de 80% des patients la présenteraient (Thakker, Weatherspoon et al. 2009). Ces lésions sont majoritairement présentes dans les **méninges et le cortex**. A un stade avancé, elles causent la nécrose des cellules musculaires lisses induisant une faiblesse du tissu. Ceci peut conduire à des **hémorragies cérébrales**. Enfin, il est important de noter que la majorité de l'Aβ déposé dans les vaisseaux sanguins est sous la forme 40 acides aminés (Yamada 2015) et non 42 acides aminés, la forme la plus toxique d'Aβ (voir partie IV.B.3).

5. Causes et facteurs de risque

La MA est classiquement divisée en deux catégories : **Les formes familiales** ou génétiques définies comme ayant un âge de déclaration de la maladie avant 65 ans, et **les formes sporadiques se déclarant après 65 ans**. Ces dernières représentent la **vaste majorité des cas** (95 à 99% des cas). Plusieurs facteurs influencent l'apparition de ces deux formes. La première est due à des **mutations** dans deux composants clés de la préformation du peptide Aβ. Les formes sporadiques sont elles aussi influencées par des causes génétiques mais de nombreux autres facteurs environnementaux favorisent son développement.

a. Mutations des formes familiales : l'APP et les présénilines

Comme mentionné ci-dessus, les formes familiales de la MA sont des **formes héréditaires et donc transmissibles**. Elles représentent une **minorité de patients** touchés par maladie (1 à 5%) mais ont permis au Dr Alois Alzheimer d'identifier cette maladie au début du XXème siècle. Bien que cette découverte n'a pu être pour le moment confirmée, sa patiente, Auguste Deter, aurait selon une étude récente une mutation dans **le gène PSEN1** (Muller, Winter et al. 2013, Rupp, Beyreuther et al. 2014). De plus, au vu de l'âge auquel la pathologie a pu être identifiée (autour de 50 ans), il est fort probable que celle-ci est été touchée par une forme familiale.

Le gène PSEN1 code pour la protéine **Préséniline 1**. Les mutations dans celle-ci et son homologue PSEN2 (Préséniline 2) sont **les plus fréquentes** dans les formes précoces de la MA (Ringman, Goate et al. 2014). Ces deux protéines forment le noyau catalytique du complexe enzymatique **γ-secrétase**. Ce dernier est un élément clé dans la génération du peptide Aβ (voir partie IV.B.3). Ces mutations augmentent ainsi l'activité catalytique du complexe et **augmentent automatiquement la quantité d'Aβ** générée (Scheuner, Eckman et al. 1996).

Les autres mutations des formes autosomiques dominantes de la MA touchent **le gène APP** codant pour la protéine APP (Amyloid Precursor Protein) et situé sur le chromosome 21. Celui-ci fut le premier à être identifié, dès 1987 (Goldgaber, Lerman et al. 1987, Kang, Lemaire et al. 1987, Robakis, Ramakrishna et al. 1987, Tanzi, Gusella et al. 1987). En effet, après la découverte de l'Aβ, des sondes spécifiques de ce peptide furent générées afin de cribler une banque d'ADNc issue de tissus cérébraux humains. La première mutation causative d'une forme précoce de la MA fut identifiée dès 1990 dans ce gène (mutation faux-sens, E693Q) (Levy, Carman et al. 1990). Comme son nom l'indique, **l'APP est la protéine précurseuse de l'Aβ** et de même manière que pour les présénilines, les mutations vont favoriser son propre clivage, en particulier vers la voie amyloïdogène, génératrice du peptide Aβ. La majorité de ces mutations se localisent en effet à proximité des sites de clivages des complexes β-secrétase et γ-secrétase et tendent

ainsi à **augmenter substantiellement la quantité d'Aβ** produit (Scheuner, Eckman et al. 1996). De manière intéressante, une **mutation protectrice** de la MA fut récemment identifiée dans la population islandaise (Jonsson, Atwal et al. 2012).

Il est ainsi important de noter que toutes les mutations impliquées dans les formes familiales de la MA touchent la voie amyloïde (menant *in fine* à la génération des plaques). En effet, à ce jour, **aucune mutation de la protéine tau** n'a pu être clairement reliée aux caractéristiques histopathologiques de la MA. Cette dissemblance explique ainsi le fait qu'une majorité de la recherche effectuée sur la MA soit focalisée sur l'amyloïde.

b. Facteurs de risques des formes sporadiques

i. Facteurs divers

Le premier facteur de risque de la MA est **l'âge**. En effet, le risque de développer la maladie augmente tous les cinq ans après 65 ans (Riedel, Thompson et al. 2016). Il a aussi été démontré que **les femmes** ont une propension plus importante à développer la MA (Payami, Zareparsi et al. 1996). La raison principale usuellement évoquée est le fait que celle-ci vivent plus longtemps que les hommes dans les pays développés mais cet

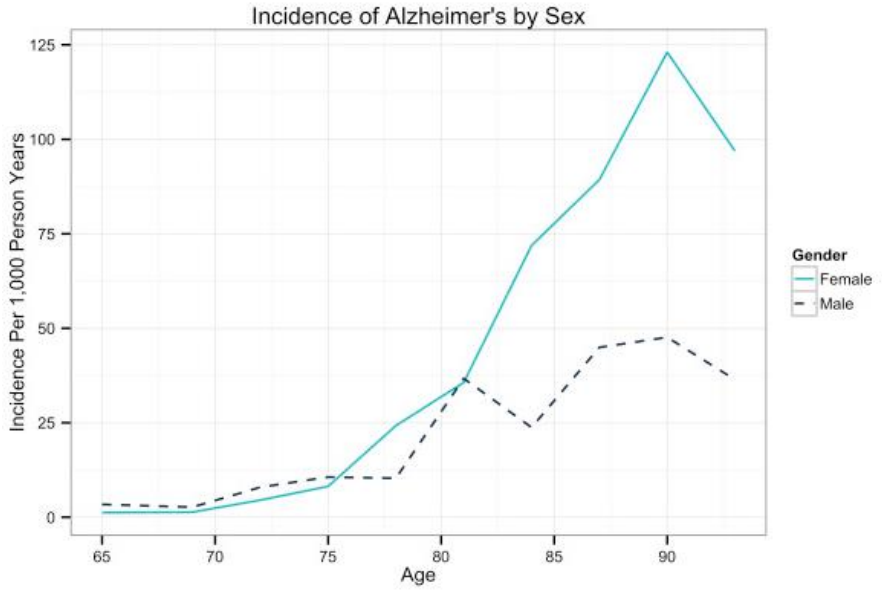

Figure 11: Incidence de la MA chez les hommes et les femmes après 65 ans. A noter le fort nombre de femmes touchées par rapport aux hommes après 80 ans. (Riedel, Thompson et al. 2016)

argument n'explique pas totalement cette différence (Figure 11). Celle-ci pourrait-être partiellement due aux hormones, et plus particulièrement à la ménopause.

Un lien a aussi été établi entre les **maladies cardiovasculaires** et la MA. Il a par exemple été montré dans la cohorte Rotterdam (4971 sujets âgés) un score MMSE plus faible chez les individus ayant eu un accident vasculaire cérébral, un infarctus du myocarde ou une artériopathie oblitérante des membres inférieurs (Breteler, Claus et al. 1994). **Le diabète de type 2** est lui aussi un facteur de risque important de développer la MA. Des études ont en effet démontré que le risque de développer la MA était augmenté de 50 à 60% pour les patients souffrant de diabète de type 2 (Talbot, Wang et al. 2012). Cette liste est bien sûr non-exhaustive puisque d'autres risques, comme le tabac par exemple, ont été évoqués par certaines études mais non confirmés sur le long terme.

ii. Facteurs de risque génétiques

Bien que les formes sporadiques de la MA ne soient pas, par définition, transmises de manière autosomique dominante, les antécédents familiaux représentent un risque important de développer la pathologie. En effet, **plusieurs facteurs de risques génétiques** ont pu être mis en évidence depuis 30 ans. Le facteur de risque génétique premier est **le gène APOE**, codant pour l'apolipoprotéine E.

ApoE est **l'apolipoprotéine la plus abondante dans le SNC** (bien qu'aussi présente dans le plasma) (Mahley 1988). Elle est produite quasi exclusivement par **les astrocytes**. Les astrocytes produisent ainsi le cholestérol et l'apolipoprotéine E qui, associés à des phospholipides, vont former des lipoprotéines de taille similaire aux lipoprotéines plasmatiques de haute densité (HDL) (Pitas, Boyles et al. 1987). Ces lipoprotéines permettront le **transfert du cholestérol des astrocytes aux neurones**. APOE est mono-allélique chez la souris mais comporte trois allèles chez l'homme ; APOEε2, APOEε3 et APOEε4. Cette différence est due à la combinaison de deux acides aminés en positions 112 et 158 (ε2:Cys112/Cys158; ε3:Cys112/Arg158; ε4:Arg112/Arg158). Le génotype d'APOE influence la susceptibilité de développer la maladie. L'allèle ε3 (comme l'allèle murin) est considéré comme neutre. **L'allèle ε4 augmente la probabilité de développer la MA** (Corder, Saunders et al. 1993): la présence d'un allèle ε4 augmente de 3 à 4 fois la probabilité de développer la maladie alors que deux allèles l'augmente de 12 fois**. L'allèle ApoE2 semble quant à lui induire une relative protection** contre la maladie (Kanekiyo, Xu et al. 2014).

Le XXIème siècle a vu l'avènement des analyses pangénomiques ou **GWAS** (Genome Wide Association Studies). Ces études de cas-témoins (sujets sains et patients atteints) regroupent actuellement des **dizaines de milliers de participants**. Ceux-ci sont ensuite génotypés sur quelques millions de variants génétiques connus du génome. Il est ensuite déterminé pour chaque variant si la fréquence allélique est altérée entre les témoins et les patients (Tosto and Reitz 2013).

Ces GWAS permirent de mettre en évidence de nombreux loci associés à la MA. Ils permirent, à l'heure actuelle, de confirmer ou d'identifier **plus de 20 gènes associés** aux formes sporadiques de la MA (Lambert, Ibrahim-Verbaas et al. 2013, Karch and Goate 2015). Outre le métabolisme de l'APP, ceux-ci peuvent être regroupés en **trois grandes voies de signalisation** regroupant la majorité des gènes influençant le développement de la pathologie (Figure 12):

- **Le métabolisme du cholestérol et le transport lipidique :** APOE, SORL1, CLU, SLC24A4 et ABCA7. La découverte d'APOE dès le début des années 1990 permit de mettre en évidence l'implication du métabolisme du cholestérol dans la MA. La découverte par les GWAS de ces autres gènes liés au métabolisme du cholestérol et de nombreuses autres études fonctionnelles ont permis de souligner son importance dans la physiopathologie de la MA (Hudry, Van Dam et al. 2010, Burlot, Braudeau et al. 2015, Djelti, Braudeau et al. 2015, Sakae, Liu et al. 2016).

- **L'immunité et l'inflammation :** TREM2, CR1, CD33, INPP5D, CLU, EPHA1 et MS4A. La neuroinflammation et l'altération du système immunitaire est une composante clé de la MA (Karch and Goate 2015). A titre d'exemple, en 2013, des variants heterozygotes rares de **TREM2** (Triggering Receptor Expressed on Myeloid cells 2) furent associés à un risque accru de développer la MA (Guerreiro, Wojtas et al. 2013, Jonsson, Stefansson et al. 2013). TREM2 code pour un récepteur exprimé notamment par **la microglie** et étant capable de **phagocyter l'Aβ** mais aussi de moduler l'inflammation (Frank, Burbach et al. 2008, Jay, Miller et al. 2015, Wang, Cella et al. 2015).

- **La transmission synaptique et l'endocytose :** CLU, PICALM, BIN1, SORL1, RIN3, PTK2B, MEF2C, EPHA1 et CD2AP. La perturbation de l'activité synaptique fait de la MA une **synaptopathie** (Perdahl, Adolfsson et al. 1984, Serrano-Pozo, Frosch et al. 2011). L'endocytose des vésicules synaptiques en est un processus clé et c'est ainsi que des gènes impliqués dans ce processus ont été associés à la MA. **PICALM** (Phosphatidylinositol binding clathrin assembly protein) fut associé dès 2009 à un risque accru de

développer la MA (Harold, Abraham et al. 2009). Cette protéine joue un rôle essentiel dans le recrutement des clathrines ainsi que dans la fusion des vésicules synaptiques à la membrane présynaptique (Zhang, Koh et al. 1998, Harel, Wu et al. 2008, Baig, Joseph et al. 2010).

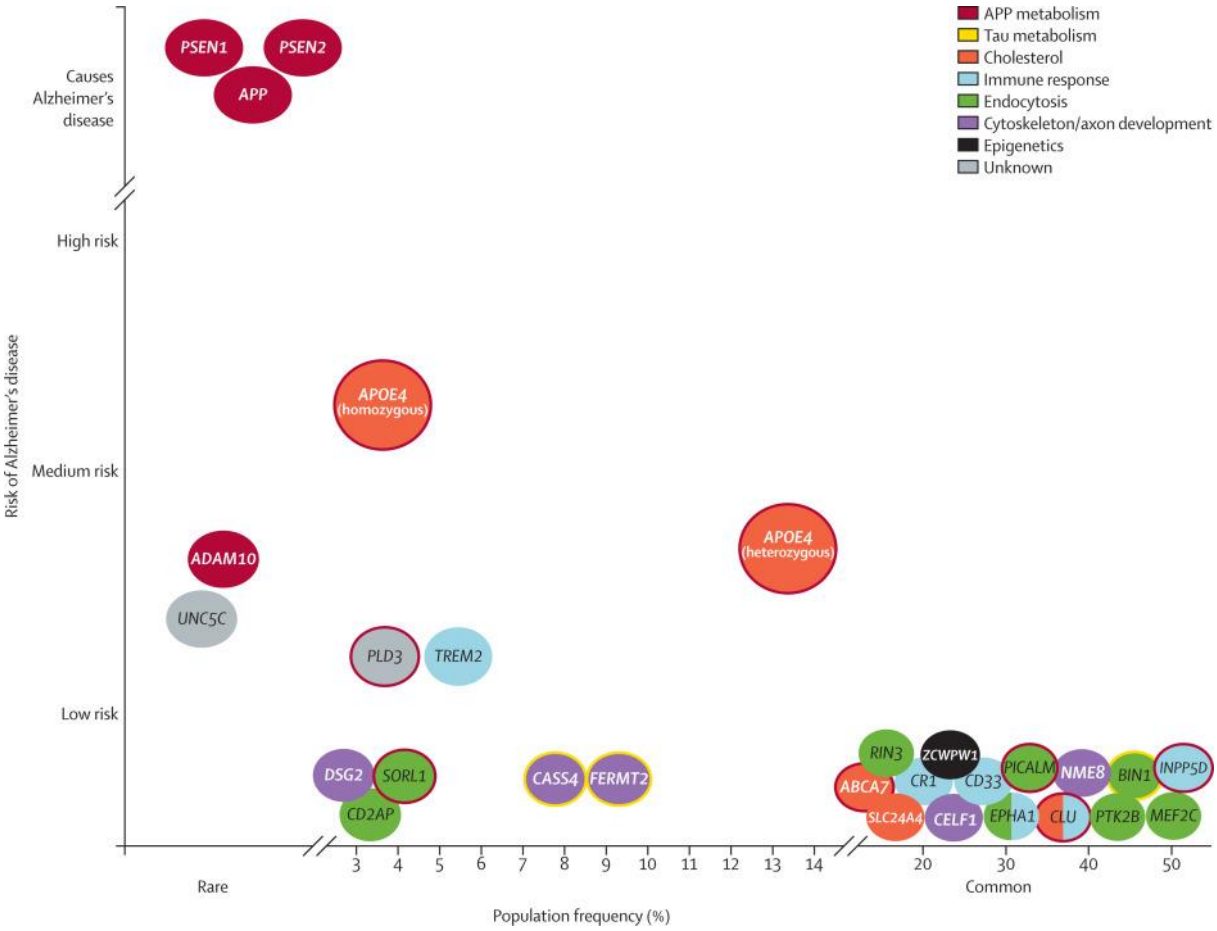

Figure 12: Vue d'ensemble des gènes impliqués dans la MA. Graphique représentant le poids du facteur de risque en fonction de sa fréquence dans la population. Les couleurs indiquent l'appartenance du gène à l'une des huit voies indiquées en légende (coin supérieur droit). (Scheltens, Blennow et al. 2016)

Il est important de noter que ces variants sont liés de manière plus ou moins forte avec la MA et n'ont **pas la même fréquence dans la population**. Le gène plus étroitement lié est sans aucun doute APOE avec une p-value inférieure à 10^{-50}.

Le défi actuel est de confirmer fonctionnellement et mécanistiquement, par des études in vitro et in vivo, l'implication de ces gènes dans la pathologie. Ainsi, la création de nouveaux modèles animaux afin d'étudier l'implication de ces gènes dans la pathogénèse de la MA semble être une approche intéressante.

6. La MA d'un point de vue clinique

Comme discuté précédemment, la pathologie se manifeste par des troubles mnésiques, moteurs et gestuels mais aussi une capacité de reconnaissance réduite. Dans cette partie, nous verrons brièvement les **outils diagnostics** à la disposition des cliniciens ainsi que les **traitements actuels**. Seront ensuite détaillés quelques **essais cliniques** et les cibles thérapeutiques actuellement développées par l'industrie pharmaceutique.

Une fois le diagnostic de la MA posée, l'espérance de vie du patient oscille entre **8 et 10 ans**. Cependant, à l'heure actuelle, ce diagnostic est un diagnostic de probabilité, le diagnostic de certitude ne pouvant être posé qu'après analyse anatomo-pathologique post-mortem. A terme, le patient décède des suites de sa perte d'autonomie, entrainant chutes ou infections, comme la pneumonie. A ce jour, **aucun traitement curatif** n'est encore disponible pour la MA. Seuls des traitements palliatifs sont utilisés comme les inhibiteurs d'acétylcholinestérase. Il est donc impératif de **développer des stratégies thérapeutiques préventives et/ou curatives** afin d'enrayer les conséquences sanitaires et socio-économiques de la MA.

a. Diagnostic

Afin d'améliorer la rapidité de prise en charge des patients, la pose d'un diagnostic précoce et efficace reste un **enjeu crucial** (Hampel, Lista et al. 2014). Bien qu'il n'existe toujours pas de traitement curatif de la MA, la prise en charge médicale et médicosociale permet de ralentir l'évolution de la maladie et la manifestation des symptômes. On estime en France, comme dans les autres pays développés que seul **un patient sur deux** atteint de la MA serait diagnostiqué (Gallez 2005, Dubois 2015).

Selon la HAS (Haute Autorité de Santé), un diagnostic doit être proposé :

- En priorité en cas de **troubles de la mémoire**
- Aux personnes se plaignant de ressentir une modification récente de leur cognition ou de leur état psychique

- Aux personnes chez lesquelles l'entourage remarque l'apparition ou l'aggravation de troubles cognitifs ou un changement psycho-comportemental non expliqué par une pathologie psychiatrique identifiée
- Aux patients venant consulter ou étant hospitalisés pour un symptôme pouvant accompagner, révéler ou provoquer un déclin cognitif : chute, syndrome confusionnel, accident vasculaire cérébral, etc…
- A l'entrée et en cours de séjour en structure d'hébergement.

En 2007 a été proposé par le groupe de travail IWG (International Working Group for New Research Criteria for the Diagnosis of Alzheimer's Disease) la possibilité d'un diagnostic au stade prodromal (symptômes limités notamment à la mémoire récente, et donc en absence de démence). Celui-ci fut révisé en 2014 (Dubois, Feldman et al. 2014) et établit grâce à une combinaison de critères cliniques et biologiques (Figure 13).

Tableau 1 Critères de l'IWG-2 pour maladie d'Alzheimer typique.
Criteria IWG-2 for typical Alzheimer's disease.

Phénotype clinique spécifique, e.g. présence de difficultés précoces et significatives de la mémoire épisodique qui incluent (1) changements graduels et progressifs de la mémoire selon le patient ou ses proches depuis plus de 6 mois ; (2) mise en évidence d'un syndrome amnésique de type hippocampique
Présence in vivo de biomarqueurs de pathologie de type Alzheimer, un parmi (1) diminution de la concentration du peptide Aβ42 et augmentation de la concentration de protéines T-tau, totale ou hyperphosphorylée, dans le LCR ; (2) augmentation de la rétention de traceur lors d'une TEP à l'amyloïde ; (3) mutation autosomale dominante de type PSEN1, PSEN2 ou APP

Figure 13: Tableau des critères de l'IWG2 pour le diagnostic précoce de la MA. Le diagnostic est posé après évaluation des critères cliniques et biologiques (Dubois, Feldman et al. 2014).

Les potentiels troubles cognitifs sont classiquement évalués en clinique grâce au test **MMSE** (Mini Mental State Examination) (Folstein, Folstein et al. 1975). Ce **test de 30 questions** permet d'évaluer le **niveau cognitif et mental** d'une personne dans le cadre d'une suspicion de démence. Dans le détail, il explore l'orientation temporelle et spatiale, l'apprentissage et la transcription des informations, l'attention et le calcul, le rappel et la rétention mnésique, le langage et la praxie constructive. L'âge et le niveau de scolarité sont deux paramètres pris en compte lors de l'interprétation du résultat du

test. De la même manière, il est aussi important de citer **l'épreuve des cinq mots** qui permet en deux étapes de rapidement contrôler l'encodage des informations à retenir et la mémorisation de celles-ci (Dubois 2002).

Les critères biologiques pris en compte dans l'évaluation globale repose sur la mesure de **biomarqueurs** caractéristiques de la MA. Le biomarqueur est un marqueur biologique (le plus souvent une molécule comme une protéine, une enzyme ou un métabolite) dont la concentration permet de mettre en évidence un statut physiopathologique particulier. Un biomarqueur diagnostic doit être reproductible, précis, peu coûteux, et dont le geste est modérément invasif. C'est ainsi que dans le cadre de la MA, les biomarqueurs utilisés sont les **marqueurs d'imagerie** et les marqueurs biologiques issus du **LCR** (Liquide Céphalo-Rachidien).

L'IRM (Imagerie par Résonnance Magnétique) permet de mettre en avant l'atrophie cérébrale globale ou de structures plus spécifiques comme l'hippocampe. En effet, l'atrophie hippocampique apparait relativement tôt dans la pathologie et est corrélée aux troubles de la mémoire (Henneman, Sluimer et al. 2009). **La TEP** (Tomographie par Emission de Positons) permet, grâce à l'utilisation de radioligants spécifiques, de marquer spécifiquement les plaques amyloïdes. En utilisant le FDG, glucose radiomarqué, il est possible de mettre en évidence des déficits métaboliques survenant dans le cerveau des patients (Mosconi, Berti et al. 2010, Ishii 2014).

Comme indiqué précédemment, le LCR des patients, obtenu après réalisation d'une ponction lombaire diagnostique, est aussi utilisé afin de doser deux marqueurs clés de la pathologie : l'**Aβ** et la protéine **tau**. Plus particulièrement, il est observé chez les patients une diminution de la concentration du peptide Aβ42, correspondant à une diminution de la clairance cérébrale vers le LCR. Au contraire, une augmentation de celle de la protéine tau totale et hyperphosphorylée est observée (Blennow 2004, Johansson, Mattsson et al. 2011).

L'étude approfondie des biomarqueurs cités ci-dessus ainsi que leur corrélation aux défauts cognitifs ont permis de mettre au point des **modèles d'évolution de la MA** (Figure 14). Ainsi, bien que le diagnostic de certitude soit actuellement posé post-mortem, ces modèles permettent de s'en rapprocher mais aussi déterminer le stade clinique du patient et prédire la progression de la pathologie.

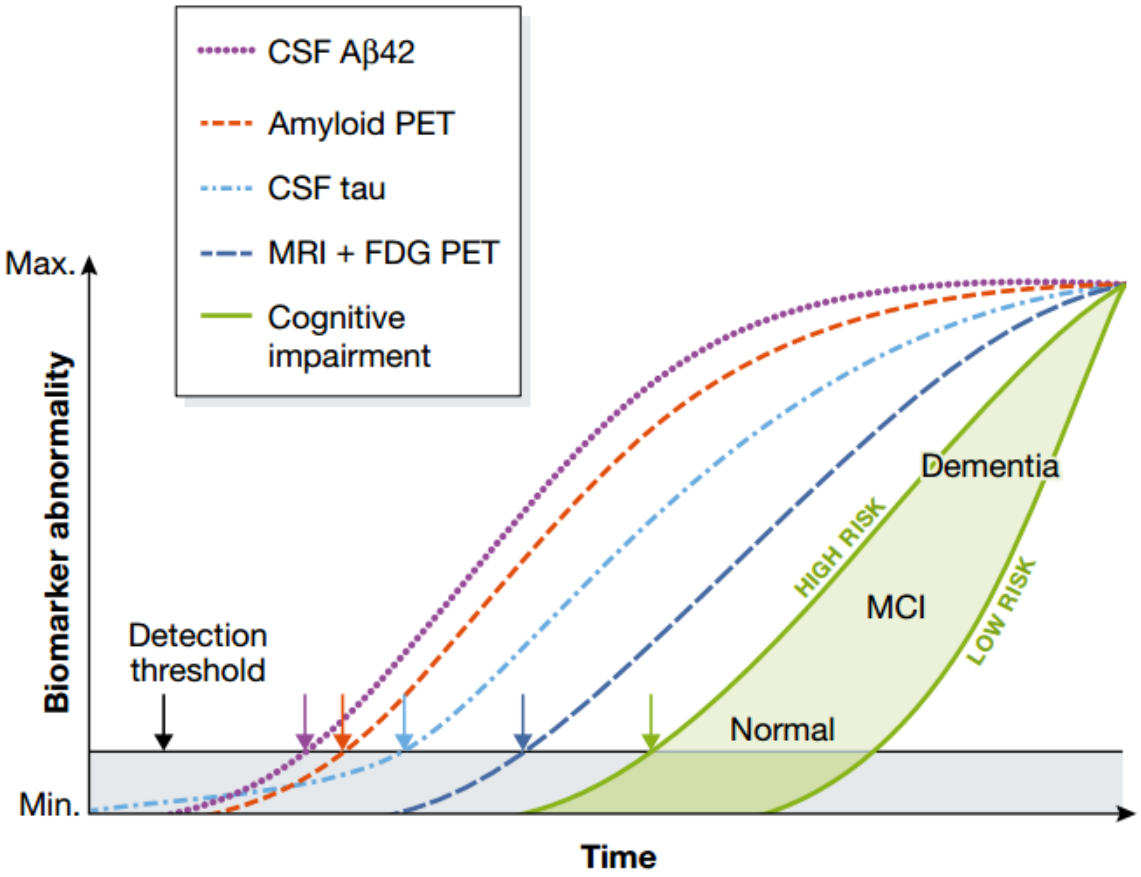

Figure 14: Modèle hypothétique d'évolution de la MA. Les premiers éléments détectés sont liés à l'amyloïde (diminution d'Aβ42 dans le LCR et plaques amyloïdes en IRM). S'en suit l'hyperphosphorylation de tau dans le LCR, l'altération métabolique et *in fine*, les troubles mnésiques et cognitifs. (Selkoe and Hardy 2016). MCI : Mild Cognitive Impairement.

b. Traitements actuels

Bien que des essais cliniques prometteurs voient actuellement le jour, aucun traitement curatif de la MA n'est actuellement disponible. Cependant **quatre molécules** sont actuellement sur le marché permettant ainsi un relatif ralentissement de la progression de la MA. Il est important de noter qu'elles n'empêchent en aucun cas la dégénérescence et la mort neuronale. Trois d'entre elles sont des **anticholinestérasiques** et permettent de contrecarrer la baisse d'acéthylcholine : l'Aricept® (donepezil), le Reminyl® (galantamine) et l'Exelon® (rivastigmine). Le 4ème est l'Ebixa® (mémantine) qui est un **antagoniste des récepteurs NMDA** (acide N-méthyl-D-aspartique) du glutamate.

c. Essais cliniques : les cibles thérapeutiques actuellement testées

Un nombre très important d'essais cliniques ont pu être recensés pour la MA à travers le monde. En effet, selon le site clinicaltrials.gov, **1764 essais ont été réalisés** depuis 2000 et ce, jusqu'au printemps 2016. Ce chiffre est tout de même à relativiser par rapport à d'autres grandes pathologies. En effet, 7317 essais cliniques sur le VIH et 7333 pour le cancer du sein sont à dénombrer sur la même période. **521 essais cliniques** relatifs à la MA sont actuellement en cours dans le monde. Parmi ceux-ci, plus de deux tiers sont localisés aux Etats-Unis ou en Europe (Figure 15).

Le marché des traitements pharmaceutiques pour la MA est actuellement estimé à **6,5 milliards de dollars** ce qui représente 5% du marché de toute la partie système nerveux. Il est cependant attendu que ce marché **progresse de plus de 200%** d'ici à 2023 et l'introduction potentielle de nouvelles thérapies (Qian, Hamad et al. 2015). Ainsi, il va sans dire que ce marché représente un enjeu économique majeur pour les grandes sociétés pharmaceutiques (la « big pharma »).

Les dernières avancées cliniques sur la MA sont chaque année présentées au congrès CTAD (Clinical Trial on Alzheimer's Disease). Afin de discuter les données les plus récentes, je vais exposer en quelques paragraphes les résultats d'essais marquants présentés lors du dernier **CTAD de novembre 2015 à Barcelone**.

- Le **Nuedexta** (ou Zenvia) est une thérapie développée par Avanir Pharmaceuticals, une société américaine filiale d'Otsuka pharmaceutical. Ce traitement est une combinatoire de **deux molécules** d'ores et déjà sur le marché. La première est le dextromethorphan, molécule active de la majorité des sirops pour la toux. Celle-ci est un **antagoniste des récepteurs NMDA** (comme la mémantine) mais aussi des récepteurs sigma 1, protéines d'échafaudages localisées à la membrane du réticulum endoplasmique. La seconde est la quinidine, prescris dans le cadre d'irrégularité cardiaque. Celle-ci va permettre d'augmenter la biodisponibilité du dextromethorphan en favorisant notamment son passage de la barrière hémato-encéphalique. Ainsi le mécanisme d'action du Nuedexta est similaire à la mémantine, c'est-à-dire une **réduction de l'éxcitotoxicité du glutamate**. Une étude de phase 2 révéla récemment une diminution de l'agitation des patients atteints de la MA traités avec le Nuedexta (Cummings, Lyketsos et al. 2015). Il est ainsi important de noter que cette thérapie, comme les traitements actuels, n'est pas curative mais cible les symptômes de la MA.

- Le **Levetiracetam** est développé par la société AgeneBio basée aux Etats-Unis. La molécule, un pyrrolidone acetamide, est un modulateur de la protéine des **vésicules synaptiques SV2A** et fut premièrement développée pour traiter

les troubles épileptiques (Lynch, Lambeng et al. 2004). Le brevet a d'ores et déjà expiré et le composé est ainsi généricqué. Des études plus récentes montrèrent le potentiel thérapeutique du composé dans des souris transgéniques de la MA (Sanchez, Zhu et al. 2012). Le composé démontra ensuite son efficacité dans une phase 2 sur des patients présentant un déficit cognitif léger (Bakker, Krauss et al. 2012) mais aussi sur des patients atteints de la MA et souffrant de crises d'épilepsie (Cumbo and Ligori 2010). Enfin récemment, de nouvelles données appuient le fait que le Levetiracetam réduit l'hyperactivité hippocampique et **améliore les fonctions mnésiques** des patients souffrant d'un déficit cognitif léger (Bakker, Albert et al. 2015). Une étude de phase 3 est d'ores et déjà programmée.

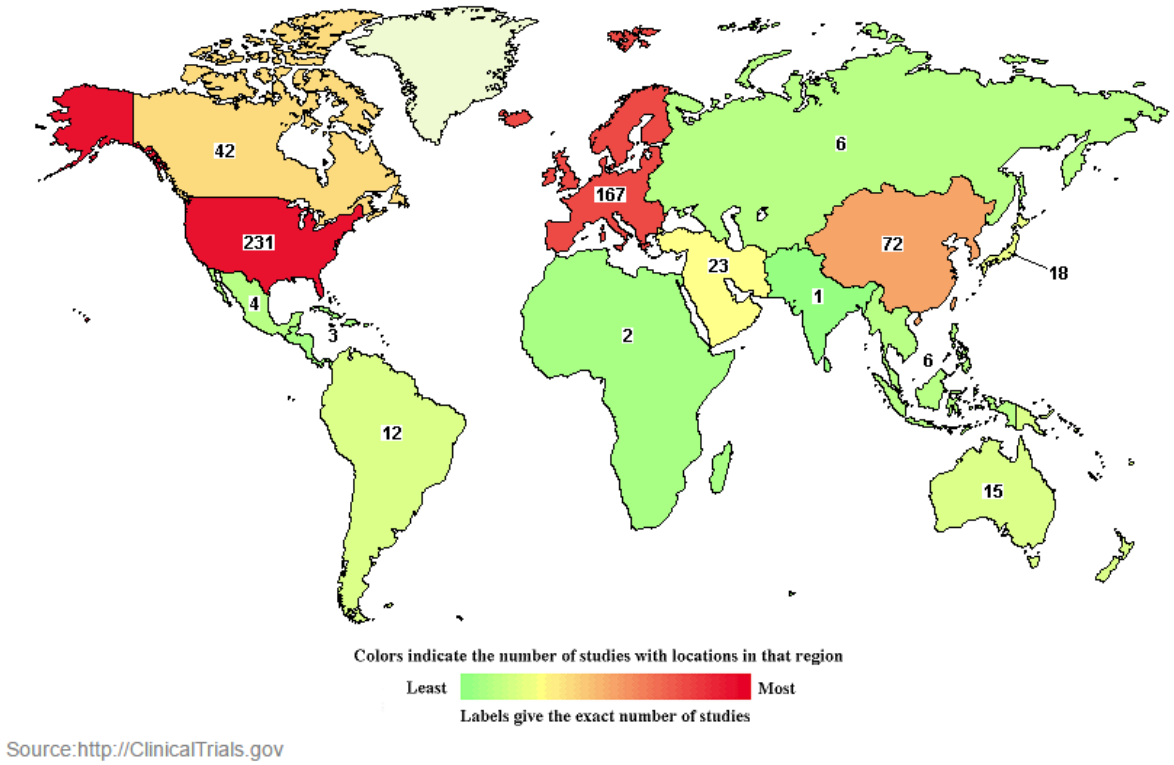

Figure 15: Les essais cliniques sur la MA en cours dans le monde. A noter que les deux tiers de ces essais sont réalisés soit aux Etats-Unis soit en Europe.

- Depuis le début des années 2000, les **anticorps anti-Aβ** sont une cible de choix pour la big pharma. En effet, Eli Lilly développe par exemple le **Solanezumab**, actuellement en phase 3. Conjointement avec Janssen, Pfizer développa jusqu'en 2012 le **Bapineuzumab**, stoppé en phase 3 faute de bénéfice probant. La société suisse Roche n'échappe pas à la tendance, avec son propre composé, le **Gantenerumab**, un anticorps humain IgG1 ayant la capacité de se lier à l'Aβ fibrillisé. Cependant, après là aussi des résultats décevants, la société stoppa son essai intitulé « SCarlet RoAD ». Malgré cela,

Roche présenta des résultats encourageants lors du dernier CTAD. En effet, le traitement semblait avoir un effet sur les patients déclinant le plus rapidement. Que ce soit au congrès de l'AAIC (Alzheimer's Association International Congress) de Washington ou au CTAD de Barcelone, les résultats de **Biogen** furent de loin les plus attendus dans le domaine de l'immunothérapie. En effet, cette société américaine a développé sa propre IgG1 humaine ciblant un épitope conformationnel de l'Aβ ; **l'Aducanumab**. Des résultats plus qu'encourageant sur la diminution des plaques et la cognition lors d'une phase 1b furent d'abord dévoilées lors de la conférence AD/PD (Alzheimer's Disease/Parkinson's Disease) de Nice en mars 2015. Durant l'été 2015, le composé rentra en phase 3 et de nouvelles données furent présentées au CTAD de Barcelone mitigeant cependant les premiers résultats puisque ne montrant pas d'effet cognitifs sur tous les tests réalisés (Alzforum). L'Aducanumab est tout même actuellement considéré, par les scientifiques, médecins et investisseurs comme l'anticorps anti-Aβ le plus prometteur (Alzforum).

- Après s'être intéressé de près aux anticorps spécifiquement dirigés contre l'Aβ, la big pharma s'essaie désormais à **l'immunisation contre la protéine tau**. Deux essais cliniques de phase 1 sont en cours. L'un mené conjointement par AC Immune et Janssen, l'autre par la société Axon Neuroscience, société autrichienne. Cette dernière développe l'**AADvac-1** qui consiste en une vaccination active grâce à l'injection d'un peptide synthétique dérivé d'un fragment de la protéine tau. En 2014, des données dans un modèle rat de la MA indiquaient une amélioration de la pathologie tau (Kontsekova, Zilka et al. 2014). La première étude de phase 1 débuta en 2013 sur une cohorte de 30 patients atteints de la MA. Les premiers résultats montrèrent une bonne tolérance ainsi qu'un score cognitif stable. Une phase 2 débuta en décembre 2015 pour une durée totale de trois ans.

- Sangamo Biosciences est la première société à avoir lancé un essai clinique en utilisant la **thérapie génique**. Cette technique repose sur l'utilisation d'acides nucléiques et leur pénétration dans cellules d'un patient afin de traiter une pathologie (voir partie IV.D). Dans ce cas précis, la molécule d'intérêt est le **NGF** (Nerve Growth Factor), principal facteur de croissance du système nerveux et la thérapie fut nommée CERE-110. Une étude pilote démontra tout d'abord la faisabilité, la sureté et un potentiel bénéfice à long terme du NGF délivré grâce à des fibroblastes génétiquement modifiés

(Tuszynski, Thal et al. 2005). Plus récemment, le NGF fut directement délivré par injections bilatérales d'AAV2 dans le noyau basal de Meynert. Le dernier essai clinique de phase 2 démontra encore une fois une bonne tolérance chez les patients mais un effet thérapeutique nul. C'est pourquoi Sangamo Biosciences mis fin au développement du CERE-110 en avril 2015 (Sangamo).

La maladie d'Alzheimer est donc une pathologie multifactorielle complexe où les enjeux sociéto-économiques sont énormes. L'échec chronique des essais cliniques sur la MA (supérieur à 99%) devient de plus en plus problématique. Outre le problème majeur du diagnostic précoce et de l'inclusion trop tardive des patients dans les protocoles cliniques, la majorité des thérapies qui furent testées reposent majoritairement sur les mêmes postulats de base : la toxicité des dérivés de l'APP et tau. Ainsi, une meilleure compréhension de la physiologie de ces protéines devrait permettre de mieux appréhender le processus physiopathologique de la MA et le développement de stratégies efficaces.

B. L'APP : protéine centrale de la MA

L'APP est une protéine clé dans le processus physiopathologique de la MA. En effet, comme nous l'avons vu précédemment, son clivage est à l'origine de la génération du peptide Aβ menant *in fine* à son agrégation en plaques, marqueur central de la pathologie. De plus, les formes familiales de la MA, sont causées par des mutations dans l'APP ou les présénilines, ses enzymes de clivage. Ainsi, due à son rôle central dans l'amyloïdose, la physiologie de l'APP a été largement étudiée ces 25 dernières années (Selkoe and Hardy 2016). Nous allons ainsi nous intéresser dans cette partie à sa famille, sa génération, son **métabolisme** et ses **rôles physiologiques**. Nous verrons ensuite les moyens de modéliser ses différents rôles et finalement son implication dans la MA.

1. L'APP et ses homologues

L'APP est une **protéine transmembranaire** de type I dont le gène est codé par le chromosome 21. Elle fait partie d'une famille de gènes très conservée dans l'évolution. Parmi ceux-ci, on peut citer APL-1 chez Caenorhabditis elegans (Daigle and Li 1993), APPL dans la drosophile (Rosen, Martin-Morris et al. 1989) ou APPA et APPB chez le poisson zèbre (Musa, Lehrach et al. 2001). Chez les mammifères, APP possède deux homologues ; APLP1 et APLP2 (Wasco, Bupp et al. 1992, Wasco, Gurubhagavatula et al. 1993, Slunt, Thinakaran et al. 1994). Toutes ces protéines possèdent trois domaines fortement conservés : les **domaines E1, E2 et le domaine intracellulaire**. Le domaine N-terminal E1 peut lui être subdivisé en deux parties distinctes ; un domaine de liaison à l'héparine ayant des propriétés neurotrophiques (HBD) et un domaine de liaison au Cuivre et Zinc (CuBD). Le domaine E2 contient lui aussi une région permettant la liaison avec l'héparine et une séquence RERMS possédant aussi des fonctions trophiques (Ninomiya, Roch et al. 1993, Roch, Masliah et al. 1994). Juxtaposant celui-ci du côté N-terminal, on retrouve une région acide, elle-même accolée au **domaine KPI** (Kunitz-type Protease Inhibitor). Ce dernier n'est cependant présent que dans l'APP et l'APLP2 et est de plus sujet à un épissage alternatif dans ces deux protéines. La partie intracellulaire de l'APP et des APLP possède une séquence conservée « YENPTY » permettant la liaison avec d'autres protéines (Klevanski, Herrmann et al. 2015). Comme l'APP, les APLP peuvent être aussi clivés par les secrétases et le **domaine C-terminal** en résultant peut jouer un rôle dans la signalisation intracellulaire (Xu, Kim et al. 2007). Il est intéressant de noter que le peptide sAPLP2, issu d'APLP2 présente des propriétés trophiques similaires au APPsα (ou sAPPsα), dérivé de l'APP (voir la partie IV.C). De manière intéressante, le domaine le plus différent entre ces homologues est celui

juxtaposant la membrane extracellulaire ; domaine contenant la séquence du peptide Aβ. Celui-ci n'est en effet présent que dans l'APP (Figure 16).

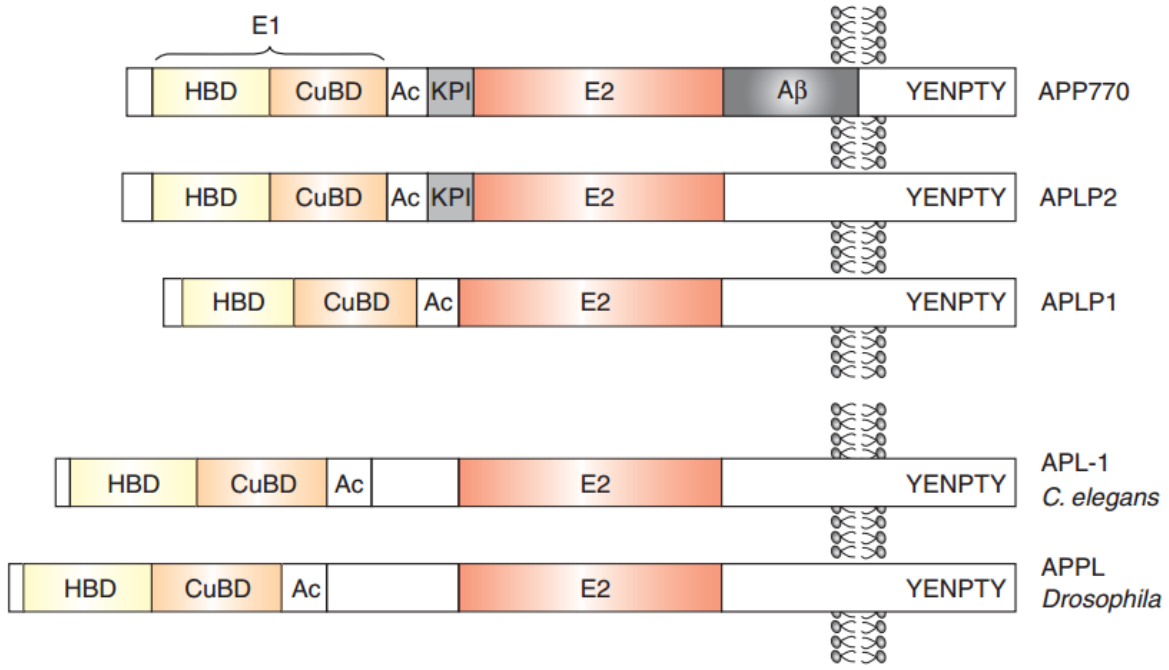

Figure 16 : L'APP et ses homologues. L'APP possède deux paralogues chez les mammifères, APLP1 et APLP2. Entre autres, elle possède aussi deux orthologues avec APL-1 chez Caenorhabditis elegans et APPL chez la drosophile (Muller and Zheng 2012).

2. Production et maturation de l'APP

Dans le cerveau humain, **trois isoformes de l'APP** sont présents et du à un épissage alternatif des exons 7, 8 et 15 : les formes 770, 751 et 695 acides aminés (Figure 17). Cette dernière est très majoritairement **exprimée par les neurones** mais minoritaire dans le cerveau (Wang, Wu et al. 2016). La forme 751 contient en plus le domaine KPI et la forme 770, en plus de ce domaine KPI contient un antigène nommé OX-2. Ces deux dernières formes sont ubiquitaires dans le cerveau, et ainsi exprimées par les cellules gliales (Menendez-Gonzalez, Perez-Pinera et al. 2005).

Le **domaine KPI** comprend 57 acides aminés et son homologie est forte avec les inhibiteurs de protéases à sérine de type Kunitz. Celles-ci sont définies par la présence d'une sérine dans leur site actif. Une de ses enzymes cibles est notamment l'acetylcholinestérase dont la concentration est corrélée avec l'APP-KPI(+) dans le LCR des patients atteints de la MA (Urakami, Takahashi et al. 1992). De manière intéressante, le ratio APP-KPI(+)/APP-total est significativement augmenté dans le cerveau des patients atteints de la MA et associé à une augmentation de l'Aβ (Palmert, Podlisny et

al. 1989, Moir, Lynch et al. 1998). A l'inverse, **l'APP 695 neuronal est réduit** notamment dans le cortex et l'hippocampe (Johnson, Rogers et al. 1989). De plus, il fut plus récemment proposé que l'homodimérisation de l'APP, responsable de signalisations intracellulaires physiologiques, soit médiée via ce domaine KPI (Ben Khalifa, Tyteca et al. 2012). Bien que les trois isoformes d'APP soient tous amyloidogéniques, il a été déterminé dans des lignées de cellules neuronales que l'APPsβ et l'Aβ étaient préférentiellement produits à partir de la forme 695 acides aminés (Belyaev, Kellett et al. 2010). Parallèlement à cela, une étude plus ancienne montra dans le cerveau et le LCR humain que l'APP-KPI(+) était préférentiellement clivé par l'α secrétase (Kametani, Tanaka et al. 1993).

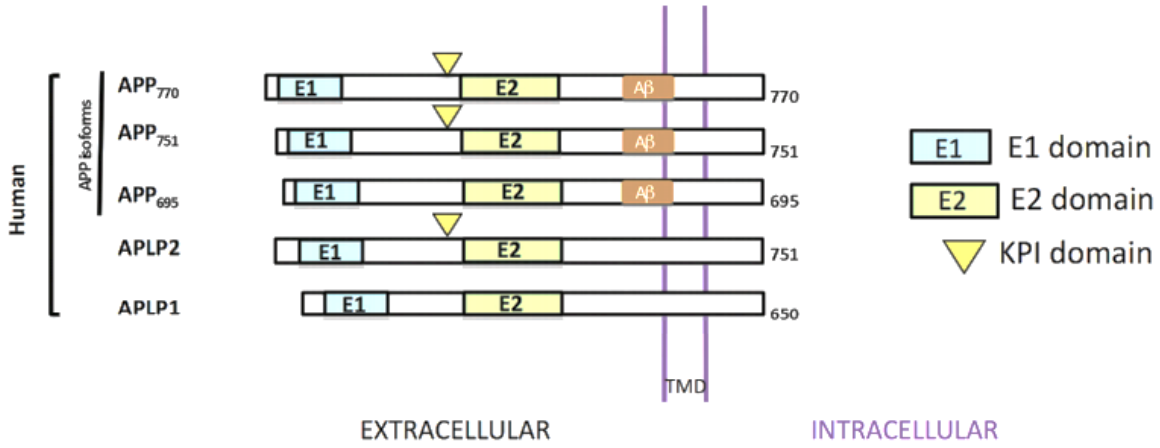

Figure 17: Les isoformes de l'APP dans le cerveau humain et ses deux paralogues. A noter que les différences majeures entre ces protéines se résument à la présence ou l'absence des domaines KPI et Aβ (Alexander, Marfil et al. 2014).

Après sa transcription, son épissage alternatif et sa traduction, l'APP va subir des modifications post-traductionnelles. L'APP est une **glycoprotéine** puisqu'elle va subir des N-glycosylations et des O-glycosylations durant son transit entre le réticulum endoplasmique et la membrane. Elle va de plus acquérir des groupements de type acide sialique et sulfate de chondroïtine (domaine CS GAG ; différentiellement exprimés par les isoformes d'APP) (Pangalos, Shioi et al. 1995, Lyckman, Confaloni et al. 1998, Jacobsen and Iverfeldt 2009). De plus, l'APP (ainsi que les membres de sa famille) va être **phosphorylé**. En particulier, les sites Tyr653, Ser655, Thr668, Ser675, Tyr682 de l'APP ont été montrés comme étant phosphorylés sur des échantillons de cerveaux humains. Le site Thr668 est un site privilégié puisque sa phosphorylation semble influencer le clivage de l'APP et la production d'Aβ (Lee, Kao et al. 2003). Cette phosphorylation induit de plus la **translocation du domaine intracellulaire** vers le noyau provoquant notamment la phosphorylation de la protéine tau (Chang, Kim et al.

2006). Parmi les nombreuses kinases impliquées dans la phosphorylation de l'APP, il est important de noter que certaines sont communes à la protéine tau comme **cdk5**, **GSK3β** ou **DYRK1A** (Suzuki and Nakaya 2008, Wegiel, Gong et al. 2011).

Finalement, seulement une petite fraction de l'APP arrive à la membrane plasmique (estimée à 10% en culture cellulaire), la majorité se localisant au niveau de l'appareil de Golgi. Il sera ensuite, grâce à son motif intracellulaire YENPTY, internalisé et localisé au niveau des endosomes. Cette localisation intracellulaire influera considérablement sur son métabolisme (Haass, Kaether et al. 2012).

3. Le métabolisme de l'APP

a. La voie non-amyloïdogène

La voie non-amyloïdogène est considérée comme **la voie physiologique** du métabolisme de l'APP puisque ne libérant pas de métabolites toxiques. De plus, dans des conditions non-pathologiques, la voie non-amyloïdogène clive près de 90% de l'APP mature, les dix derniers pourcents restant entrent dans la voie amyloïdogène (Ahmed, Holler et al. 2010). Dans cette voie physiologique, l'APP est tout d'abord clivé par l'**α secrétase**, au niveau de la surface cellulaire (Haass, Kaether et al. 2012). Celle-ci fait partie de la famille **ADAM** (A Disintegrin And Metalloprotease Domain) et cinq isoformes ont aujourd'hui été proposés comme α secrétases : ADAM8, ADAM9, ADAM10, ADAM17 et ADAM19 (Asai, Hattori et al. 2003, Naus, Reipschlager et al. 2006, Tanabe, Hotoda et al. 2007). Cependant, ADAM10 fut récemment démontrée comme étant l'isoforme constitutivement actif de l'α secrétase (Prox, Bernreuther et al. 2013). Elle conduit à la sécrétion du peptide **APPsα** (dont les propriétés seront détaillées dans la partie IV.C) et à la production du peptide C83 (α-CTF). Un clivage de ce dernier par la **γ secrétase**, dont les présénilines font parties intégrantes, mène à la production du peptide p3, non toxique et d'AICD. Par ailleurs, il est important de noter que ce peptide AICD n'est pas inerte. En effet, ce dernier peut se localiser dans le noyau et agir comme facteur de transcription (Cao and Sudhof 2001, Gao and Pimplikar 2001) mais aussi comme modificateur épigénétique (Octave, Pierrot et al. 2013).

b. La voie amyloïdogène

Le métabolisme de l'APP et plus particulièrement la voie amyloïdogène est une phase clé dans le **processus pathogène de la MA**. En effet, celle-ci est dérégulée dans la MA

et conduit à la production massive d'Aβ et finalement la génération de plaques amyloïdes. Il est cependant important de noter que cette voie permet aussi de cliver l'APP en conditions physiologiques (Muller and Zheng 2012). De plus, des individus asymptomatiques présentent, après analyse post-mortem, des plaques amyloïdes dans leur cerveau (Gibson 1983, Delaere, Duyckaerts et al. 1990, Mackenzie, McLachlan et al. 1996).

Dans cette voie, l'APP va être clivé par deux secrétases au niveau des endosomes; la **β secrétase** (BACE) et la γ secrétase. La première coupure par la β secrétase donne lieu au peptide C99 (ou β-CTF) et à l'**APPsβ**. Le second clivage par la γ secrétase libère le domaine intracellulaire AICD (APP IntraCellular Domain) et le peptide **Aβ**. Deux formes majoritaires d'Aβ sont produites suivant son clivage par la γ secrétase ; l'Aβ40 (de 40 acides aminés) dont la production est majoritaire (environ 80%) et l'**Aβ42** (comportant 42 acides aminés), le plus toxique. Les plaques amyloïdes sont donc des dépôts extracellulaires formés à partir de l'agrégation des peptides Aβ (O'Brien and Wong 2011) (Figure 18).

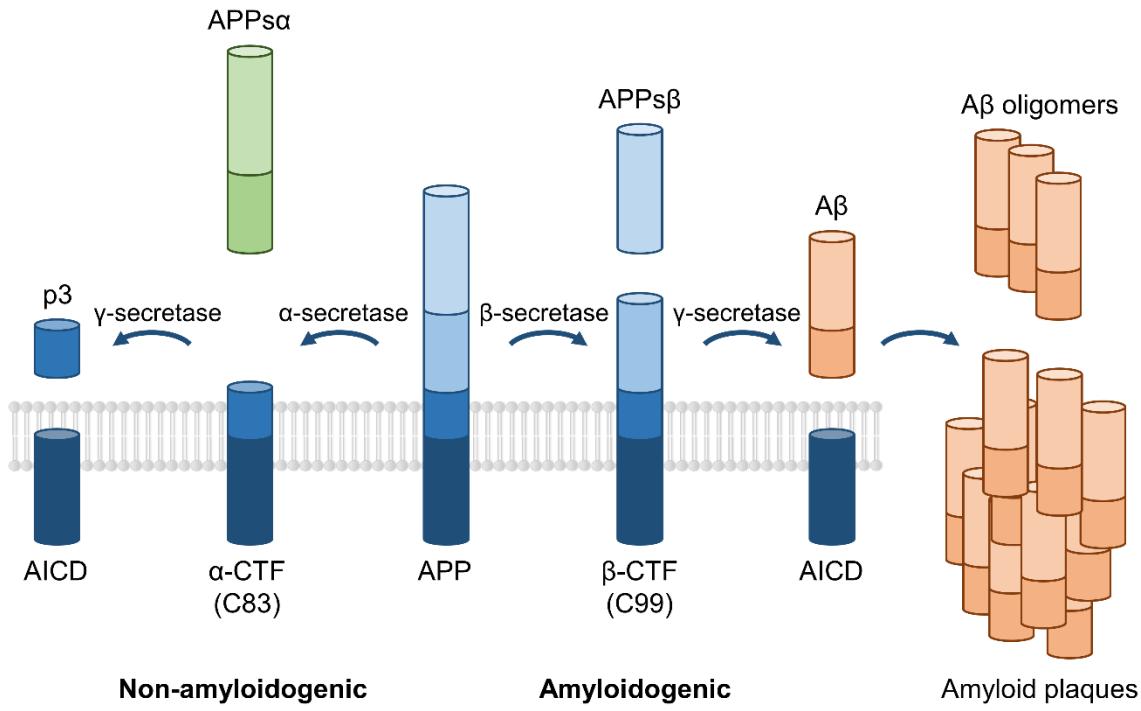

Figure 18: Le métabolisme de l'APP. L'APP est clivé selon deux voies distinctes ; la voie non-amyloïdogène, libérant notamment l'APPsα ; et la voie amyloïdogène menant à la libération d'Aβ toxique et *in fine* à la formation de plaques (Alves, Fol et al. 2016).

4. Rôles physiologiques de l'APP

Depuis le clonage de l'APP il y a plus d'un quart de siècle (Goldgaber, Lerman et al. 1987, Kang, Lemaire et al. 1987, Robakis, Ramakrishna et al. 1987, Tanzi, Gusella et al. 1987), de nombreuses études ont permis de montrer le rôle pathologique de l'Aβ. Cependant les rôles physiologiques de l'APP et la question de savoir **si sa perte de fonction contribue à la pathologie** est toujours un sujet d'actualité dans la communauté scientifique. Néanmoins, les nombreuses données génétiques et biochimiques accumulées ces vingt dernières années nous ont renseigné sur ses fonctions putatives.

a. L'adhésion cellulaire et synaptique

De par sa structure et ses nombreux domaines de liaison, l'APP peut être vu comme une **protéine d'adhésion**. En effet, l'APP a été démontré comme étant un liguant des protéines de la matrice extracellulaire comme l'héparine, le collagène ou les laminines (Kibbey, Jucker et al. 1993, Beher, Hesse et al. 1996, Clarris, Cappai et al. 1997). Ces dernières années, la capacité de l'APP à former des **homodimères** a pu être mise en évidence. Ceux-ci peuvent être dû aux domaines E1, E2 ou KPI (Wang and Ha 2004, Gralle, Oliveira et al. 2006, Dahms, Hoefgen et al. 2010, Ben Khalifa, Tyteca et al. 2012). Des études parallèles ont pu mettre en évidence ses interactions dans le cadre de la synapse, faisant de l'APP une nouvelle **molécule d'adhésion synaptique** (Soba, Eggert et al. 2005, Wang, Wang et al. 2009).

b. Des propriétés trophiques neuronales et synaptiques

Différents éléments de son promoteur (SP-1, AP-1 et AP-4) suggèrent que ce gène appartient à la classe des gènes régulant la **croissance, la prolifération et la maturation** cellulaire (Salbaum, Weidemann et al. 1988, Izumi, Yamada et al. 1992, Quitschke and Goldgaber 1992). Ainsi, de nombreuses études sont venues corroborées les fonctions de l'APP comme facteur de croissance sur les neurones et les synapses. Il a été démontré que l'expression d'APP est reliée à la synaptogénèse et la croissance neuritique durant le développement (Clarris, Key et al. 1995) et que sa diminution ou son inhibition *in vitro* conduisait à une diminution de la croissance neuritique, de la viabilité neuronale et de la transmission synaptique (Allinquant, Hantraye et al. 1995, Perez, Zheng et al. 1997, Herard, Besret et al. 2006).

Nous avons aussi récemment montré que le domaine intracellulaire de l'APP était un domaine essentiel pour la synapse, tant **dans le SNC que dans le SNP** (Klevanski, Herrmann et al. 2015). Il est ainsi probable que ses propriétés trophiques, et notamment la croissance neuritique, soient partiellement médiées par ses propriétés d'adhésion

citées ci-dessus (Small, Nurcombe et al. 1994, Qiu, Ferreira et al. 1995). Cependant, il semblerait que la majorité de ses propriétés trophiques proviennent du clivage par l'α secrétase et le relargage du **peptide neurotrophique APPsα** (voir partie IV.C). De manière opposée, une étude de Nikolaev *et coll.* indique qu'un clivage de l'APPsβ délivrant un peptide de 35kDa vient activer le récepteur de mort cellulaire DR6 et induit ainsi un signal de dégénérescence (Nikolaev, McLaughlin et al. 2009).

c. La signalisation intracellulaire

L'APP induit aussi une signalisation intracellulaire grâce au domaine intracellulaire clivé durant son métabolisme ; **AICD**. Il est ainsi important de noter que ce clivage est semblable à celui de Notch (par les présénilines), protéine de signalisation majeure (Sastre, Steiner et al. 2001). Comme indiqué précédemment, AICD peut être transloqué dans le noyau et fonctionner notamment comme facteur de transcription. Dans ce cas précis, il s'associe à Fe65 et Tip60, une histone acetyltransferase (Cao and Sudhof 2001, Gao and Pimplikar 2001). Bien que ce modèle précis fut contesté ces dernières années (Hass and Yankner 2005, Yang, Cool et al. 2006, Chen and Selkoe 2007), il semble toutefois que le triptyque APP/Fe65/Tip60 soit responsable de la transcription de nombreux gènes. Bien que ses cibles soient elles aussi contestées, on peut noter la présence de l'APP elle-même mettant ainsi en évidence une **boucle d'autorégulation** (von Rotz, Kohli et al. 2004). On peut aussi noter la présence de GSK3β, NEP, enzyme de dégradation de l'Aβ et LRP, récepteur d'APOE (Kim, Kim et al. 2003, Pardossi-Piquard, Petit et al. 2005, Liu, Zerbinatti et al. 2007).

d. Autres fonctions

D'autres fonctions physiologiques de l'APP furent proposées. L'une d'entre elles nous mène aussi à AICD et à une putative **fonction apoptotique**. En effet, il a été montré qu'un de ses gènes cibles en tant que facteur de transcription serait p53, régulateur central de l'apoptose (Checler, Sunyach et al. 2007). AICD pourrait aussi être de nouveau clivé libérant notamment le peptide C31 cytotoxique (Bertrand, Brouillet et al. 2001, Lu, Soriano et al. 2003, Park, Shaked et al. 2009). De plus, les défauts cognitifs et synaptiques d'une souris transgénique PDAPP modélisant la pathologie Alzheimer étaient restaurés avec une mutation de l'APP inhibant la libération du peptide C31 (Galvan, Gorostiza et al. 2006). Enfin, il a été montré que les neurones issues de souris transgéniques AICD sont plus susceptibles en conditions de stress (Giliberto, Zhou et al. 2008).

Enfin, un rôle de l'APP sur les phénomènes de **coagulation** fut aussi proposé dès le début des années 1990. En effet dans les plaquettes, l'APP et ses dérivés se localisent dans les granules α impliquées dans la coagulation (Van Nostrand, Schmaier et al. 1990, Van Nostrand, Schmaier et al. 1991). Il a été par ailleurs montré les formes APP-KPI(+) sont celles étant majoritaires dans le sang (Bush, Martins et al. 1990). Ainsi des études ont montré que ce domaine KPI était un puissant facteur d'inhibition de la coagulation (Smith, Higuchi et al. 1990, Schmaier, Dahl et al. 1993, Scandura, Zhang et al. 1997). Ces données furent confirmées dans les modèles animaux où les souris APP-KO présentent des hémorragies cérébrales amoindries à l'inverse des souris surexprimant l'APP qui présentent une thrombose cérébrale atténuée (Xu, Davis et al. 2005, Xu, Previti et al. 2007).

Outre son potentiel amyloïdogène, l'APP présente donc de nombreuses fonctions physiologiques. Réduire l'APP à la seule production d'Aβ est un démarche simpliste dont la recherche sur la MA semble avoir quelque peu souffert. Afin d'appréhender plus finement les mécanismes physiopathologiques de celle-ci, plusieurs souris transgéniques APP knock-out (KO) ou knock-in (KI) furent réalisées dans les années 1990.

5. Le rôle de l'APP à travers les modèles murins

a. Les souris APP-KO

L'étude des souris APP-KO a bien sûr été une étape clé dans la compréhension de la fonction de ce gène. Trois souris différentes furent générées, deux présentant une délétion complète du gène (Zheng, Jiang et al. 1995, Li, Stark et al. 1996) et la dernière avec une mutation hypomorphe (Muller, Cristina et al. 1994). La première chose à noter est que ces souris, ayant toutes trois des phénotypes semblables, sont viables indiquant que ce gène n'a **pas une fonction cruciale durant le développement** (Zheng, Jiang et al. 1995). Cependant, ces souris présentent un **déficit de poids** du corps mais aussi du cerveau (Magara, Muller et al. 1999). Au niveau comportemental, elles présentent, à un âge avancé, **des défauts d'apprentissages et mémorisation** (Seabrook, Smith et al. 1999, Senechal, Kelly et al. 2008). Des défauts du SNP, matérialisés par une activité locomotrice réduite et une faiblesse musculaire, ont aussi été observés (Muller, Cristina et al. 1994, Zheng, Jiang et al. 1995). Il n'est donc pas surprenant, à l'échelle cellulaire, de noter des **diminutions du nombre d'épines dendritiques** et de la complexité des arborisations de l'hippocampe (Lee, Moussa et al. 2010, Weyer, Zagrebelsky et al.

2014). Ces modifications sont accompagnées d'une détérioration de la transmission synaptique mise en évidence notamment par un **défaut de potentialisation à long terme (LTP)** (Seabrook, Smith et al. 1999). Ces données confirment donc l'implication de l'APP dans le fonctionnement normal du réseau synaptique et de sa plasticité.

b. Les souris transgéniques pour l'APP sauvage

Contrairement aux souris transgéniques présentant une forme mutée de l'APP (voir partie IV.B.6.d), peu d'équipes ont étudiés les conséquences de la transgénèse d'une forme sauvage. A ma connaissance, seuls deux groupes se sont intéressés à l'effet de l'introduction d'une forme humaine de l'APP dans le génome d'une souris. Les premières études furent réalisées à la fin des années 1990 à l'université californienne de San Francisco par L. Mucke *et coll.* (Mucke, Abraham et al. 1996, Masliah, Westland et al. 1997, Masliah, Raber et al. 1998, Mucke, Masliah et al. 2000). Dans les premiers articles, les auteurs comparent plusieurs souris transgéniques générées à partir de deux formes d'APP humaines ; l'APP695 et l'APP751. Ils mettent en évidence les **capacités neuroprotectrices** de celles-ci (et notamment de la forme 751 acides aminés) contre l'excitotoxicité. Dans le dernier article publié en l'an 2000, les auteurs comparent les souris transgéniques pour l'APP (hAPP695, hAPP751 et hAPP770, nommées ensuite hAPP-WT) à deux autres lignées de souris transgéniques présentant des mutations retrouvées chez les patients (Swedish et Indiana). De manière intéressante, la souris hAPP-WT, bien que produisant de l'Aβ, semble **moins enclin à produire l'Aβ42** toxique. Même à un âge avancé (15 mois), l'expression de la forme sauvage **ne permet pas la formation de plaques**, contrairement aux souris présentant des mutations familiales (Figure 19). Cependant, comparées à des souris sauvages, les souris hAPP-WT présentent un niveau moindre de synaptophysine suggérant une **altération présynatique**. Ce défaut est corrélé aux niveaux d'Aβ mais pas à ceux de l'APP ou des plaques sous-tendant ainsi la toxicité synaptique de l'Aβ et non des plaques ; un concept ardemment débattu à l'époque.

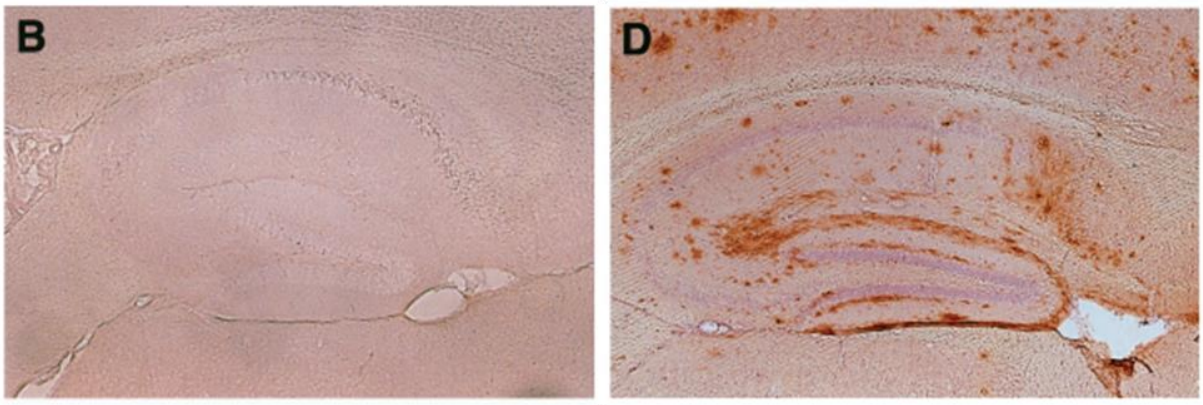

Figure 19: Hippocampes de souris transgéniques surexprimant l'APP humain. A gauche **(B)**, souris une souris surexprimant l'APP humain sauvage âgée de 15 mois. A droite **(D)**, une souris surexprimant l'APP humain muté (mutations Swedish et Indianna) âgée de 10 mois. Noter la présence abondante de plaques avec les mutations et son absence avec la forme sauvage. (Mucke, Masliah et al. 2000)

Une étude plus récente fut conduite par une équipe espagnole de l'université de Navarre (Simon, Schiapparelli et al. 2009). Les investigateurs réalisent tout d'abord une batterie de tests comportementaux comme la piscine de Morris ou la reconnaissance d'objets et mettent en évidence une **altération des performances** des souris hAPP-WT comparées à des souris sauvages à un âge relativement jeune (entre 5 et 8 mois). De manière similaire à la précédente étude, ces derniers vont comparer les niveaux d'Aβ de ces souris à d'autres présentant les mutations Swedish et Indiana (modèle J20). Les souris hAPP-WT présentent des niveaux **200 à 800 fois inférieurs** par rapport aux souris présentant une mutation. Ceci est expliqué par le fait que la majorité de l'APP est métabolisé via la voie non-amyloïdogène dans les souris hAPP-WT. Malgré cela, les auteurs mettent aussi en évidence une **hyperphosphorylation de la protéine tau** et des **niveaux diminués de nombreux marqueurs synaptiques**.

Ces résultats suggèrent ainsi que l'expression d'une forme sauvage de l'APP humaine n'est pas anodine dans la souris. Malgré un faible niveau d'Aβ42 produit et la propension à métaboliser l'APP de manière non-amyloïdogène, l'APP humain sauvage induit notamment un affaiblissement de la synapse menant in fine à des défauts de comportement. La surexpression d'une forme d'APP taille entière ne semble pas être une stratégie thérapeutique envisageable pour la MA.

6. L'APP dans la MA; La cascade amyloïde

L'hypothèse de la cascade amyloïde fut formulée dès 1992, par John Hardy et Gerald Higgins et est actuellement **la base de toute la recherche** effectuée sur la MA (Hardy and Higgins 1992). Comme son nom l'indique, elle met au centre de la pathologie **l'accumulation du peptide Aβ** comme initiateur de la cascade pathologique survenant dans la MA (Hardy and Allsop 1991). La grande majorité des modèles animaux (de type APP et/ou PS1) mais aussi des thérapeutiques actuellement testées en clinique (comme l'immunisation anti-Aβ ou les inhibiteurs de BACE) sont ainsi basés sur cette hypothèse. Malgré cela, elle est constamment débattue et remise en cause depuis plus de vingt ans, ce que nous verrons dans une dernière partie.

a. L'hypothèse de la cascade amyloïde

La composante tau de la maladie d'Alzheimer a souvent été opposée à la composante amyloïde. Cependant, l'hypothèse de la cascade amyloïde a permis d'unifier les deux éléments. Néanmoins, les auteurs énoncent la composante amyloïde comme l'**élément initial** dans le déclenchement de le MA. Cette hypothèse repose sur les études des formes familiales de la MA (moins de 5% des cas), ainsi que sur les données démontrant la toxicité cellulaire du peptide Aβ42 (Glenner and Wong 1984, Gilbert 2014). Comme indiqué précédemment, les trois gènes identifiés dans les formes familiales précoces (APP, PSEN1 et PSEN2) sont impliqués dans la production du peptide Aβ.

Dans ces formes familiales, les mutations génétiques conduisent à **une accumulation d'Aβ42 toxique** dans le cerveau. Dans les formes sporadiques de la MA, ce ne sont pas des mutations autosomales dominantes qui vont déclencher la survenue de la pathologie, mais là aussi, l'augmentation d'Aβ42 en est l'élément central, unifiant ainsi les deux formes de la maladie. Selon les auteurs, cette augmentation est la conséquence d'un défaut d'élimination, de la présence d'un allèle APOE4 dans le génome ou d'autres variants trouvés dans les analyses pangénomiques.

Dans les deux cas les peptides Aβ vont, de manière soluble ou oligomérique, causer notamment des **défauts synaptiques** et homéostastiques dans les cellules. L'agrégation de l'Aβ en plaques va causer l'activation des cellules gliales ainsi qu'une réponse inflammatoire dans le cerveau. Cette cascade pathologique mène *in fine* à la formation de DNF, la **perte neuronale**, l'atrophie et **la démence** (Figure 20). L'unification des deux marqueurs anatomo-pathologiques de la MA, à savoir les plaques et la DNF, fut un élément important dans l'approbation de théorie par la communauté scientifique. Cependant, l'éternel débat pour savoir si l'augmentation d'Aβ précède la

phosphorylation de tau ou *vice versa* reste d'actualité. Nous verrons plus en détails dans les deux prochaines parties les processus pathologiques découlant de ces deux phénomènes.

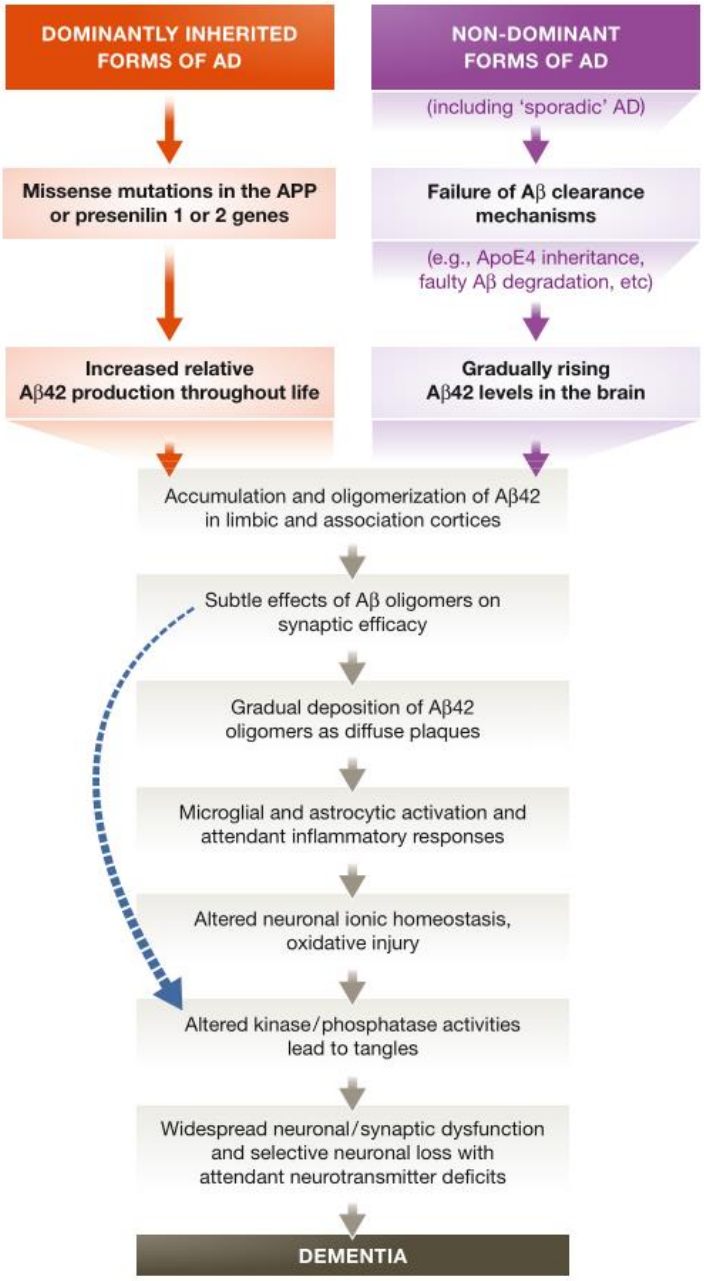

Figure 20: La version actuelle de la cascade amyloïde. Qu'elle soit d'origine familiale (présence de mutations dans l'APP ou les présénilines) ou dû à un vieillissement pathologique (formes sporadiques), la MA se caractérise par une accumulation du niveau d'Aβ42 conduisant ainsi à une réaction en chaîne d'événements conduisant au final à la démence. (Selkoe and Hardy 2016)

b. La voie amyloïde

Jusqu'au début des années 2000, les plaques amyloïdes étaient peut-être plus considérées comme l'élément central de la cascade amyloïde que le peptide Aβ (Mucke, Masliah et al. 2000, Hardy and Selkoe 2002). Des études ont cependant montré que les plaques ne **corrèlent pas avec l'atteinte cognitive** (Terry, Masliah et al. 1991) et que leur **toxicité est faible** dans des modèles expérimentaux (Klein, Krafft et al. 2001, Cheng, Scearce-Levie et al. 2007). La nocivité de l'Aβ est maintenant au cœur de la cascade amyloïde. Ce dernier fut inculpé dès le début des années 1990, peu de temps après son isolation par George Glenner (Glenner 1983, Glenner and Wong 1984). L'Aβ est un peptide d'environ 4kDa dont les **fonctions physiologiques sont mal connues**. Quelques études ont cependant montré que le peptide pouvait réguler le transport et le métabolisme du cholestérol (Yao and Papadopoulos 2002) ou encore agir en tant que facteur de transcription (Bailey, Maloney et al. 2011). Dans le cadre de la MA, celui-ci peut être retrouvé sous différentes formes : des **monomères, oligomères ou protofibrilles**. Les fibrilles matures forment quant à elles, les fameuses plaques amyloïdes (Glabe 2008).

De nombreuses études *in vitro* et *in vivo* suggèrent que les **formes oligomériques** sont les plus enclines à induire des défauts au niveau synaptique et neuronal (Cheng, Scearce-Levie et al. 2007, Tomiyama, Matsuyama et al. 2010). Ainsi, la **LTP** (évaluant la force de la transmission synaptique) est impactée par la charge en peptides (Shankar, Li et al. 2008). La région CA1 de l'hippocampe de souris est le modèle le plus couramment utilisé afin de mesurer la LTP, phénomène reposant majoritairement sur l'activation des récepteurs aux glutamates NMDA. Cependant dans le cadre de la MA, ceux-ci voient leur nombre diminué en présence d'Aβ (Snyder, Nong et al. 2005). Cette toxicité a aussi été mise en évidence grâce à la **réduction du nombre d'épines dendritiques** dans les modèles murins (Hsieh, Boehm et al. 2006). L'Aβ provoque aussi la formation **d'espèces réactives de l'oxygène** toxiques et l'augmentation du niveau d'ions calcium menant à la mort cellulaire (Behl, Davis et al. 1994). Enfin au niveau mnésique, de nombreuses études ont pu faire un lien direct entre l'Aβ et **les altérations cognitives** chez des modèles rongeurs (Hsiao, Chapman et al. 1996, Nakamura, Murayama et al. 2001). Ces données ne sont bien sûr pas exhaustives mais renseignent sur le fort potentiel pathogène du peptide et donne ainsi des arguments pour les défenseurs de la cascade amyloïde (Figure 21).

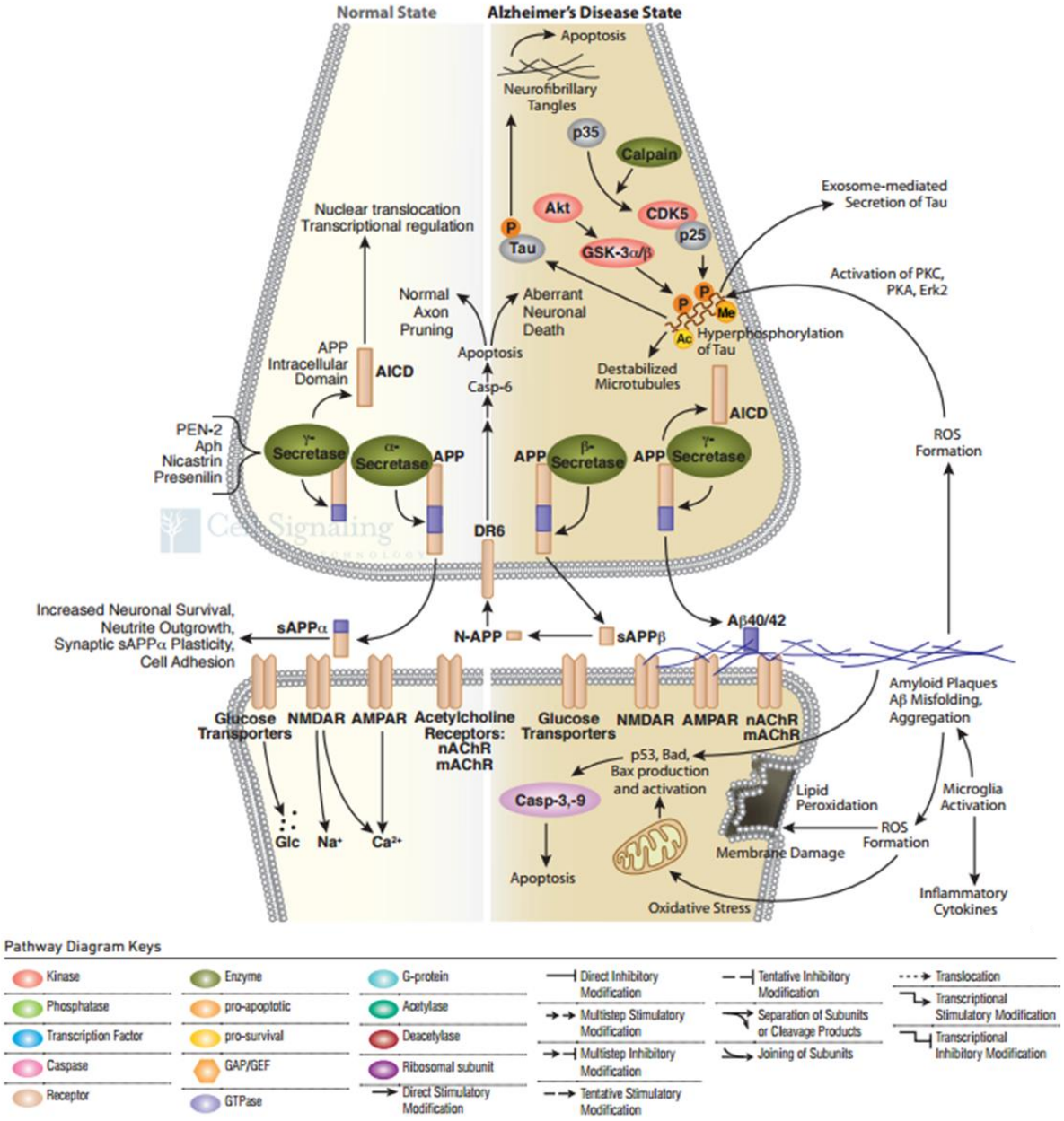

Figure 21: La synapse en conditions physiologiques et dans le cadre pathologique de la MA. Schéma non exhaustif des mécanismes physiopathologiques de la synapse. Source : Cell Signaling.

Dans les formes tardives sporadiques de la MA, plus qu'une augmentation de la production du peptide, un **défaut de clairance de l'Aβ** est considéré comme étant moteur de la pathologie. Deux enzymes sont responsables en conditions physiologiques d'une grande partie de la dégradation du peptide. **Neprilysin** (NEP) est une métalloprotéase notamment active au niveau extracellulaire. L'Insulin Degrading Enzyme (**IDE**) est aussi une métalloprotéase mais majoritairement présente au niveau cérébral dans la **microglie** (Miners, Barua et al. 2011), cellules immunitaires participant à la dégradation des plaques amyloïdes en conditions pathologiques (Prokop, Miller et

al. 2013). Cependant, dans ce contexte, il a été montré que les deux protéines sont diminuées avec l'âge et dans les régions affectées par la MA (Caccamo, Oddo et al. 2005).

Au cours des trois dernières décennies, la toxicité de l'Aβ42 a bien été démontrée et confirmée ; elle est indéniable. Mais n'a-t-on pas trop insisté sur le gain de fonction toxique de l'APP en négligeant sa perte de fonction physiologique ?

c. La voie Tau

Afin de ne pas surcharger ce manuscrit, je serai volontairement bref sur un sujet que je n'ai que très partiellement abordé pendant ma thèse. Il m'est cependant impossible de faire abstraction de cette protéine contribuant aussi grandement au processus pathologique de la MA. Dans le cerveau, tau est codée par le gène MAPT (*Microtubule Associated Protein Tau*) présent sur le chromosome 17. De manière similaire à l'APP, tau subit un épissage alternatif permettant la génération de six isoformes chez l'homme (Buee, Bussiere et al. 2000). Dans son fonctionnement physiologique, tau est une des plus importantes **protéines associées aux microtubules**. Au fil des années, différentes fonctions de la phosphoprotéine ont pu être mises en évidence et confirmées. Tout d'abord sa faculté d'assemblage des tubulines en microtubules et leur stabilisation (Weingarten, Lockwood et al. 1975). Elle est aussi impliquée dans la neurotransmission à travers la voie de signalisation Fyn (Lee, Thangavel et al. 2004, Roberson, Halabisky et al. 2011). Son **degré de phosphorylation** impacte grandement sa fonction. En effet, sa fonction d'assemblage des microtubules est régulée par celui-ci. Cependant, une **hyperphosphorylation** de la protéine annihile cette activité (Lindwall and Cole 1984, Alonso, Zaidi et al. 1994) et permet la formation de la DNF qui est une des deux grandes caractéristiques de la MA au même titre que les plaques amyloïdes (Figure 22).

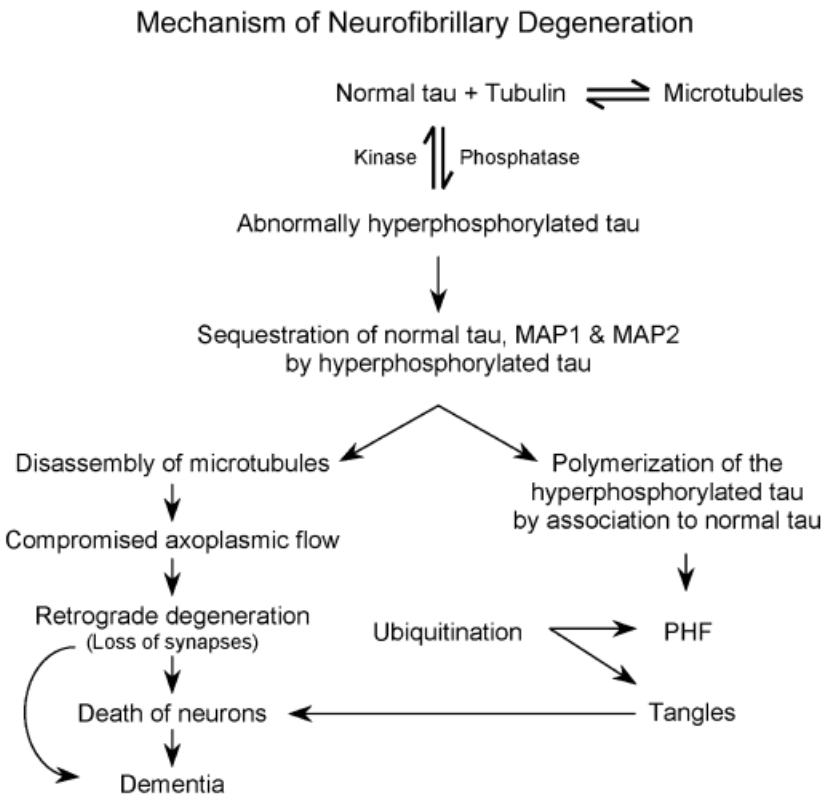

Figure 22: Processus pathologique induit par la protéine tau hyperphosphorylée. L'équilibre entre les activités kinases et phosphatases est essentiel dans l'initiation de la cascade pathologique (Iqbal, Alonso Adel et al. 2005).

Tau possède potentiellement 85 sites phosphorylables sur des sérines/thréonines (en majorité) ou des tyrosines (Buee, Bussiere et al. 2000). De nombreuses kinases ont été montrées comme étant responsable de ces phosphorylations ; les plus courantes étant **CDK5, GSK3β et DYRK1A** (cette dernière étant tyrosine-spécifique). A l'opposé, **PP2A** est sa phosphatase principale. Jusqu'à 40% du réservoir total de tau est hyperphosphorylé dans le cerveau des patients de la MA (Iqbal, Liu et al. 2016). La communauté scientifique a longtemps pensé que la DNF était responsables de la toxicité de tau. Cependant, et comme pour le couple Aβ/plaques, il est de plus en plus admis que les **formes oligomériques** solubles seraient les plus nocives (Gendreau and Hall 2013, Fa, Puzzo et al. 2016). Enfin, il est à noter que l'hyperphosphorylation de la protéine est aussi retrouvée dans d'autres pathologies regroupées sous le terme de «**tauopathies** ». Parmi celle-ci, on peut citer la démence frontro-temporale qui peut-être une tauopathie pure en faisant ainsi un « modèle d'étude » de choix de la cascade pathologique induite par la protéine tau (Iqbal, Alonso Adel et al. 2005). Afin d'étudier celle-ci, des modèles rongeurs transgéniques pour tau ont été générés. Nous avons par exemple utilisé au laboratoire la souris thy-tau22 développée par Luc Buée (Schindowski, Bretteville et al. 2006, Burlot, Braudeau et al. 2015). Il faut cependant noter qu'une grande partie des modèles transgéniques pour la MA sont basés sur des gènes impliqués dans

l'amyloïdose. Je terminerai ce paragraphe en rappelant que l'APP et tau collaborent synergiquement afin d'induire la MA (Bloom 2014). De nombreuses études sont venues corroborer cette théorie et donc la véracité de cette partie de la cascade amyloïde. On peut par exemple citer le fait qu'une forme mutée d'APP va accélérer la formation de tangles (Lewis, Dickson et al. 2001).

d. Les souris transgéniques pour l'APP muté

Depuis l'émission de l'hypothèse de cascade amyloïde, l'extrême majorité des modèles de la MA générés se sont concentrés sur les mutations des formes familiales de l'APP. Ainsi, sur les 119 modèles souris de la maladie d'Alzheimer référencés sur la base de données Alzforum, **77 présentent comme transgènes l'APP, la PS1 et/ou la PS2**. La plupart des souris modèles générées l'ont été par transgénèse, c'est-à-dire avec insertion dans le génome d'une ou plusieurs copies d'un ou plusieurs transgènes. Ces modèles sont ainsi fréquemment **remis en question** par la communauté scientifique et ce, à juste titre. En effet, comme indiqué précédemment, les formes familiales ne représente qu'une très faible minorité des cas de la MA ; l'évaluation préclinique se fait donc sur des formes familiales de la MA et les essais cliniques en majorité sur des formes sporadiques ce qui relève de l'incohérence. De plus, ces modèles familiaux caricaturent les formes génétiques de la MA, puisque très peu de patients (7% des familles génétiquement touchés par la MA en France) présentent une augmentation de l'expression (par duplication par exemple) d'APP (Rovelet-Lecrux, Hannequin et al. 2006). Celle-ci aboutit à une évolution extrêmement rapide de la pathologie chez le rongeur, puisque la majorité de ceux-ci développent des symptômes dans le premier tiers de leur vie. Il est donc important d'être vigilant quant aux interprétations des études sur ces modèles.

Malgré cela la variété des modèles générés au cours des 25 dernières années reste impressionnante si bien qu'aucune revue ne peut être exhaustive à ce sujet. Allant de modèles cellulaires aux souris transgéniques en passant par la drosophile et les modèles rats par injection d'Aβ, une certaine diversité est présente (Urani, Romieu et al. 2004). Notre équipe a aussi récemment créé un nouveau modèle souris de la MA grâce au transfert de gènes de l'APP muté et de la PS1 (Audrain, Fol et al. 2016). Un modèle rat, suivant la même méthodologie) est aussi en cours de préparation (Audrain, Souchet et al. en préparation).

Ce paragraphe est aussi l'occasion de présenter le modèle d'étude sur lequel j'ai effectué la majorité des études lors de ma thèse : **la souris APP/PS1ΔE9**, un modèle d'étude de la MA très courant. Cette souris fut développée par l'équipe de David Borchelt, déjà auteur de la première souris transgénique APP/PS1 à la fin des 1990 (Borchelt, Thinakaran et al. 1996, Borchelt, Ratovitski et al. 1997). La souris APP/PS1ΔE9 fut

quant à elle développée quelques années plus tard en collaboration avec l'équipe de Steven Younkin (Jankowsky, Slunt et al. 2001, Jankowsky, Fadale et al. 2004). Comme son nom complet l'indique (APPsw/PSEN1ΔE9), ce modèle repose sur la transgénèse de l'APP présentant la **double mutation Swedish** (KM670/671NL) et la **PS1 sans son exon 9** dans un fond mixte C57Bl/6-C3H. L'APPswe humanisée (afin de coder la séquence Aβ humaine) est sous sa forme neuronale 695 acides aminés et est, comme la PS1ΔE9, exprimé grâce au promoteur prion murin MoPrP.

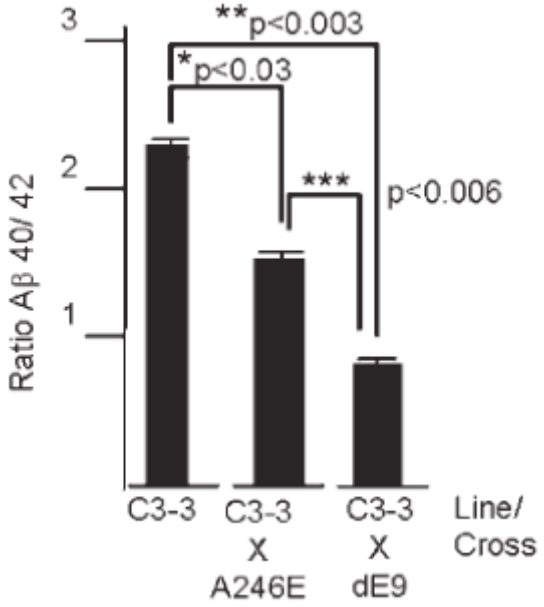

Figure 23: Comparaison du ratio Aβ40/Aβ42 des souris APP/PS1ΔE9 comparés à deux autres souris transgéniques. Les souris C3-3 présentent seulement un APP muté Swedish alors que les souris C3-3 x A246E ont en plus une PS1 muté (A246E). (Jankowsky, Fadale et al. 2004)

Dans cette souris, les niveaux d'Aβ augmentent de manière croissante avec l'âge et les premières plaques sont observables à partir de 6 mois. De manière intéressante, la publication princeps nous indique un **ratio Aβ40/Aβ42** inférieure à un suggérant ainsi une production forte de peptides Aβ42 toxiques (Figure 23). Il est aussi à noter que les femelles présentent une pathologie amyloïde plus forte que les mâles (Janus, Flores et al. 2015). Les premières **altérations synaptiques** furent observées très tôt, dès 3 mois, mettant en évidence une pathologie agressive (Volianskis, Kostner et al. 2010). Bien que des défauts de mémoire contextuelle peuvent être observés dans les 6 premiers mois (Kilgore, Miller et al. 2010), les altérations de la **mémoire spatiale** sont généralement observées après 13 mois (Volianskis, Kostner et al. 2010, Fol, Braudeau et al. 2016) (Figure 24). Il est cependant important de rappeler que ces défauts sont hautement

dépendants des conditions et des expérimentateurs et qu'ainsi, les variations inter-études sont inévitables.

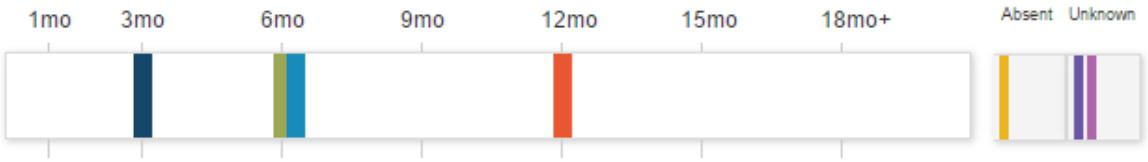

Plaques	Occasional Aβ deposits can be found by 6 months with abundant plaques in the hippocampus and cortex by 9 months (Jankowsky et al., 2004) and a progressive increase in plaques up to 12 months (Garcia-Alloza et al., 2006).
Tangles	Absent.
Neuronal Loss	Unknown.
Gliosis	Minimal astrocytosis at 3 months; significant astrocytosis by 6 months, especially in areas around plaques. Extensive GFAP+ staining at 15 months and later throughout the cortex (Kamphuis et al., 2012).
Synaptic Loss	Unknown.
Changes in LTP/LTD	Transient long term potentiation (t-LTP) is reduced by 3 months. The degree of impairment is not related to age from 3 to 12 months (Volianskis et al., 2008).
Cognitive Impairment	Impairment in the Morris water maze at 12 months, specifically during acquisition of the hidden platform sub-task and the probe trial but not in the visible platform test (Lalonde et al., 2005). At 13 months the mice commit more errors in the Morris water maze, but not at 7 months (Volianskis et al., 2008).

Figure 24: Caractéristiques physiopathologiques de la souris APP/PS1ΔE9. Les défauts électrophysiologiques (notamment en termes de LTP) apparaissent dès 3 mois, avant l'apparition des plaques et de la réactivité gliale à 6 mois. Les premiers défauts cognitifs apparaissent bien plus tard, à au moins 12 mois. Ni la pathologie tau, ni la perte neuronale a pu être mise en évidence dans cette souris. Source : Alzforum

e. Nouvelles données et remise en cause de la cascade amyloïde

Peu de questions dans le domaine biomédical ont généré ces quarante dernières années autant d'attrait pour les scientifiques mais aussi de controverses que la MA. La théorie de la cascade amyloïde a finalement émergé relativement rapidement après le vrai départ de la recherche dans ce domaine, au milieu des années 1980. Cette théorie, aussi élégante soit-elle, est quelque peu simpliste mais fut ainsi adoptée par une majorité de la

communauté scientifique. Les arguments de poids allant en sa faveur sont notamment la présence de plaques dans le cerveau des patients, les mutations du métabolisme amyloïdogène dans les formes familiales, les défauts de la mémoire des souris surexprimant l'APP et l'allèle APOE4 qui trouble la clairance de l'Aβ et influence le risque de développer la MA (Hardy and Selkoe 2002, Selkoe and Hardy 2016).

Ainsi, la majorité des essais cliniques des vingt dernières années ont été basés sur cette hypothèse. Le moins que l'on puisse dire est que ces derniers furent quelque peu décevants puisqu'aucune nouvelle thérapeutique fut mise sur le marché. Rappelons ainsi que les quatre molécules actuellement disponibles (voir IV.A.6) sont génériqués suggérant que la mise au point de nouveaux traitement stagne depuis 25 ans. Les essais cliniques les plus ancrés dans la cascade amyloïde reste ceux concernant l'immunisation (passive ou active) anti-Aβ ou l'inhibition de BACE. Bien que certains résultats semblent encourageants, on aurait tort de se réjouir trop vite. Un engouement fabuleux est né en mars 2015 lors de l'AD/PD pour la société Biogen et sa stratégie d'immunisation active avec l'Aducanumab. Cependant, celui-ci est retombé dès la fin de l'année, lorsque la société a revu à la baisse ses critères d'évaluation cognitive des patients. Enfin, pour terminer sur ces stratégies anti-Aβ, il est important de ne pas parler d'échec mais bien de succès. En effet, ces thérapeutiques furent mises au point afin de diminuer la charge amyloïde, ce qu'ils ont parfaitement réussi à faire. Cependant, force est de constater qu'en retour, l'impact cognitif est faible (Qian, Hamad et al. 2015, Underwood 2015).

Depuis sa conceptualisation, de nombreuses voix s'élèvent contre la théorie de la cascade amyloïde, jugée trop linéaire. Karl Herrup est l'auteur d'une très belle revue en 2015 (Herrup 2015). L'argument premier en faveur de la cascade est la présence de mutations des présénilines et de l'APP dans les formes précoces de la MA. Herrup note de manière intéressante dans sa revue que ces mutations impliquent donc l'APP et son métabolisme dans la MA mais **en aucun cas impliquent l'Aβ dans le processus pathologique**. Un de ses arguments est notamment de mettre en avant le fait qu'aucune mutation de BACE ou d'ADAM n'a été découverte comme influençant, de manière positive ou négative, le développement de formes familiales de la MA. Ce postulat est cependant à mitiger puisque deux SNPs furent récemment liés au développement d'une forme héréditaire de la MA (Suh, Choi et al. 2013). D'autres études récentes vont ainsi dans ce sens comme la découverte d'une nouvelle voie de métabolisme de l'APP, potentiellement pathologique, impliquant une η-secrétase et un nouveau fragment Aη (Willem, Tahirovic et al. 2015).

Nous l'avons discuté précédemment, l'Aβ présente des propriétés toxiques certaines. Mais n'a-t-il pas été trop mis en avant dans le processus pathologique de la MA ? Puisque le métabolisme de l'APP peut peut-être plus justement briguer la position de l'Aβ, qu'en est-il des autres métabolites issus de son clivage ? Nous verrons ainsi dans la prochaine partie le degré d'implication et le potentiel thérapeutique dans la MA des formes solubles de l'APP issues des voies non-amyloïdogènes et amyloïdogènes.

C. Les formes solubles de l'APP comme cibles thérapeutiques

1. Le rôle de la voie non-amyloïdogène dans la MA

De plus en plus de données générées ces dernières années permettent d'envisager une **perte d'efficacité du métabolisme non-amyloïdogène** comme contributive à la MA. Que l'on rejette ou accepte l'hypothèse de la cascade amyloïde, l'implication de la voie amyloïdogène dans la pathologie est indiscutable. Partant de ce constat, deux types de stratégies thérapeutiques peuvent être envisagés. Soit s'attaquer directement à cette voie amyloïdogène et ses métabolites, comme le font une majorité d'essais cliniques actuels. On peut naturellement citer les inhibiteurs de la β-secrétase ou l'immunisation anti-Aβ (voir IV.A.6). La seconde option serait de **restaurer la balance voie amyloïdogène / voie non-amyloïdogène**, clairement en défaveur de cette dernière dans la MA. Il va ainsi de soi que la génération des peptides issus de la voie non-amyloïdogène inhibent *de facto* la formation des peptides de la voie amyloïdogène et notamment l'Aβ.

ADAM10 est l'α secrétase constitutive et permet d'initier le clivage non-amyloïdogène de l'APP (Figure 18). Comme cité précédemment, chez l'homme, des mutations atténuant sa fonction furent associées avec une forme héréditaire de la MA (Suh, Choi et al. 2013). Chez la souris, son invalidation génétique est létale au stade embryonnaire, principalement dû au fait qu'ADAM10 a comme autre substrat que l'APP Notch, crucial durant le processus développemental (Hartmann, de Strooper et al. 2002). L'invalidation conditionnelle d'ADAM10 à l'âge adulte a permis de mettre en avant ses fonctions essentielles dans l'apprentissage, la mémoire, la plasticité et l'efficacité synaptique (Prox, Bernreuther et al. 2013). Il est cependant important de noter que ces caractéristiques ne sont pas entièrement dépendantes de son interaction avec l'APP puisqu'ADAM10 a aussi comme substrats de nombreuses molécules d'adhésions synaptiques comme Neuroligin-1 ou N-Cadherin (Reiss, Maretzky et al. 2006, Suzuki, Hayashi et al. 2012). D'autres souris transgéniques furent générées afin de muter spécifiquement le site de clivage α de l'APP. Celles-ci présentent une sensibilité accrue à l'excitotoxicité et des troubles comportementaux, ce qui renforce le rôle physiologique de la voie de clivage non-amyloïdogène (Moechars, Lorent et al. 1996, Moechars, Lorent et al. 1998).

A l'opposé, des **souris surexprimant ADAM10** ont aussi été générées et croisées avec des souris transgéniques APP mutées (Postina, Schroeder et al. 2004). Les auteurs notent tout d'abord une augmentation substantielle de l'APPsα ainsi que la prévention de formation de plaques amyloïdes. De manière intéressante, la réorientation du métabolisme de l'APP dans les souris transgéniques s'accompagne d'une **restauration comportementale** et de la plasticité synaptique. Cette étude a permis d'établir une base

pour la surexpression de la voie non-amyloïdogène afin de contrer l'évolution de la MA. Cependant, une étude plus récente du même groupe compare l'expression, grâce à des puces à ARN, des souris transgéniques ADAM10 aux souris sauvages (Prinzen, Trumbach et al. 2009). Les auteurs trouvent ainsi 355 gènes différemment régulés par la surexpression d'ADAM10. Cette étude confirme que cette **surexpression n'est pas anodine** et potentiellement délétère. De plus, la surexpression d'ADAM10 a aussi été impliquée dans les mécanismes de tumorigénèse (Prox, Rittger et al. 2012).

Si nous considérons que l'effet thérapeutique d'ADAM10 passe par l'élévation du niveau d'APPsα, il pourrait-être intéressant d'envisager sa surexpression thérapeutique afin d'éviter les écueils potentiellement délétères de celle d'ADAM10.

2. L'APPsα : une cible prometteuse

a. Rôles physiologiques

Comme indiqué précédemment, l'une des fonctions physiologiques essentielles de l'APP est notamment son **rôle trophique** et sa capacité à promouvoir croissance neuritique et synaptogénèse. Ainsi, l'accumulation des nombreuses données au cours des vingt dernières années indiquent que la majorité de ces propriétés seraient dû au peptide APPsα issu du clivage de l'APP par l'α secrétase. Les premiers indices pointaient le rôle du motif « RERMS » du domaine E2 de l'APP, capable d'induire la prolifération de fibroblastes *in vitro* (Saitoh, Sundsmo et al. 1989). De plus, l'infusion du peptide RERMS permet d'augmenter la densité synaptique chez le rongeur (Roch, Masliah et al. 1994). Ce domaine est contenu dans les deux formes solubles de l'APP mais la majorité des études suivantes se sont concentrées sur l'APPsα afin d'approfondir la compréhension de ses rôles et mécanismes d'action.

L'APPsα issu de la forme neuronale de l'APP (695 acides aminés) contient ses 612 acides aminés situés dans la **partie N-terminale**. Il contient donc les domaines E1 et E2 (avec le motif RERMS) de l'APP. La détermination de la structure 3D de l'APPsα a permis de mettre en évidence des ponts disulfures, essentiels à sa fonction (Young-pearse 2007). L'APPsα peut aussi former des dimères grâce à sa liaison avec l'héparine. Cette propriété est possible grâce aux domaines E1 et E2 et participerait à ses propriétés de croissance neuritique (Small, Nurcombe et al. 1994, Gralle, Oliveira et al. 2006). L'APPsα possède les deux sites de liaisons aux métaux (cuivre et zinc) de l'APP suggérant qu'il pourrait être physiologiquement **un transporteur neuronal de métaux**.

Ainsi, il est intéressant de noter qu'une augmentation de cuivre ingéré par des souris modélisant la pathologie amyloïde (souris APP23) induit une diminution de la charge en Aβ (Bayer, Schafer et al. 2003).

Les **propriétés neurotrophiques** de l'APPsα furent mises en évidence dès les années 1990. Différents fragments furent tour à tour impliqués dans les phénomènes de croissance neuritique. Tout d'abord, comme cités précédemment, les domaines de liaison à l'héparine, capables notamment de lier des protéoglycanes de la matrice extracellulaire et induire la neuritogénèse (Clarris, Nurcombe et al. 1994, Small, Nurcombe et al. 1994, Clarris, Cappai et al. 1997). Le seul domaine RERMS fut lui aussi démontré comme ayant de telles propriétés (Jin, Ninomiya et al. 1994, Roch, Masliah et al. 1994). Toutes ces études pointent vers un rôle proéminant du peptide soluble physiologiquement généré par l'APP. Les fonctions trophiques de l'APPsα furent d'autant plus confirmées par une étude menée par Meziane et collaborateurs en 1998. L'injection intra-cerebroventriculaire de l'APPsα dérivé des formes 695 et 751 acides aminés de l'APP induit une amélioration mnésique des souris. De plus, l'injection permit aussi de restaurer les troubles de mémoire induits par la scopolamine (Meziane, Dodart et al. 1998). En plus de ses effets sur la croissance neuritique, l'APPsα permet aussi d'induire la **neurogénèse** *in vivo*, à l'âge adulte, dans la zone sous-ventriculaire. Ces deux propriétés sont médiées par le facteur de croissance épidermique (EGF) et la voie de signalisation MAP/ERK (Caille, Allinquant et al. 2004, Chasseigneaux, Dinc et al. 2011).

De manière physiologique, l'APPsα semble aussi être une protéine essentielle pour la **synapse**. L'injection d'un petit peptide issu de l'APPsα dans des rats sauvages permet d'améliorer substantiellement leur capacité de mémorisation mais aussi d'augmenter de 20% la densité présynaptique (Roch, Masliah et al. 1994). Plus récemment, la déplétion ou l'infusion de l'APPsα dans l'hippocampe de rats conduit à la modulation de la **LTP** via notamment les récepteurs NMDA (Ishida, Furukawa et al. 1997, Taylor, Ireland et al. 2008). L'un des mécanismes évoqué par ces mêmes auteurs est la capacité de l'APPsα à induire la synthèse de protéines au niveau de la synapse (Claasen, Guevremont et al. 2009).

L'étude des **modèles animaux** fut aussi importante dans la compréhension des rôles physiologiques de l'APPsα. Ainsi, le groupe d'Ulrike Müller publia deux souris **APPsα-KI** dans des fonds APP-KO (Ring, Weyer et al. 2007) et APP/APLP2 doubles KO (Weyer, Klevanski et al. 2011). De manière intéressante, le premier knock-in permet une **restauration complète du phénotype des souris APP-KO** à savoir le déficit de poids, la mémoire spatiale et la LTP. Comparées aux souris APP/APLP2-KO, les souris APPsα-KI dans ce même fond, sont viables mais présentent une faiblesse musculaire due à une détérioration de la transmission neuromusculaire. Au niveau cérébral, l'apprentissage et la mémoire hippocampe-dépendante ainsi que la LTP sont toutes deux

impactées. Il est ainsi important de noter que **le seul APPsα ne peut restaurer le double KO de l'APP et d'APLP2**. Par ailleurs, nous avons récemment publié un article suggérant que le domaine C-terminal de l'APP est essentiel à la **fonction neuromusculaire** (Klevanski, Herrmann et al. 2015).

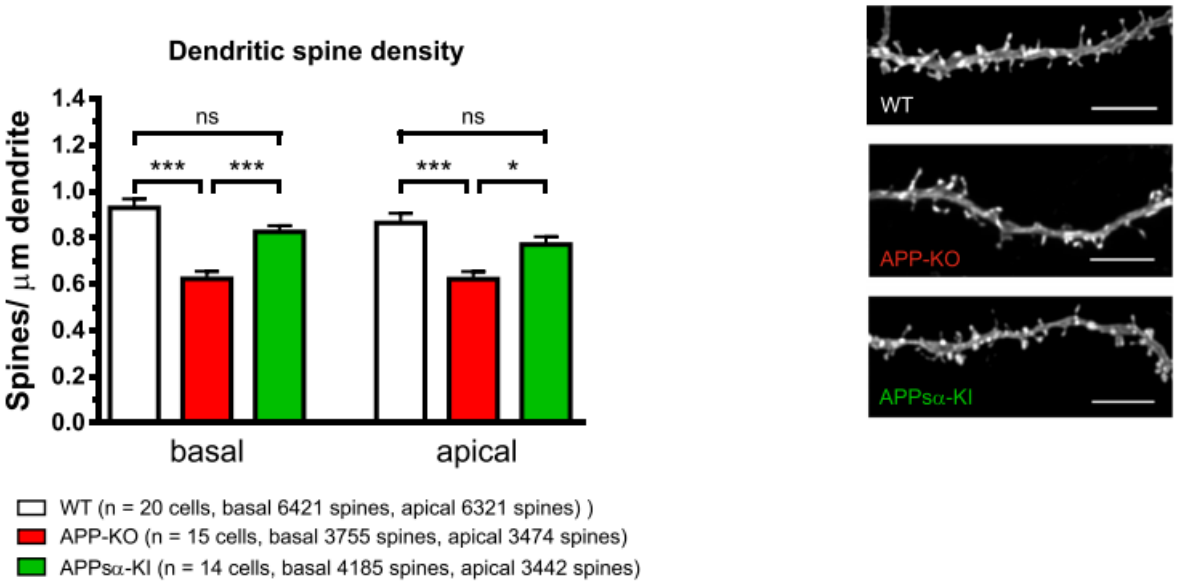

Figure 25: Le Knock-In de l'APPsα dans une souris APP-KO restaure le nombre d'épines dendritiques. Cette restauration est mise ici en évidence dans la région CA1 de l'hippocampe, au niveau basal et apical (Weyer, Zagrebelsky et al. 2014).

Quelques études se sont attachées à démontrer le rôle de l'APPsα dans les **mécanismes immunitaires**. Ainsi les plaquettes, les lymphocytes CD4 et CD8 sont capables de secréter l'APPsα (Van Nostrand, Schmaier et al. 1991, Monning, Konig et al. 1992). Il est important de noter que l'isoforme présent dans les leucocytes est spécifique de ceux-ci dû à un épissage alternatif de l'exon 15. Cet isoforme, est aussi présent et relargué de la part des astrocytes et de la microglie, cellule immunitaire du système nerveux central. De manière intéressante, dans le cerveau, une étude démontra la capacité de l'APPsα à **stimuler la microglie** (Barger and Harmon 1997). Cependant, cette activation microgliale semble délétère puisqu'induisant la sécrétion de neurotoxines. Parmi toutes les études citées précédemment, cette dernière reste la seule évoquant un rôle potentiellement délétère de l'APPsα.

b. Mécanisme d'action de l'APPsα

Malgré les données accumulées sur les rôles neurotrophiques et synaptotrophiques de l'APPsα et sur son bénéfice mnésique, peu d'études ont réellement pu mettre le doigt

sur un mécanisme d'action. Comme cité précédemment, **la voie MAP/ERK** a été impliquée dans la régulation de l'APPsα dans de nombreuses études (Greenberg and Kosik 1995, Gakhar-Koppole, Hundeshagen et al. 2008). Le groupe de Bernadette Allinquant mis en évidence qu'Egr1, régulé par cette même voie MAP/ERK, est essentiel à l'induction de la croissance neuritique par l'APPsα (Chasseigneaux, Dinc et al. 2011). L'activation de la voie de signalisation c-Jun N-terminal kinase (JNK) notamment impliquée dans la neurodégénération, est quant à elle contrecarrée par la sécrétion d'APPsα (Copanaki, Chang et al. 2010). De façon intéressante, **l'inhibition de cette seule voie JNK** permet de mimer les effets bénéfiques de l'APPsα suggérant qu'une grande partie de ses effets puissent passer par l'inhibition de cette voie (Eckert, Chang et al. 2011). Enfin, d'autres voies de signalisation comme Phosphatidylinositol-3-kinase-Akt kinase (PI3K/Akt) ou NF-κB ont aussi été ponctuellement mises en évidence (Cheng, Yu et al. 2002). Il est cependant important de noter que pour le moment, **aucun récepteur de l'APPsα n'a pu être mis en évidence**. Ainsi, son hétérodimérisation avec l'APP ou ses homologues apparait comme un mécanisme crédible pour sa signalisation intracellulaire (Kogel, Deller et al. 2012).

Il y a déjà 20 ans, il fut montré que l'APPsα active les récepteurs au potassium afin de limiter la surcharge de calcium excitotoxique dans les neurones (Furukawa, Barger et al. 1996). De manière intéressante, la sécrétion de l'APPsα est activité-dépendante et peut être augmentée via stimulation électrique et activation de récepteurs comme les récepteurs au glutamate ou à l'acétylcholine (Nitsch, Farber et al. 1993). Ces données indiquent que l'expression de l'APPsα pourrait être augmentée dans le cadre d'une d'**excitotoxicité**. Ainsi, ce mécanisme suggère une boucle d'autorégulation de la sécrétion de l'APPsα qui pourrait **protéger les neurones dans des conditions délétères**.

Les données accumulées au cours des trois dernières décennies permettent donc d'envisager un bénéfice thérapeutique de l'APPsα, notamment dans le cadre de la MA.

c. Potentiel thérapeutique de l'APPsα

L'APPsα présente des propriétés neuroprotectrices contre un nombre important de stress cellulaires et d'agressions macroscopiques. *In vitro*, des études montrèrent les **fonctions neuroprotectrices** de l'APPsα contre une privation de glucose, l'excitotoxicité du glutamate ou le stress oxydatif (Mattson, Cheng et al. 1993, Goodman and Mattson 1994, Murakami, Yamaki et al. 1998, Van den Heuvel, Blumbergs et al. 1999, Ramirez, Heslop et al. 2001, Leyssen, Ayaz et al. 2005). L'addition d'APPsα en culture permet

de contrecarrer la **dégénérescence neuronale** due à une inactivation du protéasome ou due à une irradiation aux U.V (Copanaki, Chang et al. 2010). *In vivo*, l'APPsα permet de protéger les neurones hippocampiques de rats contre les dégâts consécutifs à une ischémie cérébrale (Smith-Swintosky, Pettigrew et al. 1994). De manière plus récente, l'APPsα fut démontré comme protecteur contre les dégâts dus à un traumatisme crânien chez des souris APP-KO (Thornton, Vink et al. 2006, Corrigan, Vink et al. 2012).

La perte des capacités cognitives dans la MA, en particulier durant les phases précoces, est fondamentalement causée par un affaiblissement de la transmission synaptique, qui est suivie par une dégénérescence neuronale et la mort des neurones à des stades ultérieurs de la maladie. De manière classique et courante, la pathologie est principalement attribuée à l'accumulation de l'Aβ oligomérique (voir partie IV.B.6). Mais plus récemment, des preuves que **la perte de la fonction physiologique d'APPsα contribue considérablement à la pathogenèse** se sont accumulées. Tout d'abord, et de manière importante, les niveaux d'APPsα, d'ADAM10 et de son activité sont **diminués dans le liquide céphalo-rachidien** (LCR) des patients atteints de la MA. A l'inverse BACE et son activité sont augmentés dans la MA, faisant ainsi pencher la balance du clivage de l'APP du côté amyloïdogène. La diminution des niveaux d'APPsα dans le LCR sont corrélés avec des performances mnésiques amoindries chez les patients humains mais aussi chez le rat âgé (Palmert, Usiak et al. 1990, Lannfelt, Basun et al. 1995, Almkvist, Basun et al. 1997, Anderson, Holtz et al. 1999, Fahrenholz 2007, Endres and Fahrenholz 2012, Dobrowolska, Kasten et al. 2014).

Plusieurs études semblent indiquer que l'APPsα agit sur les deux composantes clés de la MA : **l'Aβ et tau**. Dans une étude de 2012, les auteurs montrent les effets de la surexpression d'APPsα sur la voie de clivage amyloïdogène de l'APP (Obregon, Hou et al. 2012). *In vitro* tout d'abord, des doses croissantes du peptide diminuent considérablement la génération d'Aβ. Celle-ci serait due à une interaction directe avec BACE1. De manière encore plus frappante, les auteurs montrent une diminution de la pathologie amyloïde chez des **souris transgéniques APP/PS1ΔE9 croisées avec des souris transgéniques surexprimant APPsα** (Figure 26). Très récemment, le même groupe analysa la phosphorylation de tau chez ces mêmes souris mais aussi dans des lignées cellulaires (Deng, Habib et al. 2015). Dans cette seconde condition, les auteurs démontrent qu'une dose croissante d'APPsα induit une phosphorylation inhibitrice de GSK3β, l'une des principales kinases de tau. Ceci conduit à une **diminution de la phosphorylation de tau** dans un modèle cellulaire surexprimant celle-ci mais aussi dans les souris APP/PS1ΔE9/APPsα. D'autres groupes avaient par ailleurs pu mettre en évidence le lien entre l'APPsα et les deux kinases principales de tau, GSK3β et CDK5 (Han, Dou et al. 2005, Jimenez, Torres et al. 2011). Ainsi, ces récentes études confirment et appuient le **potentiel thérapeutique de l'APPsα dans le cadre de la MA**.

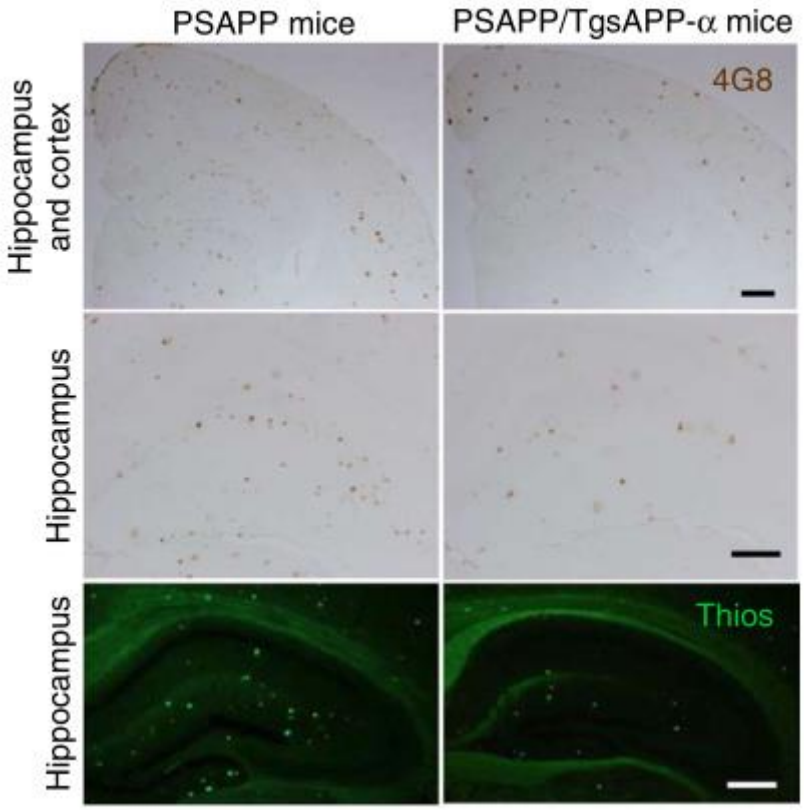

Figure 26: Le transgène APPsα inséré dans le génome de souris APP/PS1ΔE9 (PSAPP) permet de diminuer la charge amyloïde dans le cortex et l'hippocampe. L'anticorps 4G8 et la thioflavine S furent utilisées afin de marquer les plaques amyloïdes (Obregon, Hou et al. 2012).

Indépendamment du fait que la perte de fonction de l'APPsα soit une composante du processus pathologique de la MA, ses fonctions physiologiques bien établies dans la synaptogenèse, la plasticité synaptique, la croissance neuritique et la neuroprotection suggèrent que la surexpression ou la restauration de niveaux physiologiques d'APPsα serait bénéfique afin de contrecarrer la progression de la MA. La perte des épines dendritiques, les déficits de la plasticité synaptique et de la cognition sont des caractéristiques altérées dans la pathologie. Ainsi les effets de l'APPsα seraient particulièrement prometteurs dans le cadre de la MA.

3. Côté amyloïdogène; l'APPsβ

Contrairement à l'APPsα, beaucoup moins de données ont été générées concernant son pendant dans la voie amyloïdogène, l'APPsβ. Ceci est très probablement dû au fait que les premières études sur celui-ci n'aient pu mettre en évidence des propriétés trophiques similaires à l'APPsα. De plus, une augmentation de la concentration en APPsβ indique mécaniquement une accentuation du clivage amyloïdogène de l'APP et donc, une accumulation d'Aβ toxique. Structurellement, les deux formes solubles de l'APP diffèrent de seulement **16 acides aminés**. Ceux-ci, sont absents sur le APPsβ et représente la **partie N-terminale de l'Aβ (**Figure 27).

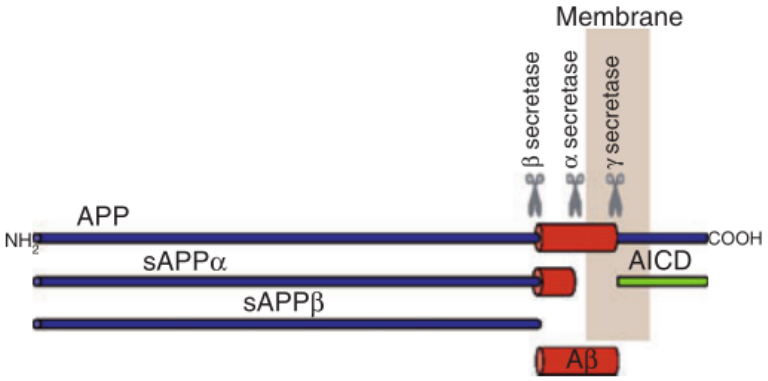

Figure 27: Similitudes et différences entre l'APP, l'APPsα et l'APPsβ. La différence entre les deux derniers se résument aux 16 acides aminés C-terminaux présents sur l'APPsα (Chasseigneaux and Allinquant 2012).

Une étude de 1996 comparant les deux peptides solubles dérivés de l'APP, suggère que les propriétés neuroprotectrices de l'APPsβ seraient extrêmement limitées (Furukawa, Sopher et al. 1996). En cultures, les neurones confrontés à une excitotoxicité, une privation de glucose ou face à l'Aβ, sont approximativement **100 fois moins protégés par l'APPsβ** par rapport à l'APPsα. Ainsi, dans la plupart des études postérieures, APPsβ est utilisé comme « contrôle négatif » par rapport à l'évaluation des propriétés trophiques de l'APPsα. De plus, l'APPsβ n'est pas capable de protéger les neurones de l'apoptose induite par le stress du protéasome (Copanaki, Chang et al. 2010). L'expression d'APPsβ ne permet pas non plus de corriger les défauts de LTP induits par l'inhibition de l'α secrétase ou dans des souris KO-conditionnelles pour APLP2 et APP (Weyer, Klevanski et al. 2011) (Figure 28). Des **souris APPsβ-KI** dans un fond double KO APP/APLP2 furent aussi générées (Li, Wang et al. 2010). A l'inverse de l'APPsα, APPsβ n'est pas capable de restaurer la létalité périnatale de ces souris ni de corriger leurs défauts au niveau de la synapse neuromusculaire.

Cependant, comme pour APPsα, APPsβ semble être capable de **stimuler la microglie**, au moins *in vitro* (Barger and Harmon 1997). Et de la même manière, cette stimulation semble délétère puisqu'affectant la viabilité des neurones en co-culture. Une seconde étude plus récente suggère un rôle apoptotique de l'APPsβ (Nikolaev, McLaughlin et al. 2009). En effet, grâce à sa liaison au récepteur DR6, celui-ci induirait la mort cellulaire.

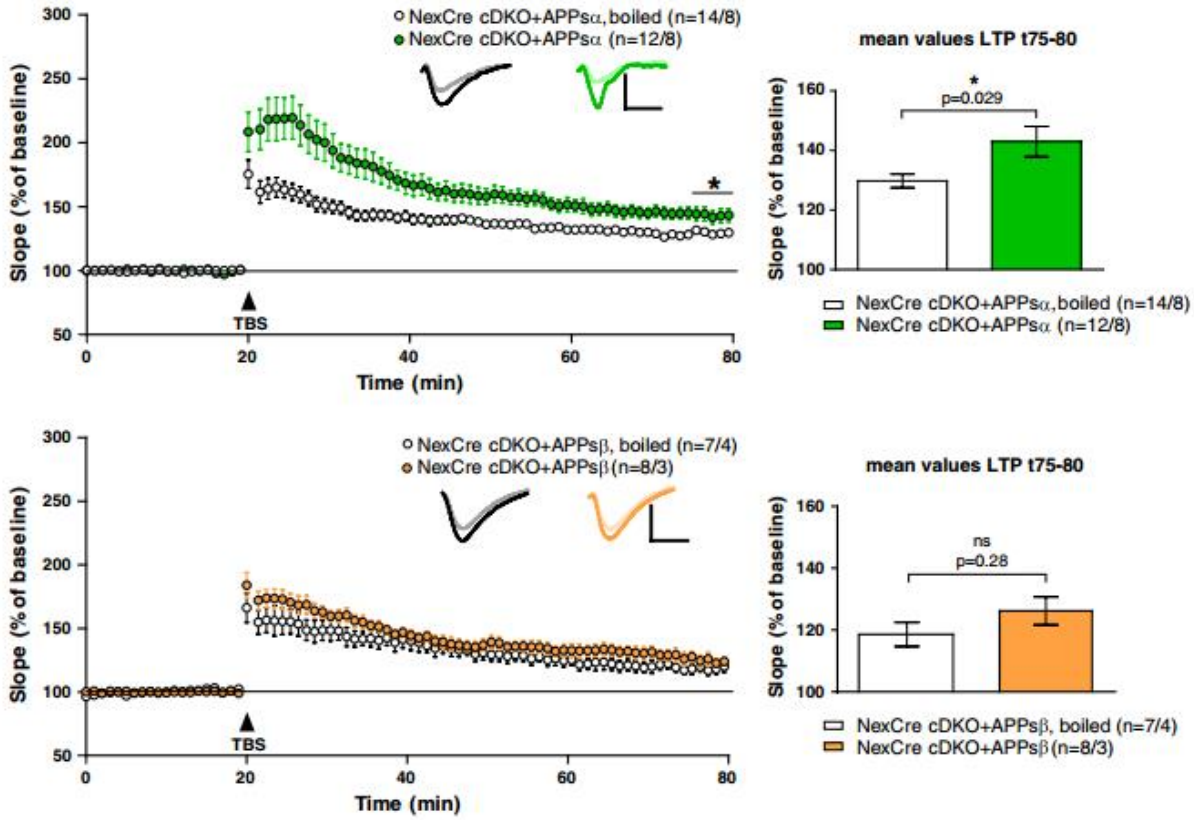

Figure 28: Contrairement à l'APPsα, l'APPsβ n'est pas capable de restaurer les défauts de LTP des souris double KO conditionnels APP/APLP2. (Weyer, Klevanski et al. 2011)

Malgré cela, une étude montra le potentiel de l'APPsβ à **favoriser la différenciation neuronale** de cellules souches embryonnaires humaines, et ce, de manière plus importante que l'APPsα (Freude, Penjwini et al. 2011). Enfin, il fut aussi montré que l'APPsβ était capable comme l'APPsα, d'**induire la croissance neuritique** en culture (Chasseigneaux, Dinc et al. 2011). Chez le patient, aucune étude n'a pu montrer un changement des niveaux d'APPsβ dans le LCR (Olsson, Hoglund et al. 2003). Aucune équipe n'a pour le moment montré un **effet putatif de l'expression d'APPsβ sur la MA** et en particulier sur les autres peptides de la voie amyloïdogène comme l'Aβ et les plaques amyloïdes.

Ce peptide est donc l'un des moins étudié parmi les produits de clivage de l'APP. L'éclaircissement de ses fonctions physiologiques ainsi que son rôle putatif dans la MA reste ainsi un enjeu important.

D. La thérapie génique

1. Le transfert de gènes

Le transfert de gènes consiste à insérer une ou plusieurs copies de gènes exogènes dans un organisme hôte. Celui-ci peut-être intégratif (l'ADN est inséré directement dans le génome hôte) ou non-intégratif, c'est-à-dire directement exprimé sous forme épisomique. Le transfert de gêne intégratif a notamment permis la génération d'**animaux transgéniques** grâce à la micro-injection dans l'ovule fécondé. La thérapie génique utilise le transfert de gènes afin de **traiter un individu malade**. Le but est soit d'introduire une copie fonctionnelle d'un allèle défectueux du génome soit de **surexprimer un gène thérapeutique**. La thérapie génique nécessite l'utilisation d'un vecteur afin d'assurer un transfert optimal de l'ADN/ARN exogène dans les cellules ou tissus hôtes. **Différents types de vecteurs** sont actuellement disponibles et utilisés en cliniques. Parmi ceux-ci, il est important de citer les lipoplexes (capsules lipidiques chargées positivement), la technique d'électroporation (utilisant une décharge électrique courte), ou les nanoparticules comme le phosphate de calcium. Cependant, les vecteurs viraux restent les plus couramment utilisés.

2. Les vecteurs viraux

Comparés aux méthodes physiques et chimiques, l'utilisation de vecteurs viraux induit le plus clair du temps une **efficacité de transfection supérieure**. C'est pourquoi ceux-ci sont utilisés par la plupart des essais cliniques réalisés à ce jour (Cavazzana-Calvo, Hacein-Bey et al. 2000, Cartier, Hacein-Bey-Abina et al. 2009, Cavazzana-Calvo, Payen et al. 2010). L'inconvénient majeur de leur utilisation est leur **immunogénicité** majoritairement prépondérante quelques semaines après leur injection. Les virus thérapeutiques sont dérivés de virus infectieux pour l'homme mais avant leur utilisation, le matériel génétique pathogène est remplacé par le gène thérapeutique. Cependant, les vecteurs intégratifs, de type lentivirus par exemple, peuvent s'insérer dans des oncogènes du génome ce qui peut entrainer des conséquences délétères (Hacein-Bey-Abina, von Kalle et al. 2003).

Ces deux conséquences potentiellement délétères (immunogénicité et mutagénèse insertionnelle) sont contournées par l'utilisation des **virus adéno-associés (AAV)** qui gardent tout de même leur forte efficacité d'infection (Gaj, Epstein et al. 2016). Les AAVs appartiennent à la famille des parovirus et sont reconnus pour leur stabilité d'expression dans les cellules post-mitotiques. La majorité des AAVs thérapeutiques

utilisés sont basés sur l'AAV2 où les modifications de capsides lui permettent de cibler la majorité des organes mammifères (Lisowski, Tay et al. 2015). Durant ma thèse, j'ai utilisé très majoritairement l'AAV2.9 (plus communément appelé **AAV9**). Celui-ci possède un tropisme important pour les **cellules cérébrales**, que ce soit les neurones ou la glie (Fol, Braudeau et al. 2016) et fut déjà utilisé en clinique pour traiter une maladie neurodégénérative rare, le syndrome de Sanfilippo (Figure 29).

Capsid use in a selection of clinical trials

Disease	AAV	Gene	Target tissue	Identifier[a]	References
Cystic fibrosis	AAV2	CFTR	Airway	*NCT00004533*	N/A
Parkinson's disease	AAV2	GAD, AADC, NRTN or GDNF	Brain	*NCT00195143*, *NCT00643890*, NCT00229736, NCT01973543, NCT00252850, NCT00400634, NCT00985517	Bartus *et al.* [34]; Lonser RR [53]
AADC deficiency	AAV2	AADC	Brain	NCT01395641, NCT01621581	Hwu *et al.* [59]
Alzheimer's disease	AAV2	NGF	Brain	*NCT00087789*	Rafii *et al.* [60]
Batten disease	AAV2	CLN2	Brain	NCT00151216	Worgall *et al.* [61]
Batten disease	AAVrh10	CLN2	Brain	NCT01414985, NCT01161576	N/A
MLD	AAVrh10	ARSA	Brain	NCT01801709	N/A
Sanfilippo type A	AAVrh10	SGSH and SUMF1	Brain	NCT01474343	N/A
Sanfilippo type B	AAV9	NAGLU	Brain	N/A (proposed trial)	Abeona[b]
Spinal muscular atrophy 1	AAV9	SMN	Cns	NCT02122952	N/A
Leber congenital amaurosis	AAV2	RPE65	Eye	NCT00643747, NCT00481546, NCT00516477, NCT00749957, NCT00999609	Boye *et al.* [33]
Leber congenital amaurosis	AAV4	RPE65	Eye	N/A	Le Meur *et al.* [62]
Aged macular degeneration	AAV2	sFLT1	Eye	NCT01024998[j], NCT01494805	N/A
Choroideremia	AAV2	REP1	Eye	NCT01461213, NCT02341807, NCT02077361, NCT02407678	MacLaren *et al.* [63]
X-linked juvenile retinoschisis	AAV8	RS1	Eye	NCT02317887	N/A
AAT deficiency	AAV2	AAT	Muscle	NCT00377416, *NCT00430768*	Flotte *et al.* [64]
AAT deficiency	AAV1	AAT	Muscle	NCT01054339	Flotte *et al.* [65]
DMD	AAV2.5	minidystrophin	Muscle	*NCT00428935*	Bowles *et al.* [66]
LGMDT2C	AAV1	αSG or γSG	Muscle	*NCT00494195*, *NCT01344798*	Mendell *et al.* [67]
familial LPL deficiency	AAV1	LPL	Muscle	NCT01109498[k], *NCT00891306*	Scott [68]
Pompe disease	AAV9	GAA	Muscle	NCT02240407, NCT00976352	Smith *et al.* [69]
Inflammatory arthritis	AAV2	TNFR:Fc	Joints	*NCT00617032*, *NCT00126724*	Heald *et al.* [70]
Heart failure	AAV1	SERCA2a	Heart	*NCT00454818*, NCT01643330, NCT02346422, NCT01966887	Greenberg [35]
Hemophilia B	AAV2	Factor IX	Liver	*NCT00076557*[l]	Manno *et al.* [71]
Hemophilia B	AAV2	Factor IX	Liver	NCT00515710	Long term functional study
Hemophilia B	AAV8	Factor IX	Liver	NCT00979238, NCT01620801	Nathwani *et al.* [28]; Nathwani *et al.* [72]
Hemophilia B	AAV5	Factor IX	Liver	NCT02396342	Miesbach *et al.* [73]
Acute intermittent porphyria	AAV5	PBGD	Liver	*NCT02082860*	UniQure[c]

Figure 29: Sélection d'AAVs utilisés en clinique. Ceux-ci sont majoritairement basés sur l'AAV2. Ainsi, un « AAV9 » correspond de manière plus juste à un « AAV2.9 » (Lisowski, Tay et al. 2015)

Il est important de noter que l'expression cellulaire n'est pas seulement due à la capside mais aussi au choix du **promoteur**. Ainsi, grâce au même AAV9, nous avons pu exprimer deux protéines thérapeutiques dans deux types cellulaires distincts ; APPsα/β dans les neurones grâce au promoteur de la synapsine (Fol, Braudeau et al. 2016) et APOE2 dans les astrocytes grâce au promoteur GFA2, dérivé du promoteur de la GFAP (Fol, Audrain et al. en préparation) (Figure 30). Cependant, un désavantage majeur de

l'utilisation des AAVs est leur **faible capacité de stockage**. Dans leur forme modifiée, il est possible d'insérer jusqu'à 6kb d'ADN simple brin et 3kb d'ADN double brin. Seules les séquences terminales inversées (ITRs) sont conservées. Celles-ci font l'identité de l'AAV et ce sont donc les **ITRs de l'AAV2** qui sont le plus couramment utilisées. Après modifications, l'AAV va aussi perdre sa capacité réplicative ce qui est essentiel pour la sûreté clinique.

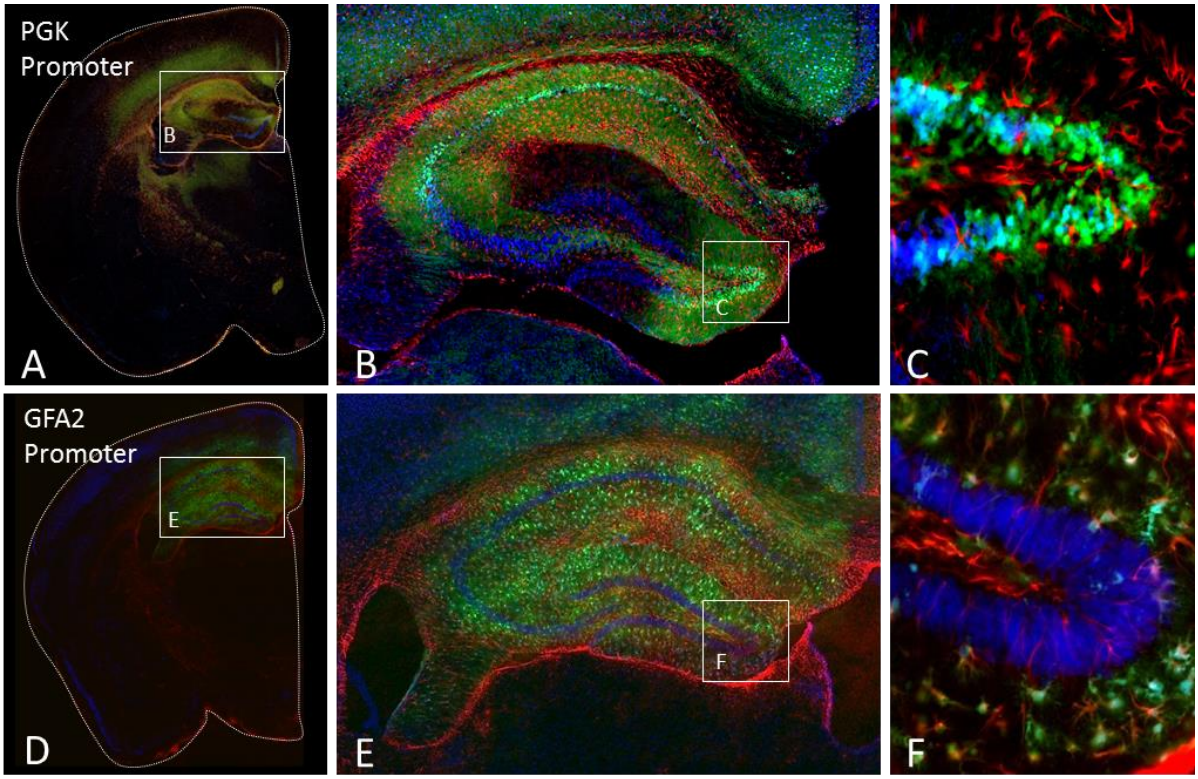

Figure 30: Expression de la GFP dans l'hippocampe de souris injectées avec un AAV9. Le promoteur PGK (phosphoglycérate kinase) permet une expression neuronale alors que le promoteur GFA2 permet de cibler les astrocytes (Fol, Audrain et al. en préparation).

3. L'injection stéréotaxique

Afin de modéliser les pathologies du SNC ou de démontrer la faisabilité d'une thérapie génique *in vivo*, la technique d'injection stéréotaxique intracérébrale reste la plus utilisée. Grâce à un **cadre stéréotaxique** (Figure 31), aussi utilisé en neurochirurgie humaine, cette technique permet de cibler très efficacement la structure cérébrale d'intérêt. A MIRCen, les différentes équipes ont déjà ciblé différentiellement ou conjointement, l'hippocampe, le cortex, le striatum ou les bulbes olfactifs. Le transgène est ainsi exprimé très majoritairement dans la zone ciblée et peut même **diffuser dans le cadre d'une protéine sécrétée** (APPsα/β, APOE).

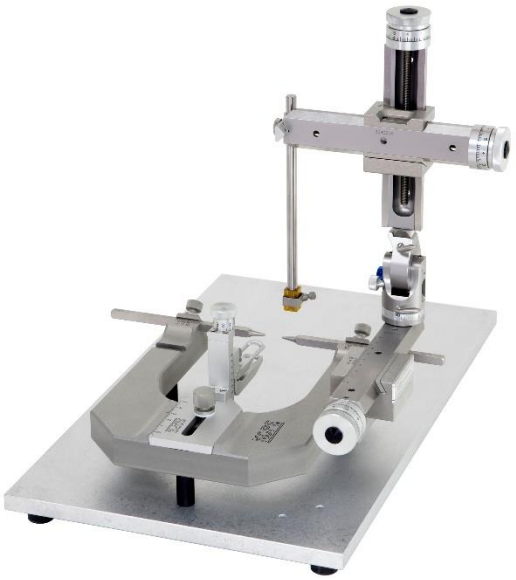

Figure 31: Un cadre stéréotaxique pour rongeurs. Source : Phymep

Il est aussi intéressant de noter que l'injection de vecteurs viraux peut se faire en périphérique. Au laboratoire, le Dr B. Gautier a développé une technique d'injection **intratéchale** afin de cibler à distance le cerveau. Le Dr. S. Alves a quant à lui injecté un AAV contenant IL-2 en **intraveineux** (Alves, Churlaud et al. en soumission). Dans ce cas-là cependant, le taux de passage de la barrière hémato-encéphalique (BHE) reste faible. Différentes solutions permettent de contourner cet écueil comme l'injection périnatale, l'ouverture de barrière grâce aux ultrasons ou des AAVs spécialement modifiés pour passer la BHE. Durant mon travail de thèse, je n'ai cependant directement travaillé que sur l'injection intraparenchymateuse dans l'hippocampe de rongeurs adultes.

4. Exemples d'applications à la MA

Dans le cadre de la MA, le transfert de gêne a permis d'un côté de reproduire la maladie, en créant des **modèles d'étude**. Ce même transfert de gènes permet aussi d'effectuer de la **thérapie génique**. Je serais volontairement bref sur cette partie puisque nous avons très récemment publié une revue concernant la thérapie génique pour la maladie d'Alzheimer (Alves, Fol et al. 2016) qui se trouve en dernière partie de l'introduction (voir partie IV.E). Je vais donc me concentrer sur les nombreuses applications réalisées au laboratoire ces dernières années.

Deux stratégies de modélisation furent employées dans notre laboratoire. La première représente le travail de thèse du Dr F. Djelti qui injecta dans l'hippocampe de souris sauvages un AAV5 codant pour un ARN d'interférence dirigé contre CYP46A1, enzyme intervenant dans le métabolisme du cholestérol intracérébral. Sa déplétion entraîne un phénotype drastique avec notamment une perte neuronale responsable d'une atrophie cérébrale et de défauts comportementaux (Djelti, Braudeau et al. 2015). Durant ma thèse, j'eu la chance de participer la création d'un autre modèle de la MA. En effet, le Dr M. Audrain réalisa un modèle par injection d'AAV10 codant pour l'APP *swedish london* et la PS1 M146L dans l'hippocampe de souris et de rats sauvages. Ces rongeurs présentent un phénotype physiopathologique unique, beaucoup plus proche de la pathologie humaine que les souris transgéniques actuellement utilisées. Cette coinjection permet d'induire les pathologies amyloïdes et tau avec un décours temporel calqué sur la MA humaine (Audrain, Fol et al. 2016) (Audrain, Souchet et al. en préparation). Ces caractéristiques font de celui-ci un modèle de choix pour l'étude des **phases précoces de la MA** et leur ciblage par des molécules pharmacologiques. Ceci est actuellement le travail de thèse de B. Souchet, qui teste sur le modèle rat des inhibiteurs de la kinase DYRK1A (Souchet et al. en préparation). La génération de ces modèles a permis l'élaboration d'un projet de création de société nommée Agent, développée par le Dr J. Braudeau.

J'ai aussi eu la chance de pouvoir participer aux autres développements de stratégies thérapeutiques par transfert de gènes dans le laboratoire. La même enzyme CYP46A1 fut surexprimée dans le cerveau de souris modélisant la pathologie amyloïde et la pathologie tau (Hudry, Van Dam et al. 2010, Burlot, Braudeau et al. 2015). Dans les deux cas, cette surexpression montra des effets bénéfiques intéressants (notamment une restauration comportementale). Le Dr S. Alves est actuellement en cours d'amélioration de la stratégie (Alves et al. en préparation) dans le but d'effectuer un essai clinique à moyen terme à travers la société Brainvectis. Enfin, ce dernier développa aussi une stratégie thérapeutique grâce à l'injection intraveineuse d'AAV2 codant pour IL-2 dans des souris amyloïdogènes. Celle-ci induit une réponse immunitaire bénéfique dans le cerveau, permettant de réduire la charge amyloïde et d'impacter positivement le comportement (Alves, Churlaud et al. en soumission).

E. Revue : Thérapie génique et maladie d'Alzheimer

Gene Therapy Strategies for Alzheimer's Disease: An Overview

Sandro Alves, Romain Fol, and Nathalie Cartier*

INSERM U1169/MIRCen CEA 92265 Fontenay aux Roses and Université Paris-Sud, Université Paris-Saclay, Orsay, France.

Key neuropathological hallmarks of Alzheimer's disease (AD) are extracellular amyloid plaques and intracellular accumulation of hyperphosphorylated Tau protein. The mechanisms underlying these neuropathological changes remain unclear. So far, research on AD therapy has had limited success in terms of symptomatic treatments although it has also had several failures for disease-modifying drugs. Gene transfer strategies to the brain have contributed to evaluate in animal models many interesting tracks, some of which should deserve clinical applications in AD patients in the future.

INTRODUCTION

ALZHEIMER'S DISEASE (AD), the most frequent cause of dementia, is a progressive neurodegenerative disease characterized by memory defects and decline of cognitive functions. Key neuropathological hallmarks of AD are extracellular amyloid plaques and intracellular accumulation of hyperphosphorylated Tau protein, a microtubule assembly protein, forming neurofibrillary tangles (NFTs).[1–3] Plaques are made of amyloid peptides produced from the metabolism of the amyloid precursor protein (APP) and are often surrounded by dystrophic neurites.[4] Plaques and tangles are associated with reactive astrogliosis and loss of synapses and neurons (Fig. 1). The mechanisms underlying these neuropathological changes remain unclear, but are probably caused by a combination of both environmental and genetic factors.[5]

Genetics and disease mechanism

Based on one's age at onset, AD is classified into early onset AD (EOAD, onset <65 years), accounting for 1–5% of all cases, and late onset AD (LOAD, onset >65 years), accounting for >95% of patients. EOAD is usually associated with a more rapid progression and a Mendelian pattern of inheritance. Three genes (*APP, PSEN1,* and *PSEN2*) that all encode proteins involved in APP metabolism and Aβ generation have been identified in the pathophysiology of EOAD, underlying the role of the amyloid pathway in its mechanism (Fig. 2). Mutations in these genes are mostly autosomal dominantly inherited and lead to Aβ aggregation and early onset disease.[6–9]

Several genes are involved in LOAD. They increase disease risk in a non-Mendelian fashion. First-degree relatives of patients with LOAD have twice the risk of people without an AD-affected first-degree relative. The first identified gene and major genetic risk factor is the *APOE* ε4 allele.[10,11] APOE is a lipid-binding protein expressed in humans as three common isoforms coded for by three alleles, APOEε2, ε3, and ε4. A single APOE-ε4 allele is associated with a 2–3-fold increased risk, and two copies increase the risk to 5-fold or more. Each allele lowers the age at onset by 6–7 years.[8]

Among thousands of candidate-gene-based association studies aiming to identify additional susceptibility *loci*, the only gene that could be identified and consistently implicated in AD was the sortilin-related receptor (*SORL1*). SORL1 is involved in vesicle trafficking from the cell surface to the Golgi-ER. SORL1 directs APP to endocytic pathways for recycling and plays an important role in Aβ generation. Interestingly, SORL1 is also a receptor that binds lipoproteins, including APOE-containing particles.[12–15] Recently, high-throughput genome-wide arrays allowed large hypothesis-free analysis of LOAD and identified more than 20 novel risk loci.[16] Most identified genes cluster in specific pathways: APP processing (*SORL1*, *CASS4*), Tau pathology (*CASS4, FERMT2*), immune response

*Correspondence: Dr. Nathalie Cartier, INSERM U1169-CEA MIRCen 18 Route du Panorama 92265 Fontenay aux Roses, France. E-mail: nathalie.cartier@inserm.fr

DOI: 10.1089/hum.2016.017

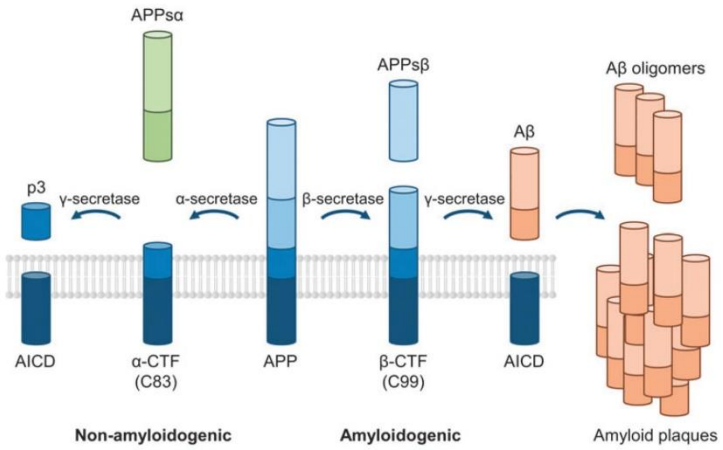

Figure 1. Scheme depicting the amyloid precursor protein (APP) processing. The APP can be proteolytically cleaved following two competing pathways. The nonamyloidogenic pathway involves the α-secretase cleaving the APP and giving rise to the soluble APPα (APPsα), which displays neurotrophic properties and the α carboxy-terminal fragment (α-CTF or C83). The last one is then processed by the γ-secretase liberating the p3 peptide and the APP intracellular domain (AICD) thought to function as a transcription factor. In the amyloidogenic pathway, APP is cleaved by the β-secretase inducing the release of the soluble APPβ (APPsβ) and the β carboxy-terminal fragment (β-CTF or C99) having cytotoxic effects. Finally, this peptide is processed by γ-secretase generating AICD and the amyloid β (Aβ), a soluble harmful peptide whose accumulation will form toxic oligomers and at later stages of the pathology, the amyloid plaques, hallmark of Alzheimer's disease patients' brains. Not drawn in proportion.

(*HLA-DRB5/DRB1, INPP5D, MEF2C, CR1, CD33, TREM2*), cell migration (*PTK2B*), endocytosis (*SORL1, PICALM, BIN1, CD2AP, EPHA1*), and lipid transport (*APOE, ABCA7, CLU*), strongly reinforcing the importance of these pathways in LOAD etiology.[12,17]

Therapeutic strategies for AD

Research into AD therapy has succeeded in developing at least partly efficacious symptomatic relief, but has failed in terms of developing disease-modifying therapies. Drugs approved for AD treatment are limited to acetylcholinesterase inhibitors (donepezil, rivastagmine, galantamine) or NMDA receptor antagonists (memantine).[18] They potentially improve cognition, behavior, and general clinical state, but their efficacy is very limited.

Among disease-modifying drugs that were evaluated, the most numerous trials concern passive immunosuppression. Results from animal studies have shown that anti-Aβ antibodies can prevent oligomer formation and reduce brain amyloid load with improvement in cognitive functions. Several monoclonal antibodies are being currently tested.[18] However, early clinical trials have been disappointing, leading to the initiation of clinical trials in which treatment is initiated in presymptomatic patients or in patients at a very early stage of the disease.[19] There remains a great unmet need to identify therapies with the potential to slow disease progression and improve cognitive function in AD.

GENE THERAPY STRATEGIES FOR AD

Acting directly on APP metabolism

Inhibiting secretase activity to decrease amyloid pathway. Anti-BACE1: Given the pivotal role BACE1 plays in Aβ production, it is an obvious therapeutic target. Small-molecule inhibitors of BACE1 have been in development, and many are now at various stages of clinical trials. Lowering BACE1 levels using lentiviral vectors expressing siRNAs reduced amyloid production and the neurodegenerative and behavioral deficits in AD mice. However, recent results showed unexpected and undesirable effects of BACE1 inhibition on synaptic function and cognition. In addition to the well-documented neurotoxic effects of Aβ, there is evidence that Aβ has neuroprotective properties and positive role on mechanisms underlying cognition at low or physiologic levels, raising the possibility that inhibiting BACE1 in wild-type animals may reduce endogenous Aβ production to such levels that its neurotrophic and synaptotrophic properties are lost.[20–22]

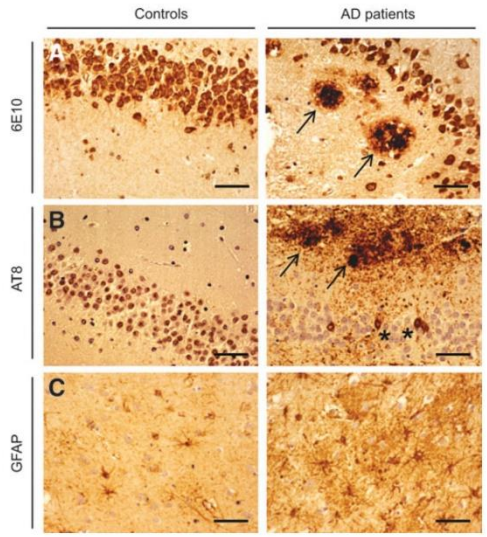

Figure 2. Alzheimer's disease (AD) neuropathology in the AD hippocampus. **(A)** Diaminobenzidine (DAB) staining using the 6E10 antibody in hippocampal slices showing the presence of dense-core amyloid-positive plaques (arrows), which are absent in controls. **(B)** Immunohistochemistry with the AT8 antibody also shows AT8-positive senile plaques (arrows) and neurofibrillary tangles (asterisk), also revealing fiber-like structures resembling distorted neurites. **(C)** GFAP immunostaining reveals the presence of astrocytes with normal fine radial processes in the control brain; in the contrary, in the hippocampus of AD patients, several clusters of astrocytes with thick radial processes are observed. Scale bars = 20 μm.

Inhibiting gamma secretase activity. γ-Secretase is a membrane protease carrying out cleavage of more than 100 single transmembrane-spanning proteins, including APP, Notch, and N-cadherin. Presenilin subunit is the catalytic component: mutations in the presenelin gene are a major cause of early onset familial AD (FAD)[8] because they lead to an increase in the production of the highly amyloidogenic Aβ42 isoform. Drugs aimed at γ-secretase are considered to be promising therapeutic targets for AD. However, inhibition of γ-secretase can cause severe adverse events, particularly because of the blockage of other pathways particularly the Notch signaling process.[23,24]

Increasing amyloid degrading enzymes: ECE, IDE, and NEP. Several proteases, including neprilysin (NEP), endothelin converting enzyme (ECE), and insulin degrading enzyme (IDE), have been shown to cleave Aβ.[25] AAV5-ECE-1 administration was evaluated in APP/PS1 transgenic mice. Strong expression was obtained in areas surrounding the injection sites, allowing Aβ and plaques decrease in the anterior cortex and hippocampus.[26]

Another study compared AAV-induced increased expression of NEP and IDE. AAV vectors expressed either native forms of NEP (NEP-n) or IDE (IDE-n), or engineered secreted forms of NEP (NEP-s) or IDE (IDE-s). In a six-week study, total Aβ and plaques were decreased in animals receiving the NEP-n and NEP-s but not for IDE-n or IDE-s in either the hippocampus or cortex. Thus, NEP, but not IDE, may be a good candidate for AD gene therapy.[27]

Delivering anti-amyloid antibodies. Monoclonal antibodies or polyclonal immunoglobulins targeting Aβ have been used to promote its clearance. Results from animal studies have shown that anti-Aβ antibodies can prevent oligomer formation and reduce brain amyloid load with improvement in cognitive functions. Several studies are ongoing to evaluate the tolerance and the efficacy of these strategies in human patients.[19,28]

A gene therapy strategy was also used based on the delivery of AAV encoding anti-Aβ single chain antibody (scFv) injected into the corticohippocampal regions of AD mouse models. One year after injection, expression of scFv was detectable in the neurons of the hippocampus. Amyloid deposits were strongly decreased at the injection sites with no sign of neurotoxicity.[29]

Increasing physiological APP pathway. The proteolytic processing of APP can be achieved following two competing pathways: the amyloidogenic and the nonamyloidogenic pathways[4] (Fig. 1). The last one not only prevents the production of amyloid toxic forms, but also enables the release of the soluble APPsα. APP has important physiological functions, many of which are thought to be mediated via the secretion of the APPsα.[30] *In vivo* the administration of APPsα enhances memory performance and long-term potentiation (LTP) in rodents, and displays crucial physiological properties for synaptic plasticity and hippocampal function.[31] In APP-KO mice, APPsα knock-in completely rescued spatial learning.[32]

The idea emerged that, beside the well-established neurotoxic and synaptotoxic properties of β-CTF and soluble and oligomeric Aβ, loss of the neuroprotective APPsα also contributes considerably to the development of AD. APPsα levels are decreased in the cerebrospinal fluid of AD patients, in both genetic and sporadic forms, which is correlated with poor memory performance.[33,34] APPsα was also shown to inhibit tau phosphorylation through GSK3β modulation.[35]

This suggests that overexpression of APPsα could be of great interest to alleviate AD-related symptoms. One way to do this would consist of overexpressing the α-secretase (ADAM10). However, ADAM10 was shown to have many substrates and its upregulation was implicated in tumorigenesis, thereby precluding a human clinical trial.[36] APPsα was overexpressed by means of AAV virus in hippocampal neurons of an aged AD mouse model (APP/PS1).[37] Two months after gene therapy, APPsα partially rescued spatial memory defects, restored synaptic plasticity and spine density, and decreased soluble Aβ and amyloid plaques. This was associated with microglial activation and phagocytosis (increase of IDE and TREM2) around amyloid plaques.

Increase neurotroprotection

Nerve growth factor. Nervous system growth factors prevent neuronal death in various correlative animal models of AD.[38] Specifically, nerve growth factor (NGF) stimulates and prevents the death of the function of basal forebrain cholinergic neurons that undergo early and prominent degeneration in AD.[39]

Degeneration of cholinergic neurons is an early and prominent contributor to cell loss and cognitive decline in AD. Indeed, NGF levels in the basal forebrain region decline in AD. Previous studies in animal models of AD have shown that NGF can stimulate cholinergic neurons that are necessary for maintenance of cognitive function, and undergo atrophy in early AD and prevent their death.[40] However, growth factors can cause off-target adverse effects, necessitating a targeted delivery strategy to control their localization and spread in the brain.[41]

In a first phase I trial, NGF was delivered through transplantation of autologous fibroblasts transduced with a Moloney leukemia viral vector to express human NGF into the basal forebrain region containing cholinergic cell bodies that send their projections throughout the cortex and hippocampus. The clinical findings of the phase I *ex vivo* trial suggested possible beneficial effects over a 2-year observation period compared with pretreatment rates of cognitive decline. A second phase I clinical trial included 10 patients who received AAV2-NGF into the basal forebrain region. An escalation dose protocol was used (1.2×10^{10} to 1.2×10^{11} vector particles[42]). The brains of all 8 patients in the first phase I trial were examined. All patients exhibited a trophic response to NGF in the form of axonal sprouting toward the NGF source. Cholinergic neuronal hypertrophy occurred on the NGF-treated side. Activation of cellular signaling and functional markers was present in the 2 patients who underwent AAV2-NGF gene transfer. An overall lower rate of cognitive decline and increased cortical glucose uptake were reported; two individuals had subcortical hemorrhage during implantation. No other adverse pathological effects related to NGF were observed.

A phase II multicenter, sham-surgery-controlled trial of NGF in AD is ongoing in 49 patients with mild to moderate AD based on a single administration of AAV-NGF vector that encodes the gene for NGF (CERE-110) or an appropriate sham (placebo) surgery control treatment. Data are expected soon.[43]

Brain-derived neurotrophic factor. Brain-derived neurotrophic factor (BDNF) is expressed in multiple cortical regions, including the entorhinal cortex and hippocampus.[44] BDNF levels decline in AD.[45] Administration of BDNF using a lentiviral vector (under the control of the CAG promoter) to the entorhinal cortex in an AD mouse model (APP transgenic mouse line J20) improved learning and memory, enhanced expression of the synaptic protein synaptophysin,[38] and prevented neuronal loss with early life BDNF treatment. The lentiviral-mediated *BDNF* gene was delivered into the entorhinal cortices of mice at age 2 months, and mice were examined 5 months later. BDNF revealed neuroprotective properties. Interestingly, this beneficial effect was not accompanied by a decrease of amyloid plaques.

Glial cell-derived neurotrophic factor. Glial cell-derived neurotrophic factor (GDNF) is emerging as a potent neurotrophic factor with therapeutic potential against a range of neurodegenerative conditions, including AD. Lentiviral vectors were used to overexpress the *GDNF* gene in hippocampal astrocytes of 3xTg-AD mice *in vivo*. After 6 months of GDNF overexpression, 10-month-old 3xTg-AD mice showed preserved learning and memory. GDNF therapy did not significantly reduce amyloid and tau pathology, but upregulated the expression of BDNF and induced neuroprotection.[46]

IGF1 and IGF2. Insulin-like growth factor 2 (IGF2) plays a critical role in memory consolidation in rats and mice, and IGF2 expression decreases in the hippocampus of patients with AD. AAV-IGF2 administration in the hippocampus of aged wild-type mice enhances memory and promotes dendritic spine formation. AAV-IGF2 or AAV-IGF1 injection into the hippocampus of APP Tg2576 mice rescues behavioral deficits, promotes dendritic

spine formation, and restores synaptic transmission. IGF2, but not IGF1, injection allows significant reduction in amyloid levels. Results demonstrate that IGF2/IGF2R is involved in the extracellular Aβ degradation mechanism, and suggest that IGF2R may act as an Aβ scavenger.[47] Another study showed that intracerebroventricular infusion of IGF2 in APP/PS1 mice that express the green fluorescent protein in cholinergic neurons (APP.PS1/CHGFP) and control littermates, at 6 months, reduced the number of hippocampal amyloid plaques and increased the level of hippocampal protein ACh-synthesizing enzyme.[48]

Nrf2 antioxidant pathway activation. Oxidative injury is thought to be central in the pathogenesis of AD. Binding of the transcription factor nuclear factor E2-related factor 2 (NRF2) to the antioxidant response element (ARE) enhancer sequence is an endogenous defense system against oxidative stress, triggering the simultaneous expression of numerous protective enzymes and scavengers.

A lentiviral vector was used to deliver NRF2 bilaterally into the hippocampus of 9-month-old transgenic AD mice (APP/PS1 mice). Reduction in spatial learning deficits of aged APP/PS1 mice was achieved. Six months after injection, *NRF2* gene transfer was associated with a reduction in astrocytic, but not microglial activation, and induction of NRF2 target gene heme oxygenase 1 in hippocampal neurons.[49]

Boosting autophagy-mediated pathways

Autophagy, the major cellular pathway for degradation of long-lived proteins and protein turnover, has been implicated in AD. Evidence suggests that increasing the levels of autopagy-related proteins may have potential for therapy. Lentiviral-mediated overexpression of beclin-1 in the hippocampus and cortex of APP transgenic mice reduced both intracellular Aβ as well as extracellular β-pleated Aβ depostis.[50] Thus, restoring beclin-1 and enhancing autophagy may be a novel approach to treat AD.

Targeting inflammatory pathway

Interleukin-4. Increasing data demonstrate the role of inflammation in AD. Anti-inflammatory cytokine signaling may play an emerging role as neurotransmitters, neuromodulators, and neurohormones in the brain. IL-4 has been characterized as a potential modulator of neuronal activities in the brain. IL-4 receptors are expressed in the hippocampus, and downregulation of IL-4 causes aging-related deficits of hippocampal LTP.[51] Moreover, IL-4 stimulation of human macrophages or microglia enhances Aβ degradation. AAV-mediated expression of the mouse IL-4 gene in APP/PS1 mice attenuates AD. Vector encoding IL-4 injection into the hippocampus resulted in sustained expression of IL-4, reduced astro/microgliosis, Aβ oligomerization and deposition, enhanced neurogenesis, improved spatial learning, and promoted phosphorylation of N-methyl-D-aspartate receptor subunit 2B.[52]

Interleukin-10. Anti-inflammatory cytokines, such as IL-10, can have significant therapeutic potentials in AD. AAV-mediated neuronal expression of the mouse IL-10 gene ameliorates cognitive dysfunction in APP/PS1 mice. Sustained expression of IL-10 reduced astro/microgliosis, enhanced neurogenesis, and improved spatial learning.[53]

Triggering receptor expressed on myeloid cells 2. The triggering receptor expressed on myeloid cells 2 (*TREM2*) gene was a recently identified susceptibility gene for AD, as its low-frequency variants increase the risk of AD similar to APOE ε4 allele. The TREM2 transmembrane protein is a receptor expressed on microglia that stimulates phagocytosis and suppresses inflammation. TREM2 is trafficked to the cell surface, where it binds with several ligands. Homozygous mutations in TREM2 are associated with autosomal recessive forms of dementia.[12]

Overexpression of TREM2 using a lentiviral injection in the brain ameliorated AD-related neuropathology (Aβ deposition, neuroinflammation, and neuronal loss) in APP/PS1 mice and improved spatial cognitive functions. Upregulation of TREM2 could serve as a compensatory response to Aβ and protect against AD progression by modeling microglia functions.[54]

Modulating genes related to LIPID metabolism

Targeting APOE, the major susceptibility gene for AD. APOE is a regulator of lipoprotein metabolism in the central nervous system, and APOE plays several important roles such as cholesterol transport, neuroplasticity, and inflammation. APOE binds to Aβ and influences its clearance and Aβ aggregation.[11]

Direct intracerebral administration of lentiviral vectors expressing the three common human *APOE* isoforms differentially alters hippocampal Aβ and amyloid burden in the PDAPP mouse model of AD. Expression of *APOE* ε2 in the absence or even in the presence of mouse APOE after direct intracerebral administration of lentiviral vector expressing *APOE* ε2 in the PDAPP mouse model

markedly reduced hippocampal Aβ burden. In contrast, expression of *APOE* ε4 in the absence of mouse APOE increased hippocampal Aβ42 levels and amyloid accumulation.[55]

Recently, a gene transfer approach to target the cortex of amyloid plaque-bearing transgenic mice with *APOE* was used by injection into the lateral ventricles of AD mice an AAV vector expressing the various human *APOE* alleles to transduce the ependymal layer. Human APOE proteins diffused into the cerebrospinal fluid and interstitial fluid (ISF). Human APOE isoforms affected the concentrations of soluble oligomeric Aβ in the ISF, the pace of Aβ fibrillization and deposition, and the extent of peri-plaque neurotoxic effects. Increase in soluble Aβ, an exacerbation of synaptic loss, and an increased number of dystrophic neurites around each deposit were observed in AD mice receiving *APOE* ε4, whereas a relative protective effect was observed with *APOE* ε2. These results suggest that therapeutic approaches aimed at decreasing *APOE* ε4, or increasing *APOE* ε2, may be beneficial in AD.[56]

Decreased plaque number was also observed when overexpressing *APOE* ε2 in astrocytes, the cells that physiologically produce APOE (Fol et al., unpublished results).

Inhibiting Acyl-CoA cholesterol acyltransferase enzyme. Acyl-CoA cholesterol acyltransferase (ACAT) enzyme catalyzes the formation of cholesteryl esters and mediates storage of cholesterol and cellular cholesterol homeostasis.[57] AAVs expressing artificial microRNA (miRNA) sequence targeting Acat1 were used to test whether a specific genetic knockdown of Acat1 in the mouse brain, administered at 10 months after the onset of the disease, could benefit AD. Analysis at 12 months showed that vector administration was well tolerated and allowed to decrease the levels of brain Aβ and full-length APP to levels comparable to full genetic ablation of Acat1.[58]

Activating cholesterol 24 hydroxylase enzyme

In AD, a mechanistic link between cholesterol metabolism in the brain and progression of AD has been clearly reported and altered cholesterol metabolism seems to play a pivotal role in the formation of amyloid plaques and in tau pathologies.[59] In the brain, cholesterol is synthesized *in situ* but cannot be degraded or cross the blood–brain barrier (BBB). The major exportable form of brain cholesterol is 24-hydroxycholesterol (24S-OHC) generated by the neuronal cholesterol 24-hydroxylase enzyme (*CYP46A1*). Because there is currently no molecule able to increase CYP46A1 activity and cross the BBB, overexpression of CYP46A1 by administering an AAV vector carrying the CYP46A1 cDNA in the brain seems to be an effective strategy. The therapeutic effect of AAV5-mediated CYP46A1 overexpression on rodent models of AD with amyloid pathology (APP23 and APP/PS1 mice) has been reported, by reducing the number of amyloid plaques (Fig. 3) and by improving spatial memory.[60] The same strategy was successful in THY-Tau22 mice, in which CYP46A1 overexpression corrected cognitive deficits, impaired long-term depression, and spine defects.[61] In conclusion, restoring CYP46A1 expression improves behavioral and clinical performances *in vivo* in both amyloid and Tau mouse models. Importantly, hippocampal shRNA-mediated inhibition of Cyp46a1 induced an AD-like phenotype in normal mice characterized by an increase in neuronal cholesterol and Aβ peptides followed by cognitive deficits, apoptotic neuronal death, and hippocampal atrophy. In ad-

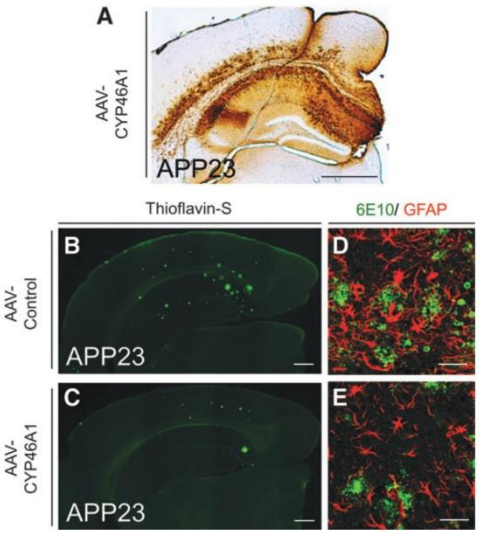

Figure 3. Overexpression of CYP46A1 in the hippocampus of AD mice decreases amyloid plaques and astrogliosis. **(A)** DAB staining using the CYP46A1 antibody showing the widespread AAV-mediated transduction of the APP23 AD mouse hippocampus. Scale bar = 1000 μm. **(B** and **C)** Thioflavin-S staining showing the reduction of thioflavin-S-positive amyloid plaques in the hippocampus of APP23 mice injected with CYP46A1 compared with age-matched APP23 mice treated with a control vector. Scale bar = 500 μm. **(D** and **E)** Laser confocal microscopy showing the reduction of amyloid-positive plaques (green/6E10 antibody) and astrocytic activation (red/GFAP) in CYP46A1-injected APP23 mice **(E)** as compared with APP23 mice treated with a control vector **(D)**. Scale bar = 20 μm.

dition, inhibition of the *CYP46A1* gene aggravated the phenotype in APP23 mice.[62] These data strongly suggest CYP46A1 as a relevant target to modulate AD progression, thus opening new avenues for treatment.

CONCLUSIONS AND FUTURE PERSPECTIVES

Research on AD therapy based on disease-modifying drugs has so far revealed limited achievements in terms of symptomatic treatments. Gene transfer strategies targeting specific regions of the brain have contributed to evaluate several potential tracks in AD animal models, some of which should deserve to be looked as potential candidates for clinical applications in AD.

As for most clinical conditions, the success of the development of new disease-modifying therapies strongly relies on critical issues, among which are the detailed knowledge of the natural history of the disease; its clinical, radiological, and biological endpoints; the selection of the patient population (EOAD, LOAD, genetic background); and the definition of valuable outcome predictors of disease evolution, but also biomarkers of treatment functionality (mechanism of action). This is particularly crucial for new innovative biotherapy strategies in which the number of patients included in phase I and phase II trials will be low. Gene therapy has a place in the battle against AD, given that it is designed to focus on one specific target and on specific delivery to affected brain regions. Moreover, it has the capacity to bring strong insight into the beneficial effects of modulating pathways to the brain that will help to better understand the physiopathology of the disease and contribute to stop its progression.

ACKNOWLEDGMENTS

This work was supported by NeurATRIS: A Translational Research Infrastructure for Biotherapies in Neurosciences, the Fondation France Alzheimer, the ANR-10-MALZ-0103 CholAD, the ERA-Net Neuron (01EW1305A), and the Fondation pour la Recherche Médicale, Bioingénierie pour la Santé 2014 "Projet DBS20140930765."

AUTHOR DISCLOSURE

N.C. is a founder and owner of founder equity of BrainVectis Therapeutics. The other authors declare that they have no competing interests.

REFERENCES

1. Hardy J, Allsop D. Amyloid deposition as the central event in the aetiology of Alzheimer's disease. Trends Pharmacol Sci 1991;12:383–388.
2. Hardy J, Bogdanovic N, Winblad B, et al. Pathways to Alzheimer's disease. J Intern Med 2014; 275:296–303.
3. Selkoe DJ. Alzheimer's disease: Genes, proteins, and therapy. Physiol Rev 2001;81:741–766.
4. Zhang YW, Thompson R, Zhang H, et al. APP processing in Alzheimer's disease. Mol Brain 2011;4:3.
5. Reitz C. Genetic diagnosis and prognosis of Alzheimer's disease: Challenges and opportunities. Expert Rev Mol Diagn 2015;15:339–348.
6. Sherrington R, Rogaev EI, Liang Y, et al. Cloning of a gene bearing missense mutations in early-onset familial Alzheimer's disease. Nature 1995; 375:754–760.
7. St George-Hyslop PH, Tanzi RE, Polinsky RJ, et al. The genetic defect causing familial Alzheimer's disease maps on chromosome 21. Science 1987; 235:885–890.
8. Bettens K, Sleegers K, Van Broeckhoven C. Genetic insights in Alzheimer's disease. Lancet Neurol 2013;12:92–104.
9. Van Broeckhoven C, Backhovens H, Cruts M, et al. Mapping of a gene predisposing to early-onset Alzheimer's disease to chromosome 14q24.3. Nat Genet 1992;2:335–339.
10. Strittmatter WJ, Saunders AM, Schmechel D, et al. Apolipoprotein E: High-avidity binding to beta-amyloid and increased frequency of type 4 allele in late-onset familial Alzheimer disease. Proc Natl Acad Sci U S A 1993;90:1977–1981.
11. Spinney L. Alzheimer's disease: The forgetting gene. Nature 2014;510:26–28.
12. Karch CM, Goate AM. Alzheimer's disease risk genes and mechanisms of disease pathogenesis. Biol Psychiatry 2015;77:43–51.
13. Lee JH, Cheng R, Honig LS, et al. Association between genetic variants in SORL1 and autopsy-confirmed Alzheimer disease. Neurology 2008;70: 887–889.
14. Rogaeva E, Meng Y, Lee JH, et al. The neuronal sortilin-related receptor SORL1 is genetically associated with Alzheimer disease. Nat Genet 2007; 39:168–177.
15. Offe K, Dodson SE, Shoemaker JT, et al. The lipoprotein receptor LR11 regulates amyloid beta production and amyloid precursor protein traffic in endosomal compartments. J Neurosci 2006;26:1596–1603.
16. Lambert JC, Ibrahim-Verbaas CA, Harold D, et al. Meta-analysis of 74,046 individuals identifies 11 new susceptibility loci for Alzheimer's disease. Nat Genet 2013;45:1452–1458.
17. Van Cauwenberghe C, Van Broeckhoven C, Sleegers K. The genetic landscape of Alzheimer disease: Clinical implications and perspectives. Genet Med 2015. doi: 10.1038/gim.2015.117. [Epub ahead of print]
18. Mangialasche F, Solomon A, Winblad B, et al. Alzheimer's disease: Clinical trials and drug development. Lancet Neurol 2010;9:702–716.
19. Godyn J, Jonczyk J, Panek D, et al. Therapeutic strategies for Alzheimer's disease in clinical trials. Pharmacol Rep 2016;68:127–138.
20. Filser S, Ovsepian SV, Masana M, et al. Pharmacological inhibition of BACE1 impairs synaptic plasticity and cognitive functions. Biol Psychiatry 2015;77:729–739.
21. Singer O, Marr RA, Rockenstein E, et al. Targeting BACE1 with siRNAs ameliorates Alzheimer disease neuropathology in a transgenic model. Nat Neurosci 2005;8:1343–1349.
22. Yan R, Vassar R. Targeting the beta secretase BACE1 for Alzheimer's disease therapy. Lancet Neurol 2014;13:319–329.

23. De Strooper B. Lessons from a failed gamma-secretase Alzheimer trial. Cell 2014;159:721–726.

24. Tan Y, Zhang Q, Wong SG, et al. Anti-Alzheimer therapeutic drugs targeting gamma-secretase. Curr Top Med Chem 2016;16:549–557.

25. Miners JS, Barua N, Kehoe PG, et al. Abeta-degrading enzymes: Potential for treatment of Alzheimer disease. J Neuropathol Exp Neurol 2011;70:944–959.

26. Carty NC, Nash K, Lee D, et al. Adeno-associated viral (AAV) serotype 5 vector mediated gene delivery of endothelin-converting enzyme reduces Abeta deposits in APP + PS1 transgenic mice. Mol Ther 2008;16:1580–1586.

27. Carty N, Nash KR, Brownlow M, et al. Intracranial injection of AAV expressing NEP but not IDE reduces amyloid pathology in APP+PS1 transgenic mice. PLoS One 2013;8:e59626.

28. Wisniewski T, Goni F. Immunotherapeutic approaches for Alzheimer's disease. Neuron 2015;85:1162–1176.

29. Fukuchi K, Tahara K, Kim HD, et al. Anti-Abeta single-chain antibody delivery via adeno-associated virus for treatment of Alzheimer's disease. Neurobiol Dis 2006;23:502–511.

30. Weyer SW, Zagrebelsky M, Herrmann U, et al. Comparative analysis of single and combined APP/APLP knockouts reveals reduced spine density in APP-KO mice that is prevented by APPsalpha expression. Acta Neuropathol Commun 2014;2:36.

31. Weyer SW, Klevanski M, Delekate A, et al. APP and APLP2 are essential at PNS and CNS synapses for transmission, spatial learning and LTP. EMBO J 2011;30:2266–2280.

32. Ring S, Weyer SW, Kilian SB, et al. The secreted beta-amyloid precursor protein ectodomain APPs alpha is sufficient to rescue the anatomical, behavioral, and electrophysiological abnormalities of APP-deficient mice. J Neurosci 2007;27:7817–7826.

33. Endres K, Fahrenholz F. Regulation of alpha-secretase ADAM10 expression and activity. Exp Brain Res 2012;217:343–352.

34. Fahrenholz F. Alpha-secretase as a therapeutic target. Curr Alzheimer Res 2007;4:412–417.

35. Deng J, Habib A, Obregon DF, et al. Soluble amyloid precursor protein alpha inhibits tau phosphorylation through modulation of GSK3beta signaling pathway. J Neurochem 2015;135:630–637.

36. Prox J, Rittger A, Saftig P. Physiological functions of the amyloid precursor protein secretases ADAM10, BACE1, and presenilin. Exp Brain Res 2012;217:331–341.

37. Fol R, Braudeau J, Ludewig S, et al. Viral gene transfer of APPsalpha rescues synaptic failure in an Alzheimer's disease mouse model. Acta Neuropathol 2016;131:247–266.

38. Nagahara AH, Merrill DA, Coppola G, et al. Neuroprotective effects of brain-derived neurotrophic factor in rodent and primate models of Alzheimer's disease. Nat Med 2009;15:331–337.

39. Kordower JH, Winn SR, Liu YT, et al. The aged monkey basal forebrain: Rescue and sprouting of axotomized basal forebrain neurons after grafts of encapsulated cells secreting human nerve growth factor. Proc Natl Acad Sci U S A 1994;91:10898–10902.

40. Counts SE, Nadeem M, Wuu J, et al. Reduction of cortical TrkA but not p75(NTR) protein in early-stage Alzheimer's disease. Ann Neurol 2004;56:520–531.

41. Malkki H. Alzheimer disease: NGF gene therapy activates neurons in the AD patient brain. Nat Rev Neurol 2015;11:548.

42. Rafii MS, Baumann TL, Bakay RA, et al. A phase 1 study of stereotactic gene delivery of AAV2-NGF for Alzheimer's disease. Alzheimers Dement 2014;10:571–581.

43. Tuszynski MH, Yang JH, Barba D, et al. Nerve growth factor gene therapy: Activation of neuronal responses in Alzheimer disease. JAMA Neurol 2015;72:1139–1147.

44. Altar CA, Cai N, Bliven T, et al. Anterograde transport of brain-derived neurotrophic factor and its role in the brain. Nature 1997;389:856–860.

45. Narisawa-Saito M, Wakabayashi K, Tsuji S, et al. Regional specificity of alterations in NGF, BDNF and NT-3 levels in Alzheimer's disease. Neuroreport 1996;7:2925–2928.

46. Revilla S, Ursulet S, Alvarez-Lopez MJ, et al. Lenti-GDNF gene therapy protects against Alzheimer's disease-like neuropathology in 3xTg-AD mice and MC65 cells. CNS Neurosci Ther 2014;20:961–972.

47. Pascual-Lucas M, Viana da Silva S, Di Scala M, et al. Insulin-like growth factor 2 reverses memory and synaptic deficits in APP transgenic mice. EMBO Mol Med 2014;6:1246–1262.

48. Mellott TJ, Pender SM, Burke RM, et al. IGF2 ameliorates amyloidosis, increases cholinergic marker expression and raises BMP9 and neurotrophin levels in the hippocampus of the APPswePS1dE9 Alzheimer's disease model mice. PLoS One 2014;9:e94287.

49. Kanninen K, Heikkinen R, Malm T, et al. Intrahippocampal injection of a lentiviral vector expressing Nrf2 improves spatial learning in a mouse model of Alzheimer's disease. Proc Natl Acad Sci U S A 2009;106:16505–16510.

50. Pickford F, Masliah E, Britschgi M, et al. The autophagy-related protein beclin 1 shows reduced expression in early Alzheimer disease and regulates amyloid beta accumulation in mice. J Clin Invest 2008;118:2190–2199.

51. Maher FO, Nolan Y, Lynch MA. Downregulation of IL-4-induced signalling in hippocampus contributes to deficits in LTP in the aged rat. Neurobiol Aging 2005;26:717–728.

52. Kiyota T, Okuyama S, Swan RJ, et al. CNS expression of anti-inflammatory cytokine interleukin-4 attenuates Alzheimer's disease-like pathogenesis in APP+PS1 bigenic mice. FASEB J 2010;24:3093–3102.

53. Kiyota T, Ingraham KL, Swan RJ, et al. AAV serotype 2/1-mediated gene delivery of anti-inflammatory interleukin-10 enhances neurogenesis and cognitive function in APP+PS1 mice. Gene Ther 2012;19:724–733.

54. Jiang T, Tan L, Zhu XC, et al. Upregulation of TREM2 ameliorates neuropathology and rescues spatial cognitive impairment in a transgenic mouse model of Alzheimer's disease. Neuropsychopharmacology 2014;39:2949–2962.

55. Dodart JC, Marr RA, Koistinaho M, et al. Gene delivery of human apolipoprotein E alters brain Abeta burden in a mouse model of Alzheimer's disease. Proc Natl Acad Sci U S A 2005;102:1211–1216.

56. Hudry E, Dashkoff J, Roe AD, et al. Gene transfer of human Apoe isoforms results in differential modulation of amyloid deposition and neurotoxicity in mouse brain. Sci Transl Med 2013;5:212ra161.

57. Chang TY, Li BL, Chang CC, et al. Acyl-coenzyme A:cholesterol acyltransferases. Am J Physiol Endocrinol Metab 2009;297:E1–E9.

58. Murphy SR, Chang CC, Dogbevia G, et al. Acat1 knockdown gene therapy decreases amyloid-beta in a mouse model of Alzheimer's disease. Mol Ther 2013;21:1497–1506.

59. Ghribi O. Potential mechanisms linking cholesterol to Alzheimer's disease-like pathology in rabbit brain, hippocampal organotypic slices, and skeletal muscle. Journal of Alzheimer's disease: JAD 2008;15:673–684.

60. Hudry E, Van Dam D, Kulik W, et al. Adeno-associated virus gene therapy with cholesterol 24-hydroxylase reduces the amyloid pathology before or after the onset of amyloid plaques in mouse models of Alzheimer's disease. Mol Ther 2010;18:44–53.

61. Burlot MA, Braudeau J, Michaelsen-Preusse K, et al. Cholesterol 24-hydroxylase defect is implicated in memory impairments associated with Alzheimer-like Tau pathology. Hum Mol Genet 2015;24:5965–5976.

62. Djelti F, Braudeau J, Hudry E, et al. CYP46A1 inhibition, brain cholesterol accumulation and neurodegeneration pave the way for Alzheimer's disease. Brain 2015;138:2383–2398.

Received for publication February 1, 2016;
accepted after revision February 1, 2016.
Published online: February 2, 2016.

F. Objectifs du travail de thèse

Nous l'avons vu précédemment, l'APP possède des rôles physiologiques dont les pertes de fonction durant le processus pathologique de la MA ont longtemps été négligées. La majorité de ces effets physiologiques, et notamment trophiques, seraient dû au peptide soluble issu du clivage de l'APP par l'α secrétase ; l'APPsα. Afin de contrecarrer les effets délétères de l'accumulation d'Aβ dans le cerveau, il semblerait que la restauration de la balance voie amyloïdogène / voie non amyloïdogène soit une approche thérapeutique prometteuse. Et même indépendamment de celle-ci, les propriétés neuroprotectrices et synaptotrophiques semblent intéressantes à exploiter dans le cadre de la MA.

Le transfert de gêne est un outil de choix afin de cibler, à un âge désiré, une structure de choix du cerveau. L'un des objectifs de ma thèse est donc d'**utiliser le transfert de gêne afin d'évaluer la surexpression thérapeutique d'APPsα** (**ARTICLE n°1**):

- Dans des souris modélisant la MA, les **APP/PS1ΔE9**. Ces souris furent injectées à douze mois, un stade avancé de la pathologie amyloïde où celles-ci présentent déjà des défauts synaptiques et une amyloïdose élevée.

- Au moyen de l'**injection stéréotaxique** intraparenchymateuse.

- Qui nous permit de cibler efficacement **l'hippocampe**, l'une des principales structure touchée dans la MA et grandement responsable de l'atteinte mnésique.

- Au moyen des vecteurs **AAV**, et en particulier l'AAV9 permettant une expression efficace et stable à long terme

- Dans les **neurones**, cellules exprimant physiologiquement l'APP.

A l'opposé, le clivage de l'APP par la β secrétase libère le peptide APPsβ. Ce dernier ne diffère que 16 acides aminés par rapport à l'APPsα. L'APPsβ étant impliqué dans voie de clivage amyloïdogène de l'APP, il a souvent été négligé comparé à son pendant non-amyloïdogène et peu de données sur ses propriétés *in vivo*, qu'elles soient bénéfiques ou délétères, ont été générées. Ainsi, **nous avons évalué de la même manière que pour APPsα, les conséquences de la surexpression hippocampique d'APPsβ dans un modèle de souris Alzheimer âgées** (**ARTICLE n°2**).

Dans les deux cas, notre but est d'évaluer les conséquences thérapeutiques de la surexpression des deux formes solubles de l'APP au niveau **comportemental** et en termes de **plasticité et densité synaptique**. Les conséquences sur la voie amyloïdogène et notamment **la charge amyloïde** sera déterminée. Les mécanismes sous-tendant les effets trophiques de l'APP et de ses dérivés étant mal connus, l'objectif est enfin de mettre en avant un potentiel **mode d'action** de ceux-ci.

V. RESULTATS

Article n°1 : Viral gene transfer of APPsα rescues synaptic failure in an Alzheimer's disease mouse model. Acta Neuropathologica, 2016. 131:247-266.

Article n°2 : Ebauche du futur article: Phenotypic differences between APPsα and APPsβ gene transfer in Alzheimer's disease mice.

A. Article n°1 : Surexpression de l'APPsα dans un modèle murin de la MA

Acta Neuropathol (2016) 131:247–266
DOI 10.1007/s00401-015-1498-9

ORIGINAL PAPER

Viral gene transfer of APPsα rescues synaptic failure in an Alzheimer's disease mouse model

Romain Fol[1,2,3] · Jerome Braudeau[1,2] · Susann Ludewig[7] · Tobias Abel[6] · Sascha W. Weyer[9] · Jan-Peter Roederer[9] · Florian Brod[6] · Mickael Audrain[1,2,3] · Alexis-Pierre Bemelmans[2,4,5] · Christian J. Buchholz[6] · Martin Korte[7,8] · Nathalie Cartier[1,2] · Ulrike C. Müller[9]

Received: 18 May 2015 / Revised: 7 October 2015 / Accepted: 15 October 2015 / Published online: 4 November 2015

Abstract Alzheimer's disease (AD) is characterized by synaptic failure, dendritic and axonal atrophy, neuronal death and progressive loss of cognitive functions. It is commonly assumed that these deficits arise due to β-amyloid accumulation and plaque deposition. However, increasing evidence indicates that loss of physiological APP functions mediated predominantly by neurotrophic APPsα produced in the non-amyloidogenic α-secretase pathway may contribute to AD pathogenesis. Upregulation of APPsα production via induction of α-secretase might, however, be problematic as this may also affect substrates implicated in tumorigenesis. Here, we used a gene therapy approach to directly overexpress APPsα in the brain using AAV-mediated gene transfer and explored its potential to rescue structural, electrophysiological and behavioral deficits in APP/PS1ΔE9 AD model mice. Sustained APPsα overexpression in aged mice with already preexisting pathology and amyloidosis restored synaptic plasticity and partially rescued spine density deficits. Importantly, AAV-APPsα treatment also resulted in a functional rescue of spatial reference memory in the Morris water maze. Moreover, we demonstrate a significant reduction of soluble Aβ species and plaque load. In addition, APPsα induced the recruitment of microglia with a ramified morphology into the vicinity of plaques and upregulated IDE and TREM2 expression suggesting enhanced plaque clearance. Collectively, these data indicate that APPsα can mitigate synaptic and cognitive deficits, despite established pathology. Increasing APPsα may therefore be of therapeutic relevance for AD.

R. Fol and J. Braudeau are joint first authors.

N. Cartier and U. C. Müller are joint senior authors.

Electronic supplementary material The online version of this article (doi:10.1007/s00401-015-1498-9) contains supplementary material, which is available to authorized users.

✉ Nathalie Cartier
nathalie.cartier@inserm.fr

✉ Ulrike C. Müller
u.mueller@urz.uni-heidelberg.de

[1] INSERM U1169/MIRCen CEA, 92265 Fontenay aux Roses, France

[2] University Paris Sud, University Paris-Saclay, 91400 Orsay, France

[3] Université Paris Descartes, 75006 Paris, France

[4] Commissariat à l'Energie Atomique et aux Energies Alternatives (CEA), Département des Sciences du Vivant (DSV), Institut d'Imagerie Biomédicale (I2BM), Molecular Imaging Research Center (MIRCen), 92260 Fontenay aux Roses, France

[5] Centre National de la Recherche Scientifique (CNRS), UMR 9199, Neurodegenerative Diseases Laboratory, 92260 Fontenay aux Roses, France

[6] Molecular Biotechnology and Gene Therapy, Paul-Ehrlich-Institut, 63225 Langen, Germany

[7] Division of Cellular Neurobiology, Zoological Institute, TU Braunschweig, Brunswick, Germany

[8] Helmholtz Centre for Infection Research, AG NIND, Inhoffenstr. 7, 38124 Brunswick, Germany

[9] Department of Bioinformatics and Functional Genomics, Institute of Pharmacy and Molecular Biotechnology, Heidelberg University, Im Neuenheimer Feld 364, 69120 Heidelberg, Germany

Keywords Alzheimer · Gene therapy · Amyloid precursor protein · APPsα · Synaptic plasticity · Spines · Behavior · Microglia · AAV

Introduction

Synaptic dysfunction, cognitive decline, and excessive accumulation of neurotoxic β-amyloid peptides (Aβ) are hallmark features of Alzheimer's disease (AD). Aβ is generated by sequential cleavage of the amyloid precursor protein (APP) by β- and γ-secretase. In the competing and physiologically predominant non-amyloidogenic pathway, α-secretase cleaves APP within the Aβ region [50, 63] thus precluding the formation of Aβ peptides. This also leads to the secretion of the neuroprotective ectodomain APPsα into the extracellular space in a process that can be stimulated by neuronal and synaptic activity [34, 35].

AD is characterized by upregulation of β-secretase (BACE-1) resulting in a shift towards amyloidogenic APP processing [2, 36]. Increasing evidence suggests that the concomitant reduction in APPsα and the loss of its physiological functions contribute to AD pathogenesis. Reduced levels of APPsα or ADAM10 were reported in patients with mild cognitive impairment and AD [22, 44] (see also review by [25]). Lowered levels of CSF APPsα were also correlated with poor memory performance in aged rats [4, 25] and moreover, in a Swedish family with AD, a strong correlation was found between low APPsα levels and poor performance in cognitive tests, whereas no association was reported for amyloid β-peptide [3]. In addition, α-secretase attenuating mutations have been associated with hereditary late-onset AD [74].

Previously, a number of in vitro studies indicated that APP and APPsα may protect cell lines and cultured neurons against various forms of stress, including growth factor withdrawal [55], apoptotic stimuli [18] and excitotoxicity [43, 48, 58, 64, 79]. In contrast, so far only few studies have addressed a protective role of APPsα in vivo and these were limited to acute forms of experimental brain injury. APPsα had beneficial effects when infused as a protein shortly after mechanical head trauma [19, 78] or after induction of ischemia in adult rats [72]. From these studies, however, it is difficult to extrapolate to the situation in neurodegenerative diseases such as AD, characterized by chronic production and accumulation of neurotoxic molecules including Aβ. Another challenge is the need for sustained expression of neurotrophic/neuroprotective factors that calls for a gene therapy approach.

Loss of function studies in APP knockout mice had indicated diverse physiological functions of APP in the PNS and CNS for neuronal morphology, synaptogenesis, adult neurogenesis, synaptic plasticity and hippocampus-dependent behavior [1, 7, 15, 33, 42, 76, 83–85]. However, it remained unclear whether deficits of mice lacking APP family members may arise due to defects (such as impaired synaptogenesis) originating in development [85]. To delineate the specific role of APPsα, we previously generated APPsα knockin (KI) mice that lack Aβ production and expresses solely the secreted APPsα ectodomain due to a stop codon insertion into the mouse APP locus behind the α-secretase cleavage site. APPsα-KI mice showed a wild-type-like phenotype lacking the LTP impairment of APP-KO mice [65]. While these early studies suggested an important role of endogenous APPsα for normal LTP, it remained unclear whether APPsα may also be of therapeutic relevance. Recently, we generated conditional double knockout (cDKO) mice lacking APP and the related APLP2 [33]. These cDKO mice revealed reduced spine density and impaired synaptic plasticity that was associated with deficits in hippocampus-dependent behaviors [33]. Interestingly, the impairment of LTP found in cDKO mice could be rescued by acute application of nanomolar amounts of recombinant APPsα, indicating a crucial role for APPsα to support synaptic plasticity in the adult brain [33]. Despite this, the question remained whether these beneficial acute effects of APPsα observed in vitro for a relatively short time of recording may also prove relevant in vivo including AD model mice.

Here, we intended to test the concept of enhancing/restoring APPsα levels using a gene therapy approach as a potential AD treatment strategy. To this end, we used direct overexpression of APPsα by AAV-mediated gene transfer into the brain to explore its potential to ameliorate or rescue structural, electrophysiological and behavioral deficits of AD model mice. We show that overexpression of APPsα in aged transgenic APP/PS1ΔE9 mice with well-established plaque pathology improves synaptic plasticity and partially rescues spine density deficits. Restoration of synaptic plasticity and increased spine density is also accompanied by a rescue of spatial reference memory. Moreover, we demonstrate that AAV-APPsα expression leads to moderately reduced Aβ levels and significantly ameliorated plaque pathology. Interestingly, in AAV-APPsα injected mice, we observed an increased number of microglia with ramified morphology in the vicinity of plaques that was associated with increased IDE and TREM2 expression which may have led to increased plaque clearance. Collectively, our data suggest that even at stages with advanced plaque deposition APPsα may mitigate Aβ induced synaptotoxic effects and improve cognitive function.

Materials and methods

AAV plasmid design and vector production

The mouse APPsα coding sequence (derived from Uniprot: P12023-2) was codon optimized (Geneart, Regensburg) and then cloned under control of the synapsin promoter into the single-stranded rAAV2-based shuttle vector pAAVSynMCS-2A-Venus [75] via NheI-HindII restriction sites. For easy detection, an N-terminal double HA-tag was inserted downstream of the APP signal peptide at the N-terminus of APPsα. The control vector (pAAV-Venus) encodes the yellow fluorescent protein Venus fused to a C-terminal farnesylation signal for membrane anchoring. All constructs were packaged into AAV9 by the MIRCen viral production platform as described [10]. Briefly, viral particles were produced by transient co-transfection of HEK-293 cells with an adenovirus helper plasmid (pXX6-80), an AAV packaging plasmid carrying the rep2 and cap9 genes, and the AAV2 transfer vector containing the above-mentioned expression cassettes. 72 h following transfection, virions were purified and concentrated from cell lysate and supernatant by ultracentrifugation on a iodixanol density gradient followed by buffer exchange to PBS, 0.01 % Pluronic via a 100kd Amicon Centrifugal filter unit (Merck-Millipore, Darmstadt, Germany). Concentration of the vector stocks was estimated by quantitative PCR according to the method described by [5]) and expressed as viral genomes per ml of concentrated stocks (vg/ml).

Animals

Sixteen APPswe/PS1ΔE9 mice (referred to as APP/PS1ΔE9; The Jackson Laboratory, Bar Harbor, USA) and seven age-matched littermate control mice were used for behavior, pathology and biochemistry. Eleven APP/PS1ΔE9 and five littermates were used for electrophysiology and spine density analysis. APP/PS1ΔE9 mice express the human APP gene carrying the *Swedish* double mutation (K595N/M596L). In addition, they express the human PS1ΔE9 variant lacking exon 9 [13, 38, 87]. Only male mice were used throughout the study. APP knockout mice have been described previously [49]. For age at AAV injection and age at analysis/sacrifice, see results section. All experiments were conducted in accordance with the ethical standards of French, German and European regulations (European Communities Council Directive of 24 November 1986).

Stereotactic injection of AAV

Mice were anesthetized by intraperitoneal injection of ketamine/xylazine (0.1/0.05 g/kg body weight) and positioned on a stereotactic frame (Stoelting, Wood Dale, USA). Vectors (either AAV-Venus or AAV-APPsα) were bilaterally injected into the hippocampus using 2 µl of viral preparation (10^{10} vg/hippocampus) at a rate of 0.2 µl/min. Two injection sites per hippocampus were used to optimize virus spreading. Stereotactic coordinates of injection sites from bregma were: anteroposterior −2 mm; mediolateral ±1 mm; dorsoventral −2.25 mm and anteroposterior −2 mm; mediolateral ±1 mm; dorsoventral −1.75 mm.

Brain samples

APP/PS1ΔE9 mice were sacrificed 5 months post-injection at 17 months of age. Following anesthesia, mice were transcardially perfused with 0.1 M phosphate-buffered saline (PBS) before dissection. For immunohistochemistry, the left cerebral hemisphere was dissected and post-fixed in 4 % paraformaldehyde (PFA) for 1 week and cryoprotected in 30 % sucrose for 24 h. 40 µm sections were cut using a freezing microtome (Leica, Wetzlar, Germany), collected in a cryoprotective solution and stored at −20 °C. The right hemisphere was dissected to segregate hippocampus and cortex for biochemical analysis. Samples were then homogenized in lysis buffer (TBS, NaCl 150 mM and Triton 1 %) containing phosphatase and protease inhibitors. After centrifugation (20 min, 13,000 rpm, 4 °C), the supernatant was collected and the protein concentration was quantified by BCA Assay (Thermo Fisher Scientific, Waltham, USA). Lysate aliquots (3 mg of protein/ml) were stored at −80 °C.

Immunostaining

Slices were washed with 0.1 M PBS and permeabilized in 0.25 % PBS-Triton before blocking in PBS-Triton 0.25 % containing 5 % goat serum for 60 min. For vector encoded HA-APPsα immunolabeling, slices were incubated with an anti-HA antibody (Covance, Princeton, USA, 1/250) overnight at 4 °C. After successive washes (PBS-Triton 0.25 %, PBS and PB 0.1 M), incubation with a biotinylated anti-mouse antibody was performed for 1 h at room temperature. For signal amplification, samples were incubated using the ABC kit (Vector laboratories, Burlingame, USA) for 1 h at room temperature. Finally, slices were incubated in Cy3-coupled streptavidin. HA-APPsα was co-immunostained overnight with the following primary antibodies: Rabbit anti-Iba1, 1/500, Wako, Richmond, USA;

Mouse-GFAP Cy3 conjugate, 1/500, Sigma-Aldrich, Saint-Louis, USA. For immunofluorescent staining of plaques, slices were stained using a 30 min incubation in 1 % thioflavin S solution, rinsed twice (1 min each) in 50 % EtOH and mounted in Vectashield fluorescent mounting media (Vector laboratories). Images were taken with a Nikon Eclipse T*i* microscope (Nikon, Tokyo, Japan) and a Leica SP8 confocal microscope (Leica). For plaque quantification, slices were incubated in 88 % formic acid solution for 15 min (antigen retrieval). To inactivate endogenous peroxidase, samples were incubated in hydrogen peroxide (30 min) before blocking and incubation with the primary antibody (4G8, Covance, 1/1000). Incubation with a horseradish-coupled secondary antibody was done at RT, developed using the DAB kit (Vector laboratories) and mounted in Eukit mounting media (Sigma-Aldrich). Images were taken with a Z6 APO macroscope (Leica). Plaques, GFAP and Iba1 immunoreactivity were quantified using ImageJ (NIH, Bethesda, USA) or Icy (Institut Pasteur, Paris, France). Laser power, numeric gain and magnification were kept constant between animals to avoid potential technical artifacts. Images were first converted to 8-bit gray scale and binary thresholded to highlight a positive staining. At least 2 sections per mouse (between −1.7 and −2.3 mm caudal to bregma) were quantified for either hippocampus or cortex. The average value per structure was calculated for each mouse. For quantification of Iba1 and GFAP immunoreactivity around plaques, a region of interest (ROI) was drawn around the center of the plaque. The diameter of the circular ROI was set as three times the diameter of the plaque. Mean fluorescence intensity values were measured for either Iba1 or GFAP immunoreactivity and were processed via Icy software (Institut Pasteur, Paris, France). Experiments and data analysis were performed blind with respect to treatments and genotypes.

Western blot analysis

Proteins were separated by SDS-PAGE using 4–12 % Bis–Tris gels (NuPAGE, Life Technologies, Carlsbad, USA) in MES SDS running buffer (NuPAGE, Life Technologies) and transferred to nitrocellulose membranes (iBlot, Life Technologies). For CTF analysis, proteins were separated using 10–20 % Tris–Tricine gradient gels (Novex, Life Technologies) and electroblotted onto 0.22 µm PVDF membrane (BioRad, Hercules, USA). After blocking in 5 % milk-PBS 0.1 M for 60 min, membranes were incubated with the primary antibodies overnight at 4 °C. The following antibodies were used: HA, 1/2000, Covance; β-actin, 1/5000, Merck Millipore; Venus (GFP), 1/1000, Vector laboratories; GAPDH, 1/4000, Abcam, Cambridge, UK; Iba1, 1/2000, Wako, Richmond, USA; GFAP, 1/4000 Dako, Glostrup, Denmark; IDE, 1/200, Santa Cruz Biotechnology, Dallas, USA; TREM2, 1/500, R&D Systems, Minneapolis, USA; APP: mouse monoclonal m3.2 and c1/6.1, 1/1000; kind gift from Paul Mathews; Y188, 1/1000, Abcam; see also Fig. S1 for a summary of anti-APP epitopes recognized by these antibodies. Membranes were then washed with TBS-T (with 0.1 % Tween), incubated with a horseradish peroxidase coupled secondary antibody and developed using enhanced chemiluminescence (ECL, GE Healthcare, Little Chalfont, UK and Super Signal, Thermo Fisher Scientific). Signals were detected with Fusion FX7 (Vilber Lourmat, Marne-la-Vallée, France) and analyzed and quantified using ImageJ.

Biochemical separation of soluble APPsα

Hippocampi were homogenized in tissue homogenization buffer (THB, 20 mM Tris–HCl, pH 7.4; 250 mM Sucrose; 1 mM EDTA; 1 mM EGTA) including phosphatase and protease inhibitors (Roche, Basel, Switzerland)) using a Potter homogenizer. After homogenization, a brief low-speed spin (5000 g, 5 min) was performed to remove remaining tissue fragments. For the detection of the soluble fragments APPsα and APPsβ, a high-speed centrifugation step (60 min at 100,000*g*) was performed and membrane-free supernatant was used for further analysis. Total brain homogenate or supernatant (20 µg protein) was used for SDS-PAGE using 12 % Tris–Tricine gels and electroblotted onto PVDF membrane (BioRad). Western blot signals were detected by enhanced chemiluminescence (Super Signal West Pico; Pierce, Rockford, USA) and imaged using the ChemiDoc Imaging System (BioRad). For quantification, all images were analyzed with the ImageLab software (BioRad).

Elisa

For quantification of APP processing products in brain samples, the following ELISA kits were employed: Human-specific APP β-CTF Assay Kit (IBL, Hamburg, Germany, JP27776), $huAPP_{SWE}$-specific ELISA (IBL, JP27733), V-PLEX Plus Aβ Peptide Panel 1 (6E10) Kit (Meso Scale Discovery, Rockville, USA) detecting at the same time $huAβ_{38}$, $huAβ_{40}$, $huAβ_{42}$, and V-PLEX Plus Aβ Peptide Panel 1 (4G8) Kit (Meso Scale Discovery) detecting hu/$muAβ_{38}$, hu/$muAβ_{40}$, and hu/$muAβ_{42}$. The procedures were performed according to the respective supplier instructions.

Morris water maze

Experiments were performed in a 120-cm-diameter, 50-cm-deep tank filled with opacified water kept at 21 °C and equipped with a 10-cm-diameter platform submerged 1 cm under the water surface. Visual clues

were disposed around the pool as spatial landmarks for the mouse and luminosity was kept at 430 lux. Training consisted of daily sessions (three trials per session) during 5 consecutive days. Start positions varied pseudo-randomly among the four cardinal points. Mean inter-trial interval was 15 min. Each trial ended when the animal reached the platform. A 60-s cutoff was used, after which mice were gently guided to the platform. Once on the platform, animals were given a 30-s rest before being returned to their cage. 72 h after the last training trial (day 8), retention was assessed during probe trial in which the platform was no longer present. Animals were video tracked using Ethovision software (Noldus, Wageningen, the Netherlands) and behavioral parameters (swim speed, traveled distance, latency, percentage of time spent in each quadrant) were automatically calculated. Experiments and statistical evaluation of data were performed by an experimentator blind to genotype and treatment group.

Statistics

Statistical analyses were performed as indicated for the respective experiments. Outliers were detected and rejected using maximum normed residual test (Grubbs' test). In most cases, data were analyzed using non-parametric Mann–Whitney *U* tests excepted for behavioral experiments. Two-way ANOVA with repeated measures were carried out when required by the experimental plan to assess statistical effects. Correlation matrices were generated using non-parametric Spearman rank correlation coefficient. For all analysis, statistical significance was set to a p value <0.05. All analyses were performed using Statistica (StatSoft Inc., Tulsa, USA) or Prism (GraphPad Software, La Jolla, USA).

Electrophysiology

In vitro extracellular recordings were performed on acute hippocampal slices of WT littermates stereotactically injected with AAV-Venus ($N = 5$), APP/PS1ΔE9 mice injected either with AAV-Venus ($N = 4$) or AAV-APPsα virus ($N = 6$) at 8 months of age. Electrophysiological recordings were performed 4–5 months later at an age of 12–13 months. In-between animals were housed in a temperature- and humidity-controlled room with a 12-h light–dark cycle and had access to food and water ad libitum.

Slice preparation

Acute hippocampal transversal slices were prepared from individuals at an age of 12–13 months. Mice were anesthetized with isoflurane and decapitated. The brain was removed and quickly transferred into ice-cold carbogenated (95 % O_2, 5 % CO_2) artificial cerebrospinal fluid (ACSF) containing 125 mM NaCl, 2 mM KCl, 1.25 mM NaH_2PO_4, 2 mM $MgCl_2$, 26 mM $NaHCO_3$, 25 mM glucose. After dissection of the two hemispheres, one was used for Golgi–Cox staining and the other for electrophysiology. The hippocampus was sectioned into 400-µm-thick transversal slices with a vibrating microtome (Leica, VT1200S). Slices were maintained in carbogenated ACSF (125 mM NaCl, 2.mM KCl, 1.25 mM NaH_2PO_4, 2 mM $MgCl_2$, 26 mM $NaHCO_3$, 2 mM $CaCl_2$, 25 mM glucose) at room temperature for at least 1.5 h before transferred into a submerged recording chamber. Before recording, each slice of the AAV-Venus injected animals was proofed for fluorescence expression of Venus in area CA1 and CA3 (Axiovert 35, Zeiss, Oberkochen, Germany). Slices absent of the fluorescence protein in the recording areas were excluded from further analysis.

Extracellular field recordings

Slices were placed in a submerged recording chamber and perfused with carbogenated ACSF (32 °C; 125 mM NaCl, 2 mM KCl, 1.25 mM NaH_2PO_4, 1 mM $MgCl_2$, 26 mM $NaHCO_3$, 2 mM $CaCl_2$, 25 mM glucose) at a rate of 1.2–1.5 ml/min. Field excitatory postsynaptic potentials (fEPSPs) were recorded in stratum radiatum of CA1 region with a borosilicate glass micropipette (resistance 2–4 MΩ) filled with 3 M NaCl at a depth of ~150–200 µm. Monopolar tungsten electrodes were used for stimulating the Schaffer collaterals at a frequency of 0.1 Hz. Stimulation intensity was adjusted to 40 % of maximum fEPSP slope for 20 min baseline recording. LTP was induced by applying theta-burst stimulation (TBS: 10 trains of 4 pulses at 100 Hz in an 200 ms interval, repeated 3 times). Basal synaptic transmission properties were analyzed via input–output (IO) measurements and short-term plasticity was examined via paired pulse facilitation (PPF). The IO measurements were performed either by application of defined current values (25–175 µA) or by adjusting the stimulus intensity to certain fiber volley (FV) amplitudes (0.1–0.7 mV). PPF was performed by applying a pair of two closely spaced stimuli in different inter-stimulus intervals (ISI) ranging from 10 to 160 ms. After completion of electrophysiological measurements, we performed anti-HA staining to monitor HA-APPsα expression or Venus expression (blind to genotype). Only well-transduced sections as evidenced by either Venus immunofluorescence or HA staining were included in the electrophysiological data analysis.

Dendrite and spine analysis

Golgi–Cox staining

Golgi staining was done using the Rapid Golgi Staining Kit (FD NeuroTechnologies, Columbia, USA) according to the manufacturer's instructions. All procedures were performed under dark conditions. One hemisphere of each mouse was used for electrophysiology and the other one for Golgi–Cox staining. Hemispheres were immersed in 2 ml mixtures of equal parts of kit solutions A and B and stored at RT for 2 weeks. Afterwards, brain tissues were stored in solution C at 4 °C for at least 48 h and up to 7 days before sectioning. Solutions AB and C were renewed within the first 24 h. Coronal sections of 200 µm were cut with a vibrating microtome (Leica, VT1200S) while embedded in 2 % Agar in 0.1 M PBS. Each section was mounted with Solution C on an adhesive microscope slide pre-coated with 1 % gelatin/0.1 % chromalaun on both sides and stained according to the manufacturer´s protocol with the exception that ApliClear (AppliChem) was used instead of xylene. Finally, slices were cover-slipped with Permount (Thermo Fisher Scientific).

Imaging and analysis of spine density in Golgi–Cox stained slices

Imaging of second- or third-order dendritic branches of hippocampal pyramidal neurons of area CA3 and CA1 was done with an Axioplan 2 imaging microscope (Zeiss) using a 63× oil objective and a z-stack thickness of 0.5 µm under reflected light. The number of spines was determined per micrometer of dendritic length (in total 100 µm) at apical and basal compartments using ImageJ (1.48v, National Instruments of Health, USA). At minimum four animals per genotype and four neurons per animal were analyzed blinded to genotype and injected virus.

Data analysis

Data of electrophysiological recordings were collected, stored and analyzed with LABVIEW software (National Instruments, Austin, USA). The initial slope of fEPSPs elicited by stimulation of the Schaffer collaterals was measured over time, normalized to baseline and plotted as average ± SEM. Analysis of the PPF data was performed by calculating the ratio of the slope of the second fEPSP divided by the slope of the first one and multiplied by 100. Data of Golgi–Cox staining were analyzed using GraphPad Prism (Version, 5.01) software. Spine density is expressed as mean ± SEM. Differences between genotypes were detected with one-way analysis of variance (ANOVA) followed by Bonferroni's post hoc test using IBM SPSS Statistics 21.

Fig. 1 Widespread expression of APPsα throughout the hippocampus and in parahippocampal cortex in AAV-APPsα injected APP/PS1ΔE9 mice. APP/PS1ΔE9 and non-transgenic littermate control mice (LM) were injected either with AAV-Venus or AAV-APPsα at 12 months of age and sacrificed at 17 months of age. (LM: AAV-Venus $n = 3$, AAV-APPsα $n = 4$; APP/PS1ΔE9 mice: AAV-Venus $n = 8$, AAV-APPsα $n = 8$; all males). **a** Schematic representation of AAV9 constructs enabling the neuron-specific expression of Venus (Control) and HA-tagged APPsα. ITR: inverted terminal repeat; SP: APP signal peptide; HA: Human influenza hemagglutinin tag; WPRE: Woodchuck hepatitis virus posttranscriptional regulatory element. **b** Scheme of the hippocampus with coordinates of the two injection sites (*red stars*). **c** High magnification of the hippocampus of an APP/PS1ΔE9 mouse injected with the AAV-APPsα. APPsα is detectable throughout the hippocampus and the proximal cortex. *Scale bar*, 500 µm. Injection sites indicated by *white stars*. **d** Scheme representing anteroposterior coordinates of coronal sections depicted in **e–h**. **e–h** Immunostaining of APPsα (anti-HA tag, *red*) and NeuN (*green*) at different anteroposterior coordinates. *Scale bar*, 500 µm. **i–l** Double immunostaining of CA1 pyramidal cells from the area boxed in **c** expressing APPsα (anti-HA tag, *red*) and specific neuronal (NeuN, *green*, **i**, **j**), microglial (Iba1, *green*, **k**) or astrocytic (GFAP, *green*, **l**) markers. *Scale bar*, 50 µm (**i**, **k**, **l**), 20 µm (**j**). Note that AAV-mediated APPsα expression is restricted to neurons. **m** Western blot analysis of Venus, muAPP and HA-muAPPsα expression in APP/PS1ΔE9 and LM hippocampi of mice injected with AAV-Venus or AAV-APPsα vectors. Note that antibody m3.2 is specific for muAPP and recognizes endogenous muAPP and HA-muAPPsα (see also Fig. S1 for antibody epitopes) **n** Analysis of extracellular muAPPsα in APP-KO mice injected with AAV-APPsα ($n = 4$) in comparison to endogenous muAPPsα produced in non-injected WT mice ($n = 4$). *Left panels* Homogenates of hippocampi were subjected to ultracentrifugation (UC) to separate soluble proteins. The C-terminal anti-APP antibody (c1/6.1) was used to confirm the separation of soluble APPsα from membrane bound full-length APP. **o** Quantification of muAPPsα (m3.2 immuoreactivity) normalized to β-actin. Data represent mean ± SEM, Student's *t* test, $^{**}p < 0.01$

Results

AAV-APPsα injection mediates efficient and long-lasting neuronal expression of APPsα in the hippocampus of APP/PS1ΔE9 mice

To assess the therapeutic potential of APPsα, we used AAV-mediated overexpression of APPsα in the brain of aged (12-month-old) APP/PS1ΔE9 mice. APP/PS1ΔE9 mice show progressive plaque deposition starting at about 5–6 months of age and highly abundant plaques are observed at 12 months of age [38, 87]. AAV9 vectors expressing either Venus or codon-optimized HA-tagged murine APPsα (HA-APPsα) under the control of the neuronal synapsin promoter (further referred to as AAV-Venus and AAV-APPsα, Fig. 1a) were bilaterally injected into the stratum lacunosum moleculare region of the dorsal hippocampus and into

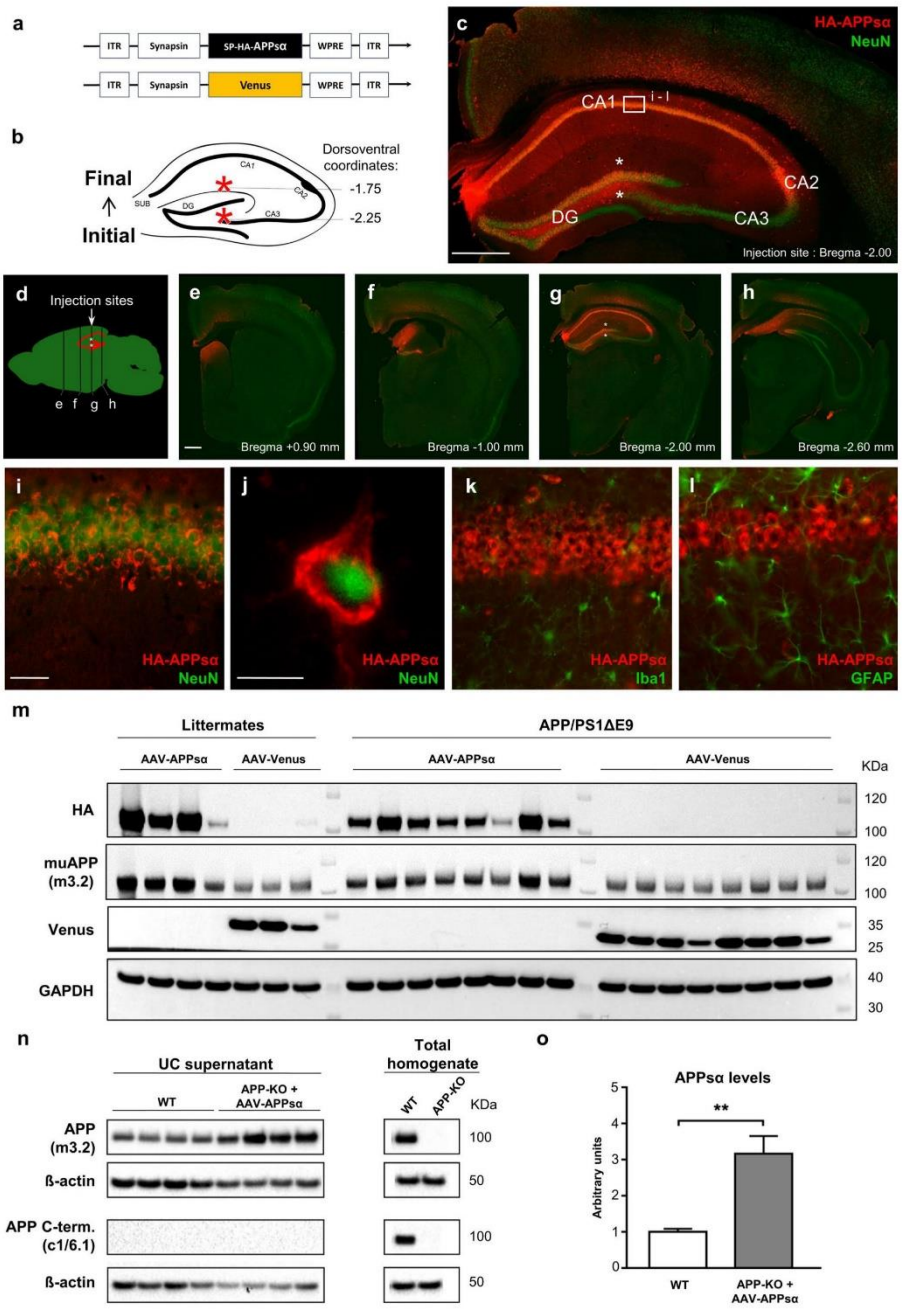
a
ITR
Synapsin
SP-HA-APPsα
WPRE
ITR
ITR
Synapsin
Venus
WPRE
ITR
b
Final
Initial
Dorsoventral coordinates:
-1.75
-2.25
SUB
DG
CA1
CA2
CA3
c
HA-APPsα
NeuN
CA1
i - l
CA2
DG
CA3
Injection site : Bregma -2.00
d
Injection sites
e f g h
e
Bregma +0.90 mm
f
Bregma -1.00 mm
g
Bregma -2.00 mm
h
Bregma -2.60 mm
i
HA-APPsα
NeuN
j
HA-APPsα
NeuN
k
HA-APPsα
Iba1
l
HA-APPsα
GFAP
m
Littermates
APP/PS1ΔE9
AAV-APPsα
AAV-Venus
AAV-APPsα
AAV-Venus
KDa
HA
muAPP (m3.2)
Venus
GAPDH
120
100
120
100
35
25
40
30
n
UC supernatant
Total homogenate
WT
APP-KO + AAV-APPsα
WT
APP-KO
KDa
APP (m3.2)
ß-actin
APP C-term. (c1/6.1)
ß-actin
100
50
100
50
o
APPsα levels
**
Arbitrary units
0
1
2
3
4
5
WT
APP-KO + AAV-APPsα

the dentate gyrus (Fig. 1b) of 12-month-old male APP/PSΔE9 mice. To monitor vector-mediated Venus and APPsα expression, mice were sacrificed 5 months after injection. Immunohistochemistry using an HA-tag-specific antibody revealed widespread expression of HA-APPsα not only in the hippocampus, but also in the cortical layers above the injected hippocampus (Fig. 1c). Analysis of serial anteroposterior coronal sections demonstrated widespread HA-APPsα immunoreactivity (over 3.5 mm) in the hippocampus from −2.6 mm posterior to +0.9 mm anterior from the injection site (Fig. 1d–h) and in the adjacent cortex. More detailed analysis showed prominent expression of vector-mediated HA-APPsα in the pyramidal cells of the subiculum, in the CA1, CA2 regions and in granular neurons of dentate gyrus (Fig. 1c). Within the CA3 subfield HA-APPsα expression was detectable but considerably lower. As APPsα expression was driven by the neuron-specific synapsin promoter, HA-APPsα expression was restricted to neuronal cells as revealed by double immunostaining against NeuN (Fig. 1i, j). Consistently, no expression was detectable in microglia (Iba1, Fig. 1k) or in astrocytes (GFAP, Fig. 1l). The AAV-Venus expression pattern was largely similar to that of AAV-APPsα. Western blot analysis of hippocampal extracts confirmed vector-mediated HA-APPsα protein expression in all injected animals. Comparable levels of either HA-APPsα or Venus were detected in hippocampi of injected APP/PS1ΔE9 mice or non-transgenic littermates, respectively (Fig. 1m). To quantify vector-mediated muAPPsα overexpression blots were also probed with an antibody (m3.2) directed against a mouse-specific APP epitope located between the β- and α-secretase site (see middle panel in Fig. 1m; see also Fig. S1 for antibody epitopes) that detects endogenous full-length muAPP, endogenously secreted muAPPsα and vector-derived AAV-muAPPsα. This analysis indicated an increase in muAPP species (m3.2 immunoreactivity) of about 1.73 ± 0.13 fold ($p < 0.0001$, t test) in AAV-APPsα injected mice ($n = 12$) as compared to the control group receiving AAV-Venus ($n = 11$). This analysis does, however, not allow to distinguish between soluble extracellular APPsα and cell bound muAPP species (including transmembrane muAPP and muAPPsα still present in compartments of the secretory machinery). To specifically determine the amount of soluble muAPPsα that is produced by AAV-APPsα injection, we employed APP knockout mice. Four weeks after injection hippocampi of injected APP-KO and non-injected WT mice were dissected, homogenized and ultracentrifugation was used to separate AAV encoded secreted, soluble APPsα from cell bound APPsα. Comparison to wild-type mice indicated that AAV-mediated soluble APPsα expression is increased by about 3.1-fold ($p < 0.01$, t test) in hippocampi of AAV-vector injected mice as compared to endogenous soluble muAPPsα (Fig. 1o) in wild-type mice. In summary, we demonstrate that our AAV-based approach leads to efficient and long-lasting APPsα expression in the hippocampus and adjacent cortex.

Fig. 2 APPsα overexpression enhances Morris water maze performance in WT mice and rescues the spatial memory deficit of APP/PS1ΔE9 mice. Transgenic APP/PS1ΔE9 mice ($n = 8$ per group) or littermate (LM) controls ($n = 3$–4 per group) were either injected with AAV-Venus or AAV-APPsα vectors at 12 months of age and tested 2 months later at 14 months of age. **a** Training phase consisted of daily sessions (three trials per session: T1, T2 and T3) during five consecutive days (D1–D5). 72 h (D8) after the last trial the platform was removed and memory retention was assessed during the probe trial. *Insert* water maze configuration during training sessions. PF: platform (*white*); TQ: target quadrant (*small segment*); OQ: other quadrants (*large segment*). **b** Swim speed and **c** escape latency of littermate controls or APP/PS1ΔE9 mice injected either with AAV-Venus or AAV-APPsα. Swim speed was similar between the different groups (2-way ANOVA: group effect: $F_{3,100} = 2.40$; ns; time effect: $F_{4,100} = 1.41$; ns; group × time interaction: $F_{12,100} < 1$; ns). **c** Littermates injected with AAV-APPsα showed improved performance, as indicated by reduced escape latency (2-way ANOVA: time effect: $F_{4,100} = 7.138$; $p < 0.0001$; group effect: $F_{3,100} = 7.247$; $p = 0.0002$, followed by Tukey post hoc test: APP/PS1ΔE9 mice injected with AAV-APPsα versus each of the other groups, $p < 0.013$). **d** Probe trial performance at 72 h. 2-way ANOVA, group effect: $F_{3,17} = 3.356$; $p < 0.04$; quadrant effect: $F_{1,17} = 23.54$; $p < 0.007$; group × quadrant interaction effect: $F_{3,17} = 3.356$; $p < 0.04$. APP/PS1ΔE9 mice injected with AAV-Venus were impaired in comparison to littermate mice injected with AAV-Venus (Tukey post hoc test: $p = 0.023$) confirmed by no preference for the trained target quadrant. Strikingly, AAV-APPsα treated APP/PS1ΔE9 mice spent more time in the target quadrant compared to APP/PS1ΔE9 mice injected with AAV-Venus (Tukey post hoc test: $p = 0.017$). Data represent mean ± SEM and were analyzed by 2-way ANOVA (genotype and group as factors) with repeated measures followed by Tukey post hoc test. $^*p < 0.05$ **e** Representative occupancy plots during the probe trial show a more random search strategy for AAV-Venus injected APP/PS1ΔE9 mice. Note that AAV-APPsα injected transgenic mice show directionality towards the platform (indicated by *segment*) similar to littermate controls. Values represent mean ± SEM

AAV-APPsα treatment rescues the spatial memory impairment of APP/PS1ΔE9 mice

To analyze the consequences of AAV-APPsα or AAV-Venus injection for spatial learning and memory, mice were tested in the Morris water maze place navigation task (Fig. 2). To this end, transgenic APP/PS1ΔE9 mice ($n = 8$ per group) or non-transgenic littermate controls ($n = 3$–4 per group) were injected either with AAV-Venus or AAV-APPsα vectors at 12 months of age and tested 2 months later at 14 months of age. Swim speed was comparable in all groups of animals (Fig. 2b) over the 5 days of training, thus excluding impairments in motor performance. While all four groups of mice did show learning, as evidenced by reduced latency to reach the platform over the 5 days of training, we observed a group effect resulting from an overall significantly increased performance in non-transgenic littermates that had received AAV-APPsα (Fig. 2c). Injection of AAV-APPsα did not, however, improve the performance of

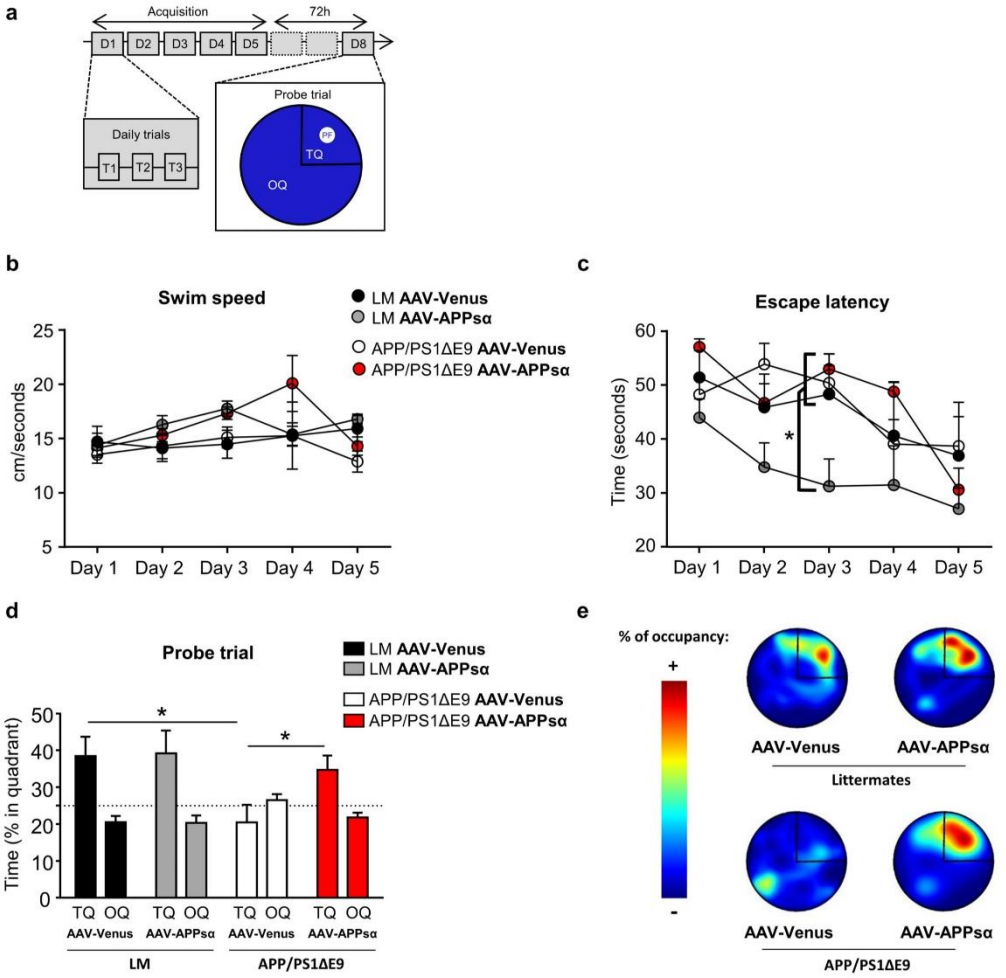

APP/PS1ΔE9 mice (Fig. 2c). Similar results were obtained when analyzing the path length to reach the platform (data not shown). During the probe trial that assesses spatial reference memory and was conducted 72 h after the last trial of training APP/PS1ΔE9 mice injected with AAV-Venus were strongly impaired (Fig. 2d) in comparison to littermate mice injected with AAV-Venus and showed no preference for the trained target quadrant (Fig. 2d; paired *t* test: $t_7 = 0.96$; $p = 0.37$). Strikingly, APP/PS1ΔE9 mice that had been injected with AAV-APPsα showed a clear preference for the trained target quadrant (Fig. 2d; paired *t* test: $t_7 = 2.516$; $p = 0.045$), that was statistically indistinguishable from the performance of littermate controls (Fig. 2d; $p > 0.84$, 2-way ANOVA followed by Tukey's post hoc test). To get further insight into the search strategy of individual mice we also analyzed spatial occupancy plots of individual mice during the probe trial (Fig. 2e). Transgenic APP/PS1ΔE9 mice injected with control vector frequently showed a rather random occupancy of the swimming arena and no preference for the trained target quadrant, indicating an impaired spatial reference memory 3 days after training. In contrast, occupancy plots of AAV-APPsα injected transgenic mice revealed clear directionality towards the trained platform similar to non-transgenic littermates injected with AAV-Venus or AAV-APPsα (Fig. 2e). Thus, vector-mediated APPsα expression rescued the spatial memory

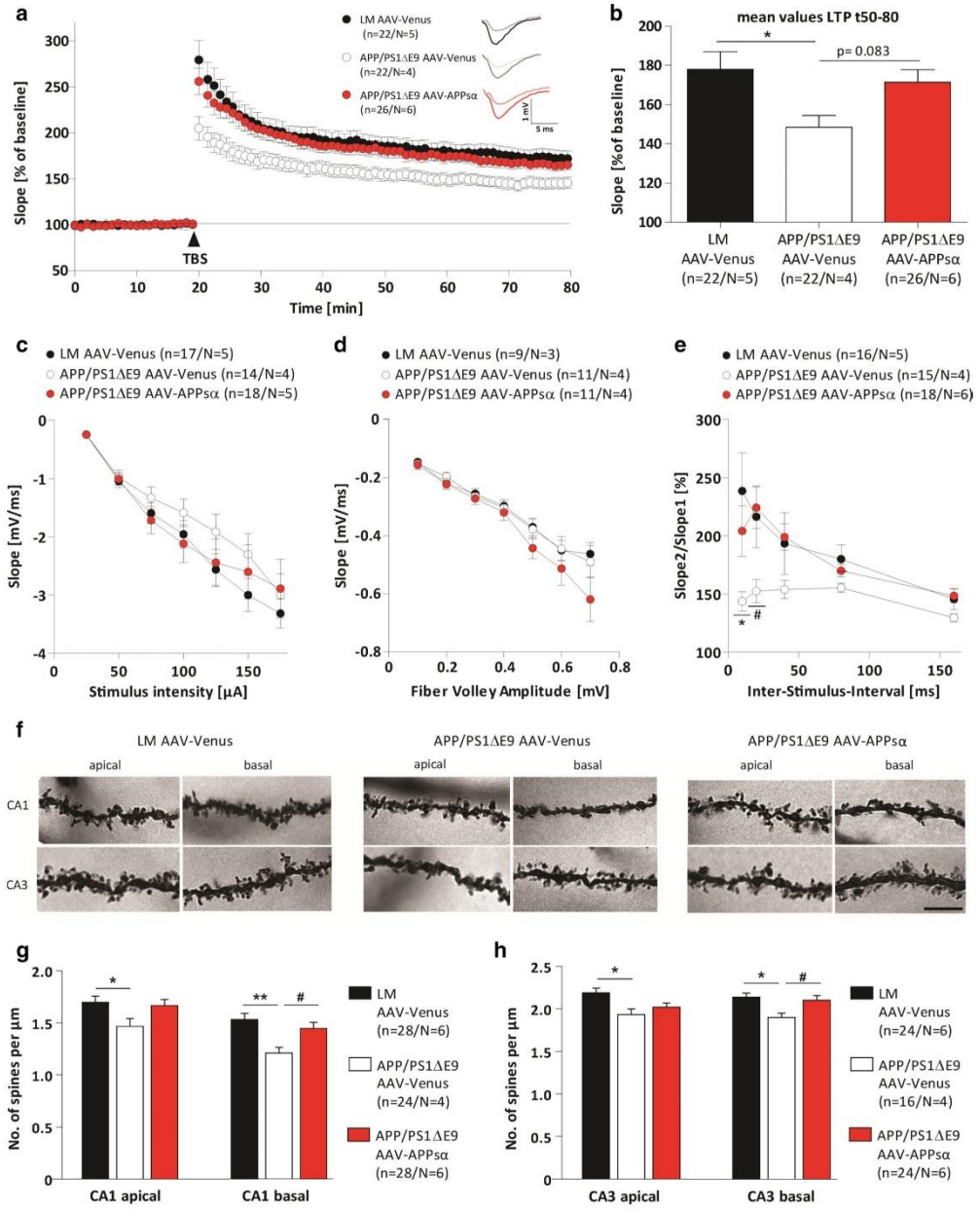
a
LM AAV-Venus (n=22/N=5)
APP/PS1ΔE9 AAV-Venus (n=22/N=4)
APP/PS1ΔE9 AAV-APPsα (n=26/N=6)
1 mV
5 ms
Slope [% of baseline]
TBS
Time [min]
b
mean values LTP t50-80
*
p= 0.083
Slope [%of baseline]
LM AAV-Venus (n=22/N=5)
APP/PS1ΔE9 AAV-Venus (n=22/N=4)
APP/PS1ΔE9 AAV-APPsα (n=26/N=6)
c
LM AAV-Venus (n=17/N=5)
APP/PS1ΔE9 AAV-Venus (n=14/N=4)
APP/PS1ΔE9 AAV-APPsα (n=18/N=5)
Slope [mV/ms]
Stimulus intensity [µA]
d
LM AAV-Venus (n=9/N=3)
APP/PS1ΔE9 AAV-Venus (n=11/N=4)
APP/PS1ΔE9 AAV-APPsα (n=11/N=4)
Slope [mV/ms]
Fiber Volley Amplitude [mV]
e
LM AAV-Venus (n=16/N=5)
APP/PS1ΔE9 AAV-Venus (n=15/N=4)
APP/PS1ΔE9 AAV-APPsα (n=18/N=6)
Slope2/Slope1 [%]
Inter-Stimulus-Interval [ms]
f
LM AAV-Venus
APP/PS1ΔE9 AAV-Venus
APP/PS1ΔE9 AAV-APPsα
apical
basal
CA1
CA3
g
No. of spines per µm
CA1 apical
CA1 basal
LM AAV-Venus (n=28/N=6)
APP/PS1ΔE9 AAV-Venus (n=24/N=4)
APP/PS1ΔE9 AAV-APPsα (n=28/N=6)
h
No. of spines per µm
CA3 apical
CA3 basal
LM AAV-Venus (n=24/N=6)
APP/PS1ΔE9 AAV-Venus (n=16/N=4)
APP/PS1ΔE9 AAV-APPsα (n=24/N=6)

◀**Fig. 3** APP/PS1ΔE9 mice reveal structural and functional synaptic impairments that are ameliorated by APPsα expression. **a**, **b** LTP was induced by TBS at hippocampal CA3-CA1 synapses after 20 min baseline recordings (*arrowhead*). Acute slices of AAV-Venus injected APP/PS1ΔE9 animals (*open circles*) exhibited significant lower induction and maintenance of LTP compared to littermate controls (LM, black circles) showing similar expression of Venus (averaged potentiation minutes t50–80: 148.47 ± 6.04 % vs. 178.01 ± 8.98 %, $p = 0.021$). Viral expression of APPsα (*red circles*) restored potentiation after TBS (171.48 ± 6.29 %) in transgenic animals and resulted in an LTP curve progression comparable to that of LM controls. The LTP induction rate is shown as percentage % of mean baseline slope, n = number of slices, N = number of mice. **c**, **d** Input–Output strength of all AAV-injected mice showed no alterations between genotypes at any fiber volley (FV) amplitude or stimulus intensity tested. **e** Altered PPF at the 10 ms ISI revealed a significant impairment in the pre-synapse of APP/PS1ΔE9 mice injected with AAV-Venus in comparison to LM controls ($^{*}p = 0.030$) that was restored after AAV-APPsα injection ($^{\#}p = 0.047$). **f** Detailed segments of 2nd or 3rd order dendritic branches of apical and basal dendrites of CA1 and CA3 neurons after Golgi–Cox staining, *scale bar* 8 µm. **g** APP/PS1ΔE9 Venus injected mice had significantly less spines at apical ($p = 0.043$) and basal ($p = 0.002$) dendrites in comparison to their littermate controls. APPsα overexpression partially restored the spine density deficit at apical and completely at basal compartments ($p = 0.019$). **h** Reduced spine density at CA3 apical ($p = 0.014$) and basal ($p = 0.011$) dendritic segments of APP/PS1ΔE9 AAV-Venus injected mice that is partially rescued at apical and completely at basal dendrites ($p = 0.039$) by APPsα. N = number of animals, n = number of neurons, Data represent mean ± SEM and were analyzed by one-way ANOVA followed by Bonferroni's post hoc test. Significant differences between littermates and APP/PS1ΔE9 animals injected with AAV-Venus are indicated by *asterisk*; *ash* indicates comparison between APP/PS1ΔE9 animals injected by AAV-Venus or AAV-APPsα

impairment in aged APP/PS1ΔE9 mice despite established plaque deposition.

Impaired synaptic plasticity and reduced spine density of APP/PS1ΔE9 mice are rescued by AAV-APPsα expression

Having established that AAV-APPsα expression restored the spatial memory deficits of APP/PS1ΔE9 mice we evaluated whether these improvements were also reflected at the functional neuronal network level. We analyzed synaptic plasticity which is considered to represent the basis of newly formed declarative memory, 4–5 months after AAV injection at an age of 12–13 months. To this end, we induced long-term potentiation (LTP) at the Schaffer collateral to CA1 pathway by theta-burst stimulation (TBS) after baseline recording (Fig. 3a). Consistent with our previous results in non-injected APP/PS1ΔE9 mice [32], AAV-Venus injected APP/PS1ΔE9 mice exhibited significantly lower induction and maintenance of LTP ($n = 22$ slices), as compared to AAV-Venus injected littermate controls ($n = 22$, Fig. 3a). Non-transgenic control slices showed at the stable phase of LTP (t50–80 min after TBS) a potentiation of 178.01 ± 8.98 %, that was significantly reduced to only 148.47 ± 6.04 % in AAV-Venus injected APP/PS1ΔE9 mice (Fig. 3b; $p = 0.021$, 1-way ANOVA followed by Bonferroni's post hoc test). In contrast, the LTP curve recorded from AAV-APPsα injected APP/PS1ΔE9 slices ($n = 26$) closely overlapped with and was statistically indistinguishable (1-way ANOVA for t50–80, $p > 1$) from that of non-transgenic littermate controls (Fig. 3a). AAV-mediated expression of APPsα largely ameliorated LTP deficits of APP/PS1ΔE9 mice as evidenced by nearly identical average potentiation at t50–80 in AAV-APPsα treated APP/PS1ΔE9 mice (171.48 ± 6.29 %) and littermate controls (178.01 ± 8.98 %) receiving AAV-Venus control virus (Fig. 3b). While basal synaptic transmission was comparable in all groups (Fig. 3c, d), short-term synaptic plasticity evaluated by paired pulse facilitation (PPF, Fig. 3e) was significantly impaired in APP/PS1ΔE9 mice. Transgenic animals injected with AAV-Venus showed an overall lowered response towards the second stimulus in the PPF paradigm, reaching significance at an inter-stimulus interval (ISI) of 10 ms compared to littermate controls ($p = 0.03$; 1-way ANOVA followed by Bonferroni's post hoc test). Strikingly, AAV-APPsα treatment completely rescued presynaptic functionality in APP/PS1ΔE9 animals, as evidenced by PPF values statistically indistinguishable from littermate controls and significantly different from that of AAV-Venus injected transgenic animals [$p(ISI_{20ms}) = 0.047$; Fig. 3e].

Next, we evaluated spine density as a correlate of excitatory synapses in the same set of animals as used for electrophysiology. Previous studies had indicated reduced spine density in various AD mouse models, presumably due to Aβ-mediated toxic effects (reviewed in [73]). Spine density of basal and mid-apical dendritic segments of hippocampal CA1 and CA3 pyramidal cells was assessed using Golgi staining (Fig. 3f). Consistent with the literature, we found an overall reduction in spine density of APP/PS1ΔE9 mice at both dendritic compartments of CA1 and CA3 neurons in comparison to littermate controls similarly injected with AAV-Venus. At CA1 neurons, the effect was even more pronounced in the basal ($p = 0.002$, 1-way ANOVA followed by Bonferroni´s post hoc test) than in the apical ($p = 0.04$) dendritic segment (Fig. 3g). Analysis of CA3 neurons revealed significantly fewer spines in both basal ($p = 0.01$) and apical ($p = 0.014$) dendritic segments when comparing AAV-Venus expressing APP/PS1ΔE9 mice and non-transgenic littermates controls. Importantly, AAV-APPsα overexpression partially restored spine density in apical compartments of CA1 ($n = 28$) and CA3 segments ($n = 24$). A complete rescue of the spine density deficit was achieved in basal dendrites of CA1 ($p = 0.019$, Fig. 3g) and CA3 dendrites ($p = 0.039$, Fig. 3h) of APP/PS1ΔE9 mice. Together, these data indicate that APPsα expression

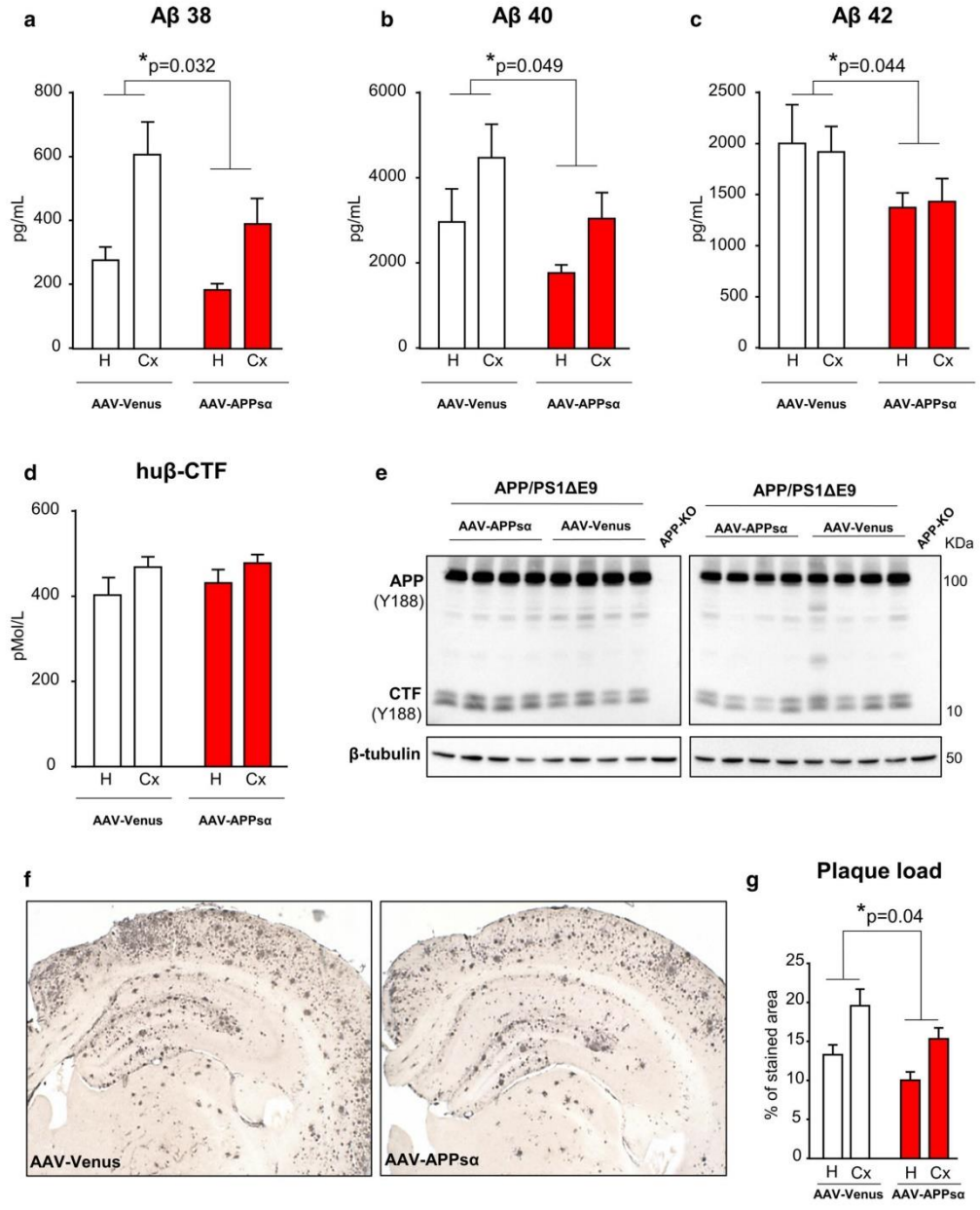
a
Aβ 38
*p=0.032
pg/mL
800
600
400
200
0
H Cx H Cx
AAV-Venus
AAV-APPsα
b
Aβ 40
*p=0.049
pg/mL
6000
4000
2000
0
H Cx H Cx
AAV-Venus
AAV-APPsα
c
Aβ 42
*p=0.044
pg/mL
2500
2000
1500
1000
500
0
H Cx H Cx
AAV-Venus
AAV-APPsα
d
huβ-CTF
pMol/L
600
400
200
0
H Cx H Cx
AAV-Venus
AAV-APPsα
e
APP/PS1ΔE9
AAV-APPsα
AAV-Venus
APP-KO
APP/PS1ΔE9
AAV-APPsα
AAV-Venus
APP-KO
KDa
APP
(Y188)
CTF
(Y188)
β-tubulin
100
10
50
f
AAV-Venus
AAV-APPsα
g
Plaque load
*p=0.04
% of stained area
25
20
15
10
5
0
H Cx H Cx
AAV-Venus
AAV-APPsα

◀ **Fig. 4** AAV-APPsα injection decreases Aβ and plaques load. **a–c** Quantification (4G8 based MSD immunoassay detecting both mu/huAβ species) of TBS soluble Aβ38 (group effect: $F_{1,14} = 5.110$, $p = 0.032$ (−35 %), Aβ40 [group effect: $F_{1,14} = 4215$, $p = 0.049$ (−36 %)] and Aβ42 (group effect: $F_{1,14} = 4.461$, $p = 0.044$ (−28 %); region effect: Aβ38 $F_{1,14} = 15.22$, $p = 0.0005$, Aβ40 $F_{1,14} = 4.760$, $p = 0.0377$, Aβ40 $F_{1,14} < 1$, ns; group × region interaction effect: $F_{1,14} < 1$, ns) in hippocampus and cortex of APP/PS1ΔE9 mice. Note that AAV-APPsα injected animals show significantly reduced levels of Aβ in both anatomical regions analyzed (hippocampus and cortex). **d** ELISA quantification of huβ-CTF in hippocampus (H) and cortex (Cx) of APP/PS1ΔE9 mice. No difference was detectable between AAV-Venus and AAV-APPsα injected animals. **e** Western blot analysis showing unaltered CTF level in the hippocampus of AAV-APPsα or AAV-Venus injected APP/PS1ΔE9 mice. For quantification CTF signal intensities (C-terminal antibody Y188, see also Fig. S1 for epitope) were normalized to β-tubulin ($p > 0.05$, ns, $n = 8$/group, t test). **f** Representative images of hippocampus and cortex of APP/PS1ΔE9 mice injected either with AAV-Venus or AAV-APPsα. **g** Quantification of 4G8 immunolabeled area in hippocampus and cortex [2-way ANOVA: group effect: $F_{1,13} = 5.50$, $p = 0.04$ (−24 %); region effect: $F_{1,13} = 22.89$, $p = 0.0004$; group × region interaction effect: $F_{1,13} < 1$, ns]. Note that 4G8 immunoreactive plaque area is significantly reduced in AAV-APPsα treated animals. Number of animals $n = 8$/group. Data represent mean ± SEM and were analyzed by 2-way ANOVA (Genotype, group and region as factors) with repeated measures followed by Tukey post hoc test. *$p < 0.05$

substantially ameliorates both structural and functional synaptic impairments of aged AD model mice.

AAV-APPsα expression decreases Aβ levels and plaque deposition in aged APP/PS1dE9 mice

APPsα had previously been reported to bind to BACE-1 and thereby reduce Aβ production [60]. We therefore evaluated if beneficial effects of AAV-APPsα overexpression on synaptic plasticity and cognitive function were associated with reduced amyloidogenic processing of APP. Employing a sensitive electrochemiluminescence ELISA, we quantified the products of amyloidogenic metabolism Aβ, secreted APPsβ and β-CTF (APP C-terminal fragment produced by β-secretase cleavage) in the cortex (Cx) and hippocampus (H) of 17 months old APP/PS1ΔE9 mice ($n = 8$/group), 5 months after viral vector injection. Using an (4G8 based) ELISA that detects both human and mouse Aβ species, we observed a significant decrease in soluble Aβ40 (reduced by about 36 % vs control, $p = 0.049$, 2-way ANOVA followed by Tukey's post hoc test, Fig. 4b) and, Aβ42 (−28 %, $p = 0.044$, Fig. 4c) in both cortex and hippocampus of APP/PS1ΔE9 mice injected with AAV-APPsα vector, as compared to AAV-Venus control injections (Fig. 4a–c). In addition, we also assessed specifically human Aβ species in transgenic mice employing a (6E10 based) human-specific ELISA (Fig. S2). We found a comparable reduction of huAβ42 (−33 %, $p = 0.04$, Fig. S2c) in both cortex and hippocampus of APP/PS1ΔE9 mice injected with AAV-APPsα vector, as compared to AAV-Venus control injections. Similarly, we found a trend towards decreased amounts of huAβ38 and huAβ40 that did, however, not reach statistical significance (Fig. S2a, b). Consistent with previous data [65] endogenous Aβ levels in non-transgenic littermates were much lower (Fig. S2). Upon AAV-APPsα injection, muAβ40 and muAβ42 were decreased, but not significantly different from Aβ levels of AAV-Venus injected littermate controls (Fig. S2d–f). In contrast to the reduction of Aβ, the amount of secreted transgene derived huAPPsβ-$_{SWE}$ that was assessed by ELISA was not significantly different in APP/PS1ΔE9 mice injected with AAV-APPsα vector, as compared to control injected mice (Fig. S2g). Similarly, we found no significant alterations in human β-CTF levels measured by ELISA (Fig. 4d) or CTFs measured by Western blot analysis (Fig. 4c) in APP/PS1ΔE9 mice injected with AAV-APPsα or control vector. To assess the impact of APPsα overexpression on amyloid deposition, we used 4G8 immunostaining to quantify the area covered by plaques both in the hippocampus and cortex of 17-month-old APP/PS1ΔE9 mice injected with viral vectors (Fig. 4f, g). Interestingly, AAV-APPsα injection ($n = 8$) resulted in a significantly reduced plaque area both in cortex and hippocampus as compared to AAV-Venus injected controls ($p = 0.04$, 2-way ANOVA followed by Tukey's post hoc test, Fig. 4g). Together, these results indicate that AAV-mediated APPsα overexpression moderately reduces both Aβ generation and amyloid plaque load in APP/PS1ΔE9 mice not only in the AAV-injected hippocampus but also in distant cortical areas.

AAV-APPsα induces microglia recruitment and activation in the vicinity of amyloid plaques

Accumulation of amyloid plaques in APP/PS1ΔE9 mice has previously been shown to be accompanied by microgliosis and astrocytosis notably at advanced stages of plaque pathology [41, 62]. Here, we evaluated the expression of GFAP (as an astrocyte-specific marker) and Iba1 (as a microglial marker) by Western blot analysis (Fig. 5a, b) and IHC (Fig. 5c–h) in the hippocampus of 17-month-old APP/PS1ΔE9 mice treated either with AAV-APPsα or control vector. While no significant difference was detectable for the astroglial marker GFAP, AAV-APPsα treatment lead to a significant increase in Iba1 expression (about +44 %; t test, $p = 0.003$; Fig. 5a, b), as compared to AAV-Venus control injections. Staining of brain sections further confirmed these data (Fig. 5c, d) at the cellular level. We went on and quantified GFAP and Iba1 immunoreactivity around amyloid plaques in the hippocampus. Consistent with Western blot analysis, GFAP immunoreactivity was not affected by AAV-APPsα injection (Fig. 5c, e). In contrast, the reduction of amyloid deposits observed after injection

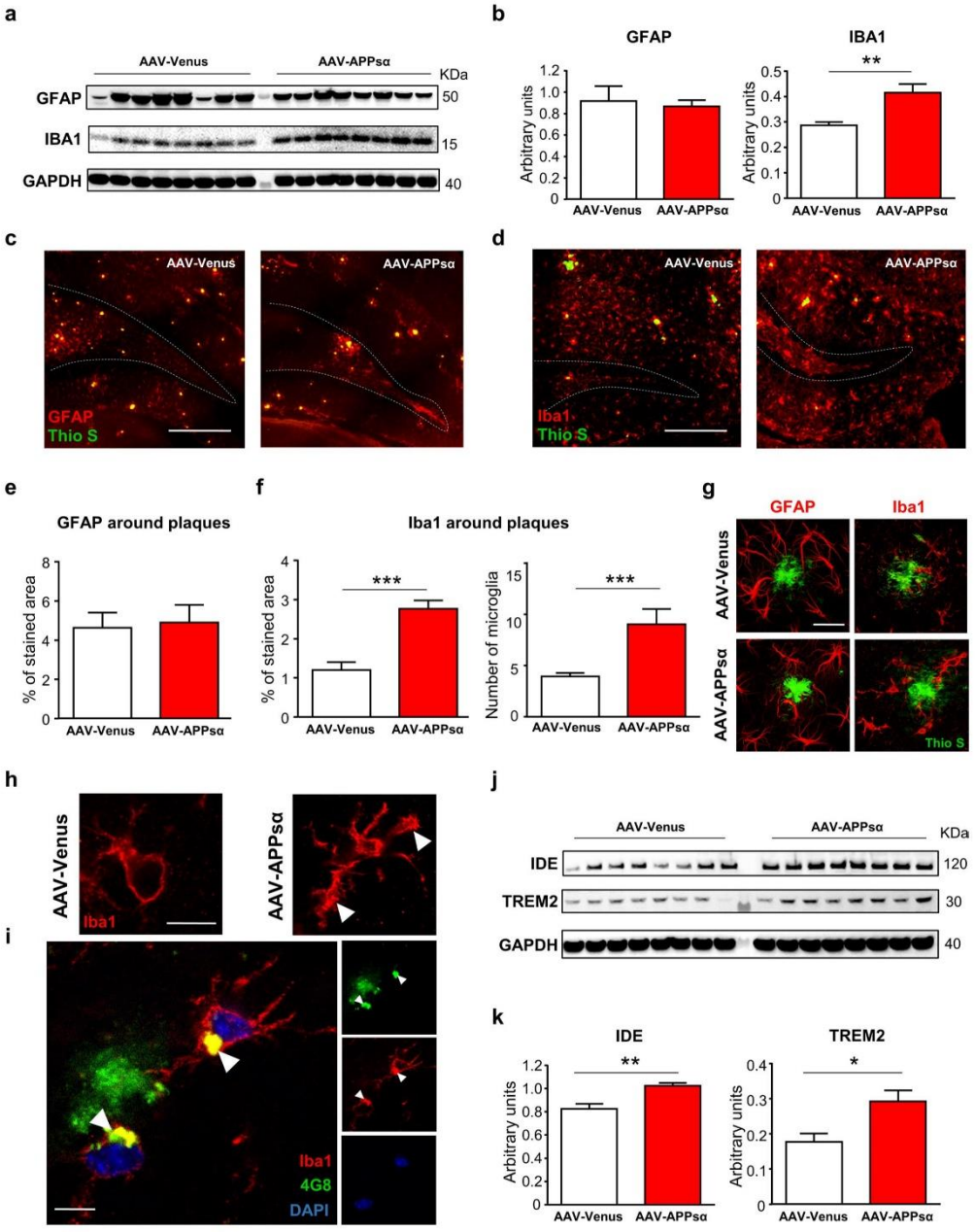
a
AAV-Venus
AAV-APPsα
KDa
GFAP
IBA1
GAPDH
50
15
40
b
GFAP
IBA1
Arbitrary units
**
AAV-Venus
AAV-APPsα
c
AAV-Venus
AAV-APPsα
GFAP
Thio S
d
AAV-Venus
AAV-APPsα
Iba1
Thio S
e
GFAP around plaques
% of stained area
f
Iba1 around plaques
% of stained area
***
Number of microglia
g
GFAP
Iba1
AAV-Venus
AAV-APPsα
Thio S
h
AAV-Venus
AAV-APPsα
Iba1
i
Iba1
4G8
DAPI
j
AAV-Venus
AAV-APPsα
KDa
IDE
TREM2
GAPDH
120
30
40
k
IDE
TREM2
Arbitrary units
**
*

◀**Fig. 5** AAV-APPsα promotes microglia recruitment around plaques in APP/PS1ΔE9 mice. **a**, **b** Western blot analysis showing the expression of GFAP and Iba1 in the hippocampus of AAV-Venus or AAV-APPsα injected APP/PS1ΔE9 mice ($n = 8$/group). **b** For quantification signal intensities were normalized to GAPDH used as a loading control. AAV-APPsα treatment specifically increased Iba1 (microglial marker) expression (*t* test: $t_{14} = 3.586$; $p = 0.003$), whereas the astrocyte marker GFAP was not affected. **c**, **d** Co-staining of amyloid plaques (Thioflavin S, *green*) and GFAP (**c**, *red*) or Iba1 (**d**, *red*) in hippocampus (DG subfield) of APP/PS1ΔE9 transgenic mice. *Dotted line* indicates the granular layer of the DG. *Scale bar*, 500 µm. **e**, **f** Whereas the distribution of GFAP positive astrocytes is unaltered, increased recruitment of Iba1 positive microglia is observed in the vicinity of amyloid plaques. **f** Significant increase was found for the Iba1 stained area (*t* test, $p < 0.0001$) and the number of Iba1 + microglia (*t* test, $p < 0.0002$) in the vicinity of plaques. **g** Higher magnification of co-staining depicting amyloid plaques (Thioflavin S, *green*) and astrocytes (GFAP, *red*) or microglia (Iba1, *red*). *Scale bar*, 20 µm. **h** Morphology of microglia in the hippocampus of AAV-injected APP/PS1ΔE9 mice. Increased ramified profile is observed in microglia of AAV-APPsα injected mice (*right*, indicated by *arrow heads*). *Scale bar*, 10 µm. **i** Co-immunostaining of Iba1 (*red*) and 4G8 (β amyloid, *green*) in AAV-APPsα injected APP/PS1ΔE9 mice indicating the uptake of Aβ (*arrow heads*) in plaque-associated microglia. *Scale bar*, 10 µm. **j**, **k** Western blot analysis showing the expression of IDE and TREM2 in the hippocampus of AAV-Venus or AAV-APPsα injected APP/PS1ΔE9 mice. Both Aβ clearance related proteins are significantly upregulated (IDE: *t* test, $p = 0.0014$; TREM2: *t* test, $p = 0.010$) following AAV-APPsα treatment. Values represent mean ± SEM. $^{***}p < 0.001$, $^{**}p < 0.01$, $^{*}p < 0.05$

of the AAV-APPsα vector in APP/PS1ΔE9 mice was paralleled by a 2.3-fold increase in Iba1 immunoreactivity and a similar increase in the number of microglia in the vicinity of plaques (Fig. 5d, f, g). Moreover, we observed an altered morphology of microglia in AAV-APPsα treated mice characterized by increased ramifications in AAV-APPsα versus control vector injected APP/PS1ΔE9 mice (Fig. 5g, h). Previously, it had been reported that AAV-mediated delivery of Aβ42 or β-CTF to the hippocampus lead to significant leakiness of the blood–brain barrier (BBB) [24], as evidenced by increased mouse IgG immunoreactivity. We therefore incubated sections of AAV-APPsα or AAV-Venus injected transgenic APP/PS1ΔE9 mice with DAPI to stain for nuclei or NeuN (to reveal neuronal cell bodies) and in addition with secondary anti-mouse IgG antibody. Overall, only very few stained cells were detectable and there was no increase in sections of AAV-APPsα injected mice (Fig. S3) indicating that AAV-APPsα injection did not result in a major BBB breakdown. We therefore conclude that microglia activation in the vicinity of plaques is not secondary to AAV-APPsα induced BBB leakiness.

Microglia contribute to Aβ clearance and are thought to play a protective role at least during early stages of AD [62], while they may acquire a senescence-like stage during disease progression [62]. Indeed, plaque-associated microglia (from both AAV-APPsα and AAV-Venus treated mice) were also engaged in Aβ uptake as evidenced by Iba1/4G8 double staining (Figs. 5i, S4). Recently, genetic variants of TREM2 (Triggering Receptor Expressed on Myeloid cells) have been associated with an increased risk for AD [31, 40]. Although the precise role of TREM2 for AD pathogenesis and Aβ pathology is still controversial [39, 82] TREM2 expression has been consistently detected in plaque-associated $Iba1^{+}$ cells in AD model mice [26, 39]. Consistent with an increase in plaque-associated microglia, we detected a significant increase of TREM2 expression (about 60 % vs control, *t* test, $p < 0.01$) by Western blot analysis in hippocampi of APP/PS1ΔE9 mice injected with AAV-APPsα versus controls (Fig. 5j, k, $n = 8$ per group). We also determined the expression of neprilysin (NEP) and insulin-degrading enzyme (IDE) that are proteases produced by microglia that contribute to Aβ clearance [56]. Expression of NEP was identical in APP/PS1ΔE9 mice injected with AAV-APPsα versus control (not shown). However, a significant increase (of about +20 %, *t* test, $p < 0.0014$) in IDE expression was observed after AAV-HA-APPsα vector injection (Fig. 5j, k). Together, these data suggest that AAV-mediated APPsα expression induces microglia recruitment, activation and possibly also phagocytic function which may lead to enhanced Aβ and plaque clearance.

Discussion

Despite a recent shift of research efforts towards preventive strategies, there is still an urgent lack of an effective treatment of patients with clinically established AD. So far, many therapeutic approaches targeted the secretases processing APP. However, since all secretases act on many different substrates besides APP [63, 80], these strategies have major drawbacks for clinical application. γ-secretase is physiologically essential and current clinical trials to develop γ-secretase inhibitors have been abrogated due to serious side effects, likely resulting from impaired Notch signaling [23]. Also systemic upregulation of the major α-secretase ADAM10 to boost APPsα production is problematic, as this may enhance cleavage of substrates implicated in tumorigenesis (reviewed by [59, 63]). Thus, direct overexpression of APPsα in the brain may be more promising than pharmacological upregulation of α-secretase.

Here, we explored a gene therapy approach and used AAV-based gene transfer to overexpress APPsα in the brain of transgenic APP/PS1ΔE9 mice, that have been widely used in experimental studies assessing the efficacy of AD therapies. Bigenic APP_{SWE}/PS1ΔE9 mice express a chimeric mouse/human APP (with Swedish double mutation) and a mutant human PS1 gene (PS1ΔE9) both associated with familial forms of AD. They produce high amounts of huAβ leading to amyloid deposition starting at 5–6 months

and pronounced progression of plaque pathology with age [68] that is associated with impairments in cognitive behavior [68]. Using bilateral injection of AAV-APPsα vector particles, we achieved highly efficient and widespread expression of APPsα throughout the whole hippocampus and also in adjacent cortical areas. We attribute this on one hand to the well-established spreading/diffusion of small AAV particles, particularly along the injection needle track [16] and on the other hand to the secretion of APPsα that may diffuse in the brain parenchyma. In this study, a single bilateral injection of AAV-APPsα particles was sufficient to mediate long-lasting APPsα expression over 5 months that was well tolerated without apparent adverse effects. This was a crucial prerequisite to study potential therapeutic efficacy of AAV-APPsα overexpression. To this end, we used aged (12-month-old) APP/PS1ΔE9 mice with preexisting amyloidosis to mimic the situation in AD patients that are usually clinically diagnosed many years after the onset of pathology [81].

Taken together, we demonstrate that in aged APP/PS1ΔE9 AD model mice AAV-APPsα could rescue or ameliorate key aspects of AD pathology: (1) defective synaptic plasticity (LTP and PPF), (2) reduced synaptic density and most importantly (3) impaired spatial reference memory.

There is a strong correlation between synapse loss and cognitive decline in AD and synaptic dysfunction is thought to underlay early stages of the disease [69, 77]. The ability of synapses to undergo long-term potentiation and thus increase their synaptic strength is considered as a cellular mechanism underlying learning and memory. Indeed, defects in LTP have not only been reported in several AD mouse models with Aβ overexpression (see, e.g., review by [73]) but also upon application of synthetic or native Aβ oligomers from AD patients to hippocampal slices (e.g. [70, 71]). Interestingly, we observed that deficits of 12- to 13-month-old APP/PS1ΔE9 mice in the induction and maintenance phase of LTP were largely rescued upon AAV-APPsα overexpression despite the presence of high amounts of soluble Aβ and extensive Aβ deposition (see Fig. 4, see also Fig. 3 regarding LTP) at this age. Given that AAV-APPsα did not affect basal synaptic transmission, but completely rescued the defects in paired pulse facilitation of APP/PS1ΔE9 mice this suggests that restoration of presynaptic function may contribute to the LTP rescue. In this regard, it is noteworthy that APP has been localized to synaptic sites, including the presynaptic active zone [45, 86]. Our present findings are perfectly in line and further extend the previously demonstrated physiological role of APP and APPsα in synaptic plasticity. Consistent with a presynaptic role of APP, we previously found a reduction in quantal content and readily releasable pool at neuromuscular synapses of APP/APLP2 mutant mice [84]. In the CNS, APP-KO mice showed altered GABAergic short-term plasticity and disturbed Ca^{2+}-homeostasis [88]. In addition, APPsα knockin mice that lack transmembrane APP and express solely secreted APPsα completely rescued the LTP impairment of APP-KO mice [65].

Previously, indirect evidence suggested that APPsα may have synaptotrophic properties not only under physiological, but also under pathological conditions. Studies involving transgenic mice with moderate overexpression of human WT APP [57], or indirect upregulation of APPsα by transgenic expression of the α-secretase ADAM10 [9], that is enriched at synaptic contacts [52], all led to increased synaptic density. In Tg2576 mice expression of mutant huAPP decreased spine density in aged animals, whereas an increase in spine density was observed in young mice prior to plaque deposition pointing towards a possibly trophic effect of APPsα [46]. Here, we now directly demonstrate that in addition to its beneficial effects on synaptic plasticity, AAV-APPsα overexpression ameliorates spine density defects associated with Aβ accumulation in aged APP/PS1ΔE9 mice, and restores normal spine density in basal dendritic segments of CA1 and CA3 neurons. Most importantly, increases in spine counts and restored synaptic plasticity were also reflected in significantly improved behavior. Although, we detected no positive effects during the acquisition phase of Morris water maze (MWM) spatial navigation AAV-APPsα treatment completely rescued the impaired probe trial performance of transgenic mice as evidenced by a significant increase in the time spent in the target quadrant that was statistically indistinguishable from AAV-Venus injected littermate controls. Moreover, AAV-APPsα injected transgenic mice showed clear directionality towards the trained platform. Together, this further supports the notion that AVV-APPsα expression improved the cognitive performance of mice and restored spatial reference memory in APP/PS1ΔE9 mice. A similar phenotype with no difference in MWM acquisition, but significant difference in probe trial performance has previously been reported for several other AD mouse models, including homozygous 3 × TG mice (APP_{SWE} × P301L × PS1M146 V) that developed early cognitive deficits in probe trial performance while MWM acquisition learning was unaffected [11]. Also, TauP301L overexpressing mice tested at 6 months of age showed impaired probe trail performance while both MWM acquisition learning and reversal learning were normal, consistent with normal working memory, as assessed by the Y-maze [61]. In addition, our results are also in agreement with findings in rats with experimentally induced lesion of the hippocampal CA3 subfield that resulted in deficits in memory retrieval [67]. Of note, the CA3 area is not only affected by plaque deposition in our APP/PS1ΔE9 mice but this was also associated with deficits in spine density which might thus lead to compromised properties of the

hippocampal network. Together, it is possible that spatial working memory is conserved longer than spatial reference memory. Of note, we also observed reduced escape latency during acquisition learning in wild-type controls injected with AAV-APPsα. These data suggest that APPsα could not only play a role in behaviorally impaired AD model mice, but might also enhance learning in normal WT mice. Future studies with larger cohorts of mice are needed to further substantiate these findings.

Although the precise role of APPsα at the synapse is still unknown, there is a large body of evidence that APPsα affects several pathways that likely contribute to its beneficial effects in APP/PS1ΔE9 mice. In vitro studies using WT rats showed that exogenous APPsα application can shift the frequency dependence of LTD and enhance LTP [37]. Moreover, intra-hippocampal infusion of recombinant APPsα (rec APPsα) increased in vivo LTP recorded at the dentate gyrus of adult rats [76] and infusion of APPsα or peptides derived from it enhances memory in mice, chicks and rats [14, 53, 54, 66]. Mechanistically, the effects on LTP may involve modulation of NMDA receptor function as recAPPsα was shown to facilitate tetanically evoked NMDA receptor-mediated currents in vitro [76]. Immunoprecipitation studies indicated that transmembrane APP interacts with GluN1/GluN2 NMDARs and enhances their cell surface expression in vitro [20, 21], but it is presently unclear whether this also holds true for extracellular APPsα. Moreover, recAPPsα has been shown to increase synaptodendritic de novo protein synthesis, an important mechanism for normal plasticity [17].

Although in this study we did not investigate neuronal death, it is noteworthy that in vitro studies had implicated APPsα in neuroprotective signaling relevant to AD pathogenesis, including protection against excitotoxic stress resulting from glutamate receptor overactivation [28] and notably also Aβ induced toxicity [27, 29, 30]. Intriguingly, a recent study identified cell surface holo-APP as the receptor that binds APPsα and confers neuroprotection via G protein-coupled activation of the Akt stress signaling pathway [55]. While these data established holo-APP as a receptor mediating prosurvial/antiapoptotic signaling, it is also clear, however, that the very rapid effects of APP on synaptic plasticity must be mediated by a receptor distinct from APP. In this respect, we recently showed that the LTP impairments of conditional DKO mice, lacking both APP and APLP2 can be rescued by a brief (30 min) pre-incubation with nanomolar amounts of APPsα [33].

In addition to beneficial effects on synaptic morphology and function, we also detected significantly reduced levels of soluble Aβ species and a significant (about 25 %) decrease in plaque load upon AAV-APPsα treatment that may contribute to the rescue of synaptic failure. Our results of reduced Aβ levels following AAV-APPsα treatment are further supported by a recent study indicating that APPsα may bind to BACE-1 and thereby reduce Aβ production [60]. In that study, classical germline APPsα transgenic (TgAPPsα) mice were generated and APP processing was investigated after crossing to APP/PS1ΔE9 mice [60]. Whereas TgAPPsα/APP/PS1ΔE9 mice revealed a reduction in both huAβ and in huβ-CTFs (consistent with BACE inhibition), we were unable to detect besides reduced Aβ levels significant alterations of other proteolytic fragments of the amyloidogenic pathway such as huAPPsβ-$_{SWE}$ and β-CTFs. These apparent differences might be related to the more variable AAV-mediated APPsα overexpression (see Fig. 1) and the fact that in TgAPPsα mice, APPsα was expressed from early development onwards (as opposed to expression in aged mice in this study). In addition, Obregon et al. assessed APP processing much earlier (at 8 months of age), when huAβ build up is considerably lower [60]. Importantly, and in contrast to our study, the functional consequences of APPsα overexpression on neuronal morphology, synaptic function and behavior had, however, not been assessed in that study [60]. In addition, we now provide evidence suggesting that AAV-APPsα may also improve pathology in a mechanism unrelated to BACE inhibition. While previous co-culture studies of neurons with microglial cell lines or primary microglia indicated that secreted APPsβ and APPsα can activate microglia and may thus indirectly affect neuronal metabolism and survival in vitro (e.g., [6, 8, 12]), the consequences of selective APPsα expression in vivo have not been studied so far. Here, we observed that AAV-APPsα treatment lead to the recruitment of microglia with ramified morphology, believed to indicate an activated state [62] towards plaques. This was paralleled by an increase in TREM2 expression. TREM2 receptor was recently shown to sustain the microglial response to Aβ and suggested to function as a sensor for anionic lipids exposed during Aβ deposition and on damaged neurons [82]. In addition, we demonstrate an upregulation of the proteolytic enzyme IDE that is produced by microglia and was previously shown to enhance Aβ and plaques clearance [32, 47]. Together, our data strongly suggest that APPsα-mediated activation and recruitment of microglia may contribute to the ameliorated Aβ pathology in APP/PS1ΔE9 mice.

AD pathogenesis is complex, still incompletely understood and multiple factors contribute to pathogenesis. Therefore, the concept of synaptic repair has recently been put forward, e.g., to tackle/ameliorate pathophysiology and improve clinical outcome as an alternative to eliminating toxic factors [51]. Notably, due to the highly plastic nature of synapses, synaptic dysfunction and synapse loss are reversible processes. Here, we provide several converging lines of evidence that viral vector-mediated APPsα expression rescues synaptic failure in AD model mice with established Aβ deposition, indicating its potential as a novel

therapeutic strategy even in the presence of pathogenic factors.

Acknowledgments This work was supported by the Deutsche Forschungsgemeinschaft Grants (MU 1457/9-1, 9-2 to UCM; KO 1674/3-1, 3-2 to MK), the ERA-Net Neuron (01EW1305A to CJB, NC and UCM), and the LOEWE Center for Cell and Gene Therapy Frankfurt funded by Hessisches Ministerium für Wissenschaft und Kunst (III L 4- 518/17.004 (2010)) to CJB.

Compliance with ethical standards

Conflict of interest The authors declare no conflict of interest.

References

1. Abramov E, Dolev I, Fogel H, Ciccotosto GD, Ruff E, Slutsky I (2009) Amyloid-beta as a positive endogenous regulator of release probability at hippocampal synapses. Nat Neurosci 12:1567–1576. doi:10.1038/nn.2433
2. Ahmed RR, Holler CJ, Webb RL, Li F, Beckett TL, Murphy MP (2010) BACE1 and BACE2 enzymatic activities in Alzheimer's disease. J Neurochem 112:1045–1053. doi:10.1111/j.1471-4159.2009.06528.x
3. Almkvist O, Basun H, Wagner SL, Rowe BA, Wahlund LO, Lannfelt L (1997) Cerebrospinal fluid levels of alpha-secretase-cleaved soluble amyloid precursor protein mirror cognition in a Swedish family with Alzheimer disease and a gene mutation. Arch Neurol 54:641–644
4. Anderson JJ, Holtz G, Baskin PP et al (1999) Reduced cerebrospinal fluid levels of alpha-secretase-cleaved amyloid precursor protein in aged rats: correlation with spatial memory deficits. Neuroscience 93:1409–1420 **(pii: S0306-4522(99)00244-4)**
5. Aurnhammer C, Haase M, Muether N et al (2012) Universal real-time PCR for the detection and quantification of adeno-associated virus serotype 2-derived inverted terminal repeat sequences. Human Gene Therapy Methods 23:18–28. doi:10.1089/hgtb.2011.034
6. Austin SA, Combs CK (2008) Mechanisms of microglial activation by amyloid precursor protein and its proteolytic fragments. In: Lane TE, Carson M, Bergmann C, Wyss-Coray T (eds) Central nervous system diseases and inflammation. Springer US, New York, pp 13–32
7. Aydin D, Weyer SW, Muller UC (2012) Functions of the APP gene family in the nervous system: insights from mouse models. Exp Brain Res 217:423–434. doi:10.1007/s00221-011-2861-2
8. Barger SW, Harmon AD (1997) Microglial activation by Alzheimer amyloid precursor protein and modulation by apolipoprotein E. Nature 388:878–881. doi:10.1038/42257
9. Bell KF, Zheng L, Fahrenholz F, Cuello AC (2008) ADAM-10 over-expression increases cortical synaptogenesis. Neurobiol Aging 29:554–565. doi:10.1016/j.neurobiolaging.2006.11.004
10. Berger A, Lorain S, Josephine C et al (2015) Repair of rhodopsin mRNA by spliceosome-mediated RNA trans-splicing: a new approach for autosomal dominant retinitis pigmentosa. Mol Ther. doi:10.1038/mt.2015.11
11. Billings LM, Oddo S, Green KN, McGaugh JL, LaFerla FM (2005) Intraneuronal Abeta causes the onset of early Alzheimer's disease-related cognitive deficits in transgenic mice. Neuron 45:675–688. doi:10.1016/j.neuron.2005.01.040
12. Bodles AM, Barger SW (2005) Secreted beta-amyloid precursor protein activates microglia via JNK and p38-MAPK. Neurobiol Aging 26:9–16. doi:10.1016/j.neurobiolaging.2004.02.022
13. Borchelt DR, Ratovitski T, van Lare J et al (1997) Accelerated amyloid deposition in the brains of transgenic mice coexpressing mutant presenilin 1 and amyloid precursor proteins. Neuron 19:939–945
14. Bour A, Little S, Dodart JC, Kelche C, Mathis C (2004) A secreted form of the beta-amyloid precursor protein (sAPP695) improves spatial recognition memory in OF1 mice. Neurobiol Learn Mem 81:27–38 **(pii: S1074742703000716)**
15. Caille I, Allinquant B, Dupont E et al (2004) Soluble form of amyloid precursor protein regulates proliferation of progenitors in the adult subventricular zone. Development 131:2173–2181
16. Casanova F, Carney PR, Sarntinoranont M (2014) Effect of needle insertion speed on tissue injury, stress, and backflow distribution for convection-enhanced delivery in the rat brain. PLoS One 9:e94919. doi:10.1371/journal.pone.0094919
17. Claasen AM, Guevremont D, Mason-Parker SE et al (2009) Secreted amyloid precursor protein-alpha upregulates synaptic protein synthesis by a protein kinase G-dependent mechanism. Neurosci Lett 460:92–96. doi:10.1016/j.neulet.2009.05.040
18. Copanaki E, Chang S, Vlachos A et al (2010) sAPPalpha antagonizes dendritic degeneration and neuron death triggered by proteasomal stress. Mol Cell Neurosci 44:386–393. doi:10.1016/j.mcn.2010.04.007
19. Corrigan F, Vink R, Blumbergs PC, Masters CL, Cappai R, van den Heuvel C (2012) sAPPalpha rescues deficits in amyloid precursor protein knockout mice following focal traumatic brain injury. J Neurochem 122:208–220. doi:10.1111/j.1471-4159.2012.07761.x
20. Cousins SL, Hoey SE, Anne Stephenson F, Perkinton MS (2009) Amyloid precursor protein 695 associates with assembled NR2A- and NR2B-containing NMDA receptors to result in the enhancement of their cell surface delivery. J Neurochem 111:1501–1513. doi:10.1111/j.1471-4159.2009.06424.x
21. Cousins SL, Innocent N, Stephenson FA (2013) Neto1 associates with the NMDA receptor/amyloid precursor protein complex. J Neurochem 126:554–564. doi:10.1111/jnc.12280
22. Dobrowolska JA, Kasten T, Huang Y et al (2014) Diurnal patterns of soluble amyloid precursor protein metabolites in the human central nervous system. PLoS One 9:e89998. doi:10.1371/journal.pone.0089998
23. Doody RS, Raman R, Farlow M et al (2013) A phase 3 trial of semagacestat for treatment of Alzheimer's disease. N Engl J Med 369:341–350. doi:10.1056/NEJMoa1210951
24. Drummond ES, Muhling J, Martins RN, Wijaya LK, Ehlert EM, Harvey AR (2013) Pathology associated with AAV mediated expression of beta amyloid or C100 in adult mouse hippocampus and cerebellum. PLoS One 8:e59166. doi:10.1371/journal.pone.0059166
25. Endres K, Fahrenholz F (2012) Regulation of alpha-secretase ADAM10 expression and activity. Exp Brain Res 217:343–352. doi:10.1007/s00221-011-2885-7
26. Frank S, Burbach GJ, Bonin M et al (2008) TREM2 is upregulated in amyloid plaque-associated microglia in aged APP23 transgenic mice. Glia 56:1438–1447. doi:10.1002/glia.20710
27. Furukawa K, Barger SW, Blalock EM, Mattson MP (1996) Activation of K + channels and suppression of neuronal activity by secreted beta-amyloid-precursor protein. Nature 379:74–78. doi:10.1038/379074a0
28. Furukawa K, Mattson MP (1998) Secreted amyloid precursor protein alpha selectively suppresses *N*-methyl-D-aspartate currents in hippocampal neurons: involvement of cyclic GMP. Neuroscience 83:429–438 **(pii: S0306452297003989)**
29. Furukawa K, Sopher BL, Rydel RE et al (1996) Increased activity-regulating and neuroprotective efficacy of alpha-secretase-derived secreted amyloid precursor protein conferred by a C-terminal heparin-binding domain. J Neurochem 67:1882–1896

30. Goodman Y, Mattson MP (1994) Secreted forms of beta-amyloid precursor protein protect hippocampal neurons against amyloid beta-peptide-induced oxidative injury. Exp Neurol 128:1–12. doi:10.1006/exnr.1994.1107
31. Guerreiro R, Wojtas A, Bras J et al (2013) TREM2 variants in Alzheimer's disease. N Engl J Med 368:117–127. doi:10.1056/NEJMoa1211851
32. Heneka MT, Kummer MP, Stutz A et al (2013) NLRP3 is activated in Alzheimer's disease and contributes to pathology in APP/PS1 mice. Nature 493:674–678. doi:10.1038/nature11729
33. Hick M, Herrmann U, Weyer SW et al (2015) Acute function of secreted amyloid precursor protein fragment APPsalpha in synaptic plasticity. Acta Neuropathol 129:21–37. doi:10.1007/s00401-014-1368-x
34. Hoe HS, Lee HK, Pak DT (2012) The upside of APP at synapses. CNS Neurosci Ther 18:47–56. doi:10.1111/j.1755-5949.2010.00221.x
35. Hoey SE, Williams RJ, Perkinton MS (2009) Synaptic NMDA receptor activation stimulates alpha-secretase amyloid precursor protein processing and inhibits amyloid-beta production. J Neurosci 29:4442–4460. doi:10.1523/JNEUROSCI.6017-08.2009
36. Holsinger RM, McLean CA, Beyreuther K, Masters CL, Evin G (2002) Increased expression of the amyloid precursor beta-secretase in Alzheimer's disease. Ann Neurol 51:783–786. doi:10.1002/ana.10208
37. Ishida A, Furukawa K, Keller JN, Mattson MP (1997) Secreted form of beta-amyloid precursor protein shifts the frequency dependency for induction of LTD, and enhances LTP in hippocampal slices. NeuroReport 8:2133–2137
38. Jankowsky JL, Fadale DJ, Anderson J et al (2004) Mutant presenilins specifically elevate the levels of the 42 residue beta-amyloid peptide in vivo: evidence for augmentation of a 42-specific gamma secretase. Hum Mol Genet 13:159–170. doi:10.1093/hmg/ddh019
39. Jay TR, Miller CM, Cheng PJ et al (2015) TREM2 deficiency eliminates TREM2+ inflammatory macrophages and ameliorates pathology in Alzheimer's disease mouse models. J Exp Med 212:287–295. doi:10.1084/jem.20142322
40. Jonsson T, Stefansson H, Steinberg S et al (2013) Variant of TREM2 associated with the risk of Alzheimer's disease. N Engl J Med 368:107–116. doi:10.1056/NEJMoa1211103
41. Kamphuis W, Mamber C, Moeton M et al (2012) GFAP isoforms in adult mouse brain with a focus on neurogenic astrocytes and reactive astrogliosis in mouse models of Alzheimer disease. PLoS One 7:e42823. doi:10.1371/journal.pone.0042823
42. Klevanski M, Saar M, Baumkotter F, Weyer SW, Kins S, Muller UC (2014) Differential role of APP and APLPs for neuromuscular synaptic morphology and function. Mol Cell Neurosci 61C:201–210. doi:10.1016/j.mcn.2014.06.004
43. Kogel D, Deller T, Behl C (2012) Roles of amyloid precursor protein family members in neuroprotection, stress signaling and aging. Exp Brain Res 217:471–479. doi:10.1007/s00221-011-2932-4
44. Lannfelt L, Basun H, Wahlund LO, Rowe BA, Wagner SL (1995) Decreased alpha-secretase-cleaved amyloid precursor protein as a diagnostic marker for Alzheimer's disease. Nat Med 1:829–832
45. Lassek M, Weingarten J, Einsfelder U, Brendel P, Muller U, Volknandt W (2013) Amyloid precursor proteins are constituents of the presynaptic active zone. J Neurochem 127:48–56. doi:10.1111/jnc.12358
46. Lee KJ, Moussa CE, Lee Y et al (2010) Beta amyloid-independent role of amyloid precursor protein in generation and maintenance of dendritic spines. Neuroscience 169:344–356. doi:10.1016/j.neuroscience.2010.04.078
47. Leissring MA, Farris W, Chang AY et al (2003) Enhanced proteolysis of beta-amyloid in APP transgenic mice prevents plaque formation, secondary pathology, and premature death. Neuron 40:1087–1093
48. Leyssen M, Ayaz D, Hebert SS, Reeve S, De Strooper B, Hassan BA (2005) Amyloid precursor protein promotes post-developmental neurite arborization in the Drosophila brain. EMBO J 24:2944–2955. doi:10.1038/sj.emboj.7600757
49. Li ZW, Stark G, Gotz J et al (1996) Generation of mice with a 200-kb amyloid precursor protein gene deletion by Cre recombinase-mediated site-specific recombination in embryonic stem cells. Proc Natl Acad Sci USA 93:6158–6162
50. Lichtenthaler SF, Haass C, Steiner H (2011) Regulated intramembrane proteolysis–lessons from amyloid precursor protein processing. J Neurochem 117:779–796. doi:10.1111/j.1471-4159.2011.07248.x
51. Lu B, Nagappan G, Guan X, Nathan PJ, Wren P (2013) BDNF-based synaptic repair as a disease-modifying strategy for neurodegenerative diseases. Nat Rev Neurosci 14:401–416. doi:10.1038/nrn3505
52. Marcello E, Gardoni F, Mauceri D et al (2007) Synapse-associated protein-97 mediates alpha-secretase ADAM10 trafficking and promotes its activity. J Neurosci 27:1682–1691. doi:10.1523/JNEUROSCI.3439-06.2007
53. Meziane H, Dodart JC, Mathis C et al (1998) Memory-enhancing effects of secreted forms of the beta-amyloid precursor protein in normal and amnestic mice. Proc Natl Acad Sci USA 95:12683–12688
54. Mileusnic R, Lancashire CL, Rose SP (2004) The peptide sequence Arg-Glu-Arg, present in the amyloid precursor protein, protects against memory loss caused by A beta and acts as a cognitive enhancer. Eur J Neurosci 19:1933–1938. doi:10.1111/j.1460-9568.2004.03276.x
55. Milosch N, Tanriover G, Kundu A et al (2014) Holo-APP and G-protein-mediated signaling are required for sAPPalpha-induced activation of the Akt survival pathway. Cell Death Dis 5:e1391. doi:10.1038/cddis.2014.352
56. Miners JS, Barua N, Kehoe PG, Gill S, Love S (2011) Abeta-degrading enzymes: potential for treatment of Alzheimer disease. J Neuropathol Exp Neurol 70:944–959. doi:10.1097/NEN.0b013e3182345e46
57. Mucke L, Abraham CR, Masliah E (1996) Neurotrophic and neuroprotective effects of hAPP in transgenic mice. Ann N Y Acad Sci 777:82–88
58. Murakami N, Yamaki T, Iwamoto Y et al (1998) Experimental brain injury induces expression of amyloid precursor protein, which may be related to neuronal loss in the hippocampus. J Neurotrauma 15:993–1003
59. Nhan HS, Chiang K, Koo EH (2015) The multifaceted nature of amyloid precursor protein and its proteolytic fragments: friends and foes. Acta Neuropathol 129:1–19. doi:10.1007/s00401-014-1347-2
60. Obregon D, Hou H, Deng J et al (2012) Soluble amyloid precursor protein-alpha modulates beta-secretase activity and amyloid-beta generation. Nat Commun 3:777. doi:10.1038/ncomms1781ncomms1781
61. Pennanen L, Wolfer DP, Nitsch RM, Gotz J (2006) Impaired spatial reference memory and increased exploratory behavior in P301L tau transgenic mice. Genes Brain Behav 5:369–379. doi:10.1111/j.1601-183X.2005.00165.x
62. Prokop S, Miller KR, Heppner FL (2013) Microglia actions in Alzheimer's disease. Acta Neuropathol 126:461–477
63. Prox J, Rittger A, Saftig P (2012) Physiological functions of the amyloid precursor protein secretases ADAM10, BACE1, and Presenilin. Exp Brain Res 217:331–341. doi:10.1007/s00221-011-2952-0
64. Ramirez MJ, Heslop KE, Francis PT, Rattray M (2001) Expression of amyloid precursor protein, tau and presenilin RNAs in

rat hippocampus following deafferentation lesions. Brain Res 907:222–232
65. Ring S, Weyer SW, Kilian SB et al (2007) The secreted beta-amyloid precursor protein ectodomain APPs alpha is sufficient to rescue the anatomical, behavioral, and electrophysiological abnormalities of APP-deficient mice. J Neurosci 27:7817–7826. doi:10.1523/JNEUROSCI.1026-07.2007
66. Roch JM, Masliah E, Roch-Levecq AC et al (1994) Increase of synaptic density and memory retention by a peptide representing the trophic domain of the amyloid beta/A4 protein precursor. Proc Natl Acad Sci USA 91:7450–7454
67. Roozendaal B, Phillips RG, Power AE, Brooke SM, Sapolsky RM, McGaugh JL (2001) Memory retrieval impairment induced by hippocampal CA3 lesions is blocked by adrenocortical suppression. Nat Neurosci 4:1169–1171. doi:10.1038/nn766
68. Savonenko A, Xu GM, Melnikova T et al (2005) Episodic-like memory deficits in the APPswe/PS1dE9 mouse model of Alzheimer's disease: relationships to beta-amyloid deposition and neurotransmitter abnormalities. Neurobiol Dis 18:602–617. doi:10.1016/j.nbd.2004.10.022
69. Selkoe DJ (2002) Alzheimer's disease is a synaptic failure. Science 298:789–791. doi:10.1126/science.1074069
70. Shankar GM, Bloodgood BL, Townsend M, Walsh DM, Selkoe DJ, Sabatini BL (2007) Natural oligomers of the Alzheimer amyloid-beta protein induce reversible synapse loss by modulating an NMDA-type glutamate receptor-dependent signaling pathway. J Neurosci 27:2866–2875. doi:10.1523/JNEUROSCI.4970-06.2007
71. Shankar GM, Li S, Mehta TH et al (2008) Amyloid-beta protein dimers isolated directly from Alzheimer's brains impair synaptic plasticity and memory. Nat Med 14:837–842. doi:10.1038/nm1782
72. Smith-Swintosky VL, Pettigrew LC, Craddock SD, Culwell AR, Rydel RE, Mattson MP (1994) Secreted forms of beta-amyloid precursor protein protect against ischemic brain injury. J Neurochem 63:781–784
73. Spires-Jones T, Knafo S (2012) Spines, plasticity, and cognition in Alzheimer's model mice. Neural Plast 2012:319836. doi:10.1155/2012/319836
74. Suh J, Choi SH, Romano DM et al (2013) ADAM10 missense mutations potentiate beta-amyloid accumulation by impairing prodomain chaperone function. Neuron 80:385–401. doi:10.1016/j.neuron.2013.08.035
75. Tang W, Ehrlich I, Wolff SB et al (2009) Faithful expression of multiple proteins via 2A-peptide self-processing: a versatile and reliable method for manipulating brain circuits. J Neurosci 29:8621–8629. doi:10.1523/JNEUROSCI.0359-09.2009
76. Taylor CJ, Ireland DR, Ballagh I et al (2008) Endogenous secreted amyloid precursor protein-alpha regulates hippocampal NMDA receptor function, long-term potentiation and spatial memory. Neurobiol Dis 31:250–260. doi:10.1016/j.nbd.2008.04.011
77. Terry RD, Masliah E, Salmon DP et al (1991) Physical basis of cognitive alterations in Alzheimer's disease: synapse loss is the major correlate of cognitive impairment. Ann Neurol 30:572–580. doi:10.1002/ana.410300410
78. Thornton E, Vink R, Blumbergs PC, Van Den Heuvel C (2006) Soluble amyloid precursor protein alpha reduces neuronal injury and improves functional outcome following diffuse traumatic brain injury in rats. Brain Res 1094:38–46. doi:10.1016/j.brainres.2006.03.107
79. Van den Heuvel C, Blumbergs PC, Finnie JW et al (1999) Upregulation of amyloid precursor protein messenger RNA in response to traumatic brain injury: an ovine head impact model. Exp Neurol 159:441–450. doi:10.1006/exnr.1999.7150
80. Vassar R, Kuhn PH, Haass C et al (2014) Function, therapeutic potential and cell biology of BACE proteases: current status and future prospects. J Neurochem 130:4–28. doi:10.1111/jnc.12715
81. Villemagne VL, Burnham S, Bourgeat P et al (2013) Amyloid beta deposition, neurodegeneration, and cognitive decline in sporadic Alzheimer's disease: a prospective cohort study. Lancet Neurol 12:357–367. doi:10.1016/S1474-4422(13)70044-9
82. Wang Y, Cella M, Mallinson K et al (2015) TREM2 lipid sensing sustains the microglial response in an Alzheimer's disease model. Cell 160:1061–1071. doi:10.1016/j.cell.2015.01.049
83. Wang Z, Wang B, Yang L et al (2009) Presynaptic and postsynaptic interaction of the amyloid precursor protein promotes peripheral and central synaptogenesis. J Neurosci 29:10788–10801. doi:10.1523/JNEUROSCI.2132-09.2009
84. Weyer SW, Klevanski M, Delekate A et al (2011) APP and APLP2 are essential at PNS and CNS synapses for transmission, spatial learning and LTP. EMBO J 30:2266–2280. doi:10.1038/emboj.2011.119
85. Weyer SW, Zagrebelsky M, Herrmann U et al (2014) Comparative analysis of single and combined APP/APLP knockouts reveals reduced spine density in APP-KO mice that is prevented by APPsalpha expression. Acta Neuropathol Commun 2:36. doi:10.1186/2051-5960-2-36
86. Wilhelm BG, Mandad S, Truckenbrodt S et al (2014) Composition of isolated synaptic boutons reveals the amounts of vesicle trafficking proteins. Science 344:1023–1028. doi:10.1126/science.1252884
87. Xiong H, Callaghan D, Wodzinska J et al (2011) Biochemical and behavioral characterization of the double transgenic mouse model (APPswe/PS1dE9) of Alzheimer's disease. Neurosci Bull 27:221–232. doi:10.1007/s12264-011-1015-7
88. Yang L, Wang Z, Wang B, Justice NJ, Zheng H (2009) Amyloid precursor protein regulates Cav1.2 L-type calcium channel levels and function to influence GABAergic short-term plasticity. J Neurosci 29:15660–15668. doi:10.1523/JNEUROSCI.4104-09.2009

Acta Neuropathologica

Electronic Supplementary Material

Viral gene transfer of APPsα rescues synaptic failure in an Alzheimers disease mouse model

Romain Fol[1,2,3], Jerome Braudeau [1,2], Susann Ludewig [6], Tobias Abel [5], Sascha W. Weyer [8], Jan-Peter Roederer [8], Florian Brod [5], Mickael Audrain [1,2,3], Alexis-Pierre Bemelmans [4], Christian J. Buchholz [5], Martin Korte[6,7], Nathalie Cartier [1,2] and Ulrike C. Müller [8]

Inventory of Electronic Supplementary Material

1. Supplementary Data
Figure S1

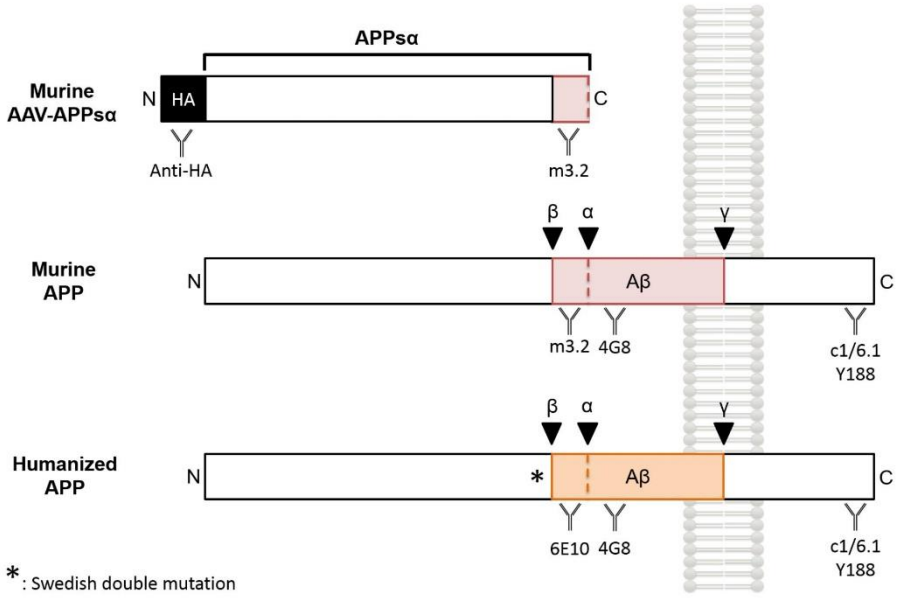

Figure S1: Scheme depicting constructs and epitopes of APP antibodies used

AAV-APPsα (top panel) encodes HA-tagged muAPPsα. Trangenic APP/PS1ΔE9 mice express endogenous murine APP (middle panel) and in addition a chimeric mouse/human APP transgene encoding murine APP_{695} with a humaized Aβ domain and the Swedish double mutation (K595N; M596L, indicated by an asterisk, bottom panel) (Borchelt et al., 1996,). Cleavage sites for the secretases (α, β and γ) are indicate by arrowheads. The Aβ region is highlighted in red (murine) or in orange (human). Epitopes of antibodies used in this study are indicated below constructs. Please note that antibody 6E10 is specific for huAβ.

Figure S2

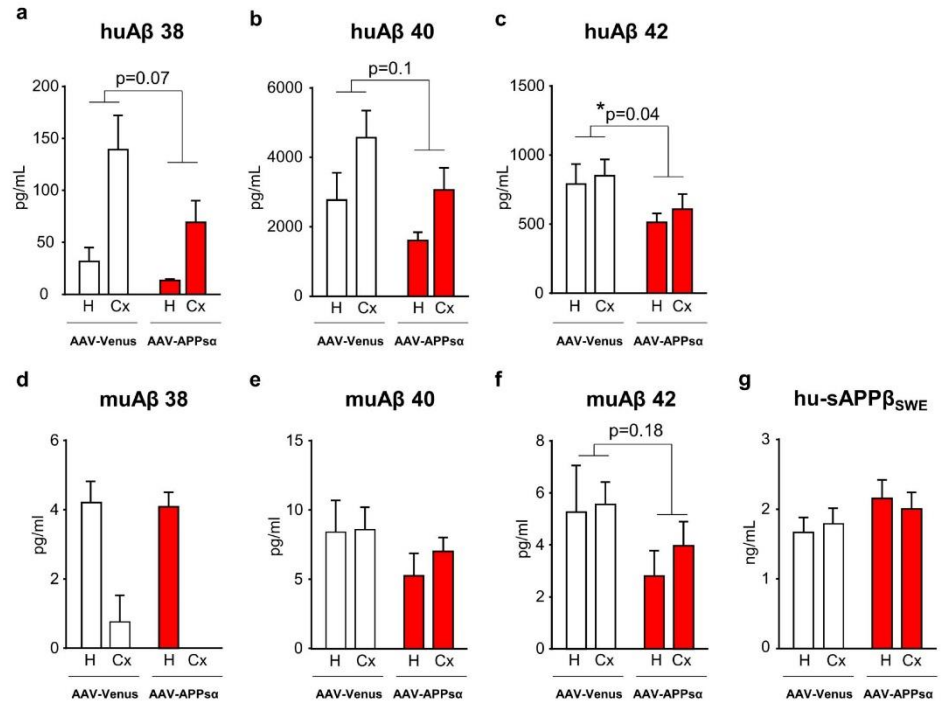

Figure S2: AAV-APPsα injection decreases both human and murine Aβ

(a-c) Quantification (using a human-specific 6E10 based MSD immunoassay) of TBS soluble human transgenic Aβ38 (Group effect: $F_{1,14}$=3.879, p=0.07 (-36%), Aβ40 (Group effect: $F_{1,14}$=3.094, p=0.10 (-32%)) and Aβ42 (Group effect: $F_{1,14}$=5.211, p=0.04 (-33%); region effect: $F_{1,14}$<1, ns; Group x region interaction effect: $F_{1,14}$<1, ns) in hippocampus and cortex of APP/PS1ΔE9 mice. Note that AAV-APPsα injected animals show reduced levels of Aβ in both in hippocampus (H) and cortex (Cx). **(d-f)** Quantification (4G8 based MSD immunoassay) of TBS soluble murine Aβ species in hippocampus and cortex of wild type littermate mice. Aβ38 (Group effect: $F_{1,4}$=0.506, p=0.52), Aβ40 (Group effect: $F_{1,4}$=1.674, p=0.26 (-28%)) and Aβ42 (Group effect: $F_{1,4}$=2.561, p=0.18 (-38%)); region effect: Aβ38 $F_{1,4}$=78.43, p=0,0009, Aβ40 and Aβ42 $F_{1,4}$<1, ns; Group x region interaction effect: $F_{1,4}$<1, ns). Note that AAV-APPsα injected animals show a trend toward reduction of Aβ42 in both hippocampus and cortex. **(g)** ELISA quantification of transgenic secreted APPsβ$_{SWE}$ in hippocampus (H) and cortex (Cx) of APP/PS1ΔE9 mice. No difference was detectable between AAV-Venus and AAV-APPsα injected animals. Number of animals: (a-c, g) n=8/group; (d-f) n=3-4/group. 2-way ANOVA (Genotype, treatment and region as factors) followed by Tukey *post-hoc* test: *p < 0.05. Values represent means ±SEM.

Figure S3

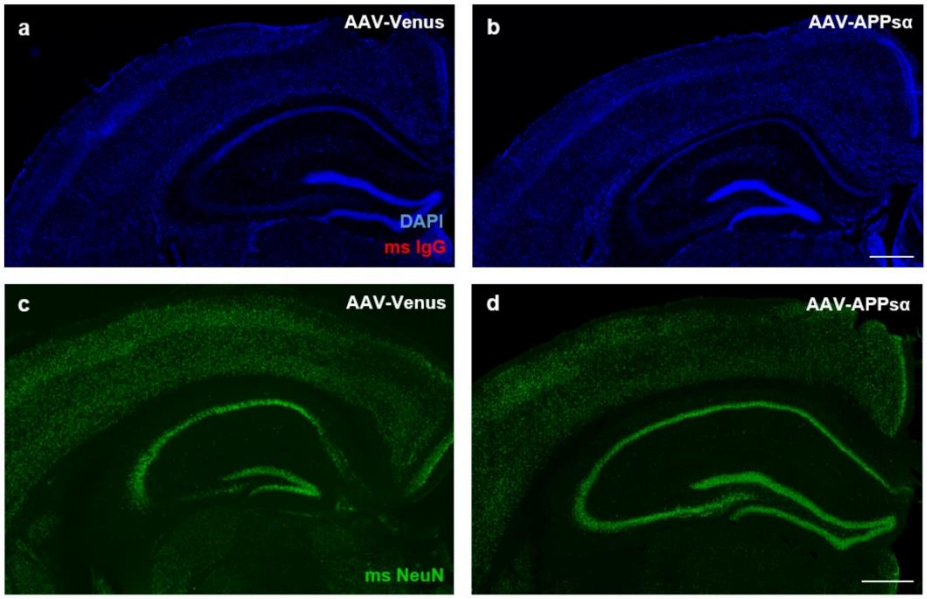

Figure S3: AAV-APPsα injection does not lead to blood brain barrier leakiness

(a-b) Sections of APP-PS1ΔE9 brains injected either with AAV-Venus (a) or AAV-APPsα (b) were labeled with anti-mouse secondary fluorescent antibody (red). DAPI blue. Scale bar=500µm. **(c-d)** APP-PS1ΔE9 brains sections injected either with AAV-Venus (c) or AAV-APPsα (d) labeled with a mouse NeuN primary antibody and an anti-mouse secondary antibody (green). Time point of analysis: 5 months after vector injection. Scale bar, 500µm. Note the absence of obvious msIgG staining. Slides depicted are examples from IHC control experiments and not precisely anatomically matched.

Figure S4

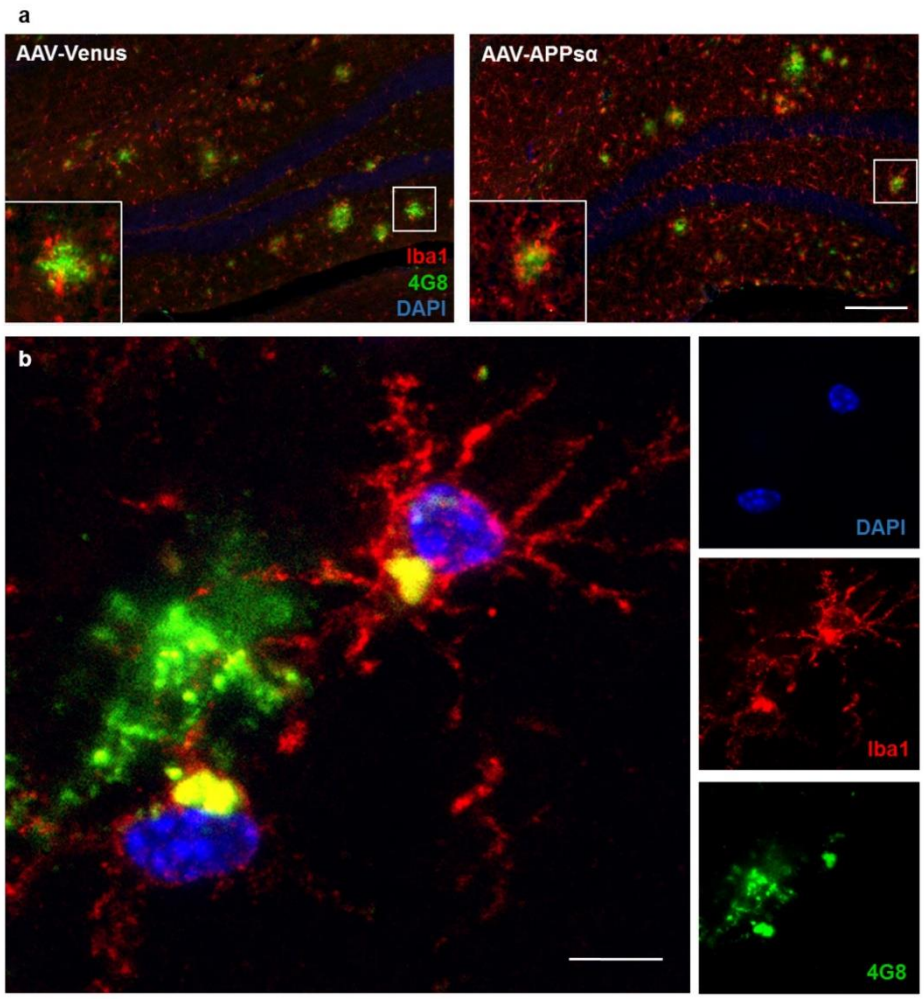

Figure S4: AAV-APPsα promotes microglia recruitment in the vicinity of plaques in APP/PS1ΔE9 mice

(a) Immunostaining of Iba1 (red) and 4G8 (amyloid-β plaques, green) in hippocampus (DG subfield) of APP/PS1ΔE9 transgenic mice. DAPI (blue) depicts the granular cell layer. Scale bar, 250 µm. **(b) Individual confocal** Z-stack of of Iba1 and 4G8 Co-immunostaining depicted in Figure 5i. Scale bar, 10 µm.

Supplementary references:

1. Borchelt DR, Davis J, Fischer M, Lee MK, Slunt HH, Ratovitsky T *et al.* A vector for expressing foreign genes in the brains and hearts of transgenic mice. *Genetic analysis : biomolecular engineering* 1996; **13**(6)**:** 159-163.

B. Article n°2 : Ebauche du futur article sur la surexpression d'APPsβ dans un modèle murin de la MA

Manuscrit en cours de préparation : Résultats préliminaires confidentiels

DISCRENPENCIES BETWEEN APPSα AND APPSβ GENE TRANSFER IN AN ALZHEIMER'S MOUSE MODEL

Fol R[1,2], Braudeau J[1], Ludewig S[3,4], Abel T[5], Weyer SW[6], Audrain M[1,2], Bemelmans AP[7], Buchholz CJ[5], Korte M[3,4], Müller UC[6], Cartier N[1]

1) INSERM U1169 / MIRCen CEA Fontenay aux Roses 92265 France, and Université Paris-Sud, 91400 Orsay, France

2) Université Paris Descartes, 75006 Paris, France

3) Zoological Institute, Division of Cellular Neurobiology, TU Braunschweig, Braunschweig, Germany

4) Helmholtz Centre for Infection Research, AG NIND, Inhoffenstr. 7, 38124 Braunschweig, Germany

5) Molecular Biotechnology and Gene Therapy, Paul-Ehrlich-Institut, 63225 Langen, Germany.

6) Department of Bioinformatics and Functional Genomics, Institute of Pharmacy and Molecular Biotechnology, Heidelberg University, Im Neuenheimer Feld 364, D-69120 Heidelberg, Germany

7) CNRS UMR9199 MIRCen CEA Fontenay aux Roses 92265, France

ABSTRACT:

Alzheimer's disease (AD) is characterized by an imbalanced processing of the amyloid precursor protein (APP) leading to an accumulation of the toxic Aβ peptide. However, the APP physiological function is yet poorly understood but most of it are thought to be mediated by the non-amyloidogenic pathway and the production of a soluble form: the APPsα. We recently showed that APPsα overexpression in the hippocampus alleviate the detrimental phenotype of APP/PS1ΔE9 mice. In the other hand, little is known about the slightly shorter APPsβ peptide, soluble APP form produced through the amyloidogenic pathway. We thereby overexpressed APPsβ in hippocampal neurons of aged APP/PS1ΔE9 mice by the mean of AAV viruses. Oppositely to APPsα, the efficient APPsβ expression in the hippocampus neither improve spatial reference memory in the Morris water maze nor synaptic plasticity nor spines number in the hippocampus. However, APPsβ was able to decrease soluble Aβ load without microglial activation. We therefore postulate that APPsα injection benefic consequences are only partially due to the decrease of Aβ which reinforces its crucial trophic function for brain physiology. The use of the 17 amino acids differing between the two soluble forms might be of therapeutic relevance.

Key words: Alzheimer, gene therapy, AAV, Amyloid Precursor Protein, APPsα, APPsβ, behavior, synaptic plasticity, spines, microglia

INTRODUCTION:

Alzheimer's disease (AD), the most common form of aged-related dementia is characterized by two main features: intracellular neurofibrillary tangles (aggregated of hyperphosphorylated Tau protein) and extracellular senile plaques constituted of amyloid-β peptides (Aβ). Elevated levels of soluble and aggregated Aβ are thought to hinder synaptic transmission and neuronal network which ultimately lead to cognitive disorders. The mechanism by which amyloidosis occurs in some individuals remains poorly understood but recent data suggest that the pathology initiate from an imbalance of the amyloid precursor protein (APP) processing (Selkoe and Hardy 2016; Sery et al. 2013; Gilbert 2014).

In vivo, the APP is cleaved following two independent and competing pathways. The non-amyloidogenic pathway is considered as being the physiological pathway, processing more than 80% of mature APP in non-pathological conditions. In this pathway, APP is sequentially cleaving by the α secretase (within the Aβ region) and then by the γ secretase. The first cut leads to the release of the APP soluble α fragment (APPsα)(Alves, Fol, and Cartier-Lacave 2016). The latter is secreted and displays neuroprotective and trophic properties. An increasing number of studies confirmed its protective effects on neurons and various macroscopic aggressions such as traumatic brain injury or strokes (reviewed in (Chasseigneaux and Allinquant 2012; Muller and Zheng 2012)). We recently showed that gene delivery of APPsα directly into the hippocampus of APP/PS1ΔE9 mice improves spatial reference memory, electrophysiological deficits and spines density (Fol et al. 2016).

In the non-amyloidogenic pathway, ultimately releasing the Aβ peptide, the β secretase initiate the APP cleavage. This gives rise to another APP soluble form, the APPsβ. Compared to APPsα, APPsβ is shorter of the 17 amino acids present at N-terminal position of the Aβ peptide (Muller and Zheng 2012). The most striking difference between the two peptides came from the study of Nikolaev et al., stating that only APPsβ undergoes a further cleavage. This produces a 35 kDa APP peptide which binds to the death receptor DR6 and mediates neurodegeneration under deleterious conditions (Nikolaev et al. 2009).

However, few studies focused on its physiological role and most of the recent studies used it as negative control to show APPsα beneficial role (Copanaki et al. 2010; Hick et al. 2015). Early on, its neuroprotective potential was shown to be significantly lower compared to its α-secretase-generated homolog (Furukawa et al. 1996). However, APPsβ seems more potent than APPsα to induce the neuronal differentiation of pluripotent stem cells (Freude et al. 2011). It was also shown to stimulate the activation of microglia but also promote neurite outgrowth *in vitro (Chasseigneaux et al. 2011; Barger and Harmon 1997)*. Nonetheless, little is known about a possible involvement into the pathologic process of AD or oppositely, a putative counterbalance to Aβ toxicity.

In the following study, we aimed to overexpress APPsβ by the mean of AAV9 vectors into the hippocampus of APP/PS1ΔE9 mice and compared its consequences to APPsα overexpression. We intended to evaluate its effects on electrophysiological, structural and behavioral deficits of this AD mouse model. APPsβ was efficiently and durably expressed into the neurons of the hippocampus. We first showed that APPsβ was unable to improve spatial reference memory of APP/PS1ΔE9 as APPsα does. Similarly, neither LTP nor spines density of the hippocampus were restored following APPsβ gene transfer. However, a significant reduction of soluble Aβ load, independent of microglia activation was observed. In contrast to APPsα, APPsβ gene transfer do not seems of therapeutic relevance to treat AD.

Materials and Methods:

AAV plasmid design and vector production

The mouse APPsα and APPsβ coding sequences were codon optimized (Geneart, Regensburg) and then cloned under control of the synapsin promoter into the single stranded rAAV2-based shuttle vector pAAVSynMCS-2A-Venus (Tang et al. 2009) via NheI-HindII restriction sites. For easy detection, an N-terminal double HA-tag was inserted downstream of the APP signal peptide at the N-terminus of APPsα and APPsβ. The control vector (pAAV-Venus) encodes the yellow fluorescent protein Venus fused to a C-terminal farnesylation signal for membrane anchoring. All constructs were packaged into AAV9 by the MIRCen viral production platform as described (Berger et al. 2015). Briefly, viral particles were produced by transient co-transfection of HEK-293 cells with an adenovirus helper plasmid (pXX6-80), an AAV packaging plasmid carrying the rep2 and cap9 genes, and the AAV2 transfer vector containing the above mentioned expression cassettes. 72 hours following transfection, virions were purified and concentrated from cell lysate and supernatant by ultracentrifugation on a iodixaniol density gradient followed by dialysis against PBSMK (0.5 mM MgCl2 and 1.25 mM KCl in PBS). Concentration of the vector stocks was estimated by quantitative-PCR according to the method described by (Aurnhammer et al. 2012)) and expressed as viral genomes per ml of concentrated stocks (vg/ml).

Animals

Twenty three APPswe/PS1ΔE9 mice (referred as APP/PS1ΔE9; Jackson Laboratories) and three age-matched littermate control mice were used for behavior, pathology and biochemistry. Thirteen APP/PS1ΔE9 and five littermates were used for electrophysiology. APP/PS1ΔE9 mice express the human APP gene carrying the *Swedish* double mutation (K595N/M596L). In addition, they express the human PS1ΔE9 variant lacking exon 9 (Borchelt et al. 1997; Jankowsky et al. 2004; Xiong et al. 2011). Only male mice were used throughout the study. For age at AAV injection and age at analysis/sacrifice see results section. All experiments were conducted in accordance with the ethical standards of French, German and European regulations (European Communities Council Directive of 24 November 1986).

Stereotactic injection of AAV

Mice were anesthetized by intraperitoneal injection of ketamine/xylazine (0.1/0.05 g/kg body weight) and positioned on a stereotactic frame (Stoelting, Wood Dale, USA). Vectors (either AAV-Venus or AAV-APPsα) were bilaterally injected into the hippocampus using 2 µl of viral preparation (10^{10} vg/hippocampus) at a rate of 0.2 µl/minute. Two injection sites per hippocampus were used to optimize virus

spreading. Stereotactic coordinates of injection sites from bregma were: anteroposterior -2 mm; mediolateral +/-1 mm; dorsoventral -2.25 mm and anteroposterior -2mm; mediolateral +/-1mm; dorsoventral -1.75mm.

Brain samples

APP/PS1ΔE9 mice were sacrificed 5 months post-injection at 17 months of age. Following anesthesia, mice were transcardially perfused with 0.1 M phosphate buffered saline (PBS) before dissection. For immunohistochemistry, the left cerebral hemisphere was dissected and post-fixed in 4% paraformaldehyde (PFA) for 1 week and cryoprotected in 30% sucrose for 24 hours. 40 µm sections were cut using a freezing microtome (Leica, Wetzlar, Germany), collected in a cryoprotective solution and stored at -20°C. The right hemisphere was dissected to segregate hippocampus and cortex for biochemical analysis. Samples were then homogenized in lysis buffer (TBS, NaCl 150mM and Triton 1%) containing phosphatase and protease inhibitors. After centrifugation (20 min, 13 000 rpm, 4°C), the supernatant was collected and the protein concentration was quantified by BCA Assay (Thermo Fisher Scientific, Waltham, USA). Lysate aliquots (3 mg of protein/ml) were stored at -80°C.

Immunostaining

Slices were washed with 0.1 M PBS and permeabilized in 0.25% PBS-Triton before blocking in PBS-Triton 0.25% containing 5% goat serum for 60 minutes. For vector encoded HA-APPsβ and HA-APPsα immunolabeling, slices were incubated with an anti-HA antibody (Covance, Princeton, USA, 1/250) overnight at 4°C. After successive washes (PBS-Triton 0.25%, PBS and PB 0.1 M), incubation with a biotinylated anti-mouse antibody was performed for one hour at room temperature. For signal amplification, samples were incubated using the ABC kit (Vector laboratories, Burlingame, USA) for one hour at room temperature. Finally, slices were incubated in Cy3-coupled streptavidine. HA-APPsβ or HA-APPsα were co-immunostained overnight with the following primary antibodies: Rabbit anti-Iba1,1/500, Wako, Richmond, USA; Mouse-GFAP Cy3 conjugate, 1/500, Sigma-Aldrich, Saint-Louis, USA; Rabbit anti-NeuN, 1/1000, Abcam, Cambridge, UK. For plaque quantification, slices were incubated in 88% formic acid solution for 15 min (antigen retrieval). To inactivate endogenous peroxidase, samples were incubated in hydrogen peroxide (30 min) before blocking and incubation with the primary antibody (4G8, Covance, 1/1000). Incubation with a horseradish coupled secondary antibody was done at RT, developed using the DAB kit (Vector laboratories) and mounted in Eukit mounting media (Sigma-Aldrich, Saint-Louis, USA). Images were taken with a Z6 APO macroscope (Leica). Plaques and Iba1 immunoreactivity were quantified using ImageJ (NIH, Bethesda, USA) or Icy (Institut Pasteur, Paris, France). Laser power, numeric gain and magnification were kept constant between animals to avoid potential technical artefacts. Images were first converted to 8-bit gray scale and binary thresholded to

highlight a positive staining. At least 2 sections per mouse (between −1.7 mm to −2.3 mm caudal to bregma) were quantified for either hippocampus or cortex. The average value per structure was calculated for each mouse. Experiments and data analysis were performed blind with respect to treatments and genotypes.

Western blot analysis

Proteins were separated by SDS-PAGE using 4-12% Bis-Tris gels (NuPAGE, Life Technologies, Carlsbad, USA) in MES SDS running buffer (NuPAGE, Life Technologies) and transferred to nitrocellulose membranes (iBlot, Life Technologies). After blocking in 5% milk-PBS 0.1M for 60 minutes, membranes were incubated with the primary antibodies overnight at 4°C. the following antibodies were used: HA, 1/2000, Covance, Princeton, USA; Venus (GFP), 1/1000, Vector laboratories Burlingame, USA; GAPDH, 1/4000, Abcam; Iba1, 1/2000, Wako, Richmond, USA. Membranes were then washed with TBS-T (with 0.1% Tween), incubated with a horseradish peroxidase coupled secondary antibody and developed using enhanced chemiluminescence (ECL, GE Healthcare, Little Chalfont, UK and Super Signal, Thermo Fisher Scienfitic). Signals were detected with Fusion FX7 (Vilber Lourmat, Marne-la-Vallée, France) and analyzed and quantified using ImageJ.

ELISA

For quantification of APP processing products in brain samples the following ELISA kits were employed: Human-specific APP β-CTF Assay Kit (IBL, Hamburg, Germany, JP27776) and V-PLEX Plus Aβ Peptide Panel 1 (4G8) Kit (Meso Scale Discovery, Rockville, USA) detecting at the same time hu/muAβ_{38}, hu/muAβ_{40}, and hu/muAβ_{42}. The procedures were performed according to the respective supplier instructions.

Morris Water Maze

Experiments were performed in a 120-cm diameter, 50 cm deep tank filled with opacified water kept at 21°C and equipped with a 10 cm diameter platform submerged 1 cm under the water surface. Visual clues were disposed around the pool as spatial landmarks for the mouse and luminosity was kept at 430 lux. Training consisted of daily sessions (three trials per session) during 5 consecutive days. Start positions varied pseudo-randomly among the four cardinal points. Mean inter-trial interval was 15 min. Each trial ended when the animal reached the platform. A 60 second cut-off was used, after which mice were gently guided to the platform. Once on the platform, animals were given a 30-second rest before being returned to their cage. 72 hours after the last training trial (day 8), retention was assessed during probe trial in which the platform was no longer present. Animals were video tracked using Ethovision software (Noldus, Wageningen, Netherlands) and behavioral parameters (swim speed,

travelled distance, latency, percentage of time spent in each quadrant) were automatically calculated. Experiments and statistical evaluation of data were performed by an experimentator blind to genotype and treatment group.

Statistics

Statistical analyses were performed as indicated for the respective experiments. Outliers were detected and rejected using maximum normed residual test (Grubbs' test). In most cases, data were analyzed using non-parametric Mann-Whitney U tests excepted for behavioral experiments. Two-way ANOVA with repeated measures were carried out when required by the experimental plan to assess statistical effects. Correlation matrices were generated using non-parametric Spearman rank correlation coefficient. For all analysis statistical significance was set to a p-value <0.05. All analyses were performed using Statistica (StatSoft Inc., Tulsa, USA) or Prism (GraphPad Software, La Jolla, USA).

Electrophysiology

In vitro extracellular recordings were performed on acute hippocampal slices of WT littermates stereotactically injected with the AAV-Venus (N= 5), APP/PS1ΔE9 mice injected either with AAV-Venus (N= 4), AAV-APPsβ orAAV-APPsα virus (N= 4) at 8-9 months of age. Electrophysiological recordings were performed 4-5 months later at an age of 12-13 months. In-between animals were housed in a temperature- and humidity-controlled room with a 12h light-dark cycle and had access to food and water *ad libitum*.

Work in progress.

Dendrite and spine analysis

Work in progress.

RESULTS

AAV-APPs injections induce an efficient and durable expression of hippocampal neurons in APP/PS1ΔE9 mice

In order to assess the consequences of APPsβ overexpression into an AD mouse model, we used viral-mediated gene transfer. Recent strategies for brain gene therapy transfer are now coalescing around AAV viruses which are non-pathogenic and induce low inflammation. We used AAV9 viruses to inject the hippocampus of APP/PS1ΔE9 mice. We aimed to restrain the APPs expression to their neurons by the use of the synapsin promoter. AAV9-Venus or AAV9-APPsβ and AAV9-APPsα both hemaglutinine tagged (thereafter referred as AAV-Venus, AAV-APPsβ and AAV-APPsα) (**Figure 1a**) were injected into the brain of aged APP/PS1ΔE9 mice (12 months) already displaying memory, synapses dysfunctions and substantial amyloidosis (Volianskis et al. 2010; Jankowsky et al. 2004). The *stratum lacunosum moleculare* and the dentate gyrus regions of the hippocampus were targeted by the bilateral injection (**Figure 1b**). Mice were sacrificed at 17 months old, 5 months post-injection to evaluate the expression of both APPsβ. We first show an efficient transduction of the hippocampus (especially in the CA1, CA2 and dentate gyrus). Moreover, APPsβ expression also diffused into the peri-hippocampal cortex (**Figure 1c**).The pattern of expression in the hippocampus was similar in AAV-APPsα injected mice (**Figure 1l**). The APPsβ expression showed also a nice diffusion from rostral to caudal coordinates in both cortex and hippocampus (**Figure 1d-h**). Further cellular analysis of the CA1 layer confirmerd that the synapsin promoter allowed us to specifically and efficiently transduce neurons without any transduction of neither astrocytes nor microglia (**Figure 1i-k**). We also analyzed the hippocampus of these mice by the mean of western blots. Levels of expression of APPsβ-HA and APPsα-HA were very close and consistent in every single animal injected. AAV-Venus control animals also displayed a similar level of Venus in-between them (**Figure 1m**). We therefore confirm the long lasting efficiency and specificity of our viral-mediated APPs delivery in mice.

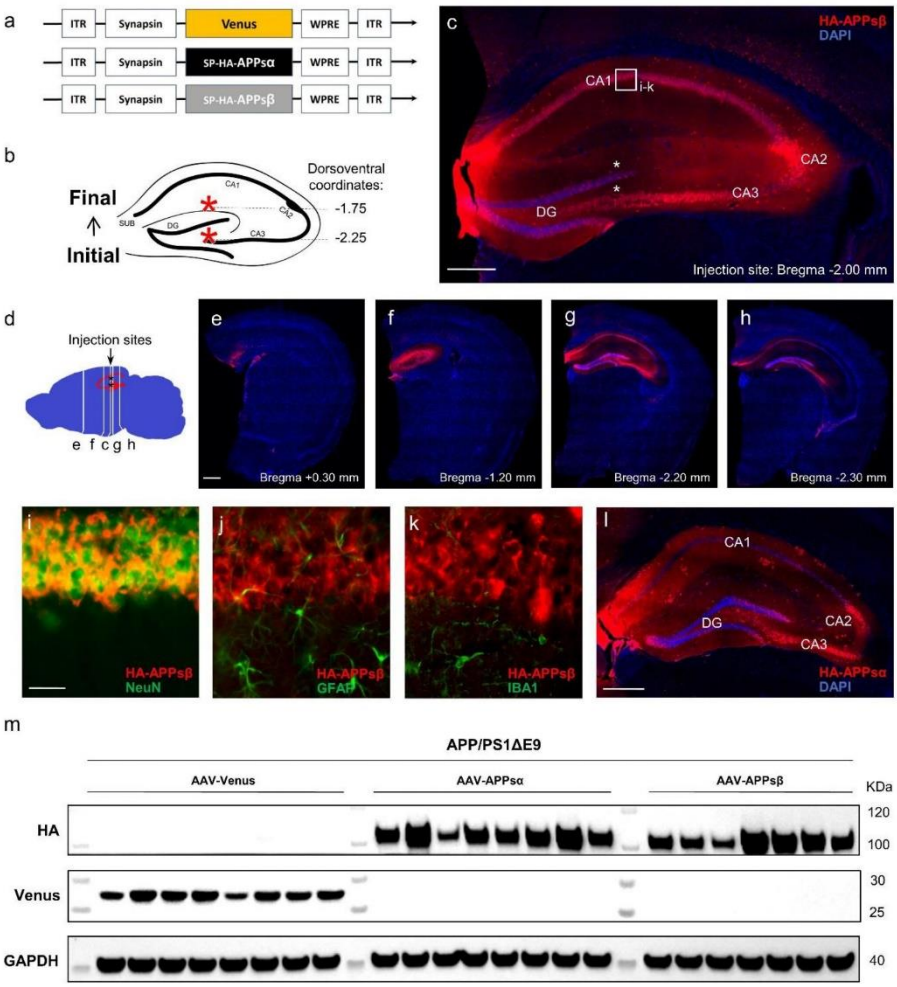

Figure 1: Widespread expression of APPsβ throughout the hippocampus in APP-PS1ΔE9 mice. APP/PS1ΔE9 and non-transgenic littermate control mice (LM) were injected either with AAV-Venus, AAV-APPsα or AAV-APPsβ at 12 months of age and sacrificed at 17 months of age. (LM: AAV-Venus *n* = 3; APP/PS1ΔE9 mice: AAV-Venus *n* = 8, AAV-APPsα *n* = 8, AAV-APPsβ n = 7; all males). **a** Schematic representation of AAV9 constructs enabling the neuron-specific expression of Venus (Negative control), HA-tagged APPsα (Positive control) and HA-tagged APPsβ. ITR: inverted terminal repeat; SP: APP signal peptide; HA: Human influenza hemagglutinin tag; WPRE: Woodchuck hepatitis virus posttranscriptional regulatory element. **b** Scheme of the hippocampus with coordinates of the two injection sites (*red stars*). **c** High magnification of the hippocampus of an APP/PS1ΔE9 mouse injected with the AAV-APPsβ. APPsβ i(anti-HA tag, *red*) is detectable throughout the hippocampus. *Scale bar*, 500 µm. Injection sites indicated by *white stars*. **d** Scheme representing anteroposterior coordinates of coronal sections depicted in **c**, **e–h**. Injection sites indicated by *black stars*. **e–h** Immunostaining of APPsβ at different anteroposterior coordinates.

Scale bar, 500 µm. **i-k** Double immunostaining of CA1 pyramidal cells from the area boxed in **c** expressing APPsβ (anti-HA tag, *red*) and specific neuronal (NeuN, *green*, **i**), astrocytic (GFAP, *green*, **j**) or microglial (IBA1, *green*, **k**) markers. *Scale bar*, 50 µm. Note that AAV-mediated APPsβ expression is restricted to neurons. **l** High magnification of the hippocampus of an APP/PS1ΔE9 mouse injected with the AAV-APPsβ. APPsβ i(anti-HA tag, *red*) is detectable throughout the hippocampus. *Scale bar*, 500 µm. Injection sites indicated by *white stars*. **m** Western blot analysis of HA-muAPPsα/β, muAPP and Venus expression in APP/PS1ΔE9 hippocampi of mice injected with AAV-Venus, AAV-APPsα or AAV-APPsβ vectors. Note that antibody m3.2 is specific for muAPP and recognizes endogenous muAPP and HA-muAPPsα but not HA-muAPPsβ.

AAV-APPsβ does not improve spatial reference memory of aged APP/PS1ΔE9

We used the Morris water maze to evaluate the spatial reference of the APP/PS1ΔE9 mice. Transgenic mice (AAV-Venus (n=8), AAV-APPsα (n=8) or AAV-APPsβ (n=7)) or littermate controls (AAV-Venus (n=3)) were injected at 12 months old and assessed 2 months later at 14 months of age. The procedure comprise five days of training were the platform is hidden under the water surface in the target quadrant (TQ, **Figure 2a**). During this phase, every group of animals showed an efficient learning of the platform position highlighted by a decreased distance to find it over the five days (**Figure 2b**). 72 hours after the last training session, the platform is removed in order to assess spatial reference memory evidenced by the distance spent in the TQ (**Figure 2c**). APP/PS1ΔE9 control mice injected with AAV-Venus showed an impaired memory as compared to AAV-Venus injected littermate mice (Tukey post-hoc test: p=0.04). AAV-APPsα injection in transgenic mice improved spatial reference memory as previously shown (p= 0.01). However, AAV-APPsβ treatment did not display such effect as the time spent in the TQ was equivalent to AAV-Venus mice (p= 0.99) and significantly different compared to AAV-APPsα mice (p= 0.02). The lack of efficiency of AAV-APPsβ to restore an efficient search strategy is highlighted by the occupancy plots (**Figure 2d**). Together, these results demonstrate that, oppositely to AAV-APPsα, AAV-APPβ injection is not able to restore memory deficits of APP/PS1ΔE9.

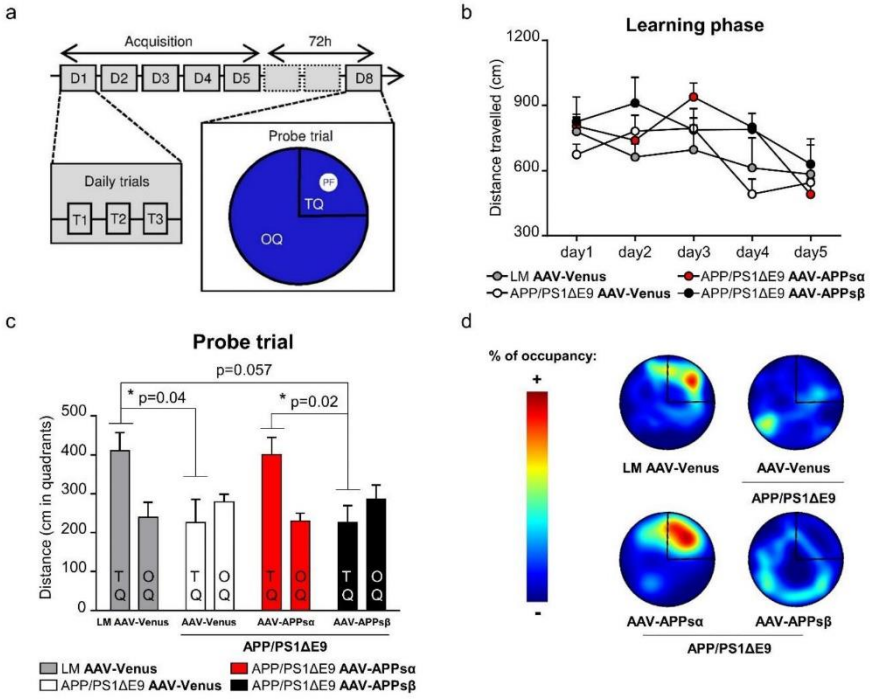

Figure 2: Unlike APPsα, APPsβ overexpression does not rescue spatial memory deficit of APP/PS1ΔE9 mice in the Morris water maze. Littermate (LM) controls injected with Venus (n = 3) or transgenic APP/PS1ΔE9 mice (n = 7-8 per group) either injected with AAV-Venus, AAV-APPsα or AAV-APPsβ vectors at 12 months of age were tested 2 months later at 14 months of age. **a** Training phase consisted of daily sessions (three trials per session: T1, T2 and T3) during five consecutive days (D1–D5). 72 h (D8) after the last trial the platform was removed and memory retention was assessed during the probe trial. *Insert* water maze configuration during training sessions. PF: platform (*white*); TQ: target quadrant (*small segment*); OQ: other quadrants (*large segment*). **b** Distance to platform of littermate controls or APP/PS1ΔE9 mice injected either with AAV-Venus, AAV-APPsα or AAV-APPsβ. Learning phase was similar between the different groups (2-way ANOVA: group effect: $F3,23 = 1.50$; ns; time effect: $F4,92 = 7.50$; $p < 0.0001$; group × time interaction: $F12,92 = 1.62$; ns). **c** Probe trial performance at 72 h. 2-way ANOVA, group × quadrant interaction effect: $F3,19 = 4.04$; $p = 0.02$. APP/PS1ΔE9 mice injected with AAV-Venus were impaired in comparison to littermate mice injected with AAV-Venus (Tukey post hoc test: $p = 0.04$) confirmed by no preference for the trained target quadrant. Unlike AAV-APPsα treatment in APP/PS1ΔE9 mice which restored time spent in the target quadrant (Tukey post hoc test: $p = 0.011$), AAV-APPsβ did not improve their performances compared to APP/PS1ΔE9 mice injected with AAV-Venus (Tukey post hoc test: $p > 0.99$). Data represent mean ± SEM and were analyzed by 2-way ANOVA (genotype and group as factors) with repeated measures followed by Tukey post hoc test. $^*p < 0.05$. **d** Representative occupancy plots during the probe trial show a more random search strategy for AAV-Venus injected APP/PS1ΔE9 mice. Note that AAV-APPsα injected transgenic mice show directionality towards the platform (indicated by *segment*) similar to littermate

controls. AAV-APPsβ injected APP/PS1ΔE9 mice do not show any preference for the target quadrant.

Preliminary results on APP/PS1ΔE9 synaptic plasticity analysis.

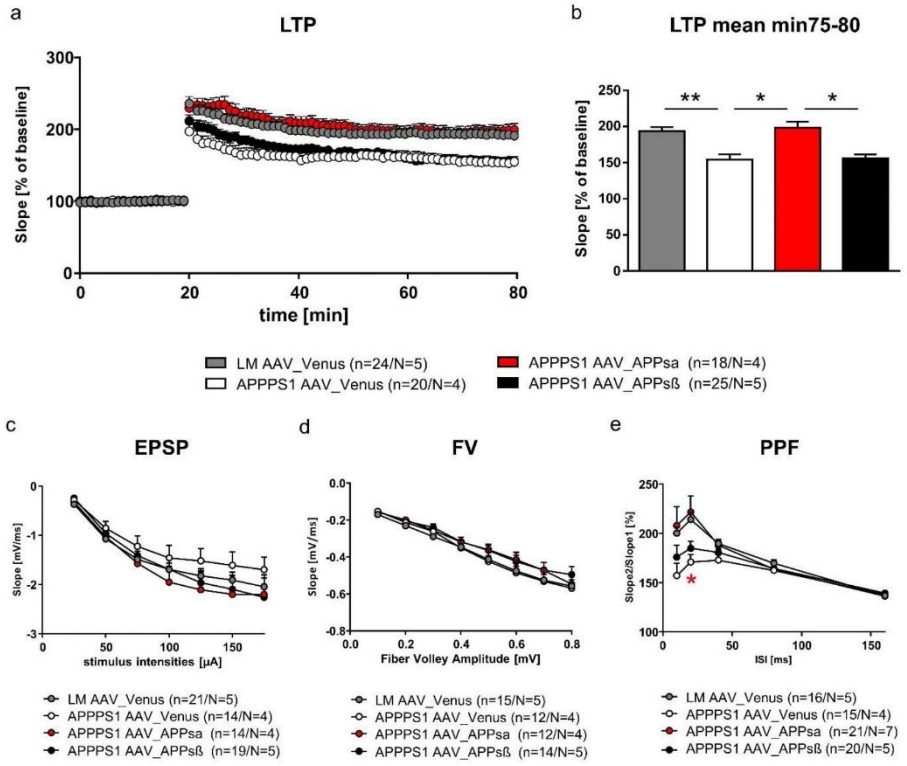

Figure 3: AAV-APPsβ injection do not restore long term potentiation in the hippocampus of aged APP/PS1ΔE9 mice. a, b LTP was induced by TBS at hippocampal CA3-CA1 synapses after 20 min baseline recordings. Acute slices of AAV-Venus (open circles) injected APP/PS1ΔE9 animals exhibited significant lower induction and maintenance of LTP compared to littermate controls (LM, grey circles) indicating a significant impairment of the transgenic mice. Viral expression of APPsα (red circles) restored potentiation after TBS in transgenic animals and resulted in an LTP curve progression comparable to that of LM controls. However, AAV-APPsβ injection (black circles) did not restore APP/PS1ΔE9 mice which show a similar level compared to AAV-Venus transgenic mice. The LTP induction rate is shown as percentage % of mean baseline slope, n = number of slices, N = number of mice. **c, d** Input–Output strength of all AAV-injected mice showed no alterations between genotypes at any fiber volley (FV) amplitude or stimulus intensity tested. **e** Altered PPF at the 10 ms ISI revealed a significant impairment in the pre-synaptic compartment of APP/PS1ΔE9 mice injected with AAV-Venus in comparison to LM controls. This parameter was restored after AAV-APPsα injection but not with AAV-APPsβ.

AAV-APPsβ and AAV-APPsα injections decrease soluble Aβ levels in aged APP/PS1ΔE9.

We then assessed the APP amyloidogenic processing of the APP/PS1ΔE9 mice injected at 12 months of age either with AAV-Venus, AAV-APPsα or AAV-APPsβ and sacrificed 5 months later. By the mean of an electrochemiluminescent ELISA, we first measured both murine and human Aβ38, Aβ40 and Aβ42 soluble levels in the hippocampus and cortex of the transgenic mice. We first confirm the ability of AAV-APPsα gene transfer to decrease all three forms of Aβ (Tukey's post-hoc test, Aβ38, p=0.009; Aβ40, p=0.02; Aβ42, p=0.04). Strikingly, AAV-APPsβ injection was also able to decrease soluble Aβ38 (p=0.03), Aβ40 (p=0.03) and Aβ42 (p=0.06) levels (**Figure 4a,b,c**). However, human β-CTF levels were neither altered by AAV-APPsα nor AAV-APPsβ injection (**Figure 4d**). Finally, we confirmed the efficiency of AAV-APPsα injection to decrease Aβ plaques in hippocampus and cortex (Tukey's post-hoc test, p=0.003). This effect could not be seen after AAV-APPsβ treatment (**Figure 4e,f**). These data suggest that APPsβ overexpression is able to decrease soluble Aβ in the hippocampus but also in distant cortex due to its diffusion. However, in contrast to AAV-APPsα, it could not decrease the aggregated form Aβ as amyloid plaques.

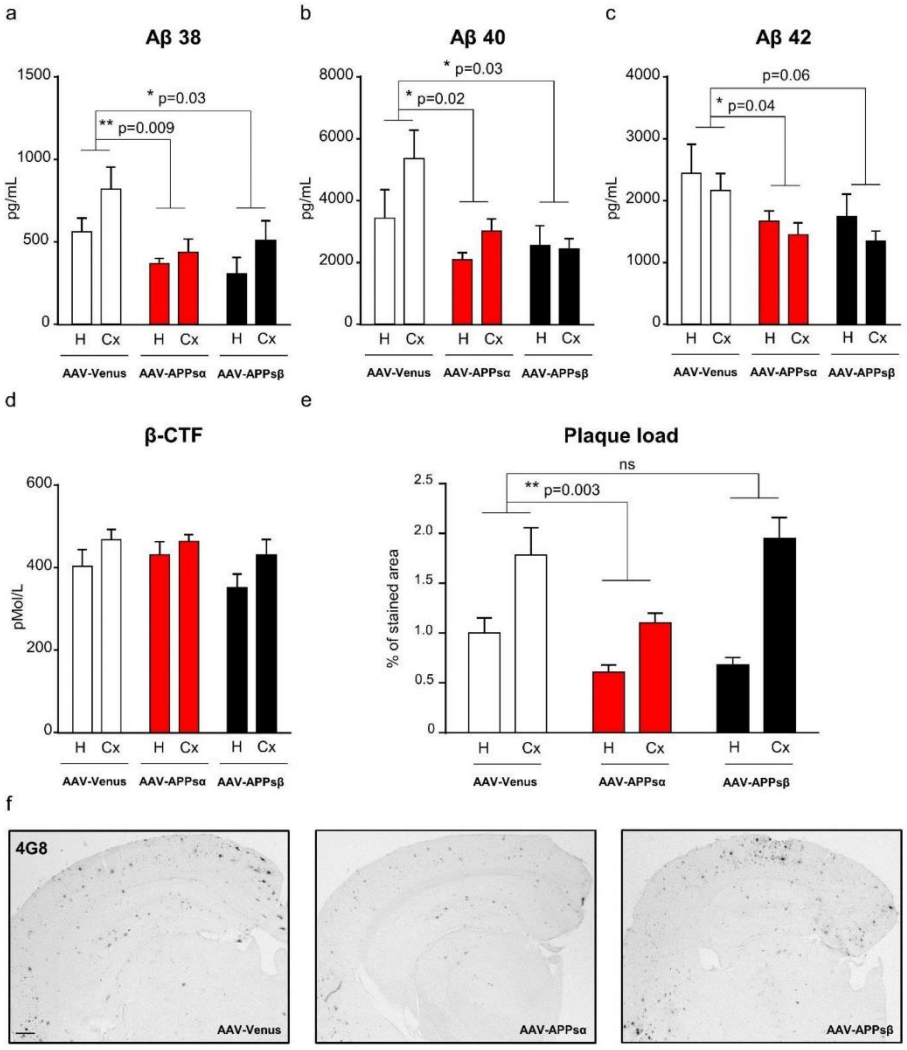

Figure 4: AAV-APPsβ injection decreases Aβ but not plaques load. a-c Quantification (4G8 based immunoassay detecting both mu/huAβ species) of TBS soluble Aβ38 (group effect: $F2,36 = 6.187$, $p = 0.0049$), Aβ40 (group effect: $F2,36 = 5.292$, $p = 0.0097$) and Aβ42 (group effect: $F2,36 = 4.225$, $p = 0.023$; region effect: Aβ38 $F1,36 = 4.97$, $p = 0.032$, Aβ40 $F1,36 = 2.58$, $p = 0.12$, Aβ42 $F1,36 = 1.36$, ns; group × region interaction effect: $F2,36 < 2$, ns) in hippocampus (H) and cortex (Cx) of APP/PS1ΔE9 mice. Note that AAV-APPsα and AAV-APPsβ injected animals show reduced levels of Aβ in both anatomical regions analyzed (hippocampus and cortex). Data were analyzed by 2-way ANOVA (Genotype, group and region as factors) with repeated measures followed by Tukey post hoc test. **d** ELISA quantification of huβ-CTF in hippocampus and cortex of APP/PS1ΔE9 mice. No difference was detectable between AAV-Venus, AAV-APPsα and AAV-APPsβ injected animals. **e** Quantification of 4G8 immunolabeled area in hippocampus and cortex (group effect:

$F2,147 = 6.151$, $p = 0.0027$; region effect: $F1,147 = 35.17$, $p < 0.0001$; group × region interaction effect: $F2,147 = 2.273$, ns). Note that 4G8 immunoreactive plaque area do not decrease in AAV-APPsβ compared to AAV-Venus treated animals (p = 0.87; ns). Number of animals $n = 7/8$ per group. Data were analyzed by one-way ANOVA followed by Tukey's post-hoc test. Data represent mean ± SEM. $^{**}p < 0.01$, $^{*}p < 0.05$. f Representative images of hippocampus and cortex of APP/PS1ΔE9 mice injected either with AAV-Venus, AAV-APPsα or AAV-APPsβ. Scale bar, 500 µm.

AAV-APPsβ does not activate microglia *in vivo*

In order to potentially explain the discrepancy between AAV-APPsα and AAV-APPsβ regarding amyloid plaques degradation, we assessed microglial activation. We previously showed that APPsα was able activate microglia which in turns internalize Aβ and upregulate the amyloid degrading enzyme IDE and the receptor TREM2 (Fol et al. 2016). We first confirm this activation evidenced by the Iba1 marker upregulation in both western blot and immunohistochemistry. However, such effect could not be evidenced with AAV-APPsβ compared to AAV-Venus injected control mice (**Figure 5a-d**).This results might indicate that the AAV-APPsα effects on soluble Aβ in one hand and amyloid plaques in the other hand are mediated by two independent mechanisms. Finally, the lack of activation following APPsβ injection could explain why plaques levels are not impacted.

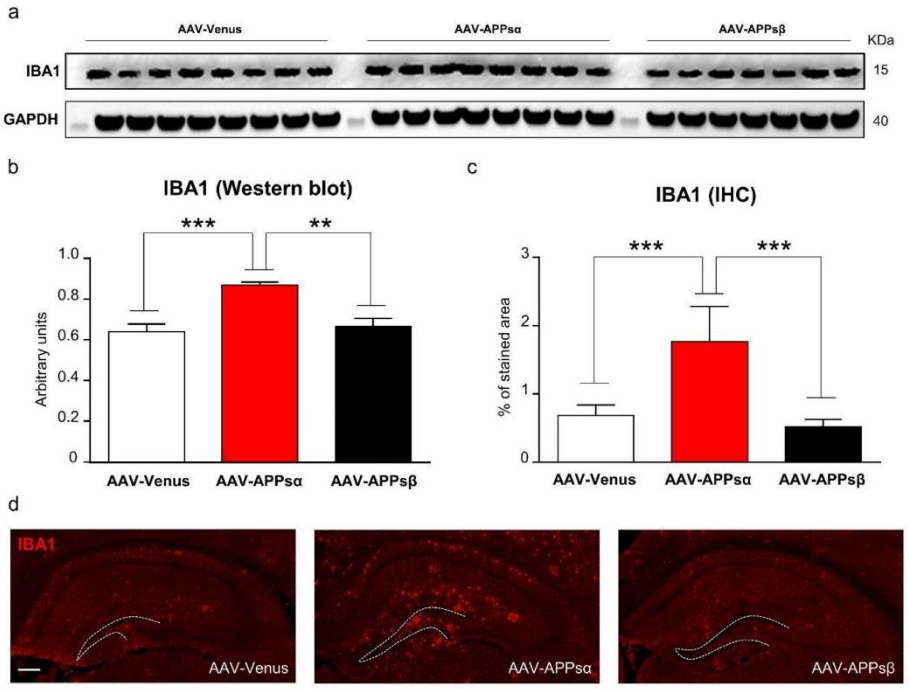

Figure 5: AAV-APPsβ injection does not activate microglia. a Western blot analysis showing the expression of IBA1 (microglial marker) in the hippocampus of AAV-Venus, AAVAPPsα or AAV-APPsβ injected APP/PS1ΔE9 mice (n = 7/8 per group). **b** For quantification signal intensity was normalized to GAPDH used as a loading control (One-way ANOVA: group effect: $F2,19 = 14.38$, $p = 0.0002$). AAV-APPsα treatment specifically increased IBA1 expression (p = 0.0002) whereas AAV-APPsβ did not (p = 0.82). **c** Quantification of IBA1 signal in the hippocampus following immunohistochemistry in APP/PS1ΔE9 mice injected either with AAV-Venus, AAV-APPsα or AAV-APPsβ (One-way ANOVA: group effect: $F2,41 = 14.12$, $p < 0.0001$). As seen in western blot, AAV-APPsβ injection is unable to rise IBA1 levels compared to AAV-Venus treated mice. Values represent mean ± SEM. $^{***}p < 0.001$, $^{**}p < 0.01$. **d** Representative images of hippocampi immunolabeled with IBA1. Scale bar, 500µm.

DISCUSSION

Work in progress.

REFERENCES

Alves, S., R. Fol, and N. Cartier-Lacave. 2016. 'Gene Therapy Strategies for Alzheimer's Disease: An Overview', *Hum Gene Ther*.

Aurnhammer, C., M. Haase, N. Muether, M. Hausl, C. Rauschhuber, I. Huber, H. Nitschko, U. Busch, A. Sing, A. Ehrhardt, and A. Baiker. 2012. 'Universal real-time PCR for the detection and quantification of adeno-associated virus serotype 2-derived inverted terminal repeat sequences', *Hum Gene Ther Methods*, 23: 18-28.

Barger, S. W., and A. D. Harmon. 1997. 'Microglial activation by Alzheimer amyloid precursor protein and modulation by apolipoprotein E', *Nature*, 388: 878-81.

Berger, A., S. Lorain, C. Josephine, M. Desrosiers, C. Peccate, T. Voit, L. Garcia, J. A. Sahel, and A. P. Bemelmans. 2015. 'Repair of Rhodopsin mRNA by Spliceosome-Mediated RNA Trans-Splicing: A New Approach for Autosomal Dominant Retinitis Pigmentosa', *Mol Ther*.

Borchelt, D. R., T. Ratovitski, J. van Lare, M. K. Lee, V. Gonzales, N. A. Jenkins, N. G. Copeland, D. L. Price, and S. S. Sisodia. 1997. 'Accelerated amyloid deposition in the brains of transgenic mice coexpressing mutant presenilin 1 and amyloid precursor proteins', *Neuron*, 19: 939-45.

Chasseigneaux, S., and B. Allinquant. 2012. 'Functions of Abeta, sAPPalpha and sAPPbeta : similarities and differences', *J Neurochem*, 120 Suppl 1: 99-108.

Chasseigneaux, S., L. Dinc, C. Rose, C. Chabret, F. Coulpier, P. Topilko, G. Mauger, and B. Allinquant. 2011. 'Secreted amyloid precursor protein beta and secreted amyloid precursor protein alpha induce axon outgrowth in vitro through Egr1 signaling pathway', *PLoS One*, 6: e16301.

Copanaki, E., S. Chang, A. Vlachos, J. A. Tschape, U. C. Muller, D. Kogel, and T. Deller. 2010. 'sAPPalpha antagonizes dendritic degeneration and neuron death triggered by proteasomal stress', *Mol Cell Neurosci*, 44: 386-93.

Fol, R., J. Braudeau, S. Ludewig, T. Abel, S. W. Weyer, J. P. Roederer, F. Brod, M. Audrain, A. P. Bemelmans, C. J. Buchholz, M. Korte, N. Cartier, and U. C. Muller. 2016. 'Viral gene transfer of APPsalpha rescues synaptic failure in an Alzheimer's disease mouse model', *Acta Neuropathol*, 131: 247-66.

Freude, K. K., M. Penjwini, J. L. Davis, F. M. LaFerla, and M. Blurton-Jones. 2011. 'Soluble amyloid precursor protein induces rapid neural differentiation of human embryonic stem cells', *J Biol Chem*, 286: 24264-74.

Furukawa, K., B. L. Sopher, R. E. Rydel, J. G. Begley, D. G. Pham, G. M. Martin, M. Fox, and M. P. Mattson. 1996. 'Increased activity-regulating and neuroprotective efficacy of alpha-secretase-derived secreted amyloid precursor protein conferred by a C-terminal heparin-binding domain', *J Neurochem*, 67: 1882-96.

Gilbert, B. J. 2014. 'Republished: the role of amyloid beta in the pathogenesis of Alzheimer's disease', *Postgrad Med J*, 90: 113-7.

Hick, M., U. Herrmann, S. W. Weyer, J. P. Mallm, J. A. Tschape, M. Borgers, M. Mercken, F. C. Roth, A. Draguhn, L. Slomianka, D. P. Wolfer, M. Korte, and U. C. Muller. 2015. 'Acute function of secreted amyloid precursor protein fragment APPsalpha in synaptic plasticity', *Acta Neuropathol*, 129: 21-37.

Jankowsky, J. L., D. J. Fadale, J. Anderson, G. M. Xu, V. Gonzales, N. A. Jenkins, N. G. Copeland, M. K. Lee, L. H. Younkin, S. L. Wagner, S. G. Younkin, and D. R. Borchelt. 2004. 'Mutant presenilins specifically elevate the levels of the 42 residue beta-amyloid peptide in vivo: evidence for augmentation of a 42-specific gamma secretase', *Hum Mol Genet*, 13: 159-70.

Muller, U. C., and H. Zheng. 2012. 'Physiological functions of APP family proteins', *Cold Spring Harb Perspect Med*, 2: a006288.

Nikolaev, A., T. McLaughlin, D. D. O'Leary, and M. Tessier-Lavigne. 2009. 'APP binds DR6 to trigger axon pruning and neuron death via distinct caspases', *Nature*, 457: 981-9.

Selkoe, D. J., and J. Hardy. 2016. 'The amyloid hypothesis of Alzheimer's disease at 25 years', *EMBO Mol Med*.

Sery, O., J. Povova, I. Misek, L. Pesak, and V. Janout. 2013. 'Molecular mechanisms of neuropathological changes in Alzheimer's disease: a review', *Folia Neuropathol*, 51: 1-9.

Tang, W., I. Ehrlich, S. B. Wolff, A. M. Michalski, S. Wolfl, M. T. Hasan, A. Luthi, and R. Sprengel. 2009. 'Faithful expression of multiple proteins via 2A-peptide self-processing: a versatile and reliable method for manipulating brain circuits', *J Neurosci*, 29: 8621-9.

Volianskis, A., R. Kostner, M. Molgaard, S. Hass, and M. S. Jensen. 2010. 'Episodic memory deficits are not related to altered glutamatergic synaptic transmission and plasticity in the CA1 hippocampus of the APPswe/PS1deltaE9-deleted transgenic mice model of ss-amyloidosis', *Neurobiol Aging*, 31: 1173-87.

Xiong, H., D. Callaghan, J. Wodzinska, J. Xu, M. Premyslova, Q. Y. Liu, J. Connelly, and W. Zhang. 2011. 'Biochemical and behavioral characterization of the double transgenic mouse model (APPswe/PS1dE9) of Alzheimer's disease', *Neurosci Bull*, 27: 221-32.

VI. DISCUSSION ET PERSPECTIVES

Mon travail de thèse porta sur les rôles fonctionnels des formes solubles de l'APP et leur potentiel thérapeutique dans le cadre de la MA. Ainsi, j'ai pu tester la surexpression de l'APPsα et de l'APPsβ dans un modèle murin de la MA. Je discuterai dans une première partie des conséquences de la surexpression de l'APPsα, de son potentiel thérapeutique et des différences que l'on a pu mettre en évidence avec l'APPsβ. Une seconde partie sera consacrée aux perspectives.

A. Discussion des résultats

1. Les outils de l'étude : les souris transgéniques, les AAV et le promoteur neuronal

Les conditions dans laquelle l'étude a été effectuée sont intimement liées aux conclusions que l'on en tire à sa fin. Ainsi, il me semble important de discuter de celles-ci avant d'évoquer les conclusions de mon travail de thèse. Les deux études se sont ainsi intéressées à l'analyse comportementale, électrophysiologique, structurale, biochimique et histologique des **souris APP/PS1ΔE9**. Comme mentionné précédemment (voir partie IV.B.6), ce modèle murin est très populaire parmi la communauté scientifique travaillant sur le versant amyloïde de la maladie. En effet, celui-ci possède les avantages classiques des souris transgéniques, à savoir une évolution rapide de l'amyloïdose et des conséquences fonctionnelles robustes, très rapidement détectables et quantifiables. Nous avons ainsi pu confirmer une amyloïdose croissante avec l'âge (Figure 32) associée à de la glie réactive, l'altération de la LTP, du nombre d'épines dendritiques et des défauts de mémoire spatiale après douze mois. Nous avons aussi **volontairement injecté ces souris à un âge relativement avancé**. A douze mois, ces souris présentaient déjà toutes les perturbations citées précédemment. Malgré l'évolution des outils diagnostiques, ce stade de la pathologie représente au mieux le degré d'altération du patient lors de leur inclusion dans les protocoles cliniques actuels (Villemagne, Burnham et al. 2013).

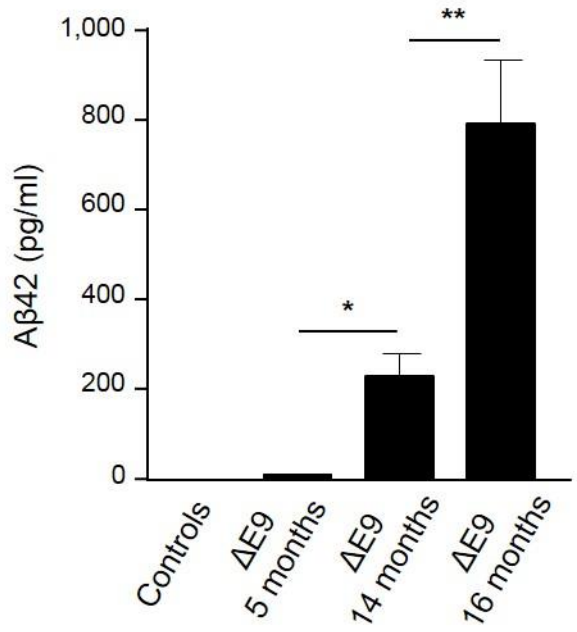

Figure 32: Les souris APP/PS1ΔE9 présentent des quantités Aβ solubles croissantes en fonction de l'âge. Niveaux d'Aβ42 chez les souris APP/PS1ΔE9 à 5, 14 et 16 mois (données internes).

Ces modèles sont donc très pratiques mais d'un autre côté très **caricaturaux de ce qu'est réellement la MA chez l'homme** (Duyckaerts, Potier et al. 2008). En effet, l'augmentation de l'APP taille entière, l'amyloïdose massive, les défauts synaptiques prématurés, l'absence de mort neuronale et de pathologie tau sont les points de différence majeurs avec l'homme. Mais ce sont ces modèles qui sont utilisés dans 90% des cas, faute de mieux pour le moment. Ceci peut expliquer, en partie, les échecs des essais cliniques lors des 25 dernières années. Les résultats thérapeutiques avec l'APPsα dans ce modèle sont donc encourageants mais doivent être pris avec précaution concernant un transfert chez l'homme. Néanmoins, d'autres modèles plus proches de la physiopathologie ont récemment été développés comme les souris knock-in APP *Swedish, Beyreuther/Iberian* ou notre propre modèle par transfert de gènes, qui permet notamment d'étudier les phases précoces de la MA (Saito, Matsuba et al. 2014, Audrain, Fol et al. 2016).

Les formes solubles de l'APP furent ensuite surexprimées dans ces souris au moyen d'un **vecteur AAV**, plus précisément d'un AAV9 (voir partie IV.D.2). C'est un vecteur classiquement utilisé dans notre laboratoire, que ce soit pour l'expression hippocampique d'APPsα, d'APOE2 ou de CYP46A1 mais aussi le transfert de l'APP et la PS1 pour la création d'un modèle rat. Ainsi, que ce soit l'expression de l'APP *swedish london* ou des formes solubles APPsα et APPsβ, l'utilisation d'un AAV nous permet

une transduction efficace de l'hippocampe. De manière intéressante, celui-ci nous permit de concentrer fortement l'expression de ces trois formes dans **le *subiculum* et le CA2** (Figure 33). De plus, nous observons une bonne expression de l'APPsα dans le cortex para-hippocampique, très probablement responsable de la diminution d'Aβ soluble dans cette structure. Ainsi, nous attribuons en partie ce phénomène à la diffusion de l'AAV9, sans négliger la diffusion de l'APPsα depuis ses sites de productions hippocampiques.

Enfin, pour terminer sur les outils principaux de l'étude, je souhaite rapidement revenir sur le **choix du promoteur**. Avant le début de l'étude, trois choix s'offraient à nous : le promoteur SFFV (Spleen Focus-Forming Virus), promoteur viral fort utilisé en culture par notre collaborateur Christian Buchholz, le promoteur CAG (Cytomegalovirus βActin βGlobin), promoteur fort classiquement utilisé dans notre laboratoire et le promoteur synapsine (Kugler, Kilic et al. 2003, Gonzalez-Murillo, Lozano et al. 2010). Nous avons finalement choisi ce dernier puisqu'il représente un bon compromis entre **niveau d'expression et spécificité neuronale**. Cependant, le promoteur CAG a toujours démontré une expression exclusivement neuronale dans nos mains (Figure 33). Nous avons ainsi récemment produit un plasmide codant l'APPsα sous le contrôle de ce promoteur, l'objectif étant de tester le potentiel d'une surexpression plus forte de l'APPsα dans l'hippocampe de souris APP/PS1ΔE9. Enfin, bien que l'expression physiologique de l'APP soit majoritairement neuronale dans le cerveau, nous pouvons nous demander si la surexpression ubiquitaire d'APPsα, par le biais d'un promoteur de type PGK (PhosphoGlycerate Kinase), pourrait-être intéressante dans le cadre de la MA.

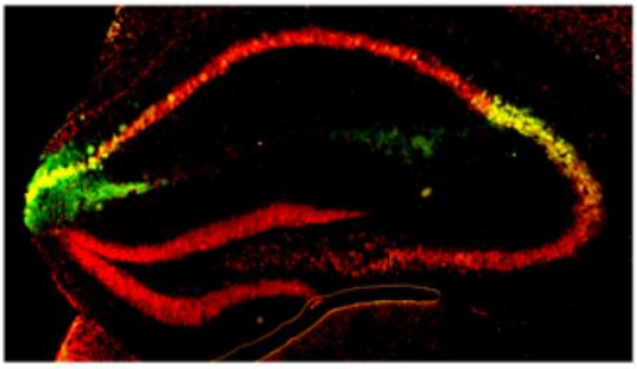

Figure 33: Expression de l'APP humaine sous le contrôle du promoteur CAG dans un cerveau de souris. L'APP humaine *swedish london* fut injectée au moyen d'un AAV10 dans l'hippocampe de souris C57Bl6/j. Noter la localisation de l'APP humaine (vert) avec les neurones des couches pyramidales (rouges). (Audrain, Fol et al. 2016)

2. Le rééquilibrage du métabolisme de l'APP comme cible thérapeutique

Nous avons choisi la surexpression du peptide APPsα afin de restaurer la balance du clivage de l'APP vers un équilibre physiologique. Dû à ses propriétés neurotrophiques et neuroprotectrices mais aussi à sa diffusibilité, ce fragment est une cible de choix pour la thérapie génique intracérébrale. Cependant, il est important d'indiquer que la surexpression directe de l'APPsα n'est **pas le seul moyen de rééquilibrer le métabolisme de l'APP**. Nous avons par exemple déjà évoqué la surexpression d'ADAM lors de l'introduction (voir partie IV.C.1) et je ne reviendrai pas donc sur ces éventuels effets indésirables dû à ses multiples autres cibles (Prox, Rittger et al. 2012). Cependant, la **stimulation de nombreux récepteurs** permet une augmentation de son activité et ainsi un relargage accru de l'APPsα. Dès le début des années 1990, il fut montré que les récepteurs couplés aux protéines G, comme par exemple les récepteurs muscariniques, contrôlent la production d'APPsα (Nitsch, Slack et al. 1992). Plus récemment, les récepteurs sérotoninergiques 5-HT_4 ont été montrés comme pouvant favoriser le clivage de l'APP par ADAM10 et ainsi le relargage d'APPsα (Robert, Zugaza et al. 2001, Cochet, Donneger et al. 2013). L'utilisation d'un agoniste de ceux-ci permet de notamment augmenter la production de l'APPsα (Giannoni, Gaven et al. 2013). Cependant, cette famille de récepteurs n'est pas la seule impliquée dans la régulation de la voie non-amyloïdogène. En effet, l'activation des récepteurs purinergiques P2X7 permettent le relargage du peptide APPsα (Delarasse, Auger et al. 2011, Darmellah, Rayah et al. 2012). Celle-ci est médiée par le biais de la voie MAP/ERK, précédemment impliquée dans le métabolisme non-amyloïdogène de l'APP (Chasseigneaux, Dinc et al. 2011). La stimulation de ces récepteurs peut donc être d'intérêt thérapeutique, en particulier dans le cadre de la MA.

3. Surexprimer l'APPsα dans la MA : une approche intéressante

Je vais ici discuter des résultats de l'article n°1 avec des arguments semblables à la discussion de ce dernier (Fol, Braudeau et al. 2016). Je traiterai tout d'abord des conséquences fonctionnelles de la surexpression de l'APPsα dans le modèle murin de la MA. J'aborderai dans une seconde partie les possibles mécanismes par lesquels passe le bénéfice thérapeutique mis en évidence.

a. Conséquences fonctionnelles

Nous avons spécifiquement surexprimé l'APPsα au moyen d'un vecteur viral dans l'hippocampe de souris modélisant le versant amyloïde de la pathologie Alzheimer. Bien que le peptide diffuse dans les structures synaptiques adjacentes, ce système reste un modèle d'étude des **conséquences hippocampiques** de la restauration du métabolisme de l'APP. Ainsi, nous avons restauré (partiellement ou totalement) dans cette structure, la densité synaptique, la LTP et la facilitation neuronale (Paired Pulsed Facilitation, PPF) et finalement la mémoire spatiale des souris APP/PS1ΔE9. Il y a bien sûr une **corrélation forte entre ces trois paramètres** et les répercussions fonctionnelles (LTP et mémoire spatiale) peuvent être ainsi directement expliquées par la normalisation structurelle du nombre d'épines dendritiques dans l'hippocampe. Chez l'homme, le couple troubles mnésiques/altérations synaptiques et leur forte corrélation est considéré comme étant un moteur prépondérant dans l'évolution de la pathologie (Terry, Masliah et al. 1991, Selkoe 2002).

L'effet de l'APPsα sur la **densité synaptique** a pu être entrevu indirectement lors de précédentes études. En effet, la transgénèse d'ADAM10 ou la surexpression d'une forme sauvage de l'APP dans un modèle Tg2576 de la MA améliorent tous deux la genèse d'épines dendritiques (Bell, Zheng et al. 2008, Lee, Moussa et al. 2010). Cependant, notre étude montre pour la première fois une **restauration de ce paramètre dans un contexte pathologique** par la surexpression directe d'APPsα. Nous avons ainsi pu mettre en évidence une amélioration de la densité synaptique dans deux zones de l'hippocampe ; le CA1 et le CA3. Cette étude confirme ainsi le rôle synaptotrophique de l'APPsα mais aussi sa capacité à contrecarrer les conséquences néfastes d'une surcharge importante d'Aβ.

La **LTP** de l'hippocampe est une mesure de la force synaptique qui a bien sûr été exclusivement étudiée chez les animaux de laboratoire. Cependant, il est couramment admis que celle-ci sous-tend l'apprentissage et la mémoire (Sweatt 2016). Ainsi chez la souris, l'extrême majorité des modèles de la MA présente cette atteinte de la LTP et des défauts de mémoire (Alzforum). De manière intéressante, dans nos souris APP/PS1ΔE9 âgées de douze mois au moment de l'injection, nous avons été capables de complètement restaurer la LTP mais aussi la PPF qui représente le degré de **l'altération présynaptique**. Ce dernier paramètre contribue à la mesure de la LTP globale et sa restauration influe grandement sur celle de la LTP. Il est aussi intéressant de noter que ce compartiment présynaptique est détérioré chez les patients atteints de la MA (Shankar and Walsh 2009). Les effets d'APPsα sur la LTP ne sont pas ici démontrés pour la première fois (Ishida, Furukawa et al. 1997, Ring, Weyer et al. 2007, Taylor, Ireland et al. 2008, Hick, Herrmann et al. 2015), mais aucune étude électrophysiologique de ce type n'avait été effectuée dans un modèle présentant une amyloïdose forte. De par cette restauration, il peut être envisageable de penser que l'APPsα a, à un moment ou un autre, été localisé au niveau de la fente synaptique. Cette observation est en accord avec le fait

que de manière générale, l'APP et ses dérivés se retrouvent localisés au niveau de cette zone présynaptique et joue un rôle dans la transmission synaptique (Ring, Weyer et al. 2007, Lassek, Weingarten et al. 2013).

Les deux composantes précédemment citées, densité synaptique et LTP, ont bien sûr une conséquence sur la troisième : **l'apprentissage et la mémoire** des souris APP/PS1ΔE9. En testant celles-ci grâce à la piscine de Morris, nous n'avons pu mettre en évidence une amélioration de l'apprentissage des souris transgéniques après injection de l'APPsα. Cependant, au cours des cinq jours d'entrainement, quand la plateforme est présente dans le quadrant cible, l'injection de l'APPsα dans les souris sauvages améliore grandement leur performance par rapport aux souris sauvages contrôles. Cette donnée confirme ainsi que même dans un cadre physiologique, la surexpression de l'APPsα semble **bénéfique pour les capacités d'apprentissage**. Dans une seconde phase, nous testâmes la mémoire des souris en retirant la plateforme et évaluant le temps qu'elles passèrent à chercher celle-ci dans le quadrant cible. La surexpression de l'APPsα dans les souris transgéniques nous permit d'**améliorer significativement les performances mnésiques** de celles-ci en comparaison avec les souris injectées avec Venus. Nous n'avons cependant pas pu mettre en évidence un effet promnésiant chez les souris sauvages, comme nous avons pu le faire lors de la phase d'apprentissage. L'APPsα apparait ainsi comme une cible intéressante afin de contrecarrer la dégradation mnésique typique de la MA.

Nous n'avons cependant pas observé de défauts d'apprentissage chez les souris APP/PS1ΔE9 alors que celles-ci présentaient, lors de la phase de restitution, un fort trouble de la mémoire. Toutefois, cette différence qui peut sembler surprenante au premier abord, est loin d'être un phénomène rare lors de l'étude de souris transgéniques modélisant la MA. Ainsi, cette différence entre apprentissage et mémorisation a par exemple été observée auparavant chez la souris « 3xTg » APP/PS1/Tau ou chez le rat présentant une lésion du CA3 de l'hippocampe (Roozendaal, Phillips et al. 2001, Billings, Oddo et al. 2005). En outre, cette dernière étude marque l'importance du CA3 dans le processus de mémorisation. Nous avons montré une diminution du nombre d'épines dendritiques des souris APP/PS1ΔE9 âgées de douze dans cette région. Et de manière intéressante, notre injection d'APPsα induit une restauration de la densité synaptique pouvant expliquer, au moins partiellement, l'amélioration des capacités mnésiques.

b. Mécanismes d'action possibles

L'amélioration de la LTP grâce à l'APPsα avait pu être mise en évidence précédemment soit *in vitro* (Ishida, Furukawa et al. 1997) ou bien *in vivo* (Ring, Weyer et al. 2007,

Taylor, Ireland et al. 2008, Hick, Herrmann et al. 2015). L'étude issue du laboratoire du Cliff Abraham montre d'ailleurs que la modulation de la LTP passe par un **effet de l'APPsα sur les récepteurs NMDA**, plus particulièrement dans le gyrus denté. Des études d'immunoprécipitation montrèrent que l'APP taille entière interagit directement avec les récepteurs NMDA et augmente leur disponibilité synaptique *in vitro* (Cousins, Hoey et al. 2009, Cousins, Innocent et al. 2013). Il convient maintenant de savoir si ses formes solubles extracellulaires, et plus particulièrement l'APPsα, sont tout aussi capables d'induire ce phénomène.

Comme indiqué précédemment, la surexpression et la sécrétion de l'APPsα peut être induite via **l'activation des récepteurs couplés aux protéines G**. Une étude *in vitro* montra récemment que les effets neuroprotecteurs induits par l'APPsα étaient médiés par contact direct avec **l'APP taille entière, qui serait finalement le propre récepteur de ses formes solubles**. Cette dernière va, au moyen des récepteurs aux protéines G induire la signalisation de la voie Akt (Milosch, Tanriover et al. 2014). Cette hypothèse fournit ainsi un autre mode d'action possible de l'APPsα qui reste à explorer plus en détail. Néanmoins, les travaux du groupe d'Ulrike Müller démontra aussi que l'injection d'APPsα restaure les défauts de LTP dans une souris APP/APLP2 double KO suggérant que l'APP n'est pas le seul récepteur d'APPsα (Hick, Herrmann et al. 2015). L'identification précise de ses récepteurs est un enjeu crucial dans la compréhension du signalement physiologique induit par l'APPsα mais aussi sa possible stimulation pharmacologique dans un cadre thérapeutique (Figure 34).

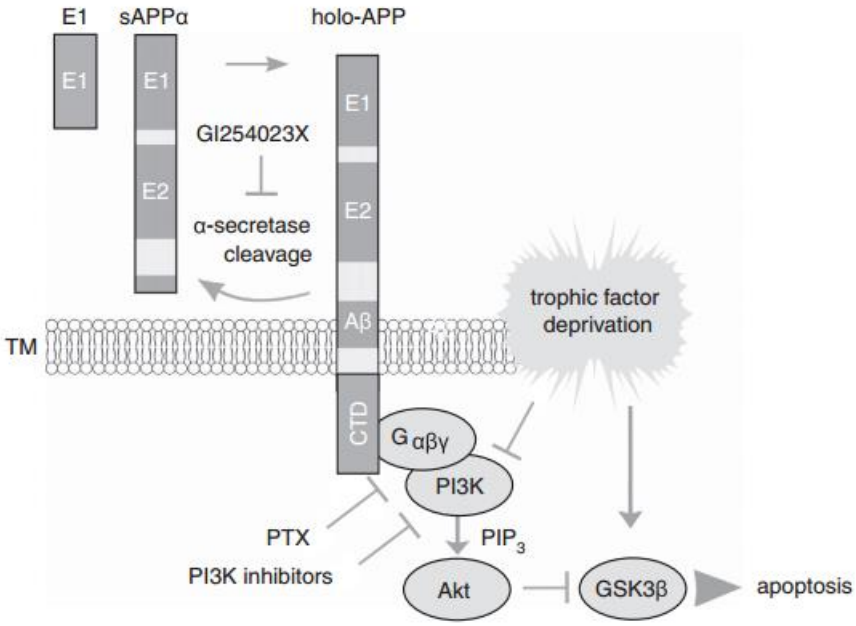

Figure 34: Mécanisme d'action possible de l'effet neuroprotecteur de l'APPsα. Le schéma ci-dessus postule que l'APP taille entière et ancré à la membrane serait le récepteur d'APPsα et permettrait de médier ses effets bénéfiques. (Milosch, Tanriover et al. 2014)

Outre les effets les effets bénéfiques entrevus au niveau de la synapse, nous avons aussi pu mettre en évidence une **diminution d'Aβ38, 40 et 42 supérieure à 30%**. Il est important de noter que l'injection d'APPsα murin permit la diminution aussi bien des formes endogènes murines que les formes transgéniques humaines dans l'hippocampe et le cortex. Cette même injection induisit aussi une **baisse du niveau des plaques amyloïdes de l'ordre de 25%**, là aussi dans l'hippocampe et le cortex. Les propriétés diffusibles du peptide prennent ainsi tout leur sens et permettent, avec une seule injection intra-hippocampe de diminuer la charge amyloïde **dans les structures adjacentes**. Il est ainsi fort probable que la baisse de la concentration en Aβ soluble toxique et de l'encombrement stérique induit par les plaques participe à l'amélioration de la force synaptique et de la mémoire spatiale des souris.

Une diminution de l'amyloïdose fut aussi observée après transgénèse de l'APPsα dans ces mêmes souris APP/PS1Δ9. Les auteurs clament que la **liaison directe entre l'APPsα et BACE1** induirait cette baisse (Obregon, Hou et al. 2012). Dans notre étude, nous n'avons ni pu mettre en évidence une diminution du β-CTF ni de l'APPsβ*swe* après injection d'APPsα. Cette différence peut être expliquée par différents arguments comme le mode d'expression de l'APPsα (transgénèse ubiquitaire versus transfert viral hippocampique et neuronal dans notre cas), la durée de l'expression (*in utero* versus cinq mois à partir du milieu de vie) ou l'âge du sacrifice (huit mois versus dix-sept mois

où l'amyloïdose est bien plus conséquente). Cependant, nous suggérons ici un potentiel mécanisme d'action complémentaire.

La capacité de l'APPsα à activer la microglie fut mise en évidence en culture dès les années 1990 (Barger and Harmon 1997, Bodles and Barger 2005). Ce mécanisme fut longtemps considéré comme délétère mais la stimulation de la population microgliale du cerveau est apparu récemment comme une cible de choix pour le traitement de la MA (McGeer and McGeer 2015). Plus généralement, la recrudescence d'études sur les rôles de la microglie dans la MA nous ont permis de mieux connaître ce type cellulaire. Du côté pathogénique, la « dark microglia » qui représenterait un stade ultime de pathogénicité, notamment dans les souris APP/PS1, fut récemment mise en évidence (Bisht, Sharma et al. 2016). D'un autre côté, la microglie semble essentielle à la physiologie du cerveau et peut être surtout bénéfique, selon son type d'activation, dans la MA (Tremblay, Stevens et al. 2011, McGeer and McGeer 2015). Ainsi, deux types d'activation furent décrits par le passé : les profils M1 et M2 (Tang and Le 2016). La conversion d'un profil M1 (inflammatoire et neurotoxique) vers un phénotype d'activation M2, moins inflammatoire et présentant une capacité accrue de phagocyter l'Aβ, est une piste thérapeutique majeure pour le traitement de la MA.

Nous montrons ainsi que l'injection d'APPsα induit un changement morphologique de la microglie caractéristique de son activation (Prokop, Miller et al. 2013). Son activation est maximale autour des plaques amyloïdes de l'hippocampe et induit une phagocytose intracellulaire de l'Aβ. Nous postulons ainsi que la diminution de la charge en plaques amyloïdes est, au moins partiellement, induite par cette activation. De plus, TREM2, récepteur microglial associé à la MA, fut récemment montré comme pouvant lier et internaliser l'Aβ (Wang, Cella et al. 2015). Il est ainsi plausible de penser que ce phénomène soit responsable de la diminution d'Aβ. **L'activation microgliale induite par APPsα va donc permettre de diminuer l'Aβ soluble comme fibrillisé et induire leur dégradation grâce notamment à la surexpression d'IDE, enzyme de dégradation de l'Aβ.** Ce mécanisme est responsable d'une diminution de l'amyloïdose hippocampique (mais aussi corticale) et en partie responsable des bénéfices synaptiques et mnésiques mis en évidence chez les souris APP/PS1ΔE9.

4. Point sur l'étude de l'APPsβ : 16 acides aminés, ça compte ?

Après avoir étudié les conséquences de la surexpression d'APPsα dans l'hippocampe de souris atteintes de la MA, nous nous sommes intéressés à son homologue de la voie amyloïdogénique, l'APPsβ. Comme indiqué dans l'introduction (voir partie IV.C.3) très peu d'études se sont attachées à étudier ce peptide. Ainsi, son éventuelle implication dans le processus pathogénique de la MA ou au contraire son possible rôle protecteur

sont inconnus. De la même manière que pour la première étude, nous avons surexprimé l'APPsβ au moyen d'AAV9 dans l'hippocampe de souris APP/PS1ΔE9 âgées de douze mois. Nous avons tout d'abord pu mettre en évidence **une magnitude d'expression similaire à l'APPsα**, exclusivement neuronale et diffusant jusque dans le cortex. Ainsi nous avons pu comparer les effets des deux peptides dans le reste de l'étude et étudier pour la première fois les conséquences de la surexpression *in vivo* d'APPsβ.

Au niveau fonctionnel, nous montrons qu'APPsβ n'est **pas capable de restaurer la LTP et la PPF** des souris APP/PS1ΔE9 âgées de douze mois. Toujours de manière opposée à l'injection d'APPsα, APPsβ n'est **pas capable de restaurer les défauts de mémoire spatiale** des souris transgéniques lors du test en piscine de Morris. Ces données préliminaires nous montre donc que, contrairement à l'APPsα, la surexpression d'APPsβ ne permet de restaurer les fonctions mnésiques hippocampe-dépendante détériorées par une surcharge amyloïde. Notre étude renforce donc des données *in vitro* suggérant l'absence d'effet neuroprotecteur de l'APPsβ (Furukawa, Sopher et al. 1996, Copanaki, Chang et al. 2010). L'étude du nombre d'épines dendritiques dont les résultats sont attendus prochainement sera intéressante afin de compléter ces données.

Notre étude montre aussi pour la première fois l'influence de la surexpression d'APPsβ sur le métabolisme amyloïdogénique de l'APP. Cette injection induit la **diminution de l'Aβ 38, 40 et 42** d'origine murine et humaine, dans l'hippocampe et le cortex des souris APP/PS1ΔE9 **sans avoir de répercussions sur la charge en plaques amyloïdes**. De la même manière que pour l'APPsα, nous n'avons pu mettre en évidence une baisse de la concentration en β-CTF suggérant que l'activité et/ou l'expression de BACE1 n'est pas altérée. Cependant, l'injection d'APPsβ n'est-elle **pas capable d'induire une réactivité microgliale** dans l'hippocampe. L'étude approfondie de ce mécanisme doit se poursuivre dans les prochaines semaines avec notamment l'étude spécifique en périphérie des plaques amyloïdes, la morphologie microgliale, la phagocytose d'Aβ et l'exploration des marqueurs TREM2 et IDE.

Ainsi, ces données préliminaires suggèrent trois points importants :

- Premièrement, elles sous-entendent que **l'activation de la microglie**, mise en évidence après injection d'APPsα est **responsable de la baisse de la charge en plaques amyloïdes**. Nous confirmerons ces résultats prochainement en étudiant le marquage Iba1 en périphérie des plaques après injection d'APPsβ.

- Deuxièmement, ces résultats suggèrent que la **diminution d'Aβ induite par la surexpression d'APPsβ passe par un autre phénomène que l'activation microgliale**. Il sera donc important de mesurer les niveaux d'APPsβ humain

de cette souris, pour confirmer que l'activité/l'expression de BACE1 n'est pas altérée. Si celle-ci est confirmée, il pourrait être intéressant de s'intéresser à la γ secrétase qui pourrait possiblement être modulée aussi bien par APPsβ qu'à APPsα.

- Finalement, l'interprétation de ces données sous-entend que **les effets fonctionnels bénéfiques mis en évidence après injection d'APPsα seraient principalement dû à un effet synaptrophique** et non à la diminution de l'amyloïdose chez ces souris APP/PS1ΔE9.

La comparaison de mes deux études suggère donc deux mécanismes indépendants suivant l'injection d'APPsα. Tout d'abord un effet **trophique bénéfique** pour la synapse (densité synaptique et LTP restaurée) induisant une restauration mnésique. Puis, d'un autre côté, une **diminution de l'amyloïdose** cérébrale, en partie due à l'activation microgliale. Même si cette dernière ne semble pas cruciale pour l'amélioration de la mémoire spatiale, on peut penser qu'elle ne soit pas délétère dans le cadre d'un traitement pour la MA.

Pour terminer, il semblerait donc qu'à ce point de l'étude de la surexpression d'APPsβ, bien que capable de diminuer les formes solubles d'Aβ, celle-ci ne soit pas suffisante pour envisager un réel bénéfice thérapeutique. Ainsi, l'étude approfondie des 16 acides C-terminaux de l'APPsα, absents sur l'APPsβ semble crucial pour la compréhension des fonctions physiologiques et thérapeutiques des formes solubles de l'APP.

B. Perspectives : Orientations futures et autres projets

Dans cette seconde partie de la discussion, je discuterai brièvement de différentes pistes d'études qui seront entreprises dans les mois à venir ou qui me sembleraient intéressantes de traiter à moyen terme.

1. Utiliser l'APPsα à des fins thérapeutiques ; les prochaines étapes

L'injection intra-hippocampique d'APPsα nous permit pour la première fois de mettre en évidence **l'activation microgliale** induite par ce peptide *in vivo*. La **voie de signalisation par laquelle l'APPsα induit cette stimulation reste cependant méconnue**. Une étude *in vitro* publiée par le groupe de Steven Barger suggère que celle-ci est induite par la voie des MAP kinases (Bodles and Barger 2005). Cette étude suggère cependant un rôle délétère de cette activation notamment due à une production d'iNOS, enzyme productrice d'oxyde nitrique. Notre étude suggère cependant le contraire à travers une phagocytose des plaques et possiblement d'Aβ. Cependant, le profil complet de ces cellules microgliales en pourtour de plaques amyloïdes reste à explorer en détails. Il conviendra ainsi de déterminer à quel type d'activation, M1 ou M2, conduit la stimulation de l'APPsα. Ceci pourrait être réalisé *in vitro* soit après tri de la microglie de souris APP/PS11ΔE9 injectées avec l'APPsα soit transfection directe de ce dernier dans la microglie en culture. Cette stratégie pourrait aussi permettre de caractériser finement le lien entre APPsα et TREM2, qui pourrait être le moteur potentiel de cette activation microgliale. L'étude de la cascade de signalisation induite par TREM2 avec notamment son partenaire DAP12, pourrait être intéressante (Ulland, Wang et al. 2015).

Si le profil M2 est mis en évidence grâce à l'étude citée ci-dessus, il pourrait être envisageable de **cibler l'expression d'APPsα directement dans cette population microgliale**. Deux solutions sont possibles. Soit l'injection intracérébrale directe grâce à un AAV et un promoteur microglial comme par exemple CD68 ou F4/80 (Cucchiarini, Ren et al. 2003). Soit le recours aux **cellules souches hématopoïétiques** qui réinjectées après le transfert de gène de l'APPsα *ex vivo*, vont induire la formation de cellules microgliales dans le cerveau. Cette dernière stratégie est en cours de développement dans notre laboratoire par le Dr Satoru Tada (Asheuer, Pflumio et al. 2004, Cartier, Lewis et al. 2014).

Nous avons aussi délibérément choisi d'injecter l'APPsα à un stade relativement avancé de la pathologie. En effet, comme je l'ai décrit précédemment, les souris APP/PS1ΔE9 âgées de douze mois présentent une concentration d'Aβ importante, une charge en plaques élevée et des altérations de la mémoire spatiale dans la piscine de Morris. Cet

état corrèle globalement avec le stade auquel les patients atteints de la MA sont inclus dans les protocoles cliniques (Villemagne, Burnham et al. 2013). Il serait cependant intéressant de tester la capacité de l'APPsα à **prévenir la pathologie amyloïde ainsi que les défauts électrophysiologiques et comportementaux**. L'injection de ces mêmes souris APP/PS1ΔE9 à un stade plus précoce est une piste à explorer, tout comme le recours à un second modèle de la pathologie présentant des propriétés physiopathologiques différentes. Cette seconde option est actuellement explorée dans le cadre du consortium nEUAPPs (voir partie VI.B.5).

Il serait réducteur de définir la MA à travers la seule composante amyloïde. Le versant tau est en effet crucial dans la physiopathologie de la maladie (voir partie IV.B.6.c). Je n'ai volontairement pas abordé ce sujet en détail dans ma thèse puisqu'il ne constitue pas le cœur de celle-ci. Cependant, si l'on considère que les effets bénéfiques de l'APPsα sont médiés par un effet trophique et non par la seule modulation de la pathologie amyloïde, **il pourrait être envisageable de tester sa surexpression neuronale dans un modèle de tauopathie**. Dans le laboratoire, nous avons précédemment utilisé le même type de développement préclinique pour CYP46A1, enzyme de conversion du cholestérol. Ainsi, après avoir testé sa surexpression dans un modèle amyloïde (Hudry, Van Dam et al. 2010), sa surexpression dans un modèle tau fut testée (Burlot, Braudeau et al. 2015). Les souris THY-Tau22 (Schindowski, Bretteville et al. 2006), développées par Luc Buée pourraient elle aussi être utilisées afin d'évaluer les effets de la surexpression de l'APPsα sur la pathologie tau.

Enfin, je souhaite rappeler ici que la version murine de l'APPsα fut utilisée dans notre étude. En effet, s'il on considère que les effets trophiques et amyloïdo-protecteurs passent par la liaison du peptide soluble à un récepteur, il y a bien sûr de plus forte chance que sa version murine soit plus affine pour les récepteurs murins. Cependant, dans le cadre d'un développement préclinique, il conviendra de **tester la version humaine** de l'APPsα, qui présente tout de même 97% d'homologie avec la version souris. Les plasmides (toujours avec le promoteur synapsine) et les virus (AAV9) ont d'ores et déjà été produits et seront testés dans les mois à venir.

2. Vers un transfert clinique de l'APPsα ?

Nous l'avons vu dans l'introduction, les propriétés neuroprotectrices de l'APPsα furent largement démontrées au cours de ces 20 dernières années (voir partie IV.C.2). Notre étude constitue une étape centrale du développement préclinique, seconde étape clé dans le processus d'innovation thérapeutique. La troisième est bien sûr le test chez l'homme, l'essai clinique. Cependant, il existe un fossé entre les phases précliniques et cliniques et les étapes intermédiaires sont nombreuses. Nous venons d'ailleurs de voir, selon moi,

les prochaines études à effectuer (sans compter la toxicologie voire l'injection chez le gros animal) avant d'envisager de tester la surexpression de l'APPsα chez l'homme. Cependant, une question majeure reste ; **La thérapie génique est-elle envisageable chez le patient âgé, atteint de la MA ?**

Un seul essai clinique de thérapie génique dans le cadre de la MA fut réalisé à ce jour (voir partie IV.A.6). La phase 1 fut réalisée il y a plus de 15 ans, au début des années 2000. Le gène d'intérêt était le **Nerve Growth Factor (NGF)**, principale neurotrophine du SNC. Il est important de noter que la correction génétique fut réalisée *ex vivo* avant réimplantation de fibroblastes génétiquement modifiés dans le cerveau (Tuszynski, Thal et al. 2005). L'AAV2 codant pour le NGF fut ensuite directement injecté dans le noyau de Meynert, sans bénéfice thérapeutique, ce qui causa l'arrêt de l'essai clinique. Ainsi, pour revenir à notre cas, est-il toujours envisageable d'effectuer une injection directe de plusieurs heures chez des patients âgés de plus de 65 ans ? Il semblerait qu'une autorisation de la part de l'ANSM et/ou de la FDA soit difficile à obtenir notamment dû au fait que les conditions d'autorisation d'essai clinique se sont durcies ces dernières années et devrait continuer dans ce sens suite à « l'affaire Biotrial » (Butler and Callaway 2016). Il serait peut-être même aussi difficile d'obtenir cette autorisation pour des personnes atteintes de formes génétiques et touchées plus précocement.

Deux solutions sont envisageables selon moi afin de contourner cet écueil. J'ai déjà évoqué la première un peu plus haut mais le recours aux **cellules souches hématopoïétiques** me semble intéressant. Celles-ci peuvent même être prélevées dans la circulation périphérique grâce une stimulation au G-CSF (Granulocyte Colony-Stimulating Factor) afin d'éviter une chirurgie trop lourde (Hosing 2012). De plus, contrairement au traitement d'une leucémie, les cellules souches résidentes n'ont pas besoin d'être entièrement déplétées avant réintroduction des cellules transduites avec l'APPsα. Deuxièmement, la stimulation pharmacologique de la production et du relargage de l'APPsα semble être une approche envisageable pour le traitement de la MA. Celle-ci pourrait notamment passer par l'utilisation de **molécules pharmacologiques** afin de stimuler les récepteurs 5-HT_4 (Figure 35). Une étude récente menée par Patrick Dallemagne montra le potentiel thérapeutique d'une molécule (le Donecopride) ayant la double propriété de stimuler la production d'APPsα (comme la RS 67333) et d'inhiber l'acétylcholinestérase (Giannoni, Gaven et al. 2013, Lecoutey, Hedou et al. 2014, Rochais, Lecoutey et al. 2015).

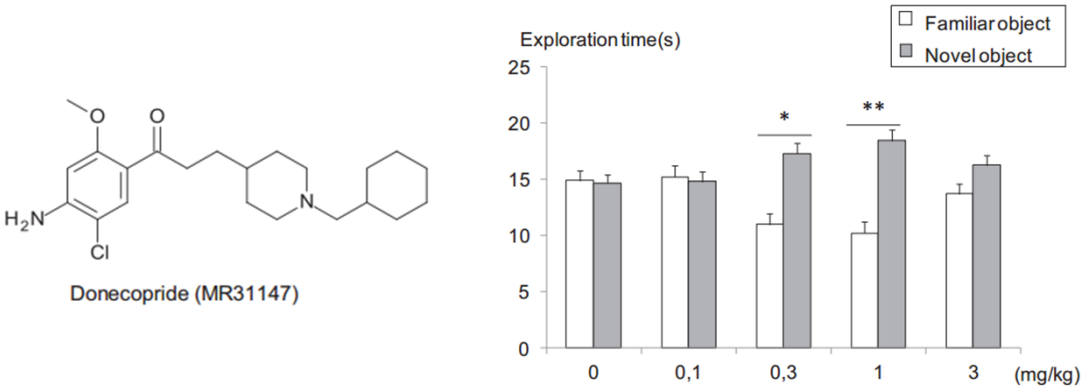

Figure 35 : Le Donecopride et son bénéfice comportemental. A gauche, schéma de la molécule. A droite, ses effets cognitifs sur les souris dans le test de la reconnaissance d'objets. Noter qu'à 0,3 et 1mg/kg, les souris montrent une préférence pour le nouvel objet. (Lecoutey, Hedou et al. 2014)

3. Autres pistes thérapeutiques dérivées de l'APPsα

L'un des principaux écueils dans le traitement des pathologies du SNC est le passage de la **Barrière Hémato-Encéphalique** (BHE). La thérapie génique permet bien sûr de contourner ce problème mais reste, on l'a vu, très invasive. La méthode la plus populaire est bien sûr le recours aux petites molécules pharmacologiques ayant la capacité de passer cette BHE, comme le Donecopride.

Nous avons montré les effets neuroprotecteurs de l'APPsα en comparaison avec l'APPsβ qui lui semble, pour le moment, inerte pour les fonctions mnésiques. Ainsi, la différence entre ces deux peptides est la présence de **16 acides aminés en position C-terminale de l'APPsα**. On peut ainsi logiquement se poser la question de savoir si ce seul petit peptide « DAEFRHDSGYEVHHQK » pourrait induire des effets bénéfiques dans le cadre de la MA. Notre collaboratrice Ulrike Müller a d'ores et déjà initié une étude *in vitro* afin d'**évaluer le potentiel trophique de cette séquence**. Cependant, même si celui-ci démontre des effets similaires à l'APPsα, avec 2000 daltons, il dépasse d'ores et déjà la limite de passage de la BHE, estimée à 500 Daltons. On peut toutefois imaginer que des techniques de **passage actif de la BHE**, comme le recours aux ultrasons (développée par la société Carthera), pourraient être plus efficaces avec des peptides de cette taille que l'APPsα, de l'ordre de 100kDA (Leinenga and Gotz 2015). Enfin, dans le cadre d'un premier test préclinique, nous pouvons aussi imaginer le recours à la même stratégie que pour APPsα/β. L'injection intra-hippocampique d'un AAV encapsidant la courte séquence sous le contrôle d'un promoteur neuronal pourrait être une première phase rapidement envisageable.

Comme je l'ai déjà indiqué lors de l'introduction (voir partie IV.B.6), une nouvelle voie de clivage de l'APP fut mise en évidence très récemment : la **voie de la η secrétase** (Figure 36) (Willem, Tahirovic et al. 2015). Cette voie physiologique induit la genèse de quatre nouveaux peptides. Tout d'abord, le η-CTF, premier peptide ayant été détecté par les auteurs de par son fort poids moléculaire. Deux peptides sont issus de ce dernier ; l'Aη-α et l'Aη-β respectivement issus des clivages du η-CTF par l'α secrétase ou la β secrétase. Le dernier fragment est la partie N-terminale de l'APP généré après clivage de la η secrétase : l'**APPsη**. Ce dernier est donc plus court que l'APPsβ mais ses propriétés méritent cependant d'être testées comme nous l'avons fait pour ces homologues. En outre, je souhaite revenir sur l'étude de l'Aη-α réalisée par les auteurs qui nous donne un indice sur les propriétés de la partie C-terminale de l'APPsα. Les auteurs décrivent que ce peptide nuit à la LTP alors que son homologue, l'Aη-β est neutre. L'étude des 16 acides aminés C-terminaux de l'APPsα devient donc, selon moi, encore plus intrigante.

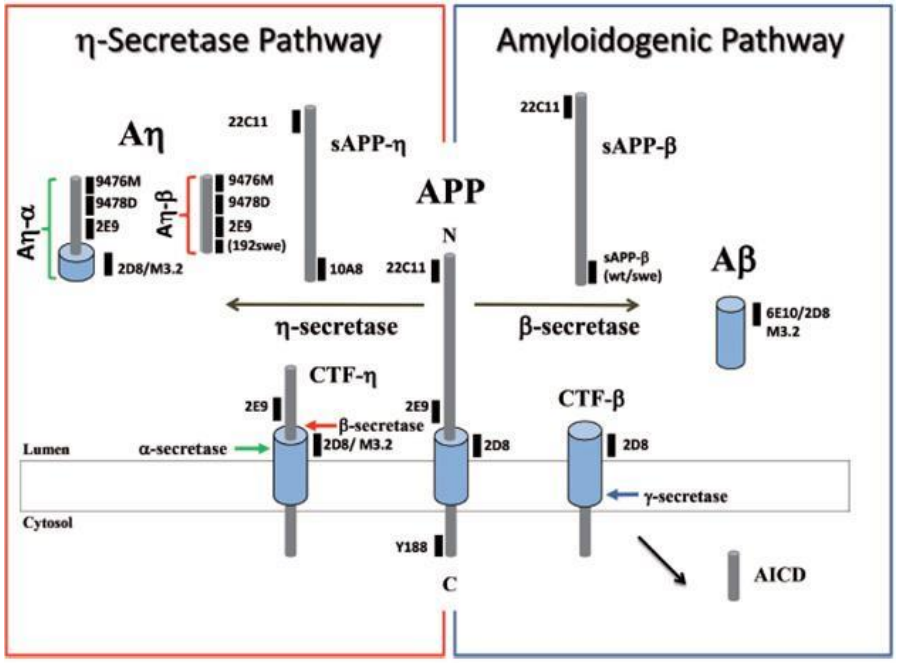

Figure 36: Une nouvelle voie de clivage de l'APP. A gauche, voie de clivage de la η secrétase, qui génère quatre nouveaux fragments ; l'APPsη, le η-CTF, l'Aη-α et l'Aη-β. (Willem, Tahirovic et al. 2015)

Enfin, je terminerai ce paragraphe en rappelant que l'APPsα n'a pas le monopole neurotrophique dans sa famille. En effet, la forme soluble issue du clivage d'APLP2, le **sAPLP2** présente lui aussi de telles propriétés (Cappai, Mok et al. 1999). La comparaison de ces effets *in vivo* sur un modèle de la MA pourrait être tout aussi intéressant à évaluer.

4. Les challenges de l'étude d'APPsβ

Le premier enjeu des mois à venir sera de compléter l'étude de l'APPsβ. Comme indiqué dans la partie précédente, plusieurs expériences restent encore à réaliser afin d'obtenir une idée globale du rôle que pourrait jouer la surexpression du peptide dans le contexte d'une amyloïdose avancée. L'analyse des **épines dendritiques**, basales et apicales, dans les régions CA1 et CA3 de l'hippocampe sera une donnée importante. Une incapacité de l'APPsβ à améliorer ce paramètre confirmera son inaptitude à induire une restauration fonctionnelle chez des souris transgéniques âgées. L'un des challenges intéressant à relever, sera d'**expliquer par quel mécanisme passe la diminution d'Aβ** soluble suivant l'injection d'APPsβ. Il conviendra tout d'abord de confirmer que BACE1 n'est pas affecté par APPsβ en mesurant son activité et la concentration d'APPsβ*swe* humain. Si tel est le cas, la caractérisation de l'expression et/ou de l'activité γ secrétase sera une première piste à étudier. Enfin, l'étude fine de la microglie hippocampique, similaire à ce que nous avons fait pour l'APPsα, et son possible rôle dans la diminution des plaques amyloïdes sera l'ultime objectif de cette étude.

5. Le consortium nEUAPPS et ses autres projets

Mes deux projets de thèse principaux, c'est-à-dire les études des surexpressions d'APPsα et d'APPsβ sont le fruit d'une **collaboration européenne** à travers le programme ERA-NET Neuron. Celui-ci a jalonné l'ensemble de ma thèse puisqu'il débuta en 2013 et se terminera en cette fin d'année 2016. En plus de la nôtre, trois autres équipes font partie du consortium « nEUAPPS » ; l'équipe belge du Pr Anton Roebroek et les équipes allemandes du Pr Christian Buchholz et du Pr Ulrike Müller. Nous pouvons aussi compter sur la collaboration de l'équipe du Pr Martin Korte pour les analyses électrophysiologiques et dendritiques. Outre les surexpressions *in vivo* des formes solubles de l'APP dans le modèle APP/PS1ΔE9 réalisées et analysées en grande partie par mes soins, l'équipe du Pr Roebroek analyse la **surexpression de l'APPsα dans le modèle murin APP$_{v717I}$**. Ces souris présentent une pathologie plus agressive que les souris APP/PS1ΔE9 avec notamment des défauts cognitifs avant l'apparition de plaques amyloïdes (Moechars, Dewachter et al. 1999). L'élégance de cette étude porte aussi sur le fait qu'une construction bicistronique codant pour APPsα et Venus fut utilisée ici. Celle-ci est exprimée grâce au même virus que le nôtre, l'AAV9 que nous avons fait produire à MIRCen par le Dr Alexis Bemelmans. Cette construction bicistronique permettra une analyse fonctionnelle fine, permettant de cibler l'analyse cellulaire uniquement aux cellules transduites.

Le consortium s'intéressa aussi à la **physiologie de l'APP**. L'équipe d'Ulrike Müller caractérisa ainsi des souris KO, associés ou non, pour l'APP, APLP1 et/ou APLP2 (Weyer, Zagrebelsky et al. 2014, Hick, Herrmann et al. 2015). Nous avons aussi conjointement publié un article s'intéressant au rôle physiologique de la **partie C-terminale de l'APP**. Nous avons démontré que celle-ci est essentielle pour la synapse tant dans le SNC (et ainsi la mémoire hippocampique) que dans le SNP, au niveau de la synapse neuromusculaire (Klevanski, Herrmann et al. 2015). Bien que cette étude ne représente pas le cœur de ma thèse, il me semble important d'indiquer qu'outre les formes solubles de l'APP (partie N-terminale), les fonctions physiologiques de l'APP C-terminale ne sont pas à négliger. Cet article est inséré en annexe de ma thèse (voir partie VIII.A).

VII. CONCLUSION GENERALE

Mes travaux de thèse permettent une meilleure compréhension des formes solubles de l'APP et leur potentiel thérapeutique pour traiter l'amyloïdose de la MA. La surexpression d'APPsβ dans les neurones hippocampiques d'une souris modèle de la MA semble neutre au niveau fonctionnel. Elle n'induisit pas de modifications mnésiques et électrophysiologiques mais en revanche, diminua la concentration en Aβ. J'ai surtout pu démontrer pour la première fois que la surexpression d'APPsα était une stratégie de choix pour le traitement de la MA. Ainsi, l'injection intracérébrale d'APPsα permit de restaurer les défauts de mémoire, de LTP et d'épines dendritiques des souris APP/PS1ΔE9. Celles-ci s'accompagnèrent d'une diminution d'Aβ et des plaques amyloïdes probablement induites par l'activation microgliale. Ces résultats méritent d'être explorés plus en détails, que ce soit dans d'autres contextes (prévention de la pathologie amyloïde ou tauopathie) ou par d'autres voies d'abord (cellules souches hématopoïétiques ou molécules pharmacologiques). Ainsi, que ce soit par le biais de la thérapie génique ou non, mon travail ouvre la voie à une exploitation clinique de l'APPsα.

VIII. ANNEXES

A. Article additionnel

16018 • The Journal of Neuroscience, December 9, 2015 • 35(49):16018–16033

Neurobiology of Disease

The APP Intracellular Domain Is Required for Normal Synaptic Morphology, Synaptic Plasticity, and Hippocampus-Dependent Behavior

Maja Klevanski,[1]* Ulrike Herrmann,[2]* Sascha W. Weyer,[1]* Romain Fol,[3,4] Nathalie Cartier,[3] David P. Wolfer,[5] John H. Caldwell,[6] Martin Korte,[2,7] and Ulrike C. Müller[1]

[1]Department of Bioinformatics and Functional Genomics, Institute of Pharmacy and Molecular Biotechnology, Heidelberg University, 69120 Heidelberg, Germany, [2]Zoological Institute, TU Braunschweig, 38106 Braunschweig, Germany, [3]INSERM U1169/MIRCen CEA Fontenay aux Roses, 92265, and Université Paris-Sud, University Paris-Saclay, Orsay 94100, France, [4]Université Paris Descartes, 75006 Paris, France, [5]Institute of Anatomy, University of Zurich and Institute of Human Movement Sciences, ETH Zurich, 8057 Zurich, Switzerland, [6]Department of Cell and Developmental Biology, University of Colorado, Aurora, Colorado 80045, and [7]AG NIND, Helmholtz Centre for Infection Research, 38124 Braunschweig, Germany

The amyloid precursor protein family (APP/APLPs) has essential roles for neuromuscular synapse development and for the formation and plasticity of synapses within the CNS. Despite this, it has remained unclear whether APP mediates its functions primarily as a cell surface adhesion and signaling molecule or via its numerous proteolytic cleavage products. To address these questions, we followed a genetic approach and used APPΔCT15 knockin mice lacking the last 15 amino acids of APP, including the highly conserved YENPTY protein interaction motif. To circumvent functional compensation by the closely related APLP2, these mice were bred to an APLP2-KO background to generate APPΔCT15-DM double mutants. These APPΔCT15-DM mice were partially viable and displayed defects in neuromuscular synapse morphology and function with impairments in the ability to sustain transmitter release that resulted in muscular weakness. In the CNS, we demonstrate pronounced synaptic deficits including impairments in LTP that were associated with deficits in spatial learning and memory. Thus, the APP-CT15 domain provides essential physiological functions, likely via recruitment of specific interactors. Together with the well-established role of APPsα for synaptic plasticity, this shows that multiple domains of APP, including the conserved C-terminus, mediate signals required for normal PNS and CNS physiology. In addition, we demonstrate that lack of the APP-CT15 domain strongly impairs Aβ generation *in vivo*, establishing the APP C-terminus as a target for Aβ-lowering strategies.

Key words: Alzheimer's disease; amyloid precursor protein; behavior; knockin; signaling; synaptogenesis

Significance Statement

Synaptic dysfunction and cognitive decline are early hallmark features of Alzheimer's disease. Thus, it is essential to elucidate the *in vivo* function(s) of APP at the synapse. At present, it is unknown whether APP family proteins function as cell surface receptors, or mainly via shedding of their secreted ectodomains, such as neurotrophic APPsα. Here, to dissect APP functional domains, we used APP mutant mice lacking the last 15 amino acids that were crossed onto an APLP2-KO background. These APPΔCT15-DM mice showed defects in neuromuscular morphology and function. Synaptic deficits in the CNS included impairments of synaptic plasticity, spatial learning, and memory. Collectively, this indicates that multiple APP domains, including the C-terminus, are required for normal nervous system function.

Introduction

The amyloid precursor protein (APP) is central to the pathogenesis of Alzheimer's disease (AD), as APP processing gives rise to Aβ peptides accumulating in the brains of AD patients. Preceding plaque deposition, AD is characterized by diminished synaptic contacts that are correlated with cognitive deficits. It is therefore crucial to elucidate the normal *in vivo* role of APP at the synapse

Received May 25, 2015; revised Sept. 7, 2015; accepted Oct. 1, 2015.

Author contributions: J.H.C., M. Korte, and U.C.M. designed research; M. Klevanski, U.H., S.W.W., R.F., and J.H.C. performed research; M. Klevanski, U.H., S.W.W., R.F., N.C., D.P.W., J.H.C., M. Korte, and U.C.M. analyzed data; M. Klevanski, D.P.W., J.H.C., M. Korte, and U.C.M. wrote the paper.

This work was supported by Deutsche Forschungsgemeinschaft Grants MU548 1457/8-1 and MU 1457/9-1,9-2 to U.C.M. and KO 1674/3-1,3-2 to M. Korte, the ERA-Net Neuron 01EW1305A to U.C.M. and N.C., and the Breuer Stiftung to U.C.M., D.P.W. is a member of the Zurich Center of Integrative Human Physiology ZIHP and the Neuroscience Center Zurich. We thank Julia Gobbert, Claudia Meyer, and Inger Drescher for excellent technical

and to assess whether loss of physiological APP functions contributes to AD pathogenesis.

APP belongs to a gene family that comprises, in addition to APP, the two amyloid precursor-like proteins, APLP1 and APLP2. Although the Aβ domain is unique for APP, APLPs undergo similar processing by α-, β-, and γ-secretases (Aydin et al., 2012). APP and APLPs are highly expressed in brain, including hippocampus, and are localized to postsynaptic and presynaptic sites both at the neuromuscular junction (Wang et al., 2009; Caldwell et al., 2013; Klevanski et al., 2014) and at CNS synapses (Laßek et al., 2013; Wilhelm et al., 2014). APP family proteins have been implicated in numerous processes, including transcription, neuronal differentiation and migration, neurite outgrowth, and synaptogenesis. Presently, it is not clear whether APP family proteins mainly function as surface-bound synaptic signaling receptors and/or adhesion molecules (Wang et al., 2009; Baumkötter et al., 2014; Bourdet et al., 2015) or act through their shedded ectodomains, such as APPsα, that have well-established functions in neuroprotection (Kögel et al., 2012) and in synaptic plasticity (Taylor et al., 2008; Korte et al., 2012; Hick et al., 2015). The APP C-terminus contains highly conserved protein interaction domains, notably the YENPTY motif that mediates APP internalization and was reported to regulate APP trafficking, processing, and likely signaling (Aydin et al., 2012; van der Kant and Goldstein, 2015). Moreover, this motif binds numerous cytosolic proteins, including Dab1, Shc, Grb, Mint/X11 proteins, and Fe65 family proteins (Aydin et al., 2012; van der Kant and Goldstein, 2015). The *in vivo* relevance of conserved APP domains, however, including the relevance of the multitude of interactors has remained challenging to dissect, as APP functions may be compensated by APLPs. Mice lacking single APP family members are viable, whereas APP/APLP2 double knock-out (DKO) or APLP1/APLP2-DKO mice die perinatally (Magara et al., 1999; Heber et al., 2000; Herms et al., 2004) due to impaired neuromuscular transmission (Wang et al., 2005; Weyer et al., 2011; Caldwell et al., 2013; Klevanski et al., 2014). Recently, we generated conditional DKO mice (cDKO mice) lacking APP in excitatory forebrain neurons (Hick et al., 2015). These fully viable cDKO mice revealed a crucial role of APP family proteins for dendritic length and branching, spine density, synaptic plasticity, and hippocampus-dependent behavior (Hick et al., 2015). While these studies corroborated essential *in vivo* functions of APP/APLP2 also in the CNS, crucial questions remained: which APP domain(s) or proteolytic fragments are required to mediate these functions and which signaling pathways are involved? To dissect APP functional domains, we previously generated C-terminally truncated APP knockin (KI) alleles: APPsα-KI mice produce only APPsα, whereas APPΔCT15-KI mice lack the last 15 amino acids, including the YENPTY motif (Ring et al., 2007). Interestingly, both KI lines showed a WT-like phenotype and lacked the impairments in LTP and behavior seen in APP-KO mice. These and other studies (Hornsten et al., 2007; Wentzell et al., 2012) suggested that APP functions are primarily mediated by the secreted fragment APPsα. However, analysis of APPsα-DM (double mutants) obtained by crossing APPsα-KI with APLP2-KO mice revealed a more complex picture (Weyer et al., 2011). To test whether C-terminal APP domains may be required for APP functions, we now generated double mutant mice (APPΔCT15-DM) that lack APLP2 and the last 15 amino acids of APP. Similarly to APPsα-DM mice, APPΔCT15-DM mice proved partially viable and showed aberrant morphology of neuromuscular synapses, defective transmitter release, and muscular weakness. Pronounced synaptic deficits in the CNS included impairments of synaptic plasticity and hippocampus-dependent behavior. Collectively, this indicates that the APP-CT15 domain provides essential functions, likely via recruitment of specific proteins mediating signals required for normal PNS and CNS physiology.

Materials and Methods

Mice. APP-KO (Li et al., 1996), APPΔCT15-KI (Ring et al., 2007), APLP2-KO mice (von Koch et al., 1997), and APP/APLP2-DKO mice (Heber et al., 2000) were described previously. Briefly, APPΔCT15-KI mice expressing a truncated form of APP that lacks the last 15 C-terminal amino acids were generated by inserting a stop codon into the terminal part of APP exon 18. APP$^{-/-}$APLP2$^{-/-}$ (APP/ALP2-DKO) and APP$^{\Delta/\Delta}$APLP2$^{-/-}$ (APPΔCT15-DM) mice were generated by intercrossing APP$^{+/-}$APLP2$^{-/-}$ or APP$^{\Delta/+}$APLP2$^{-/-}$ mice, respectively. APPΔCT15-DM mice were genotyped using primers reported previously (Ring et al., 2007). Survival of APPΔCT15-DM and APP/APLP2-DKO mice backcrossed to C57BL/6 animals either once (R1) or at least six times (R6) was determined at weaning. To assess the genotype distribution, χ^2 test was applied. Mice used for phenotyping were backcrossed to C57BL/6 animals for at least six generations (R6).

Measurement of Aβ. Mice were killed by CO_2 euthanasia and immediately perfused transcardially with PBS (0.1 M, pH 7.4). The brain was dissected, the olfactory bulbs and the cerebellum were removed, and both hemispheres were separated. The tissue was shock-frozen in liquid nitrogen and kept at −80°C until use. For brain homogenates, a Tris-buffered saline-based lysis buffer (20 mM Tris-base, pH 7.4, 150 mM NaCl, 1% Triton X-100) containing protease (Complete, Roche) and phosphatase inhibitors (PhosSTOP, Roche) was used. Mouse brain hemispheres were homogenized using a Potter homogenizer and centrifuged at 15,700 × *g* for 20 min. Supernatant was used for further analysis. Total protein was determined using BCA method, and homogenates were adjusted to 10 mg protein per milliliter. Mouse brain $A\beta_{40}$ and $A\beta_{42}$ levels were measured by electrochemiluminescence using the V-Plex Aβ Panel kit from Meso Scale Discovery. The assay was performed as outlined by the manufacturer's instructions. Statistical significance was calculated using one-way ANOVA followed by Tukey's multiple-comparison test. Number of animals: WT, $n = 5$; APLP2-KO, $n = 6$; APPDCT15-DM, $n = 6$. Age at analysis: 5–6 months, all male.

Western blot analysis. For Western blot analysis, specific antibodies directed against full-length APP and APPsα (M3.2; 1:1000; kind gift from Paul Mathews), the APP C-terminus (C1/6.1; 1:1000; provided by Paul Mathews), APPsβ (IBL, #JP18957), and β-tubulin (MAB3408; 1:10,000; Millipore) were used. Brain dissection was done as described above. Mouse brain hemispheres were homogenized in tissue homogenization buffer (20 mM Tris-HCl, pH 7.4, 250 mM sucrose, 1 mM EDTA, 1 mM EGTA), including phosphatase and protease inhibitors (Roche) using a Potter homogenizer. After homogenization, a brief low-speed spin (5000 × *g*, 5 min) was performed to remove remaining tissue fragments. For the detection of the soluble fragments APPsα and APPsβ, a high-speed centrifugation step (60 min at 100,000 × *g*) was performed, and membrane-free supernatant was used for further analysis. Total brain homogenate (30 μg protein) or supernatant (20 μg protein) was used for SDS-PAGE using 4–12% Bis-Tris gels (Novex). For the detection of APP β-CTFs, the membrane pellet of the high-speed centrifugation (60 min at 100,000 × *g*) was solubilized in 1% Triton X-100. Proteins were separated by PAGE using 10–20% Tris-Tricine gradient gels (Novex, Invitrogen). After blocking in 5% nonfat milk powder in PBS-T for 1 h, membranes were incubated with primary antibodies at 4°C overnight.

assistance; Paul Mathews for kindly providing the M3.2 and C1/6.1 antibody; and the Nikon Imaging Center (University of Heidelberg) for support with confocal microscopy.

The authors declare no competing financial interests.

*M.K., U.H., and S.W.W. contributed equally to this work.

Correspondence should be addressed to Dr. Ulrike C. Müller, Department of Bioinformatics and Functional Genomics, Institute of Pharmacy and Molecular Biotechnology, Heidelberg University, 69120 Heidelberg, Germany. E-mail: u.mueller@urz.uni-hd.de.

DOI:10.1523/JNEUROSCI.2009-15.2015

 0270-6474/15/3516019-16$15.00/0

M3.2 was used to detect full-length APP, APPsα, and β-CTFs. Western blot signals were detected by enhanced chemiluminescence (Super Signal West Pico, Pierce or for β-CTFs with SignalFire, Synaptic Systems) and imaged using the ChemiDoc Imaging System (Bio-Rad). For quantification, all images were analyzed with the ImageLab software (Bio-Rad).

Immunohistochemistry and microscopy. Diaphragms of adult (2 months old) WT, APLP2-KO, and APPΔCT15-DM mice were obtained and stained as previously described (Weyer et al., 2011). To avoid tissue stretching, the following procedures (up to the permeabilization step) were performed when the diaphragm muscle was still present within the dissected costal arch. Briefly, tissue was incubated in 1 mg/ml Type IA collagenase (Sigma-Aldrich) in PBS supplemented with 0.036 mM $CaCl_2$ for 15 min at room temperature (RT), rinsed in PBS, and fixed in 1% formaldehyde/PBS for 1 h at RT. After applying 0.1 M glycine blocking solution overnight at 4°C, tissue was permeabilized in 1% Triton X-100/PBS (6 h at RT). Subsequently, the diaphragm muscle was excised along the border of the costal arch, and tissue was permeabilized (1% Triton X-100/PBS) and incubated with synaptophysin antibody (1:50; rabbit polyclonal, Invitrogen) in 2% BSA/PBS at 4°C for 48 h. After three washing steps in PBS, the diaphragm was stained with MFP-488-conjugated goat α-rabbit antibody (1:100; Molecular Biotechnology) and rhodamine-conjugated α-bungarotoxin (1:500; Invitrogen) in 2% BSA/PBS at 4°C. For newborn mice, a modified protocol was used (Klevanski et al., 2014). The costal arch containing the diaphragm muscle was dissected from P0 mice and fixed for 15 min in 1% formaldehyde/PBS solution at RT. Tissue was briefly rinsed in PBS and incubated for 2.5 h in 0.1 M glycine blocking solution at RT. The diaphragm muscle was dissected from the costal arch, permeabilized with 1% Triton X-100/PBS for 10 min at RT, and incubated with the primary antibody solution (see above) overnight at 4°C. The diaphragm was rinsed in PBS, and the solution containing the secondary antibody and the labeled bungarotoxin was applied overnight at 4°C. After the staining procedure, diaphragms from both adult and newborn mice were washed in PBS and mounted in Mowiol 4–88 (Carl Roth). Images were obtained with a Nikon A1 laser scanning confocal microscope.

Quantification of synapse distribution. The endplate analysis was performed as described previously (Klevanski et al., 2014). As a baseline for further quantitative analyses, we determined the left–right (lr) extension of the diaphragm. For this, we acquired nonconfocal overview images in the channel used for synaptophysin (newborn pups) or neurofilament staining (adult animals). For the subsequent determination of the precise position of the synapse band relative to the inner border of the muscle, we also acquired overview images in the bungarotoxin channel (AChRs). Subsequently, the confocal maximum projection of the synapse band was superimposed onto the nonconfocal overview images (bungarotoxin channel) using well-discernible synapses as guideposts. The lr extension parameter corresponds to the distance between the inner muscle border of the diaphragm and the regression line of the synapse band (see below). Confocal image stacks were obtained in the bungarotoxin channel using a 20× objective (NA: 0.7; *z*-step: 1.5 μm) for tissue from P0 mice or 10× objective (NA: 0.45; *z*-step: 2 μm) for adult mice and projected into one plane. Multiple maximum intensity projections were merged to one large image using ImageJ (National Institutes of Health) software. For the analysis of newborn mice, we selected a 728 μm high region within the left hemidiaphragm (S2), located ~550 μm ventral to the entry point of the phrenic nerve (see also Klevanski et al., 2014). To obtain a comparable area in adult mice, the region was scaled and positioned accordingly. The coordinates of individual synapses were determined and imported to Excel software (Microsoft). A regression line describing the backbone of the synapse band was determined using a least squares linear fit. To quantify the area covered by AChR clusters, the region selected for analysis was subdivided into 8 segments oriented perpendicularly to the synapse band regression line. Subareas were calculated within each segment as a product of the segment height and the width determined by the most distal synapses within each segment. Total synapse band area was calculated as the sum of the 8 resulting subareas. Synapse density was calculated as number of synapses per subarea. To determine the width of the synapse band, 8 equidistant narrow segments (height: ~1/5th of the height used for the subarea determination) were positioned perpendicularly to the regression line of the synapse band. The width was determined by the most distant synapses within each segment. The average band width was calculated from these 8 segments. At least 4–7 mice were examined per genotype. To account for differences in diaphragm size, all data were normalized according to the diaphragm extension parameters described above. Comparison of group means was performed using one-way ANOVA with Bonferroni *post hoc* test.

Quantification of synapse morphology. Morphological analysis of individual synapses was performed within the ventral part of the right hemidiaphragm (S3) as previously described (Klevanski et al., 2014). In brief, confocal image stacks (*z*-step: 0.25 μm) were obtained using a 60× oil-immersion objective (NA: 1.4) and merged into maximum intensity projections. Only en face images of endplates were used to determine the area of presynaptic and postsynaptic specializations. Area of AChR clusters was measured using the "Particle Analyzer" tool of ImageJ. Synaptophysin area was quantified within the border of the AChR-occupied region. Degree of synaptophysin-AChR colocalization was determined using Manders' overlap coefficient described by Dunn et al. (2011) using the "Colocalization Analysis" tool of ImageJ. At least 10–20 synapses were analyzed from each mouse, and 4–7 animals were examined per genotype. Comparison of group means was performed using one-way ANOVA with Bonferroni *post hoc* test.

PNS electrophysiology. Electrophysiological recordings were performed as previously described (Ring et al., 2007; Weyer et al., 2011). Briefly, the diaphragm with 5–10 mm of the attached phrenic nerve was dissected from adult mice (6–7 weeks old), mounted in a Sylgard-lined dish, and superfused with oxygenated (95% O_2, 5% CO_2) modified Tyrode's solution (in mM as follows: 125 NaCl, 5.37 KCl, 24 $NaHCO_3$, 1 $MgCl_2$, 1.8 $CaCl_2$, 11 glucose, pH 7.4) for at least 1 h before recording. Recordings were obtained from the left hemidiaphragm in region S2. A tight-fitting glass suction electrode was used for nerve stimulation (stimulus duration 0.1 ms, amplitude 0.1–1 V). Intracellular muscle fiber recordings were made at room temperature (20°C–22°C) with 20–30 MΩ resistance glass microelectrodes filled with 3 M potassium acetate. Muscles were paralyzed with μ-conotoxin (1 μM; Bachem) to block skeletal muscle but not axonal voltage-gated sodium channels. Data were acquired with custom-written MATLAB (The MathWorks) programs and digitized at 5 kHz with DAQCard-1200 (National Instruments). Data were analyzed with Clampfit 9 (Molecular Devices) and Origin 6.1 (OriginLab). Endplate potentials (EPPs) and quantal content were corrected for nonlinear summation (McLachlan and Martin, 1981). EPPs were not corrected for extracellular field potentials sometimes generated by neighboring muscle fibers. Spontaneous activity was typically recorded for 1 min, except for those fibers with very low spontaneous release, for which recordings were made for 2–3 min. Quantal content was calculated from the average of 50–100 EPPs at a stimulation rate of 0.5 Hz. Because of the pulse-to-pulse variability in the EPP amplitude during trains of 20 Hz stimuli, the EPP amplitude during rundown experiments (data not shown) was calculated as the average of five EPPs closest to each data point (equivalent to an average response within a window duration of 200 ms). Comparison of group means was performed using Student's *t* test or one-way ANOVA with Bonferroni *post hoc* test.

CNS electrophysiology. Acute hippocampal slices were prepared from 9- to 12-month-old APPΔCT15-DM mice and APLP2-KO littermate controls as previously described (Weyer et al., 2011; Hick et al., 2015). In brief, mice were anesthetized and decapitated; the brain was quickly transferred into ice-cold carbogenated (95% O_2, 5% CO_2) ACSF for 3 min. The ACSF used for electrophysiological recordings contained 125 mM NaCl, 2.5 mM KCl, 1.25 mM NaH_2PO_4, 2 mM $MgCl_2$, 26 mM $NaHCO_3$, 2 mM $CaCl_2$, and 25 mM glucose. Hippocampi were cut with a vibrating microtome (VT 1200S; Leica) into 400-μm-thick transversal slices. Recordings were performed at 32°C.

After placing the slices in a submerged recording chamber, field EPSPs (fEPSPs) were recorded in the stratum radiatum of the CA1 region with a glass micropipette (resistance: 3–15 MΩ) filled with 3 M NaCl at a depth of ~150–200 μm. Monopolar tungsten electrodes were used for stimulation of Schaffer collaterals at a frequency of 0.1 Hz. Stimulation was set to elicit an fEPSP with a slope of ~40% of maximum for LTP recordings.

After 20 min of baseline stimulation, LTP was induced by applying theta-burst stimulation (TBS), in which a burst consisted of 4 pulses at 100 Hz, which were repeated 10 times in a 200 ms interval (5 Hz). Three such trains were used to induce LTP at 0.1 Hz. Basic synaptic transmission and presynaptic properties were analyzed via input–output (IO) measurements and paired-pulse facilitation. The IO measurements were performed by application of a defined value of current (25–250 μA in steps of 25 μA). Paired-pulse facilitation was performed by applying a pair of two stimuli spaced by different interstimulus intervals ranging from 10, 20, 40, 80, to 160 ms. Data were collected, stored, and analyzed with LABVIEW software (National Instruments). The initial slope of fEPSPs elicited by stimulation of the Schaffer collaterals was measured over time, normalized to baseline, and plotted as average ± SEM. Statistical analyses were performed using Student's *t* test.

Behavior. Behavioral analysis was performed according to the protocols previously published (Weyer et al., 2011). All behavioral procedures were approved by animal welfare authorities. A total of 34 mice of both sexes were analyzed in a blinded manner: APPΔCT15, $n = 17$ (11 female, 6 male); APLP2-KO controls, $n = 17$ (11 female, 6 male). The mice were transferred to single cages before the beginning of the experimental period and tested under dim light (~12 lux) during the dark phase of the cycle (lights on between 8:00 P.M. and 8:00 A.M.). Standard mouse chow, water, and nesting material were available *ad libitum*. The home cage rack was brought to the test room at least 30 min before each experiment. Mice at the age of 5.5–7 months were analyzed over 4 weeks in the following order of tests: home cage activity, open field, grip strength, rotarod, T-maze, nesting, burrowing, and the radial maze. Criteria for postexperiment exclusions before statistical comparisons are run were technical failures, aberrant nonperformant behavior, and data values 3 SDs above mean (applies to all behavioral experiments). T-maze: one female APPΔCT15-DM was excluded as nonperformer (no choices). Radial maze: one female APLP2-KO was excluded as nonperformer (too many bait and arm neglects).

Grip strength. Forepaw grip strength was measured as described previously (Ring et al., 2007) using a Newton meter (maximum force: 300 g) that was positioned horizontally and attached to a metallic ring of 5.5 cm diameter and 3 mm thickness. Mice were held by the tail and allowed to grasp the ring with both forepaws. They were then gently pulled back until they released the ring. Five measurements were obtained each on 2 consecutive days and averaged.

Home cage activity. Home cage activity was recorded as described previously (Madani et al., 2003) using a cage rack equipped with one passive IR sensor per mouse (ActiviScope, New Behavior). The sensors detected any locomotion and remained silent only when the mice were sleeping or grooming. Recording started after a habituation period of at least 18 h, and circadian profiles were calculated by averaging data from at least 4 recording days.

Open field. Activity was tested as described previously (Madani et al., 2003). In brief, the open field was a dimly lit circular arena (150 cm diameter) in which the mice were observed and tracked using Noldus EthoVision 3.1 software (Noldus Information Technology) for 10 min each on 2 consecutive days. The arena was divided into a wall zone (18% of surface, 7 cm wide), a center zone (50%), and a transition zone in between.

Radial maze. The working memory procedure on the 8-arm radial maze was performed as described previously (Hick et al., 2015). The apparatus was constructed of gray polyvinyl chloride. Eight arms (7 × 38 cm) with clear Perspex sidewalls (5 cm high) extended from an octagonal center platform (diameter: 18.5 cm, distance between platform center and end of arm: 47 cm). It was placed 38 cm above the floor in a dimly lit room (4 × 40 W bulbs, 12 lux) rich in salient extramaze cues (same room as for water-maze testing). Small cereal pellets (~6 mg) were placed as baits in small metal cups (3 cm diameter, 1 cm deep) at the end of each arm, in such a way that the mouse could not see them without completely entering the arm. A reversed box of clear Perspex served to confine the mouse on the center platform before each test session during which the mice were allowed to move freely in the maze. Mice were gradually reduced to and maintained at 85% of their free-feeding body weight using a premeasured amount of chow each day. Water was available *ad libitum*. Mice performed one trial per day lasting maximally 10 min or until the animal had collected all pellets. They began with two habituation sessions during which they were accustomed to collect pellets from the maze that were distributed all over the maze. During the following 10 training trials, each cup was baited only with one pellet. While trials were video-tracked using a Noldus EthoVision 3.1 system (www.noldus.com), consumption of each pellet was registered by pressing a designated key on the keyboard. Using this information, we calculated the number of correct choices among the first eight, as well as the number of reentry errors as a function of trial and of baits already collected.

T-maze. Spontaneous alternation on the T-maze was assessed as described previously (Deacon and Rawlins, 2006). The T-maze was made of gray PVC. Each arm measured 30 × 10 cm. A removable central partition extended from the center of the back goal wall of the T to 7 cm into the start arm. This totally prevented the mouse from seeing or smelling the nonchosen arm during the sample run, thus minimizing interfering stimuli. The entrance to each goal arm was fitted with a guillotine door. Each trial consisted of an information-gathering sample run, followed immediately by a choice run. For the sample run, a mouse was placed in the start arm, facing away from the choice point with the central partition in place. It was allowed to choose a goal arm and confined there for 30 s by lowering the guillotine door. Then the central partition was removed, the mouse replaced to the start arm, and the guillotine door was raised. Alternation was defined as entering the opposite arm to that entered on the sample trial (whole body, including tail). Three trials were run per day with an intertrial interval of ~60 min. Each mouse received 6 trials in total; and for data analysis, the percentage of correct choices was calculated.

Nesting test. Nest building was studied as described previously (Deacon, 2006b). At the beginning of the dark phase, mice were placed in individual testing cages (Type II, 267 × 207 × 140 mm), containing regular bedding and a Nestlet of 3 g compressed cotton (Ancare). After 24 h, the nests were assessed on a rating scale of 1–5: 1 = Nestlet >90% intact; 2 = Nestlet 50–90% intact; 3 = Nestlet mostly shredded but no identifiable nest site; 4 = identifiable but flat nest; 5 = crater-shaped nest.

Burrowing test. Burrowing was studied as described previously (Deacon, 2006a). A gray plastic tube (inner diameter: 6.3 cm; length: 18.2 cm) was filled with 350 g standard diet food pellets (Kliba Nafag 3430, Provimi Kliba; ~3 g each) and placed at a slight angle into a large standard transparent mouse cage (Type III, 425 × 266 × 155 mm). The lower end of the tube was closed, resting on the cage floor. The open end was supported 3.5 cm above the floor by two metal bolts. The cage floor was covered with fresh standard bedding material, and a cardboard environmental enrichment tube was also placed in the test cage. At the beginning of the dark period, mice were placed individually in test cages and left in their familiar animal room for an observation period of 4 h after which the amount of nondisplaced food was measured. This was followed by a second observation period of 20 h. Water was available *ad libitum* during the entire period. It was assumed that the amount of food eaten per mouse (2 ± 0.5 g) was a very small portion of the 350 g available and approximately equal across the groups.

Data were analyzed using mixed ANOVA models with genotype (APPΔCT15-DM, APLP2-KO control) as between-subject factor and within-subject factors to explore the dependence of genotype effects on place, time, or response type. Sex factor is not reported because there were no genotype × sex interactions. Significant interactions and, where necessary, significant main effects were further explored by Tukey–Kramer's *post hoc* tests or by splitting the ANOVA model, as appropriate. One-sample *t* tests were used for follow-up comparisons against chance levels. Variables known to produce strongly skewed distributions and/or frequent outliers were subjected to a $\log(1 + x)$ transformation before ANOVA as indicated. The significance threshold was set at $p = 0.05$. The false discovery rate control procedure of Hochberg was applied to groups of conceptually related variables within single tests to correct significance thresholds for multiple comparisons.

Results

APPΔCT15 only partially rescues the postnatal lethality of APP/APLP2 double knock-out mice

To assess in more detail the specific role of the APP C-terminus for early postnatal development and in the adult CNS, we crossed

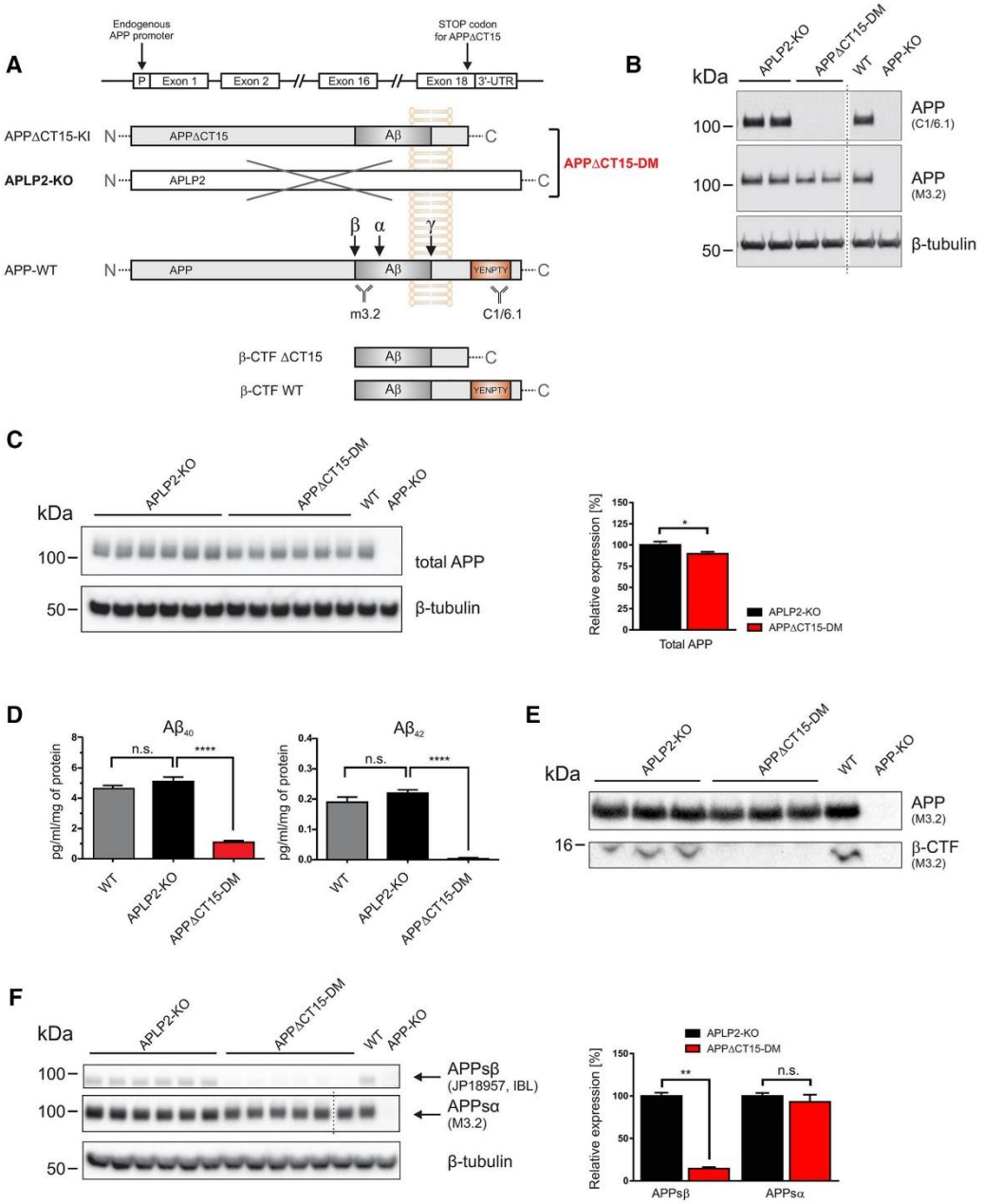

Figure 1. Analysis of APP processing in APPΔCT15-DM mice. ***A***, Scheme depicting APP, WT, and APPΔCT15 truncation. A stop codon was inserted into APP exon18 leading to the deletion of the last 15 amino acids, including the YENPTY interaction motif. The APPΔCT15 variant is expressed under the control of the endogenous APP promoter. APPΔCT15-DM mice were generated by crossing APPΔCT15 knockin (KI) mice with APLP2-KO mice; for final heterozygous intercrosses, APP $^{\Delta/+}$ APLP2-KO mice were used. APLP2-KO mice served as internal littermate controls. ***B***, Expression of APP and antibody specificity was analyzed in brain homogenates from APLP2-KO littermate controls, APPΔCT15-DM, WT, and APP-KO mice. No signal is detected using C1/6.1 antibody directed against the APP C-terminus (top; for antibody epitopes, see ***A***). M3.2 antibody detects both APP-WT and APPΔCT15, whereas no signal is obtained in APP-KO brain. β-tubulin staining served as a loading control. ***C***, Western blot of total APP (M3.2 antibody) in adult mouse brain homogenates (left). Quantification (right) showed slightly reduced total APP levels (*Figure legend continues.*)

Table 1. Genotype distribution and survival of APPΔCT15-DM and APP/APLP2-DKO mice at weaning

Matings (genetic background)	Genotype (expected frequency)	Total offspring	Obtained (frequency)	Obtained of expected	χ^2 test
$APP^{+/\Delta}APLP2^{-/-}$ (R1)	$APP^{\Delta/\Delta}APLP2^{-/-}$ (25%)	583	66 (11.3%)	45.3%	***
	$APP^{+/\Delta}APLP2^{-/-}$ (50%)		329 (56.4%)		
	$APP^{+/+}APLP2^{-/-}$ (25%)		188 (32.2%)		
$APP^{+/-}APLP2^{-/-}$ (R1)	$APP^{-/-}APLP2^{-/-}$ (25%)	813	39 (4.8%)	19.2%	
	$APP^{+/-}APLP2^{-/-}$ (50%)		467 (57.4%)		
	$APP^{+/+}APLP2^{-/-}$ (25%)		307 (37.8%)		
$APP^{+/\Delta}APLP2^{-/-}$ (R6)	$APP^{\Delta/\Delta}APLP2^{-/-}$ (25%)	1189	80 (6.7%)	26.9%	***
	$APP^{+/\Delta}APLP2^{-/-}$ (50%)		699 (58.8%)		
	$APP^{+/+}APLP2^{-/-}$ (25%)		410 (34.5%)		
$APP^{+/-}APLP2^{-/-}$ (R6)	$APP^{-/-}APLP2^{-/-}$ (25%)	798	14 (1.8%)	7%	
	$APP^{+/-}APLP2^{-/-}$ (50%)		485 (60.8%)		
	$APP^{+/+}APLP2^{-/-}$ (25%)		299 (37.5%)		

APPΔCT15-DM and APP/APLP2-DKO mice were obtained from heterozygous $APP^{+/\Delta}APLP2^{-/-}$ and $APP^{+/-}APLP2^{-/-}$ intercrosses. The survival rate of mutant mice varied depending on the genetic background. Mice with a mixed genetic background (R1 = 129/Ola × C57BL/6) showed a higher survival rate than mice backcrossed at least 6 times to C57BL/6 (R6). Depending on the genetic background, ~27% (R6) to ~45% (R1) of expected APPΔCT15-DM mice were obtained at weaning (P21-P28), whereas only 7% (R6) to ~19% (R1) of APP/APLP2-DKO mice were viable. Statistical significance was calculated using χ^2 test with regard to the expected Mendelian genotype distribution (***$p < 0.001$) for each of the given matings; data not shown) or between the different genotypes.

APPΔCT15-KI mice lacking the last 15 amino acids of APP with APLP2-deficient mice. Double mutants (designated APPΔCT15-DM) were obtained from heterozygous $APP^{\Delta/+}APLP2^{-/-}$ intercrosses (Fig. 1*A*; Table 1). For comparison, DKOs were generated in parallel by intercrossing heterozygous $APP^{-/+}APLP2^{-/-}$ mice (Table 1). As the genetic background may influence the penetrance and severity of knock-out phenotypes (Wolfer and Lipp, 2000; Aydin et al., 2011), we also investigated whether the genetic background may affect survival rates. To this end, we compared genotype distributions in animals of mixed genetic background (129/OLA × C57BL/6) that had been backcrossed only once to C57BL/6 (designated R1) and animals backcrossed to C57BL/6 for >6 generations (designated R6; Table 1). Newborn homozygous APPΔCT15-DMs showed a Mendelian-like genotype distribution (χ^2 test, $p = 0.238$, R1 background, $n = 244$ newborns) similarly as previously shown for APP/APLP2-DKO mice (von Koch et al., 1997; Heber et al., 2000), thus excluding prenatal lethality. At weaning, we obtained a considerable proportion of surviving homozygous APPΔCT15-DM mice, however, significantly (χ^2 test, $p < 0.001$) less than expected from Mendelian frequency: ~45.3% of expected homozygous APPΔCT15-DM mice survived on mixed (R1) background (66 of 583 total offspring), whereas we found a lower survival rate of 26.9% of expected (80 of 1189 total offspring) on backcrossed C57BL/6 (R6) background (Table 1). Earlier studies reported a small number of surviving APP/APLP2-DKO "escape" mutants (von Koch et al., 1997; Heber et al., 2000). Here, we analyzed survival more systematically in a large set of offspring (cumulating data over several years) and found that either 19.2% of the expected DKOs (R1) or only 7% of backcrossed DKOs (R6) survived (Table 1). Importantly, however, for both genetic backgrounds (R1 and R6), the percentage of surviving APPΔCT15-DM mice was significantly and considerably higher (~2.3- to 3.8-fold) than the percentage of viable DKO animals (χ^2 test, $p < 0.001$; Table 1). Together, these data clearly indicate that the APPΔCT15 allele is able to only partially rescue the lethality of DKO mutants and that genetic background modulates postnatal survival rates of APP/APLP mutants. To avoid potentially confounding effects of background alleles, the subsequent phenotypic analysis of surviving adult APPΔCT15-DM mice was performed in backcrossed (R6) animals.

Lack of the APP C-terminus impairs Aβ generation in APPΔCT15-DM mice

We then investigated the role of the APP C-terminus for endogenous APP processing *in vivo* (Fig. 1). As a baseline for further experiments, we confirmed the lack of the APP C-terminus in APPΔCT15-DM mice by Western blot analysis (Fig. 1*A*,*B*) using a C-terminus specific antibody (C1/6.1) and APP-KO mice as a negative control. Expression of total APPΔCT15 was slightly reduced (89.6% of control, $p = 0.0411$; Fig. 1*C*) due to somewhat reduced expression at the mRNA level in KI mice (Ring et al., 2007). Previously, we had shown in APPΔCT15-KI single mutants (Ring et al., 2007) that lack of the APP-CT15 domain, which contains the YENPTY consensus motif for clathrin-mediated endocytosis, enhances APP cell surface expression and reduces cellular APP turnover, likely via reducing endosomal β/γ-secretase processing (Perez et al., 1999). Consistent with our previous analysis of APP mutants (Ring et al., 2007), Aβ40 levels (determined by a sensitive electrochemiluminescence ELISA) were highly reduced (to ~21.3 ± 2.2% of littermate control levels; Fig. 1*D*) in cortical brain lysates of APPΔCT15-DM mice. Similarly, while Aβ42 was readily detectable in littermate controls, Aβ42 levels were close to the detection limit in APPΔCT15-DM brain (Fig. 1*D*). Likewise, although we could detect β-CTFs (β-secretase generated C-terminal fragments) in membrane-enriched fractions of wild-type mice and littermate controls, we failed to detect them in APPΔCT15-DM mice (Fig. 1*E*). Next, we assessed whether lack of the APP-CT15 domain affects APPs ectodomain shedding (Fig. 1*F*). Consistent with reduced Aβ and β-CTF levels, we detected also a pronounced reduction of soluble APPsβ

←

(*Figure legend continued.*) in APPΔCT15-DM mice (~89.6% of APLP2-KO set as 100%). ***D***, $A\beta_{40}$ and $A\beta_{42}$ were quantified by ELISA. $A\beta_{40}$ and $A\beta_{42}$ levels were similar in APLP2-KO and WT mice. In contrast, $A\beta_{40}$ and $A\beta_{42}$ were severely reduced in APPΔCT15-DM mice. $A\beta_{40}$: ANOVA, $F_{(2,14)} = 99{,}37$; $p < 0.0001$ with Tukey's *post hoc* test; $A\beta_{42}$: ANOVA, $F_{(2,14)} = 119.3$; $p < 0.0001$ with Tukey's *post hoc* test; WT, $n = 5$; APLP2-KO, $n = 6$; APPΔCT15-DM, $n = 6$. ***E***, β-CTF is detected in membrane fractions obtained from cortices of adult APLP2-KO littermate and WT mice using antibody M3.2 directed against the N-terminus of the Aβ-region. No β-CTFs were detectable in APPΔCT15-DM mice or APP-KO mice that served as a negative control. Short exposure of the same gel is shown for detection of full-length APP (top), long exposure (bottom) for β-CTF detection. ***F***, Analysis of soluble APP fragments indicated highly reduced APPsβ (14.4% of APLP2 control mice) but only nonsignificant, minor reduction of APPsα (93.2%). Dotted line indicates that samples were run on the same gel but not in adjacent lanes. ***C***, ***F***, APLP2-KO, $n = 6$; APPΔCT15-DM, $n = 6$. Values are mean ± SEM. ****$p < 0.0001$ (*t* test). **$p < 0.01$ (*t* test). *$p < 0.05$ (*t* test). n.s., Not significant.

(to 14.4% of control, $p = 0.0022$, Student's t test; Fig. 1*F*), whereas APPsα levels (93.2% of control; $p = 0.2381$, Student's t test) were not significantly different in APPΔCT15-DM mice. Together, these data indicate that lack of the APP-CT15 domain in APPΔCT15-DM mice strongly impairs amyloidogenic APP processing *in vivo*, whereas APPsα levels are similar to littermate controls.

APPΔCT15-DM mice exhibit a widened endplate band with smaller and fragmented neuromuscular synapses

Previously, aberrant neuromuscular synaptic morphology was found in newborn lethal APP/APLP2-DKO mice (Wang et al., 2005; Klevanski et al., 2014) and also in adult APPsα-DM mice lacking transmembrane APP and expressing solely APPsα (Weyer et al., 2011). To investigate whether the APP-CT15 domain is required for proper neuromuscular junction (NMJ) morphology, we studied the diaphragm from surviving young adult APPΔCT15-DMs compared with APLP2-KO littermates and WT controls (Fig. 2). Endplate topology was visualized by bungarotoxin rhodamine staining of AChRs. In adult (2-month-old) APPΔCT15-DM mice, endplates were distributed over a much larger muscle area (Fig. 2*A*), although the size of the diaphragm along the left–right body axis was not altered in mutant mice (Fig. 2*B*). Quantification of synapse distribution also showed a significant increase of endplate band width (Fig. 2*C*) and a concomitant reduction in synapse density with no change in the total synapse number (Fig. 2*D*,*E*). To assess the severity of endplate widening, we also studied diaphragms of newborn APPΔCT15-DM compared with lethal DKO mice (Fig. 2*F–J*). The synapse band widths of newborn APPΔCT15-DM and DKO mice were significantly increased to a similar extent compared with controls (Fig. 2*F*,*H–J*). This was also associated with a similar degree of nerve terminal sprouting in mice of both genotypes (Fig. 2*G*). Next, we studied the morphology of individual synapses at high magnification (Fig. 3). In adult surviving APPΔCT15-DM mice, we found that both the postsynaptic area covered by AChRs and the size of synaptophysin-immunoreactive presynaptic specializations were significantly reduced compared with APLP2 and WT controls (Fig. 3*A–C*). Interestingly, we also noted a gradual, significant reduction already in APLP2-KO single mutants compared with WT (Fig. 3*A–C*). In addition, many endplates of APPΔCT15-DM mice appeared fragmented, consisting of several small discontinuous islands contrasting with the typical "pretzel"-like pattern found in adult WT mice (Fig. 3*A*). Computer-assisted quantification confirmed a highly increased degree of fragmentation in APPΔCT15-DM mice (Fig. 3*D*). Again, we asked whether the phenotype might be similar or ameliorated in APPΔCT15-DM mice compared with completely APP/APLP2-deficient DKOs. Analysis of newborn mice (Fig. 3*E–H*) indicated significantly reduced presynaptic and postsynaptic area in both APPΔCT15-DM and DKO mutants (Fig. 3*F*,*G*), with a slightly more pronounced reduction in DKO mice that did, however, not reach statistical significance. In addition, presynaptic and postsynaptic apposition was found to be significantly reduced to a similar extent in synapses of APPΔCT15-DM and DKO pups, as evidenced by Manders' overlap coefficients (Fig. 3*H*). These data indicate that, although a proportion of APPΔCT15-DM mice survive up to weaning, NMJ morphology is compromised and closely resembles that of lethal DKO mice, suggesting a crucial role of the last 15 amino acids for NMJ formation and maintenance.

Impaired neuromuscular transmission and motor performance in surviving APPΔCT15-DM mice

Next, we examined whether impaired neuromuscular morphology is associated with functional deficits. APP and APLPs have been localized to presynaptic and postsynaptic compartments at the NMJ (Wang et al., 2005; Klevanski et al., 2014) and in the CNS to the presynaptic active zone (Laßek et al., 2013). Moreover, biochemical studies had indicated that APP binds via the YENPTY motif to several adaptors, including Fe65 and Mint proteins that, in turn, bind to Munc18 and may thus link APP to the vesicle release machinery (Weyer et al., 2011). Spontaneous transmitter release recorded from the diaphragm was, however, not affected in adult APPΔCT15-DM mice, as evidenced by lack of significant differences in miniature endplate potential (MEPP) frequency or amplitudes (Fig. 4*A*,*B*). We also studied potential differences in evoked transmitter release. Although quantal content (e.g., the response to a single action potential) was unaffected (Fig. 4*C*), APPΔCT15-DM mice revealed a significantly reduced readily releasable pool (Fig. 4*D*) determined according to Elmqvist and Quastel (1965), which implies a reduction in the number of presynaptic release sites and is consistent with the decrease in presynaptic area shown in Figure 3. The probability of synaptic vesicle release was increased (Fig. 4*E*), which may explain why the quantal content was unchanged (Fig. 4*C*; quantal content is the product of the readily releasable pool and the probability of release). Short-term plasticity was studied by measuring paired-pulse facilitation and was normal (data not shown). Notably, when stimulating the phrenic nerve for 10 s with 20 Hz trains of action potentials, APPΔCT15-DM mice displayed significant deficits to sustain transmitter release over prolonged periods of stimulation (Fig. 4*F*). Consistent with these findings, we observed a pronounced grip strength deficit in APPΔCT15-DM mice (Fig. 4*G*). As a baseline for subsequent cognitive tests, we studied spontaneous locomotor activity in a familiar home cage where APPΔCT15-DM mice showed increased activity (Fig. 4*H*). In the open field that assesses locomotor and exploratory behavior in a novel environment, APPΔCT15-DMs displayed increased locomotion and lacked habituation observed in APLP2-KO littermate controls (Fig. 4*I*). In addition, APPΔCT15-DMs showed significantly reduced avoidance of the center field (Fig. 4*J*). This, together with the highly abnormal time course of activity in the home cage and the open field, is likely related to hippocampal dysfunction (see also below). Together, our data indicate that, whereas APPΔCT15-DM mice show deficits in demanding motor tasks involving sustained muscle contraction, basal locomotion is not impaired.

Impaired synaptic plasticity and hippocampus-dependent behavior

As we have previously shown an impairment in synaptic plasticity in aged APP-KO mice, we explored whether lack of the APP-CT15 domain may affect LTP. LTP induction by TBS led to an overall increase in synaptic strength in both APPΔCT15-DMs and APLP2-KO littermate controls (Fig. 5*A*). APPΔCT15-DMs revealed significantly decreased potentiation already at early time points after TBS during the induction phase of post tetanic potentiation (Fig. 5*A*). This defect proceeded into the maintenance phase of the LTP, showing a significant reduction of average potentiation at 55–60 min after TBS of 129 ± 6.0% ($n = 15/4$ corresponding to 15 slices from 4 mice) for APPΔCT15-DM mice compared with 160 ± 9.7% ($n = 16/5$) for littermate controls (Fig. 5*B*; $p = 0.015$, t test). To assess whether this defect persists also at later phases of protein synthesis-dependent LTP (termed late-LTP), responses were recorded 3 h after TBS, and the mean

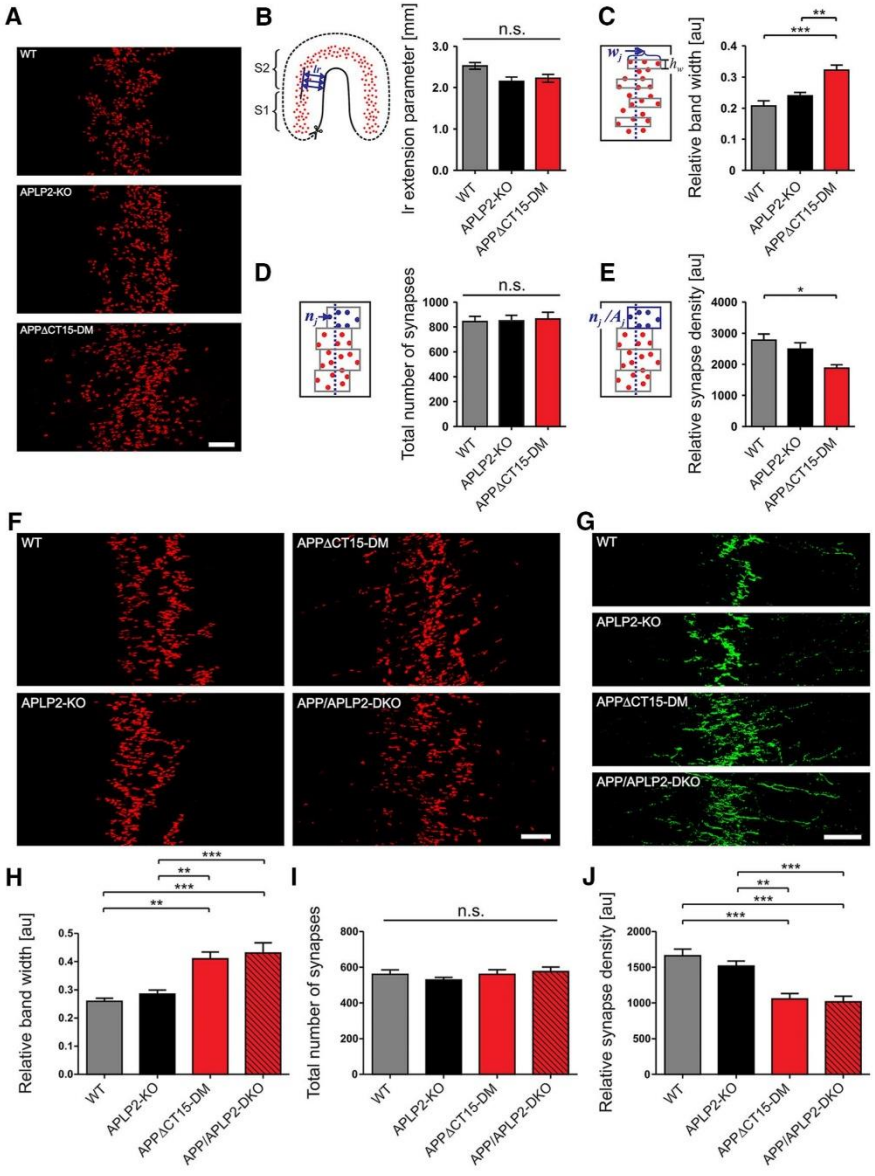

Figure 2. Widening of the endplate band and excessive branching of the phrenic nerve in APPΔCT15-DM mice. ***A***, Representative images of whole-mount bungarotoxin staining of diaphragm muscles from adult (2-month-old) mice. ***B***, Left–right (lr) extension of the diaphragm was measured as distance of synapse band from muscle border. The lr extension was not altered in mutant mice. ***C–E***, Quantitative analysis of endplate distribution. ***C***, The width (w) of the synapse band was calculated from 8 equidistantly positioned endplate-containing segments. Note the widening of the endplate band in adult APPΔCT15-DM mice. ***D***, Total synapse numbers (n) quantified from 8 band subareas are unaffected among all genotypes analyzed. ***E***, Synapse density calculated as synapse number (shown in ***C***) per subarea (n/A) is significantly reduced in APPΔCT15-DM adult mice compared with WT. ***F–J***, Analysis of endplate distribution in newborn (P0) mice. ***F***, Whole-mount bungarotoxin staining revealed widening of the endplate band already in newborn APPΔCT15-DMs to an extent similar to newborn APP/APLP2-DKO mice. ***G***, Exemplary panels demonstrating excessive nerve terminal branching, visualized by synaptophysin immunostaining (green), in both APPΔCT15-DM and APP/APLP2-DKO newborns. Quantification of synapse band parameters reveals that both APPΔCT15-DM and APP/APLP2-DKO P0 mice exhibit a significantly increased synapse band width (***H***) accompanied by a reduced synapse density (***J***) while the total number of synapses per comparable area was equal for the genotypes analyzed (***I***). Number of mice analyzed in ***C–E*** (age: 2 months): WT, $n = 5$; APLP2-KO, $n = 7$; APPΔCT15-DM, $n = 4$; in ***H–J*** (age: P0): WT, $n = 5$; APLP2-KO, $n = 8$; APPΔCT15-DM, $n = 5$; APP/APLP2-DKO, $n = 5$. Error bars indicate mean ± SEM. One-way ANOVA with Bonferroni *post hoc* test: $^{***}p < 0.001$, $^{**}p < 0.01$, $^{*}p < 0.05$, n.s., not significant. Scale bars: ***A***, ***F***, 100 μm; ***G***, 200 μm.

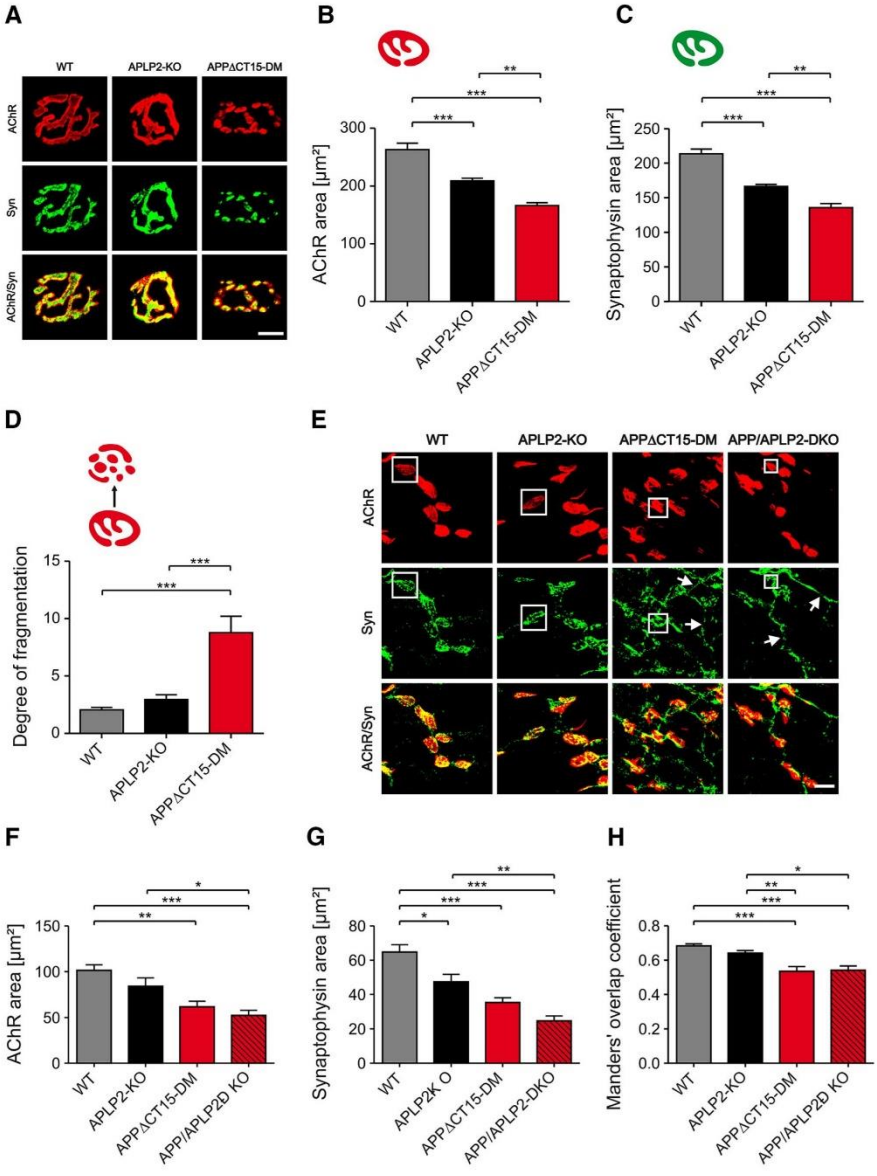

Figure 3. APPΔCT15-DM mice show abnormal synaptic morphologies and deficits in presynaptic/postsynaptic apposition. ***A***, Synaptic morphology of adult mice. Postsynaptic AChRs were labeled by bungarotoxin (red), presynaptic specializations by synaptophysin staining (Syn, green). Quantitative analysis indicates a significant reduction of both the area covered by AChRs (***B***) as well as the synaptophysin-occupied area (***C***) in APPΔCT15-DM mice. Representative images of bungarotoxin-stained AChR clusters (see ***A***) and computer-based quantification (***D***) reveal that endplates of adult APPΔCT15-DM mice appear fragmented, consisting of a significantly increased number of islands, whereas WT synapses show a typical pretzel-like shape. ***E***, ***F***, Morphological NMJ abnormalities in newborn APPΔCT15-DM mice are similar to those observed in APP/APLP2-DKOs. ***E***, White boxes highlight presynaptic and postsynaptic specializations. Arrows indicate nerve terminal overgrowth in APPΔCT15-DM and APP/APLP2-DKO animals. Quantification reveals significantly reduced areas of presynapses (***F***) and postsynapses (***G***) in both newborn APPΔCT15-DM and APP/APLP2-DKO mice and (***H***) a significantly reduced colocalization between AChR- and Syn-positive areas. Total number of synapses and number of mice analyzed in ***B–D*** (age: 2 months): WT, $n = 213/5$ (corresponding to 213 synapses from 5 mice); APLP2-KO, $n = 218/6$; APPΔCT15-DM, $n = 106/4$; in ***F–H*** (age: P0): WT, $n = 119/6$; APLP2-KO, $n = 80/5$; APPΔCT15-DM, $n = 75/4$; APP/APLP2-DKO, $n = 75/4$. Bars represent mean ± SEM. One-way ANOVA with Bonferroni *post hoc* test: $^{***}p < 0.001$, $^{**}p < 0.01$, $^{*}p < 0.05$. Scale bars: ***D***, 10 µm; ***E***, 15 µm.

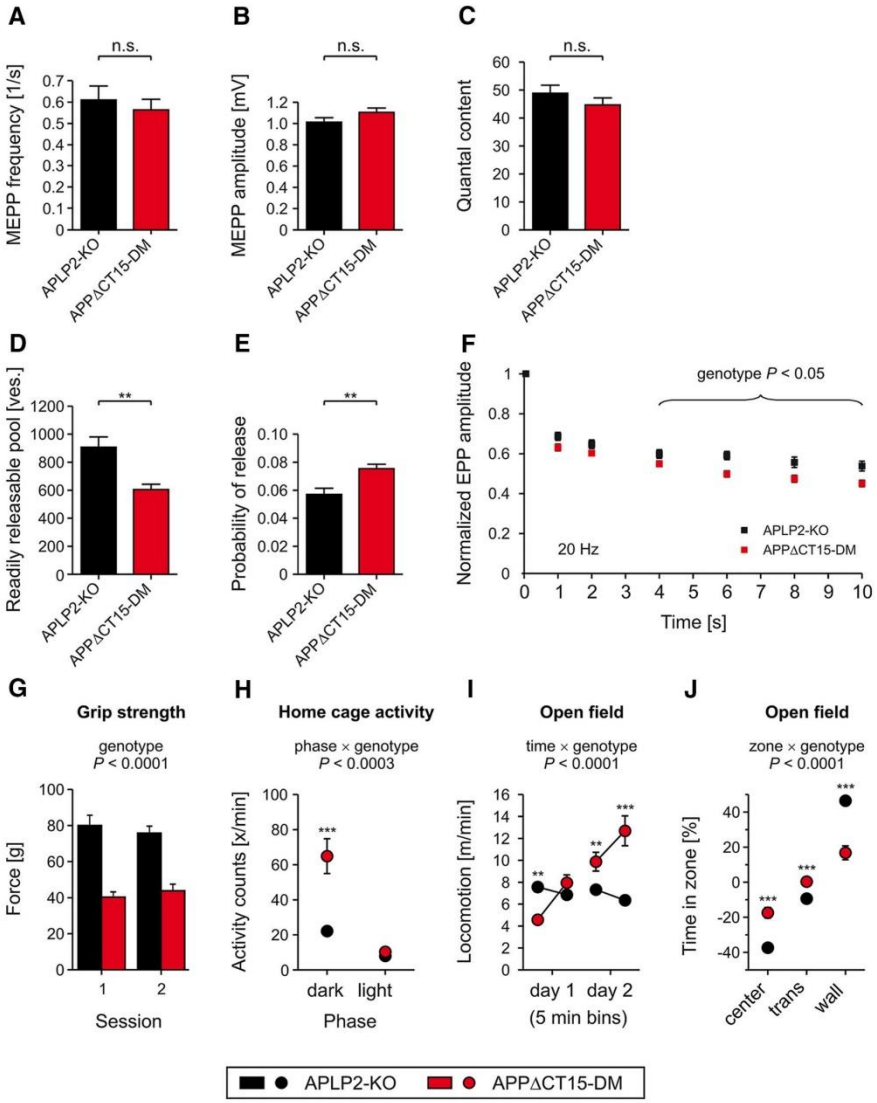

Figure 4. Impaired neuromuscular transmission and motor performance in APPΔCT15-DM mice. Mean MEPP frequency (***A***) and amplitude (***B***) reflecting spontaneous vesicle release are not affected in surviving APPΔCT15-DM mice compared with APLP2-KO littermate controls. ***C–F***, Evoked vesicle release. ***C***, Quantal content of APPΔCT15-DM mice is not significantly altered. However, APPΔCT15-DMs display a significantly decreased pool of readily releasable vesicles (ves.) (***D***) paralleled by an increased probability of vesicle release (***E***). ***E***, Probability of release was calculated as the ratio of the quantal content of the first response of a train divided by the readily releasable pool of that synapse. ***F***, Endplate potentials were measured at six time points (1, 2, 4, 6, 8, and 10 s) during a total stimulation period of 10 s (at 20 Hz). For each data point, five responses occurring during a 200 ms window were averaged. The evoked postsynaptic responses in APPΔCT15-DM mice were significantly ($p < 0.05$) reduced between 4 and 10 s of stimulation. Total number of myofibers and number of mice analyzed in ***A***: APLP2-KO, $n = 49/5$ (corresponding to 49 myofibers from 5 mice); APPΔCT15-DM, $n = 54/5$; in ***B***: APLP2-KO, $n = 50/5$; APPΔCT15-DM, $n = 54/5$; in ***C***: APLP2-KO, $n = 30/5$; APPΔCT15-DM, $n = 54/5$; in ***D***, ***E***: APLP2-KO, $n = 29/3$; APPΔCT15-DM, $n = 47/5$; in ***F***: APLP2-KO, $n = 29/3$; APPΔCT15-DM, $n = 46/5$. ***G***, Significantly decreased grip strength of APPΔCT15-DMs indicates impaired muscular performance. ***H***, Home cage activity of APPΔCT15-DM mice was significantly increased during the dark but unaltered during the light phase. ***I***, Exploratory behavior of mice was tested in a circular open field. In a new environment, the locomotion activity of APPΔCT15-DM animals increased during 2 consecutive days, which differs from the habituation behavior of APLP2-KO controls. ***J***, In contrast to the WT-like zone preference of APLP2-KOs, APPΔCT15-DM mice showed significantly reduced avoidance of the center and the transition (trans) zone. Number of mice analyzed in ***G***: APLP2-KO, $n = 17$; APPΔCT15-DM, $n = 15$; and in ***H–J***: APLP2-KO, $n = 17$; APPΔCT15-DM, $n = 17$. Bars, circles, and squares represent mean ± SEM. Statistical analysis was performed using Student's *t* test in ***A–F*** or ANOVA, genotype, $F_{(1,28)} = 59.3$, $p < 0.0001$ (***G***), phase × genotype, $F_{(1,30)} = 50.7$, $p < 0.0003$ (***H***), time × genotype, $F_{(3,90)} = 40.4$, $p < 0.0001$ (***I***), zone × genotype, $F_{(2,60)} = 31.1$, $p < 0.0001$ (***J***) with Tukey's *post hoc* test in ***G–J***: ***$p < 0.001$, **$p < 0.01$, n.s., not significant. Age at analysis: ***A–F***, ~6–8 weeks; and ***G–J***, 5.5–7 months.

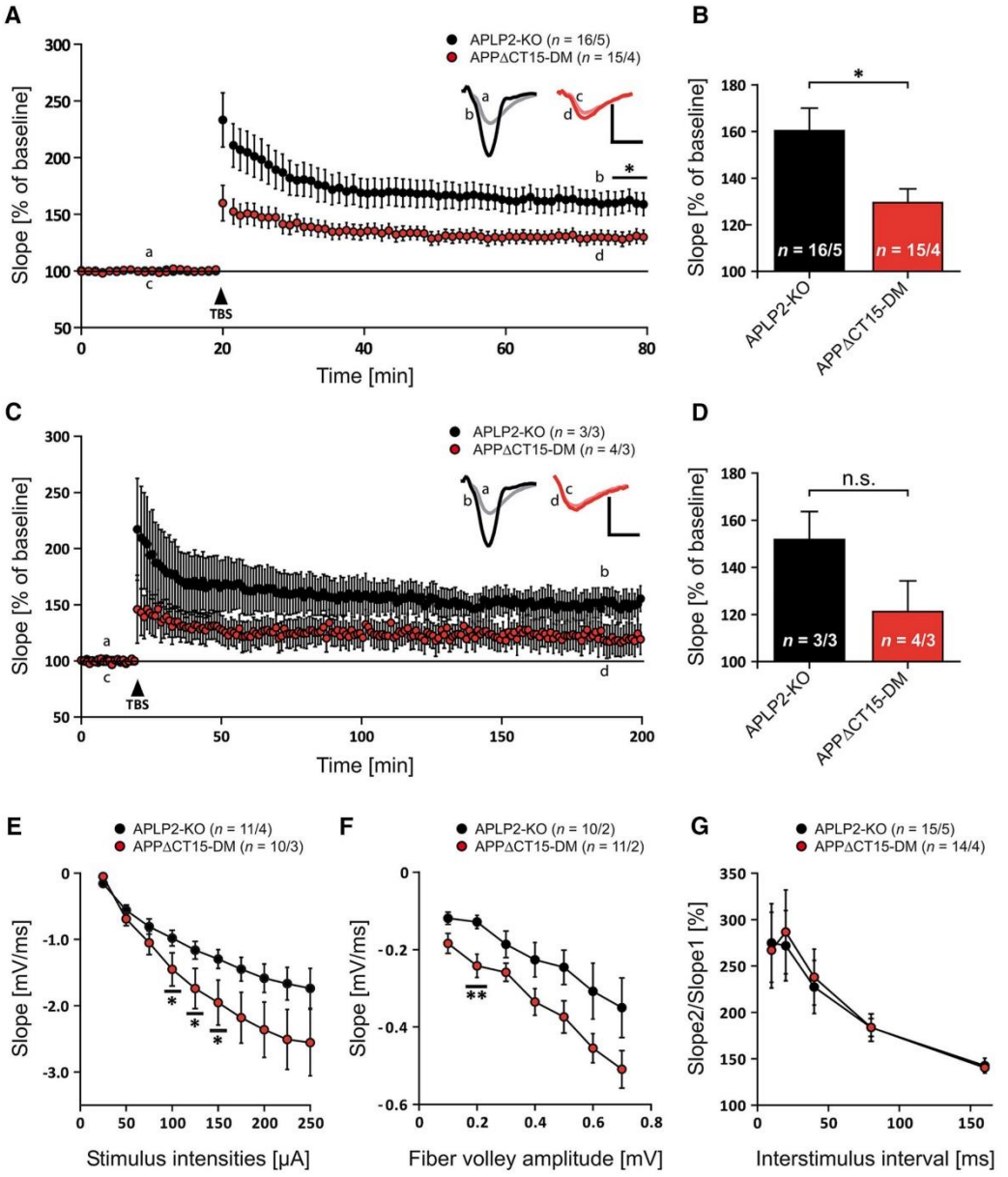

Figure 5. APPΔCT15-DM mice display impaired synaptic plasticity. ***A***, After 20 min of baseline recording, LTP was successfully induced by TBS (arrow). After TBS application, LTP is significantly impaired in APPΔCT15-DMs (red circles) compared with littermate controls (black circles). ***B***, Average fEPSP values for the last 5 min of LTP recording. With a mean of 129 ± 6.0%, APPΔCT15-DMs show significantly lower potentiation levels than littermate controls with 160 ± 9.7% ($p = 0.015$, Student's t test). ***C***, Recording time was prolonged to 3 h after TBS to investigate protein synthesis-dependent late-LTP. Progression of late-LTP displayed a trend comparable with LTP recordings. ***D***, However, no significant difference was observed between mean fEPSP values of APPΔCT15-DMs and of littermate controls for the last 5 min of recording ($p = 0.215$, Student's t test). ***E***, APPΔCT15-DM mice show significantly reduced input ouput (IO) strength at defined stimulus intensities of 100 μA ($p = 0.046$), 125 μA ($p = 0.042$), and 150 μA ($p = 0.048$, Student's t test). ***F***, The fEPSP slope of APPΔCT15-DM animals was significantly steeper than that of APLP2-KO mice at a fiber volley amplitude of 0.2 mV ($p = 0.007$, Student's t test). ***G***, APPΔCT15-DMs show unaffected paired-pulse facilitation. ***A***, ***C***, Insets, Original traces of representative individual experiments. Calibration: vertical, 1 mV; horizontal, 5 ms. Error bars indicate ± SEM. Age at analysis: ~9–12 months.

of the last 5 min was analyzed. Indeed, a similar trend was observed for APPΔCT15-DM with 121 ± 13.0% (n = 4/3) and littermate control with 151 ± 11.9% of potentiation (n = 3/3), although it did not reach significance (Fig. 5*C*,*D*; $p = 0.215$, t test). To test whether the defect is accompanied by an altered basal synaptic transmission, we also measured input ouput (IO) strength. The correlation of the fEPSP slope to defined stimulus intensities (Fig. 5*E*) revealed a larger fEPSP slope in double mutants than in controls, which was significant at currents ranging from 100 μA ($p = 0.046$, t test), 125 μA ($p = 0.042$), to 150 μA ($p = 0.048$). Comparable results were obtained when measuring the slope size at given fiber volley amplitudes (Fig. 5*F*). Again, the slope size was increased in relation to values from littermate controls over the complete measurement, although this difference became only significant for a fiber volley amplitude of 0.2 mV ($p = 0.007$, t test). As a second approach, the presynaptic functionality and short-term plasticity were probed by the paired-pulse facilitation paradigm. To this end, two pulses with defined interstimulus intervals were applied, and the ratio of the second to first slope was calculated, revealing no significant difference (Fig. 5*G*). Overall, this points to a postsynaptic, but not presynaptic defect, which might in turn affect LTP induction and maintenance.

As APPΔCT15-DMs exhibit reduced muscle strength, we used dry mazes (instead of the Morris water maze) to study hippocampus-dependent behavior. To assess spatial working memory, mice underwent testing in the 8-arm radial maze (Fig. 6*A–C*). Whereas APLP2-KO littermate controls learned the test well and made on average 7 correct among the first 8 choices at the end of training, APPΔCT15-DMs showed a significantly reduced performance with only 5 or 6 correct choices (Fig. 6*A*) after 10 d of training. Likewise, when collecting baits from the arms of the maze, the number of reentry errors into previously visited arms was much higher for APPΔCT15-DMs (Fig. 6*B*). In both groups, the number of reentry errors increased with the number of baits already collected, reflecting the increasing working memory load, but in APPΔCT15-DM mice this increase was significantly steeper (Fig. 6*C*). To examine whether performance of APPΔCT15-DM mice on the radial maze was compromised by hyperactivity, we evaluated three error measures, which we expected to be increased as a result of hyperactive behavior: nonchoices (partial arm entries without the mouse placing all 4 paws into the arm), aborted choices (arm entries with the animal returning before reaching the bait area), and procedural errors (complete entries of a still baited arm without consuming the bait). These errors occurred in very low numbers mainly during the first 2 d and were not more frequent in APPΔCT15-DM mice (data not shown). Nonchoices were even slightly more numerous in APLP2-KO controls (ANOVA genotype, $F_{(1,29)} = 11.15$, $p < 0.0023$) (data not shown). Also, in the T-maze, which assesses spontaneous alternation between two T-shaped arms, APPΔCT15-DMs were severely impaired (Fig. 6*D*) and performed only at chance level. Finally, mice underwent testing in two species-typical hippocampus-dependent behaviors (nesting behavior and burrowing behavior), which have previously been shown to be severely impaired by hippocampal lesions (Deacon et al., 2002). In both tests, APPΔCT15-DMs were drastically impaired (Fig. 6*E*,*F*). Together, we are providing converging evidence from four independent behavioral tests (T-maze, radial maze, and the tests for species specific behavior) for impairments in hippocampus-dependent behavior in APPΔCT15-DM mice. Collectively, these data indicate that lack of the APP-CT15 domain severely impairs synaptic plasticity and is associated with impairments in spatial working memory and hippocampus-dependent behavior.

Discussion

The vast majority of studies of APP biology have focused on its role for AD pathogenesis. Accumulating evidence indicates, however, that loss of physiological APP-mediated functions may contribute to the clinical symptoms of disease, most notably synaptic dysfunction and loss of cognitive abilities (Taylor et al., 2008; Suh et al., 2013; Hick et al., 2015). As such, it is crucial to dissect which APP domain(s) and/or fragments mediate its various functions in the developing and adult nervous system. Here, we used a genetic approach and demonstrate that lack of the APP-CT15 domain on an APLP2-KO background affects postnatal viability and leads to defective neuromuscular synapse development and function. Moreover, we also demonstrate a crucial role of the APP-CT15 domain for postnatal PNS and CNS physiology, with APPΔCT15-DM mice exhibiting synaptic deficits, including impaired LTP and behavioral deficits that indicate hippocampal dysfunction.

The analysis of large cohorts of offspring allowed us to clearly distinguish rescue effects due to expression of C-terminally truncated APP in APPΔCT15-DM mice compared with the significantly lower survival rates of complete DKO mice. Depending on the genetic background, between ~27% and 45% of APPΔCT15-DM mice survived into adulthood. These survival rates closely resemble those of previously generated APPsα-DM mice (Weyer et al., 2011) and thus identify the APP-CT15 domain as the crucial domain for proper neuromuscular function, which is a prerequisite for survival. Indeed, morphological defects of newborn APPΔCT15-DM and APP/APLP2-DKO mice were remarkably similar with comparable degrees of endplate widening, nerve terminal sprouting, reductions in presynaptic and postsynaptic area, and reduced apposition of presynaptic and postsynaptic specializations. Surviving adult APPΔCT15-DM mice exhibited a large number of fragmented synapses, indicating a role of the APP-CT15 domain for postnatal NMJ maintenance, consistent with similar findings in APPsα-DM mice (Weyer et al., 2011). Recordings of synaptic transmission at the diaphragm of adult APPΔCT15-DM mice revealed deficits in the readily releasable pool and impaired sustained transmitter release upon repetitive stimulations that were also reflected in reduced grip force. Interestingly, electrophysiological impairments of APPΔCT15-DM mice were less pronounced compared with APPsα-DM mice that showed, in addition, severely reduced quantal content and altered MEPP frequencies, suggesting that other motifs (e.g., more membrane proximal regions or transmembrane APP anchoring) are also required for normal physiology. Overall, our studies indicate a requirement of the C-terminus for both early stages (synaptic patterning and nerve growth) of neuromuscular development and postnatal NMJ maturation and function.

What might be the mechanism how lack of the APP-CT15 domain leads to PNS and CNS deficits? Lack of the APP-CT15 domain may abolish the binding of and signaling mediated by interactors of the YENPTY motif, including Dab1, Shc, Grb, Mint/X11 proteins, and most notably Fe65 family proteins (Aydin et al., 2012; van der Kant and Goldstein, 2015), which may provide a link to Ena/VASP proteins involved in actin organization. In this regard, it is striking that Fe65/Fe65L1-DKO mice exhibit remarkably similar neuromuscular deficits characterized by reduced size and apposition of presynaptic and postsynaptic elements, fragmented synapse topology in adult mice, and grip strength deficits (Kins et al., 2015; S. Kins, personal communication), suggesting that an APP/APLP2/Fe65L1 complex may be

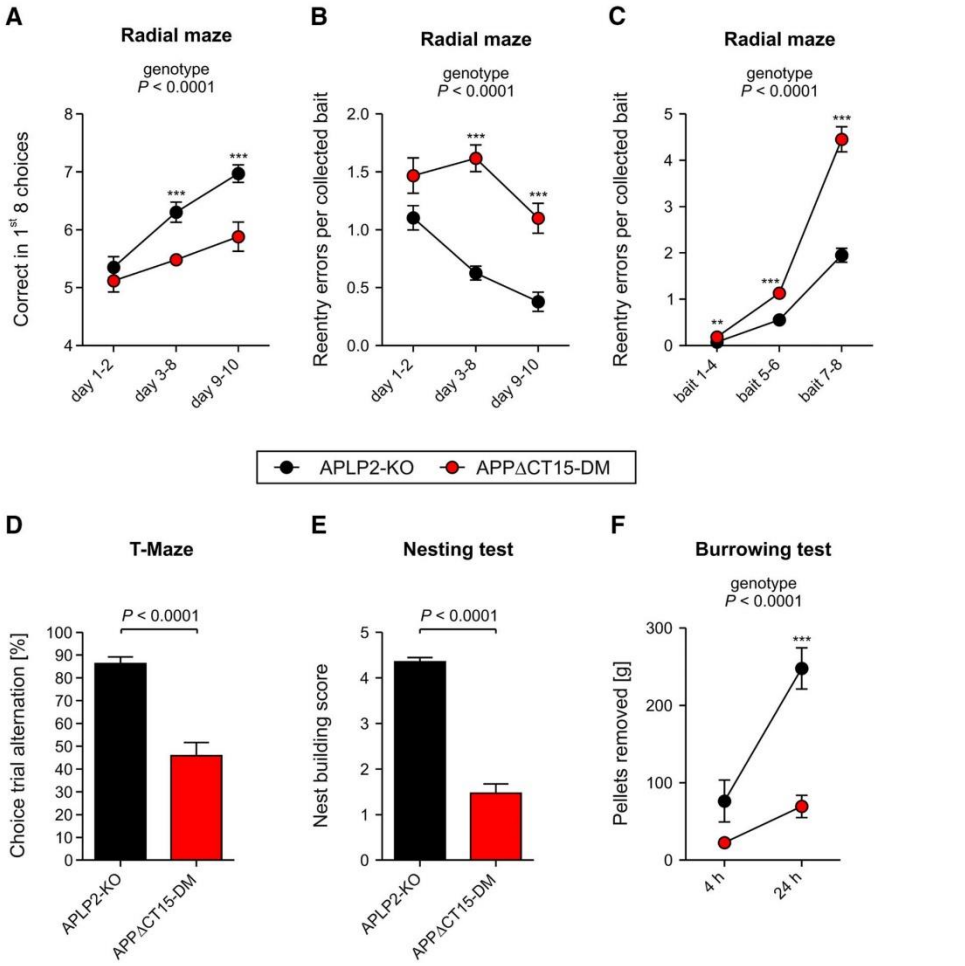

Figure 6. Hippocampus-related cognitive deficits and impaired species-typical behavior in APPΔCT15-DM mice. Spatial working memory evaluated in the radial maze (***A–C***). ***A***, APPΔCT15-DM animals made fewer correct choices and showed less improvement during consecutive testing intervals. ***B***, To evaluate learning progress, reentry errors per collected bait were averaged within days and analyzed as a function of time. Double mutants made more errors per bait during days 3–10. ***C***, To evaluate the impact of memory load on error number, reentry errors per collected bait were averaged across days and analyzed as a function of bait number. With increasing number of already collected baits, double mutant mice showed progressively higher error rates than control animals, indicating working memory deficits. ***D***, APPΔCT15-DMs show abolished spontaneous alternation in the T-maze, with 50% being the chance level. Alternation is calculated as the average percentage from 6 trials per genotype. ***E***, The ability to build nests was significantly impaired in APPΔCT15-DMs. Scale: worst (1) to best (5) performance. ***F***, APPΔCT15-DMs removed substantially less pellets than APLP2-KO after 5 and 24 h of testing. Number of mice analyzed in ***A–C***: APLP2-KO, $n = 16$; APPΔCT15-DM, $n = 17$; in ***D***: APLP2-KO, $n = 17$; APPΔCT15-DM, $n = 16$; in ***E***, ***F***: APLP2-KO, $n = 17$; APPΔCT15-DM, $n = 17$. Bars and circles represent mean ± SEM. Statistical analysis was performed using ANOVA, genotype $F_{(1,29)} = 30.6$, $p < 0.0001$ (***A***), genotype $F_{(1,29)} = 60.4$, $p < 0.0001$ (***B***), genotype $F_{(1,29)} = 93.9$, $p < 0.0001$ (***C***), $F_{(1,29)} = 45.7$, $p < 0.0001$ (***D***), $F_{(1,30)} = 147$, $p < 0.0001$ (***E***), genotype $F_{(1,30)} = 20$, $p < 0.0001$ (***F***). Tukey's *post hoc* test: $^{***}p < 0.001$, $^{**}p < 0.01$. Age at analysis: ~5.5–7 months.

crucially involved in APP transmembrane signal transduction. Consistent with this model, APP^{Y682G} knockin abrogates Fe65 binding and newborn APP^{Y682G}APLP2-KO mice exhibited deficits in neuromuscular morphology (Barbagallo et al., 2011). It is also clear, however, that lack of Fe65 signaling alone cannot fully account for APP/APLP2 functions at the NMJ as lethality of APP/APLP2-DKO mice is highly penetrant (e.g., 93% on C57BL6 background), whereas the majority of Fe65/Fe65L1-DKO mice proved viable (Guénette et al., 2006). In turn, this implicates other interactors and/or APP domains as being required for proper NMJ function. Consistent with this, we and others have previously shown that APP binds Mint/X11 proteins, which may provide a functional link to Munc18 and thus the machinery for transmitter release (Weyer et al., 2011). Of note, the recently identified cytoplasmic G_0 binding site that links APP to Akt signaling (Deyts et al., 2012; Ramaker et al., 2013; Milosch et al., 2014) is still present in APPΔCT15 mutants, excluding a role of this pathway for NMJ deficits.

Partial viability of DM mice also allowed us to investigate CNS functions. Although APPΔCT15-KI single mutants exhibit a WT-like phenotype (Ring et al., 2007), we show here that, in the absence of APLP2, the APPΔCT15 variant is not sufficient to confer normal synaptic plasticity and behavior; this highlights again the importance of APLP2, which is often neglected in the AD field. The behavioral phenotype of APPΔCT15-DMs with defects in spatial working memory (impairments in T-maze and radial maze performance) indicates hippocampal dysfunction (Deacon and Rawlins, 2006), which is further supported by impaired species-typic behaviors (nesting and burrowing) that are highly sensitive to hippocampal lesions (Deacon et al., 2002). This notion is further supported by hyperactivity and lack of habituation in the open field (Roberts et al., 1962). Although basal synaptic transmission was largely normal, impaired hippocampus-dependent behaviors were also reflected in impairments in both the induction and maintenance of LTP. Normal short-term plasticity, assessed by paired-pulse facilitation, indicated that presynaptic functions, including transmitter release are normal, implicating postsynaptic defects as the major underlying cause of LTP deficits in APPΔCT15-DM mutant mice. Recently, we observed impairments in paired-pulse facilitation (that may indicate a deficit in the control of presynaptic Ca^{2+}) in NexCre cDKO mice completely lacking APP and APLP2 (Hick et al., 2015), suggesting that also extracellular and/or membrane domains of APP contribute to its presynaptic function. In addition, an upregulation of presynaptic L-type Ca^{2+} channels ($Ca_{v1.2}$) and altered short-term plasticity were found in GABAergic striatal APP-KO neurons (Yang et al., 2009). Thus, it appears that APP family proteins mediate crucial presynaptic and postsynaptic functions at both PNS and CNS synapses.

Overall, the phenotype of APPΔCT15-DM mice closely resembles that of previously generated APPsα-DM mice, which suggests an important role of APP transmembrane signaling for synaptic function. Consistently, recent analysis of Fe65-KO, Fe65L1-KO, and Fe65/Fe65L1-DKO mice also revealed similar CNS phenotypes, including defects in learning tasks and most notably LTP (Kins et al., 2015; S. Kins personal communication), strongly supporting the view that APP and Fe65 family proteins function in a common signaling pathway.

However, lack of the APP-CT15 domain not only abolishes binding of interactors, such as proteins of the Fe65 family, but also may indirectly affect APP physiology via altering the amounts/ratio of APP fragments being produced. Here, we unequivocally show that lack of the APP-CT15 domain strongly impairs Aβ generation *in vivo*, establishing the APP C-terminus as a target for Aβ lowering strategies. Our findings of reduced amyloidogenic processing contrasts with previous studies of APP/hAβ/mutC knockin mice with C-terminal APP truncations (Li et al., 2010b) that were, however, confounded due to the cointroduction of three FAD-related mutations (Swedish, Arctic, and London), including the Swedish double mutation known to lead to highly elevated Aβ levels. Given that young adult APP-KO mice lacking Aβ production are normal and that APPsβ cannot rescue the lethality of APP/APLP2-DKO mice (Li et al., 2010a) and may even be neurotoxic (Nikolaev et al., 2009), we doubt that insufficient amyloidogenic APP processing causes the observed phenotypic abnormalities. The importance of the APP C-terminus for APP processing is also evident from APP^{Y682G}-KI mice (that can no longer bind Fe65), which produce highly elevated APPsα levels (Barbagallo et al., 2010). Whereas young animals were normal, aged APP^{Y682G}-KI mice developed impaired cognitive function and spine loss (Matrone et al., 2012), which may indicate a dominant negative role of the APP^{Y682G} mutation or that massive chronic overproduction of APPsα might have adverse effects.

Here, we show that APPsα production in APPΔCT15-DM mice is not significantly altered compared with the phenotypically normal littermate controls, thus excluding potentially adverse effects due to APPsα overexpression. It is also conceivable, however, that the precise regulation of APPsα secretion at the synapse that occurs correlated with synaptic activity (Hoey et al., 2009; Hoe et al., 2012) may be lost in the absence of the APP-CT15 domain (and similarly also in APPsα-DM mice). Several findings indicated that secreted APPsα is crucially involved in synaptic functions (Ishida et al., 1997; Meziane et al., 1998; Bour et al., 2004; Bell et al., 2008; Prox et al., 2013; Weyer et al., 2014). Notably, intracerebral infusion of APPsα-specific antibodies or pharmacological inhibition of α-secretase impaired LTP in adult rats (Taylor et al., 2008). Recently, to circumvent lethality due to neuromuscular impairments, we generated forebrain-specific APP/APLP2 double knock-out (cDKO) mice that exhibited reduced spine density, impaired LTP and hippocampus-dependent behaviors (Hick et al., 2015). Strikingly, the impairment of LTP of adult cDKO mice could be rescued by acute application of nanomolar amounts of recombinant APPsα (but not APPsβ), indicating a crucial role for APPsα to support synaptic plasticity on a rapid time scale in adult brain (Hick et al., 2015). Clearly, more work, in particular the identification of the still elusive APPsα receptor, is needed to fully understand the precise synaptic role of the APP gene family. Consistent with our data, a recent study from *Drosophila* implicated both secreted APPLs (the fly homologs of APP) and a noncleavable transmembrane APPL isoform in memory formation (Bourdet et al., 2015). Collectively, these studies and our present analysis of APPΔCT15-DM mice show the complex and multifaceted nature of APP/APLP physiological functions and indicate that not only secreted APPsα but also transmembrane APP signaling is required for normal PNS and CNS function, which needs to be taken into account when studying the pathophysiology of APP with respect to Alzheimer's disease.

References

Aydin D, Filippov MA, Tschäpe JA, Gretz N, Prinz M, Eils R, Brors B, Müller UC (2011) Comparative transcriptome profiling of amyloid precursor protein family members in the adult cortex. BMC Genomics 12:160. CrossRef Medline

Aydin D, Weyer SW, Müller UC (2012) Functions of the APP gene family in the nervous system: insights from mouse models. Exp Brain Res 217:423–434. CrossRef Medline

Barbagallo AP, Weldon R, Tamayev R, Zhou D, Giliberto L, Foreman O, D'Adamio L (2010) Tyr(682) in the intracellular domain of APP regulates amyloidogenic APP processing in vivo. PLoS One 5:e15503. CrossRef Medline

Barbagallo AP, Wang Z, Zheng H, D'Adamio L (2011) A single tyrosine residue in the amyloid precursor protein intracellular domain is essential for developmental function. J Biol Chem 286:8717–8721. CrossRef Medline

Baumkötter F, Schmidt N, Vargas C, Schilling S, Weber R, Wagner K, Fiedler S, Klug W, Radzimanowski J, Nickolaus S, Keller S, Eggert S, Wild K, Kins S (2014) Amyloid precursor protein dimerization and synaptogenic function depend on copper binding to the growth factor-like domain. J Neurosci 34:11159–11172. CrossRef Medline

Bell KF, Zheng L, Fahrenholz F, Cuello AC (2008) ADAM-10 overexpression increases cortical synaptogenesis. Neurobiol Aging 29:554–565. CrossRef Medline

Bour A, Little S, Dodart JC, Kelche C, Mathis C (2004) A secreted form of the beta-amyloid precursor protein (sAPP695) improves spatial recognition memory in OF1 mice. Neurobiol Learn Mem 81:27–38. CrossRef Medline

Bourdet I, Preat T, Goguel V (2015) The full-length form of the *Drosophila* amyloid precursor protein is involved in memory formation. J Neurosci 35:1043–1051. CrossRef Medline

Caldwell JH, Klevanski M, Saar M, Müller UC (2013) Roles of the amyloid precursor protein family in the peripheral nervous system. Mech Dev 130:433–446. CrossRef Medline

Deacon RM (2006a) Burrowing in rodents: a sensitive method for detecting behavioral dysfunction. Nat Protoc 1:118–121. CrossRef Medline

Deacon RM (2006b) Assessing nest building in mice. Nat Protoc 1: 1117–1119. CrossRef Medline

Deacon RM, Rawlins JN (2006) T-maze alternation in the rodent. Nat Protoc 1:7–12. CrossRef Medline

Deacon RM, Croucher A, Rawlins JN (2002) Hippocampal cytotoxic lesion effects on species-typical behaviours in mice. Behav Brain Res 132: 203–213. CrossRef Medline

Deyts C, Vetrivel KS, Das S, Shepherd YM, Dupré DJ, Thinakaran G, Parent AT (2012) Novel GalphaS-protein signaling associated with membrane-tethered amyloid precursor protein intracellular domain. J Neurosci 32: 1714–1729. CrossRef Medline

Dunn KW, Kamocka MM, McDonald JH (2011) A practical guide to evaluating colocalization in biological microscopy. Am J Physiol Cell Physiol 300:C723–C742. CrossRef Medline

Elmqvist D, Quastel DM (1965) A quantitative study of end-plate potentials in isolated human muscle. J Physiol 178:505–529. CrossRef Medline

Guénette S, Chang Y, Hiesberger T, Richardson JA, Eckman CB, Eckman EA, Hammer RE, Herz J (2006) Essential roles for the FE65 amyloid precursor protein-interacting proteins in brain development. EMBO J 25: 420–431. CrossRef Medline

Heber S, Herms J, Gajic V, Hainfellner J, Aguzzi A, Rülicke T, von Kretzschmar H, von Koch C, Sisodia S, Tremml P, Lipp HP, Wolfer DP, Müller U (2000) Mice with combined gene knock-outs reveal essential and partially redundant functions of amyloid precursor protein family members. J Neurosci 20:7951–7963. Medline

Herms J, Anliker B, Heber S, Ring S, Fuhrmann M, Kretzschmar H, Sisodia S, Müller U (2004) Cortical dysplasia resembling human type 2 lissencephaly in mice lacking all three APP family members. EMBO J 23:4106–4115. CrossRef Medline

Hick M, Herrmann U, Weyer SW, Mallm JP, Tschäpe JA, Borgers M, Mercken M, Roth FC, Draguhn A, Slomianka L, Wolfer DP, Korte M, Müller UC (2015) Acute function of secreted amyloid precursor protein fragment APPsalpha in synaptic plasticity. Acta Neuropathol 129:21–37. CrossRef Medline

Hoe HS, Lee HK, Pak DT (2012) The upside of APP at synapses. CNS Neurosci Ther 18:47–56. CrossRef Medline

Hoey SE, Williams RJ, Perkinton MS (2009) Synaptic NMDA receptor activation stimulates alpha-secretase amyloid precursor protein processing and inhibits amyloid-beta production. J Neurosci 29:4442–4460. CrossRef Medline

Hornsten A, Lieberthal J, Fadia S, Malins R, Ha L, Xu X, Daigle I, Markowitz M, O'Connor G, Plasterk R, Li C (2007) APL-1, a *Caenorhabditis elegans* protein related to the human beta-amyloid precursor protein, is essential for viability. Proc Natl Acad Sci U S A 104:1971–1976. CrossRef Medline

Ishida A, Furukawa K, Keller JN, Mattson MP (1997) Secreted form of beta-amyloid precursor protein shifts the frequency dependency for induction of LTD, and enhances LTP in hippocampal slices. Neuroreport 8: 2133–2137. CrossRef Medline

Kins S, Strecker P, Schilling S, Schmidt N, Baumkötter F, Herz J, Korte M, Ludewig S, Rust M, Eggert S, Guénette S (2015) Amyloid Precursor Protein synaptic function involves trans-dimerization and Fe65/Fe65L1 signaling. In: 12th international conference on Alzheimer's and Parkinson's diseases. Nice, France.

Klevanski M, Saar M, Baumkötter F, Weyer SW, Kins S, Müller UC (2014) Differential role of APP and APLPs for neuromuscular synaptic morphology and function. Mol Cell Neurosci 61C:201–210. CrossRef Medline

Kögel D, Deller T, Behl C (2012) Roles of amyloid precursor protein family members in neuroprotection, stress signaling and aging. Exp Brain Res 217:471–479. CrossRef Medline

Korte M, Herrmann U, Zhang X, Draguhn A (2012) The role of APP and APLP for synaptic transmission, plasticity, and network function: lessons from genetic mouse models. Exp Brain Res 217:435–440. CrossRef Medline

Laßek M, Weingarten J, Einsfelder U, Brendel P, Müller U, Volknandt W (2013) Amyloid precursor proteins are constituents of the presynaptic active zone. J Neurochem 127:48–56. CrossRef Medline

Li H, Wang B, Wang Z, Guo Q, Tabuchi K, Hammer RE, Südhof TC, Zheng H (2010a) Soluble amyloid precursor protein (APP) regulates transthyretin and Klotho gene expression without rescuing the essential function of APP. Proc Natl Acad Sci U S A 107:17362–17367. CrossRef Medline

Li H, Wang Z, Wang B, Guo Q, Dolios G, Tabuchi K, Hammer RE, Südhof TC, Wang R, Zheng H (2010b) Genetic dissection of the amyloid precursor protein in developmental function and amyloid pathogenesis. J Biol Chem 285:30598–30605. CrossRef Medline

Li ZW, Stark G, Götz J, Rülicke T, Gschwind M, Huber G, Müller U, Weissmann C (1996) Generation of mice with a 200-kb amyloid precursor protein gene deletion by Cre recombinase-mediated site-specific recombination in embryonic stem cells. Proc Natl Acad Sci U S A 93: 6158–6162. CrossRef Medline

Madani R, Kozlov S, Akhmedov A, Cinelli P, Kinter J, Lipp HP, Sonderegger P, Wolfer DP (2003) Impaired explorative behavior and neophobia in genetically modified mice lacking or overexpressing the extracellular serine protease inhibitor neuroserpin. Mol Cell Neurosci 23:473–494. CrossRef Medline

Magara F, Müller U, Li ZW, Lipp HP, Weissmann C, Stagljar M, Wolfer DP (1999) Genetic background changes the pattern of forebrain commissure defects in transgenic mice underexpressing the beta-amyloid-precursor protein. Proc Natl Acad Sci U S A 96:4656–4661. CrossRef Medline

Matrone C, Luvisetto S, La Rosa LR, Tamayev R, Pignataro A, Canu N, Yang L, Barbagallo AP, Biundo F, Lombino F, Zheng H, Ammassari-Teule M, D'Adamio L (2012) Tyr682 in the Abeta-precursor protein intracellular domain regulates synaptic connectivity, cholinergic function, and cognitive performance. Aging Cell 11:1084–1093. CrossRef Medline

McLachlan EM, Martin AR (1981) Non-linear summation of end-plate potentials in the frog and mouse. J Physiol 311:307–324. CrossRef Medline

Meziane H, Dodart JC, Mathis C, Little S, Clemens J, Paul SM, Ungerer A (1998) Memory-enhancing effects of secreted forms of the beta-amyloid precursor protein in normal and amnestic mice. Proc Natl Acad Sci U S A 95:12683–12688. CrossRef Medline

Milosch N, Tanriöver G, Kundu A, Rami A, François JC, Baumkötter F, Weyer SW, Samanta A, Jäschke A, Brod F, Buchholz CJ, Kins S, Behl C, Müller UC, Kögel D (2014) Holo-APP and G-protein-mediated signaling are required for sAPPalpha-induced activation of the Akt survival pathway. Cell Death Dis 5:e1391. CrossRef Medline

Nikolaev A, McLaughlin T, O'Leary DD, Tessier-Lavigne M (2009) APP binds DR6 to trigger axon pruning and neuron death via distinct caspases. Nature 457:981–989. CrossRef Medline

Perez RG, Soriano S, Hayes JD, Ostaszewski B, Xia W, Selkoe DJ, Chen X, Stokin GB, Koo EH (1999) Mutagenesis identifies new signals for beta-amyloid precursor protein endocytosis, turnover, and the generation of secreted fragments, including Abeta42. J Biol Chem 274:18851–18856. CrossRef Medline

Prox J, Bernreuther C, Altmeppen H, Grendel J, Glatzel M, D'Hooge R, Stroobants S, Ahmed T, Balschun D, Willem M, Lammich S, Isbrandt D, Schweizer M, Horré K, De Strooper B, Saftig P (2013) Postnatal disruption of the disintegrin/metalloproteinase ADAM10 in brain causes epileptic seizures, learning deficits, altered spine morphology, and defective synaptic functions. J Neurosci 33:12915–12928. CrossRef Medline

Ramaker JM, Swanson TL, Copenhaver PF (2013) Amyloid precursor proteins interact with the heterotrimeric G protein Go in the control of neuronal migration. J Neurosci 33:10165–10181. CrossRef Medline

Ring S, Weyer SW, Kilian SB, Waldron E, Pietrzik CU, Filippov MA, Herms J, Buchholz C, Eckman CB, Korte M, Wolfer DP, Müller UC (2007) The secreted beta-amyloid precursor protein ectodomain APPs alpha is sufficient to rescue the anatomical, behavioral, and electrophysiological abnormalities of APP-deficient mice. J Neurosci 27:7817–7826. CrossRef Medline

Roberts WW, Dember WN, Brodwick M (1962) Alternation and exploration in rats with hippocampal lesions. J Comp Physiol Psychol 55: 695–700. CrossRef Medline

Suh J, Choi SH, Romano DM, Gannon MA, Lesinski AN, Kim DY, Tanzi RE (2013) ADAM10 missense mutations potentiate beta-amyloid accumulation by impairing prodomain chaperone function. Neuron 80:385–401. CrossRef Medline

Taylor CJ, Ireland DR, Ballagh I, Bourne K, Marechal NM, Turner PR, Bilkey DK, Tate WP, Abraham WC (2008) Endogenous secreted amyloid pre-

cursor protein-alpha regulates hippocampal NMDA receptor function, long-term potentiation and spatial memory. Neurobiol Dis 31:250–260. CrossRef Medline

van der Kant R, Goldstein LS (2015) Cellular functions of the amyloid precursor protein from development to dementia. Dev Cell 32:502–515. CrossRef Medline

von Koch CS, Zheng H, Chen H, Trumbauer M, Thinakaran G, van der Ploeg LH, Price DL, Sisodia SS (1997) Generation of APLP2 KO mice and early postnatal lethality in APLP2/APP double KO mice. Neurobiol Aging 18:661–669. CrossRef Medline

Wang P, Yang G, Mosier DR, Chang P, Zaidi T, Gong YD, Zhao NM, Dominguez B, Lee KF, Gan WB, Zheng H (2005) Defective neuromuscular synapses in mice lacking amyloid precursor protein (APP) and APP-Like protein 2. J Neurosci 25:1219–1225. CrossRef Medline

Wang Z, Wang B, Yang L, Guo Q, Aithmitti N, Songyang Z, Zheng H (2009) Presynaptic and postsynaptic interaction of the amyloid precursor protein promotes peripheral and central synaptogenesis. J Neurosci 29:10788–10801. CrossRef Medline

Wentzell JS, Bolkan BJ, Carmine-Simmen K, Swanson TL, Musashe DT, Kretzschmar D (2012) Amyloid precursor proteins are protective in *Drosophila* models of progressive neurodegeneration. Neurobiol Dis 46:78–87. CrossRef Medline

Weyer SW, Klevanski M, Delekate A, Voikar V, Aydin D, Hick M, Filippov M, Drost N, Schaller KL, Saar M, Vogt MA, Gass P, Samanta A, Jäschke A, Korte M, Wolfer DP, Caldwell JH, Müller UC (2011) APP and APLP2 are essential at PNS and CNS synapses for transmission, spatial learning and LTP. EMBO J 30:2266–2280. CrossRef Medline

Weyer SW, Zagrebelsky M, Herrmann U, Hick M, Ganss L, Gobbert J, Gruber M, Altmann C, Korte M, Deller T, Müller UC (2014) Comparative analysis of single and combined APP/APLP knockouts reveals reduced spine density in APP-KO mice that is prevented by APPsalpha expression. Acta Neuropathol Commun 2:36. CrossRef Medline

Wilhelm BG, Mandad S, Truckenbrodt S, Kröhnert K, Schäfer C, Rammner B, Koo SJ, Claßen GA, Krauss M, Haucke V, Urlaub H, Rizzoli SO (2014) Composition of isolated synaptic boutons reveals the amounts of vesicle trafficking proteins. Science 344:1023–1028. CrossRef Medline

Wolfer DP, Lipp HP (2000) Dissecting the behaviour of transgenic mice: is it the mutation, the genetic background, or the environment? Exp Physiol 85:627–634. CrossRef Medline

Yang L, Wang Z, Wang B, Justice NJ, Zheng H (2009) Amyloid precursor protein regulates Cav1.2 L-type calcium channel levels and function to influence GABAergic short-term plasticity. J Neurosci 29:15660–15668. CrossRef Medline

B. Brevet

METHODS AND PHARMACEUTICAL COMPOSITION FOR THE TREATMENT OF ALZHEIMER'S DISEASE

FIELD OF THE INVENTION:

The present invention relates to methods and pharmaceutical compositions for the treatment of Alzheimer's disease.

BACKGROUND OF THE INVENTION:

Synaptic dysfunction, cognitive decline, and excessive accumulation of neurotoxic β-amyloid peptides (Aβ), are hallmark features of Alzheimers disease (AD). Aβ is generated by sequential cleavage of the amyloid precursor protein (APP) by β- and γ-secretase. In the competing and physiologically predominant non-amyloidogenic pathway α-secretase cleaves APP within the Aβ region (Lichtenthaler et al, 2011; Prox et al, 2012) thus precluding the formation of Aβ peptides. This leads to the secretion of the neuroprotective ectodomain APPsα, into the extracellular space in a process that can be stimulated by neuronal and synaptic activity (Hoe et al, 2012; Hoey et al, 2009).

AD is characterized by upregulation of β-secretase (BACE-1) resulting in a shift towards amyloidogenic APP processing (Ahmed et al, 2010; Holsinger et al, 2002). Increasing evidence suggests that the concomitant reduction in APPsα and the loss of its physiological functions contributes to AD pathogenesis. Reduced levels of APPsα or ADAM10 were reported in patients with amyloid deposits and AD (Dobrowolska et al, 2014; Lannfelt et al, 1995) and reviewed in (Endres & Fahrenholz, 2012). Lowered levels of CSF APPsα were also correlated with poor memory performance in both human patients and aged rats (reviewed in Endres & Fahrenholz, 2012). Moreover, α-secretase attenuating mutations have been associated with hereditary late-onset AD (Suh et al, 2013). Interestingly, APPsα has recently also been shown to reduce Aβ generation by binding to and thereby inhibiting BACE-1 activity (Obregon et al, 2012).

Substantial evidence has implicated APP and APPsα in protecting cultured neurons in vitro against various forms of stress (Kogel et al, 2012). In vivo, APP was found upregulated in response to brain injury suggesting a role in damage response (Leyssen et al, 2005; Murakami et al, 1998; Ramirez et al, 2001; Van den Heuvel et al, 1999). Moreover, APPsα was shown to ameliorate pathology and to improve cognitive function following traumatic brain injury in adult mice and rats (Corrigan et al, 2012; Thornton et al, 2006). Importantly, in

addition to neuroprotection APPsα has prominent physiological functions for neurite outgrowth, synaptogenesis, adult neurogenesis, synaptic plasticity and hippocampus-dependent behavior (Aydin et al, 2012). Previously, we generated APP-KO mice that showed impaired long term potentiation (LTP) and spatial learning that was fully rescued in APPsα knockin mice expressing solely APPsα from the endogenous APP locus (Ring et al, 2007). Recently, to avoid functional redundancy within the APP gene family (reviewed in (Aydin et al, 2012), we generated conditional double knockout mice (cDKO) lacking APP and the close homologue APLP2 in excitatory forebrain neurons (Hick et al, 2015). These cDKO mice revealed reduced spine density and impaired synaptic plasticity that was associated with deficits in hippocampus dependent behaviors (Hick et al 2015). Strikingly, the impairment of LTP of adult cDKO mice could be rescued by acute application of nanomolar amounts of recombinant APPsα (but not APPsβ), indicating a crucial role for APPsα to support synaptic plasticity on a rapid time scale in the adult brain (Hick et al, 2015). Even if these results appear promising, there is still a need in an effective and safe AD treatment strategy.

SUMMARY OF THE INVENTION:

The present invention relates to methods and pharmaceutical compositions for the treatment of Alzheimer's disease. In particular, the present invention is defined by the claims.

DETAILED DESCRIPTION OF THE INVENTION:

Here, the inventors used direct overexpression of APPsα by AAV-mediated gene transfer into the brain to explore its potential to ameliorate or rescue structural, electrophysiological and behavioral deficits of AD model mice. They show that overexpression of APPsα in aged transgenic APP/PS1ΔE9 mice with well-established plaque pathology improves synaptic plasticity and partially rescues spine density deficits. Restoration of synaptic plasticity and increased spine density is also accompanied by a rescue of spatial memory. Moreover, they demonstrated that AAV-APPsα expression leads to moderately reduced Aβ levels and significantly ameliorated plaque pathology. Interestingly, in AAV-APPsα injected mice, they observed an increased recruitment of microglia towards plaques which may have led to increased plaque clearance. Collectively, these data suggest, that even at stages with advanced plaque deposition APPsα may counteract Aβ induced synaptotoxic effects and restores cognitive functions.

Accordingly, a first object of the present invention relates to a method of treating Alzheimer's disease in a subject in need thereof comprising administering to the subject a therapeutically effective amount of a vector which comprises a nucleic acid molecule encoding for a polypeptide which is a soluble member of the APP (amyloid precursor protein) family.

As used herein, the term "subject" denotes a mammal, such as a rodent, a feline, a canine, and a primate. Preferably a subject according to the invention is a human. In the context of the present invention, a "subject in need thereof" denotes a subject, preferably a human, with Alzheimer's disease.

As used herein, the term "Alzheimer's disease" has its general meaning in the art and denotes chronic neurodegenerative disease that usually starts slowly and gets worse over time. Alzheimer's disease (AD) is characterized by amyloid deposits, intracellular neurofibrillary tangles, neuronal loss and a decline in cognitive function. The most common early symptom is difficulty in remembering recent events (short-term memory loss). As the disease advances, symptoms can include: problems with language, disorientation (including easily getting lost), mood swings, loss of motivation, not managing self-care, and behavioural issues. AD is undoubtedly multifactorial, but the amyloid protein precursor (APP) is a key element in its development. The physiological functions of APP of its first cleavage product APPsα are unclear, but it has been shown to play crucial roles in spine density, morphology and plasticity.

As used herein, the term "treatment" or "treat" refer to both prophylactic or preventive treatment as well as curative or disease modifying treatment, including treatment of subjects at risk of contracting the disease or suspected to have contracted the disease as well as subjects who are ill or have been diagnosed as suffering from a disease or medical condition, and includes suppression of clinical relapse. The treatment may be administered to a subject having a medical disorder or who ultimately may acquire the disorder, in order to prevent, cure, delay the onset of, reduce the severity of, or ameliorate one or more symptoms of a disorder or recurring disorder, or in order to prolong the survival of a subject beyond that expected in the absence of such treatment. By "therapeutic regimen" is meant the pattern of treatment of an illness, e.g., the pattern of dosing used during therapy. A therapeutic regimen may include an induction regimen and a maintenance regimen. The phrase "induction

regimen" or "induction period" refers to a therapeutic regimen (or the portion of a therapeutic regimen) that is used for the initial treatment of a disease. The general goal of an induction regimen is to provide a high level of drug to a subject during the initial period of a treatment regimen. An induction regimen may employ (in part or in whole) a "loading regimen", which may include administering a greater dose of the drug than a physician would employ during a maintenance regimen, administering a drug more frequently than a physician would administer the drug during a maintenance regimen, or both. The phrase "maintenance regimen" or "maintenance period" refers to a therapeutic regimen (or the portion of a therapeutic regimen) that is used for the maintenance of a subject during treatment of an illness, e.g., to keep the subject in remission for long periods of time (months or years). A maintenance regimen may employ continuous therapy (e.g., administering a drug at a regular intervals, e.g., weekly, monthly, yearly, etc.) or intermittent therapy (e.g., interrupted treatment, intermittent treatment, treatment at relapse, or treatment upon achievement of a particular predetermined criteria [e.g., disease manifestation, etc.]).

In particular, the method of the present invention is particularly suitable for rescuing memory impairment, synaptic plasticity and/or spine density, ameliorating both structural and functional synaptic impairments, decreasing Aβ levels and plaque deposition, inducing microglia recruitment and activation in the vicinity of amyloid plaques, enhancing Aβ and plaque clearance and/or restoring cognitive functions.

As used herein the “amyloid precursor protein (APP) family” has its general meaning in the art and represents integral membrane proteins expressed in many tissues and concentrated in the synapses of neurons. Amyloid precursor proteins include APP, APLP1 (amyloid beta (A4) precursor-like protein 1) and APLP2 (amyloid beta (A4) precursor-like protein 1). Soluble members of the amyloid precursor protein (APP) family include the form cleaved by secretases. The soluble members thus include APPsα, APLP1s and APLP2s.

In some embodiments, the vector of the present invention comprises a nucleic acid encoding for a APPsα polypeptide.

As used herein the term “APPsα” has its general meaning in the art and refers to the protein formed by the cleavage of the amyloid precursor protein (APP) by the α-secretase.

The APPsα is then secreted into the extracellular space. Exemplary amino acid sequences of APPsα include sequences a set forth in SEQ ID NO:1 and SEQ ID NO:2.

SEQ ID NO1: amino acid sequence of the murine APPsα protein

LEVPTDGNAGLLAEPQIAMFCGKLNMHMNVQNGKWESDPSGTKTCIGTKEGI
LQYCQEVYPELQITNVVEANQPVTIQNWCKRGRKQCKTHTHIVIPYRCLVGEFVSDA
LLVPDKCKFLHQERMDVCETHLHWHTVAKETCSEKSTNLHDYGMLLPCGIDKFRGV
EFVCCPLAEESDSVDSADAEEDDSDVWWGGADTDYADGGEDKVVEVAEEEEVADV
EEEEADDDEDVEDGDEVEEEAEEPYEEATERTTSTATTTTTTESVEEVVRVPTTAAS
TPDAVDKYLETPGDENEHAHFQKAKERLEAKHRERMSQVMREWEEAERQAKNLPK
ADKKAVIQHFQEKVESLEQEAANERQQLVETHMARVEAMLNDRRRLALENYITALQ
AVPPRPHHVFNMLKKYVRAEQKDRQHTLKHFEHVRMVDPKKAAQIRSQVMTHLRV
IYERMNQSLSLLYNVPAVAEEIQDEVDELLQKEQNYSDDVLANMISEPRISYGNDAL
MPSLTETKTTVELLPVNGEFSLDDLQPWHPFGVDSVPANTENEVEPVDARPAADRGL
TTRPGSGLTNIKTEEISEVKMDAEFGHDSGFEVRHQK

SEQ ID NO:2: amino acid sequence of the human APPsα protein

LEVPTDGNAGLLAEPQIAMFCGRLNMHMNVQNGKWDSDPSGTKTCIDTKEGI
LQYCQEVYPELQITNVVEANQPVTIQNWCKRGRKQCKTHPHFVIPYRCLVGEFVSDA
LLVPDKCKFLHQERMDVCETHLHWHTVAKETCSEKSTNLHDYGMLLPCGIDKFRGV
EFVCCPLAEESDNVDSADAEEDDSDVWWGGADTDYADGSEDKVVEVAEEEEVAEV
EEEEADDDEDDEDGDEVEEEAEEPYEEATERTTSIATTTTTTESVEEVVRVPTTAAS
TPDAVDKYLETPGDENEHAHFQKAKERLEAKHRERMSQVMREWEEAERQAKNLPK
ADKKAVIQHFQEKVESLEQEAANERQQLVETHMARVEAMLNDRRRLALENYITALQ
AVPPRPRHVFNMLKKYVRAEQKDRQHTLKHFEHVRMVDPKKAAQIRSQVMTHLRV
IYERMNQSLSLLYNVPAVAEEIQDEVDELLQKEQNYSDDVLANMISEPRISYGNDAL
MPSLTETKTTVELLPVNGEFSLDDLQPWHSFGADSVPANTENEVEPVDARPAADRGL
TTRPGSGLTNIKTEEISEVKMDAEFRHDSGYEVHHQK

In some embodiments, the vector of the present invention comprises a nucleic acid molecule encoding for a APPsα polypeptide comprising an amino acid sequence having at least 90% of identity with the sequence as set forth in SEQ ID NO:1 or 2.

According to the invention a first amino acid sequence having at least 90% of identity with a second amino acid sequence means that the first sequence has 90; 91; 92; 93; 94; 95; 96; 97; 98; 99 or 100% of identity with the second amino acid sequence.

Sequence identity is frequently measured in terms of percentage identity (or similarity or homology); the higher the percentage, the more similar are the two sequences. Methods of alignment of sequences for comparison are well known in the art. Various programs and alignment algorithms are described in: Smith and Waterman, Adv. Appl. Math., 2:482, 1981; Needleman and Wunsch, J. Mol. Biol., 48:443, 1970; Pearson and Lipman, Proc. Natl. Acad. Sci. U.S.A., 85:2444, 1988; Higgins and Sharp, Gene, 73:237-244, 1988; Higgins and Sharp, CABIOS, 5:151-153, 1989; Corpet et al. Nuc. Acids Res., 16:10881-10890, 1988; Huang et al., Comp. Appls Biosci., 8:155-165, 1992; and Pearson et al., Meth. Mol. Biol., 24:307-31, 1994). Altschul et al., Nat. Genet., 6:119-129, 1994, presents a detailed consideration of sequence alignment methods and homology calculations. By way of example, the alignment tools ALIGN (Myers and Miller, CABIOS 4:11-17, 1989) or LFASTA (Pearson and Lipman, 1988) may be used to perform sequence comparisons (Internet Program® 1996, W. R. Pearson and the University of Virginia, fasta20u63 version 2.0u63, release date December 1996). ALIGN compares entire sequences against one another, while LFASTA compares regions of local similarity. These alignment tools and their respective tutorials are available on the Internet at the NCSA Website, for instance. Alternatively, for comparisons of amino acid sequences of greater than about 30 amino acids, the Blast 2 sequences function can be employed using the default BLOSUM62 matrix set to default parameters, (gap existence cost of 11, and a per residue gap cost of 1). When aligning short peptides (fewer than around 30 amino acids), the alignment should be performed using the Blast 2 sequences function, employing the PAM30 matrix set to default parameters (open gap 9, extension gap 1 penalties). The BLAST sequence comparison system is available, for instance, from the NCBI web site; see also Altschul et al., J. Mol. Biol., 215:403-410, 1990; Gish. & States, Nature Genet., 3:266-272, 1993; Madden et al. Meth. Enzymol., 266:131-141, 1996; Altschul et al., Nucleic Acids Res., 25:3389-3402, 1997; and Zhang & Madden, Genome Res., 7:649-656, 1997.

As used herein, the term "nucleic acid molecule" has its general meaning in the art and refers to a DNA or RNA molecule. However, the term captures sequences that include any of the known base analogues of DNA and RNA such as, but not limited to 4-acetylcytosine, 8-

hydroxy-N6-methyladenosine, aziridinylcytosine, pseudoisocytosine, 5-(carboxyhydroxylmethyl) uracil, 5-fiuorouracil, 5-bromouracil, 5-carboxymethylaminomethyl-2-thiouracil, 5-carboxymethyl-aminomethyluracil, dihydrouracil, inosine, N6-isopentenyladenine, 1 -methyladenine, 1 -methylpseudouracil, 1-methylguanine, 1- methylinosine, 2,2-dimethylguanine, 2-methyladenine, 2-methylguanine, 3-methylcytosine, 5- methylcytosine, N6-methyladenine, 7-methylguanine, 5-methylaminomethyluracil, 5-methoxyamino-methyl-2-thiouracil, beta-D-mannosylqueosine, 5'-methoxycarbonylmethyluracil, 5-methoxyuracil, 2-methylthio-N6-isopentenyladenine, uracil-5-oxyacetic acid methylester, uracil-5-oxyacetic acid, oxybutoxosine, pseudouracil, queosine, 2-thiocytosine, 5-methyl-2-thiouracil, 2-thiouracil, 4-thiouracil, 5-methyluracil, -uracil-5-oxyacetic acid methylester, uracil-5-oxyacetic acid, pseudouracil, queosine, 2-thiocytosine, and 2,6-diaminopurine.

In some embodiments, the nucleic acid molecule of the present invention comprises a sequence having at least 70% of identity with the nucleic acid sequence as set forth in SEQ ID NO:3, or SEQ ID NO:4.

According to the invention a first nucleic acid sequence having at least 70% of identity with a second nucleic acid sequence means that the first sequence has 70; 71; 72; 73; 74; 75; 76; 77; 78; 79; 80; 81; 82; 83; 84; 85; 86; 87; 88; 89; 90; 91; 92; 93; 94; 95; 96; 97; 98; 99 or 100% of identity with the second nucleic acid sequence.

SEQ ID NO:3: codon-optimized nucleic acid sequence encoding for the murine form of the APPsα:

ttggaggtgcccaccgacggcaacgctggactgctggctgaaccccagatcgccatgttctgcggcaagctgaacatgca
catgaacgtgcagaacggcaagtgggagagcgaccccagcggcaccaagacctgcatcggcaccaaagagggcatcctgcagtat
tgccaggaagtgtaccccgagctgcagatcaccaacgtggtggaagccaaccagcccgtgaccatccagaactggtgcaagaggg
gcagaaagcagtgcaagacccacacccacatcgtgatcccttacagatgcctcgtgggcgagttcgtgtccgacgctctgctggtgcc
cgacaagtgcaagttcctgcatcaggaacggatggacgtgtgcgagacacatctgcactggcacaccgtggccaaagagacatgca
gcgagaagtccaccaacctgcacgactacggcatgctgctgccctgcggcatcgacaagttcagaggcgtggaattcgtgtgctgcc
ccctggccgaggaatccgactctgtggatagcgccgacgccgaagaggacgactctgacgtgtggtggggcggagccgacacaga
ttacgctgatggcggcgaggacaaggtggtggaagtggctgaagaggaagaggtggccgacgtggaagaagaaggccgacga
cgacgaggatgtggaagatggcgacgaggtggaagaggaagccgaggaaccctacgaggaagccaccgagagaaccaccagca
ccgccaccacaaccaccaccactaccgagagcgtggaagaggtcgtgcgggtgccaacaacagccgcctctacacctgacgccgt

ggacaagtacctggaaaccccaggcgacgagaacgagcacgcccacttccagaaggctaaagagagactggaagctaagcaccg
cgagagaatgagccaagtgatgagagagtgggaggaagctgagagacaggccaagaacctgcccaaggccgacaagaaagccg
tgatccagcacttccaggaaaaggtggaaagcctggaacaggaagctgccaacgagagacagcagctggtggaaacccacatggc
cagagtggaagctatgctgaacgacagaagaaggctggccctggaaaactacatcaccgctctgcaggccgtgccccccagacctc
accacgtgttcaacatgctgaagaaatacgtgcgggccgagcagaaggacagacagcacaccctgaagcacttcgagcacgtgcgg
atggtggaccccaagaaggccgcccagatcagatcccaagtgatgacccacctgagagtgatctacgagaggatgaaccagagcct
gagcctgctgtacaacgtgcccgccgtggccgaagaaatccaggatgaggtggacgagctgctgcagaaagagcagaactacagc
gacgacgtgctggccaacatgatcagcgagcccagaatcagctacggcaacgacgccctgatgcccagcctgaccgagacaaaga
ccaccgtggaactgctgcccgtgaacggcgagttcagcctggatgacctgcagccctggcacccttteggcgtggactctgtgcctgc
caacacagagaacgaagtggaacccgtggacgccagacctgccgctgatagaggcctgaccacaagacctggcagcggcctgac
aaacatcaagaccgaagagatcagcgaagtgaagatggacgccgagttcgggcacgacagcggctttgaagtgcggcaccagaaa

SEQ ID NO:4: codon-optimized nucleic acid sequence encoding for the human form of the APPsα:

ttggaggtgcccaccgacggcaacgccggactgctggccgagccccagatcgccatgttctgcggcagactgaacatgc
acatgaacgtgcagaacggcaagtgggacagcgaccccagcggcaccaagacctgcatcgacaccaaagagggcatcctgcagta
ttgccaagaagtgtaccccgagctgcagatcaccaacgtggtggaagccaaccagcccgtgaccatccagaactggtgcaagcggg
gcagaaagcagtgcaagacccacccccacttcgtgatcccttacagatgcctcgtgggcgagttcgtgtccgacgccctgctggtgcc
cgacaagtgcaagttcctgcatcaagaacggatggacgtgtgcgagacacatctgcactggcacaccgtggccaaagagacatgca
gcgagaagtccaccaacctgcacgactacggcatgctgctgccctgcggcatcgacaagttccggggcgtggaattcgtgtgctgcc
ccctggccgaggaatccgacaacgtggacagcgccgacgccgaagaggacgacagcgacgtgtggtggggcggagccgacacc
gattacgccgacggcagcgaggacaaggtggtggaagtggctgaagaggaagaggtggccgaggtcgaggaagaggaagccga
cgacgacgaggatgacgaggacggcgacgaggtggaagaagaggccgaggaaccctacgaggaagccaccgagcggaccacc
tctatcgccaccaccaccacaaccactaccgagagcgtggaagaggtcgtgcgggtgccaaccaccgccgcctctacccccgacgc
cgtggacaagtacctggaaaccccctggcgacgagaacgagcacgcccacttccagaaggccaaagagcggctggaagccaagca
ccgcgagcggatgagccaggtcatgagagagtgggaagaagccgagcggcaggccaagaacctgcccaaggccgacaagaaag
ccgtgatccagcacttccaagaaaaggtcgagagcctggaacaagaagccgccaacgagcggcagcagctggtggaaacccacat
ggccagagtggaagccatgctgaacgaccggcggagactggccctggaaaactacatcaccgctctgcaggccgtgccccccaga
ccccggcacgtgttcaacatgctgaagaaatacgtgcgggccgagcagaaggaccggcagcacaccctgaagcacttcgagcacgt
gcggatggtggaccccaagaaggccgcccagatccgctctcaggtcatgacccacctgagagtgatctacgagagaatgaaccaga
gcctgagcctgctgtacaacgtgcccgccgtggccgaagaaatccaggatgaggtggacgagctgctgcagaaagagcagaactac
agcgacgacgtgctggccaacatgatcagcgagccccggatcagctacggcaacgacgccctgatgcccagcctgaccgagacaa
agaccaccgtggaactgctgcccgtgaacggcgagttcagcctggacgacctgcagccctggcacagcttcggcgctgatagcgtg
cccgccaacaccgagaatgaggtggaacccgtggacgccagacctgccgccgatagaggcctgaccacaagacctggcagcggc

ctgaccaacatcaagaccgaagagatcagcgaagtgaagatggacgccgagttccggcacgacagcggctacgaggtgcaccacc
agaaa

As used herein, the term "vector" has its general meaning in the art and refers to the vehicle by a nucleic acid molecule can be introduced into a host cell, so as to transform the host and promote expression (e.g. transcription and translation) of the introduced sequence. The terms “Gene transfer” or “gene delivery” refer to methods or systems for reliably inserting foreign DNA into host cells. Such methods can result in transient expression of non-integrated transferred DNA, extrachromosomal replication and expression of transferred replicons (e.g. episomes), or integration of transferred genetic material into the genomic DNA of host cells.

In some embodiments, the vector of the present invention is a non-viral vector. Typically, the non-viral vector may be a plasmid which includes the nucleic acid molecule of the present invention.

In some embodiments, the vector of the present invention is a viral vector. Gene delivery viral vectors useful in the practice of the present invention can be constructed utilizing methodologies well known in the art of molecular biology. Typically, viral vectors carrying transgenes are assembled from polynucleotides encoding the transgene, suitable regulatory elements and elements necessary for production of viral proteins which mediate cell transduction. Examples of viral vector include but are not limited to adenoviral, retroviral, lentiviral, herpesvirus and adeno-associated virus (AAV) vectors.

In some embodiments, the vector of the present invention is an adeno-associated viral (AAV) vector. By an "AAV vector" is meant a vector derived from an adeno-associated virus serotype, including without limitation AAV1, AAV2, AAV3, AAV4, AA5, AAV6, AAV7, AAV8, AAV9, AAV10 or any other serotypes of AAV that can infect humans, monkeys or other species. AAV vectors can have one or more of the AAV wild-type genes deleted in whole or part, preferably the rep and/or cap genes, but retain functional flanking ITR sequences. Functional ITR sequences are necessary for the rescue, replication and packaging of the AAV virion. Thus, an AAV vector is defined herein to include at least those sequences required in cis for replication and packaging (e. g., functional ITRs) of the virus. The ITRs need not be the wild-type nucleotide sequences, and may be altered, e. g by the insertion,

deletion or substitution of nucleotides, so long as the sequences provide for functional rescue, replication and packaging. AAV expression vectors are constructed using known techniques to at least provide as operatively linked components in the direction of transcription, control elements including a transcriptional initiation region, the nucleic acid molecule of the present invention and a transcriptional termination region. The control elements are selected to be functional in a mammalian cell. The resulting construct which contains the operatively linked components is bounded (5' and 3') with functional AAV ITR sequences. By "adeno-associated virus inverted terminal repeats " or "AAV ITRs" is meant the art-recognized regions found at each end of the AAV genome which function together in cis as origins of DNA replication and as packaging signals for the virus. AAV ITRs, together with the AAV rep coding region, provide for the efficient excision and rescue from, and integration of a nucleotide sequence interposed between two flanking ITRs into a mammalian cell genome. The nucleotide sequences of AAV ITR regions are known. See, e.g., Kotin, 1994; Berns, KI "Parvoviridae and their Replication" in Fundamental Virology, 2nd Edition, (B. N. Fields and D. M. Knipe, eds.) for the AAV-2 sequence. As used herein, an "AAV ITR" does not necessarily comprise the wild-type nucleotide sequence, but may be altered, e.g., by the insertion, deletion or substitution of nucleotides. Additionally, the AAV ITR may be derived from any of several AAV serotypes, including without limitation, AAV-1, AAV-2, AAV-3, AAV-4, AAV-5, AAV-6, etc. Furthermore, 5' and 3' ITRs which flank a selected nucleotide sequence in an AAV vector need not necessarily be identical or derived from the same AAV serotype or isolate, so long as they function as intended, i.e., to allow for excision and rescue of the sequence of interest from a host cell genome or vector, and to allow integration of the heterologous sequence into the recipient cell genome when AAV Rep gene products are present in the cell. Additionally, AAV ITRs may be derived from any of several AAV serotypes, including without limitation, AAV-1, AAV-2, AAV-3, AAV-4, AAV 5, AAV-6, etc. Furthermore, 5 'and 3' ITRs which flank a selected nucleotide sequence in an AAV expression vector need not necessarily be identical or derived from the same AAV serotype or isolate, so long as they function as intended, i. e., to allow for excision and rescue of the sequence of interest from a host cell genome or vector, and to allow integration of the DNA molecule into the recipient cell genome when AAV Rep gene products are present in the cell. In some embodiments, the AAV vector of the present invention is selected from vectors derived from AAV serotypes having tropism for and high transduction efficiencies in cells of the mammalian central and peripheral nervous system, particularly neurons, neuronal progenitors, astrocytes, oligodendrocytes and glial cells. In some embodiments, the AAV

vector is an AAV4, AAV9 or an AAV10 that have been described to well transduce brain cells especially neurons. In some embodiments, the AAV vector of the present invention is a double-stranded, self-complementary AAV (scAAV) vector. Alternatively to the use of single-stranded AAV vector, self-complementary vectors can be used. The efficiency of AAV vector in terms of the number of genome-containing particles required for transduction, is hindered by the need to convert the single-stranded DNA (ssDNA) genome into double-stranded DNA (dsDNA) prior to expression. This step can be circumvented through the use of self-complementary vectors, which package an inverted repeat genome that can fold into dsDNA without the requirement for DNA synthesis or base-pairing between multiple vector genomes. Resulting self-complementary AAV (scAAV) vectors have increased resulting expression of the transgene. For an overview of AAV biology, ITR function, and scAAV constructs, see McCarty D M. Self-complementary AAV vectors; advances and applications. Mol. Ther. 2008 October; 16 (10): at pages 1648-51, first full paragraph, incorporated herein by reference for disclosure of AAV and scAAV constructs, ITR function, and role of ΔTRS ITR in scAAV constructs. A rAAV vector comprising a ΔTRS ITR cannot correctly be nicked during the replication cycle and, accordingly, produces a self-complementary, double-stranded AAV (scAAV) genome, which can efficiently be packaged into infectious AAV particles. Various rAAV, ssAAV, and scAAV vectors, as well as the advantages and drawbacks of each class of vector for specific applications and methods of using such vectors in gene transfer applications are well known to those of skill in the art (see, for example, Choi V W, Samulski R J, McCarty D M. Effects of adeno-associated virus DNAhairpin structure on recombination. J. Virol. 2005 June; 79(11):6801-7; McCarty D M, Young S M Jr, Samulski R J. Integration of adeno-associated virus (AAV) and recombinant AAV vectors. Annu Rev Genet. 2004; 38:819-45; McCarty D M, Monahan P E, Samulski R J. Self-complementary recombinant adeno-associated virus (scAAV) vectors promote efficient transduction independently of DNA synthesis. Gene Ther. 2001 August; 8(16):1248-54; and McCarty D M. Self-complementary AAV vectors; advances and applications. Mol. Ther. 2008 October; 16(10):1648-56; all references cited in this application are incorporated herein by reference for disclosure of AAV, rAAV, and scAAV vectors).

The AAV vector of the present invention can be constructed by directly inserting the selected sequence (s) into an AAV genome which has had the major AAV open reading frames ("ORFs") excised therefrom. Other portions of the AAV genome can also be deleted, so long as a sufficient portion of the ITRs remain to allow for replication and packaging

functions. Such constructs can be designed using techniques well known in the art. See, e. g. U. S. Patents Nos. 5,173, 414 and 5,139, 941; International Publications Nos. WO 92/01070 (published 23 January 1992) and WO 93/03769 (published 4 March 1993); Lebkowski et al., 1988 ; Vincent et al., 1990; Carter, 1992 ; Muzyczka, 1992 ; Kotin,1994; Shelling and Smith, 1994 ; and Zhou et al., 1994. Alternatively, AAV ITRs can be excised from the viral genome or from an AAV vector containing the same and fused 5' and 3' of a selected nucleic acid construct that is present in another vector using standard ligation techniques. AAV vectors which contain ITRs have been described in, e. g. U. S. Patent no. 5,139, 941. In particular, several AAV vectors are described therein which are available from the American Type Culture Collection ("ATCC") under Accession Numbers 53222,53223, 53224,53225 and 53226. Additionally, chimeric genes can be produced synthetically to include AAV ITR sequences arranged 5' and 3' of one or more selected nucleic acid sequences. Preferred codons for expression of the chimeric gene sequence in mammalian CNS and PNS cells can be used. The complete chimeric sequence is assembled from overlapping oligonucleotides prepared by standard methods. See, e. g., Edge, 1981 ; Nambair et al., 1984 ; Jay et al., 1984. In order to produce AAV virions, an AAV expression vector is introduced into a suitable host cell using known techniques, such as by transfection. A number of transfection techniques are generally known in the art. See, e. g. , Graham et al., 1973;, Sambrook et al. (1989) Molecular Cloning, a laboratory manual, Cold Spring Harbor Laboratories, New York, Davis etal. (1986) Basic Methods in Molecular Biology, Elsevier, and Chu et al., 1981. Particularly suitable transfection methods include calcium phosphate co-precipitation (Graham et al., 1973), direct microinjection into cultured cells (Capecchi, 1980), electroporation (Shigekawa et al., 1988), liposome mediated gene transfer (Mannino et al., 1988), lipid-mediated transduction (Felgner et al., 1987), and nucleic acid delivery using high-velocity microprojectiles (Klein et al., 1987).

Typically the vector of the present invention comprises an expression cassette. The term “expression cassette”, as used herein, refers to a nucleic acid construct comprising nucleic acid elements sufficient for the expression of the nucleic acid molecule of the present invention. Typically, an expression cassette comprises the nucleic acid molecule of the present invention operatively linked to a promoter sequence. The term “operatively linked” refers to the association of two or more nucleic acid fragments on a single nucleic acid fragment so that the function of one is affected by the other. For example, a promoter is operatively linked with a coding sequence when it is capable of affecting the expression of

that coding sequence (e.g., the coding sequence is under the transcriptional control of the promoter). Encoding sequences can be operatively linked to regulatory sequences in sense or antisense orientation. In some embodiments, the promoter is a heterologous promoter. The term "heterologous promoter", as used herein, refers to a promoter that is not found to be operatively linked to a given encoding sequence in nature. In some embodiments, an expression cassette may comprise additional elements, for example, an intron, an enhancer, a polyadenylation site, a woodchuck response element (WRE), and/or other elements known to affect expression levels of the encoding sequence. As used herein, the term "promoter" refers to a nucleotide sequence capable of controlling the expression of a coding sequence or functional RNA. In general, the nucleic acid molecule of the present invention is located 3 of a promoter sequence. In some embodiments, a promoter sequence consists of proximal and more distal upstream elements and can comprise an enhancer element. An "enhancer" is a nucleotide sequence that can stimulate promoter activity and may be an innate element of the promoter or a heterologous element inserted to enhance the level or tissue-specificity of a promoter. In some embodiments, the promoter is derived in its entirety from a native gene. In some embodiments, the promoter is composed of different elements derived from different naturally occurring promoters. In some embodiments, the promoter comprises a synthetic nucleotide sequence. It will be understood by those skilled in the art that different promoters will direct the expression of a gene in different tissues or cell types, or at different stages of development, or in response to different environmental conditions or to the presence or the absence of a drug or transcriptional co-factor. Ubiquitous, cell-type-specific, tissue-specific, developmental stage-specific, and conditional promoters, for example, drug-responsive promoters (e.g. tetracycline-responsive promoters) are well known to those of skill in the art. Examples of promoter include, but are not limited to, the phophoglycerate kinase (PKG) promoter, CAG, NSE (neuronal specific enolase), synapsin or NeuN promoters, the SV40 early promoter, mouse mammary tumor virus LTR promoter; adenovirus major late promoter (Ad MLP); a herpes simplex virus (HSV) promoter, a cytomegalovirus (CMV) promoter such as the CMV immediate early promoter region (CMVIE), SFFV promoter, rous sarcoma virus (RSV) promoter, synthetic promoters, hybrid promoters, and the like. The promoters can be of human origin or from other species, including from mice. In addition, sequences derived from nonviral genes, such as the murine metallothionein gene, will also find use herein. Such promoter sequences are commercially available from, e. g. Stratagene (San Diego, CA).

In some embodiments, the expression cassette comprises an appropriate secretory signal sequence that will allow the secretion of the polypeptide encoded by the nucleic acid molecule of the present invention. As used herein, the term "secretory signal sequence" or variations thereof are intended to refer to amino acid sequences that function to enhance (as defined above) secretion of an operably linked polypeptide from the cell as compared with the level of secretion seen with the native polypeptide. As defined above, by "enhanced" secretion, it is meant that the relative proportion of the polypeptide synthesized by the cell that is secreted from the cell is increased; it is not necessary that the absolute amount of secreted protein is also increased. In some embodiments, essentially all (i.e., at least 95%, 97%, 98%, 99% or more) of the polypeptide is secreted. It is not necessary, however, that essentially all or even most of the polypeptide is secreted, as long as the level of secretion is enhanced as compared with the native polypeptide. Generally, secretory signal sequences are cleaved within the endoplasmic reticulum and, in some embodiments, the secretory signal sequence is cleaved prior to secretion. It is not necessary, however, that the secretory signal sequence is cleaved as long as secretion of the polypeptide from the cell is enhanced and the polypeptide is functional. Thus, in some embodiments, the secretory signal sequence is partially or entirely retained. The secretory signal sequence can be derived in whole or in part from the secretory signal of a secreted polypeptide (i.e., from the precursor) and/or can be in whole or in part synthetic. The length of the secretory signal sequence is not critical; generally, known secretory signal sequences are from about 10-15 to 50-60 amino acids in length. Further, known secretory signals from secreted polypeptides can be altered or modified (e.g., by substitution, deletion, truncation or insertion of amino acids) as long as the resulting secretory signal sequence functions to enhance secretion of an operably linked polypeptide. The secretory signal sequences of the invention can comprise, consist essentially of or consist of a naturally occurring secretory signal sequence or a modification thereof (as described above). Numerous secreted proteins and sequences that direct secretion from the cell are known in the art. The secretory signal sequence of the invention can further be in whole or in part synthetic or artificial. Synthetic or artificial secretory signal peptides are known in the art, see e.g., Barash et al., "Human secretory signal peptide description by hidden Markov model and generation of a strong artificial signal peptide for secreted protein expression," Biochem. Biophys. Res. Comm. 294:835-42 (2002); the disclosure of which is incorporated herein in its entirety.

In some embodiments, the vector of the present invention comprises the nucleic acid sequence set forth in SED ID NO:5 or 6.

SEQ ID NO:5: complete sequence of the expression cassette of the AAV transfer vector encoding codon-optimized mouse APPsα

ggggggggggggggggggttggccactccctctctgcgcgctcgctcgctcactgaggccgggcgaccaaaggtcgcc
cgacgcccgggctttgcccgggcggcctcagtgagcgagcgagcgcgcagagagggagtggccaactccatcactagggggttcct
agatctaggatcacgcgttctagaaatattaaggtacgggaggtacttggagcggccgcaataaaatatctttattttcattacatctgtgtg
ttggttttttgtgtgaatcgatagtactaacatacgctctccatcaaaacaaaacgaaacaaaacaaactagcaaaataggctgtccccag
tgcaagtgggttttaggaccaggatgaggcggggtgggggtgcctacctgacgaccgaccccgacccactggacaagcacccaac
ccccattccccaaattgcgcatcccctatcagagaggggggaggggaaacaggatgcggcgaggcgcgtgcgcactgccagcttcag
caccgcggacagtgccttcgccccgcctggcggcgcgcgccaccgccgcctcagcactgaaggcgcgctgacgtcactcgccgg
tcccccgcaaactcccctttcccggccaccttggtcgcgtccgcgccgccgccggcccagccggaccgcaccacgcgaggcgcgag
atagggggggcacgggcgcgaccatctgcgctgcggcgccggcgactcagcgctgcctcagtctgcggtgggcagcggaggagtc
gtgtcgtgcctgagagcgcagtcgaattgctagcggggatccaccggtcgccaccatgctgccttctctggctttgctgctgctggccg
cttggacagtgcgggcctacccttacgacgtgcccgactacgcttacccctacgatgtgcctgattatgcattggaggtgcccaccgac
ggcaacgctggactgctggctgaaccccagatcgccatgttctgcggcaagctgaacatgcacatgaacgtgcagaacggcaagtg
ggagagcgaccccagcggcaccaagacctgcatcggcaccaaagagggcatcctgcagtattgccaggaagtgtaccccgagctg
cagatcaccaacgtggtggaagccaaccagcccgtgaccatccagaactggtgcaagaggggcagaaagcagtgcaagacccaca
cccacatcgtgatcccttacagatgcctcgtgggcgagttcgtgtccgacgctctgctggtgcccgacaagtgcaagttcctgcatcag
gaacggatggacgtgtgcgagacacatctgcactggcacaccgtggccaaagagacatgcagcgagaagtccaccaacctgcacg
actacggcatgctgctgccctgcggcatcgacaagttcagaggcgtggaattcgtgtgctgccccctggccgaggaatccgactctgt
ggatagcgccgacgccgaagaggacgactctgacgtgtggtggggcggagccgacacagattacgctgatggcggcgaggacaa
ggtggtggaagtggctgaagaggaagaggtggccgacgtggaagaagaagaggccgacgacgacgaggatgtggaagatggcg
acgaggtggaagaggaagccgaggaaccctacgaggaagccaccgagagaaccaccagcaccgccaccacaaccaccaccact
accgagagcgtggaagaggtcgtgcgggtgccaacaacagccgcctctacacctgacgccgtggacaagtacctggaaaccccag
gcgacgagaacgagcacgcccacttccagaaggctaaagagagactggaagctaagcaccgcgagagaatgagccaagtgatga
gagagtgggaggaagctgagagacaggccaagaacctgcccaaggccgacaagaaagccgtgatccagcacttccaggaaaagg
tggaaagcctggaacaggaagctgccaacgagagacagcagctggtggaaacccacatggccagagtggaagctatgctgaacga
cagaagaaggctggccctggaaaactacatcaccgctctgcaggccgtgccccccagacctcaccacgtgttcaacatgctgaagaa
atacgtgcgggccgagcagaaggacagacagcacaccctgaagcacttcgagcacgtgcggatggtggaccccaagaaggccgc
ccagatcagatcccaagtgatgacccacctgagagtgatctacgagaggatgaaccagagcctgagcctgctgtacaacgtgcccgc
cgtggccgaagaaatccaggatgaggtggacgagctgctgcagaaagagcagaactacagcgacgacgtgctggccaacatgatc
agcgagcccagaatcagctacggcaacgacgccctgatgcccagcctgaccgagacaaagaccaccgtggaactgctgcccgtga

acggcgagttcagcctggatgacctgcagccctggcacccttt cggcgtggactctgtgcctgccaacacagagaacgaagtggaac
ccgtggacgccagacctgccgctgatagaggcctgaccacaagacctggcagcggcctgacaaacatcaagaccgaagagatcag
cgaagtgaagatggacgccgagttcgggcacgacagcggctttgaagtgcggcaccagaaatagaagcttatcgataatcaacctct
ggattacaaaatttgtgaaagattgactggtattcttaactatgttgctccttttacgctatgtggatacgctgctttaatgcctttgtatcatgct
attgcttcccgtatggctttcattttctcctccttgtataaatcctggttgctgtctctttatgaggagttgtggcccgttgtcaggcaacgtggc
gtggtgtgcactgtgtttgctgacgcaacccccactggttggggcattgccaccacctgtcagctcctttccgggactttcgctttccccct
ccctattgccacggcggaactcatcgccgcctgccttgcccgctgctggacaggggctcggctgttgggcactgacaattccgtggtgt
tgtcggggaagctgacgtcctttccatggctgctcgcctgtgttgccacctggattctgcgcgggacgtccttctgctacgtcccttcggc
cctcaatccagcggaccttccttcccgcggcctgctgccggctctgcggcctcttccgcgtcttcgccttcgccctcagacgagtcggat
ctccctttgggccgcctccccgcctgatcgataccgtcgactagagctcgctgatcagcctcgactgtgccttctagttgccagccatctg
ttgtttgcccctcccccgtgccttccttgaccctggaaggtgccactcccactgtcctttcctaataaaatgaggaaattgcatcgcattgtc
tgagtaggtgtcattctattctgggggggtggggtggggcaggacagcaagggggaggattgggaagacaatagcaggcatgctggg
gagagatctgaggaacccctagtgatggagttggccactccctctctgcgcgctcgctcgctcactgaggccgcccgggcaaagccc
gggcgtcgggcgacctttggtcgcccggcctcagtgagcgagcgagcgcgcagagagggagtggccaacccccccccccccccc
c

SEQ ID NO:6: complete sequence of the expression cassette of the AAV transfer vector encoding codon-optimized human APPsα

Gggggggggggggggggttggccactccctctctgcgcgctcgctcgctcactgaggccgggcgaccaaaggtcgc
ccgacgcccgggctttgcccgggcggcctcagtgagcgagcgagcgcgcagagagggagtggccaactccatcactagggttcc
tagatctaggatcacgcgttctagaaatattaaggtacgggaggtacttggagcggccgcaataaaatatctttatttttcattacatctgtgt
gttggttttttgtgtgaatcgatagtactaacatacgctctccatcaaaacaaaacgaaacaaaacaaactagcaaaataggctgtcccca
gtgcaagtgggttttaggaccaggatgaggcggggtgggggtgcctacctgacgaccgaccccgacccactggacaagcacccaa
cccccattccccaaattgcgcatcccctatcagagaggggggaggggaaacaggatgcggcgaggcgcgtgcgcactgccagcttca
gcaccgcggacagtgccttcgccccgcctggcggcgcgcgccaccgccgcctcagcactgaaggcgcgctgacgtcactcgccg
gtcccccgcaaactcccctcccggccaccttggtcgcgtccgcgccgccgccggcccagccggaccgcaccacgcgaggcgcga
gataggggggcacgggcgcgaccatctgcgctgcggcgccggcgactcagcgctgcctcagtctgcggtgggcagcggaggagt
cgtgtcgtgcctgagagcgcagtcgaattgctagcggggatccaccggtcgccacc
atgctgcctggactggctctgctgctgctggccgcctggacagccagagcctacccctacgacgtgcccgactacgcctacccttatg
atgtgcctgactatgcattggaggtgcccaccgacggcaacgccggactgctggccgagccccagatcgccatgttctgcggcagac
tgaacatgcacatgaacgtgcagaacggcaagtgggacagcgaccccagcggcaccaagacctgcatcgacaccaaagagggcat
cctgcagtattgccaagaagtgtaccccgagctgcagatcaccaacgtggtggaagccaaccagcccgtgaccatccagaactggtg
caagcggggcagaaagcagtgcaagacccacccccacttcgtgatcccttacagatgcctcgtgggcgagttcgtgtccgacgccct
gctggtgcccgacaagtgcaagttcctgcatcaagaacggatggacgtgtgcgagacacatctgcactggcacaccgtggccaaaga

gacatgcagcgagaagtccaccaacctgcacgactacggcatgctgctgccctgcggcatcgacaagttccggggcgtggaattcgt
gtgctgcccccctggccgaggaatccgacaacgtggacagcgccgacgccgaagaggacgacagcgacgtgtggtggggcggag
ccgacaccgattacgccgacggcagcgaggacaaggtggtggaagtggctgaagaggaagaggtggccgaggtcgaggaagag
gaagccgacgacgacgaggatgacgaggacggcgacgaggtggaagaagaggccgaggaaccctacgaggaagccaccgagc
ggaccacctctatcgccaccaccaccacaaccactaccgagagcgtggaagaggtcgtgcgggtgccaaccaccgccgcctctacc
cccgacgccgtggacaagtacctggaaaccccctggcgacgagaacgagcacgcccacttccagaaggccaaagagcggctggaa
gccaagcaccgcgagcggatgagccaggtcatgagagagtgggaagaagccgagcggcaggccaagaacctgcccaaggccga
caagaaagccgtgatccagcacttccaagaaaaggtcgagagcctggaacaagaagccgccaacgagcggcagcagctggtgga
aacccacatggccagagtggaagccatgctgaacgaccggcggagactggccctggaaaactacatcaccgctctgcaggccgtgc
cccccagaccccggcacgtgttcaacatgctgaagaaatacgtgcgggccgagcagaaggaccggcagcacaccctgaagcactt
cgagcacgtgcggatggtggaccccaagaaggccgcccagatccgctctcaggtcatgacccacctgagagtgatctacgagagaa
tgaaccagagcctgagcctgctgtacaacgtgcccgccgtggccgaagaaatccaggatgaggtggacgagctgctgcagaaaga
gcagaactacagcgacgacgtgctggccaacatgatcagcgagccccggatcagctacggcaacgacgccctgatgcccagcctg
accgagacaaagaccaccgtggaactgctgcccgtgaacggcgagttcagcctggacgacctgcagccctggcacagcttcggcg
ctgatagcgtgcccgccaacaccgagaatgaggtggaacccgtggacgccagacctgccgccgatagaggcctgaccacaagacc
tggcagcggcctgaccaacatcaagaccgaagagatcagcgaagtgaagatggacgccgagttccggcacgacagcggctacga
ggtgcaccaccagaaatagaagcttatcgataatcaacctctggattacaaaatttgtgaaagattgactggtattcttaactatgttgctcc
ttttacgctatgtggatacgctgctttaatgcctttgtatcatgctattgcttcccgtatggctttcattttctcctccttgtataaatcctggttgct
gtctctttatgaggagttgtggcccgttgtcaggcaacgtggcgtggtgtgcactgtgtttgctgacgcaacccccactggttggggcatt
gccaccacctgtcagctcctttccgggactttcgctttcccctccctattgccacggcggaactcatcgccgcctgccttgcccgctgct
ggacaggggctcggctgttgggcactgacaattccgtggtgttgtcggggaagctgacgtcctttccatggctgctcgcctgtgttgcca
cctggattctgcgcgggacgtccttctgctacgtcccttcggccctcaatccagcggaccttccttcccgcggcctgctgccggctctgc
ggcctcttccgcgtcttcgccttcgccctcagacgagtcggatctcccttgggccgcctccccgcctgatcgataccgtcgactagagc
tcgctgatcagcctcgactgtgccttctagttgccagccatctgttgtttgcccctcccccgtgccttccttgaccctggaaggtgccactc
ccactgtcctttcctaataaaatgaggaaattgcatcgcattgtctgagtaggtgtcattctattctgggggggtggggtggggcaggacag
caaggggggaggattgggaagacaatagcaggcatgctggggagagatctgaggaacccctagtgatggagttggccactccctctct
gcgcgctcgctcgctcactgaggccgcccgggcaaagcccgggcgtcgggcgacctttggtcgcccggcctcagtgagcgagcga
gcgcgcagagagggagtggccaacccccccccccccccc

By a "therapeutically effective amount" of the vector of the present invention is meant a sufficient amount of the vector for the treatment of Alzheimer's disease. It will be understood, however, that the total daily usage of the vector of the present invention will be decided by the attending physician within the scope of sound medical judgment. The specific therapeutically effective dose level for any particular subject will depend upon a variety of

factors including the disorder being treated and the severity of the disorder; activity of the specific compound employed; the specific composition employed, the age, body weight, general health, sex and diet of the subject; the time of administration, route of administration, and rate of excretion of the specific compound employed; the duration of the treatment; drugs used in combination or coincidental with the specific vector employed; and like factors well known in the medical arts. For example, it is well within the skill of the art to start doses of the compound at levels lower than those required to achieve the desired therapeutic effect and to gradually increase the dosage until the desired effect is achieved. Typically, from 10^8 to 10^{10} viral genomes (vg) are administered per dose in mice. Typically, the doses of AAV vectors to be administered in humans may range from 10^{10} to 10^{12} vg.

Typically, the vector of the present invention is delivered directly and specifically into selected brain regions by intracerebral injections into the cerebellum, the dentate nucleus, the striatum, the cortex and particularly the entorhinal cortex, or the hippocampus. In some embodiments, the vector of the present invention is delivered by intrathecal delivery. In some embodiments, the vector of the present invention is delivered into the brain by intracerebral injection and/ blood by intravenously injection, in the spinal fluid by intrathecal delivery, by or intracerebroventricular injection or by intra-nasal injection. Particularly, any routes of administration that allow an important expression of the vector in the spinal cord, brain, cortex, hippocampus, dentate nucleus and, purkinje and granular cerebellar cells can be used in the invention.

In some embodiments, the vector of the present invention is administrated to the subject in need thereof one time, two times, three times or more. In some embodiments, the vector of the present invention is administrated to the subject in need thereof one time and readministered several months or years later to said subject.

The vectors used herein may be formulated in any suitable vehicle for delivery. For instance they may be placed into a pharmaceutically acceptable suspension, solution or emulsion. Suitable mediums include saline and liposomal preparations. More specifically, pharmaceutically acceptable carriers may include sterile aqueous of non-aqueous solutions, suspensions, and emulsions. Examples of non-aqueous solvents are propylene glycol, polyethylene glycol, vegetable oils such as olive oil, and injectable organic esters such as ethyl oleate. Aqueous carriers include water, alcoholic/aqueous solutions, emulsions or

suspensions, including saline and buffered media. Intravenous vehicles include fluid and nutrient replenishers, electrolyte replenishers (such as those based on Ringer's dextrose), and the like. Preservatives and other additives may also be present such as, for example, antimicrobials, antioxidants, chelating agents, and inert gases and the like. A colloidal dispersion system may also be used for targeted gene delivery. Colloidal dispersion systems include macromolecule complexes, nanocapsules, microspheres, beads, and lipid-based systems including oil-in-water emulsions, micelles, mixed micelles, and liposomes.

The invention will be further illustrated by the following figures and examples. However, these examples and figures should not be interpreted in any way as limiting the scope of the present invention.

FIGURES:

Figure 1: Widespread expression of APPsα throughout the hippocampus and in parahippocampal cortex in AAV-APPsα injected APP/PS1ΔE9 mice. APP/PS1ΔE9 and nontransgenic littermate control mice (LM) were injected either with AAV-Venus or AAV-APPsα at 12 months of age and sacrificed at 17 months of age. (LM: AAV-Venus n=3, AAV-APPsα n=4; APP/PS1ΔE9 mice: AAV-Venus n=8, AAV-APPsα n=8; all males). **(A)** Schematic representation of AAV9 constructs enabling the neuron-specific expression of Venus (Control) and HA-tagged APPsα. ITR: inverted terminal repeat; SP: APP signal peptide; HA: Human influenza hemagglutinin tag; WPRE: Woodchuck hepatitis virus posttranscriptional regulatory element. **(B)** Scheme of the hippocampus with coordinates of the two injection sites (red stars). **(C)** High magnification of the hippocampus of a APP/PS1ΔE9 mouse injected with the AAV-APPsα. APPsα is detectable throughout the hippocampus and the proximal cortex. Scale bar, 500 µm. Injection sites indicated by white stars. **(D)** Scheme representing antero-posterior coordinates of coronal sections depicted in E to H. **(E-H)** Immunostaining of APPsα (anti-HA tag, red) and NeuN (green) at different antero-posterior coordinates. Scale bar, 500 µm. **(I-L)** Double immunostaining of CA1 pyramidal cells from the area boxed in C expressing APPsα (anti-HA tag, red) and specific neuronal (NeuN, green, I, J), microglial (Iba1, green, K) or astrocytic (GFAP, green; L) markers. Scale bar, 50 µm (I, K, L), 20µm (J). Note that AAV-mediated APPsα expression is restricted to neurons. **(M)** Western blot analyis of Venus and HA-APPsα expression in APP/PS1ΔE9 and LM hippocampi of mice injected with AAV-Venus or AAV-APPsα

vectors.

Figure 2: APPsα overexpression enhances Morris water maze performance in WT mice and rescues the spatial memory deficit of APP/PS1ΔE9 mice. Transgenic APP/PS1ΔE9 mice (n=8 per group) or littermate (LM) controls (n=3-4 per group) were either injected with AAV-Venus or AAV-APPsα vectors at 12 months of age and tested 2 months later at 14 months of age. **(A)** Training phase consisted of daily sessions (three trials per session: T1, T2 and T3) during 5 consecutive days (D1 to D5). 72 hours (D8) after the last trial the platform was removed and memory retention was assessed during the probe trial. Insert: Water maze configuration during training sessions. PF: Platform; TQ: Target Quadrant (white); OQ: Other Quandrants (grey). **(B)** Escape latency and **(C)** swim speed of littermate controls or APP/PS1ΔE9 mice injected either with AAV-Venus or AAV-APPsα. Swim speed was similar between the different groups (2-way ANOVA: Group effect: $F_{3,100}=2.40$; ns; Time effect: $F_{4,100}=1.41$; ns; Group x Time interaction: $F_{12,100}<1$; ns). Littermates injected with AAV-APPsα showed improved performance, as indicated by reduced escape latency (2-way ANOVA: Time effect: $F_{4,100}=7.138$; $p<0.0001$; Group effect: $F_{3,100}=7.247$; $p=0.0002$, followed by Tukey post-hoc test: APP/PS1ΔE9 mice injected with AAV-APPsα versus each of the other groups, $p<0.013$). **(D)** Probe trial performance at 72h. 2-way ANOVA, Group effect: $F_{3,17}=3.356$; $p<0.04$; quadrant effect: $F_{1,17}=23.54$; $p<0.007$; Group x quadrant interaction effect: $F_{3,17}=3.356$; $p<0.04$. APP/PS1ΔE9 mice injected with AAV-Venus were impaired in comparison to littermate mice injected with AAV-Venus (Tukey *post-hoc* test: $p=0.023$) confirmed by no preference for the trained target quadrant. Strikingly, AAV-APPsα treated APP/PS1ΔE9 mice spent more time in the target quadrant compared to APP/PS1ΔE9 mice injected with AAV-Venus (Tukey *post-hoc* test: $p=0.017$). Statistics: 2-way ANOVA (genotype and group as factors) with repeated measures followed by Tukey *post-hoc* test: *< 0.05. Values represent means ±SEM.

Figure 3: APP/PS1ΔE9 mice reveal structural and functional synaptic impairments that are ameliorated by APPsα expression. (A, B) LTP was induced by TBS at hippocampal CA3-CA1 synapses after 20 min baseline recordings (arrowhead). Acute slices of AAV-Venus injected APP/PS1ΔE9 animals (open circles) exhibited significant lower induction and maintenance of LTP compared to littermate controls (LM, black circles) showing similar expression of Venus (averaged potentiation minutes t50-80: 148.47 ± 6.04% vs. 178.01 ± 8.98%, p= 0.021). Viral expression of APPsα (red circles) restored potentiation

after TBS (171.48 ± 6.29%) in transgenic animals and resulted in an LTP curve progression comparable to that of LM controls. The LTP induction rate is shown as percentage % of mean baseline slope, n = number of slices, N = number of mice. **(C, D)** Input-Output strength of all AAV-injected mice showed no alterations between genotypes at any fiber volley (FV) amplitude or stimulus intensity tested. **(E)** Altered PPF at the 10 ms ISI revealed a significant impairment in the pre-synapse of APP/PS1ΔE9 mice injected with AAV-Venus in comparison to LM controls (*p= 0.030) that was restored after AAV-APPsα injection (#p= 0.047). **(F)** Detailed segments of 2nd or 3rd order dendritic branches of apical and basal dendrites of CA1 and CA3 neurons after Golgi-Cox staining, scale bar 8 µm. **(G)** No differences in spine density at CA1 apical neurons between groups, but significantly less spines at basal dendrites of APP/PS1ΔE9 Venus injected mice (p=0.040). APPsα overexpression partially restored the spine density deficit. **(H)** Reduced spine density at CA3 apical (p=0.014) and basal (p=0.011) dendritic segments of APP/PS1ΔE9 AAV-Venus injected mice that is partially rescued at apical and completely at basal dendrites (p= 0.039) by APPsα. N = number of neurons, N = number of animals. Data represent mean ± SEM and were analyzed by one-way ANOVA followed by Bonferroni´s post-hoc test.

Figure 4: AAV-APPsα injection decreases Aβ and plaques load. (A) ELISA quantification of β-CTF in hippocampus (H) and cortex (Cx) of APP/PS1ΔE9 mice. No difference was detectable between AAV-Venus and AAV-APPsα injected animals. **(B-D)** Quantification (MSD immunoassay) of TBS soluble Aβ38 (Group effect: $F_{1,14}$=3.879, p=0.07 (-36%), Aβ40 (Group effect: $F_{1,14}$=3.094, p=0.10 (-32%)) and Aβ42 (Group effect: $F_{1,14}$=5.211, p=0.04 (-33%); region effect: $F_{1,14}$<1, ns; Group x region interaction effect: $F_{1,14}$<1, ns) in hippocampus and cortex of APP/PS1ΔE9 mice. Note that AAV-APPsα injected animals show reduced levels of Aβ in both anatomical regions analyzed (hippocampus and cortex). **(E-F)** Representative images of hippocampus and cortex of APP/PS1ΔE9 mice injected either with AAV-Venus **(E)** or AAV-APPsα **(F). (G)** Quantification of 4G8 immunolabeled area in hippocampus and cortex (2-way ANOVA: Treatment effect: $F_{1,13}$=5.50, p=0.04 (-24%); region effect: $F_{1,13}$=22.89, p=0.0004; Treatment x region interaction effect: $F_{1,13}$<1, ns). Note that 4G8 immunoreactive plaque area is significantly reduced in AAV-APPsα treated animals. Number of animals n=8/group. 2-way ANOVA (Genotype, treatment and region as factors) followed by Tukey *post-hoc* test: *p < 0.05. Values represent means ±SEM.

Figure 5: AAV-APPsα promotes microglia recruitment around plaques in APP/PS1ΔE9 mice. (A-B) Western blot analysis showing the expression of GFAP and Iba1 in the hippocampus of AAV-Venus or AAV-APPsα injected APP/PS1ΔE9 mice (n=8/group). **(B)** For quantification signal intensities were normalized to GAPDH used as a loading control. AAV-APPsα treatment specifically increased Iba1 (microglial marker) expression (t-test: t_{14}=3.586; p=0.003), whereas the astrocyte marker GFAP was not affected. **(C, D)** Immunostaining of GFAP **(C)** or Iba1 **(D)** in hippocampus (DG subfield) of APP/PS1ΔE9 transgenic mice. Dotted line indicates the granular layer of the DG. Scale bar, 500 µm. **(E)** Whereas the distribution of GFAP positive astrocytes is unaltered, increased recruitment of Iba1 positive microglia is observed in the vicinity of amyloid plaques (t-test: t_{16}=5.441; p<0.0001). **(F)** Co-staining of amyloid plaques (Thioflavin S, green) and GFAP (red) or Iba1 (red). Scale bar, 20 µm. **(G)** Morphology of microglia in the hippocampus of AAV-injected APP/PS1ΔE9 mice. Increased ramified profile is observed in microglia of AAV-APPsα injected mice (bottom, indicated by arrow heads). Scale bar, 10 µm. **(H)** Co-immunostaining of Iba1 (red) and 4G8 (β amyloid, green) in AAV-APPsα injected APP/PS1ΔE9 mice indicating the uptake of Aβ (arrow heads) in plaque associated microglia. Scale bar, 10 µm. **(I, J)** Western blot analysis showing the expression of IDE and TREM2 in the hippocampus of AAV-Venus or AAV-APPsα injected APP/PS1ΔE9 mice. Both Aβ clearance related proteins are significantly upregulated (IDE: t-test: t_{14}=3.984; p=0.0014; TREM2: t-test: t_{14}=2.947; p=0.010) following AAV-APPsα treatment. Values represent means ±SEM. ***$P < 0.001$, **$P < 0.01$, *$P < 0.05$.

EXAMPLE:

Material & Methods

AAV plasmid design and vector production

The mouse APPsα coding sequence (derived from Uniprot: P12023-2) was codon optimized (Geneart, Regensburg) and then cloned under control of the synapsin promoter into the single stranded, rAAV2-based transfer vector pAAVSynMCS-2A-Venus (Tang et al, 2009) via NheI-HindIII restriction sites. For easy detection, an N-terminal double HA-tag was inserted downstream of the APP signal peptide at the N-terminus of APPsα. The control vector (pAAV-Venus) encodes the yellow fluorescent protein Venus fused to a C-terminal

farnesylation signal for membrane anchoring. All constructs were packaged into AAV9 by the MIRCen viral production platform as described (Berger et al, 2015).

Animals

Sixteen APPswe/PS1ΔE9 mice (referred as APP/PS1ΔE9; Jackson Laboratories) and seven age-matched littermate control mice were used for behavior, pathology and biochemistry. Eleven APP/PS1ΔE9 and five littermates were used for electrophysiology and spine density analysis. APP/PS1ΔE9 mice express the human APP gene carrying the *Swedish* double mutation (K595N/M596L). In addition, they express the human PS1ΔE9 variant lacking exon 9 (Borchelt et al, 1997; Jankowsky et al, 2004; Xiong et al, 2011). Only male mice were used throughout the study. For age at AAV injection and age at analysis/sacrifice see results section. All experiments were conducted in accordance with the ethical standards of French, German and European regulations (European Communities Council Directive of 24 November 1986).

Stereotactic injection of AAV

Mice were anesthetized by intraperitoneal injection of ketamine/xylazine (0.1/0.05 g/kg body weight) and positioned on a stereotactic frame (Stoelting, Wood Dale, USA). Vectors (either AAV-Venus or AAV-APPsα) were bilaterally injected into the hippocampus using 2 µl of viral preparation (10^{10} vg/site) at a rate of 0.2 µl/minute. Two injections sites per hippocampus were used to optimize virus spreading. Stereotactic coordinates of injection sites from bregma were: anteroposterior -2 mm; mediolateral +/-1 mm; dorsoventral -2.25 mm and anteroposterior -2mm; mediolateral +/-1mm; dorsoventral -1.75mm.

Brain samples

APP/PS1ΔE9 mice were sacrificed 5 months post-injection at 17 months of age. Following anesthesia, mice were transcardially perfused with 0.1 M phosphate buffered saline (PBS) before dissection. For immunohistochemistry, the left cerebral hemisphere was dissected and post-fixed in 4% paraformaldehyde (PFA) for 1 week and cryoprotected in 30% sucrose for 24 hours. 40 µm sections were cut using a freezing microtome (Leica, Wetzlar, Germany), collected in a cryoprotective solution and stored at -20°C. The right hemisphere was dissected to segregate hippocampus and cortex for biochemical analysis. Samples were then homogenized in lysis buffer (TBS, NaCl 150mM and Triton 1%) containing phosphatase

and protease inhibitors. After centrifugation (20 min, 13 000 rpm, 4°C), the supernatant was collected and the protein concentration was quantified by BCA Assay (Thermo Fisher Scientific, Waltham, USA). Lysate aliquots (3 mg of protein/ml) were stored at -80°C.

Immunostaining

Slices were washed with 0.1 M PBS and permeabilized in 0.25% PBS-Triton before blocking in PBS-Triton 0.25% containing 5% goat serum for 60 minutes. For vector encoded HA-APPsα immunolabeling, slices were incubated with an anti-HA antibody (Covance, Princeton, USA, 1/250) overnight at 4°C. After successive washes (PBS-Triton 0.25%, PBS and PB 0.1 M), incubation with a biotinylated anti-mouse antibody was performed for one hour at room temperature. For signal amplification, samples were incubated using the ABC kit (Vector laboratories, Burlingame, USA) for one hour at room temperature. Finally, slices were incubated in Cy3-coupled streptavidine. HA-APPsα was co-immunostained overnight with the following primary antibodies: Rabbit anti-Iba1,1/500, Wako, Richmond, USA; Mouse-GFAP Cy3 conjugate, 1/500, Sigma-Aldrich, Saint-Louis, USA. For immunofluorescent staining of plaques, slices were stained using a 30 min incubation in 1% thioflavin-S solution, rinsed twice (1 min each) in 50% EtOH and mounted in Vectashield fluorescent mounting media (Vector laboratories). Images were taken with a Nikon Eclipse T*i* microscope (Nikon, Tokyo, Japan) and a Leica SP8 confocal microscope (Leica). For plaque quantification, slices were incubated in 88% formic acid solution for 15 min (antigen retrieval). To inactivate endogenous peroxidase, samples were incubated in hydrogen peroxide (30 min) before blocking and incubation with the primary antibody (4G8, Covance, 1/1000). Incubation with a horseradish coupled secondary antibody was done at RT, developed using the DAB kit (Vector laboratories) and mounted in Eukitt mounting media (Sigma-Aldrich, Saint-Louis, USA). Images were taken with a Z6 APO macroscope (Leica). Plaques, GFAP and Iba1 immunoreactivity were quantified using ImageJ (NIH, Bethesda, USA) or Icy (Institut Pasteur, Paris, France). Laserpower, numeric gain and magnification were kept constant between animals to avoid potential technical artefacts. Images were first converted to 8-bit gray scale and binary thresholded to highlight a positive staining. At least 2 sections per mouse (between −1.7 mm to −2.3 mm caudal to bregma) were quantified for either hippocampus or cortex. The average value per structure was calculated for each mouse. For quantification of Iba1 and GFAP immunoreactivity around plaques, a region of interest (ROI) was drawn around the center of the plaque. The diameter of the circular ROI was set as 3 times the diameter of the plaque. Mean fluorescence intensity values were measured for

either Iba1 or GFAP immunoreactivity and were processed via Icy software (Institut Pasteur, Paris, France). Experimentators and data managers were blind with respect to treatments and genotypes.

Western blot analysis

Proteins were separated by electrophoresis using 4-12% SDS-PAGE (NuPAGE, Life Technologies, Carlsbad, USA) in MOPS buffer (NuPAGE, Life Technologies) and transferred to nitrocellulose membranes (iBlot, Life Technologies). After blocking in 5% milk-PBS 0.1M for 60 minutes, membranes were incubated with the primary antibodies overnight at 4°C (HA, 1/2000, Covance, Princeton, USA; Venus (GFP), 1/1000,Vector laboratories Burlingame, USA; GAPDH, 1/4000 Abcam, Cambridge, UK; Iba1, 1/2000, Wako, Richmond, USA; GFAP, 1/4000 Dako, Glostrup, Denmark; IDE, 1/200, Santa Cruz Biotechnology, Dallas, USA; TREM2, 1/500, R&D Systems, Minneapolis, USA). Membranes were then washed with TBS-T (with 0.1% Tween), incubated with a horseradish peroxidase coupled secondary antibody and developed using enhanced chemiluminescence (ECL, GE Healthcare, Little Chalfont, UK and Super Signal, Thermo Fisher Scienfitic). Signals were detected with Fusion FX7 (Vilber Lourmat, Marne-la-Vallée, France) and analyzed and quantified using ImageJ.

ELISA

APPsα, β-CTF, and Aβ were quantified using the sAPPα kit (Meso Scale Discovery, Rockville, USA), Human APP β-CTF Assay Kit (IBL, Hamburg, Germany), V-PLEX Plus Aβ Peptide Panel 1 (6E10) Kit (Meso Scale Discovery). The procedures were performed according to the respective supplier instructions.

Morris Water Maze

Experiments were performed in a 120-cm diameter, 50 cm deep tank filled with opacified water kept at 21°C and equipped with a 10 cm diameter platform submerged 1 cm under the water surface. Visual clues were disposed around the pool as spatial landmarks for the mouse and luminosity was kept at 430 lux. Training consisted of daily sessions (three trials per session) during 5 consecutive days. Start positions varied pseudo-randomly among the four cardinal points. Mean inter-trial interval was 15 min. Each trial ended when the animal reached the platform. A 60 second cut-off was used, after which mice were gently guided to the platform. Once on the platform, animals were given a 30-second rest before

being returned to their cage. 72 hours after the last training trial (day 8), retention was assessed during probe trial in which the platform was no longer present. Animals were video tracked using Ethovision software (Noldus, Wageningen, Netherlands) and behavioral parameters (swim speed, travelled distance, latency, percentage of time spend in each quadrant) were automatically calculated. Experiments and statistical evaluation of data were performed by an experimentator blind to genotype and treatment group.

Statistics

Statistical analyses were performed as indicated for the respective experiments. Outliers were detected and rejected using maximum normed residual test (Grubbs' test). In most cases, data were analyzed using non-parametric Mann-Whitney U tests excepted for behavioral experiments. Two-way ANOVA with repeated measures were carried out when required by the experimental plan to assess statistical effects. Correlation matrices were generated using non-parametric Spearman rank correlation coefficient. For all analysis statistical significance was set to a p-value <0.05. All analyses were performed using Statistica (StatSoft Inc., Tulsa, USA) or Prism (GraphPad Software, La Jolla, USA).

Electrophysiology

In vitro extracellular recordings were performed on acute hippocampal slices of WT littermates stereotactically injected with the AAV-Venus (N= 5), APP/PS1ΔE9 mice injected either with AAV-Venus (N= 4) or AAV-APPsα virus (N= 6) at 8 months of age. Electrophysiological recordings were performed 4-5 months later at an age of 12-13 months. In-between animals were housed in a temperature- and humidity-controlled room with a 12h light-dark cycle and had access to food and water ad libitum.

Slice preparation

Acute hippocampal transversal slices were prepared from individuals at an age of 12 to 13 months. Mice were anesthetized with isoflurane and decapitated. The brain was removed and quickly transferred into ice-cold carbogenated (95% O_2, 5% CO_2) artificial cerebrospinal fluid (ACSF) containing 125 mM NaCl, 2 mM KCl, 1.25 mM NaH_2PO_4, 2 mM $MgCl_2$, 26 mM $NaHCO_3$, 25 mM glucose. After dissection of the two hemispheres one was used for Golgi-Cox staining and the other for electrophysiology. The hippocampus was sectioned into 400 µm thick transversal slices with a vibrating microtome (Leica, VT1200S). Slices were maintained in carbogenated ACSF (125 mM NaCl, 2.mM KCl, 1.25 mM

NaH_2PO_4, 2 mM $MgCl_2$, 26 mM $NaHCO_3$, 2 mM $CaCl_2$, 25 mM glucose) at room temperature for at least 1.5 h before transferred into a submerged recording chamber. Before recording, each slice of the AAV-Venus injected animals was proofed for fluorescence expression of Venus in area CA1 and CA3 (Zeiss, Axiovert 35). Slices absent of the fluorescence protein in the recording areas were excluded from further analysis.

Extracellular field recordings

Slices were placed in a submerged recording chamber and perfused with carbogenated ACSF (32°C; 125 mM NaCl, 2 mM KCl, 1.25 mM NaH_2PO_4, 1 mM $MgCl_2$, 26 mM $NaHCO_3$, 2 mM $CaCl_2$, 25 mM glucose) at a rate of 1.2 to 1.5 ml/min. Field excitatory postsynaptic potentials (fEPSPs) were recorded in stratum radiatum of CA1 region with a borosilicate glass micropipette (resistance 2-4 MΩ) filled with 3 M NaCl at a depth of ~150-200 µm. Monopolar tungsten electrodes were used for stimulating the Schaffer collaterals at a frequency of 0.1 Hz. Stimulation intensity was adjusted to 40% of maximum fEPSP slope for 20 minutes baseline recording. LTP was induced by applying theta-burst stimulation (TBS: 10 trains of 4 pulses at 100 Hz in an 200 ms interval, repeated 3 times). Basal synaptic transmission properties were analyzed via input-output-(IO) measurements and short-term plasticity was examined via paired pulse facilitation (PPF). The IO- measurements were performed either by application of a defined current values (25 - 175 µA) or by adjusting the stimulus intensity to certain fiber volley (FV) amplitudes (0.1 – 0.7 mV). PPF was performed by applying a pair of two closely spaced stimuli in different inter-stimulus-intervals (ISI) ranging from 10 to 160 ms.

Dendrite and spine analysis

Golgi-Cox staining

Golgi staining was done using the FD Rapid GolgiStain™ Kit according to the manufacturer's instructions. All procedures were performed under dark conditions. One hemisphere of each mouse was used for electrophysiology and the other one for Golgi-Cox staining. Hemispheres were immersed in 2 ml mixtures of equal parts of kit solutions A and B and stored at RT for 2 weeks. Afterwards brain tissues were stored in solution C at 4°C for at least 48 h and up to 7 days before sectioning. Solutions AB and C were renewed within the first 24 h. Coronal sections of 200 µm were cut with a vibrating microtome (Leica, VT1200S) while embedded in 2% Agar in 0.1 M PBS. Each section was mounted with Solution C on an adhesive microscope slide pre-coated with 1% gelatin/0.1% chromalaun on both sides and

stained according to the manufacturer´s protocol with the exception that AppliClear (AppliChem) was used instead of xylene. Finally slices were cover-slipped with Permount (Fisher Scientific).

Imaging and analysis of spine density in Golgi-Cox stained slices

Imaging of 2nd or 3rd order dendritic branches of hippocampal pyramidal neurons of area CA3 and CA1 was done with an Axioplan 2 imaging microscope (Zeiss) using a 63x oil objective and a z-stack thickness of 0.5 µm under reflected light. The number of spines was determined per micrometer of dendritic length (in total 100 µm) at apical and basal compartments using ImageJ (1.48v, National Instruments of Health, USA). At minimum 4 animals per genotype and 4 neurons per animal were analyzed blinded to genotype and injected virus.

Data analysis

Data of electrophysiological recordings were collected, stored and analyzed with LABVIEW software (National Instruments, Austin, TX). The initial slope of fEPSPs elicited by stimulation of the Schaffer collaterals was measured over time, normalized to baseline and plotted as average ± SEM. Analysis of the PPF data was performed by calculating the ratio of the slope of the second fEPSP divided by the slope of the first one and multiplied by 100. Data of Golgi-Cox staining were analyzed using GraphPad Prism (Version, 5.01) software. Spine density is expressed as mean ± SEM. Differences between genotypes were detected with one-way analysis of variance (ANOVA) followed by Bonferroni´s *post hoc* test using IBM SPSS Statistics 21.

Results

AAV-APPsα injection mediates efficient and long lasting neuronal expression of APPsα in the hippocampus of APP/PS1ΔE9 mice

To assess the therapeutic potential of APPsα we used AAV-mediated overexpression of APPsα in the brain of aged (12 month-old) APP/PS1ΔE9 mice. APP/PS1ΔE9 mice show progressive plaque deposition starting at about 5-6 months of age and highly abundant plaques are observed at 12 months of age (Jankowsky et al, 2004; Xiong et al, 2011). AAV9 vectors expressing either Venus or codon optimized HA-tagged murine APPsα (HA-APPsα) under the control of the neuronal synapsin promoter (further referred to as AAV-Venus and

AAV-APPsα, Fig. 1A) were bilaterally injected into the stratum lacunosum moleculare region of the dorsal hippocampus and into the dentate gyrus (Fig. 1B) of 12 month-old male APP/PSΔE9 mice.

To monitor vector-mediated Venus and APPsα expression, mice were sacrificed 5 months after injection. Immunohistochemistry using an HA-tag specific antibody revealed widespread expression of HA-APPsα not only in the hippocampus, but also in the cortical layers above the injected hippocampus (Fig.1C). Analysis of serial anteroposterior coronal sections demonstrated widespread HA-APPsα immunoreactivity (over 3.5 mm) in the hippocampus from -2.6 mm posterior to +0.9 mm anterior from the injection site (Fig. 1D-H) and in the adjacent cortex. More detailed analysis showed prominent expression of vector-mediated HA-APPsα in the pyramidal cells of the subiculum, in the CA1, CA2 regions and in granular neurons of dentate gyrus (Fig. 1C). Within the CA3 subfield HA-APPsα expression was detectable but considerably lower. As APPsα expression was driven by the neuron-specific synapsin promotor, HA-APPsα expression was restricted to neuronal cells as revealed by double immunostaining against NeuN (Fig. 1 I-J). Consistently, no expression was detectable in microglia (Iba1, Fig. 1K) or in astrocytes (GFAP, Fig. 1L). The AAV-Venus expression pattern was largely similar to that of AAV-APPsα.

Western blot analysis of hippocampal extracts confirmed vector-mediated HA-APPsα protein expression in all injected animals. Comparable levels of either HA-APPsα or Venus were detected in injected APP/PS1ΔE9 mice or nontransgenic littermates, respectively (Fig. 1M). Altogether we demonstrate that our AAV based approach leads to efficient and long lasting APPsα expression in the hippocampus and adjacent cortex.

AAV-APPsα treatment rescues the spatial memory impairment of APP/PS1ΔE9 mice

To analyze the consequences of AAV-APPsα or AAV-Venus injection for spatial learning and memory, mice were tested in the Morris water maze place navigation task (Fig. 2). To this end, transgenic APP/PS1ΔE9 mice (n=8 per group) or nontransgenic littermate controls (n=3-4 per group) were either injected with AAV-Venus or AAV-APPsα vectors at 12 months of age and tested 2 months later at 14 months of age. Swim speed was comparable in all groups of animals (Fig. 2B) over the 5 days of training, thus excluding impairments in motor performances. While all 4 groups of mice did show learning, as evidenced by reduced latency to reach the platform over the 5 days of training, we observed a group effect resulting from an overall significantly increased performance in nontransgenic littermates that had

received AAV-APPsα (Fig. 2C). Injection of AAV-APPsα did not, however, improve the performance of APP/PS1ΔE9 mice (Fig. 2C). Similar results were obtained when analyzing the path length to reach the platform (data not shown). During the probe trial that assesses spatial reference memory and was conducted 72 hours after the last trial of training APP/PS1ΔE9 mice injected with AAV-Venus were strongly impaired (Fig. 2D) in comparison to littermate mice injected with AAV-Venus and showed no preference for the trained target quadrant (Fig. 2D; paired t-test: t_7=0.96; p=0.37). Strikingly, APP/PS1ΔE9 mice that had been injected with AAV-APPsα showed a clear preference for the trained target quadrant (Fig. 2D; paired t-test: t_7=2.516; p=0.045), that was statistically indistinguishable from the performance of littermate controls (Fig 2D; p> 0.84, 2-way ANOVA followed by Tukey's *post-hoc* test). Thus, vector mediated APPsα expression rescued the spatial memory impairment in aged APP/PS1ΔE9 mice despite established plaque deposition.

Impaired synaptic plasticity and reduced spine density of APP/PS1 Δ E9 mice are rescued by AAV-APPsα expression

Having established that AAV-APPsα expression restored the spatial memory deficits of APP/PS1ΔE9 mice we evaluated whether these improvements were also reflected at the functional neuronal network level. We analyzed synaptic plasticity which is considered to represent the basis of newly formed declarative memory, 4-5 months after AAV injection at an age of 12-13 months. To this end, we induced long term potentiation (LTP) at the Schaffer collateral to CA1 pathway by theta-burst stimulation (TBS) after baseline recording (Fig. 3A). Consistent with our previous results in noninjected APP/PS1ΔE9 mice (Heneka et al, 2013) AAV-Venus injected APP/PS1ΔE9 mice exhibited significantly lower induction and maintenance of LTP (n= 22 slices), as compared to AAV-Venus injected littermate controls (n=22, Fig 3A). Nontransgenic control slices showed at the stable phase of LTP (t50-80 min after TBS) a potentiation of 178.01 ± 8.98%, that was significantly reduced to only 148.47 ± 6.04% in AAV-Venus injected APP/PS1ΔE9 mice (Fig. 3B; p=0.021, 1-way ANOVA followed by Bonferroni´s post-hoc test). In contrast, the LTP curve recorded from AAV-APPsα injected APP/PS1ΔE9 slices (n=26) closely overlapped with and was statistically indistinguishable (1-Way ANOVA for t50-80, p>1) from that of nontransgenic littermate controls (Fig. 3A). AAV mediated expression of APPsα largely ameliorated LTP deficits of APP/PS1ΔE9 mice as evidenced by nearly identical average potentiation at t50-80 in AAV-APPsα treated APP/PS1ΔE9 mice (171.48 ± 6.29%) and littermate controls (178.01 ± 8.98%) receiving AAV-Venus control virus (Fig. 3B). While basal synaptic transmission was

comparable in all groups (Fig. 3C and D), short-term synaptic plasticity evaluated by paired pulse facilitation (PPF, Fig. 3E) was significantly impaired in APP/PS1ΔE9 mice. Transgenic animals injected with AAV-Venus showed an overall lowered response towards the second stimulus in the PPF paradigm, reaching significance at an inter-stimulus interval (ISI) of 10 ms compared to littermate controls ($p= 0.03$; 1-way ANOVA followed by Bonferroni´s post-hoc test). Strikingly, AAV-APPsα treatment completely rescued presynaptic functionality in APP/PS1ΔE9 animals, as evidenced by PPF values statistically indistinguishable from littermate controls and significantly different from that of AAV-Venus injected transgenic animals ($p(ISI_{20ms})= 0.047$; Fig. 3E).

Next we evaluated spine density as a correlate of excitatory synapses in the same set of animals as used for electrophysiology. Previous studies had indicated reduced spine density in various AD mouse models, presumably due to Aβ mediated toxic effects (reviewed in (Spires-Jones & Knafo, 2012). Spine density of basal and mid-apical dendritic segments of hippocampal CA1 and CA3 pyramidal cells was assessed using Golgi staining (Fig 3F). Apical dendrites of CA1 neurons showed comparable spine density between experimental groups, whereas significantly reduced spine density was observed in the basal dendrites of CA1 neurons from APP/PS1ΔE9 mice (n=16 neurons) as compared to littermates controls (n=24 neurons, both treated with AAV-Venus, Fig 3G). Analysis of CA3 neurons revealed significantly fewer spines in both basal (t-test, $p=0.01$) and apical ($p=0.014$) dendritic segments when comparing AAV-Venus expressing APP/PS1ΔE9 mice and nontransgenic littermates controls. Importantly, AAV-APPsα overexpression partially restored spine density in CA3 apical segments (n=24) and completely rescued the spine density deficit in basal dendrites of CA3 neurons from APP/PS1ΔE9 mice ($p=0.031$; Fig. 3H). Together, these data indicate that APPsα expression substantially ameliorates both structural and functional synaptic impairments of aged AD model mice.

AAV-APPsα expression decreases Aβ levels and plaque deposition in aged APP/PS1dE9 mice

APPsα had previously been reported to bind to BACE-1 and thereby reduce Aβ production (Obregon et al, 2012). We therefore evaluated if beneficial effects of AAV-APPsα overexpression on synaptic plasticity and cognitive function were associated with reduced amyloidogenic processing of APP. Employing a sensitive electrochemiluminescence ELISA we quantified products of amyloidogenic metabolism (Aβ and β-CTF) in the cortex (Cx) and hippocampus (H) of 17 months old APP/PS1ΔE9 mice (n=8/group), 5 months after viral

vector injection. No significant difference in β-CTF levels were detectable in APP/PS1ΔE9 mice injected with AAV-APPsα vector, as compared to mice injected with AAV-Venus control vector (Fig. 4A). In contrast, we observed a significant decrease in soluble Aβ42 (reduced by about 33% vs control, Fig 4D) in both cortex and hippocampus of APP/PS1ΔE9 mice injected with AAV-APPsα vector, as compared to AAV-Venus control injections. Similarly, we found a trend towards decreased amounts of Aβ38 and Aβ40 that did, however, not reach statistical significance (Fig. 4B, C).

In order to assess the impact of APPsα overexpression on amyloid deposition, we used 4G8 immunostaining to quantify the area covered by plaques both in the hippocampus and cortex of 17 months old APP/PS1ΔE9 mice injected with viral vectors (Fig. 4E-F). Interestingly, AAV-APPsα injection (n=8) resulted in a significantly reduced plaque area both in cortex and hippocampus as compared to AAV-Venus injected controls (Fig. 4G). Together, these results indicate that AAV-mediated APPsα overexpression moderately reduces both Aβ generation and amyloid plaque load in APP/PS1ΔE9 mice not only in the AAV injected hippocampus but also in distant cortical areas.

AAV-APPsα induces microglia recruitment and activation in the vicinity of amyloid plaques

Accumulation of amyloid plaques in APP/PS1ΔE9 mice has previously been shown to be accompanied by microgliosis and astrocytosis notably at advanced stages of plaque pathology (Kamphuis et al, 2012; Prokop et al, 2013). Here we evaluated the expression of GFAP (as an astrocyte-specific marker) and Iba1 (as a microglial marker) by Western blot analysis (Fig. 5A,B) and IHC (Fig. 5C-H) in the hippocampus of 17 month old APP/PS1ΔE9 mice treated either with AAV-APPsα or control vector. While no significant difference was detectable for the astroglial marker GFAP, AAV-APPsα treatment lead to a significant increase in Iba1 expression (about +44%; t-test, p=0.003; Fig. 5A,B), as compared to AAV-Venus control injections. Staining of brain sections further confirmed these data (Fig. 5C,D) at the cellular level. We went on and quantified GFAP and Iba1 immunoreactivity around amyloid plaques in the hippocampus. Consistent with Western blot analysis, GFAP immunoreactivity was not affected by AAV-APPsα injection (Fig. 5E,F). In contrast, the reduction of amyloid deposits observed after injection of the AAV-APPsα vector in APP/PS1ΔE9 mice was accompanied by a 2.3-fold increase in Iba1 immunoreactivity in the vicinity of plaques (Fig. 5D,E). Moreover, we observed an altered morphology of microglia in AAV-APPsα treated mice characterized by increased ramifications in AAV-APPsα versus

control vector injected APP/PS1ΔE9 mice (Fig 5F,G). Microglia contribute to Aβ clearance and are thought to play a protective role at least during early stages of AD (Prokop et al, 2013). Indeed, plaque associated microglia (from both AAV-APPsα and AAV-Venus treated mice) were also engaged in Aβ uptake as evidenced by Iba1/4G8 double staining (Fig 5H). Recently, genetic variants of TREM2 (Triggering Receptor Expressed on Myeloid cells) have been associated with an increased risk for AD (Guerreiro et al, 2013; Jonsson et al, 2013).Although the precise role of TREM2 for AD pathogenesis and Aβ pathology is still controversial (Jay et al, 2015; Wang et al, 2015) TREM2 expression has been consistently detected in plaque associated $Iba1^+$ cells in AD model mice (Frank et al, 2008; Jay et al, 2015). Consistent with an increase in plaque associated microglia we detected a significant increase of TREM2 expression (about 60% of control, t-test, $p<0.05$) by Western blot analysis in hippocampi of APP/PS1ΔE9 mice injected with AAV-APPsα versus controls (Fig. 5I-J, n=8 per group). We also determined the expression of neprilysin (NEP) and insulin-degrading enzyme (IDE) that are proteases produced by microglia that contribute to Aβ clearance (Tang 2008). Expression of NEP was identical in APP/PS1ΔE9 mice injected with AAV-APPsα versus control (not shown). However a significant increase (of about +20%, t-test, $p< 0.001$) in IDE expression was observed after AAV-HA-APPsα vector injection (Fig. 5I,J). Together these data suggest that AAV mediated APPsα expression induces microglia recruitment, activation and possibly also phagocytic function which may lead to enhanced Aβ and plaque clearance.

Discussion

Despite a recent shift of research efforts towards preventive strategies, there is still an urgent lack of an effective treatment of patients with clinically established AD. So far, many therapeutic approaches targeted the secretases processing APP. However, since all secretases act on many different substrates besides APP (Prox et al, 2012; Vassar et al, 2014), these strategies have major drawbacks for clinical application. γ-secretase is physiologically essential and current clinical trials to develop γ-secretase inhibitors have been abrogated due to serious side effects, likely resulting from impaired Notch signalling (Doody et al, 2013). Also systemic upregulation of the major α-secretase ADAM10 to boost APPsα production is problematic, as this may enhance cleavage of substrates implicated in tumorigenesis (reviewed by Nhan et al, 2015; Prox et al, 2012). Thus, direct overexpression of APPsα in the brain may be more promising than pharmacological upregulation of α-secretase.

Here, we explored a gene therapeutic approach and used AAV based gene transfer to overexpress APPsα in the brain of transgenic APP/PS1ΔE9 mice, that have been widely used in experimental studies assessing the efficacy of AD therapies. Bigenic APP_{SWE}/PS1ΔE9 mice express a chimeric mouse/human APP (with Swedish double mutation) and a mutant human PS1 gene (PS1ΔE9) both associated with familial forms of AD. They produce high amounts of huAβ leading to amyloid deposition starting at 5-6 months and pronounced progression of plaque pathology with age that is associated with impairments in cognitive behavior (Savonenko et al, 2005). Using bilateral injection of AAV-APPsα vector particles we achieved highly efficient and widespread expression of APPsα throughout the whole hippocamus and also in adjacent cortical areas. We attribute this on one hand to the well-established spreading/diffusion of small AAV particles, particularly along the injection needle track (Casanova et al, 2014) and on the other hand to the secretion of APPsα that may diffuse in the brain parenchyma. In this study, a single bilateral injection of AAV-APPsα particles was sufficient to mediate long-lasting APPsα expression over five months that was well tolerated without apparent adverse effects. This was a crucial prerequisite to study potential therapeutic efficacy of AAV-APPsα overexpression. To this end, we used aged (12 month old) APP/PS1ΔE9 mice with preexisting amyloidosis to mimic the situation in AD patients that are usually clinically diagnosed many years after the onset of pathology (Villemagne et al, 2013) .

Taken together, we demonstrate that in aged APP/PS1ΔE9 AD model mice AAV-APPsα could rescue or ameliorate key aspects of AD pathology: i) defective synaptic plasticity (LTP and PPF), ii) reduced synaptic density and most importantly iii) impaired spatial memory.

There is a strong correlation between synapse loss and cognitive decline in AD and synaptic dysfunction is thought to underlie early stages of the disease (see e.g. Selkoe, 2002; Terry et al, 1991). The ability of synapses to undergo long-term potentiation and thus increase their synaptic strength is considered as a cellular mechanism underlying learning and memory. Indeed, defects in LTP have not only been reported in several AD mouse models with Aβ overexpression (see e.g. review by Spires-Jones & Knafo, 2012) but also upon application of synthetic or native Aβ oligomers from AD patients to hippocampal slices (e.g. Shankar et al, 2007; Shankar et al, 2008). Interestingly, we observed that deficits of 12-13 month-old APP/PS1ΔE9 mice in the induction and maintenance phase of LTP were largely rescued upon AAV-APPsα overexpression despite the presence of high amounts of soluble Aβ and extensive Aβ deposition (see Fig. 4) at this age. Given that AAV-APPsα did not affect

basal synaptic transmission, but completely rescued the defects in paired pulse fascilitation of APP/PS1ΔE9 mice this suggests that restoration of presynaptic function may contribute to the LTP rescue. In this regard, it is noteworthy that APP has been localized to synaptic sites, including the presynaptic active zone (Lassek et al, 2013; Wilhelm et al, 2014). Our present findings are perfectly in line and further extend the previously demonstrated physiological role of APP and APPs in synaptic plasticity. Consistent with a presynaptic role of APP, we previously found a reduction in quantal content and readily releasable pool at neuromuscular synapses of APP/APLP2 mutant mice (Weyer et al, 2011). In the CNS, APP-KO mice showed altered GABAergic short-term plasticity and disturbed Ca^{2+}-homeostasis (Yang et al, 2009). In addition, APPsα knockin mice that lack transmembrane APP and express solely secreted APPsα completely rescued the LTP impairment of APP-KO mice (Ring et al, 2007).

Previously, indirect evidence suggested that APPsα may have synaptotrophic properties not only under physiological, but also under pathological conditions. Studies involving transgenic mice with moderate overexpression of human WT APP (Mucke et al, 1996), or indirect up-regulation of APPsα by transgenic expression of the α-secretase ADAM10 (Bell et al, 2008), that is enriched at synaptic contacts (Marcello et al, 2007), all led to increased synaptic density. In Tg2576 mice expression of mutant huAPP decreased spine density in aged animals, whereas an increase in spine density was observed in young mice prior to plaque deposition pointing towards a possibly trophic effect of APPsα (Lee et al, 2010). Here, we now directly demonstrate that in addition to its beneficial effects on synaptic plasticity, AAV-APPsα overexpression ameliorates spine density defects associated with Aβ accumulation in aged APP/PS1ΔE9 mice, and restores normal spine density in basal dendritic segments of CA3 neurons. Most importantly, increases in spine counts and restored synaptic plasticity were also reflected in significantly improved cognition, as evidenced by a complete rescue of Morris water maze probe trial performance, that assess spatial long-term memory. While APPsα expression somewhat improved the performance of nontransgenic littermates during the acquisition phase, we did not observe measurable effects on the performance of APP/PS1ΔE9 mice. However, one should keep in mind that acquisition performance is not always correlated with probe trial performance (Wolfer et al, 1998). In any event, our data clearly indicate that APPsα specifically improves retention of spatial reference memory in aged APP/PS1ΔE9 mice.

Although the precise role of APPsα at the synapse is still unknown, there is a large body of evidence that APPsα affects several pathways that likely contribute to its beneficial effects in APP/PS1ΔE9 mice. *In vitro* studies using WT rats showed that exogenous APPsα

application can shift the frequency dependence of LTD and enhance LTP (Ishida et al, 1997). Moreover, intra-hippocampal infusion of recombinant APPsα (rec APPsα) increased *in vivo* LTP recorded at the dentate gyrus of adult rats (Taylor et al, 2008) and infusion of APPsα or peptides derived from it enhances memory in mice, chicks and rats (Bour et al, 2004; Meziane et al, 1998; Mileusnic et al, 2004; Roch et al, 1994). Mechanistically, the effects on LTP may involve modulation of NMDA-receptor function as recAPPsα was shown to facilitate tetanically evoked NMDA receptor-mediated currents *in vitro* (Taylor et al, 2008). Immunoprecipitation studies indicated that transmembrane APP interacts with GluN1/GluN2 NMDARs and enhances their cell surface expression *in vitro* (Cousins et al, 2009; Cousins et al, 2013), but it is presently unclear whether this also holds true for extracellular APPsα. Moreover, recAPPsα has been shown to increase synaptodendritic *de novo* protein synthesis, an important mechanism for normal plasticity (Claasen et al, 2009).

Although in this study we did not investigate neuronal death, it is noteworthy that *in vitro* studies had implicated APPsα in neuroprotective signalling relevant to AD pathogenesis, including protection against excitotoxic stress resulting from glutamate receptor overactivation (Furukawa & Mattson, 1998) and notably also Aβ induced toxicity (Goodman & Mattson, 1994; Furukawa et al, 1996). Intriguingly, a recent study identified cell surface holo-APP as the receptor that binds APPsα and confers neuroprotection via G protein-coupled activation of the Akt stress signalling pathway (Milosch et al, 2014). While these data established holo-APP as a receptor mediating prosurvial/antiapoptotic signaling, it is also clear, however, that the very rapid effects of APP on synaptic plasticity must be mediated by a receptor distinct from APP. In this respect, we recently showed that the LTP impairments of conditional DKO mice, lacking both APP and APLP2 can be rescued by a brief (30 min) pre-incubation with nanomolar amounts of APPsα (Hick et al, 2015).

In addition to beneficial effects on synaptic morphology and function we also detected reduced levels of soluble Aβ species and a significant (about 25%) decrease in plaque load upon AAV-APPsα treatment. In APP/PS1ΔE9 mice Aβ production is massively shifted towards Aβ42 (with a ratio Aβ42/40 of about 2:1, see (Jankowsky et al, 2004; Xiong et al, 2011)) which may explain why we detected a significant reduction in A 42 (by about 33%) and a trend towards lowering A 40. Our results of reduced Aβ levels following AAV-APPsα treatment are further supported by a study using classical germline transgenic mice to express APPsα on an APP/PS1ΔE9 background (Obregon et al, 2012). In contrast to our study, Obregon et al. did not investigate, however, the functional consequences of APPsα overexpression on synaptic plasticity and behavior. Whereas Obregon and coworkers reported

in TgAPPs /APP/PS1ΔE9 mice also a reduction in β-CTFs (supporting the concept that APPsα inhibits BACE) we found no significant alterations in β-CTFs, as assessed by a sensitive ELISA. These apparent differences might be related to the fact that in TgAPPsα mice, APPsα was expressed from early development onwards (as opposed to expression in aged mice in this study) and that Obregon et al. assessed APP processing much earlier (at 8 month of age), when Aβ build up is considerably lower (Obregon et al, 2012). In addition, we now provide evidence suggesting that AAV-APPsα may also improve pathology in a mechanism unrelated to BACE inhibition. In this regard, and consistent with previous data from the literature (Austin & Combs, 2008; Bodles & Barger, 2005), we observed that AAV-APPsα treatment lead to the recruitment of microglia with ramified morphology (believed to indicate an activated state) towards plaques, that was paralleled by an increase in TREM2 expression. TREM2 receptor was recently shown to sustain the microglial response to Aβ and suggested to function as a sensor for anionic lipids exposed during Aβ deposition and on damaged neurons (Wang et al, 2015). In addition we demonstrate an upregulation of the proteolytic enzyme IDE, that is produced by microglia and was previously shown to enhance Aβ and plaques clearance (Heneka et al, 2013; Leissring et al, 2003). Together, our data strongly suggest that APPsα mediated activation and recruitment of microglia may contribute to the ameliorated Aβ pathology in APP/PS1ΔE9 mice.

AD pathogenesis is complex, still incompletely understood and multiple factors contribute to pathogenesis. Therefore, the concept of synaptic repair has recently been put forward, e.g. to tackle/ameliorate pathophysiology and improve clinical outcome as an alternative to eliminating toxic factors (Lu et al, 2013). Notably, due to the highly plastic nature of synapses, synaptic dysfunction and synapse loss are reversible processes. Here, we provide several converging lines of evidence that viral vector mediated APPsα expression rescues synaptic failure in AD model mice with established Aβ deposition, indicating its potential as a novel therapeutic strategy even in the presence of pathogenic factors.

REFERENCES:

Throughout this application, various references, including United States patents and patent applications, describe the state of the art to which this invention pertains. The disclosures of these references are hereby incorporated by reference in entirety into the present disclosure.

Ahmed RR, Holler CJ, Webb RL, Li F, Beckett TL, Murphy MP (2010) BACE1 and BACE2 enzymatic activities in Alzheimer's disease. J Neurochem 112: 1045-1053

Austin SA, Combs CK (2008) Mechanisms of Microglial Activation by Amyloid precursor Protein and its Proteolytic Fragments. In Central Nervous System Diseases and Inflammation, Lane TE, Carson M, Bergmann C, Wyss-Coray T (eds) pp 13-32. Springer US

Aydin D, Weyer SW, Muller UC (2012) Functions of the APP gene family in the nervous system: insights from mouse models. Exp Brain Res 217: 423-434

Bell KF, Zheng L, Fahrenholz F, Cuello AC (2008) ADAM-10 over-expression increases cortical synaptogenesis. Neurobiol Aging 29: 554-565

Berger A, Lorain S, Josephine C, Desrosiers M, Peccate C, Voit T, Garcia L, Sahel JA, Bemelmans AP (2015) Repair of Rhodopsin mRNA by Spliceosome-Mediated RNA Trans-Splicing: A New Approach for Autosomal Dominant Retinitis Pigmentosa. Mol Ther

Bodles AM, Barger SW (2005) Secreted beta-amyloid precursor protein activates microglia via JNK and p38-MAPK. Neurobiol Aging 26: 9-16

Borchelt DR, Ratovitski T, van Lare J, Lee MK, Gonzales V, Jenkins NA, Copeland NG, Price DL, Sisodia SS (1997) Accelerated amyloid deposition in the brains of transgenic mice coexpressing mutant presenilin 1 and amyloid precursor proteins. Neuron 19: 939-945

Bour A, Little S, Dodart JC, Kelche C, Mathis C (2004) A secreted form of the beta-amyloid precursor protein (sAPP695) improves spatial recognition memory in OF1 mice. Neurobiol Learn Mem 81: 27-38

Caille I, Allinquant B, Dupont E, Bouillot C, Langer A, Muller U, Prochiantz A (2004) Soluble form of amyloid precursor protein regulates proliferation of progenitors in the adult subventricular zone. Development 131: 2173-2181

Casanova F, Carney PR, Sarntinoranont M (2014) Effect of needle insertion speed on tissue injury, stress, and backflow distribution for convection-enhanced delivery in the rat brain. PloS one 9: e94919

Claasen AM, Guevremont D, Mason-Parker SE, Bourne K, Tate WP, Abraham WC, Williams JM (2009) Secreted amyloid precursor protein-alpha upregulates synaptic protein synthesis by a protein kinase G-dependent mechanism. Neurosci Lett 460: 92-96

Corrigan F, Vink R, Blumbergs PC, Masters CL, Cappai R, van den Heuvel C (2012) sAPPalpha rescues deficits in amyloid precursor protein knockout mice following focal traumatic brain injury. J Neurochem 122: 208-220

Cousins SL, Hoey SE, Anne Stephenson F, Perkinton MS (2009) Amyloid precursor protein 695 associates with assembled NR2A- and NR2B-containing NMDA receptors to result in the enhancement of their cell surface delivery. J Neurochem 111: 1501-1513

Cousins SL, Innocent N, Stephenson FA (2013) Neto1 associates with the NMDA receptor/amyloid precursor protein complex. J Neurochem 126: 554-564

Dobrowolska JA, Kasten T, Huang Y, Benzinger TL, Sigurdson W, Ovod V, Morris JC, Bateman RJ (2014) Diurnal patterns of soluble amyloid precursor protein metabolites in the human central nervous system. PloS one 9: e89998

Doody RS, Raman R, Farlow M, Iwatsubo T, Vellas B, Joffe S, Kieburtz K, He F, Sun X, Thomas RG et al (2013) A phase 3 trial of semagacestat for treatment of Alzheimer's disease. N Engl J Med 369: 341-350

Endres K, Fahrenholz F (2012) Regulation of alpha-secretase ADAM10 expression and activity. Exp Brain Res 217: 343-352

Frank S, Burbach GJ, Bonin M, Walter M, Streit W, Bechmann I, Deller T (2008) TREM2 is upregulated in amyloid plaque-associated microglia in aged APP23 transgenic mice. Glia 56: 1438-1447

Furukawa K, Mattson MP (1998) Secreted amyloid precursor protein alpha selectively suppresses N-methyl-D-aspartate currents in hippocampal neurons: involvement of cyclic GMP. Neuroscience 83: 429-438

Furukawa K, Sopher BL, Rydel RE, Begley JG, Pham DG, Martin GM, Fox M, Mattson MP (1996) Increased activity-regulating and neuroprotective efficacy of alpha-secretase-derived secreted amyloid precursor protein conferred by a C-terminal heparin-binding domain. J Neurochem 67: 1882-1896

Goodman Y, Mattson MP (1994) Secreted forms of beta-amyloid precursor protein protect hippocampal neurons against amyloid beta-peptide-induced oxidative injury. Exp Neurol 128: 1-12

Guerreiro R, Wojtas A, Bras J, Carrasquillo M, Rogaeva E, Majounie E, Cruchaga C, Sassi C, Kauwe JS, Younkin S et al (2013) TREM2 variants in Alzheimer's disease. N Engl J Med 368: 117-127

Hardy, J. and D. Allsop (1991). "Amyloid deposition as the central event in the aetiology of Alzheimer's disease." Trends Pharmacol Sci 12(10): 383-388.

Heneka MT, Kummer MP, Stutz A, Delekate A, Schwartz S, Vieira-Saecker A, Griep A, Axt D, Remus A, Tzeng TC et al (2013) NLRP3 is activated in Alzheimer's disease and contributes to pathology in APP/PS1 mice. Nature 493: 674-678

Hick M, Herrmann U, Weyer SW, Mallm JP, Tschape JA, Borgers M, Mercken M, Roth FC, Draguhn A, Slomianka L et al (2015) Acute function of secreted amyloid precursor protein fragment APPsalpha in synaptic plasticity. Acta Neuropathol 129: 21-37

Hick, M., U. Herrmann, S. W. Weyer, J. P. Mallm, J. A. Tschape, M. Borgers, M. Mercken, F. C. Roth, A. Draguhn, L. Slomianka, D. P. Wolfer, M. Korte and U. C. Muller (2015). "Acute function of secreted amyloid precursor protein fragment APPsalpha in synaptic plasticity." Acta Neuropathol 129(1): 21-37.

Hoe HS, Lee HK, Pak DT (2012) The upside of APP at synapses. CNS Neurosci Ther 18: 47-56

Hoey SE, Williams RJ, Perkinton MS (2009) Synaptic NMDA receptor activation stimulates alpha-secretase amyloid precursor protein processing and inhibits amyloid-beta production. J Neurosci 29: 4442-4460

Holsinger RM, McLean CA, Beyreuther K, Masters CL, Evin G (2002) Increased expression of the amyloid precursor beta-secretase in Alzheimer's disease. Annals of neurology 51: 783-786

Ishida A, Furukawa K, Keller JN, Mattson MP (1997) Secreted form of beta-amyloid precursor protein shifts the frequency dependency for induction of LTD, and enhances LTP in hippocampal slices. Neuroreport 8: 2133-2137

Jankowsky JL, Fadale DJ, Anderson J, Xu GM, Gonzales V, Jenkins NA, Copeland NG, Lee MK, Younkin LH, Wagner SL et al (2004) Mutant presenilins specifically elevate the levels of the 42 residue beta-amyloid peptide in vivo: evidence for augmentation of a 42-specific gamma secretase. Hum Mol Genet 13: 159-170

Jay TR, Miller CM, Cheng PJ, Graham LC, Bemiller S, Broihier ML, Xu G, Margevicius D, Karlo JC, Sousa GL et al (2015) TREM2 deficiency eliminates TREM2+ inflammatory macrophages and ameliorates pathology in Alzheimer's disease mouse models. J Exp Med 212: 287-295

Jonsson T, Stefansson H, Steinberg S, Jonsdottir I, Jonsson PV, Snaedal J, Bjornsson S, Huttenlocher J, Levey AI, Lah JJ et al (2013) Variant of TREM2 associated with the risk of Alzheimer's disease. N Engl J Med 368: 107-116

Jonsson, T., J. K. Atwal, S. Steinberg, J. Snaedal, P. V. Jonsson, S. Bjornsson, H. Stefansson, P. Sulem, D. Gudbjartsson, J. Maloney, K. Hoyte, A. Gustafson, Y. Liu, Y. Lu, T. Bhangale, R. R. Graham, J. Huttenlocher, G. Bjornsdottir, O. A. Andreassen, E. G. Jonsson, A. Palotie, T. W. Behrens, O. T. Magnusson, A. Kong, U. Thorsteinsdottir, R. J. Watts and K.

Stefansson (2012). "A mutation in APP protects against Alzheimer's disease and age-related cognitive decline." Nature 488(7409): 96-99.

Kamphuis W, Mamber C, Moeton M, Kooijman L, Sluijs JA, Jansen AH, Verveer M, de Groot LR, Smith VD, Rangarajan S et al (2012) GFAP isoforms in adult mouse brain with a focus on neurogenic astrocytes and reactive astrogliosis in mouse models of Alzheimer's disease. PloS one 7: e42823

Klevanski M, Saar M, Baumkotter F, Weyer SW, Kins S, Muller UC (2014) Differential role of APP and APLPs for neuromuscular synaptic morphology and function. Mol Cell Neurosci 61C: 201-210

Kogel D, Deller T, Behl C (2012) Roles of amyloid precursor protein family members in neuroprotection, stress signaling and aging. Exp Brain Res 217: 471-479

Lannfelt L, Basun H, Wahlund LO, Rowe BA, Wagner SL (1995) Decreased alpha-secretase-cleaved amyloid precursor protein as a diagnostic marker for Alzheimer's disease. Nat Med 1: 829-832

Lassek M, Weingarten J, Einsfelder U, Brendel P, Muller U, Volknandt W (2013) Amyloid precursor proteins are constituents of the presynaptic active zone. J Neurochem 127: 48-56

Lee KJ, Moussa CE, Lee Y, Sung Y, Howell BW, Turner RS, Pak DT, Hoe HS (2010) Beta amyloid-independent role of amyloid precursor protein in generation and maintenance of dendritic spines. Neuroscience 169: 344-356

Leissring MA, Farris W, Chang AY, Walsh DM, Wu X, Sun X, Frosch MP, Selkoe DJ (2003) Enhanced proteolysis of beta-amyloid in APP transgenic mice prevents plaque formation, secondary pathology, and premature death. Neuron 40: 1087-1093

Leyssen M, Ayaz D, Hebert SS, Reeve S, De Strooper B, Hassan BA (2005) Amyloid precursor protein promotes post-developmental neurite arborization in the Drosophila brain. EMBO J 24: 2944-2955

Lichtenthaler SF, Haass C, Steiner H (2011) Regulated intramembrane proteolysis--lessons from amyloid precursor protein processing. J Neurochem 117: 779-796

Lu B, Nagappan G, Guan X, Nathan PJ, Wren P (2013) BDNF-based synaptic repair as a disease-modifying strategy for neurodegenerative diseases. Nat Rev Neurosci 14: 401-416

Marcello E, Gardoni F, Mauceri D, Romorini S, Jeromin A, Epis R, Borroni B, Cattabeni F, Sala C, Padovani A et al (2007) Synapse-associated protein-97 mediates alpha-secretase ADAM10 trafficking and promotes its activity. J Neurosci 27: 1682-1691

Meziane H, Dodart JC, Mathis C, Little S, Clemens J, Paul SM, Ungerer A (1998) Memory-enhancing effects of secreted forms of the beta-amyloid precursor protein in normal and amnestic mice. Proc Natl Acad Sci U S A 95: 12683-12688

Mileusnic R, Lancashire CL, Rose SP (2004) The peptide sequence Arg-Glu-Arg, present in the amyloid precursor protein, protects against memory loss caused by A beta and acts as a cognitive enhancer. Eur J Neurosci 19: 1933-1938

Milosch N, Tanriover G, Kundu A, Rami A, Francois JC, Baumkotter F, Weyer SW, Samanta A, Jaschke A, Brod F et al (2014) Holo-APP and G-protein-mediated signaling are required for sAPPalpha-induced activation of the Akt survival pathway. Cell Death Dis 5: e1391

Mucke L, Abraham CR, Masliah E (1996) Neurotrophic and neuroprotective effects of hAPP in transgenic mice. Ann N Y Acad Sci 777: 82-88

Murakami N, Yamaki T, Iwamoto Y, Sakakibara T, Kobori N, Fushiki S, Ueda S (1998) Experimental brain injury induces expression of amyloid precursor protein, which may be related to neuronal loss in the hippocampus. J Neurotrauma 15: 993-1003

Nhan HS, Chiang K, Koo EH (2015) The multifaceted nature of amyloid precursor protein and its proteolytic fragments: friends and foes. Acta Neuropathol 129: 1-19

Obregon D, Hou H, Deng J, Giunta B, Tian J, Darlington D, Shahaduzzaman M, Zhu Y, Mori T, Mattson MP et al (2012) Soluble amyloid precursor protein-alpha modulates beta-secretase activity and amyloid-beta generation. Nat Commun 3: 777

Prokop S, Miller KR, Heppner FL (2013) Microglia actions in Alzheimer's disease. Acta Neuropathol 126: 461-477

Prox J, Rittger A, Saftig P (2012) Physiological functions of the amyloid precursor protein secretases ADAM10, BACE1, and Presenilin. Exp Brain Res 217: 331-341

Ramirez MJ, Heslop KE, Francis PT, Rattray M (2001) Expression of amyloid precursor protein, tau and presenilin RNAs in rat hippocampus following deafferentation lesions. Brain Res 907: 222-232

Ring S (2007) Phenotypic analysis to define physiolocically essential functional domains of APP family proteins. In Institut für Phramazie und molekulare Biotechnologie - Funktionelle Genomik. Heidelberg: Universität Heidelberg

Ring S, Weyer SW, Kilian SB, Waldron E, Pietrzik CU, Filippov MA, Herms J, Buchholz C, Eckman CB, Korte M et al (2007) The secreted beta-amyloid precursor protein ectodomain APPs alpha is sufficient to rescue the anatomical, behavioral, and electrophysiological abnormalities of APP-deficient mice. J Neurosci 27: 7817-7826

Roch JM, Masliah E, Roch-Levecq AC, Sundsmo MP, Otero DA, Veinbergs I, Saitoh T (1994) Increase of synaptic density and memory retention by a peptide representing the trophic domain of the amyloid beta/A4 protein precursor. Proc Natl Acad Sci U S A 91: 7450-7454

Savonenko A, Xu GM, Melnikova T, Morton JL, Gonzales V, Wong MP, Price DL, Tang F, Markowska AL, Borchelt DR (2005) Episodic-like memory deficits in the APPswe/PS1dE9 mouse model of Alzheimer's disease: relationships to beta-amyloid deposition and neurotransmitter abnormalities. Neurobiol Dis 18: 602-617

Selkoe DJ (2002) Alzheimer's disease is a synaptic failure. Science 298: 789-791

Selkoe, D. J. (2001). "Alzheimer's disease: genes, proteins, and therapy." Physiol Rev 81(2): 741-766.

Shankar GM, Bloodgood BL, Townsend M, Walsh DM, Selkoe DJ, Sabatini BL (2007) Natural oligomers of the Alzheimer amyloid-beta protein induce reversible synapse loss by modulating an NMDA-type glutamate receptor-dependent signaling pathway. J Neurosci 27: 2866-2875

Shankar GM, Li S, Mehta TH, Garcia-Munoz A, Shepardson NE, Smith I, Brett FM, Farrell MA, Rowan MJ, Lemere CA et al (2008) Amyloid-beta protein dimers isolated directly from Alzheimer's brains impair synaptic plasticity and memory. Nat Med 14: 837-842

Spires-Jones T, Knafo S (2012) Spines, plasticity, and cognition in Alzheimer's model mice. Neural Plast 2012: 319836

Suh J, Choi SH, Romano DM, Gannon MA, Lesinski AN, Kim DY, Tanzi RE (2013) ADAM10 missense mutations potentiate beta-amyloid accumulation by impairing prodomain chaperone function. Neuron 80: 385-401

Tang W, Ehrlich I, Wolff SB, Michalski AM, Wolfl S, Hasan MT, Luthi A, Sprengel R (2009) Faithful expression of multiple proteins via 2A-peptide self-processing: a versatile and reliable method for manipulating brain circuits. J Neurosci 29: 8621-8629

Taylor CJ, Ireland DR, Ballagh I, Bourne K, Marechal NM, Turner PR, Bilkey DK, Tate WP, Abraham WC (2008) Endogenous secreted amyloid precursor protein-alpha regulates hippocampal NMDA receptor function, long-term potentiation and spatial memory. Neurobiol Dis 31: 250-260

Terry RD, Masliah E, Salmon DP, Butters N, DeTeresa R, Hill R, Hansen LA, Katzman R (1991) Physical basis of cognitive alterations in Alzheimer's disease: synapse loss is the major correlate of cognitive impairment. Annals of neurology 30: 572-580

Thornton E, Vink R, Blumbergs PC, Van Den Heuvel C (2006) Soluble amyloid precursor protein alpha reduces neuronal injury and improves functional outcome following diffuse traumatic brain injury in rats. Brain Res 1094: 38-46

Van den Heuvel C, Blumbergs PC, Finnie JW, Manavis J, Jones NR, Reilly PL, Pereira RA (1999) Upregulation of amyloid precursor protein messenger RNA in response to traumatic brain injury: an ovine head impact model. Exp Neurol 159: 441-450

Vassar R, Kuhn PH, Haass C, Kennedy ME, Rajendran L, Wong PC, Lichtenthaler SF (2014) Function, therapeutic potential and cell biology of BACE proteases: current status and future prospects. J Neurochem 130: 4-28

Villemagne VL, Burnham S, Bourgeat P, Brown B, Ellis KA, Salvado O, Szoeke C, Macaulay SL, Martins R, Maruff P et al (2013) Amyloid beta deposition, neurodegeneration, and cognitive decline in sporadic Alzheimer's disease: a prospective cohort study. Lancet Neurol 12: 357-367

Wang Y, Cella M, Mallinson K, Ulrich JD, Young KL, Robinette ML, Gilfillan S, Krishnan GM, Sudhakar S, Zinselmeyer BH et al (2015) TREM2 Lipid Sensing Sustains the Microglial Response in an Alzheimer's Disease Model. Cell 160: 1061-1071

Weyer SW, Klevanski M, Delekate A, Voikar V, Aydin D, Hick M, Filippov M, Drost N, Schaller KL, Saar M et al (2011) APP and APLP2 are essential at PNS and CNS synapses for transmission, spatial learning and LTP. EMBO J 30: 2266-2280

Weyer SW, Zagrebelsky M, Herrmann U, Hick M, Ganss L, Gobbert J, Gruber M, Altmann C, Korte M, Deller T et al (2014) Comparative analysis of single and combined APP/APLP knockouts reveals reduced spine density in APP-KO mice that is prevented by APPsalpha expression. Acta Neuropathol Commun 2: 36

Wilhelm BG, Mandad S, Truckenbrodt S, Krohnert K, Schafer C, Rammner B, Koo SJ, Classen GA, Krauss M, Haucke V et al (2014) Composition of isolated synaptic boutons reveals the amounts of vesicle trafficking proteins. Science 344: 1023-1028

Wolfer DP, Stagljar-Bozicevic M, Errington ML, Lipp HP (1998) Spatial Memory and Learning in Transgenic Mice: Fact or Artifact? News Physiol Sci 13: 118-123

Xiong H, Callaghan D, Wodzinska J, Xu J, Premyslova M, Liu QY, Connelly J, Zhang W (2011) Biochemical and behavioral characterization of the double transgenic mouse model (APPswe/PS1dE9) of Alzheimer's disease. Neurosci Bull 27: 221-232

Yang L, Wang Z, Wang B, Justice NJ, Zheng H (2009) Amyloid precursor protein regulates Cav1.2 L-type calcium channel levels and function to influence GABAergic short-term plasticity. J Neurosci 29: 15660-15668

CLAIMS:

1. A method of treating Alzheimer's disease in a subject in need thereof comprising administering to the subject a therapeutically effective amount of a vector which comprises a nucleic acid molecule encoding for a polypeptide which is a soluble member of the APP (amyloid precursor protein) family.

2. The method of claim 1 wherein the vector comprises a nucleic acid molecule that encodes for a APPsα, APLP1s or APLP2s polypeptide.

3. The method of claim 1 wherein the vector comprises a nucleic acid encoding for a APPsα polypeptide.

4. The method of claim 1 wherein the nucleic acid molecule encoding for a APPsα polypeptide comprising an amino acid sequence having at least 90% of identity with the sequence as set forth in SEQ ID NO:1 or 2.

5. The method of claim 1 wherein the nucleic acid molecule comprises a sequence having at least 70% of identity with the nucleic acid sequence as set forth in SEQ ID NO:3, or SEQ ID NO:4.

6. The method of claim 1 wherein the vector is a non viral vector.

7. The method of claim 1 wherein the vector is a viral vector.

8. The method of claim 1 wherein the vector is an adeno-associated virus (AAV) vector.

9. The method of claim 8 wherein the AAV vector is selected from vectors derived from AAV serotypes having tropism for and high transduction efficiencies in cells of the mammalian central and peripheral nervous system, particularly neurons, neuronal progenitors, astrocytes, oligodendrocytes and glial cells.

10. The method of claim 8 wherein the AAV vector is an AAV4, AAV9 or an AAV10.

11. The method of claim 8 wherein the AAV vector of the present invention is a double-stranded, self-complementary AAV (scAAV) vector.

12. The method of claim 1 wherein the nucleic acid molecule is operatively linked to a promoter sequence.

13. The method of claim 1 wherein the vector comprises a secretory signal sequence.

14. The method of claim 1 wherein the vector comprises the nucleic acid sequence set forth in SED ID NO:5 or 6.

15. The method of claim 1 wherein the vector is delivered by intrathecal delivery.

ABSTRACT OF THE INVENTION

METHODS AND PHARMACEUTICAL COMPOSITION FOR THE TREATMENT AND THE PREVENTION OF ALZHEIMER'S DISEASE

The present invention relates to methods and pharmaceutical compositions for the treatment of Alzheimer's disease. In particular the present invention relates to a method of treating Alzheimer's disease in a subject in need thereof comprising administering to the subject a therapeutically effective amount of a vector which comprises a nucleic acid molecule encoding for a polypeptide which is a soluble member of the APP (amyloid precursor protein) family..

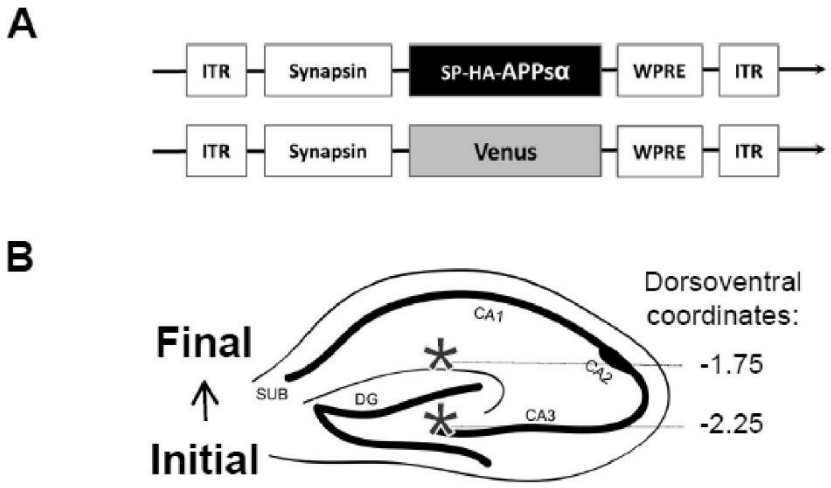

Figures 1A&1B

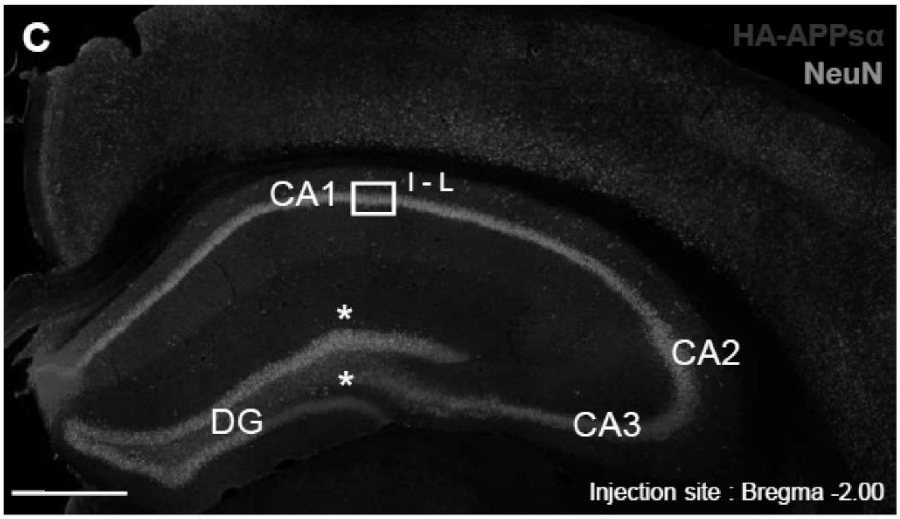

Figure 1C

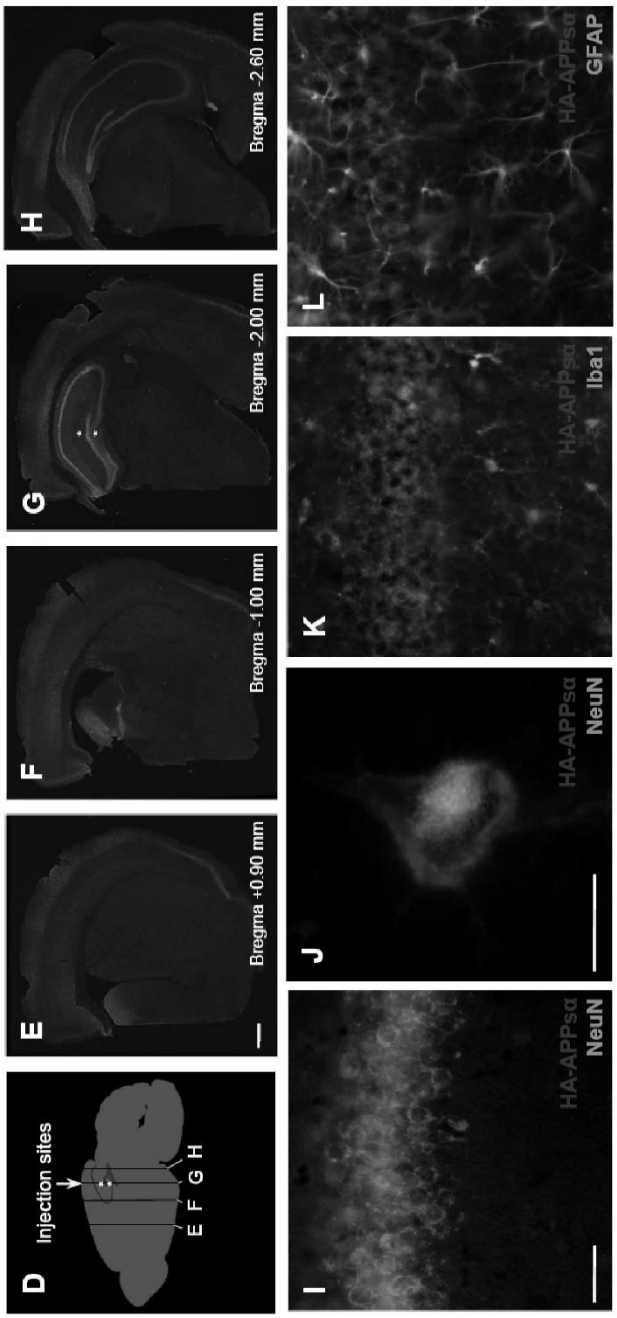
D
Injection sites
E F G H
E
Bregma +0.90 mm
F
Bregma -1.00 mm
G
Bregma -2.00 mm
H
Bregma -2.60 mm
I
HA-APPsα
NeuN
J
HA-APPsα
NeuN
K
HA-APPsα
Iba1
L
HA-APPsα
GFAP

Figures 1D-L

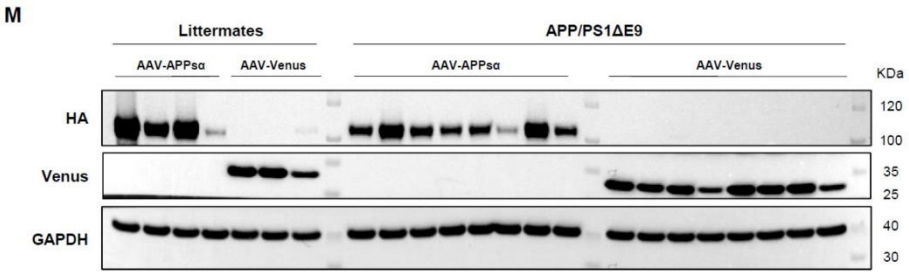

Figure 1M

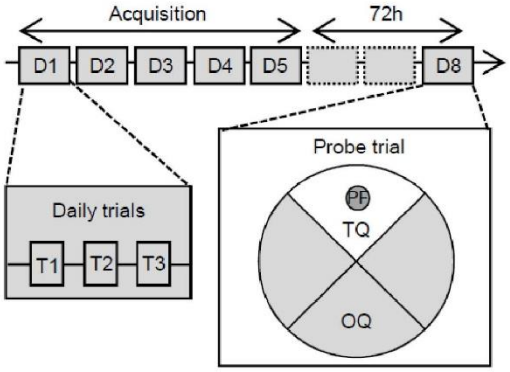

Figure 2A

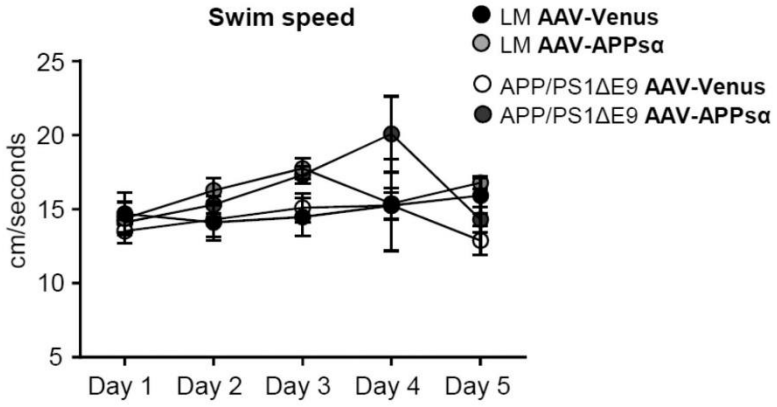

Figure 2B

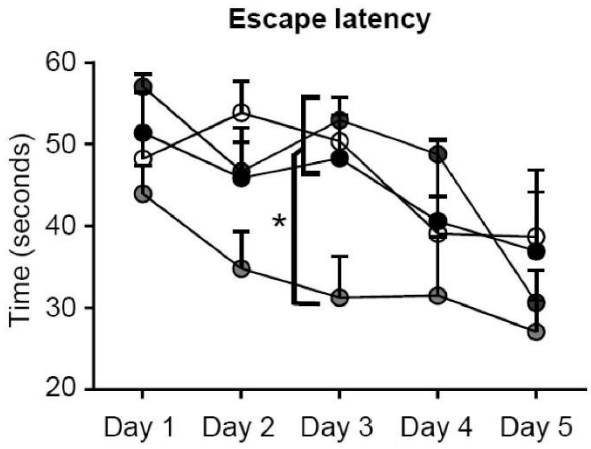

Figure 2C

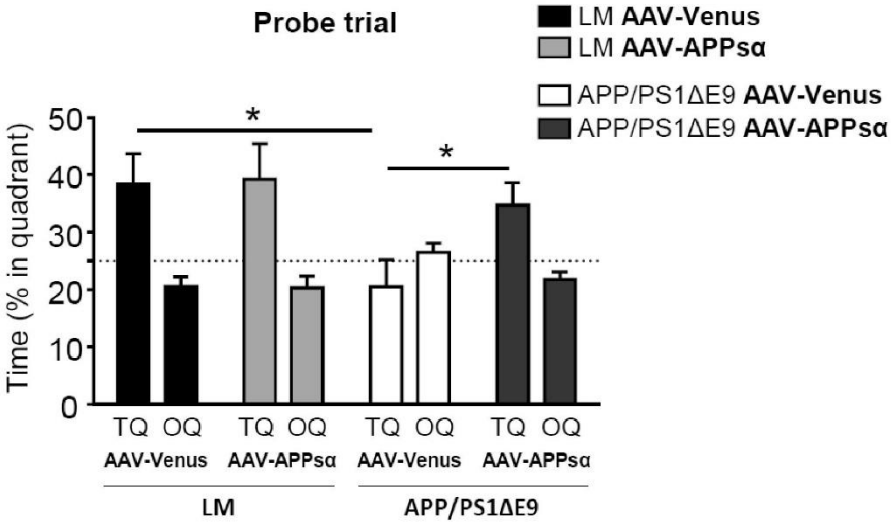

Figure 2D

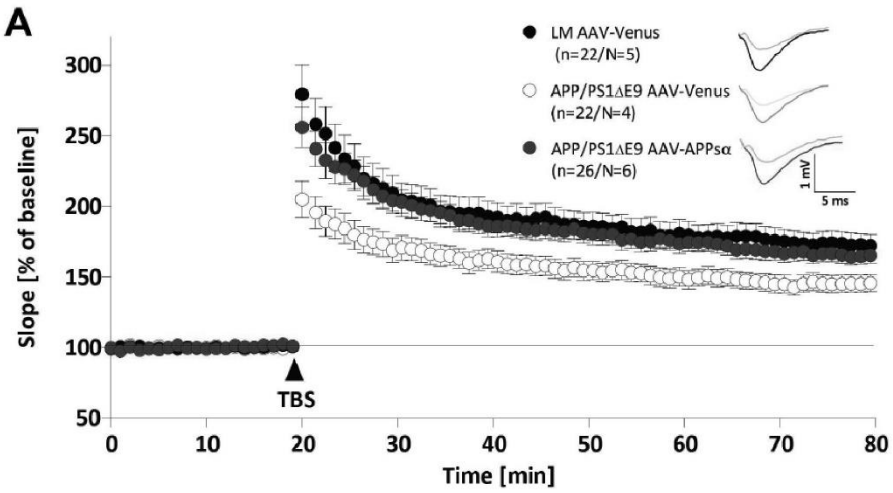

Figure 3A

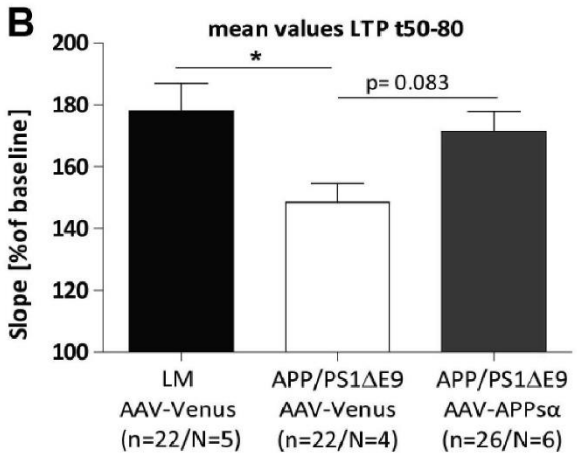

Figure 3B

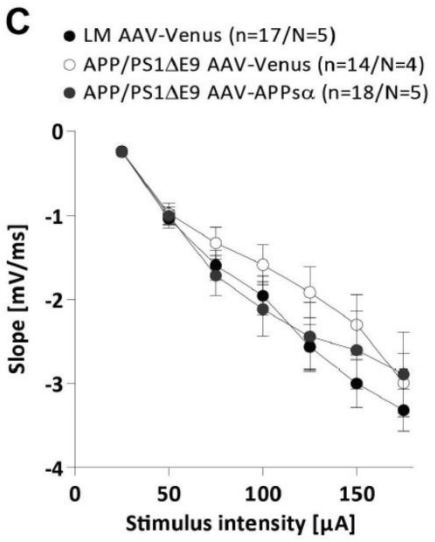

Figure 3C

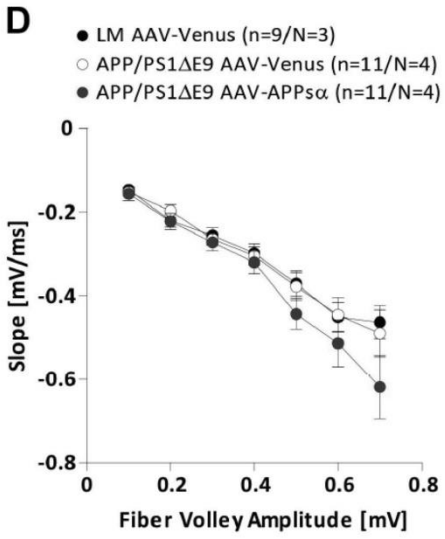

Figure 3D

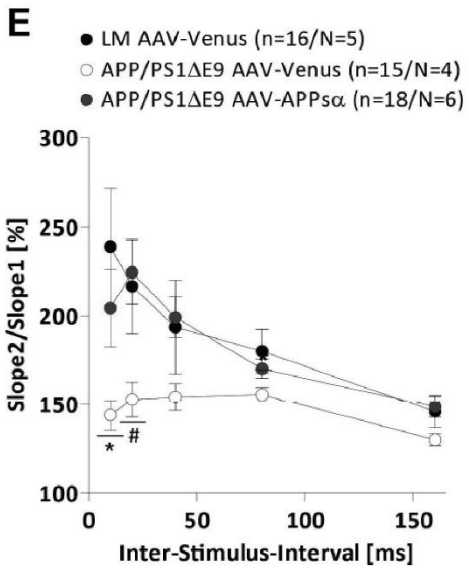
E
LM AAV-Venus (n=16/N=5)
APP/PS1ΔE9 AAV-Venus (n=15/N=4)
APP/PS1ΔE9 AAV-APPsα (n=18/N=6)
Slope2/Slope1 [%]
300
250
200
150
100
0
50
100
150
Inter-Stimulus-Interval [ms]
*
#

Figure 3E

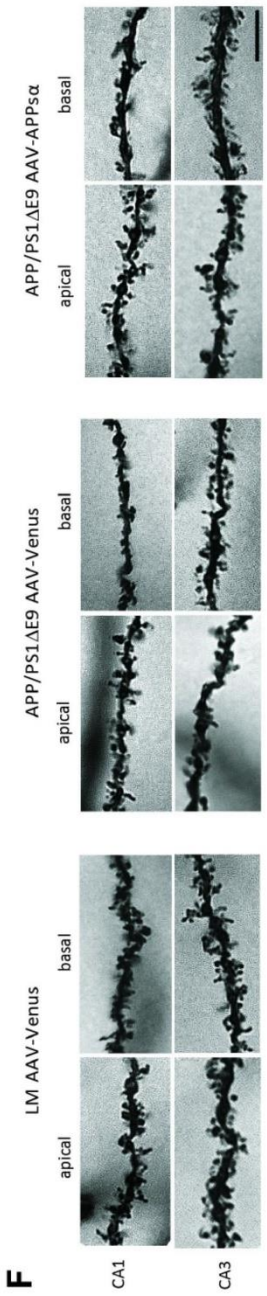
F
CA1
CA3
LM AAV-Venus
apical
basal
APP/PS1ΔE9 AAV-Venus
apical
basal
APP/PS1ΔE9 AAV-APPsα
apical
basal

Figure 3F

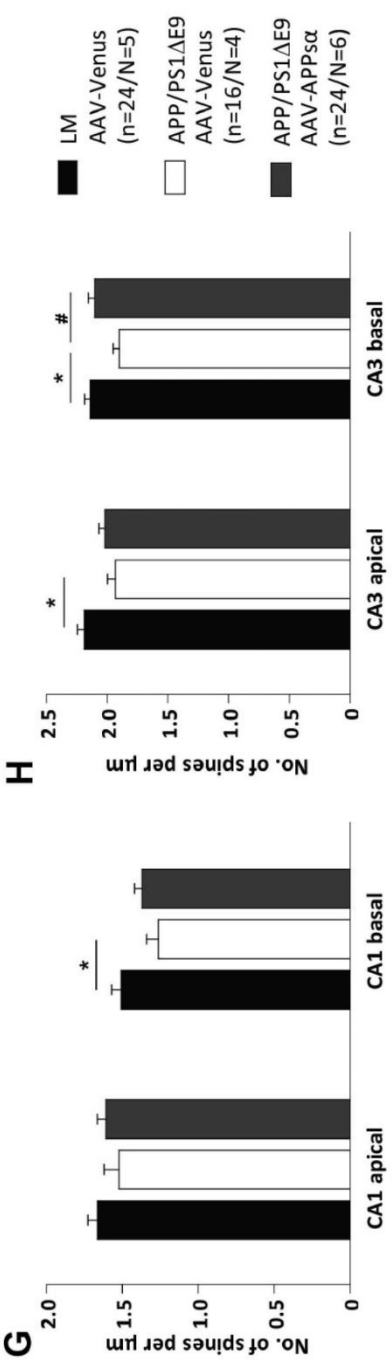

Figures 3G&3H

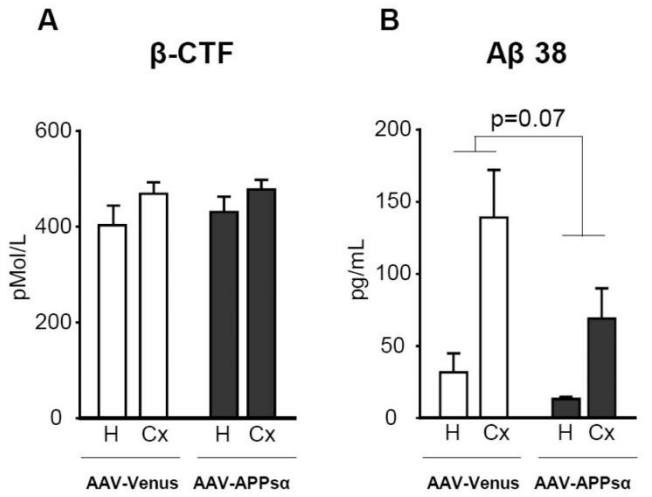

Figures 4A&B

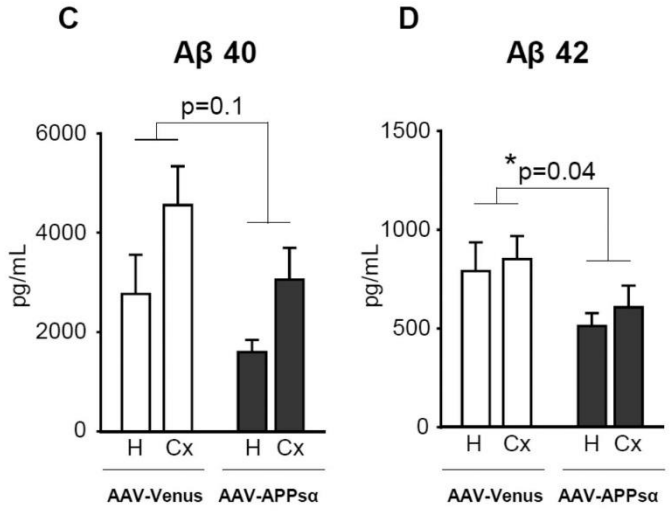

Figures 4C&D

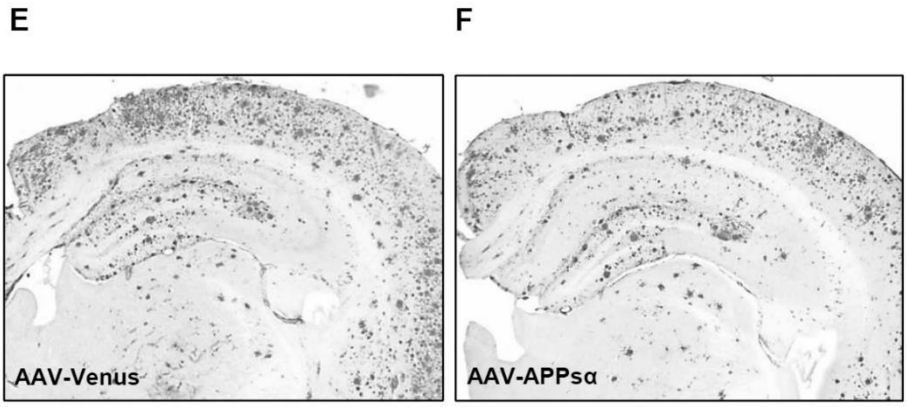

Figures 4E& F

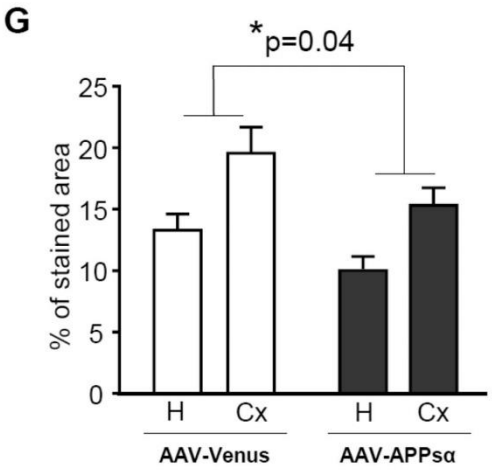

Figure 4G

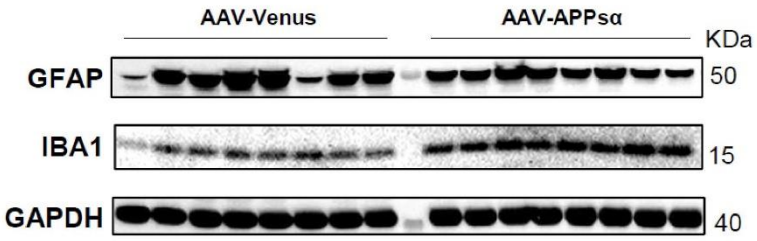

Figure 5A

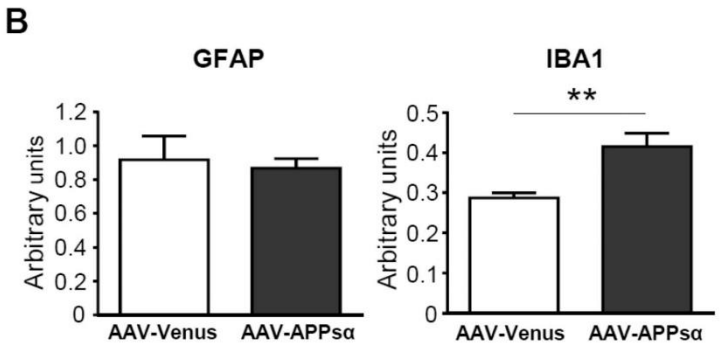

Figure 5B

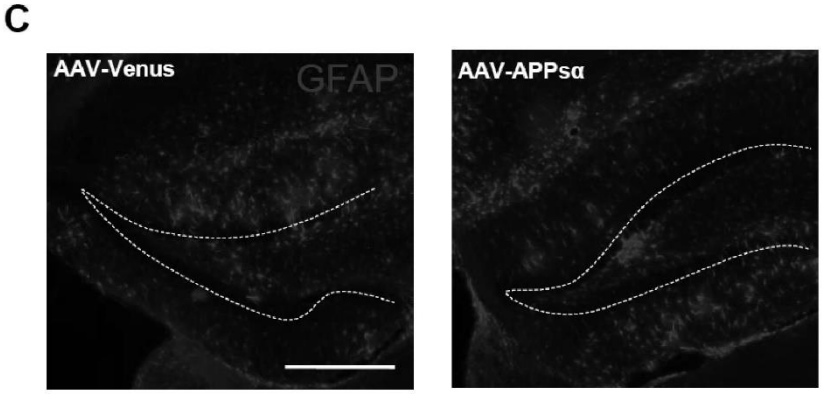

Figure 5C

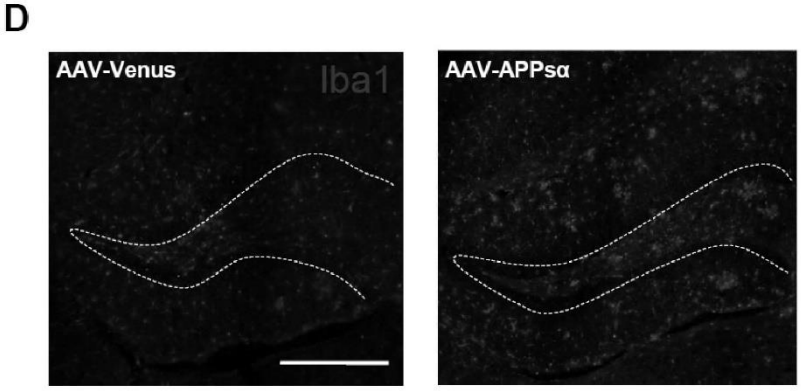

Figure 5D

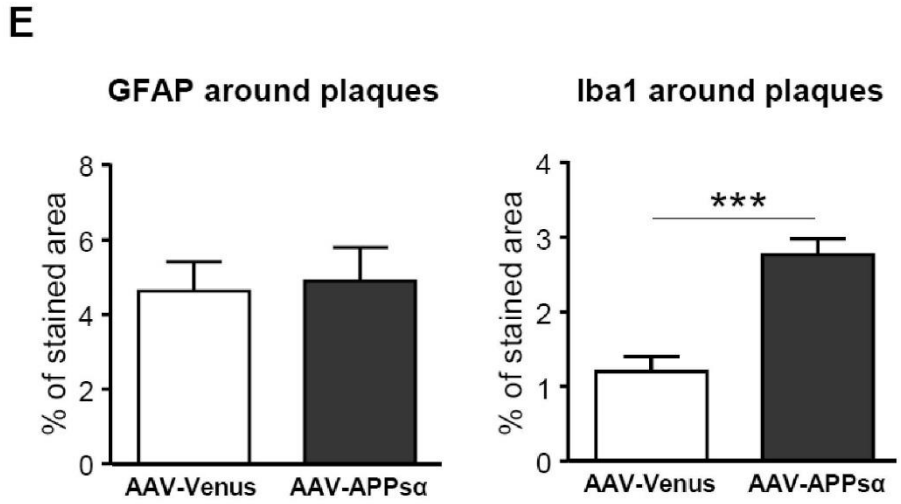

Figure 5E

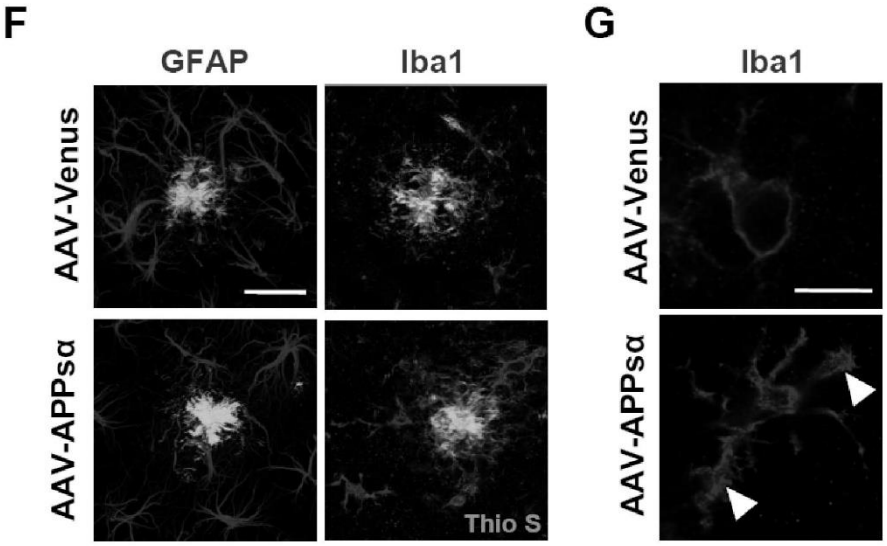

Figures 5F&G

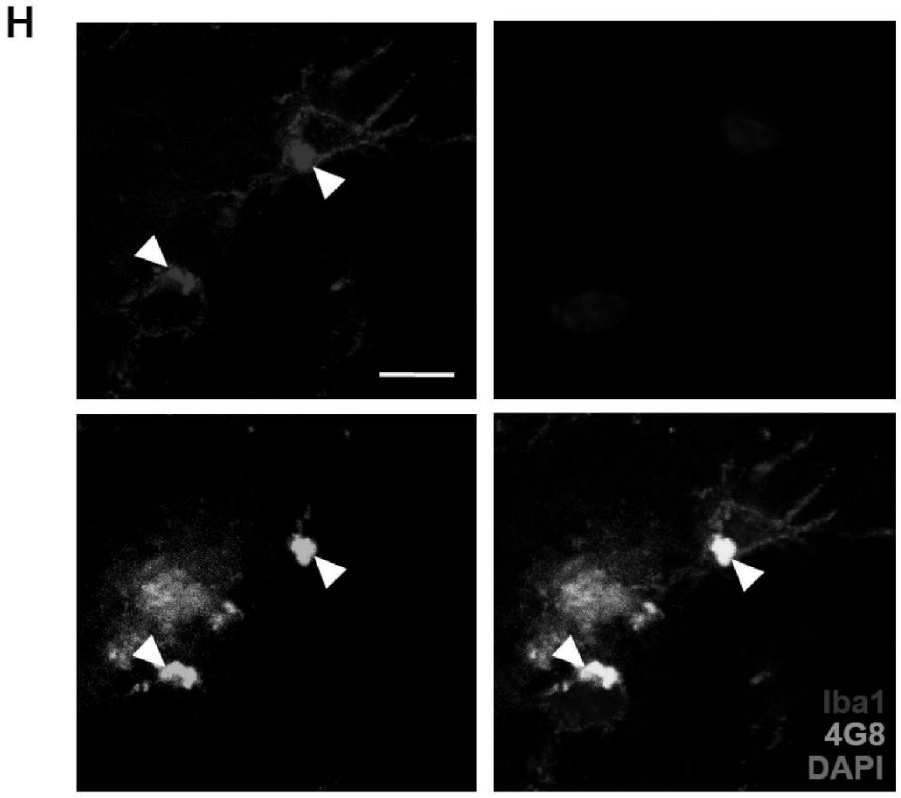

Figure 5H

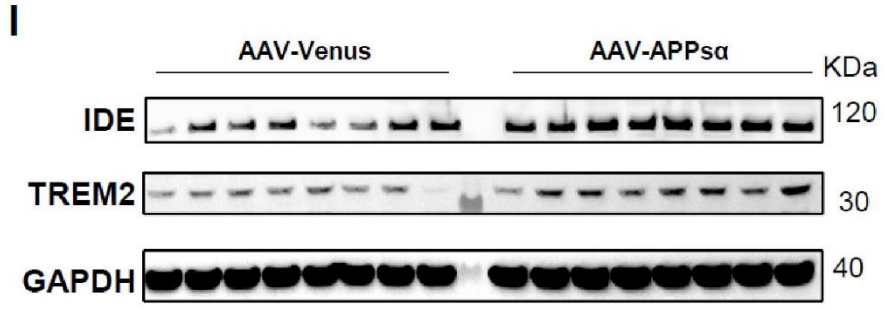

Figure 5I

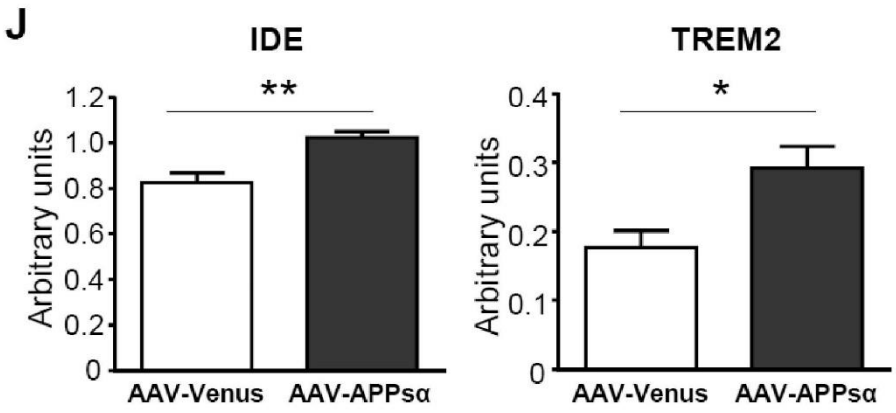
J
IDE
**
Arbitrary units
1.2
1.0
0.8
0.6
0.4
0.2
0
AAV-Venus
AAV-APPsα
TREM2
*
Arbitrary units
0.4
0.3
0.2
0.1
0
AAV-Venus
AAV-APPsα

Figure 5J

C. Communications orales

1. Présentations poster

- Forum annuel du DIM biothérapies, Paris, Novembre 2013. **Elu meilleur poster**
- Congrès annuel de la Société Française des Thérapies Cellulaires et Géniques (SFTCG), Toulouse, Mars 2014
- AAIC 2014, Copenhague (Danemark), Juillet 2014. **Finaliste pour le prix du meilleur poster**
- AAIC 2015 ; Washington DC (Etats-Unis), Juillet 2015. **Finaliste pour le prix du meilleur poster.**

2. Présentations orales

- Congrès annuel de la Société Française des Thérapies Cellulaires et Géniques (SFTCG), Toulouse, Mars 2014
- Réunion francophone sur la maladie d'Alzheimer, Montpellier, Juin 2014
- Congrès annuel de l'European Society for Gene and Cell Therapy (ESGCT), Helsinki (Finlande) Octobre 2015, **Elu meilleur résumé.**

D. Publications scientifiques

1. Publications au sein de l'unité INSERM/CEA 1169

a. Publiés

Viral gene transfer of APPsα rescues synaptic failure in an Alzheimer's disease mouse model. ARTICLE N°1

Fol R, Braudeau J, Ludewig S, Abel T, Weyer SW, Roederer JP, Brod F, Audrain M, Bemelmans AP, Buchholz CJ, Korte M, Cartier N, Müller UC.

Acta Neuropathologica. Novembre 2015

The APP Intracellular Domain Is Required for Normal Synaptic Morphology, Synaptic Plasticity, and Hippocampus-Dependent Behavior. ARTICLE ANNEXE

Klevanski M, Herrmann U, Weyer SW, **Fol R**, Cartier N, Wolfer DP, Caldwell JH, Korte M, Müller UC.

The journal of Neuroscience. Décembre 2015

Alzheimer's disease-like APP processing in wild-type mice identifies synaptic defects as initial steps of disease progression.

Audrain M, **Fol R**, Dutar P, Potier B, Billard JM, Flament J, Alves S, Burlot MA, Dufayet-Chaffaud G, Bemelmans AP, Valette J, Hantraye P, Déglon N, Cartier N, Braudeau J.

Molecular Neurodegeneration. Janvier 2016

Abstract:

BACKGROUND:

Alzheimer's disease (AD) is the most frequent form of dementia in the elderly and no effective treatment is currently available. The mechanisms triggering AD onset and progression are still imperfectly dissected. We aimed at deciphering the modifications occurring in vivo during the very early stages of AD, before the development of amyloid deposits, neurofibrillary tangles, neuronal death and inflammation. Most current AD models based on Amyloid Precursor Protein (APP) overproduction beginning from in

utero, to rapidly reproduce the histological and behavioral features of the disease within a few months, are not appropriate to study the early steps of AD development. As a means to mimic in vivo amyloid APP processing closer to the human situation in AD, we used an adeno-associated virus (AAV)-based transfer of human mutant APP and Presenilin 1 (PS1) genes to the hippocampi of two-month-old C57Bl/6 J mice to express human APP, without significant overexpression and to specifically induce its amyloid processing.

RESULTS:

The human APP, βCTF and Aβ42/40 ratio were similar to those in hippocampal tissues from AD patients. Three months after injection the murine Tau protein was hyperphosphorylated and rapid synaptic failure occurred characterized by decreased levels of both PSD-95 and metabolites related to neuromodulation, on proton magnetic resonance spectroscopy ((1)H-MRS). Astrocytic GLT-1 transporter levels were lower and the tonic glutamatergic current was stronger on electrophysiological recordings of CA1 hippocampal region, revealing the overstimulation of extrasynaptic N-methyl D-aspartate receptor (NMDAR) which precedes the loss of long-term potentiation (LTP). These modifications were associated with early behavioral impairments in the Open-field, Y-maze and Morris Mater Maze tasks.

CONCLUSIONS:

Altogether, this demonstrates that an AD-like APP processing, yielding to levels of APP, βCTF and Aβ42/Aβ40 ratio similar to those observed in AD patients, are sufficient to rapidly trigger early steps of the amyloidogenic and Tau pathways in vivo. With this strategy, we identified a sequence of early events likely to account for disease onset and described a model that may facilitate efforts to decipher the factors triggering AD and to evaluate early neuroprotective strategies.

Gene Therapy Strategies for Alzheimer's Disease: An Overview. REVUE

Alves S, **Fol R**, Cartier N.

Human Gene Therapy. Février 2016

b. Publications prochaines

Discrepencies between APPsα and APPsβ gene transfer in an Alzheimer's disease mouse model. ARTICLE N°2

Fol R, Braudeau J, Ludewig S, Abel T, Weyer SW, Audrain M, Bemelmans AP, Buchholz CJ, Korte M, Cartier N, Müller UC.

En préparation

Consequences of astrocytic APOE2 overexpression on amyloid pathology and synaptic features in an Alzheimer's mouse model

Fol R, Audrain M, Hudry E, Burlot M-A, Dufayet-Chaffaud G, Bemelmans A, Hyman H, Cartier N, Braudeau J

En préparation

Abstract :

Alzheimer's disease (AD) is characterized by an impaired clearance of the amyloid β peptide (Aβ) from the brain. This process is mediated upon its binding with the Apolipoprotein E (APOE), the most influential genetic risk factor for the late-onset form of AD. Among the 3 human APOE alleles (APOE2, APOE3 and APOE4), APOE2 is associated with a reduced probability to develop the disease. In order to evaluate therapeutic effects of APOE2 overexpression to alleviate AD physiopathological changes, we exogenously expressed human APOE2 in hippocampal astrocytes (that physiologically express ApoE) by stereotaxic intracerebral injection of adeno-associated virus (AAV) in transgenic AD mice (APP/PS1ΔE9). Injection of AAV9-GFA2-APOE2 vector resulted in sustained production and diffusion of APOE2 in the mouse brain. Five months after injection, APOE2 overexpression decreased Aβ precursors (APP and β-CTF) in both cortex and hippocampus of APP/PS1ΔE9 mice. Amyloid plaques density was diminished in the cortex. APOE2 injected APP/PS1ΔE9 mice developed early memory defects in the Morris water maze. This observation was correlated with decreased amounts of synaptic markers in the hippocampus. Similar overexpression of APOE2 in wild type mice resulted in subtle memory and synaptic consequences. Our results confirm that overexpressing APOE2 in the hippocampus of AD mice favorably affects Aβ economy in the whole brain. However, overexpression of APOE2 in the mouse hippocampus might not be as beneficial as suggested by human APOE2 carriers.

Sustained peripheral AAV-based administration of Interleukin-2 improves amyloid pathology and memory in Alzheimer's disease mice.

Alves S, Churlaud G, Audrain M, Braudeau J, **Fol R**, Dufayet-Chaffaud G, Fouquet F, Bosch F, Klatzmann D, Cartier N.

Annals of Neurology. En révision

Abstract:

Interleukin-2 (IL-2) deficient mice have cytoarchitectural hippocampal modifications and impaired learning and memory ability reminiscent of Alzheimer's disease (AD). IL-2 stimulates regulatory T cells (Tregs) which role is to control inflammation. As neuroinflammation contributes to neurodegeneration, we investigated IL-2 in AD. We first found decreased IL-2 levels in hippocampal biopsies from of AD patients. We then treated APP/PS1ΔE9 mice having established AD with IL-2 for five months. IL-2 induced systemic and brain Treg expansion and activation. In the hippocampus, IL-2 induced astrocytic activation and recruitment around amyloid plaques, decrease Aβ (42/40) ratio and amyloid plaques load, improvement of synaptic plasticity and total rescue of spine density. Noteworthy, this tissue remodeling was associated with recovery of memory deficits. Thus, IL-2 can alleviate AD in APP/PS1ΔE9 AD mice with established pathology. This should prompt the investigation of low-dose IL-2 in AD and other neuroinflammatory/neurodegenerative disorders.

Modulating cholesterol metabolism alleviates Alzheimer's disease: towards a clinical application.

Alves S, Audrain M, Aron-Badin R, Lamazière A, Michaelsen-Preusse K, **Fol R**, Braudeau J, Despres G, Fouquet F, Dufayet-Chaffaud G, Korte M, Hantraye P, Aubourg P, Cartier N

En préparation

Growing evidences suggest the role of cholesterol in Alzheimer's disease (AD) headway. Brain cholesterol is synthesized in situ and cannot be eliminated without crossing the blood-brain-barrier (BBB). In order to be translocated out of the brain, the excess of cholesterol needs to be converted into 24S-hydroxycholesterol (24-OHC). This is mediated by a key enzyme in cholesterol metabolism named 24-hydroxylase (CYP46A1), encoded by the CYP46A1 gene. Here, we first demonstrate that CYP46A1 is decreased in hippocampal biopsies from AD patients. We had previously reported the therapeutic effect of an AAV (adeno-associated vector)-5 encoding CYP46A1 in AD mice. In a therapeutic perspective and in order to find the finest vector, we compared CYP46A1 expression, mediated by AAV9 and AAVrh10 in the hippocampus of C57Bl6J mice. We then treated APP23 mice before the onset of plaque load and showed

that AAV9-CYP46A1 increases the 24-OHC content, strongly prevents amyloid plaques deposition, and decreases Aß peptides as well as astrogliosis. Noteworthy, this tissue remodeling was associated with recovery of memory deficits. Strikingly, APP/PS1 knock-in mice having severe and established early AD pathology were treated with AAV9-CYP46A1, showing reduced amyloid plaques load, reduced astrogliosis and complete rescue of impaired electrophysiological and spine defects. In addition, we also evaluated the efficacy, tropism and safety of the AAV-CYP46A1-mediated transduction of the non-human primate (NHP) hippocampus. Altogether, these results identify CYP46A1 as a relevant target to alleviate AD progression, also opening new avenues for treatment of other neurodegenerative disorders.

Early-onset Alzheimer's disease and its progression explored in a novel rat model based on gene transfer.

Audrain M, Souchet B, Haddjeri A, Alves S, **Fol R**, Déglon N, Hantraye P, Akwa Y,

Billard J-M, Potier B, Dutar P, Cartier N, Braudeau J.

En préparation.

Abstract:

Alzheimer's disease (AD) is an irreversible brain disorder characterized by a decline in cognitive function and belated hallmarks such as amyloid deposits and neurofibrillary tangles. There is increasing evidences that these markers appear late in the disease progression and thereby are not responsible of the triggering of AD. To investigate early stages of AD without transgenesis pitfall, we developed a novel AD rat model based on co-injection of two AAV vectors coding for the human mutated APP and PS1 proteins, in the hippocampus of 2 months old Wistar rats. This strategy allowed a stable and moderate expression of transgenes with equivalent levels of APP compared to human patient's hippocampi. We observed a very slow progressive AD like neuropathology where amyloid deposits and AT8 positive neurons appear only around 2.5 years old. We thereby used this model at 3 and 8 months post- injection, as an AD early-phases model, to decipher first consequences of a human-like APP processing and its consequences in the onset of memory troubles.

2. Autres publications

ABCA7 Deficiency Accelerates Amyloid-β Generation and Alzheimer's Neuronal Pathology.

Sakae N, Liu CC, Shinohara M, Frisch-Daiello J, Ma L, Yamazaki Y, Tachibana M, Younkin L, Kurti A, Carrasquillo MM, Zou F, Sevlever D, Bisceglio G, Gan M, **Fol R**, Knight P, Wang M, Han X, Fryer JD, Fitzgerald ML, Ohyagi Y, Younkin SG, Bu G, Kanekiyo T.

The journal of Neuroscience. Mars 2016

Abstract:

In Alzheimer's disease (AD), the accumulation and deposition of amyloid-β (Aβ) peptides in the brain is a central event. Aβ is cleaved from amyloid precursor protein (APP) by β-secrétase and γ-secrétase mainly in neurons. Although mutations in APP, PS1 or PS2 cause early-onset familial AD, ABCA7 encoding ATP-binding cassette transporter A7 is one of the susceptibility genes for late-onset AD (LOAD), in which its loss-of-function variants increase the disease risk. ABCA7 is homologous to a major lipid transporter ABCA1 and is highly expressed in neurons and microglia in the brain. Here, we show that ABCA7 deficiency altered brain lipid profile and impaired memory in ABCA7 knock-out (Abca7(-/-)) mice. When bred to amyloid model APP/PS1 mice, plaque burden was exacerbated by ABCA7 deficit. *In vivo* microdialysis studies indicated that the clearance rate of Aβ was unaltered. Interestingly, ABCA7 deletion facilitated the processing of APP to Aβ by increasing the levels of β-site APP cleaving enzyme 1 (BACE1) and sterol regulatory element-binding protein 2 (SREBP2) in primary neurons and mouse brains. Knock-down of ABCA7 expression in neurons caused endoplasmic reticulum stress highlighted by increased level of protein kinase R-like endoplasmic reticulum kinase (PERK) and increased phosphorylation of eukaryotic initiation factor 2α (eIF2α). In the brains of APP/PS1; Abca7(-/-) mice, the level of phosphorylated extracellular regulated kinase (ERK) was also significantly elevated. Together, our results reveal novel pathways underlying the association of ABCA7 dysfunction and LOAD pathogenesis.

IX. BIBLIOGRAPHIE

Ahmed, R. R., C. J. Holler, R. L. Webb, F. Li, T. L. Beckett and M. P. Murphy (2010). "BACE1 and BACE2 enzymatic activities in Alzheimer's disease." J Neurochem **112**(4): 1045-1053.

Akiyama, H., C. Schwab, H. Kondo, H. Mori, F. Kametani, K. Ikeda and P. L. McGeer (1996). "Granules in glial cells of patients with Alzheimer's disease are immunopositive for C-terminal sequences of beta-amyloid protein." Neurosci Lett **206**(2-3): 169-172.

Alexander, A. G., V. Marfil and C. Li (2014). "Use of Caenorhabditis elegans as a model to study Alzheimer's disease and other neurodegenerative diseases." Front Genet **5**: 279.

Allinquant, B., P. Hantraye, P. Mailleux, K. Moya, C. Bouillot and A. Prochiantz (1995). "Downregulation of amyloid precursor protein inhibits neurite outgrowth in vitro." J Cell Biol **128**(5): 919-927.

Almkvist, O., H. Basun, S. L. Wagner, B. A. Rowe, L. O. Wahlund and L. Lannfelt (1997). "Cerebrospinal fluid levels of alpha-secretase-cleaved soluble amyloid precursor protein mirror cognition in a Swedish family with Alzheimer disease and a gene mutation." Arch Neurol **54**(5): 641-644.

Alonso, A. C., T. Zaidi, I. Grundke-Iqbal and K. Iqbal (1994). "Role of abnormally phosphorylated tau in the breakdown of microtubules in Alzheimer disease." Proc Natl Acad Sci U S A **91**(12): 5562-5566.

Alves, S., R. Fol and N. Cartier-Lacave (2016). "Gene Therapy Strategies for Alzheimer's Disease: An Overview." Hum Gene Ther.

Alzheimer, A., R. A. Stelzmann, H. N. Schnitzlein and F. R. Murtagh (1995). "An English translation of Alzheimer's 1907 paper, "Uber eine eigenartige Erkankung der Hirnrinde"." Clin Anat **8**(6): 429-431.

Anderson, J. J., G. Holtz, P. P. Baskin, R. Wang, L. Mazzarelli, S. L. Wagner and F. Menzaghi (1999). "Reduced cerebrospinal fluid levels of alpha-secretase-cleaved amyloid precursor protein in aged rats: correlation with spatial memory deficits." Neuroscience **93**(4): 1409-1420.

Ankri, J. (2006). "Épidémiologie des démences et de la maladie d'Alzheimer." Bulletin épidémiologique hebdomadaire **5-6**.

Arends, Y. M., C. Duyckaerts, J. M. Rozemuller, P. Eikelenboom and J. J. Hauw (2000). "Microglia, amyloid and dementia in alzheimer disease. A correlative study." Neurobiol Aging **21**(1): 39-47.

Arnold, S. E., B. T. Hyman, J. Flory, A. R. Damasio and G. W. Van Hoesen (1991). "The topographical and neuroanatomical distribution of neurofibrillary tangles and neuritic plaques in the cerebral cortex of patients with Alzheimer's disease." Cereb Cortex **1**(1): 103-116.

Asai, M., C. Hattori, B. Szabo, N. Sasagawa, K. Maruyama, S. Tanuma and S. Ishiura (2003). "Putative function of ADAM9, ADAM10, and ADAM17 as APP alpha-secretase." Biochem Biophys Res Commun **301**(1): 231-235.

Asheuer, M., F. Pflumio, S. Benhamida, A. Dubart-Kupperschmitt, F. Fouquet, Y. Imai, P. Aubourg and N. Cartier (2004). "Human CD34+ cells differentiate into microglia and express recombinant therapeutic protein." Proc Natl Acad Sci U S A **101**(10): 3557-3562.

Audrain, M., R. Fol, P. Dutar, B. Potier, J. M. Billard, J. Flament, S. Alves, M. A. Burlot, G. Dufayet-Chaffaud, A. P. Bemelmans, J. Valette, P. Hantraye, N. Deglon, N. Cartier and J. Braudeau (2016). "Alzheimer's disease-like APP processing in wild-type mice identifies synaptic defects as initial steps of disease progression." Mol Neurodegener **11**(1): 5.

Augustinack, J. C., A. Schneider, E. M. Mandelkow and B. T. Hyman (2002). "Specific tau phosphorylation sites correlate with severity of neuronal cytopathology in Alzheimer's disease." Acta Neuropathol **103**(1): 26-35.

Baig, S., S. A. Joseph, H. Tayler, R. Abraham, M. J. Owen, J. Williams, P. G. Kehoe and S. Love (2010). "Distribution and expression of picalm in Alzheimer disease." J Neuropathol Exp Neurol **69**(10): 1071-1077.

Bailey, J. A., B. Maloney, Y. W. Ge and D. K. Lahiri (2011). "Functional activity of the novel Alzheimer's amyloid beta-peptide interacting domain (AbetaID) in the APP and BACE1 promoter sequences and implications in activating apoptotic genes and in amyloidogenesis." Gene **488**(1-2): 13-22.

Bakker, A., M. S. Albert, G. Krauss, C. L. Speck and M. Gallagher (2015). "Response of the medial temporal lobe network in amnestic mild cognitive impairment to therapeutic intervention assessed by fMRI and memory task performance." Neuroimage Clin **7**: 688-698.

Bakker, A., G. L. Krauss, M. S. Albert, C. L. Speck, L. R. Jones, C. E. Stark, M. A. Yassa, S. S. Bassett, A. L. Shelton and M. Gallagher (2012). "Reduction of hippocampal hyperactivity improves cognition in amnestic mild cognitive impairment." Neuron **74**(3): 467-474.

Ball, M. J. (1976). "NEUROFIBRILLARY TANGLES AND THE PATHOGENESIS OF DEMENTIA: A QUANTITATIVE STUDY." Neuropathology and Applied Neurobiology **2**(5): 395-410.

Barger, S. W. and A. D. Harmon (1997). "Microglial activation by Alzheimer amyloid precursor protein and modulation by apolipoprotein E." Nature **388**(6645): 878-881.

Bayer, T. A., S. Schafer, A. Simons, A. Kemmling, T. Kamer, R. Tepest, A. Eckert, K. Schussel, O. Eikenberg, C. Sturchler-Pierrat, D. Abramowski, M. Staufenbiel and G. Multhaup (2003). "Dietary Cu stabilizes brain superoxide dismutase 1 activity and reduces amyloid Abeta production in APP23 transgenic mice." Proc Natl Acad Sci U S A **100**(24): 14187-14192.

Beher, D., L. Hesse, C. L. Masters and G. Multhaup (1996). "Regulation of amyloid protein precursor (APP) binding to collagen and mapping of the binding sites on APP and collagen type I." J Biol Chem **271**(3): 1613-1620.

Behl, C., J. B. Davis, R. Lesley and D. Schubert (1994). "Hydrogen peroxide mediates amyloid beta protein toxicity." Cell **77**(6): 817-827.

Bell, K. F., L. Zheng, F. Fahrenholz and A. C. Cuello (2008). "ADAM-10 over-expression increases cortical synaptogenesis." Neurobiol Aging **29**(4): 554-565.

Belyaev, N. D., K. A. Kellett, C. Beckett, N. Z. Makova, T. J. Revett, N. N. Nalivaeva, N. M. Hooper and A. J. Turner (2010). "The transcriptionally active amyloid precursor protein (APP) intracellular domain is preferentially produced from the 695 isoform of APP in a {beta}-secretase-dependent pathway." J Biol Chem **285**(53): 41443-41454.

Ben Khalifa, N., D. Tyteca, C. Marinangeli, M. Depuydt, J. F. Collet, P. J. Courtoy, J. C. Renauld, S. Constantinescu, J. N. Octave and P. Kienlen-Campard (2012). "Structural features of the KPI domain control APP dimerization, trafficking, and processing." FASEB J **26**(2): 855-867.

Bertrand, E., E. Brouillet, I. Caille, C. Bouillot, G. M. Cole, A. Prochiantz and B. Allinquant (2001). "A short cytoplasmic domain of the amyloid precursor protein induces apoptosis in vitro and in vivo." Mol Cell Neurosci **18**(5): 503-511.

Bielschowsky, M. (1902). "Die Silberimprägnation der Achsencylinder." Neurologisches Zentralblatt (Leipzig) **21**: 579-584.

Bielschowsky, M. (1903). "Die Silberimprägnation der Achsencylinder." Neurologisches Zentralblatt (Leipzig) **22**: 997-1006.

Biernat, J., E. M. Mandelkow, C. Schroter, B. Lichtenberg-Kraag, B. Steiner, B. Berling, H. Meyer, M. Mercken, A. Vandermeeren, M. Goedert and et al. (1992). "The switch of tau protein to an Alzheimer-like state includes the phosphorylation of two serine-proline motifs upstream of the microtubule binding region." EMBO J **11**(4): 1593-1597.

Billings, L. M., S. Oddo, K. N. Green, J. L. McGaugh and F. M. LaFerla (2005). "Intraneuronal Abeta causes the onset of early Alzheimer's disease-related cognitive deficits in transgenic mice." Neuron **45**(5): 675-688.

Bisht, K., K. P. Sharma, C. Lecours, M. Gabriela Sanchez, H. El Hajj, G. Milior, A. Olmos-Alonso, D. Gomez-Nicola, G. Luheshi, L. Vallieres, I. Branchi, L. Maggi, C. Limatola, O. Butovsky and M. E. Tremblay (2016). "Dark microglia: A new phenotype predominantly associated with pathological states." Glia **64**(5): 826-839.

Blennow, K. (2004). "Cerebrospinal fluid protein biomarkers for Alzheimer's disease." NeuroRx **1**(2): 213-225.

Bloom, G. S. (2014). "Amyloid-beta and tau: the trigger and bullet in Alzheimer disease pathogenesis." JAMA Neurol **71**(4): 505-508.

Bodles, A. M. and S. W. Barger (2005). "Secreted beta-amyloid precursor protein activates microglia via JNK and p38-MAPK." Neurobiol Aging **26**(1): 9-16.

Borchelt, D. R., T. Ratovitski, J. van Lare, M. K. Lee, V. Gonzales, N. A. Jenkins, N. G. Copeland, D. L. Price and S. S. Sisodia (1997). "Accelerated amyloid deposition in the brains of transgenic mice coexpressing mutant presenilin 1 and amyloid precursor proteins." Neuron **19**(4): 939-945.

Borchelt, D. R., G. Thinakaran, C. B. Eckman, M. K. Lee, F. Davenport, T. Ratovitsky, C. M. Prada, G. Kim, S. Seekins, D. Yager, H. H. Slunt, R. Wang, M. Seeger, A. I. Levey, S. E. Gandy, N. G. Copeland, N. A. Jenkins, D. L. Price, S. G. Younkin and S. S. Sisodia (1996). "Familial Alzheimer's disease-linked presenilin 1 variants elevate Abeta1-42/1-40 ratio in vitro and in vivo." Neuron **17**(5): 1005-1013.

Braak, H. and E. Braak (1991). "Neuropathological stageing of Alzheimer-related changes." Acta Neuropathol **82**(4): 239-259.

Breteler, M. M., J. J. Claus, D. E. Grobbee and A. Hofman (1994). "Cardiovascular disease and distribution of cognitive function in elderly people: the Rotterdam Study." BMJ **308**(6944): 1604-1608.

Brion, J. P., A. M. Couck, E. Passareiro and J. Flament-Durand (1985). "Neurofibrillary tangles of Alzheimer's disease: an immunohistochemical study." J Submicrosc Cytol **17**(1): 89-96.

Buee, L., T. Bussiere, V. Buee-Scherrer, A. Delacourte and P. R. Hof (2000). "Tau protein isoforms, phosphorylation and role in neurodegenerative disorders." Brain Res Brain Res Rev **33**(1): 95-130.

Burlot, M. A., J. Braudeau, K. Michaelsen-Preusse, B. Potier, S. Ayciriex, J. Varin, B. Gautier, F. Djelti, M. Audrain, L. Dauphinot, F. J. Fernandez-Gomez, R. Caillierez, O. Laprevote, I. Bieche, N. Auzeil, M. C. Potier, P. Dutar, M. Korte, L. Buee, D. Blum and N. Cartier (2015). "Cholesterol 24-hydroxylase defect is implicated in memory impairments associated with Alzheimer-like Tau pathology." Hum Mol Genet **24**(21): 5965-5976.

Bush, A. I., R. N. Martins, B. Rumble, R. Moir, S. Fuller, E. Milward, J. Currie, D. Ames, A. Weidemann, P. Fischer and et al. (1990). "The amyloid precursor protein of Alzheimer's disease is released by human platelets." J Biol Chem **265**(26): 15977-15983.

Butler, D. and E. Callaway (2016). "Scientists in the dark after French clinical trial proves fatal." Nature **529**(7586): 263-264.

Caccamo, A., S. Oddo, M. C. Sugarman, Y. Akbari and F. M. LaFerla (2005). "Age- and region-dependent alterations in Abeta-degrading enzymes: implications for Abeta-induced disorders." Neurobiol Aging **26**(5): 645-654.

Caille, I., B. Allinquant, E. Dupont, C. Bouillot, A. Langer, U. Muller and A. Prochiantz (2004). "Soluble form of amyloid precursor protein regulates proliferation of progenitors in the adult subventricular zone." Development **131**(9): 2173-2181.

Cao, X. and T. C. Sudhof (2001). "A transcriptionally [correction of transcriptively] active complex of APP with Fe65 and histone acetyltransferase Tip60." Science **293**(5527): 115-120.

Cappai, R., S. S. Mok, D. Galatis, D. F. Tucker, A. Henry, K. Beyreuther, D. H. Small and C. L. Masters (1999). "Recombinant human amyloid precursor-like protein 2 (APLP2) expressed in the yeast Pichia pastoris can stimulate neurite outgrowth." FEBS Lett **442**(1): 95-98.

Cartier, N., S. Hacein-Bey-Abina, C. C. Bartholomae, G. Veres, M. Schmidt, I. Kutschera, M. Vidaud, U. Abel, L. Dal-Cortivo, L. Caccavelli, N. Mahlaoui, V. Kiermer, D. Mittelstaedt, C. Bellesme, N. Lahlou, F. Lefrere, S. Blanche, M. Audit, E. Payen, P. Leboulch, B. l'Homme, P. Bougneres, C. Von Kalle, A. Fischer, M. Cavazzana-Calvo and P. Aubourg (2009). "Hematopoietic stem cell gene therapy with a lentiviral vector in X-linked adrenoleukodystrophy." Science **326**(5954): 818-823.

Cartier, N., C. A. Lewis, R. Zhang and F. M. Rossi (2014). "The role of microglia in human disease: therapeutic tool or target?" Acta Neuropathol **128**(3): 363-380.

Cavazzana-Calvo, M., S. Hacein-Bey, G. de Saint Basile, F. Gross, E. Yvon, P. Nusbaum, F. Selz, C. Hue, S. Certain, J. L. Casanova, P. Bousso, F. L. Deist and A. Fischer (2000). "Gene therapy of human severe combined immunodeficiency (SCID)-X1 disease." Science **288**(5466): 669-672.

Cavazzana-Calvo, M., E. Payen, O. Negre, G. Wang, K. Hehir, F. Fusil, J. Down, M. Denaro, T. Brady, K. Westerman, R. Cavallesco, B. Gillet-Legrand, L. Caccavelli, R. Sgarra, L. Maouche-Chretien, F. Bernaudin, R. Girot, R. Dorazio, G. J. Mulder, A. Polack, A. Bank, J. Soulier, J. Larghero, N. Kabbara, B. Dalle, B. Gourmel, G. Socie, S. Chretien, N. Cartier, P. Aubourg, A. Fischer, K. Cornetta, F. Galacteros, Y. Beuzard, E. Gluckman, F. Bushman, S. Hacein-Bey-Abina and P. Leboulch (2010). "Transfusion independence and HMGA2 activation after gene therapy of human beta-thalassaemia." Nature **467**(7313): 318-322.

Chang, K. A., H. S. Kim, T. Y. Ha, J. W. Ha, K. Y. Shin, Y. H. Jeong, J. P. Lee, C. H. Park, S. Kim, T. K. Baik and Y. H. Suh (2006). "Phosphorylation of amyloid precursor protein (APP) at Thr668 regulates the nuclear translocation of the APP intracellular domain and induces neurodegeneration." Mol Cell Biol **26**(11): 4327-4338.

Chasseigneaux, S. and B. Allinquant (2012). "Functions of Abeta, sAPPalpha and sAPPbeta : similarities and differences." J Neurochem **120 Suppl 1**: 99-108.

Chasseigneaux, S., L. Dinc, C. Rose, C. Chabret, F. Coulpier, P. Topilko, G. Mauger and B. Allinquant (2011). "Secreted amyloid precursor protein beta and secreted amyloid precursor protein alpha induce axon outgrowth in vitro through Egr1 signaling pathway." PLoS One **6**(1): e16301.

Checler, F., C. Sunyach, R. Pardossi-Piquard, J. Sevalle, B. Vincent, T. Kawarai, N. Girardot, P. St George-Hyslop and C. A. da Costa (2007). "The gamma/epsilon-secretase-derived APP intracellular domain fragments regulate p53." Curr Alzheimer Res **4**(4): 423-426.

Chen, A. C. and D. J. Selkoe (2007). "Response to: Pardossi-Piquard et al., "Presenilin-Dependent Transcriptional Control of the Abeta-Degrading Enzyme Neprilysin by Intracellular Domains of betaAPP and APLP." Neuron 46, 541-554." Neuron **53**(4): 479-483.

Cheng, G., Z. Yu, D. Zhou and M. P. Mattson (2002). "Phosphatidylinositol-3-kinase-Akt kinase and p42/p44 mitogen-activated protein kinases mediate neurotrophic and excitoprotective actions of a secreted form of amyloid precursor protein." Exp Neurol **175**(2): 407-414.

Cheng, I. H., K. Scearce-Levie, J. Legleiter, J. J. Palop, H. Gerstein, N. Bien-Ly, J. Puolivali, S. Lesne, K. H. Ashe, P. J. Muchowski and L. Mucke (2007). "Accelerating amyloid-beta fibrillization reduces oligomer levels and functional deficits in Alzheimer disease mouse models." J Biol Chem **282**(33): 23818-23828.

Claasen, A. M., D. Guevremont, S. E. Mason-Parker, K. Bourne, W. P. Tate, W. C. Abraham and J. M. Williams (2009). "Secreted amyloid precursor protein-alpha upregulates synaptic protein synthesis by a protein kinase G-dependent mechanism." Neurosci Lett **460**(1): 92-96.

Clarris, H. J., R. Cappai, D. Heffernan, K. Beyreuther, C. L. Masters and D. H. Small (1997). "Identification of heparin-binding domains in the amyloid precursor protein of Alzheimer's disease by deletion mutagenesis and peptide mapping." J Neurochem **68**(3): 1164-1172.

Clarris, H. J., B. Key, K. Beyreuther, C. L. Masters and D. H. Small (1995). "Expression of the amyloid protein precursor of Alzheimer's disease in the developing rat olfactory system." Brain Res Dev Brain Res **88**(1): 87-95.

Clarris, H. J., V. Nurcombe, D. H. Small, K. Beyreuther and C. L. Masters (1994). "Secretion of nerve growth factor from septum stimulates neurite outgrowth and release of the amyloid protein precursor of Alzheimer's disease from hippocampal explants." J Neurosci Res **38**(3): 248-258.

Cleveland, D. W., S. Y. Hwo and M. W. Kirschner (1977). "Purification of tau, a microtubule-associated protein that induces assembly of microtubules from purified tubulin." J Mol Biol **116**(2): 207-225.

Cochet, M., R. Donneger, E. Cassier, F. Gaven, S. F. Lichtenthaler, P. Marin, J. Bockaert, A. Dumuis and S. Claeysen (2013). "5-HT4 receptors constitutively promote the non-amyloidogenic pathway of APP cleavage and interact with ADAM10." ACS Chem Neurosci **4**(1): 130-140.

Copanaki, E., S. Chang, A. Vlachos, J. A. Tschape, U. C. Muller, D. Kogel and T. Deller (2010). "sAPPalpha antagonizes dendritic degeneration and neuron death triggered by proteasomal stress." Mol Cell Neurosci **44**(4): 386-393.

Corder, E. H., A. M. Saunders, W. J. Strittmatter, D. E. Schmechel, P. C. Gaskell, G. W. Small, A. D. Roses, J. L. Haines and M. A. Pericak-Vance (1993). "Gene dose of apolipoprotein E type 4 allele and the risk of Alzheimer's disease in late onset families." Science **261**(5123): 921-923.

Corrigan, F., R. Vink, P. C. Blumbergs, C. L. Masters, R. Cappai and C. van den Heuvel (2012). "sAPPalpha rescues deficits in amyloid precursor protein knockout mice following focal traumatic brain injury." J Neurochem **122**(1): 208-220.

Cousins, S. L., S. E. Hoey, F. Anne Stephenson and M. S. Perkinton (2009). "Amyloid precursor protein 695 associates with assembled NR2A- and NR2B-containing NMDA receptors to result in the enhancement of their cell surface delivery." J Neurochem **111**(6): 1501-1513.

Cousins, S. L., N. Innocent and F. A. Stephenson (2013). "Neto1 associates with the NMDA receptor/amyloid precursor protein complex." J Neurochem **126**(5): 554-564.

Cucchiarini, M., X. L. Ren, G. Perides and E. F. Terwilliger (2003). "Selective gene expression in brain microglia mediated via adeno-associated virus type 2 and type 5 vectors." Gene Ther **10**(8): 657-667.

Cumbo, E. and L. D. Ligori (2010). "Levetiracetam, lamotrigine, and phenobarbital in patients with epileptic seizures and Alzheimer's disease." Epilepsy Behav **17**(4): 461-466.

Cummings, J. L., C. G. Lyketsos, E. R. Peskind, A. P. Porsteinsson, J. E. Mintzer, D. W. Scharre, J. E. De La Gandara, M. Agronin, C. S. Davis, U. Nguyen, P. Shin, P. N. Tariot and J. Siffert (2015). "Effect of Dextromethorphan-Quinidine on Agitation in Patients With Alzheimer Disease Dementia: A Randomized Clinical Trial." JAMA **314**(12): 1242-1254.

Dahms, S. O., S. Hoefgen, D. Roeser, B. Schlott, K. H. Guhrs and M. E. Than (2010). "Structure and biochemical analysis of the heparin-induced E1 dimer of the amyloid precursor protein." Proc Natl Acad Sci U S A **107**(12): 5381-5386.

Daigle, I. and C. Li (1993). "apl-1, a Caenorhabditis elegans gene encoding a protein related to the human beta-amyloid protein precursor." Proc Natl Acad Sci U S A **90**(24): 12045-12049.

Darmellah, A., A. Rayah, R. Auger, M. H. Cuif, M. Prigent, M. Arpin, A. Alcover, C. Delarasse and J. M. Kanellopoulos (2012). "Ezrin/radixin/moesin are required for the purinergic P2X7 receptor (P2X7R)-dependent processing of the amyloid precursor protein." J Biol Chem **287**(41): 34583-34595.

de la Monte, S. M. (1989). "Quantitation of cerebral atrophy in preclinical and end-stage Alzheimer's disease." Ann Neurol **25**(5): 450-459.

DeKosky, S. T. and S. W. Scheff (1990). "Synapse loss in frontal cortex biopsies in Alzheimer's disease: correlation with cognitive severity." Ann Neurol **27**(5): 457-464.

Delaere, P., C. Duyckaerts, C. Masters, K. Beyreuther, F. Piette and J. J. Hauw (1990). "Large amounts of neocortical beta A4 deposits without neuritic plaques nor tangles in a psychometrically assessed, non-demented person." Neurosci Lett **116**(1-2): 87-93.

Delarasse, C., R. Auger, P. Gonnord, B. Fontaine and J. M. Kanellopoulos (2011). "The purinergic receptor P2X7 triggers alpha-secretase-dependent processing of the amyloid precursor protein." J Biol Chem **286**(4): 2596-2606.

Deng, J., A. Habib, D. F. Obregon, S. W. Barger, B. Giunta, Y. J. Wang, H. Hou, D. Sawmiller and J. Tan (2015). "Soluble amyloid precursor protein alpha inhibits tau phosphorylation through modulation of GSK3beta signaling pathway." J Neurochem **135**(3): 630-637.

Divry, P. F., M. (1927). "Sur les proprietes optiques de l'amyloide." C R Soc Biol **97**: 1808–1810.

Djelti, F., J. Braudeau, E. Hudry, M. Dhenain, J. Varin, I. Bieche, C. Marquer, F. Chali, S. Ayciriex, N. Auzeil, S. Alves, D. Langui, M. C. Potier, O. Laprevote, M. Vidaud, C. Duyckaerts, R. Miles, P. Aubourg and N. Cartier (2015). "CYP46A1 inhibition, brain cholesterol accumulation and neurodegeneration pave the way for Alzheimer's disease." Brain **138**(Pt 8): 2383-2398.

Dobrowolska, J. A., T. Kasten, Y. Huang, T. L. Benzinger, W. Sigurdson, V. Ovod, J. C. Morris and R. J. Bateman (2014). "Diurnal patterns of soluble amyloid precursor protein metabolites in the human central nervous system." PLoS One **9**(3): e89998.

Dubois, B., H. H. Feldman, C. Jacova, H. Hampel, J. L. Molinuevo, K. Blennow, S. T. DeKosky, S. Gauthier, D. Selkoe, R. Bateman, S. Cappa, S. Crutch, S. Engelborghs, G. B. Frisoni, N. C. Fox, D. Galasko, M. O. Habert, G. A. Jicha, A. Nordberg, F. Pasquier, G. Rabinovici, P. Robert, C. Rowe, S. Salloway, M. Sarazin, S. Epelbaum, L. C. de Souza, B. Vellas, P. J. Visser, L. Schneider, Y. Stern, P. Scheltens and J. L. Cummings (2014). "Advancing research diagnostic criteria for Alzheimer's disease: the IWG-2 criteria." Lancet Neurol **13**(6): 614-629.

Dubois, B. M., A. (2015). "Démences." Traité de neurologie.

Dubois, B. T., J.; Portet, F.; Ousset, J-P.; Vellas, B.; Michel, B. (2002). ""Les 5 mots", épreuve simple et sensible pour le diagnostic de la maladie d'Alzheimer." La presse médicale.

Duyckaerts, C., M. C. Potier and B. Delatour (2008). "Alzheimer disease models and human neuropathology: similarities and differences." Acta Neuropathol **115**(1): 5-38.

Eckert, G. P., S. Chang, J. Eckmann, E. Copanaki, S. Hagl, U. Hener, W. E. Muller and D. Kogel (2011). "Liposome-incorporated DHA increases neuronal survival by enhancing non-amyloidogenic APP processing." Biochim Biophys Acta **1808**(1): 236-243.

Ellis, W. G. M., J. R.; Corley, C. L. (1974). "Presenile dementia in Down's syndrome." Neurology **24**: 101-106.

Endres, K. and F. Fahrenholz (2012). "Regulation of alpha-secretase ADAM10 expression and activity." Exp Brain Res **217**(3-4): 343-352.

Engelhardt, E. and M. Gomes Mda (2015). "Alzheimer's 100th anniversary of death and his contribution to a better understanding of Senile dementia." Arq Neuropsiquiatr **73**(2): 159-162.

Fa, M., D. Puzzo, R. Piacentini, A. Staniszewski, H. Zhang, M. A. Baltrons, D. D. Li Puma, I. Chatterjee, J. Li, F. Saeed, H. L. Berman, C. Ripoli, W. Gulisano, J. Gonzalez, H. Tian, J. A. Costa, P. Lopez, E. Davidowitz, W. H. Yu, V. Haroutunian, L. M. Brown, A. Palmeri, E. M. Sigurdsson, K. E. Duff, A. F. Teich, L. S. Honig, M. Sierks, J. G. Moe, L. D'Adamio, C. Grassi, N. M. Kanaan, P. E. Fraser and O. Arancio (2016). "Extracellular Tau Oligomers Produce An Immediate Impairment of LTP and Memory." Sci Rep **6**: 19393.

Fahrenholz, F. (2007). "Alpha-secretase as a therapeutic target." Curr Alzheimer Res **4**(4): 412-417.

Fol, R., J. Braudeau, S. Ludewig, T. Abel, S. W. Weyer, J. P. Roederer, F. Brod, M. Audrain, A. P. Bemelmans, C. J. Buchholz, M. Korte, N. Cartier and U. C. Muller (2016). "Viral gene transfer of APPsalpha rescues synaptic failure in an Alzheimer's disease mouse model." Acta Neuropathol **131**(2): 247-266.

Folstein, M. F., S. E. Folstein and P. R. McHugh (1975). ""Mini-mental state". A practical method for grading the cognitive state of patients for the clinician." J Psychiatr Res **12**(3): 189-198.

Forloni, G., R. Chiesa, S. Smiroldo, L. Verga, M. Salmona, F. Tagliavini and N. Angeretti (1993). "Apoptosis mediated neurotoxicity induced by chronic application of beta amyloid fragment 25-35." Neuroreport **4**(5): 523-526.

Frackowiak, J., H. M. Wisniewski, J. Wegiel, G. S. Merz, K. Iqbal and K. C. Wang (1992). "Ultrastructure of the microglia that phagocytose amyloid and the microglia that produce beta-amyloid fibrils." Acta Neuropathol **84**(3): 225-233.

Frank, S., G. J. Burbach, M. Bonin, M. Walter, W. Streit, I. Bechmann and T. Deller (2008). "TREM2 is upregulated in amyloid plaque-associated microglia in aged APP23 transgenic mice." Glia **56**(13): 1438-1447.

Fratiglioni, L., L. J. Launer, K. Andersen, M. M. Breteler, J. R. Copeland, J. F. Dartigues, A. Lobo, J. Martinez-Lage, H. Soininen and A. Hofman (2000). "Incidence of dementia and major subtypes in Europe: A collaborative study of population-based cohorts. Neurologic Diseases in the Elderly Research Group." Neurology **54**(11 Suppl 5): S10-15.

Freude, K. K., M. Penjwini, J. L. Davis, F. M. LaFerla and M. Blurton-Jones (2011). "Soluble amyloid precursor protein induces rapid neural differentiation of human embryonic stem cells." J Biol Chem **286**(27): 24264-24274.

Furukawa, K., S. W. Barger, E. M. Blalock and M. P. Mattson (1996). "Activation of K+ channels and suppression of neuronal activity by secreted beta-amyloid-precursor protein." Nature **379**(6560): 74-78.

Furukawa, K., B. L. Sopher, R. E. Rydel, J. G. Begley, D. G. Pham, G. M. Martin, M. Fox and M. P. Mattson (1996). "Increased activity-regulating and neuroprotective efficacy of alpha-secretase-derived secreted amyloid precursor protein conferred by a C-terminal heparin-binding domain." J Neurochem **67**(5): 1882-1896.

Gaj, T., B. E. Epstein and D. V. Schaffer (2016). "Genome Engineering Using Adeno-associated Virus: Basic and Clinical Research Applications." Mol Ther **24**(3): 458-464.

Gakhar-Koppole, N., P. Hundeshagen, C. Mandl, S. W. Weyer, B. Allinquant, U. Muller and F. Ciccolini (2008). "Activity requires soluble amyloid precursor protein alpha to promote neurite outgrowth in neural stem cell-derived neurons via activation of the MAPK pathway." Eur J Neurosci **28**(5): 871-882.

Gallez, C. (2005). "Rapport surla maladie d'Alzheimer et les maladies apparentées." Paris: Office parlementaire d'évaluation des politiques de santé.

Galvan, V., O. F. Gorostiza, S. Banwait, M. Ataie, A. V. Logvinova, S. Sitaraman, E. Carlson, S. A. Sagi, N. Chevallier, K. Jin, D. A. Greenberg and D. E. Bredesen (2006). "Reversal of Alzheimer's-like pathology and behavior in human APP transgenic mice by mutation of Asp664." Proc Natl Acad Sci U S A **103**(18): 7130-7135.

Gao, Y. and S. W. Pimplikar (2001). "The gamma -secretase-cleaved C-terminal fragment of amyloid precursor protein mediates signaling to the nucleus." Proc Natl Acad Sci U S A **98**(26): 14979-14984.

Gendreau, K. L. and G. F. Hall (2013). "Tangles, Toxicity, and Tau Secretion in AD - New Approaches to a Vexing Problem." Front Neurol **4**: 160.

Gervais, F. G., D. Xu, G. S. Robertson, J. P. Vaillancourt, Y. Zhu, J. Huang, A. LeBlanc, D. Smith, M. Rigby, M. S. Shearman, E. E. Clarke, H. Zheng, L. H. Van Der Ploeg, S. C. Ruffolo, N. A. Thornberry, S. Xanthoudakis, R. J. Zamboni, S. Roy and D. W. Nicholson (1999). "Involvement of caspases in proteolytic cleavage of Alzheimer's amyloid-beta precursor protein and amyloidogenic A beta peptide formation." Cell **97**(3): 395-406.

Giannoni, P., F. Gaven, D. de Bundel, K. Baranger, E. Marchetti-Gauthier, F. S. Roman, E. Valjent, P. Marin, J. Bockaert, S. Rivera and S. Claeysen (2013). "Early administration of RS 67333, a specific 5-HT4 receptor agonist, prevents amyloidogenesis and behavioral deficits in the 5XFAD mouse model of Alzheimer's disease." Front Aging Neurosci **5**: 96.

Gibson, P. H. (1983). "Form and distribution of senile plaques seen in silver impregnated sections in the brains of intellectually normal elderly people and people with Alzheimer-type dementia." Neuropathol Appl Neurobiol **9**(5): 379-389.

Gilbert, B. J. (2014). "Republished: the role of amyloid beta in the pathogenesis of Alzheimer's disease." Postgrad Med J **90**(1060): 113-117.

Giliberto, L., D. Zhou, R. Weldon, E. Tamagno, P. De Luca, M. Tabaton and L. D'Adamio (2008). "Evidence that the Amyloid beta Precursor Protein-intracellular domain lowers the stress threshold of neurons and has a "regulated" transcriptional role." Mol Neurodegener **3**: 12.

Glabe, C. G. (2008). "Structural classification of toxic amyloid oligomers." J Biol Chem **283**(44): 29639-29643.

Glenner, G. G. (1983). "Banbury Report 15: Biological Aspects of Alzheimer's Disease." Cold Spring Harbor Symposium: 137-144.

Glenner, G. G. and C. W. Wong (1984). "Alzheimer's disease and Down's syndrome: sharing of a unique cerebrovascular amyloid fibril protein." Biochem Biophys Res Commun **122**(3): 1131-1135.

Glenner, G. G. and C. W. Wong (1984). "Alzheimer's disease: initial report of the purification and characterization of a novel cerebrovascular amyloid protein." Biochem Biophys Res Commun **120**(3): 885-890.

Goedert, M., R. Jakes and E. Vanmechelen (1995). "Monoclonal antibody AT8 recognises tau protein phosphorylated at both serine 202 and threonine 205." Neurosci Lett **189**(3): 167-169.

Goldgaber, D., M. I. Lerman, O. W. McBride, U. Saffiotti and D. C. Gajdusek (1987). "Characterization and chromosomal localization of a cDNA encoding brain amyloid of Alzheimer's disease." Science **235**(4791): 877-880.

Gonzalez-Murillo, A., M. L. Lozano, L. Alvarez, A. Jacome, E. Almarza, S. Navarro, J. C. Segovia, H. Hanenberg, G. Guenechea, J. A. Bueren and P. Rio (2010). "Development of lentiviral vectors with optimized transcriptional activity for the gene therapy of patients with Fanconi anemia." Hum Gene Ther **21**(5): 623-630.

Goodman, Y. and M. P. Mattson (1994). "Secreted forms of beta-amyloid precursor protein protect hippocampal neurons against amyloid beta-peptide-induced oxidative injury." Exp Neurol **128**(1): 1-12.

Gralle, M., C. L. Oliveira, L. H. Guerreiro, W. J. McKinstry, D. Galatis, C. L. Masters, R. Cappai, M. W. Parker, C. H. Ramos, I. Torriani and S. T. Ferreira (2006). "Solution conformation and heparin-induced dimerization of the full-length extracellular domain of the human amyloid precursor protein." J Mol Biol **357**(2): 493-508.

Greenberg, S. M. and K. S. Kosik (1995). "Secreted beta-APP stimulates MAP kinase and phosphorylation of tau in neurons." Neurobiol Aging **16**(3): 403-407; discussion 407-408.

Grundke-Iqbal, I., K. Iqbal, M. Quinlan, Y. C. Tung, M. S. Zaidi and H. M. Wisniewski (1986). "Microtubule-associated protein tau. A component of Alzheimer paired helical filaments." J Biol Chem **261**(13): 6084-6089.

Grundke-Iqbal, I., K. Iqbal, Y. C. Tung, M. Quinlan, H. M. Wisniewski and L. I. Binder (1986). "Abnormal phosphorylation of the microtubule-associated protein tau (tau) in Alzheimer cytoskeletal pathology." Proc Natl Acad Sci U S A **83**(13): 4913-4917.

Grundke-Iqbal, I., A. B. Johnson, R. D. Terry, H. M. Wisniewski and K. Iqbal (1979). "Alzheimer neurofibrillary tangles: antiserum and immunohistological staining." Ann Neurol **6**(6): 532-537.

Grundke-Iqbal, I., A. B. Johnson, H. M. Wisniewski, R. D. Terry and K. Iqbal (1979). "Evidence that Alzheimer neurofibrillary tangles originate from neurotubules." Lancet **1**(8116): 578-580.

Guerreiro, R., A. Wojtas, J. Bras, M. Carrasquillo, E. Rogaeva, E. Majounie, C. Cruchaga, C. Sassi, J. S. Kauwe, S. Younkin, L. Hazrati, J. Collinge, J. Pocock, T. Lashley, J. Williams, J. C. Lambert, P. Amouyel, A. Goate, R. Rademakers, K. Morgan, J. Powell, P. St George-Hyslop, A. Singleton, J. Hardy and G. Alzheimer Genetic Analysis (2013). "TREM2 variants in Alzheimer's disease." N Engl J Med **368**(2): 117-127.

Haass, C., C. Kaether, G. Thinakaran and S. Sisodia (2012). "Trafficking and proteolytic processing of APP." Cold Spring Harb Perspect Med **2**(5): a006270.

Hacein-Bey-Abina, S., C. von Kalle, M. Schmidt, F. Le Deist, N. Wulffraat, E. McIntyre, I. Radford, J. L. Villeval, C. C. Fraser, M. Cavazzana-Calvo and A. Fischer (2003). "A serious adverse event after successful gene therapy for X-linked severe combined immunodeficiency." N Engl J Med **348**(3): 255-256.

Hampel, H., S. Lista, S. J. Teipel, F. Garaci, R. Nistico, K. Blennow, H. Zetterberg, L. Bertram, C. Duyckaerts, H. Bakardjian, A. Drzezga, O. Colliot, S. Epelbaum, K. Broich, S. Lehericy, A. Brice, Z. S. Khachaturian, P. S. Aisen and B. Dubois (2014). "Perspective on future role of biological markers in clinical therapy trials of Alzheimer's disease: a long-range point of view beyond 2020." Biochem Pharmacol **88**(4): 426-449.

Han, P., F. Dou, F. Li, X. Zhang, Y. W. Zhang, H. Zheng, S. A. Lipton, H. Xu and F. F. Liao (2005). "Suppression of cyclin-dependent kinase 5 activation by amyloid precursor protein: a novel excitoprotective mechanism involving modulation of tau phosphorylation." J Neurosci **25**(50): 11542-11552.

Hardy, J. and D. Allsop (1991). "Amyloid deposition as the central event in the aetiology of Alzheimer's disease." Trends Pharmacol Sci **12**(10): 383-388.

Hardy, J. and D. J. Selkoe (2002). "The amyloid hypothesis of Alzheimer's disease: progress and problems on the road to therapeutics." Science **297**(5580): 353-356.

Hardy, J. A. and G. A. Higgins (1992). "Alzheimer's disease: the amyloid cascade hypothesis." Science **256**(5054): 184-185.

Harel, A., F. Wu, M. P. Mattson, C. M. Morris and P. J. Yao (2008). "Evidence for CALM in directing VAMP2 trafficking." Traffic **9**(3): 417-429.

Harold, D., R. Abraham, P. Hollingworth, R. Sims, A. Gerrish, M. L. Hamshere, J. S. Pahwa, V. Moskvina, K. Dowzell, A. Williams, N. Jones, C. Thomas, A. Stretton, A. R. Morgan, S. Lovestone, J. Powell, P. Proitsi, M. K. Lupton, C. Brayne, D. C. Rubinsztein, M. Gill, B. Lawlor, A. Lynch, K. Morgan, K. S. Brown, P. A. Passmore, D. Craig, B. McGuinness, S. Todd, C. Holmes, D. Mann, A. D. Smith, S. Love, P. G. Kehoe, J. Hardy, S. Mead, N. Fox, M. Rossor, J. Collinge, W. Maier, F. Jessen, B. Schurmann, R. Heun, H. van den Bussche, I. Heuser, J. Kornhuber, J. Wiltfang, M. Dichgans, L. Frolich, H. Hampel, M. Hull, D. Rujescu, A. M. Goate, J. S. Kauwe, C. Cruchaga, P. Nowotny, J. C. Morris, K. Mayo, K. Sleegers, K. Bettens, S. Engelborghs, P. P. De Deyn, C. Van Broeckhoven, G. Livingston, N. J. Bass, H. Gurling, A. McQuillin, R. Gwilliam, P. Deloukas, A. Al-Chalabi, C. E. Shaw, M. Tsolaki, A. B. Singleton, R. Guerreiro, T. W. Muhleisen, M. M. Nothen, S. Moebus, K. H. Jockel, N. Klopp, H. E. Wichmann, M. M. Carrasquillo, V. S. Pankratz, S. G. Younkin, P. A. Holmans, M. O'Donovan, M. J. Owen and J. Williams (2009). "Genome-wide association study identifies variants at CLU and PICALM associated with Alzheimer's disease." Nat Genet **41**(10): 1088-1093.

Hartmann, D., B. de Strooper, L. Serneels, K. Craessaerts, A. Herreman, W. Annaert, L. Umans, T. Lubke, A. Lena Illert, K. von Figura and P. Saftig (2002). "The disintegrin/metalloprotease ADAM 10 is essential for Notch signalling but not for alpha-secretase activity in fibroblasts." Hum Mol Genet **11**(21): 2615-2624.

Hass, M. R. and B. A. Yankner (2005). "A {gamma}-secretase-independent mechanism of signal transduction by the amyloid precursor protein." J Biol Chem **280**(44): 36895-36904.

Heneka, M. T., M. P. Kummer and E. Latz (2014). "Innate immune activation in neurodegenerative disease." Nat Rev Immunol **14**(7): 463-477.

Henneman, W. J., J. D. Sluimer, J. Barnes, W. M. van der Flier, I. C. Sluimer, N. C. Fox, P. Scheltens, H. Vrenken and F. Barkhof (2009). "Hippocampal atrophy rates in Alzheimer disease: added value over whole brain volume measures." Neurology **72**(11): 999-1007.

Heppner, F. L., R. M. Ransohoff and B. Becher (2015). "Immune attack: the role of inflammation in Alzheimer disease." Nat Rev Neurosci **16**(6): 358-372.

Herard, A. S., L. Besret, A. Dubois, J. Dauguet, T. Delzescaux, P. Hantraye, G. Bonvento and K. L. Moya (2006). "siRNA targeted against amyloid precursor protein impairs synaptic activity in vivo." Neurobiol Aging **27**(12): 1740-1750.

Herrup, K. (2015). "The case for rejecting the amyloid cascade hypothesis." Nat Neurosci **18**(6): 794-799.

Hick, M., U. Herrmann, S. W. Weyer, J. P. Mallm, J. A. Tschape, M. Borgers, M. Mercken, F. C. Roth, A. Draguhn, L. Slomianka, D. P. Wolfer, M. Korte and U. C. Muller (2015). "Acute function of secreted amyloid precursor protein fragment APPsalpha in synaptic plasticity." Acta Neuropathol **129**(1): 21-37.

Hosing, C. (2012). "Hematopoietic stem cell mobilization with G-CSF." Methods Mol Biol **904**: 37-47.

Hsiao, K., P. Chapman, S. Nilsen, C. Eckman, Y. Harigaya, S. Younkin, F. Yang and G. Cole (1996). "Correlative memory deficits, Abeta elevation, and amyloid plaques in transgenic mice." Science **274**(5284): 99-102.

Hsieh, H., J. Boehm, C. Sato, T. Iwatsubo, T. Tomita, S. Sisodia and R. Malinow (2006). "AMPAR removal underlies Abeta-induced synaptic depression and dendritic spine loss." Neuron **52**(5): 831-843.

Hudry, E., D. Van Dam, W. Kulik, P. P. De Deyn, F. S. Stet, O. Ahouansou, A. Benraiss, A. Delacourte, P. Bougneres, P. Aubourg and N. Cartier (2010). "Adeno-associated virus gene therapy with cholesterol 24-hydroxylase reduces the amyloid pathology before or after the onset of amyloid plaques in mouse models of Alzheimer's disease." Mol Ther **18**(1): 44-53.

Iqbal, K., C. Alonso Adel, S. Chen, M. O. Chohan, E. El-Akkad, C. X. Gong, S. Khatoon, B. Li, F. Liu, A. Rahman, H. Tanimukai and I. Grundke-Iqbal (2005). "Tau pathology in Alzheimer disease and other tauopathies." Biochim Biophys Acta **1739**(2-3): 198-210.

Iqbal, K., E. Braak, H. Braak, T. Zaidi and I. Grundke-Iqbal (1991). "A silver impregnation method for labeling both Alzheimer paired helical filaments and their polypeptides separated by sodium dodecyl sulfate-polyacrylamide gel electrophoresis." Neurobiol Aging **12**(4): 357-361.

Iqbal, K., F. Liu and C. X. Gong (2016). "Tau and neurodegenerative disease: the story so far." Nat Rev Neurol **12**(1): 15-27.

Iqbal, K. and I. Tellez-Nagel (1972). "Isolation of neurons and glial cells from normal and pathological human brains." Brain Res **45**(1): 296-301.

Iqbal, K., H. M. Wisniewski, M. L. Shelanski, S. Brostoff, B. H. Liwnicz and R. D. Terry (1974). "Protein changes in senile dementia." Brain Res **77**(2): 337-343.

Ishida, A., K. Furukawa, J. N. Keller and M. P. Mattson (1997). "Secreted form of beta-amyloid precursor protein shifts the frequency dependency for induction of LTD, and enhances LTP in hippocampal slices." Neuroreport **8**(9-10): 2133-2137.

Ishii, K. (2014). "PET approaches for diagnosis of dementia." AJNR Am J Neuroradiol **35**(11): 2030-2038.

Izumi, R., T. Yamada, S. Yoshikai, H. Sasaki, M. Hattori and Y. Sakaki (1992). "Positive and negative regulatory elements for the expression of the Alzheimer's disease amyloid precursor-encoding gene in mouse." Gene **112**(2): 189-195.

Jacobsen, K. T. and K. Iverfeldt (2009). "Amyloid precursor protein and its homologues: a family of proteolysis-dependent receptors." Cell Mol Life Sci **66**(14): 2299-2318.

Jankowsky, J. L., D. J. Fadale, J. Anderson, G. M. Xu, V. Gonzales, N. A. Jenkins, N. G. Copeland, M. K. Lee, L. H. Younkin, S. L. Wagner, S. G. Younkin and D. R. Borchelt (2004). "Mutant presenilins specifically elevate the levels of the 42 residue beta-amyloid peptide in vivo: evidence for augmentation of a 42-specific gamma secretase." Hum Mol Genet **13**(2): 159-170.

Jankowsky, J. L., H. H. Slunt, T. Ratovitski, N. A. Jenkins, N. G. Copeland and D. R. Borchelt (2001). "Co-expression of multiple transgenes in mouse CNS: a comparison of strategies." Biomol Eng **17**(6): 157-165.

Janus, C., A. Y. Flores, G. Xu and D. R. Borchelt (2015). "Behavioral abnormalities in APPSwe/PS1dE9 mouse model of AD-like pathology: comparative analysis across multiple behavioral domains." Neurobiol Aging **36**(9): 2519-2532.

Jay, T. R., C. M. Miller, P. J. Cheng, L. C. Graham, S. Bemiller, M. L. Broihier, G. Xu, D. Margevicius, J. C. Karlo, G. L. Sousa, A. C. Cotleur, O. Butovsky, L. Bekris, S. M. Staugaitis, J. B. Leverenz, S. W. Pimplikar, G. E. Landreth, G. R. Howell, R. M. Ransohoff and B. T. Lamb (2015). "TREM2 deficiency eliminates TREM2+ inflammatory macrophages and ameliorates pathology in Alzheimer's disease mouse models." J Exp Med **212**(3): 287-295.

Jimenez, S., M. Torres, M. Vizuete, R. Sanchez-Varo, E. Sanchez-Mejias, L. Trujillo-Estrada, I. Carmona-Cuenca, C. Caballero, D. Ruano, A. Gutierrez and J. Vitorica (2011). "Age-dependent accumulation of soluble amyloid beta (Abeta) oligomers reverses the neuroprotective effect of soluble amyloid precursor protein-alpha (sAPP(alpha)) by modulating phosphatidylinositol 3-kinase (PI3K)/Akt-GSK-3beta pathway in Alzheimer mouse model." J Biol Chem **286**(21): 18414-18425.

Jin, L. W., H. Ninomiya, J. M. Roch, D. Schubert, E. Masliah, D. A. Otero and T. Saitoh (1994). "Peptides containing the RERMS sequence of amyloid beta/A4 protein precursor bind cell surface and promote neurite extension." J Neurosci **14**(9): 5461-5470.

Johansson, P., N. Mattsson, O. Hansson, A. Wallin, J. O. Johansson, U. Andreasson, H. Zetterberg, K. Blennow and J. Svensson (2011). "Cerebrospinal fluid biomarkers for Alzheimer's disease: diagnostic performance in a homogeneous mono-center population." J Alzheimers Dis **24**(3): 537-546.

Johnson, S. A., J. Rogers and C. E. Finch (1989). "APP-695 transcript prevalence is selectively reduced during Alzheimer's disease in cortex and hippocampus but not in cerebellum." Neurobiol Aging **10**(6): 755-760.

Jonsson, T., J. K. Atwal, S. Steinberg, J. Snaedal, P. V. Jonsson, S. Bjornsson, H. Stefansson, P. Sulem, D. Gudbjartsson, J. Maloney, K. Hoyte, A. Gustafson, Y. Liu, Y. Lu, T. Bhangale, R. R. Graham, J. Huttenlocher, G. Bjornsdottir, O. A. Andreassen, E. G. Jonsson, A. Palotie, T. W. Behrens, O. T. Magnusson, A. Kong, U. Thorsteinsdottir, R. J. Watts and K. Stefansson (2012). "A mutation in APP protects against Alzheimer's disease and age-related cognitive decline." Nature **488**(7409): 96-99.

Jonsson, T., H. Stefansson, S. Steinberg, I. Jonsdottir, P. V. Jonsson, J. Snaedal, S. Bjornsson, J. Huttenlocher, A. I. Levey, J. J. Lah, D. Rujescu, H. Hampel, I. Giegling, O. A. Andreassen, K. Engedal, I. Ulstein, S. Djurovic, C. Ibrahim-Verbaas, A. Hofman, M. A. Ikram, C. M. van Duijn, U. Thorsteinsdottir, A. Kong and K. Stefansson (2013). "Variant of TREM2 associated with the risk of Alzheimer's disease." N Engl J Med **368**(2): 107-116.

Kametani, F., K. Tanaka, T. Ishii, S. Ikeda, H. E. Kennedy and D. Allsop (1993). "Secretory form of Alzheimer amyloid precursor protein 695 in human brain lacks beta/A4 amyloid immunoreactivity." Biochem Biophys Res Commun **191**(2): 392-398.

Kanekiyo, T., H. Xu and G. Bu (2014). "ApoE and Abeta in Alzheimer's disease: accidental encounters or partners?" Neuron **81**(4): 740-754.

Kang, J., H. G. Lemaire, A. Unterbeck, J. M. Salbaum, C. L. Masters, K. H. Grzeschik, G. Multhaup, K. Beyreuther and B. Muller-Hill (1987). "The precursor of Alzheimer's disease amyloid A4 protein resembles a cell-surface receptor." Nature **325**(6106): 733-736.

Karch, C. M. and A. M. Goate (2015). "Alzheimer's disease risk genes and mechanisms of disease pathogenesis." Biol Psychiatry **77**(1): 43-51.

Kibbey, M. C., M. Jucker, B. S. Weeks, R. L. Neve, W. E. Van Nostrand and H. K. Kleinman (1993). "beta-Amyloid precursor protein binds to the neurite-promoting IKVAV site of laminin." Proc Natl Acad Sci U S A **90**(21): 10150-10153.

Kidd, M. (1963). "Paired helical filaments in electron microscopy of Alzheimer's disease." Nature **197**: 192-193.

Kilgore, M., C. A. Miller, D. M. Fass, K. M. Hennig, S. J. Haggarty, J. D. Sweatt and G. Rumbaugh (2010). "Inhibitors of class 1 histone deacetylases reverse contextual memory deficits in a mouse model of Alzheimer's disease." Neuropsychopharmacology **35**(4): 870-880.

Kim, H. S., E. M. Kim, J. P. Lee, C. H. Park, S. Kim, J. H. Seo, K. A. Chang, E. Yu, S. J. Jeong, Y. H. Chong and Y. H. Suh (2003). "C-terminal fragments of amyloid precursor protein exert neurotoxicity by inducing glycogen synthase kinase-3beta expression." FASEB J **17**(13): 1951-1953.

Kimura, T., T. Ono, J. Takamatsu, H. Yamamoto, K. Ikegami, A. Kondo, M. Hasegawa, Y. Ihara, E. Miyamoto and T. Miyakawa (1996). "Sequential changes of tau-site-specific phosphorylation during development of paired helical filaments." Dementia **7**(4): 177-181.

Klein, W. L., G. A. Krafft and C. E. Finch (2001). "Targeting small Abeta oligomers: the solution to an Alzheimer's disease conundrum?" Trends Neurosci **24**(4): 219-224.

Klevanski, M., U. Herrmann, S. W. Weyer, R. Fol, N. Cartier, D. P. Wolfer, J. H. Caldwell, M. Korte and U. C. Muller (2015). "The APP Intracellular Domain Is Required for Normal Synaptic Morphology, Synaptic Plasticity, and Hippocampus-Dependent Behavior." J Neurosci **35**(49): 16018-16033.

Kogel, D., T. Deller and C. Behl (2012). "Roles of amyloid precursor protein family members in neuroprotection, stress signaling and aging." Exp Brain Res **217**(3-4): 471-479.

Kontsekova, E., N. Zilka, B. Kovacech, P. Novak and M. Novak (2014). "First-in-man tau vaccine targeting structural determinants essential for pathological tau-tau interaction reduces tau oligomerisation and neurofibrillary degeneration in an Alzheimer's disease model." Alzheimers Res Ther **6**(4): 44.

Kosik, K. S., C. L. Joachim and D. J. Selkoe (1986). "Microtubule-associated protein tau (tau) is a major antigenic component of paired helical filaments in Alzheimer disease." Proc Natl Acad Sci U S A **83**(11): 4044-4048.

Kugler, S., E. Kilic and M. Bahr (2003). "Human synapsin 1 gene promoter confers highly neuron-specific long-term transgene expression from an adenoviral vector in the adult rat brain depending on the transduced area." Gene Ther **10**(4): 337-347.

LaFerla, F. M., B. T. Tinkle, C. J. Bieberich, C. C. Haudenschild and G. Jay (1995). "The Alzheimer's A beta peptide induces neurodegeneration and apoptotic cell death in transgenic mice." Nat Genet **9**(1): 21-30.

Lambert, J. C., C. A. Ibrahim-Verbaas, D. Harold, A. C. Naj, R. Sims, C. Bellenguez, A. L. DeStafano, J. C. Bis, G. W. Beecham, B. Grenier-Boley, G. Russo, T. A. Thorton-Wells, N. Jones, A. V. Smith, V. Chouraki, C. Thomas, M. A. Ikram, D. Zelenika, B. N. Vardarajan, Y. Kamatani, C. F. Lin, A. Gerrish, H. Schmidt, B. Kunkle, M. L. Dunstan, A. Ruiz, M. T. Bihoreau, S. H. Choi, C. Reitz, F. Pasquier, C. Cruchaga, D. Craig, N. Amin, C. Berr, O. L. Lopez, P. L. De Jager, V. Deramecourt, J. A. Johnston, D. Evans, S. Lovestone, L. Letenneur, F. J. Moron, D. C. Rubinsztein, G. Eiriksdottir, K. Sleegers, A. M. Goate, N. Fievet, M. W. Huentelman, M. Gill, K. Brown, M. I. Kamboh, L. Keller, P. Barberger-Gateau, B. McGuiness, E. B. Larson, R. Green, A. J. Myers, C. Dufouil, S. Todd, D. Wallon, S. Love, E. Rogaeva, J. Gallacher, P. St George-Hyslop, J. Clarimon, A. Lleo, A. Bayer, D. W. Tsuang, L. Yu, M. Tsolaki, P. Bossu, G. Spalletta, P. Proitsi, J. Collinge, S. Sorbi, F. Sanchez-Garcia, N. C. Fox, J. Hardy, M. C. Deniz Naranjo, P. Bosco, R. Clarke, C. Brayne, D. Galimberti, M. Mancuso, F. Matthews, I. European Alzheimer's Disease, Genetic, D. Environmental Risk in Alzheimer's, C. Alzheimer's Disease Genetic, H. Cohorts for, E. Aging Research in Genomic, S. Moebus, P. Mecocci, M. Del Zompo, W. Maier, H. Hampel, A. Pilotto, M. Bullido, F. Panza, P. Caffarra, B. Nacmias, J. R. Gilbert, M. Mayhaus, L. Lannefelt, H. Hakonarson, S. Pichler, M. M. Carrasquillo, M. Ingelsson, D. Beekly, V. Alvarez, F. Zou, O. Valladares, S. G. Younkin, E. Coto, K. L. Hamilton-Nelson, W. Gu, C. Razquin, P. Pastor, I. Mateo, M. J. Owen, K. M. Faber, P. V. Jonsson, O. Combarros, M. C. O'Donovan, L. B. Cantwell, H. Soininen, D. Blacker, S. Mead, T. H. Mosley, Jr., D. A. Bennett, T. B. Harris, L. Fratiglioni, C. Holmes, R. F. de Bruijn, P. Passmore, T. J. Montine, K. Bettens, J. I. Rotter, A. Brice, K. Morgan, T. M. Foroud, W. A. Kukull, D. Hannequin, J. F. Powell, M. A. Nalls, K. Ritchie, K. L. Lunetta, J. S. Kauwe, E. Boerwinkle, M. Riemenschneider, M. Boada, M. Hiltuenen, E. R. Martin, R. Schmidt, D. Rujescu, L. S. Wang, J. F. Dartigues, R. Mayeux, C. Tzourio, A. Hofman, M. M. Nothen, C. Graff, B. M. Psaty, L. Jones, J. L. Haines, P. A. Holmans, M. Lathrop, M. A. Pericak-Vance, L. J. Launer, L. A. Farrer, C. M. van Duijn, C. Van Broeckhoven, V. Moskvina, S. Seshadri, J. Williams, G. D. Schellenberg and P. Amouyel (2013). "Meta-analysis of 74,046 individuals identifies 11 new susceptibility loci for Alzheimer's disease." Nat Genet **45**(12): 1452-1458.

Lannfelt, L., H. Basun, L. O. Wahlund, B. A. Rowe and S. L. Wagner (1995). "Decreased alpha-secretase-cleaved amyloid precursor protein as a diagnostic marker for Alzheimer's disease." Nat Med **1**(8): 829-832.

Lassek, M., J. Weingarten, U. Einsfelder, P. Brendel, U. Muller and W. Volknandt (2013). "Amyloid precursor proteins are constituents of the presynaptic active zone." J Neurochem **127**(1): 48-56.

Lecoutey, C., D. Hedou, T. Freret, P. Giannoni, F. Gaven, M. Since, V. Bouet, C. Ballandonne, S. Corvaisier, A. Malzert Freon, S. Mignani, T. Cresteil, M. Boulouard, S. Claeysen, C. Rochais and P. Dallemagne (2014). "Design of donecopride, a dual serotonin subtype 4 receptor agonist/acetylcholinesterase inhibitor with potential interest for Alzheimer's disease treatment." Proc Natl Acad Sci U S A **111**(36): E3825-3830.

Lee, G., R. Thangavel, V. M. Sharma, J. M. Litersky, K. Bhaskar, S. M. Fang, L. H. Do, A. Andreadis, G. Van Hoesen and H. Ksiezak-Reding (2004). "Phosphorylation of tau by fyn: implications for Alzheimer's disease." J Neurosci **24**(9): 2304-2312.

Lee, K. J., C. E. Moussa, Y. Lee, Y. Sung, B. W. Howell, R. S. Turner, D. T. Pak and H. S. Hoe (2010). "Beta amyloid-independent role of amyloid precursor protein in generation and maintenance of dendritic spines." Neuroscience **169**(1): 344-356.

Lee, M. S., S. C. Kao, C. A. Lemere, W. Xia, H. C. Tseng, Y. Zhou, R. Neve, M. K. Ahlijanian and L. H. Tsai (2003). "APP processing is regulated by cytoplasmic phosphorylation." J Cell Biol **163**(1): 83-95.

Leinenga, G. and J. Gotz (2015). "Scanning ultrasound removes amyloid-beta and restores memory in an Alzheimer's disease mouse model." Sci Transl Med **7**(278): 278ra233.

Letenneur, L., D. Commenges, J. F. Dartigues and P. Barberger-Gateau (1994). "Incidence of dementia and Alzheimer's disease in elderly community residents of south-western France." Int J Epidemiol **23**(6): 1256-1261.

Levy, E., M. D. Carman, I. J. Fernandez-Madrid, M. D. Power, I. Lieberburg, S. G. van Duinen, G. T. Bots, W. Luyendijk and B. Frangione (1990). "Mutation of the Alzheimer's disease amyloid gene in hereditary cerebral hemorrhage, Dutch type." Science **248**(4959): 1124-1126.

Lewis, J., D. W. Dickson, W. L. Lin, L. Chisholm, A. Corral, G. Jones, S. H. Yen, N. Sahara, L. Skipper, D. Yager, C. Eckman, J. Hardy, M. Hutton and E. McGowan (2001). "Enhanced neurofibrillary degeneration in transgenic mice expressing mutant tau and APP." Science **293**(5534): 1487-1491.

Leyssen, M., D. Ayaz, S. S. Hebert, S. Reeve, B. De Strooper and B. A. Hassan (2005). "Amyloid precursor protein promotes post-developmental neurite arborization in the Drosophila brain." EMBO J **24**(16): 2944-2955.

Li, H., B. Wang, Z. Wang, Q. Guo, K. Tabuchi, R. E. Hammer, T. C. Sudhof and H. Zheng (2010). "Soluble amyloid precursor protein (APP) regulates transthyretin and Klotho gene expression without rescuing the essential function of APP." Proc Natl Acad Sci U S A **107**(40): 17362-17367.

Li, Z. W., G. Stark, J. Gotz, T. Rulicke, M. Gschwind, G. Huber, U. Muller and C. Weissmann (1996). "Generation of mice with a 200-kb amyloid precursor protein gene deletion by Cre recombinase-mediated site-specific recombination in embryonic stem cells." Proc Natl Acad Sci U S A **93**(12): 6158-6162.

Lindwall, G. and R. D. Cole (1984). "Phosphorylation affects the ability of tau protein to promote microtubule assembly." J Biol Chem **259**(8): 5301-5305.

Lisowski, L., S. S. Tay and I. E. Alexander (2015). "Adeno-associated virus serotypes for gene therapeutics." Curr Opin Pharmacol **24**: 59-67.

Liu, Q., C. V. Zerbinatti, J. Zhang, H. S. Hoe, B. Wang, S. L. Cole, J. Herz, L. Muglia and G. Bu (2007). "Amyloid precursor protein regulates brain apolipoprotein E and cholesterol metabolism through lipoprotein receptor LRP1." Neuron **56**(1): 66-78.

Lu, D. C., S. Soriano, D. E. Bredesen and E. H. Koo (2003). "Caspase cleavage of the amyloid precursor protein modulates amyloid beta-protein toxicity." J Neurochem **87**(3): 733-741.

Lyckman, A. W., A. M. Confaloni, G. Thinakaran, S. S. Sisodia and K. L. Moya (1998). "Post-translational processing and turnover kinetics of presynaptically targeted amyloid precursor superfamily proteins in the central nervous system." J Biol Chem **273**(18): 11100-11106.

Lynch, B. A., N. Lambeng, K. Nocka, P. Kensel-Hammes, S. M. Bajjalieh, A. Matagne and B. Fuks (2004). "The synaptic vesicle protein SV2A is the binding site for the antiepileptic drug levetiracetam." Proc Natl Acad Sci U S A **101**(26): 9861-9866.

Mackenzie, I. R., R. S. McLachlan, C. S. Kubu and L. A. Miller (1996). "Prospective neuropsychological assessment of nondemented patients with biopsy proven senile plaques." Neurology **46**(2): 425-429.

Magara, F., U. Muller, Z. W. Li, H. P. Lipp, C. Weissmann, M. Stagljar and D. P. Wolfer (1999). "Genetic background changes the pattern of forebrain commissure defects in transgenic mice underexpressing the beta-amyloid-precursor protein." Proc Natl Acad Sci U S A **96**(8): 4656-4661.

Mahley, R. W. (1988). "Apolipoprotein E: cholesterol transport protein with expanding role in cell biology." Science **240**(4852): 622-630.

Masliah, E., J. Raber, M. Alford, M. Mallory, M. P. Mattson, D. Yang, D. Wong and L. Mucke (1998). "Amyloid protein precursor stimulates excitatory amino acid transport. Implications for roles in neuroprotection and pathogenesis." J Biol Chem **273**(20): 12548-12554.

Masliah, E., C. E. Westland, E. M. Rockenstein, C. R. Abraham, M. Mallory, I. Veinberg, E. Sheldon and L. Mucke (1997). "Amyloid precursor proteins protect neurons of transgenic mice against acute and chronic excitotoxic injuries in vivo." Neuroscience **78**(1): 135-146.

Masters, C. L., G. Simms, N. A. Weinman, G. Multhaup, B. L. McDonald and K. Beyreuther (1985). "Amyloid plaque core protein in Alzheimer disease and Down syndrome." Proc Natl Acad Sci U S A **82**(12): 4245-4249.

Mattson, M. P., B. Cheng, A. R. Culwell, F. S. Esch, I. Lieberburg and R. E. Rydel (1993). "Evidence for excitoprotective and intraneuronal calcium-regulating roles for secreted forms of the beta-amyloid precursor protein." Neuron **10**(2): 243-254.

McGeer, P. L. and E. G. McGeer (2015). "Targeting microglia for the treatment of Alzheimer's disease." Expert Opin Ther Targets **19**(4): 497-506.

Menendez-Gonzalez, M., P. Perez-Pinera, M. Martinez-Rivera, M. T. Calatayud and B. Blazquez Menes (2005). "APP processing and the APP-KPI domain involvement in the amyloid cascade." Neurodegener Dis **2**(6): 277-283.

Mercken, M., M. Vandermeeren, U. Lubke, J. Six, J. Boons, A. Van de Voorde, J. J. Martin and J. Gheuens (1992). "Monoclonal antibodies with selective specificity for Alzheimer Tau are directed against phosphatase-sensitive epitopes." Acta Neuropathol **84**(3): 265-272.

Meziane, H., J. C. Dodart, C. Mathis, S. Little, J. Clemens, S. M. Paul and A. Ungerer (1998). "Memory-enhancing effects of secreted forms of the beta-amyloid precursor protein in normal and amnestic mice." Proc Natl Acad Sci U S A **95**(21): 12683-12688.

Milosch, N., G. Tanriover, A. Kundu, A. Rami, J. C. Francois, F. Baumkotter, S. W. Weyer, A. Samanta, A. Jaschke, F. Brod, C. J. Buchholz, S. Kins, C. Behl, U. C. Muller and D. Kogel (2014). "Holo-APP and G-protein-mediated signaling are required for sAPPalpha-induced activation of the Akt survival pathway." Cell Death Dis **5**: e1391.

Miners, J. S., N. Barua, P. G. Kehoe, S. Gill and S. Love (2011). "Abeta-degrading enzymes: potential for treatment of Alzheimer disease." J Neuropathol Exp Neurol **70**(11): 944-959.

Moechars, D., I. Dewachter, K. Lorent, D. Reverse, V. Baekelandt, A. Naidu, I. Tesseur, K. Spittaels, C. V. Haute, F. Checler, E. Godaux, B. Cordell and F. Van Leuven (1999). "Early phenotypic changes in transgenic mice that overexpress different mutants of amyloid precursor protein in brain." J Biol Chem **274**(10): 6483-6492.

Moechars, D., K. Lorent, B. De Strooper, I. Dewachter and F. Van Leuven (1996). "Expression in brain of amyloid precursor protein mutated in the alpha-secretase site causes disturbed behavior, neuronal degeneration and premature death in transgenic mice." EMBO J **15**(6): 1265-1274.

Moechars, D., K. Lorent, I. Dewachter, V. Baekelandt, B. De Strooper and F. Van Leuven (1998). "Transgenic mice expressing an alpha-secretion mutant of the amyloid precursor protein in the brain develop a progressive CNS disorder." Behav Brain Res **95**(1): 55-64.

Moir, R. D., T. Lynch, A. I. Bush, S. Whyte, A. Henry, S. Portbury, G. Multhaup, D. H. Small, R. E. Tanzi, K. Beyreuther and C. L. Masters (1998). "Relative increase in Alzheimer's disease of soluble forms of cerebral Abeta amyloid protein precursor containing the Kunitz protease inhibitory domain." J Biol Chem **273**(9): 5013-5019.

Monning, U., G. Konig, R. B. Banati, H. Mechler, C. Czech, J. Gehrmann, U. Schreiter-Gasser, C. L. Masters and K. Beyreuther (1992). "Alzheimer beta A4-amyloid protein precursor in immunocompetent cells." J Biol Chem **267**(33): 23950-23956.

Morishima-Kawashima, M., M. Hasegawa, K. Takio, M. Suzuki, H. Yoshida, A. Watanabe, K. Titani and Y. Ihara (1995). "Hyperphosphorylation of tau in PHF." Neurobiol Aging **16**(3): 365-371; discussion 371-380.

Mosconi, L., V. Berti, L. Glodzik, A. Pupi, S. De Santi and M. J. de Leon (2010). "Pre-clinical detection of Alzheimer's disease using FDG-PET, with or without amyloid imaging." J Alzheimers Dis **20**(3): 843-854.

Mucke, L., C. R. Abraham and E. Masliah (1996). "Neurotrophic and neuroprotective effects of hAPP in transgenic mice." Ann N Y Acad Sci **777**: 82-88.

Mucke, L., E. Masliah, G. Q. Yu, M. Mallory, E. M. Rockenstein, G. Tatsuno, K. Hu, D. Kholodenko, K. Johnson-Wood and L. McConlogue (2000). "High-level neuronal expression of abeta 1-42 in wild-type human amyloid protein precursor transgenic mice: synaptotoxicity without plaque formation." J Neurosci **20**(11): 4050-4058.

Muller, U., N. Cristina, Z. W. Li, D. P. Wolfer, H. P. Lipp, T. Rulicke, S. Brandner, A. Aguzzi and C. Weissmann (1994). "Behavioral and anatomical deficits in mice homozygous for a modified beta-amyloid precursor protein gene." Cell **79**(5): 755-765.

Muller, U., P. Winter and M. B. Graeber (2013). "A presenilin 1 mutation in the first case of Alzheimer's disease." Lancet Neurol **12**(2): 129-130.

Muller, U. C. and H. Zheng (2012). "Physiological functions of APP family proteins." Cold Spring Harb Perspect Med **2**(2): a006288.

Murakami, N., T. Yamaki, Y. Iwamoto, T. Sakakibara, N. Kobori, S. Fushiki and S. Ueda (1998). "Experimental brain injury induces expression of amyloid precursor protein, which may be related to neuronal loss in the hippocampus." J Neurotrauma **15**(11): 993-1003.

Musa, A., H. Lehrach and V. A. Russo (2001). "Distinct expression patterns of two zebrafish homologues of the human APP gene during embryonic development." Dev Genes Evol **211**(11): 563-567.

Nakamura, S., N. Murayama, T. Noshita, H. Annoura and T. Ohno (2001). "Progressive brain dysfunction following intracerebroventricular infusion of beta(1-42)-amyloid peptide." Brain Res **912**(2): 128-136.

Naus, S., S. Reipschlager, D. Wildeboer, S. F. Lichtenthaler, S. Mitterreiter, Z. Guan, M. L. Moss and J. W. Bartsch (2006). "Identification of candidate substrates for ectodomain shedding by the metalloprotease-disintegrin ADAM8." Biol Chem **387**(3): 337-346.

Nikolaev, A., T. McLaughlin, D. D. O'Leary and M. Tessier-Lavigne (2009). "APP binds DR6 to trigger axon pruning and neuron death via distinct caspases." Nature **457**(7232): 981-989.

Ninomiya, H., J. M. Roch, M. P. Sundsmo, D. A. Otero and T. Saitoh (1993). "Amino acid sequence RERMS represents the active domain of amyloid beta/A4 protein precursor that promotes fibroblast growth." J Cell Biol **121**(4): 879-886.

Nitsch, R. M., S. A. Farber, J. H. Growdon and R. J. Wurtman (1993). "Release of amyloid beta-protein precursor derivatives by electrical depolarization of rat hippocampal slices." Proc Natl Acad Sci U S A **90**(11): 5191-5193.

Nitsch, R. M., B. E. Slack, R. J. Wurtman and J. H. Growdon (1992). "Release of Alzheimer amyloid precursor derivatives stimulated by activation of muscarinic acetylcholine receptors." Science **258**(5080): 304-307.

O'Brien, R. J. and P. C. Wong (2011). "Amyloid precursor protein processing and Alzheimer's disease." Annu Rev Neurosci **34**: 185-204.

Obregon, D., H. Hou, J. Deng, B. Giunta, J. Tian, D. Darlington, M. Shahaduzzaman, Y. Zhu, T. Mori, M. P. Mattson and J. Tan (2012). "Soluble amyloid precursor protein-alpha modulates beta-secretase activity and amyloid-beta generation." Nat Commun **3**: 777.

Octave, J. N., N. Pierrot, S. Ferao Santos, N. N. Nalivaeva and A. J. Turner (2013). "From synaptic spines to nuclear signaling: nuclear and synaptic actions of the amyloid precursor protein." J Neurochem **126**(2): 183-190.

Olsson, A., K. Hoglund, M. Sjogren, N. Andreasen, L. Minthon, L. Lannfelt, K. Buerger, H. J. Moller, H. Hampel, P. Davidsson and K. Blennow (2003). "Measurement of alpha- and beta-secretase cleaved amyloid precursor protein in cerebrospinal fluid from Alzheimer patients." Exp Neurol **183**(1): 74-80.

Palmert, M. R., M. B. Podlisny, T. E. Golde, M. L. Cohen, D. M. Kovacs, R. E. Tanzi, J. F. Gusella, P. J. Whitehouse, D. S. Witker, T. Oltersdorf and et al. (1989). "The beta amyloid protein precursor: mRNAs, membrane-associated forms, and soluble derivatives." Prog Clin Biol Res **317**: 971-984.

Palmert, M. R., M. Usiak, R. Mayeux, M. Raskind, W. W. Tourtellotte and S. G. Younkin (1990). "Soluble derivatives of the beta amyloid protein precursor in cerebrospinal fluid: alterations in normal aging and in Alzheimer's disease." Neurology **40**(7): 1028-1034.

Pangalos, M. N., J. Shioi and N. K. Robakis (1995). "Expression of the chondroitin sulfate proteoglycans of amyloid precursor (appican) and amyloid precursor-like protein 2." J Neurochem **65**(2): 762-769.

Pardossi-Piquard, R., A. Petit, T. Kawarai, C. Sunyach, C. Alves da Costa, B. Vincent, S. Ring, L. D'Adamio, J. Shen, U. Muller, P. St George Hyslop and F. Checler (2005). "Presenilin-dependent transcriptional control of the Abeta-degrading enzyme neprilysin by intracellular domains of betaAPP and APLP." Neuron **46**(4): 541-554.

Park, S. A., G. M. Shaked, D. E. Bredesen and E. H. Koo (2009). "Mechanism of cytotoxicity mediated by the C31 fragment of the amyloid precursor protein." Biochem Biophys Res Commun **388**(2): 450-455.

Payami, H., S. Zareparsi, K. R. Montee, G. J. Sexton, J. A. Kaye, T. D. Bird, C. E. Yu, E. M. Wijsman, L. L. Heston, M. Litt and G. D. Schellenberg (1996). "Gender difference in apolipoprotein E-associated risk for familial Alzheimer disease: a possible clue to the higher incidence of Alzheimer disease in women." Am J Hum Genet **58**(4): 803-811.

Perdahl, E., R. Adolfsson, I. Alafuzoff, K. A. Albert, E. J. Nestler, P. Greengard and B. Winblad (1984). "Synapsin I (protein I) in different brain regions in senile dementia of Alzheimer type and in multi-infarct dementia." J Neural Transm **60**(2): 133-141.

Perez-Nievas, B. G., T. D. Stein, H. C. Tai, O. Dols-Icardo, T. C. Scotton, I. Barroeta-Espar, L. Fernandez-Carballo, E. L. de Munain, J. Perez, M. Marquie, A. Serrano-Pozo, M. P. Frosch, V. Lowe, J. E. Parisi, R. C. Petersen, M. D. Ikonomovic, O. L. Lopez, W. Klunk, B. T. Hyman and T. Gomez-Isla (2013). "Dissecting phenotypic traits linked to human resilience to Alzheimer's pathology." Brain **136**(Pt 8): 2510-2526.

Perez, R. G., H. Zheng, L. H. Van der Ploeg and E. H. Koo (1997). "The beta-amyloid precursor protein of Alzheimer's disease enhances neuron viability and modulates neuronal polarity." J Neurosci **17**(24): 9407-9414.

Pitas, R. E., J. K. Boyles, S. H. Lee, D. Foss and R. W. Mahley (1987). "Astrocytes synthesize apolipoprotein E and metabolize apolipoprotein E-containing lipoproteins." Biochim Biophys Acta **917**(1): 148-161.

Postina, R., A. Schroeder, I. Dewachter, J. Bohl, U. Schmitt, E. Kojro, C. Prinzen, K. Endres, C. Hiemke, M. Blessing, P. Flamez, A. Dequenne, E. Godaux, F. van Leuven and F. Fahrenholz (2004). "A disintegrin-metalloproteinase prevents amyloid plaque formation and hippocampal defects in an Alzheimer disease mouse model." J Clin Invest **113**(10): 1456-1464.

Prinzen, C., D. Trumbach, W. Wurst, K. Endres, R. Postina and F. Fahrenholz (2009). "Differential gene expression in ADAM10 and mutant ADAM10 transgenic mice." BMC Genomics **10**: 66.

Prokop, S., K. R. Miller and F. L. Heppner (2013). "Microglia actions in Alzheimer's disease." Acta Neuropathol **126**(4): 461-477.

Prox, J., C. Bernreuther, H. Altmeppen, J. Grendel, M. Glatzel, R. D'Hooge, S. Stroobants, T. Ahmed, D. Balschun, M. Willem, S. Lammich, D. Isbrandt, M. Schweizer, K. Horre, B. De Strooper and P. Saftig (2013). "Postnatal disruption of the disintegrin/metalloproteinase ADAM10 in brain causes epileptic seizures, learning deficits, altered spine morphology, and defective synaptic functions." J Neurosci **33**(32): 12915-12928, 12928a.

Prox, J., A. Rittger and P. Saftig (2012). "Physiological functions of the amyloid precursor protein secretases ADAM10, BACE1, and presenilin." Exp Brain Res **217**(3-4): 331-341.

Qian, X., B. Hamad and G. Dias-Lalcaca (2015). "The Alzheimer disease market." Nat Rev Drug Discov **14**(10): 675-676.

Qiu, W. Q., A. Ferreira, C. Miller, E. H. Koo and D. J. Selkoe (1995). "Cell-surface beta-amyloid precursor protein stimulates neurite outgrowth of hippocampal neurons in an isoform-dependent manner." J Neurosci **15**(3 Pt 2): 2157-2167.

Quitschke, W. W. and D. Goldgaber (1992). "The amyloid beta-protein precursor promoter. A region essential for transcriptional activity contains a nuclear factor binding domain." J Biol Chem **267**(24): 17362-17368.

Ramaroson, H., C. Helmer, P. Barberger-Gateau, L. Letenneur, J. F. Dartigues and Paquid (2003). "[Prevalence of dementia and Alzheimer's disease among subjects aged 75 years or over: updated results of the PAQUID cohort]." Rev Neurol (Paris) **159**(4): 405-411.

Ramirez, M. J., K. E. Heslop, P. T. Francis and M. Rattray (2001). "Expression of amyloid precursor protein, tau and presenilin RNAs in rat hippocampus following deafferentation lesions." Brain Res **907**(1-2): 222-232.

Reiss, K., T. Maretzky, I. G. Haas, M. Schulte, A. Ludwig, M. Frank and P. Saftig (2006). "Regulated ADAM10-dependent ectodomain shedding of gamma-protocadherin C3 modulates cell-cell adhesion." J Biol Chem **281**(31): 21735-21744.

Riedel, B. C., P. M. Thompson and R. D. Brinton (2016). "Age, APOE and Sex: Triad of Risk of Alzheimer's Disease." J Steroid Biochem Mol Biol.

Ring, S., S. W. Weyer, S. B. Kilian, E. Waldron, C. U. Pietrzik, M. A. Filippov, J. Herms, C. Buchholz, C. B. Eckman, M. Korte, D. P. Wolfer and U. C. Muller (2007). "The secreted beta-amyloid precursor protein ectodomain APPs alpha is sufficient to rescue the anatomical, behavioral, and electrophysiological abnormalities of APP-deficient mice." J Neurosci **27**(29): 7817-7826.

Ringman, J. M., A. Goate, C. L. Masters, N. J. Cairns, A. Danek, N. Graff-Radford, B. Ghetti, J. C. Morris and N. Dominantly Inherited Alzheimer (2014). "Genetic heterogeneity in Alzheimer disease and implications for treatment strategies." Curr Neurol Neurosci Rep **14**(11): 499.

Rissman, R. A., W. W. Poon, M. Blurton-Jones, S. Oddo, R. Torp, M. P. Vitek, F. M. LaFerla, T. T. Rohn and C. W. Cotman (2004). "Caspase-cleavage of tau is an early event in Alzheimer disease tangle pathology." J Clin Invest **114**(1): 121-130.

Robakis, N. K., N. Ramakrishna, G. Wolfe and H. M. Wisniewski (1987). "Molecular cloning and characterization of a cDNA encoding the cerebrovascular and the neuritic plaque amyloid peptides." Proc Natl Acad Sci U S A **84**(12): 4190-4194.

Roberson, E. D., B. Halabisky, J. W. Yoo, J. Yao, J. Chin, F. Yan, T. Wu, P. Hamto, N. Devidze, G. Q. Yu, J. J. Palop, J. L. Noebels and L. Mucke (2011). "Amyloid-beta/Fyn-induced synaptic, network, and cognitive impairments depend on tau levels in multiple mouse models of Alzheimer's disease." J Neurosci **31**(2): 700-711.

Robert, S. J., J. L. Zugaza, R. Fischmeister, A. M. Gardier and F. Lezoualc'h (2001). "The human serotonin 5-HT4 receptor regulates secretion of non-amyloidogenic precursor protein." J Biol Chem **276**(48): 44881-44888.

Roch, J. M., E. Masliah, A. C. Roch-Levecq, M. P. Sundsmo, D. A. Otero, I. Veinbergs and T. Saitoh (1994). "Increase of synaptic density and memory retention by a peptide representing the trophic domain of the amyloid beta/A4 protein precursor." Proc Natl Acad Sci U S A **91**(16): 7450-7454.

Rochais, C., C. Lecoutey, F. Gaven, P. Giannoni, K. Hamidouche, D. Hedou, E. Dubost, D. Genest, S. Yahiaoui, T. Freret, V. Bouet, F. Dauphin, J. Sopkova de Oliveira Santos, C. Ballandonne, S. Corvaisier, A. Malzert-Freon, R. Legay, M. Boulouard, S. Claeysen and P. Dallemagne (2015). "Novel multitarget-directed ligands (MTDLs) with acetylcholinesterase (AChE) inhibitory and serotonergic subtype 4 receptor (5-HT4R) agonist activities as potential agents against Alzheimer's disease: the design of donecopride." J Med Chem **58**(7): 3172-3187.

Roozendaal, B., R. G. Phillips, A. E. Power, S. M. Brooke, R. M. Sapolsky and J. L. McGaugh (2001). "Memory retrieval impairment induced by hippocampal CA3 lesions is blocked by adrenocortical suppression." Nat Neurosci **4**(12): 1169-1171.

Rosen, D. R., L. Martin-Morris, L. Q. Luo and K. White (1989). "A Drosophila gene encoding a protein resembling the human beta-amyloid protein precursor." Proc Natl Acad Sci U S A **86**(7): 2478-2482.

Rovelet-Lecrux, A., D. Hannequin, G. Raux, N. Le Meur, A. Laquerriere, A. Vital, C. Dumanchin, S. Feuillette, A. Brice, M. Vercelletto, F. Dubas, T. Frebourg and D. Campion (2006). "APP locus duplication causes autosomal dominant early-onset Alzheimer disease with cerebral amyloid angiopathy." Nat Genet **38**(1): 24-26.

Rupp, C., K. Beyreuther, K. Maurer and S. Kins (2014). "A presenilin 1 mutation in the first case of Alzheimer's disease: revisited." Alzheimers Dement **10**(6): 869-872.

Saito, T., Y. Matsuba, N. Mihira, J. Takano, P. Nilsson, S. Itohara, N. Iwata and T. C. Saido (2014). "Single App knock-in mouse models of Alzheimer's disease." Nat Neurosci **17**(5): 661-663.

Saitoh, T., M. Sundsmo, J. M. Roch, N. Kimura, G. Cole, D. Schubert, T. Oltersdorf and D. B. Schenk (1989). "Secreted form of amyloid beta protein precursor is involved in the growth regulation of fibroblasts." Cell **58**(4): 615-622.

Sakae, N., C. C. Liu, M. Shinohara, J. Frisch-Daiello, L. Ma, Y. Yamazaki, M. Tachibana, L. Younkin, A. Kurti, M. M. Carrasquillo, F. Zou, D. Sevlever, G. Bisceglio, M. Gan, R. Fol, P. Knight, M. Wang, X. Han, J. D. Fryer, M. L. Fitzgerald, Y. Ohyagi, S. G. Younkin, G. Bu and T. Kanekiyo (2016). "ABCA7 Deficiency Accelerates Amyloid-beta Generation and Alzheimer's Neuronal Pathology." J Neurosci **36**(13): 3848-3859.

Salbaum, J. M., A. Weidemann, H. G. Lemaire, C. L. Masters and K. Beyreuther (1988). "The promoter of Alzheimer's disease amyloid A4 precursor gene." EMBO J **7**(9): 2807-2813.

Sanchez, P. E., L. Zhu, L. Verret, K. A. Vossel, A. G. Orr, J. R. Cirrito, N. Devidze, K. Ho, G. Q. Yu, J. J. Palop and L. Mucke (2012). "Levetiracetam suppresses neuronal network dysfunction and reverses synaptic and cognitive deficits in an Alzheimer's disease model." Proc Natl Acad Sci U S A **109**(42): E2895-2903.

Sastre, M., H. Steiner, K. Fuchs, A. Capell, G. Multhaup, M. M. Condron, D. B. Teplow and C. Haass (2001). "Presenilin-dependent gamma-secretase processing of beta-amyloid precursor protein at a site corresponding to the S3 cleavage of Notch." EMBO Rep **2**(9): 835-841.

Scandura, J. M., Y. Zhang, W. E. Van Nostrand and P. N. Walsh (1997). "Progress curve analysis of the kinetics with which blood coagulation factor XIa is inhibited by protease nexin-2." Biochemistry **36**(2): 412-420.

Scheff, S. W., S. T. DeKosky and D. A. Price (1990). "Quantitative assessment of cortical synaptic density in Alzheimer's disease." Neurobiol Aging **11**(1): 29-37.

Scheff, S. W., D. A. Price, F. A. Schmitt and E. J. Mufson (2006). "Hippocampal synaptic loss in early Alzheimer's disease and mild cognitive impairment." Neurobiol Aging **27**(10): 1372-1384.

Scheltens, P., K. Blennow, M. M. Breteler, B. de Strooper, G. B. Frisoni, S. Salloway and W. M. Van der Flier (2016). "Alzheimer's disease." Lancet.

Scheuner, D., C. Eckman, M. Jensen, X. Song, M. Citron, N. Suzuki, T. D. Bird, J. Hardy, M. Hutton, W. Kukull, E. Larson, E. Levy-Lahad, M. Viitanen, E. Peskind, P. Poorkaj, G. Schellenberg, R. Tanzi, W. Wasco, L. Lannfelt, D. Selkoe and S. Younkin (1996). "Secreted amyloid beta-protein similar to that in the senile plaques of Alzheimer's disease is increased in vivo by the presenilin 1 and 2 and APP mutations linked to familial Alzheimer's disease." Nat Med **2**(8): 864-870.

Schindowski, K., A. Bretteville, K. Leroy, S. Begard, J. P. Brion, M. Hamdane and L. Buee (2006). "Alzheimer's disease-like tau neuropathology leads to memory deficits and loss of functional synapses in a novel mutated tau transgenic mouse without any motor deficits." Am J Pathol **169**(2): 599-616.

Schmaier, A. H., L. D. Dahl, A. J. Rozemuller, R. A. Roos, S. L. Wagner, R. Chung and W. E. Van Nostrand (1993). "Protease nexin-2/amyloid beta protein precursor. A tight-binding inhibitor of coagulation factor IXa." J Clin Invest **92**(5): 2540-2545.

Schwartz, P., J. Kurucz and A. Kurucz (1964). "RECENT OBSERVATIONS ON SENILE CEREBRAL CHANGES AND THEIR PATHOGENESIS." Journal of the American Geriatrics Society **12**(10): 908-922.

Seabrook, G. R., D. W. Smith, B. J. Bowery, A. Easter, T. Reynolds, S. M. Fitzjohn, R. A. Morton, H. Zheng, G. R. Dawson, D. J. Sirinathsinghji, C. H. Davies, G. L. Collingridge and R. G. Hill (1999). "Mechanisms contributing to the deficits in hippocampal synaptic plasticity in mice lacking amyloid precursor protein." Neuropharmacology **38**(3): 349-359.

Selkoe, D. J. (2002). "Alzheimer's disease is a synaptic failure." Science **298**(5594): 789-791.

Selkoe, D. J. and J. Hardy (2016). "The amyloid hypothesis of Alzheimer's disease at 25 years." EMBO Mol Med.

Senechal, Y., P. H. Kelly and K. K. Dev (2008). "Amyloid precursor protein knockout mice show age-dependent deficits in passive avoidance learning." Behav Brain Res **186**(1): 126-132.

Serrano-Pozo, A., M. P. Frosch, E. Masliah and B. T. Hyman (2011). "Neuropathological alterations in Alzheimer disease." Cold Spring Harb Perspect Med **1**(1): a006189.

Shankar, G. M., S. Li, T. H. Mehta, A. Garcia-Munoz, N. E. Shepardson, I. Smith, F. M. Brett, M. A. Farrell, M. J. Rowan, C. A. Lemere, C. M. Regan, D. M. Walsh, B. L. Sabatini and D. J. Selkoe (2008). "Amyloid-beta protein dimers isolated directly from Alzheimer's brains impair synaptic plasticity and memory." Nat Med **14**(8): 837-842.

Shankar, G. M. and D. M. Walsh (2009). "Alzheimer's disease: synaptic dysfunction and Abeta." Mol Neurodegener **4**: 48.

Shao, Y., M. Gearing and S. S. Mirra (1997). "Astrocyte-apolipoprotein E associations in senile plaques in Alzheimer disease and vascular lesions: a regional immunohistochemical study." J Neuropathol Exp Neurol **56**(4): 376-381.

Simon, A. M., L. Schiapparelli, P. Salazar-Colocho, M. Cuadrado-Tejedor, L. Escribano, R. Lopez de Maturana, J. Del Rio, A. Perez-Mediavilla and D. Frechilla (2009). "Overexpression of wild-type human APP in mice causes cognitive deficits and pathological features unrelated to Abeta levels." Neurobiol Dis **33**(3): 369-378.

Slunt, H. H., G. Thinakaran, C. Von Koch, A. C. Lo, R. E. Tanzi and S. S. Sisodia (1994). "Expression of a ubiquitous, cross-reactive homologue of the mouse beta-amyloid precursor protein (APP)." J Biol Chem **269**(4): 2637-2644.

Small, D. H., V. Nurcombe, G. Reed, H. Clarris, R. Moir, K. Beyreuther and C. L. Masters (1994). "A heparin-binding domain in the amyloid protein precursor of Alzheimer's disease is involved in the regulation of neurite outgrowth." J Neurosci **14**(4): 2117-2127.

Smith-Swintosky, V. L., L. C. Pettigrew, S. D. Craddock, A. R. Culwell, R. E. Rydel and M. P. Mattson (1994). "Secreted forms of beta-amyloid precursor protein protect against ischemic brain injury." J Neurochem **63**(2): 781-784.

Smith, R. P., D. A. Higuchi and G. J. Broze, Jr. (1990). "Platelet coagulation factor XIa-inhibitor, a form of Alzheimer amyloid precursor protein." Science **248**(4959): 1126-1128.

Snyder, E. M., Y. Nong, C. G. Almeida, S. Paul, T. Moran, E. Y. Choi, A. C. Nairn, M. W. Salter, P. J. Lombroso, G. K. Gouras and P. Greengard (2005). "Regulation of NMDA receptor trafficking by amyloid-beta." Nat Neurosci **8**(8): 1051-1058.

Soba, P., S. Eggert, K. Wagner, H. Zentgraf, K. Siehl, S. Kreger, A. Lower, A. Langer, G. Merdes, R. Paro, C. L. Masters, U. Muller, S. Kins and K. Beyreuther (2005). "Homo- and heterodimerization of APP family members promotes intercellular adhesion." EMBO J **24**(20): 3624-3634.

Suh, J., S. H. Choi, D. M. Romano, M. A. Gannon, A. N. Lesinski, D. Y. Kim and R. E. Tanzi (2013). "ADAM10 missense mutations potentiate beta-amyloid accumulation by impairing prodomain chaperone function." Neuron **80**(2): 385-401.

Suzuki, K., Y. Hayashi, S. Nakahara, H. Kumazaki, J. Prox, K. Horiuchi, M. Zeng, S. Tanimura, Y. Nishiyama, S. Osawa, A. Sehara-Fujisawa, P. Saftig, S. Yokoshima, T. Fukuyama, N. Matsuki, R. Koyama, T. Tomita and T. Iwatsubo (2012). "Activity-dependent proteolytic cleavage of neuroligin-1." Neuron **76**(2): 410-422.

Suzuki, T. and T. Nakaya (2008). "Regulation of amyloid beta-protein precursor by phosphorylation and protein interactions." J Biol Chem **283**(44): 29633-29637.

Sweatt, J. D. (2016). "Neural Plasticity & Behavior - Sixty Years of Conceptual Advances." J Neurochem.

Talbot, K., H. Y. Wang, H. Kazi, L. Y. Han, K. P. Bakshi, A. Stucky, R. L. Fuino, K. R. Kawaguchi, A. J. Samoyedny, R. S. Wilson, Z. Arvanitakis, J. A. Schneider, B. A. Wolf, D. A. Bennett, J. Q. Trojanowski and S. E. Arnold (2012). "Demonstrated brain insulin resistance in Alzheimer's disease patients is associated with IGF-1 resistance, IRS-1 dysregulation, and cognitive decline." J Clin Invest **122**(4): 1316-1338.

Tanabe, C., N. Hotoda, N. Sasagawa, A. Sehara-Fujisawa, K. Maruyama and S. Ishiura (2007). "ADAM19 is tightly associated with constitutive Alzheimer's disease APP alpha-secretase in A172 cells." Biochem Biophys Res Commun **352**(1): 111-117.

Tang, Y. and W. Le (2016). "Differential Roles of M1 and M2 Microglia in Neurodegenerative Diseases." Mol Neurobiol **53**(2): 1181-1194.

Tanzi, R. E., J. F. Gusella, P. C. Watkins, G. A. Bruns, P. St George-Hyslop, M. L. Van Keuren, D. Patterson, S. Pagan, D. M. Kurnit and R. L. Neve (1987). "Amyloid beta protein gene: cDNA, mRNA distribution, and genetic linkage near the Alzheimer locus." Science **235**(4791): 880-884.

Taylor, C. J., D. R. Ireland, I. Ballagh, K. Bourne, N. M. Marechal, P. R. Turner, D. K. Bilkey, W. P. Tate and W. C. Abraham (2008). "Endogenous secreted amyloid precursor protein-alpha regulates hippocampal NMDA receptor function, long-term potentiation and spatial memory." Neurobiol Dis **31**(2): 250-260.

Terry, R. D., E. Masliah, D. P. Salmon, N. Butters, R. DeTeresa, R. Hill, L. A. Hansen and R. Katzman (1991). "Physical basis of cognitive alterations in Alzheimer's disease: synapse loss is the major correlate of cognitive impairment." Ann Neurol **30**(4): 572-580.

Thakker, D. R., M. R. Weatherspoon, J. Harrison, T. E. Keene, D. S. Lane, W. F. Kaemmerer, G. R. Stewart and L. L. Shafer (2009). "Intracerebroventricular amyloid-beta antibodies reduce cerebral amyloid angiopathy and associated micro-hemorrhages in aged Tg2576 mice." Proc Natl Acad Sci U S A **106**(11): 4501-4506.

Thal, D. R., U. Rub, M. Orantes and H. Braak (2002). "Phases of A beta-deposition in the human brain and its relevance for the development of AD." Neurology **58**(12): 1791-1800.

Thompson, P. M., K. M. Hayashi, G. I. De Zubicaray, A. L. Janke, S. E. Rose, J. Semple, M. S. Hong, D. H. Herman, D. Gravano, D. M. Doddrell and A. W. Toga (2004). "Mapping hippocampal and ventricular change in Alzheimer disease." Neuroimage **22**(4): 1754-1766.

Thornton, E., R. Vink, P. C. Blumbergs and C. Van Den Heuvel (2006). "Soluble amyloid precursor protein alpha reduces neuronal injury and improves functional outcome following diffuse traumatic brain injury in rats." Brain Res **1094**(1): 38-46.

Tomiyama, T., S. Matsuyama, H. Iso, T. Umeda, H. Takuma, K. Ohnishi, K. Ishibashi, R. Teraoka, N. Sakama, T. Yamashita, K. Nishitsuji, K. Ito, H. Shimada, M. P. Lambert, W. L. Klein and H. Mori (2010). "A mouse model of amyloid beta oligomers: their contribution to synaptic alteration, abnormal tau phosphorylation, glial activation, and neuronal loss in vivo." J Neurosci **30**(14): 4845-4856.

Tosto, G. and C. Reitz (2013). "Genome-wide association studies in Alzheimer's disease: a review." Curr Neurol Neurosci Rep **13**(10): 381.

Tremblay, M. E., B. Stevens, A. Sierra, H. Wake, A. Bessis and A. Nimmerjahn (2011). "The role of microglia in the healthy brain." J Neurosci **31**(45): 16064-16069.

Tuszynski, M. H., L. Thal, M. Pay, D. P. Salmon, H. S. U, R. Bakay, P. Patel, A. Blesch, H. L. Vahlsing, G. Ho, G. Tong, S. G. Potkin, J. Fallon, L. Hansen, E. J. Mufson, J. H. Kordower, C. Gall and J. Conner (2005). "A phase 1 clinical trial of nerve growth factor gene therapy for Alzheimer disease." Nat Med **11**(5): 551-555.

Ulland, T. K., Y. Wang and M. Colonna (2015). "Regulation of microglial survival and proliferation in health and diseases." Semin Immunol **27**(6): 410-415.

Underwood, E. (2015). "NEUROSCIENCE. Alzheimer's amyloid theory gets modest boost." Science **349**(6247): 464.

Urakami, K., K. Takahashi, H. Saito, A. Okada, S. Nakamura, S. Tanaka, N. Kitaguchi, Y. Tokushima and S. Yamamoto (1992). "Amyloid beta protein precursors with kunitz-type inhibitor domains and acetylcholinesterase in cerebrospinal fluid from patients with dementia of the Alzheimer type." Acta Neurol Scand **85**(5): 343-346.

Urani, A., P. Romieu, F. J. Roman, K. Yamada, Y. Noda, H. Kamei, H. Manh Tran, T. Nagai, T. Nabeshima and T. Maurice (2004). "Enhanced antidepressant efficacy of sigma1 receptor agonists in rats after chronic intracerebroventricular infusion of beta-amyloid-(1-40) protein." Eur J Pharmacol **486**(2): 151-161.

Van den Heuvel, C., P. C. Blumbergs, J. W. Finnie, J. Manavis, N. R. Jones, P. L. Reilly and R. A. Pereira (1999). "Upregulation of amyloid precursor protein messenger RNA in response to traumatic brain injury: an ovine head impact model." Exp Neurol **159**(2): 441-450.

Van Nostrand, W. E., A. H. Schmaier, J. S. Farrow, D. B. Cines and D. D. Cunningham (1991). "Protease nexin-2/amyloid beta-protein precursor in blood is a platelet-specific protein." Biochem Biophys Res Commun **175**(1): 15-21.

Van Nostrand, W. E., A. H. Schmaier, J. S. Farrow and D. D. Cunningham (1990). "Protease nexin-II (amyloid beta-protein precursor): a platelet alpha-granule protein." Science **248**(4956): 745-748.

Vassar, P. S. and C. F. Culling (1959). "Fluorescent stains, with special reference to amyloid and connective tissues." Arch Pathol **68**: 487-498.

Villemagne, V. L., S. Burnham, P. Bourgeat, B. Brown, K. A. Ellis, O. Salvado, C. Szoeke, S. L. Macaulay, R. Martins, P. Maruff, D. Ames, C. C. Rowe, C. L. Masters, B. Australian Imaging and G. Lifestyle Research (2013). "Amyloid beta deposition, neurodegeneration, and cognitive decline in sporadic Alzheimer's disease: a prospective cohort study." Lancet Neurol **12**(4): 357-367.

Volianskis, A., R. Kostner, M. Molgaard, S. Hass and M. S. Jensen (2010). "Episodic memory deficits are not related to altered glutamatergic synaptic transmission and plasticity in the CA1 hippocampus of the APPswe/PS1deltaE9-deleted transgenic mice model of ss-amyloidosis." Neurobiol Aging **31**(7): 1173-1187.

von Rotz, R. C., B. M. Kohli, J. Bosset, M. Meier, T. Suzuki, R. M. Nitsch and U. Konietzko (2004). "The APP intracellular domain forms nuclear multiprotein complexes and regulates the transcription of its own precursor." J Cell Sci **117**(Pt 19): 4435-4448.

Wang, Y., M. Cella, K. Mallinson, J. D. Ulrich, K. L. Young, M. L. Robinette, S. Gilfillan, G. M. Krishnan, S. Sudhakar, B. H. Zinselmeyer, D. M. Holtzman, J. R. Cirrito and M. Colonna (2015). "TREM2 lipid sensing sustains the microglial response in an Alzheimer's disease model." Cell **160**(6): 1061-1071.

Wang, Y. and Y. Ha (2004). "The X-ray structure of an antiparallel dimer of the human amyloid precursor protein E2 domain." Mol Cell **15**(3): 343-353.

Wang, Y., F. Wu, H. Pan, W. Zheng, C. Feng, Y. Wang, Z. Deng, L. Wang, J. Luo and S. Chen (2016). "Lost region in amyloid precursor protein (APP) through TALEN-mediated genome editing alters mitochondrial morphology." Sci Rep **6**: 22244.

Wang, Z., B. Wang, L. Yang, Q. Guo, N. Aithmitti, Z. Songyang and H. Zheng (2009). "Presynaptic and postsynaptic interaction of the amyloid precursor protein promotes peripheral and central synaptogenesis." J Neurosci **29**(35): 10788-10801.

Wasco, W., K. Bupp, M. Magendantz, J. F. Gusella, R. E. Tanzi and F. Solomon (1992). "Identification of a mouse brain cDNA that encodes a protein related to the Alzheimer disease-associated amyloid beta protein precursor." Proc Natl Acad Sci U S A **89**(22): 10758-10762.

Wasco, W., S. Gurubhagavatula, M. D. Paradis, D. M. Romano, S. S. Sisodia, B. T. Hyman, R. L. Neve and R. E. Tanzi (1993). "Isolation and characterization of APLP2 encoding a homologue of the Alzheimer's associated amyloid beta protein precursor." Nat Genet **5**(1): 95-100.

Wegiel, J., C. X. Gong and Y. W. Hwang (2011). "The role of DYRK1A in neurodegenerative diseases." FEBS J **278**(2): 236-245.

Weingarten, M. D., A. H. Lockwood, S. Y. Hwo and M. W. Kirschner (1975). "A protein factor essential for microtubule assembly." Proc Natl Acad Sci U S A **72**(5): 1858-1862.

Weyer, S. W., M. Klevanski, A. Delekate, V. Voikar, D. Aydin, M. Hick, M. Filippov, N. Drost, K. L. Schaller, M. Saar, M. A. Vogt, P. Gass, A. Samanta, A. Jaschke, M. Korte, D. P. Wolfer, J. H. Caldwell and U. C. Muller (2011). "APP and APLP2 are essential at PNS and CNS synapses for transmission, spatial learning and LTP." EMBO J **30**(11): 2266-2280.

Weyer, S. W., M. Zagrebelsky, U. Herrmann, M. Hick, L. Ganss, J. Gobbert, M. Gruber, C. Altmann, M. Korte, T. Deller and U. C. Muller (2014). "Comparative analysis of single and combined APP/APLP knockouts reveals reduced spine density in APP-KO mice that is prevented by APPsalpha expression." Acta Neuropathol Commun **2**: 36.

Willem, M., S. Tahirovic, M. A. Busche, S. V. Ovsepian, M. Chafai, S. Kootar, D. Hornburg, L. D. Evans, S. Moore, A. Daria, H. Hampel, V. Muller, C. Giudici, B. Nuscher, A. Wenninger-Weinzierl, E. Kremmer, M. T. Heneka, D. R. Thal, V. Giedraitis, L. Lannfelt, U. Muller, F. J. Livesey, F. Meissner, J. Herms, A. Konnerth, H. Marie and C. Haass (2015). "eta-Secretase processing of APP inhibits neuronal activity in the hippocampus." Nature **526**(7573): 443-447.

Wood, J. G., S. S. Mirra, N. J. Pollock and L. I. Binder (1986). "Neurofibrillary tangles of Alzheimer disease share antigenic determinants with the axonal microtubule-associated protein tau (tau)." Proc Natl Acad Sci U S A **83**(11): 4040-4043.

Xu, F., J. Davis, J. Miao, M. L. Previti, G. Romanov, K. Ziegler and W. E. Van Nostrand (2005). "Protease nexin-2/amyloid beta-protein precursor limits cerebral thrombosis." Proc Natl Acad Sci U S A **102**(50): 18135-18140.

Xu, F., M. L. Previti and W. E. Van Nostrand (2007). "Increased severity of hemorrhage in transgenic mice expressing cerebral protease nexin-2/amyloid beta-protein precursor." Stroke **38**(9): 2598-2601.

Xu, Y., H. S. Kim, Y. Joo, Y. Choi, K. A. Chang, C. H. Park, K. Y. Shin, S. Kim, Y. H. Cheon, T. K. Baik, J. H. Kim and Y. H. Suh (2007). "Intracellular domains of amyloid precursor-like protein 2 interact with CP2 transcription factor in the nucleus and induce glycogen synthase kinase-3beta expression." Cell Death Differ **14**(1): 79-91.

Yamada, M. (2015). "Cerebral amyloid angiopathy: emerging concepts." J Stroke **17**(1): 17-30.

Yang, F., X. Sun, W. Beech, B. Teter, S. Wu, J. Sigel, H. V. Vinters, S. A. Frautschy and G. M. Cole (1998). "Antibody to caspase-cleaved actin detects apoptosis in differentiated neuroblastoma and plaque-associated neurons and microglia in Alzheimer's disease." Am J Pathol **152**(2): 379-389.

Yang, Z., B. H. Cool, G. M. Martin and Q. Hu (2006). "A dominant role for FE65 (APBB1) in nuclear signaling." J Biol Chem **281**(7): 4207-4214.

Yao, Z. X. and V. Papadopoulos (2002). "Function of beta-amyloid in cholesterol transport: a lead to neurotoxicity." FASEB J **16**(12): 1677-1679.

Zhang, B., Y. H. Koh, R. B. Beckstead, V. Budnik, B. Ganetzky and H. J. Bellen (1998). "Synaptic vesicle size and number are regulated by a clathrin adaptor protein required for endocytosis." Neuron **21**(6): 1465-1475.

Zheng, H., M. Jiang, M. E. Trumbauer, D. J. Sirinathsinghji, R. Hopkins, D. W. Smith, R. P. Heavens, G. R. Dawson, S. Boyce, M. W. Conner, K. A. Stevens, H. H. Slunt, S. S. Sisoda, H. Y. Chen and L. H. Van der Ploeg (1995). "beta-Amyloid precursor protein-deficient mice show reactive gliosis and decreased locomotor activity." Cell **81**(4): 525-531.